Brain development in fetal ventriculomegaly

Vanesa Kyriakopoulou

Imperial College London

Institute of Clinical Sciences

Submitted for the degree of PhD

Declaration of Originality

I declare that the contents of this thesis are my own work and work by others is appropriately referenced and acknowledged.

Abstract

Introduction

Fetal ventriculomegaly is the most common detectable central nervous system abnormality affecting 1% of fetuses and is associated with abnormal neurodevelopment in childhood. Neurodevelopmental outcome is partially predictable by the 2D size of the ventricles in the absence of other abnormalities while the aetiology of the dilatation remains unknown. The main aim of this study was to investigate brain development in the presence of isolated ventriculomegaly during fetal and neonatal life.

Methods

Fetal brain MRI (1.5T) was performed in 60 normal fetuses and 65 with isolated ventriculomegaly from 22-38 gestational weeks. Volumetric analysis of the ventricles and supratentorial brain structures was performed on 3D reconstructed datasets while cortical maturation was assessed using a detailed cortical scoring system. The metabolic profile of the fetal brain was assessed using magnetic resonance spectroscopy. During neonatal life, volumetric analysis of ventricular and supratentorial brain tissue was performed while white matter microstructure was assessed using Diffusion Tensor Imaging. The neurodevelopmental outcome of these children was evaluated at 1 and 2 years of age.

Results

Fetuses with isolated ventriculomegaly had significantly increased cortical volumes when compared to controls while cortical maturation of the calcarine sulcus and parieto-occipital fissure was delayed. NAA:Cho, MI:Cho and MI:Cr ratios were lower whilst Cho:Cr ratios were higher in fetuses with ventriculomegaly. Neonates with prenatally diagnosed ventriculomegaly had increased ventricular and supratentorial brain tissue volumes and reduced FA values in the splenium of the corpus callosum, sagittal striatum and corona radiata. At year 2 of age, only 37.5% of the children assessed had a normal neurodevelopment.

Conclusions

The presence of relative cortical overgrowth, delayed cortical maturation and aberrant white matter development in fetuses with ventriculomegaly may represent the neurobiological substrate for cognitive, language and behavioural deficits in these children.

Dedication

This thesis is dedicated to my mother Eleni Kyriakopoulou, my partner Michael Powner and my supervisor Mary Rutherford for their support and guidance throughout my PhD.

Contents

1 Introduction 18

1.1 Fetal Ventriculomegaly 18

1.1.1 Ventriculomegaly overview 18

1.1.2 Definition and prevalence 18

1.1.3 Causes of ventriculomegaly 21

1.1.4 Isolated ventriculomegaly 29

1.1.5 Outcome 30

1.1.6 Ventriculomegaly in childhood and adulthood 39

1.1.7 Animal models of ventriculomegaly 43

1.2 Development of the brain and ventricular system 44

1.2.1 The ventricular system 47

1.2.2 The role of embryonic CSF 49

1.2.3 Cavum septum pellucidum 51

1.2.4 Cortical development 54

1.3 Aims and Hypothesis 59

1.4 Magnetic Resonance Imaging 60

1.4.1 Physics of Magnetic Resonance Imaging 60

1.4.2 MR safety 63

1.4.3 Imaging the fetus using ultrasound and MRI 67

1.4.4 Fetal CNS assessment 68

1.4.5 Imaging the neonate 76

2 Materials and Methods 79

2.1 Ethics 79

2.2 Study population 80

2.2.1 Normal control cohort 80
2.2.2 Isolated ventriculomegaly cohort 80
2.3 Fetal Imaging 81
2.3.1 MR safety 82
2.3.2 Imaging 83
2.4 Neonatal Imaging 121
2.4.1 Patient preparation 121
2.4.2 Neonatal volumetry 123
2.4.3 Diffusion Tensor Imaging 126
2.5 Neurodevelopmental assessments 127
2.5.1 Griffiths Mental Development Scales 128
2.5.2 Bayley Scales of Infant and Toddler Development-III 129
2.5.3 Ages and Stages Questionnaires 131
2.6 Statistics 132
2.6.1 Power calculations 132
3 Results 133
3.1 Contribution of MRI in the sonographic diagnosis of ventriculomegaly 133
3.1.1 Background 133
3.1.2 Aims 133
3.1.3 Cohort 133
3.1.4 Detection of additional abnormalities on MRI 134
3.1.5 Ventricular size and risk of additional abnormalities 136
3.1.6 Discussion 138
3.2 Volumetric quantification of intracranial structures from 22-38 weeks of gestation and after birth 141
3.2.1 Background 141

3.2.2 Aims 141
3.2.3 Fetal volumetry 142
3.2.4 Neonatal volumetry 184
3.2.5 Discussion 192
3.3 Assessment of cortical development and maturation 199
3.3.2 Aims 199
3.3.3 Normal control cohort 199
3.3.4 Comparison with ventriculomegaly cohort 216
3.3.5 Statistics 235
3.3.6 Discussion 237
3.4 Assessment of metabolite ratios during gestation 242
3.4.1 Background 242
3.4.2 Aim 242
3.4.3 Reproducibility 242
3.4.4 Spectral acquisition at echo time 136ms 243
3.4.5 Spectral acquisition at echo time 270ms 247
3.4.6 Lactate presence at 136ms and 270ms 251
3.4.7 Spectral acquisition at echo time 42ms 251
3.4.8 Discussion 256
3.5 Assessment of white matter microstructure in neonates with ventriculomegaly 262
3.5.1 Background 262
3.5.2 Aim 262
3.5.3 Cohorts 263
3.5.4 FA quantification 265
3.5.5 Discussion 269
3.6 Neurodevelopmental outcome in children with antenatal ventriculomegaly 274
3.6.1 Aim 274

3.6.2 Developmental assessments at year 1 of age 274
3.6.3 Developmental assessments at year 2 of age 277
3.6.4 Discussion 281
4. Main discussion 284
5. Future work 291
5.1 Volumetric segmentation of the cerebellum in fetuses with ventriculomegaly 291
5.2 Volumetric segmentation of white matter and gray matter in neonates with ventriculomegaly 291
5.3 Neurodevelopmental follow up in children with antenatal ventriculomegaly 292
5.4 Correlation of neurodevelopmental outcome and white matter development 292
5.5 Vitamin D and brain development: a pilot study 292
Appendix 300
Appendix 1. Information Sheet for Patients 300
Appendix 2. Information Sheet for Healthy Pregnant Volunteers 305
Appendix 3. Parental Questionnaire 310
Appendix 4. Ages and Stages Questionnaire 315
Appendix 5. Detailed protocol of cortical development assessment 321
Appendix 6. Cortical development: Mean and standard deviation of GA for different development scores 329
Appendix 7. Vitamin D Questionnaire 330
References 331

Figures

Figure 1. Measurement of the atrium of the lateral ventricles 19
Figure 2. Fetal ventriculomegaly 21
Figure 3. Fetal ventriculomegaly secondary to obstruction at the foramen of monro 22
Figure 4. Agenesis of the corpus callosum 24
Figure 5. Subependymal heterotopia 25
Figure 6. Ventriculomegaly secondary to congenital infection 26
Figure 7. Ventriculomegaly secondary to haemorrhage 27
Figure 8. Ventriculomegaly secondary to brain tissue atrophy 28
Figure 9. Isolated ventriculomegaly 29
Figure 10. Ventriculomegaly and hemimegalencephaly 42
Figure 11. Early embryonic brain morphogenesis 46
Figure 12. Embryonic brain regions and equivalent adult structures 47
Figure 13. Adult brain ventricular system and CSF flow 48
Figure 14. Cavum septum pellucidum 52
Figure 15. Formation of layers in the human cerebral wall 55
Figure 16. Precession 61
Figure 17. Fetal MR imaging through the years 67
Figure 18. Example of fetal dataset before and after reconstruction 69
Figure 19. ^{1}HMRS fetal spectrum 73
Figure 20. Diffusion ellipsoids 77
Figure 21. DTI Imaging: ADC and FA maps 78
Figure 22. T2-weighted Single Shot Turbo Spin Echo 84
Figure 23. T2-weighted dynamic Single Shot Turbo Spin 84
Figure 24. T1-weighted single shot Inversion-Recovery 85
Figure 25. T2*-weighted Gradient Echo 86
Figure 26. Voxel placement in fetal ^{1}HMRS 87
Figure 27. Fetal MRI clinical examination 93
Figure 28. Fetal motion 93
Figure 29. Post-processing of MR images 95

Figure 30. Selection of voxel size for volumetric analysis 97
Figure 31. Linear measurements 98
Figure 32. Volumetric segmentation of the lateral ventricles 100
Figure 33. Volumetric segmentation of the third ventricle 100
Figure 34. Volumetric segmentation of the fourth ventricle 101
Figure 35. Volumetric segmentation of extra-cerebral CSF 102
Figure 36. Volumetric segmentation of supratentorial brain tissue 102
Figure 37. Volumetric segmentation of supratentorial brain tissue (hemispheres) 103
Figure 38. Volumetric segmentation of the cavum septum pellucidum 103
Figure 39. Volumetric segmentation basal ganglia (yellow) and thalami (pink). 104
Figure 40. Volumetric segmentation of the cortex 105
Figure 41. Cortical segmentation protocol 107
Figure 42. Cortical development scoring system 109
Figure 43. Cortical landmarks of the frontal lobe 111
Figure 44. Cortical landmarks of the frontal/parietal border 112
Figure 45. Cortical landmarks of the temporal lobe 113
Figure 46. Cortical landmarks of the parietal lobe 114
Figure 47. Cortical landmarks of the frontal/parietal/ temporal border 115
Figure 48. Cortical landmarks of the limbic lobe 116
Figure 49. Cortical landmarks of the occipital lobe 116
Figure 50. Motion corrupted fetal spectrum at echo time 136ms 118
Figure 51. Automatic volumetric analysis in a neonatal brain 125
Figure 52. Risk of additional abnormalities detected on MRI 137
Figure 53. Gestational age distribution histogram in normal controls 143
Figure 54. Atrial diameter measurements using MRI in normal controls 146
Figure 55. Lateral ventricle volumes in normal controls 147
Figure 56. Total lateral ventricular volume in normal controls 148
Figure 57. Relationship between ventricular atrial diameter and volume in normal controls 149
Figure 58. Third ventricle volumes in normal controls 150
Figure 59. Fourth ventricle volume in normal controls 151
Figure 60. Extra-cerebral CSF volumes in normal controls 152

Figure 61. Cavum septum pellucidum width in normal controls 154
Figure 62. Cavum septum pellucidum width in normal controls (weekly average) 154
Figure 63. Cavum septum pellucidum volume in normal controls 155
Figure 64. Cavum septum pellucidum volume in normal controls (weekly average) 155
Figure 65. Supratentorial brain tissue volume in normal controls 156
Figure 66. Supratentorial hemispheric brain tissue in normal controls 157
Figure 67. Cortical gray matter volume in normal controls 158
Figure 68. Thalamic volume in normal controls 159
Figure 69. Basal ganglia volumes in normal controls 160
Figure 70. White matter volumes in normal controls 161
Figure 71. Gestational age distribution histogram in ventriculomegaly and normal controls ... 163
Figure 72. Lateral ventricle volume in controls and ventriculomegaly from 22 to 38 weeks 165
Figure 73. Relationship between ventricular atrial diameter and volume in ventriculomegaly . 166
Figure 74. Relationship between ventricular atrial diameter and volume in controls and ventriculomegaly 167
Figure 75. Third ventricle volumes in ventriculomegaly and normal controls 168
Figure 76. Fourth ventricle volumes in ventriculomegaly and normal controls 169
Figure 77. Extra-cerebral CSF volumes in ventriculomegaly and normal controls 170
Figure 78. Cavum septum pellucidum width in ventriculomegaly and normal controls 171
Figure 79. Cavum septum pellucidum volumes in ventriculomegaly and normal controls 172
Figure 80. Supratentorial brain tissue volumes in ventriculomegaly and normal controls 173
Figure 81. Supratentorial hemispheric brain tissue volumes in ventriculomegaly and normal controls 174
Figure 82. Hemispheric tissue volumes in unilateral ventriculomegaly 175
Figure 83. Cortical volume in ventriculomegaly and normal controls 176
Figure 84. White matter volumes in ventriculomegaly and normal controls 177
Figure 85. Basal ganglia volumes in ventriculomegaly and normal controls 178
Figure 86. Thalamic volumes in ventriculomegaly and normal controls 179
Figure 87. Ventricular and supratentorial brain tissue changes in serial scans 181
Figure 88. Histogram of age distribution of post-menstrual age at scan in the ventriculomegaly and normal control groups 185

Figure 89. Lateral ventricle volumes in normal controls and neonates with antenatal ventriculomegaly 188
Figure 90. Total lateral ventricular volume in normal controls and neonates with antenatal ventriculomegaly 189
Figure 91. Supratentorial brain tissue volumes in normal controls and neonates with antenatal ventriculomegaly 190
Figure 92. Fetal cases with antenatal ventriculomegaly used in neonatal volumetric analysis .. 191
Figure 93. Gestational age and presence of early sulcation (score 1) of cortical landmarks in normal controls 200
Figure 94. Precentral gyrus and superior frontal gyrus development in normal controls 204
Figure 95. Superior frontal sulcus and middle frontal gyrus development in normal controls .. 205
Figure 96. Inferior frontal gyrus and inferior frontal sulcus development in normal controls ... 206
Figure 97. Central sulcus and Sylvian fissure development in normal controls 208
Figure 98. Postcentral gyrus and parieto-occipital fissure development in normal controls 210
Figure 99. Superior temporal gyrus and superior temporal sulcus development in normal controls 212
Figure 100. Middle temporal gyrus and inferior temporal gyrus development in normal controls 213
Figure 101. Calcarine sulcus and cingulate sulcus development in normal controls 215
Figure 102. Gestational age of early sulcation (score 1) of cortical landmarks in normal controls (blue) and ventriculomegaly (pink) cohorts 217
Figure 103. Precentral gyrus and frontal gyrus development in normal control and ventriculomegaly cohorts 220
Figure 104. Superior frontal sulcus and middle frontal gyrus development in normal control and ventriculomegaly cohorts 222
Figure 105. Inferior frontal gyrus and inferior frontal sulcus development in normal control and ventriculomegaly cohorts 224
Figure 106. Central sulcus and Sylvian fissure development in normal control and ventriculomegaly cohorts 226
Figure 107. Postcentral gyrus and parieto-occipital fissure development in normal control and ventriculomegaly cohorts 228

Figure 108. Superior temporal gyrus and superior temporal sulcus development in normal control and ventriculomegaly cohorts 230
Figure 109. Middle temporal gyrus and inferior temporal gyrus development in normal control and ventriculomegaly cohorts 232
Figure 110. Calcarine sulcus and cingulate sulcus development in normal control and ventriculomegaly cohorts 234
Figure 111. Fetal spectrum at 136ms of a normal control fetus at 32^{+2} gestational weeks 243
Figure 112. NAA:Cho, Cho:Cr and NAA:Cr ratios varying with gestation in normal control fetuses acquired at an echo time of 136ms 244
Figure 113. NAA:Cho, Cho:Cr and NAA:Cr ratios varying with gestation in normal control fetuses and fetuses with isolated ventriculomegaly acquired at an echo time of 136ms 246
Figure 114. Fetal spectrum at 270ms in a normal control fetus at 24^{+4} gestational weeks 247
Figure 115. NAA:Cho, Cho:Cr and NAA:Cr ratios varying with gestation in normal control fetuses acquired at an echo time of 270ms 248
Figure 116. NAA:Cho, Cho:Cr and NAA:Cr ratios varying with gestation in normal control fetuses and fetuses with isolated ventriculomegaly acquired at an echo time of 270ms 250
Figure 117. Lactate detection at 136ms and 270ms echo times 251
Figure 118. Fetal spectrum at 42ms 252
Figure 119. MI:Cho, MI:Cr and Cho:Cr ratios varying with gestation in normal control fetuses acquired at an echo time of 42ms 253
Figure 120. MI:Cho, MI:Cr and Cho:Cr ratios varying with gestation in normal control fetuses and fetuses with isolated ventriculomegaly acquired at an echo time of 42ms 255
Figure 121. Mean FA images 265
Figure 122. Mean FA skeleton 265
Figure 123. Splenium of the corpus callosum 266
Figure 124. Sagittal stratum 267
Figure 125. Posterior corona radiata 268
Figure 126. Total Vitamin D levels and ethnicity 297
Figure 127. Vitamin D status and intracranial structures in controls and fetuses with ventriculomegaly 298

Tables

Table 1. CNS malformation associated with fetal ventriculomegaly 23
Table 2. Neurodevelopmental outcome in isolated ventriculomegaly: review of the literature ... 33
Table 3. Reasons for referral for a fetal MRI scan 79
Table 4. Fetal imaging parameters 83
Table 5. Cortical landmarks assessed 110
Table 6. 1HMRS echo time and metabolite detection 120
Table 7. Neonatal MRI scanning parameters 122
Table 8. Neonatal DTI scanning parameters 122
Table 9. Griffiths Mental Development Scales 129
Table 10. Bayley Scales of Infant and Toddler Development-III 130
Table 11. Additional findings detected on MRI 135
Table 12. Discrepancy between ultrasound and MRI on the diagnosis of ventriculomegaly 135
Table 13. Normal control cohort participants 144
Table 14. Ventricular measurements using MRI in normal controls 145
Table 15. Correlation of total ventricular volume and intracranial volumetric measurements .. 162
Table 16. Ventricular measurements in ventriculomegaly 164
Table 17. Correlation of total ventricular volume and intracranial volumetric measurements .. 180
Table 18. Volumetric results for control and ventriculomegaly cohorts 182
Table 19. Normal control cohort characteristics 184
Table 20. Ventriculomegaly cohort characteristics 185
Table 21. Additional findings on neonatal MRI in the ventriculomegaly cohort 186
Table 22. Gestational age of early appearance (score 1) of cortical landmarks in normal controls 201
Table 23. Correlation of cortical development scores with GA in normal controls 202
Table 24. Correlation of height and width of cortical landmarks with GA in normal controls .. 202
Table 25. Correlation of cortical development scores with GA in ventriculomegaly 218
Table 26. Correlation of height and width of cortical landmarks with GA in ventriculomegaly 218
Table 27. Inter-group comparisons of cortical measurements 236
Table 28. Normal control cohort characteristics 263

Table 29. Ventriculomegaly cohort characteristics 264
Table 30. White matter regions and tracts 268
Table 31. Year 1 cohort characteristics..... 275
Table 32. Relationship between MR measurements and GMDS outcome scores at year 1..... 276
Table 33. Year 2 cohort characteristics..... 277
Table 34. Relationship between MR measurements and BSID-III outcome scores at year 2.... 279
Table 35. Comparison between developmental outcomes at 1 and 2 years of age in 12 cases .. 280
Table 36. Main aims and findings of this thesis 285

Abbreviations

^{1}HMRS	^{1}H Magnetic Resonance Spectroscopy
ADC	Apparent Diffusion Coefficient
ADHD	Attention-Deficit Hyperactivity Disorder
ASQ	Ages and Stages Questionnaires
B_0	External Magnetic Field
BDNF	Brain-Derived Neurotrophic factor
BSID	Bayley Scales of Infant Development
Cho	Choline
CNS	Central Nervous System
Cr	Creatine
CSF	Cerebro-Spinal Fluid
CSP	Cavum Septum Pellucidum
DQ	Developmental Quotient
DTI	Diffusion Tensor Imaging
EM	Expectation-Maximization algorithm
FA	Fractional Anisotropy
FID	Free Induction Decay
FOV	Field of View
GA	Gestational Age
GDMS	Griffiths Mental Development Scales
M_0	Net Magnetization Vector
MI	Myo-inositol
MLPV	Mislabelled Partial Volume
MRF	Markov Random Field
MRI	Magnetic Resonance Imaging
NAA	N-acetylaspartate
NGF	Nerve Growth Factor
ppm	Parts per million
PRESS	Point Resolved Spectroscopy
REC	Research Ethics Committee

RF	Radio Frequency
SAR	Specific Absorption Rate
SD	Standard Deviation
SQ	Sub-Quotient
ssFSE	Single Shot Fast Spin Echo
SVR	Snapshot MRI with Volume Reconstruction
TBSS	Tract-Based Spatial Statistics
TE	Echo Time
TR	Repetition Time
US	Ultrasonography

1 Introduction

1.1 Fetal Ventriculomegaly

1.1.1 Ventriculomegaly overview

Fetal ventriculomegaly is the most common central nervous system (CNS) abnormality occurring in 1% of the fetal population. Despite being the most frequent abnormal brain finding, counselling the parents with affected fetuses is challenging as the aetiology and neurodevelopmental outcome is variable (Gaglioti et al., 2009; Garel et al., 2003b; Mehta and Levine, 2005; Wyldes and Watkinson, 2004). 50% of ventriculomegaly cases have no additional CNS abnormalities (isolated ventriculomegaly) and the aetiology of the dilatation for these cases remains unknown (Kelly et al., 2001). The neurodevelopmental outcome in children with isolated fetal ventriculomegaly is variable and includes predominantly cognitive, language and behaviour deficits (Leitner et al., 2009; Sadan et al., 2007). The reasons for this variability are not understood. Most published research into fetal ventriculomegaly has focused on the correlation of later neurodevelopmental outcome with ventricular 2D size but the results have been variable and inconclusive (Gaglioti et al., 2009; Garel et al., 2003b; Lyall et al., 2012; Mehta and Levine, 2005; Wyldes and Watkinson, 2004). To date there is no detailed prospective study looking at whether fetal brain development is altered in the presence of isolated ventriculomegaly. The main aim of this study is to investigate changes in brain development at a macro- and micro-structural level and characterise in detail the brain phenotype of the fetus with isolated ventriculomegaly.

1.1.2 Definition and prevalence

The size of the lateral ventricles remains stable from 14 gestational weeks until birth as evaluated on ultrasound with a single linear measurement (atrial diameter) at the posterior part of the lateral ventricles (Figure 1) (Snijders and Nicolaides, 1994). Mean atrial diameter between 20 and 40 weeks as measured on ultrasound is 6.4 mm (±1.2 mm) (Almog et al., 2003). The atria of the ventricles are routinely measured during the fetal anomaly ultrasound scan, offered to all pregnant women and performed around 20 weeks gestation. Antenatal diagnosis of

ventriculomegaly is defined when the atrial diameter of one or both lateral ventricles is equal to or exceeds 10 mm (corresponding to 4 standard deviations above the mean) from 14 gestational weeks until term (Cardoza et al., 1988) (Figure 2). Atrial diameter is measured on ultrasound and MR images according to the International Society of Ultrasound in Obstetrics and Gynaecology (ISUOG) guidelines (ISUOG, 2007). Measurements between the two modalities correlate well (Griffiths et al., 2010; Leijser et al., 2007; Morris et al., 2007). According to the guidelines for performing the 'basic examination' of the fetal CNS by ISUOG, 'the ventricular atrial diameter is measured in a transverse plane at the level of the atrium perpendicular to the ventricular cavity, positioning the calipers inside the echoes of the ventricular walls' (Figure 1). The anterior aspect of the lateral ventricles is not routinely measured on ultrasound on MRI.

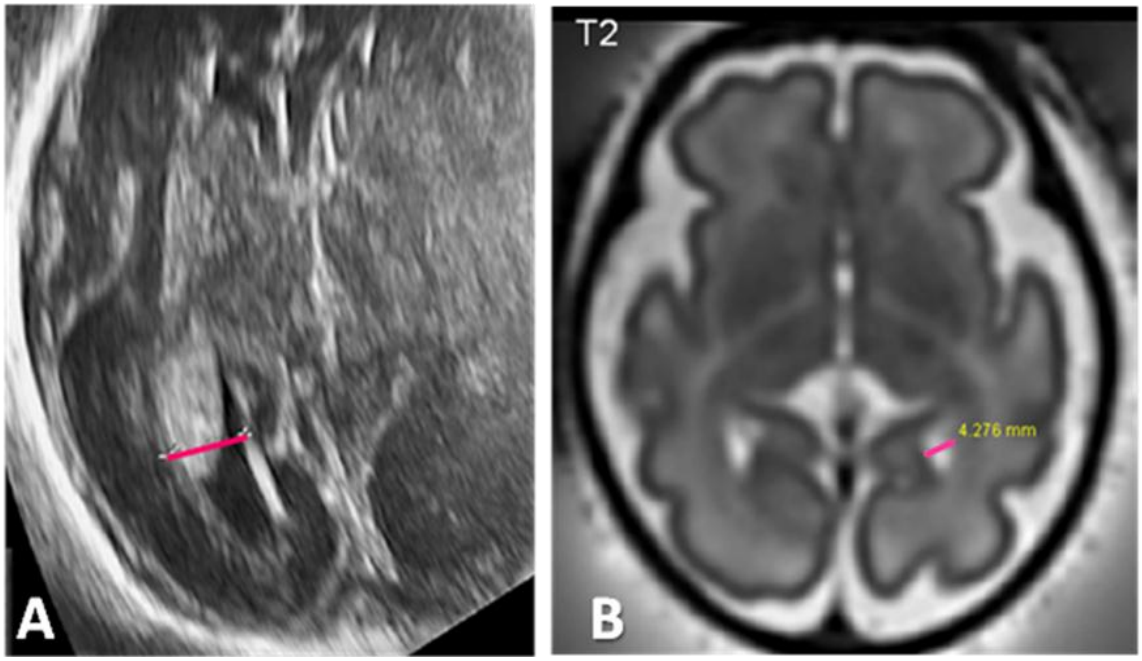


Figure 1. Measurement of the atrium of the lateral ventricles

(A) Ultrasound image of a fetal brain in a transverse plane illustrating correct positioning of callipers for the measurement of the ventricular atrial diameter (B) T2-weighted MR image of a fetal brain (30^{+5} weeks) in a transverse plane illustrating the measurement of the ventricular atrial diameter. The atrial diameter measurement is performed at the posterior part of the lateral ventricles, at the level of the low basal ganglia and perpendicular to the ventricular axis. Atrial diameter measurement is shown in pink. The calipers are placed in the low signal intensity of the ventricular wall, touching the inner edge of the ventricle and perpendicular of the long axis of the ventricle. The subependymal lining of the ventricular wall (low signal intensity) is not included. Image (A) has been reproduced from the ISUOG guidelines (ISUOG, 2007).

Ventriculomegaly is more common in boys than girls and previous studies have reported a range of male/female ratios of 1.31 to 2 (Falip et al., 2007; Ouahba et al., 2006). Ultrasound biometry studies have shown that boys have larger atrial and biparietal diameter measurements than girls (Kramer et al., 1997; Nadel and Benacerraf, 1995; Patel et al., 1995; Smulian et al., 1995), however the differences are of small magnitude. Studies have argued as to whether the 10 mm cut-off should be extended to 11 mm for male fetuses however at the present time an atrial diameter of 10 mm is the cut-off value applied to both sexes (Hilpert et al., 1995; Pretorius et al., 1986).

Ventriculomegaly is classified as isolated when there are no other CNS abnormalities detected. Depending on the degree of enlargement ventriculomegaly is classified into borderline (10 mm), mild (10.1-12 mm), moderate (12.1-15 mm) and severe (>15 mm). The current diagnosis of isolated ventriculomegaly does not require a normal karyotype or negative infection status. The prevalence of ventriculomegaly has been calculated by previous studies between 0.08% and 1% (Salomon et al., 2007; Sethna et al., 2011; Vergani et al., 1998; Weichert et al., 2010). The prevalence of isolated ventriculomegaly has been estimated at a range of 0.03% to 0.4% (Sethna et al., 2011; Vergani et al., 1998). The large discrepancy may be due to differences in imaging modality, diagnostic criteria or gestational age at diagnosis.

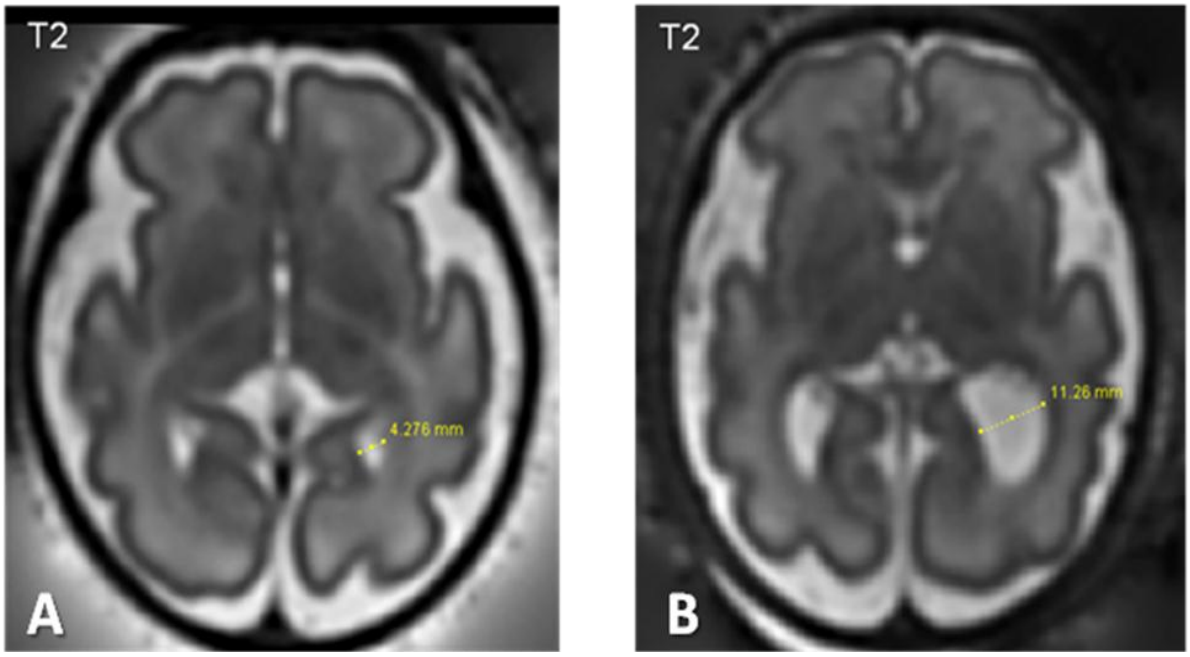


Figure 2. Fetal ventriculomegaly

T2-weighted MR image in a transverse plane of (A) a normal control fetus aged 31^{+5} weeks and (B) a fetus aged 30 weeks with ventriculomegaly. Fetal ventriculomegaly is diagnosed when the atrial diameter is equal to or exceeds 10 mm. Atrial diameter measurements are shown in yellow. It should be noted that at this level the dilatation involves only the posterior aspect of the lateral ventricles.

1.1.3 Causes of ventriculomegaly

Ventriculomegaly is a descriptive term indicating an enlargement of the lateral ventricle(s) in the developing brain.

1.1.3.1 Abnormal cerebro-spinal fluid turnover

While ventriculomegaly is a descriptive term not referring to the underlying aetiology, the term hydrocephalus has been used in the past to describe an abnormal accumulation of cerebro-spinal fluid (CSF) within the ventricles. Increase in pressure may occur due to an obstruction in the ventricular system (D'Addario et al., 2007). The reasons for the formation of an obstruction can be numerous, such as a congenital aqueduct stenosis, an inflammatory process subsequent to infection or haemorrhage, a tumour, or a CNS malformation such as Dandy-Walker (Gaglioti et

al., 2009). Most commonly seen causes postnatally are dilation secondary to haemorrhage or infection. In some rare cases increased pressure may result from overproduction of CSF as in cases of choroid plexus papilloma (Nejat et al., 2008). Although it is not possible to measure intraventricular pressure in-utero, there are specific brain features visible on MR images that would be indicative of increased pressure. Obstruction may be associated with a large or increasing occipito-frontal circumference and brain imaging appearance of ballooned ventricles with a decreased extra-cerebral space, suggestive of raised pressure within the ventricles and intracranial cavity (Figure 3). Structural obstructions may occasionally be directly visible such as a large cyst, haemorrhage or indirectly such as secondary enlargement of the 3rd ventricle due to aqueduct stenosis. In addition, alteration in the signal intensity of the adjacent white matter may be detected resulting from oedema due to the increased pressure, presumed secondary to impaired venous drainage (Del Bigio, 1993). The term hydrocephalus was extensively used in the past to describe any ventricular enlargement however it has now been replaced by the term obstructive ventricular dilatation.

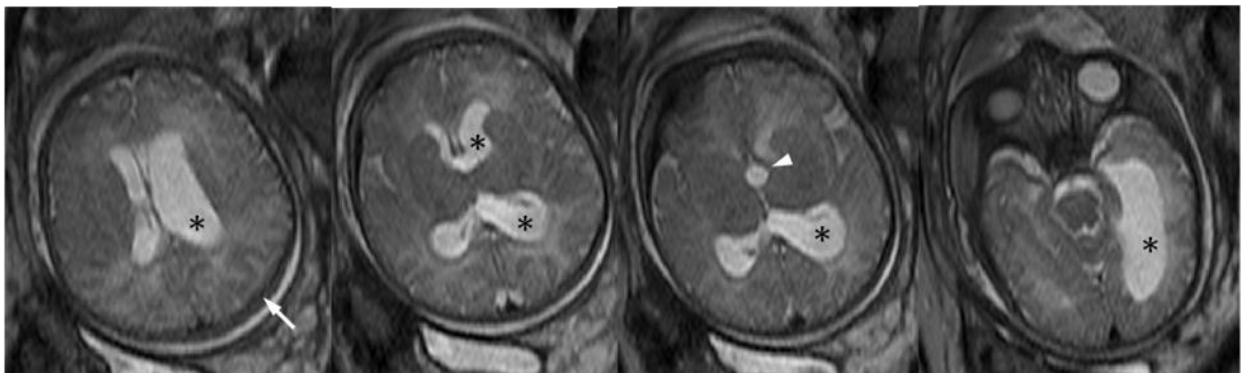


Figure 3. Fetal ventriculomegaly secondary to obstruction at the foramen of monro

T2-weighted MR images of a 39^{+6} weeks old fetus with ventriculomegaly. Lateral ventricles appear "ballooned" (asterisk). There is evidence of structural obstruction (cyst present) at the foramen of monro (arrowhead) and also decreased extra-cerebral space (arrow).

1.1.3.2 Association with other abnormalities

Presence of ventriculomegaly has been associated with a high risk of detecting additional CNS abnormalities (Gaglioti et al., 2009). Fetal MRI has been proven to be a valuable adjunct to antenatal ultrasound for the detection of additional CNS abnormalities. The risk of associated abnormalities (ventriculomegaly 10-15 mm) reported in previous studies varies from 10% to 76% (Breeze et al., 2005; Bromley et al., 1991; Gaglioti et al., 2005; Goldstein et al., 1990; Mercier et al., 2001; Morris et al., 2007; Patel et al., 1994; Pilu et al., 1999; Vergani et al., 1998). Cases with measurements above 12 mm are more likely to be associated with additional brain abnormalities (Gaglioti et al., 2005). Brain abnormalities that have been associated with ventriculomegaly are presented in Table 1 (Breeze et al., 2007; Gaglioti et al., 2005; Gaglioti et al., 2009; Gomez-Arriaga et al., 2012; Joo et al., 2008; Madazli et al., 2011; Ouahba et al., 2006; Senat et al., 1999; Sethna et al., 2011; Weichert et al., 2010; Wilhelm et al., 1998). The most commonly detected CNS abnormality associated with fetal ventriculomegaly is agenesis of the corpus callosum (Figure 4). The ventricles have a characteristic parallel pattern and appear shaped as a tear-drop posteriorly (Manfredi et al., 2010). This relative posterior dilation is termed colpocephaly. This appearance has been attributed to the fact that callosal fibres that normally cross the brain midline fail to cross the midline and form ectopic thick bundles running anterior-posteriorly (Probst bundles).

CNS malformations associated with fetal ventriculomegaly
Agenesis of the corpus callosum
Spina bifida
Holoprosencephaly
Agenesis of the cerebellar vermis
Absent septum pellucidum
Cerebral haemorrhage
Subependymal heterotopia
Schizencephaly
Arnold-Chiari malformation
Dandy-Walker syndrome
Miller-Dieker syndrome

Table 1. CNS malformation associated with fetal ventriculomegaly

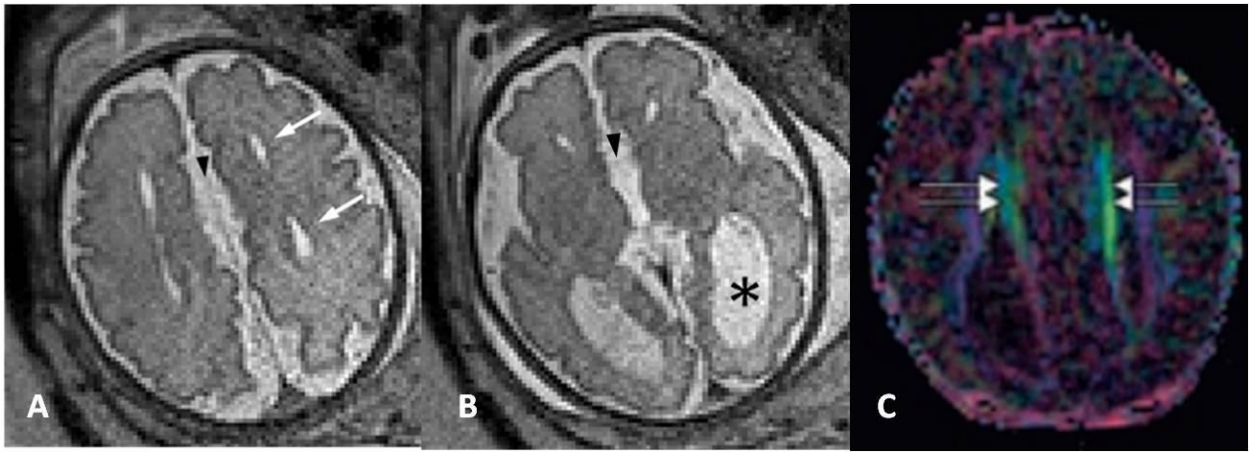


Figure 4. Agenesis of the corpus callosum

(A-B) Ventriculomegaly and agenesis of the corpus callosum in a 31 week old fetus. The intrahemispheric fissure appears wide due to agenesis of the corpus callosum (arrowhead in A). The ventricles have a characteristic parallel orientation (arrows in A) and are enlarged posteriorly (asterisk in B) and third ventricle is elevated (arrowhead in B). (C) fibres from the hemispheres fail to cross the midline and form fibre bundles running anteroposteriorly (Probst bundles-arrows) as shown in a diffusion tensor image of a 18 month old infant.

1.1.3.3 Neuronal migration disorders

Neuronal migration disorders accompanied by ventriculomegaly include periventricular subependymal heterotopia. A brain abnormality caused by defective neuronal migration with a MR appearance of ectopic neuronal "nodules" lining the lateral ventricles (Figure 5). Pathogenesis may arise due to a disruption of the radial glia scaffolding organisation and neuronal orientation (Carabalona et al., 2012). Studies in adults and children have linked subependymal heterotopia to epilepsy and impaired cognition (Raymond et al., 1994; Srour et al., 2011). Genetic mutations such as in the *FilaminA* gene may be present (Liu, 2011).

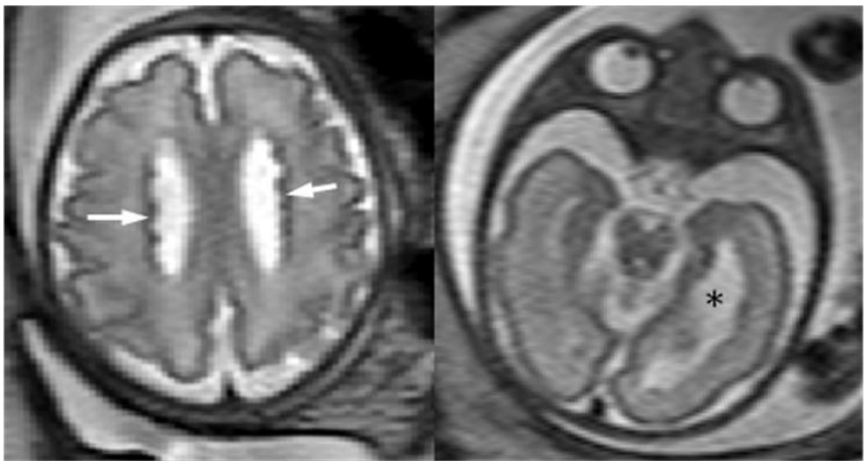


Figure 5. Subependymal heterotopia

Fetus aged 32^{+5} gestational weeks with subependymal heterotopia and superior ventricular dilatation. Characteristic ectopic neuronal nodular lining the ventricular walls (arrows). Ventricular enlargement also present posteriorly (asterisk).

1.1.3.4 Infection

As mentioned, ventriculomegaly may indicate the presence of an infection therefore TORCH infection screening is offered to all pregnant women with a diagnosis of ventriculomegaly. TORCH screening which is performed on maternal blood includes testing for Toxoplasmosis, Other (syphilis, parvovirus, hepatitits B, varicella-zoster, Epstein-Barr), Rubella, Cytomegalovirus and Herpes (Kriebs, 2008). Testing can be performed on a current blood sample or on the stored booking bloods acquired in the first 12 weeks of pregnancy. A comparison of the two samples is usually needed to confirm a recent infection. Infection screening using polymerase chain reaction (PCR) on a sample of amniotic fluid obtained through amniocentesis is also offered. The incidence of infection in ventriculomegaly has been estimated in previous studies between 0.6-2.9% (Gomez-Arriaga et al., 2012; Pier et al., 2011). According to a systematic review by Devaseelan et al., (2010) the risk of positive infection in isolated mild ventriculomegaly is 0.4% whilst in isolated mild to moderate ventriculomegaly the average rate is 1.5%. It is quite common however that the presence of infection is associated with additional abnormalities and suspicious signs on antenatal ultrasound imaging may include calcification, increased periventricular echogenicity, microcephaly, cerebellar abnormalities, abnormal signal intensity in the white matter, cortical abnormalities and periventricular pseudocysts (Figure 6)

(Malinger et al., 2003). Even in cases where antenatal brain MR imaging may only indicate isolated ventriculomegaly the progression of an infection may result in severe brain damage (Pistorius et al., 2008). The clinical outcome of these cases seems to be correlated to the extent of brain damage and can range from normal development to cognitive impairment and behavioural abnormalities, and in the severe cases to fetal or neonatal death (Malinger et al., 2011b).

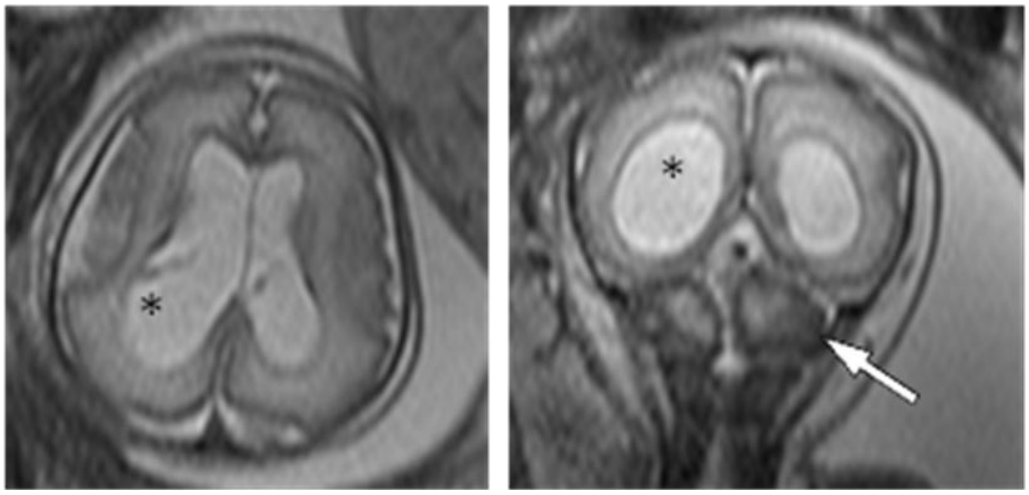


Figure 6. Ventriculomegaly secondary to congenital infection

Fetus aged 30^{+1} weeks presenting with severe ventriculomegaly (asterisk) and cerebellar haemorrhage, seen as low signal intensity around the hemisphere (arrow) secondary to parvovirus infection.

1.1.3.5 Chromosomal abnormalities

The risk of aneuploidies is higher in non-isolated ventriculomegaly regardless of the degree of dilatation (Bromley et al., 1991; Gaglioti et al., 2005; Mercier et al., 2001; Pilu et al., 1999; Vergani et al., 1998). However, the incidence is lower in severe isolated ventriculomegaly compared to mild to moderate (Nicolaides et al., 1990). In isolated cases the risk of an abnormal karyotype ranges from 3% to 14% (Bromley et al., 1991; Gaglioti et al., 2005; Graham et al., 2001; Mercier et al., 2001; Patel et al., 1994; Pilu et al., 1999; Vergani et al., 1998). In a systematic review by Devaseelan et al., (2010) it was reported that in isolated ventriculomegaly (10.1-15 mm) the risk for a chromosomal abnormality is 5% (41/923 cases). In mild isolated ventriculomegaly the risk is smaller at 3% (12/319). A recent ultrasound study measured the area of the lateral ventricles and choroid plexuses in euploid fetuses and fetuses with trisomy 21, 18 and 13 and showed that most fetuses with trisomy 13 and one third of fetuses with trisomy 18

had evidence of ventriculomegaly (Loureiro et al., 2012). The only reliable screening test for the detection of chromosomal abnormalities is karyotyping on amniotic fluid, however amniocentesis carries an approximate 1% risk of miscarriage that parents may be unwilling to take.

1.1.3.6 Germinal matrix haemorrhage

Fetal ventriculomegaly may be secondary to germinal matrix haemorrhage although this is a rare cause in a singleton fetus. As discussed haemorrhage may complicate congenital infections such as parvovirus and cytomegalovirus. In twin pregnancies complicated by twin-to-twin transfusion syndrome, haemorrhage may be seen particularly following an interventional procedure such as laser ablation of placental vessels (Figure 7). Thrombophilia screening may be indicated in fetal haemorrhage cases. Mutations in the genes for thrombotic proteins Factor-V and Factor-II and the *MTHFR* gene have been associated with thrombophilia. Patients of Mediterranean origin are a high risk group as studies have shown a high incidence of these mutations in this population (Hatzaki et al., 2003; Zoossmann-Diskin et al., 2008). Mutations in the *Col4A1* genes have also been associated with perinatal cerebral haemorrhage and porencephaly (Breedveld et al., 2006; Gould et al., 2005).

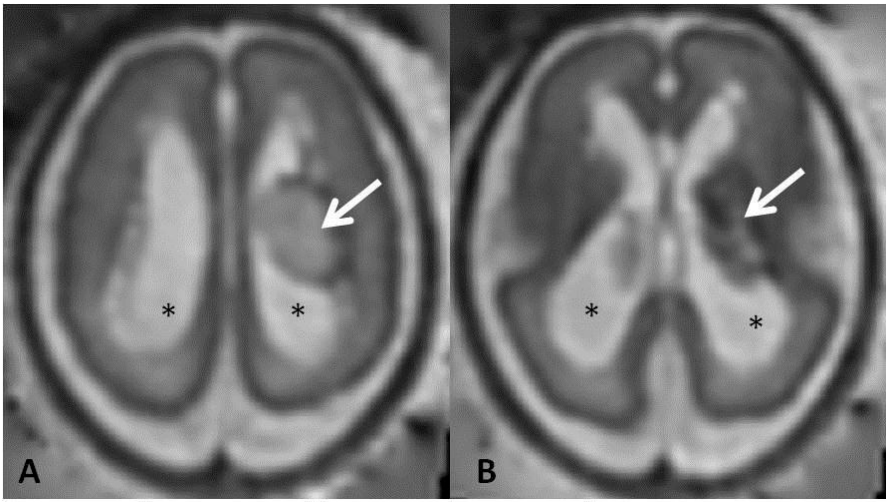


Figure 7. Ventriculomegaly secondary to haemorrhage

(A-B) Fetus aged 27^{+1} weeks showing marked ventricular dilatation and a large germinal matrix haemorrhage (arrow). Fetus shown is a twin from a diamniotic monochorionic pregnancy complicated by twin-to-twin transfusion syndrome. Laser ablation of the placental vessels was performed at 24 weeks. * = ventricular dilatation.

1.1.3.7 Brain atrophy

Rarely during fetal life and more commonly during neonatal life, ventricular enlargement may develop secondary to atrophy of the surrounding brain tissue as a consequence of brain injury (Figure 8), arising from ischemia, haemorrhage or infection (Rutherford et al., 2006). Brain tissue atrophy is evident on fetal MRI and features may include a normal or small occipito-frontal centile, decreased white matter volume and enlargement of the extra-cerebral space. Overt lesions or evidence of injury and distortion of the tissue may also be present (Leviton and Gilles, 1996).

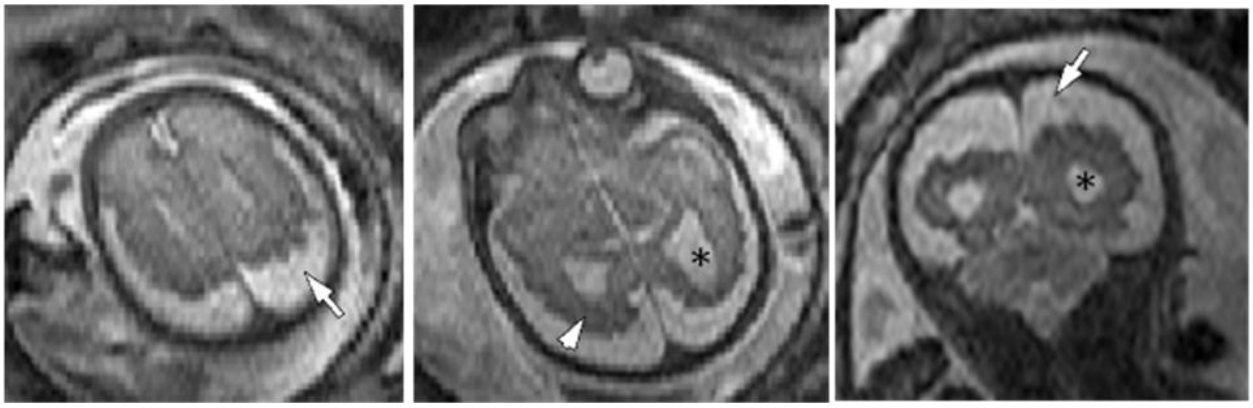


Figure 8. Ventriculomegaly secondary to brain tissue atrophy

Fetus aged 30^{+5} gestational weeks presenting with ventriculomegaly (asterisk) secondary to brain tissue atrophy. Characteristic features include increased extra-cerebral space (arrow) and distorted brain appearance and white matter loss (arrowhead). Brain size is small for gestational age while the cortex posteriorly is markedly abnormal consistent with polymicrogyria. These findings may represent an early insult to the brain.

1.1.4 Isolated ventriculomegaly

Half of the cases of ventriculomegaly however have no associated abnormality and are classified as isolated ventriculomegaly (Figure 9) (Kelly et al., 2001). In the absence of infection or chromosomal abnormality the cause of isolated ventriculomegaly is obscure. As described in future work (chapter 5.5) we are currently exploring the relationship of maternal vitamin D deficiency and fetal ventriculomegaly. The outcome of isolated ventriculomegaly is variable which poses a challenging case for consultation for clinicians and great stress to the prospective parents. For these reasons the main focus of this project is to improve our understanding of brain development in the fetuses with isolated ventriculomegaly in order to better predict outcome.

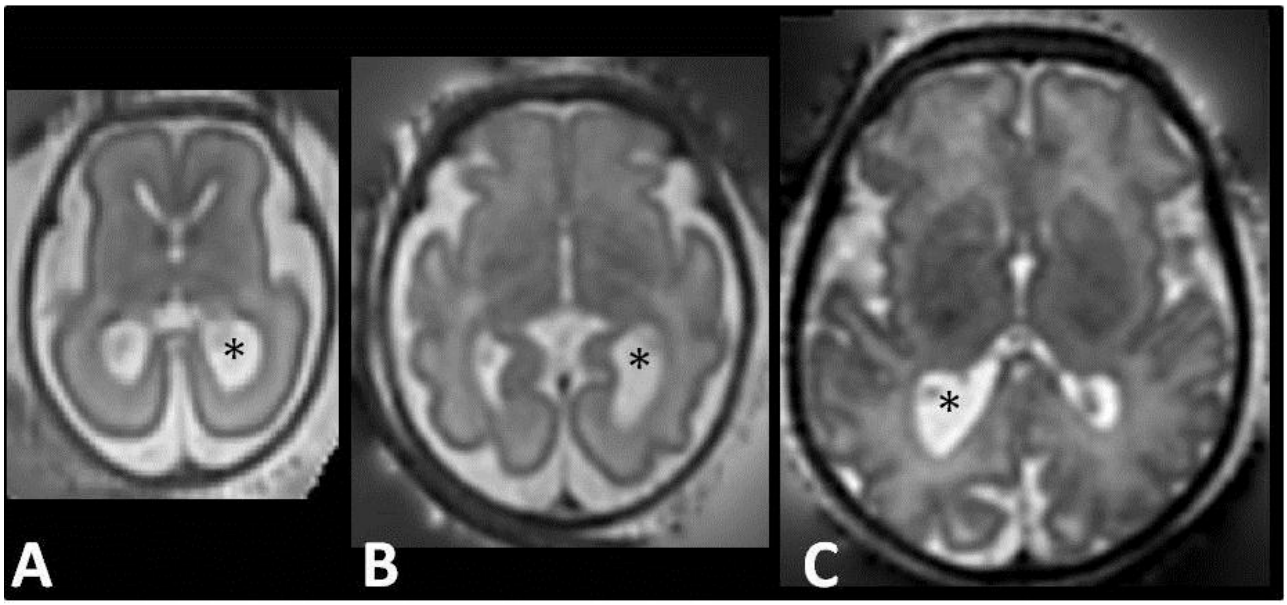


Figure 9. Isolated ventriculomegaly

Isolated ventriculomegaly presenting in three different fetal cases aged (A) 24^{+5} gestational weeks (B) 32^{+2} gestational weeks (C) 37^{+1} gestational weeks. Enlargement of the lateral ventricles is the only brain abnormality (asterisk).

1.1.5 Outcome

Prediction of the outcome of fetal ventriculomegaly is challenging partly because the aetiology of the dilation is unknown and also due to the variability of neurodevelopmental outcome. The reasons behind this spectrum in outcomes are unclear and improved understanding of the underlying causative mechanisms leading to ventriculomegaly together with an improved description of the imaging phenotype will aid outcome prediction and counselling.

Diagnosis on ultrasound is usually followed by a course of investigations which include screening for the presence of a congenital infection, karyotyping for exclusion of chromosomal abnormalities, and if available, MRI scan for the exclusion of additional brain abnormalities. Sequential ultrasound scans are recommended to monitor the size and document the progression of the dilatation. Correct differentiation between the various aetiologies of ventriculomegaly is essential to predict outcome and counselling is heavily dependent on the results of the above investigations. Numerous studies have assessed the outcome of fetuses with ventriculomegaly and variation between studies has been attributed to inhomogeneity in the cohorts assessed. We have reviewed the current literature and have extrapolated, were possible, the outcome of the isolated cases (Table 2).

Study	Imaging modality	No. cases	Ventriculomegaly size	Cohort	Assessment modality	Developmental areas assessed	Mean age	GA range	% abnormal	Specific deficits
Gaglioti 2005	US	59	Group 1: 10-12mm Group 2: 12.1-14.9mm Group 3: >15mm	isolated VM -ve TORCH euploid.	Questionnaires	Locomotor, eye and hand co-ordination, hearing and speech, learning performance.	≥ 24 m	2-12 y	Group 1: 7% Group 2: 25% Group 3: 37.5%	Language problems, nystagmus, mild intellective impairment, mild strabismus, mild neurodevelopmental delay, severe handicap. 2 cases required ventroperitoneal shunt.
Vergani 1998	US	45	10-15mm	isolated VM euploid.	Prechtl scoring system, Milani-Comparetti, Gidoni.	Cognition, motor.	28 m	3-72 m	<12mm: 3% ≥12mm: 23%	N/A
Beeghly 2010	MRI	98	Group 1: 10-12mm Group 2: >12mm	isolated VM -ve TORCH euploid.	BSID-II, Vineland Behaviour Scales, standard neurological exam.	Cognitive, motor, adaptive behaviour.	24.4 m	N/A	Group 1: mental status (8%), cranial nerves (3%), hearing/vision (0%), strength (0%), posture and tone (6%), gait (3%).	Group 2: mental status (0%), cranial nerves (8%), hearing/vision (0%), strength (0%), posture and tone (0%), gait (0%).
Leitner2009	MRI	28	10-12mm	isolated VM -ve TORCH euploid. Unilateral vs bilateral	(K-ABC), neurological examination and parental questionnaires	Neurodevelopment co-ordination, skills, speech and language, cognitive, memory, attention visuomotor.	4.4 y	3-5.9 y	unilateral: 12.5% bilateral: 33%	Cerebral palsy-left hemiparesis, deficits requiring physiotherapy, speech/ language therapy and occupational therapy. Lower scores in working memory, attention and Kaufman achievement scale.

Study	Imaging modality	No. cases	Ventriculomegaly size	Cohort	Assessment modality	Developmental areas assessed	Mean age	GA range	% abnormal	Specific deficits
Gomez-Arriaga 2012	US	18	10-12mm	isolated VM, -ve infection, euploid.	Battelle Developmental Inventory Screening Test	Personal-social, adaptive behaviour, gross/fine motor, communication, cognition.	4.9 y	1-8 y	personal/social 64%, adaptive behaviour 39%, gross motor 57%, fine motor 28%, receptive communication 39%, expressive communication 23%, cognition 17%.	Language impairment, intellectual retardation, left hemiparesis. Delayed scores in: social-personal, gross motor, adaptive behaviour (attention), communication, cognition.
Tatli 2012	US (+postnatal US)	31	10-15mm	isolated VM	BSID-III	Cognition, expressive/receptive language, gross/fine motor.	16.7 m	8-33 m	Cognitive: 16% Language: 13% Motor: 29%	Down's syndrome, tuberous sclerosis, equivarous foot deformity, cognitive/ language/ motor delay.
Pilu 1999	US	31	10-15mm	non-isolated/ isolated VM	Parental and paediatrician interviews.	N/A	33 m	21-72 m	11.5%	isolated cases all normal, non-isolated cases cognitive and motor delay/retardation.
Signorelli 2004	US	60	10-12mm	isolated VM, -ve TORCH, euploid.	Retrospective: 38 children: Parental and paediatrician interviews. Prospective: 22 children: GMDS	Cognitive, motor.	Retr. 5.4 y Prosp. 18 m	Retr. 3-10 y Prosp. 18 m	0%	-

Study	Imaging modality	No. cases	Ventriculomegaly size	Cohort	Assessment modality	Developmental areas assessed	Mean age	GA range	% abnormal	Specific deficits
Ouahba 2006	US (+MRI at 2 months and 2 years)	101	10-15mm	isolated VM -ve TORCH, euploid.	Questionnaires in 36 children. Brunet-Lezine psychomotor scale, MSCA, WPPSI-III in 65 children.	Gross/fine motor, language, social skills, memory.	54.7 m	19-127 m	11.8%	PVL+encephalopathy, encephalopathy and mental retardation, hydrocephalus, epilepsy, dyslexia, language delay, upper limb monoparia, cerebral palsy.
Sadan 2007	US	21	10-15mm	isolated VM	BSID-II, VABS.	Mental, motor, behaviour.	23.1 m	24-42 m	25%	Global developmental delay, language/communication delay, hypotonia.
Falip 2007	US (+postnatal US and MRI)	101	10-15mm	isolated VM -ve TORCH, euploid.	Brunet-Lezine psychomotor scale, MSCA, WPPSI-III	Gross/fine motor, language, social skills, memory.	24.5 m	8 m-6.5 y	9%	Neurological abnormalities, language delay, autism, behaviour disorders, severe encephalopathy, cerebral diplegia, oculomotor apraxia, language and graphic delay, seizures.
Lipitz 1998	US	25	11-15mm	isolated unilateral VM, -ve TORCH, euploid.	neonatal evaluation at birth	N/A	13 m	6-32 m	1 case	Petit mal seizures.
Bloom 1997	US	22	10-15mm	isolated VM	BSID-II, VABS.	Cognitive, motor, adaptive behaviour.	21.6 m	N/A	36.4%	Lower scores in mental and motor scales, ventriculoperitoneal shunt.

Table 2. Neurodevelopmental outcome in isolated ventriculomegaly: review of the literature

VM: ventriculomegaly, m:months, y:years, -ve: negative, MacCarthy scales of children's abilities, WPPSI: Wechsler Preschool and Primary Scale of Intelligence, K-ABC: Kaufman Assessment Battery for Children, VABS: Vineland Behaviour Scales, BSID: Bayley Scales of Infant Development, GMDS: Griffiths Mental Development Scales. No. of cases represented the number of cases that were participated in the follow-up.

1.1.5.1 Ventricular size and outcome

In non-isolated ventriculomegaly the outcome is defined by the abnormality detected. In isolated ventriculomegaly the sole predictor of outcome is the degree of enlargement (atrial diameter measurement). Other aspects that affect outcome are the evolution of ventriculomegaly with a decrease in ventricular size associated with a better outcome, whilst further enlargement has a worse prognosis (Arora et al., 1998; Gaglioti et al., 2005; Ouahba et al., 2006). Devaseelan et al., (2010) reported that the risk of neurological abnormality in isolated ventriculomegaly 10.1-15 mm and in the absence of infection or chromosomal abnormality is 12%. In mild isolated ventriculomegaly (10-12 mm) the overall risk of abnormality decreases to 4%.

In a study in 76 fetuses with isolated ventriculomegaly Gaglioti et al., (2005) divided cases into 3 groups according to atrial diameter (10-12 mm, 12.1-14.9 mm, ≥15 mm) and showed that an atrial diameter above 12 mm is less frequently associated with a normal outcome. In a study by Vergani et al., (1998) on 45 euploid fetuses with isolated ventriculomegaly it was reported that male fetuses and those with atrial measurements below 12 mm had a better prognosis. Tatli et al. (2012) studied the neurodevelopmental outcome of 31 children with antenatal borderline ventriculomegaly and reported that risk factors for an abnormal outcome included an atrial diameter >12 mm and persistence of the enlargement after birth. The study included a case diagnosed with Down's syndrome and one case with tuberous sclerosis. When excluding these cases their results showed cognitive delay (n=3), language delay (n=2) and motor delay (n=5).

Probably one of the most comprehensive imaging follow-up studies is the study by Falip et al., (2007) in a series of 101 fetuses with isolated ventriculomegaly (10-15 mm). Antenatal ultrasound and MRI were performed during the fetal period whilst brain development was followed up postnatally using cranial ultrasound at birth and MRI at 1 year, between 1 and 3 years and after the age of 3. Neurodevelopmental follow up was also performed. According to the study and as previously shown, outcome was more favourable in mild (12-11.9 mm) compared to moderate (12-15 mm) ventriculomegaly with 94% and 85% of infants with a normal outcome respectively. An interesting observation was that at the neonatal cranial ultrasound, ventriculomegaly was found in only 24 out of 64 neonates scanned. However postnatal MRI

which was performed in 76 infants, showed persisting ventriculomegaly in 58 cases. The authors suggested that the lateral ventricles were decreased as a result of vaginal delivery and decided to stop performing cranial ultrasound examinations shortly after birth as it was underestimating the progression of the dilatation.

Ouahba et al., (2006) followed 101 of children with antenatal isolated ventriculomegaly (10-15 mm) with a normal TORCH screening and a normal karyotype. Paediatric follow up included a cranial ultrasound at 3 days and a brain MRI at 2 months and at 2 years. Neurodevelopmental assessments were performed at a mean age of 54.7 months (range 19-127 months) using questionnaires (36 children) or a complete paediatric follow up including detailed developmental assessments at short time intervals (46 children) or one or more neurological and developmental assessments (19 children). Transcranial ultrasound revealed persisting ventriculomegaly in 61% of cases. Out of the 101 cases, 89 had a normal psychomotor development whilst 12 had neurological or developmental delay. Poor neurological outcome was more often associated with atrial diameter >12 mm, asymmetrical ventriculomegaly (>2 mm) and progression of the dilatation prenatally (more than 3 mm). The 12 children with abnormal outcome included cases with periventricular leucomalacia, encepahlopathy, heterotopia and hydrocephalus as diagnosed antenatally.

The group of Melchiorre et al., (2009b) evaluated the outcome of 20 children with non-progressive isolated ventriculomegaly (10-12 mm) diagnosed on antenatal ultrasound. Postnatal follow-up was performed at a mean age of 42.7 months (range 13 to 95 months) and found that 4 children had a mildly impaired neurological outcome. All children were entered into rehabilitation programs for their specific needs and 2 later recovered. Interestingly, the 2 cases that did not recover had exhibited a normal ventricular measurement on postnatal ultrasound.

1.1.5.2 Fetal ventriculomegaly and normal outcome

Signorelli et al., (2004), retrospectively assessed the neurodevelopment (range 3-10 years) of 38 children which were diagnosed with antenatal mild isolated ventriculomegaly (10-12 mm) and found no cases with an abnormal outcome. Prospectively they followed-up 22 infants with

antenatal mild isolated ventriculomegaly and found no abnormal outcome at 18 months. They suggested that mild isolated ventriculomegaly is a normal variant. Similarly Lipitz et al., (1998) evaluated the development of children with antenatal ventriculomegaly and found that all the isolated cases had a normal outcome at a mean age of 13 months.

1.1.5.3 Cognitive and behavioural delay

Sadan et al., (2007) studied 20 children with antenatal unilateral ventriculomegaly at a mean age of 32 months and found a significant difference between the ventriculomegaly and control cohorts in the mental and behaviour scale but not in the motor scale. In more detail, 20% of the ventriculomegaly group performed two SDs below average classified as significant developmental delay and another 25% had some developmental delay that required intervention. They reported that girls did better than boys in the ventriculomegaly group but there was no difference between sexes in the control group. When looking at ventriculomegaly laterality and developmental scores they reported a significant difference in the mental scale between left and right ventriculomegaly with the latter associated with a higher score in the mental scale only. As part of their study they also examined children with antenatal asymmetric ventricles (>2mm asymmetry) but below 10 mm. They reported that having ventricular asymmetry was associated with behaviour deficits but no difference was found in the mental or motor scales.

The group of Gomez-Arriaga et al., (2012) followed up 18 children with antenatal isolated ventriculomegaly (≤12mm) using parental filled questionnaires during telephone interviews at a mean age of 4.9 years (range 1-8). 64% showed a delay in social-personal skills, 56% in gross motor skills (majority were minor deviations from normality), 39% in adaptive behaviour and 28% in fine motor skills and 22% in cognitive skills.

Bloom et al. (1997) compared the development of 22 children with isolated antenatal ventriculomegaly (10-15mm) as diagnosed on ultrasound and in comparison with a control group. Children in the ventriculomegaly group scored significantly lower in the mental development index, a generalised score of development and in the motor development index. Atrial diameter and mental developmental index score correlated negatively ($r=-0.5$, $p=0.001$).

Eight children in the ventriculomegaly group and one from the control group were classified as developmentally delayed. Interestingly there was no difference in the children's behaviour.

Pilu et al., (1999) looked at the outcome of 31 fetuses with isolated ventriculomegaly (diagnosed on ultrasound, 10-15mm). Mild to moderate cognitive and motor delay was present in 11.5% of cases. However, the cohort selected included cases with chromosomal abnormalities and additional brain abnormalities diagnosed after birth.

Leitner et al., (2009) used ultrasound and MRI to diagnose isolated ventriculomegaly (10-15 mm) in 28 fetuses and followed up their cohort until a mean age of 4.4 years. Whilst most children with ventriculomegaly were within the normal range in most measurements, they reported significantly reduced attention span and working memory scores compared to controls and suggested that these specific difficulties could later influence academic performance at school. Two children had motor impairments. One child had a fixed motor deficit (cerebral palsy-left hemiparesis) and another child had multiple development difficulties requiring physiotherapy and speech and language therapy.

Beeghly et al., (2010) performed a study looking at the relationship between atrial diameter and neurodevelopmental outcome in 78 fetuses with isolated ventriculomegaly. Assessments were performed at year 1 and year 2 and evaluated the cognitive, motor and behaviour of these children. They showed no association between atrial diameter and abnormal outcome and atrial diameter did not correlate with any of the neurodevelopmental scores. They reported that while the average scores in mental, motor and behaviour development were within normal limits, individual scores in either sub-scale varied from severely or mildly delayed to within normal limits. However the majority of cases were a motor abnormality of uncertain functional significance as commented by the authors.

Falip et al., reported that 1 case with isolated antenatal ventriculomegaly was diagnosed with autism at 1.5 years of age. There are currently no studies on children with antenatal ventriculomegaly performing diagnostic assessments for autistic spectrum disorders.

1.1.5.4 Conclusions

The limitation of outcome studies using ultrasound as the sole imaging modality is that some brain abnormalities may not be detected prenatally. Several studies have shown that MRI will add information in 17% (Griffiths et al., 2010; Ouahba et al., 2006; Salomon et al., 2006) of cases after diagnosis of isolated ventriculomegaly on ultrasound. Therefore the outcome severity in "isolated" ventriculomegaly may be overestimated in these studies. In addition inclusion of cases with chromosomal abnormalities and a positive infection screen make previous studies inconclusive. There have been only 2 studies that have used MRI to confirm no additional abnormalities after an ultrasound referral of ventriculomegaly and have excluded cases with chromosomal abnormalities and positive infection screening (Beeghly et al., 2010; Leitner et al., 2009).

The variation between studies on developmental outcome can be attributed to selection of different and non-standardised developmental assessment examinations, evaluation at different and wide range of ages, follow-up rate and limited sample size. Additional bias may also be introduced due to study design with retrospective studies introducing selection and recall bias. Despite variability in outcome studies, it is apparent that developmental outcome in isolated ventriculomegaly predominantly includes language (Falip et al., 2007; Sadan et al., 2007) cognitive (Bloom et al., 1997; Gomez-Arriaga et al., 2012; Leitner et al., 2009; Sadan et al., 2007) and behavioural deficits (Falip et al., 2007; Gomez-Arriaga et al., 2012; Leitner et al., 2009; Sadan et al., 2007). Behavioural and cognitive impairments may not be obvious at 2 years of age therefore longer follow-up is essential while developmental assessment tools need to be sensitive to the impairments anticipated.

1.1.6 Ventriculomegaly in childhood and adulthood

Ventricular enlargement in adult life has been observed in many neurologic and psychiatric disorders including schizophrenia (Wright et al., 2000), epilepsy (Jackson et al., 2011), autism spectrum disorders (Palmen et al., 2005) and attention-deficit hyperactivity disorders (Lyoo et al., 1996). It is still uncertain whether these adults have always had ventriculomegaly and whether the dilatation had its origins in fetal life. It is also unknown whether fetal ventriculomegaly persists into adulthood and is a predisposing factor for adult psychiatric disorders.

1.1.6.1 Schizophrenia

Probably the most common structural brain abnormality associated with schizophrenia is ventricular enlargement and a large number of studies support a neurodevelopmental basis for this disorder (Fatemi and Folsom, 2009; Lewis and Levitt, 2002; Owen et al., 2011). A detailed meta-analysis (Wright et al., 2000) of 18 volumetric studies of patients with schizophrenia compared to controls showed increased volume of the lateral, third and fourth ventricles in patients with schizophrenia while whole brain volumes were decreased. The question arises as to whether fetal ventriculomegaly is a risk factor or a marker of increased risk of schizophrenia. Despite the association between schizophrenia and ventriculomegaly it is unclear as to when the enlargement occurs. A brain morphology study in first-episode schizophrenics revealed that ventricular enlargement was present in this population indicating that brain changes are present very early in the onset of symptoms and may not be due to medication or disease chronicity (Nopoulos et al., 1997). There is therefore no clear link between fetal ventriculomegaly and adult schizophrenia. There are no published prospective studies looking at the progression of fetal ventriculomegaly or mental status of children after school age and into adulthood and there are no retrospective studies reviewing the antenatal ultrasounds of adults with schizophrenia. Antenatal and perinatal complications have been associated with an increased risk for schizophrenia however these do not mention cases diagnosed with antenatal ventriculomegaly (Buka and Fan, 1999).

1.1.6.2 Epilepsy

Ventriculomegaly has also been observed in epileptic children. An imaging study by Kalnin et al., (2009) in 281 children with newly diagnosed seizures revealed that 87 had at least one brain abnormality. Ventricular enlargement was the most common finding present in 51% of the patients and in the majority of those cases this was an isolated finding. Similarly, Jackson et al., (2011) performed a MRI volumetric analysis of the lateral ventricles in children with new-onset paediatric epilepsy and showed a significant increase in volume compared to controls with enlargement most prominent in the frontal horns. The authors of both studies hypothesised that ventricular enlargement may be secondary to atrophy. However they did not measure brain volumes. Herman et al., (2010) performed a MRI volumetric analysis of cortical gray matter and white matter in 38 children with new-onset epilepsy and demonstrated a decrease in cortical volume and delayed growth of white matter in the epilepsy cohort (Hermann et al., 2010).

1.1.6.3 Autism

Palmen et al., (2005) performed MR volumetric analysis in 21 medication-naive high-functioning autistic children and compared the results to a healthy control group. They showed that autistic children had significantly larger total brain and lateral ventricle volumes (more than 40%) and the ventricular enlargement persisted even when correcting for cerebral volume. Enlargement was also reported in cerebral gray matter and the cerebellum. Subsequent studies have not however replicated these data. However studies investigating brain development and size in autism have been contradicting and factors that account for this variation include age at imaging, IQ, gender and medication (Courchesne et al., 2011a). The conflicting results between studies on autism are attributed to the fact that autism is not a single disorder but encompasses a wide spectrum of symptoms and may include Asperger's and pervasive developmental disorder (Johnson and Myers, 2007). The age of imaging seems to play the most important role in validation of results. The changes that are occurring in the autistic brain are evolving and age specific, therefore different brain phenotypes are observed at different ages. There are currently no studies using serial imaging in children with autism due to the difficulty in collecting MRI scans across a wide age range in autistic and healthy children. Age-related changes are statistically inferred from meta-analyses studies. The feature of the autistic brain that most

studies highlight is increased brain size. According to the study by Courchesne et al. (2011a) looking at brain growth across the life span in autism, early brain overgrowth (2-4 years) is observed in autism. This is followed by a decreased growth rate during childhood with brain volumes decreasing in autism at a faster rate than normal leading to brain sizes slightly smaller than average by 6 years of age. Retrospective studies have collected data of head circumference at birth and showed that enlargement was not present at birth. However, these are retrospectively collected data and head circumference measured after birth may not be the most reliable method of evaluating brain enlargement. At a cellular level, an excess of cerebral cortical neurons (by 67%) has been found at autopsy in a small group (n=7) of autistic patients compared to controls (Courchesne et al., 2011b). The authors suggested that such an increase in neuronal numbers can only have occurred during fetal life as there is no other time during brain development during which such a large excess of cortical neurons is generated.

1.1.6.4 Attention-deficit hyperactivity disorder

Studies looking at brain volumetry in attention-deficit hyperactivity disorder (ADHD) have also been contradictory. A MR volumetric study performed in 51 children (mean age 11.7 years and range 5-17 years) with ADHD showed increased lateral ventricles and decreased area of the splenium of the corpus callosum (Lyoo et al., 1996). In contrast, Castellanos et al., (1996) analysed brain MRIs from 57 boys with ADHD (mean age 12 years and range 5-18 years) and showed no difference in ventricular volume but reversal of normal left>right ventricular asymmetry. In addition total cerebral volumes were decreased by 4.7%. Interestingly they speculated that a fetal event affecting normal development of ventricular asymmetry might underlie their findings. IQ, medication, dyslexia and heterogeneity in the groups must all contribute to the heterogeneity in study results.

1.1.6.5 Hemimegalencephaly

Hemimegalencephaly is a congenital CNS abnormality which is characterised by enlargement of one cerebral hemisphere and its associated lateral ventricle with additional abnormal cortical gyrification (Kalifa et al., 1987) (Figure 10). Patients have intractable seizures and mental

retardation. Although the aetiology of hemimegalencephaly remains unknown, studies have shown abnormal neuronal migration and presence of giant neurons throughout the cortex and subcortical white matter (Bosman et al., 1996; Manoranjan and Provias, 2010). Post-mortem evidence demonstrates that neurons do not differentiate completely during proliferation and migration from the germinal matrix leading to a disordered arrangement of neurons in the gray and white matter (Bosman et al., 1996). Hemispheric enlargement is a result of an increased number of neurons and glia due to overproduction of neuroblasts and glioblasts or from a reduction in apoptosis. Abnormally increased levels of the neurotrophic, nerve growth factor (NGF) and brain-derived neurotrophic factor (BDNF) have been detected in brain samples from infants with hemimegalencephaly (Antonelli et al., 2004).

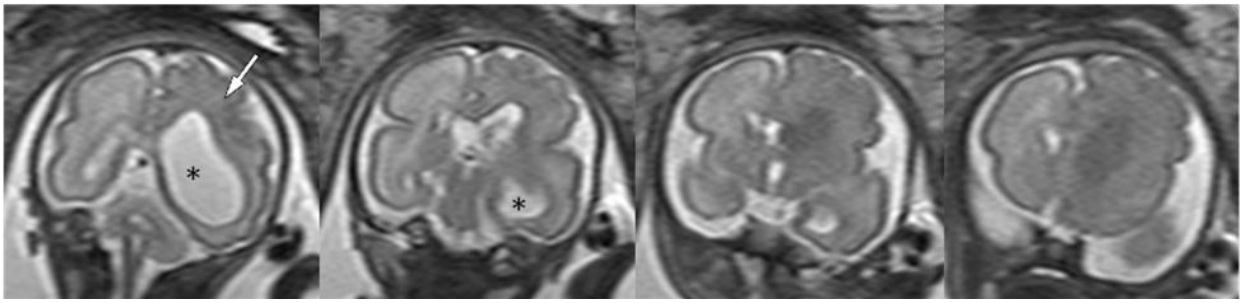


Figure 10. Ventriculomegaly and hemimegalencephaly

Fetus aged 28^{+3} gestational weeks presenting with hemimegalencephaly and ventricular enlargemnt. MR images show enlrargment of one hemisphere (arrow) and the assosciated ventricle (asterisk).

1.1.6.6 Soto's syndrome

Soto's syndrome also known as cerebral gigantism is characterised by brain and somatic overgrowth. More specifically it is characterised by macrocephaly (being the most distinctive characteristic), tall stature, advanced bone age, typical facial anomalies and mental retardation (Leventopoulos et al., 2009). Mild ventricular enlargement is a common imaging finding in patients with Soto's syndrome as indicated in imaging studies in children and fetuses with macrocephaly (Leventopoulos et al., 2009; Malinger et al., 2011a; Melo, 1999). Mutations in the *NSD*1 gene are the principal cause of Soto's syndrome affecting the regulation of transcription through histone modification (Douglas et al., 2003).

1.1.7 Animal models of ventriculomegaly

The cause and underlying mechanism of isolated ventriculomegaly is unknown, thus there are no animal models engineered specifically for the condition. The literature describes an animal model of ventriculomegaly caused by mechanically increased intraventricular pressure inside the cranium of rats representing hydrocephalus (McAllister et al., 1985; Park et al., 2011). However as mentioned previously increased intraventricular pressure is not a common feature in the fetus and such fetuses are not part of this study.

A brain phenotype of isolated ventriculomegaly has been described in a newborn rat model of gestational Vitamin D deficiency. This model was designed to create adult rats with a "schizophrenia phenotype" based on epidemiological studies showing links between low antenatal vitamin D and enhanced risk of schizophrenia. The study examined the effect of serum maternal Vitamin D deficiency throughout pregnancy on the newborn pup and showed that there were profound changes on the fetal brain (Eyles et al., 2003). The newborn pups exhibited enlarged ventricles, larger brains and an increased cortical volume whilst having a thinner cortex. Maternal deficiency altered brain gene and protein expression and disrupted the balance between neuronal stem cell proliferation and programmed cell death in the offspring (Eyles et al., 2003; Feron et al., 2005). There was no change in Vitamin D receptor expression. After re-introduction of Vitamin D to pups postnatally the brain size normalised but not the ventricular size, suggesting persisting changes in the adult brain (Feron et al., 2005). Microscopically there was a decrease in neurotrophic proteins and in proteins involved in neurotransmission and cytoskeleton maintenance (Eyles et al., 2003; Feron et al., 2005). When the rats reached adulthood they exhibited abnormal behaviour and hyperlocomotion (Burne et al., 2004; Fernandes de Abreu et al., 2010).

1.2 Development of the brain and ventricular system

Intrauterine development comprises 3 stages; the blastocyst implantation period during the first 3 gestational weeks, the embryonic period from week 4 until day 57 and lastly the fetal period ending at birth.

At 3 weeks post fertilisation the sides of the neural plate, a sheet of elongated neuroectodermal cells that will give rise to the central nervous system, start to rise up and fold inwards. By 3½ post fertilisation weeks the major subdivision of the nervous system appear. The primary vesicles of the embryonic brain consist of the prosencephalon (forebrain), mesencephalon (midbrain) and rhombencephalon (hindbrain) (Figure 11) (O'Rahilly and Muller, 2008). By week 4 the neural groove folds begin to fuse to form the neural tube which constitutes the primitive brain. The ends of the neural tube fuse and it goes through a series of folds, bends, constrictions and rotations to shape the future brain, with the anterior becoming the expanded brain, the posterior the spinal cord and the cavity of the neural tube the primitive ventricular system (Greene and Copp, 2009; O'Rahilly and Muller, 2008). These changes in shape are achieved through the continuous generation of neuroblasts and neuronal divisions from the neuroepithelium (cells lining the neural tube), to form the future forebrain, midbrain and hindbrain.

At week 6 of development, five secondary vesicles are established. Figure 12 illustrates the later subdivision of the forebrain, midbrain and hindbrain into the brain structures present in the adult brain. The prosencephalon consists of the telencephalon and diencephalon which are the precursors of the future cerebrum including the cerebral cortex, white matter and basal nuclei. The mesencephalon will become the adult midbrain region. The hindbrain consisting of the metencephalon and myelencephalon will form the cerebellum/pons and the medulla oblonganta respectively (Nichols et al., 2001). By week 8, the lateral ventricles have become c-shaped and the anterior and inferior horns are clearly established while the posterior horns have not yet been formed although their location can be determined (Blaas et al., 1998; O'Rahilly and Muller, 1990). The posterior horns become visible around week 11 of gestation and become more elongated in an anterior posterior fashion as gestation progresses (Kinoshita et al., 2001; Levene and Chervenak, 2009). Ultrasound studies have shown that the atrial diameter remains relatively stable in the second and third trimesters although an increase in absolute values is observed

(Almog et al., 2003; Snijders and Nicolaides, 1994). Fetal MRI volumetric studies have been inconclusive as to whether the volume of the lateral ventricles increases (Scott et al., 2011), decreases (Clouchoux et al., 2011) or remains stable (Kazan-Tannus et al., 2007) from 22 to 40 weeks of gestation.

Brain shaping and ventricular formation are regulated by regional cell proliferation, apoptosis and cytoskeletal rearrangements in the neuroepithelium inside the neural tube (Buss and Oppenheim, 2004; Kolega, 1986; Lecuit and Lenne, 2007). The manner in which the neural tube folds is regulated by distinct gene expression domains that control early tissue specification and therefore influence the position of the ventricles (Lumsden and Krumlauf, 1996). Regional specification of neural tissue is determined and influenced by the pattern of gene expression of neurons in each region. *Hox* genes, first described in Drosophila, coordinate the expression of a number of other genes in order to form a specific structure of each region in the embryo. Throughout the developing CNS, anterior-posterior and dorsoventral gradients of transcription factors determine regional specification (Nichols et al., 2001).

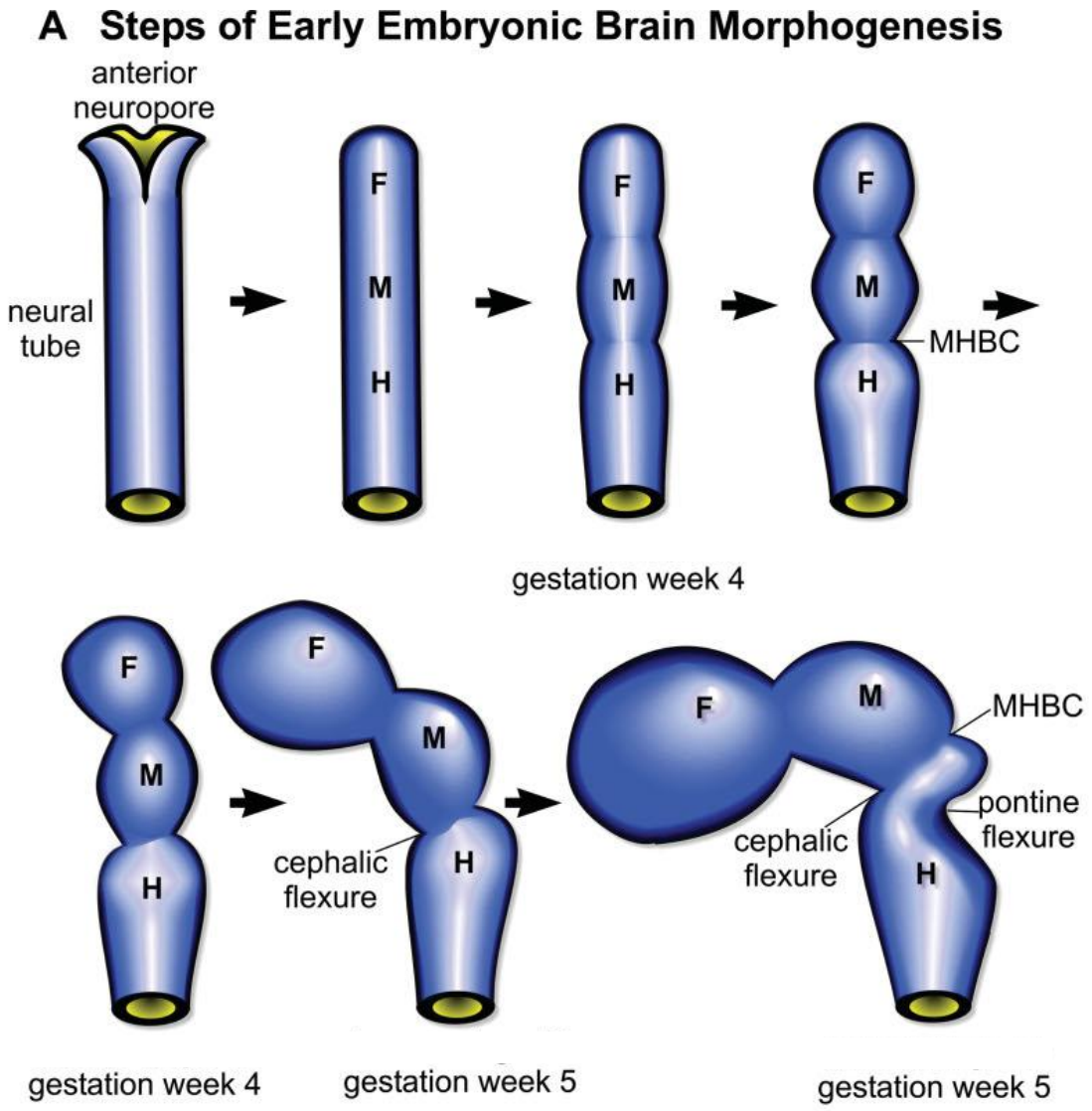


Figure 11. Early embryonic brain morphogenesis

Schematic representation of how the neural tube folds to form the embryonic brain. F, forebrain; M, midbrain; H, hindbrain; MHBC, midbrain hindbrain boundary constriction. (Image taken from Lowery and Sive 2009).

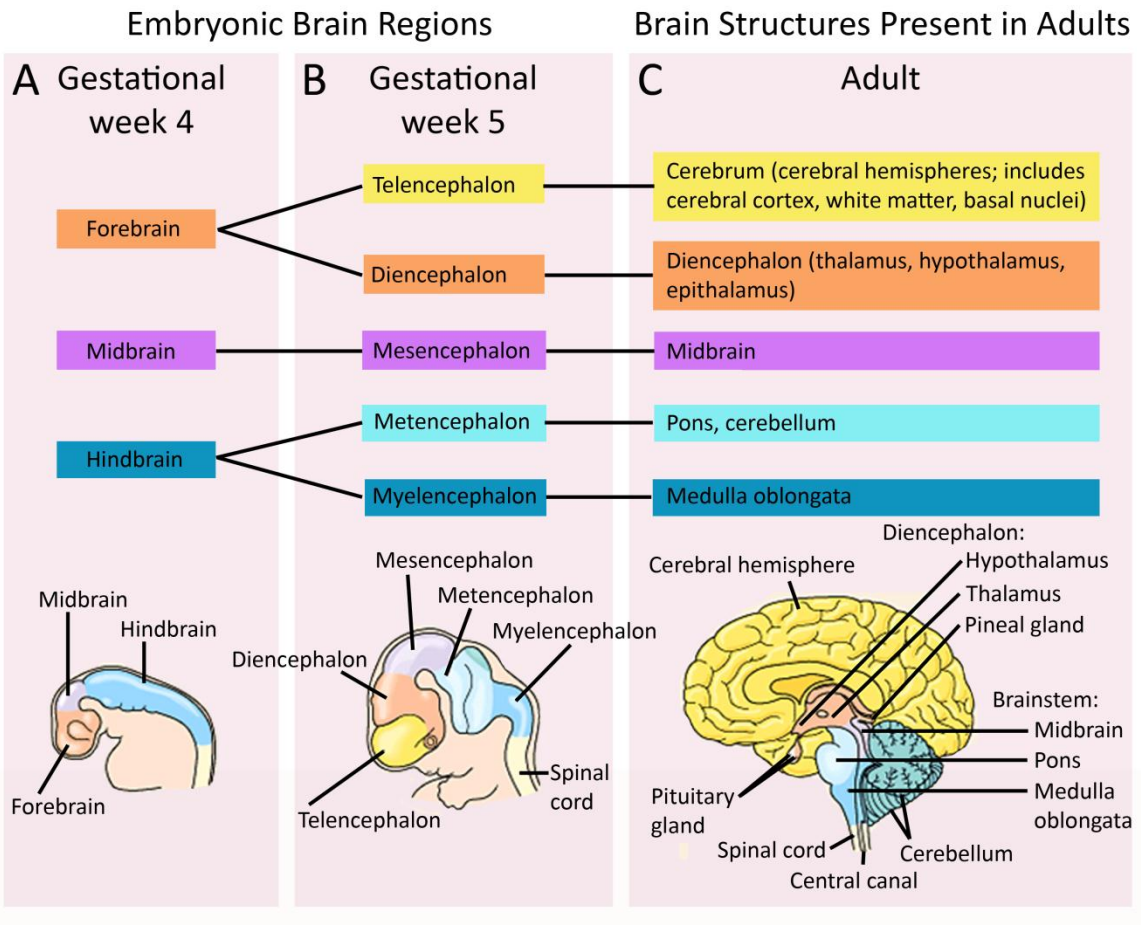


Figure 12. Embryonic brain regions and equivalent adult structures

The forebrain consists of the telencephalon and diencephalon which are the precursors of the future cerebrum including the cerebral cortex, white matter and basal nuclei. The midbrain will form the adult midbrain region. The hindbrain comprises of the metencephalon and myelencephalon which is the precursors of the pons/cerebellum and medulla oblongata respectively.

1.2.1 The ventricular system

The ventricular system consists of a series of connected cavities filled with CSF extending through all the major divisions of the central nervous system (Figure 13). The two lateral ventricles in the cerebrum, which are c-shaped, are connected to the third ventricle in the diencephalon which is in turn connected to the fourth ventricle (via the cerebral aqueduct) located between the cerebellum and the pons (Davson and Segal, 1996; Millen and Woollam, 1962). The fourth ventricle is then connected to the spinal cord canal and the subarachnoid space that surrounds the brain. During development, ultrasound studies have shown that the atrial

diameter remains relatively stable in the second and third trimester although an increase in absolute values is observed (Almog et al., 2003). The width of the third ventricle remains relatively stable from 12 until 27 gestational weeks and increases thereafter (Sari et al., 2005; Snijders and Nicolaides, 1994). As shown on ultrasound the configuration of the third ventricle also varies during gestation, starting as a single line and evolving to two parallel lines and eventually to a v-shaped configuration. MRI data indicate that the width of the third ventricle is relatively stable throughout gestation despite some fluctuation in values. When corrected for brain growth the third ventricle decreases with gestation in proportion to the fetal brain (Garel, 2004). The anterio-posterior diameter of the fourth ventricle increases through gestation however this growth is proportional to the fetal brain (Garel, 2004).

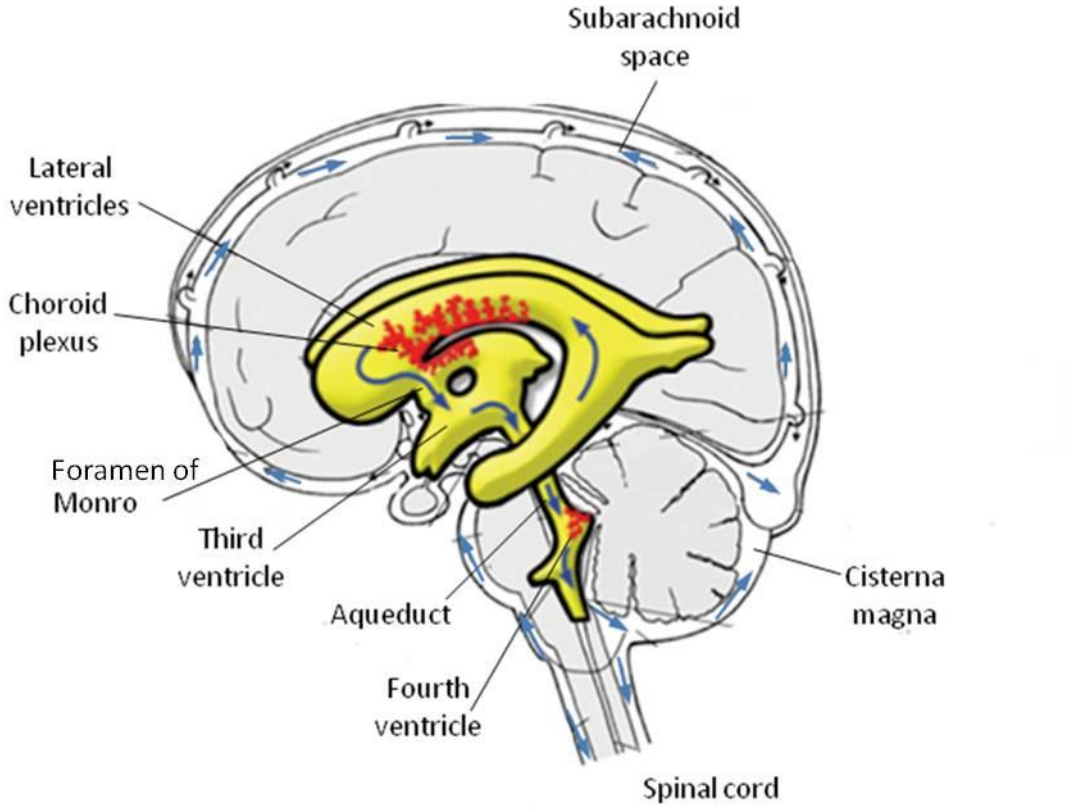


Figure 13. Adult brain ventricular system and CSF flow

CSF is produced by the choroid plexuses present in the lateral, 3rd and 4th ventricles. CSF flows from the lateral ventricles through the foramen of monro to the 3rd ventricle and then through the cerebral aqueduct into the 4th ventricle. LV, Lateral ventricles, 3V, third ventricle, 4V, fourth ventricle. (Image adapted from from Lowery and Sive 2009 and Oresković and Klarica 2010).

In adults, CSF flows from the lateral ventricles to the third and fourth ventricles and then enters the subarachnoid space at the base of the brain, it then ascends surrounding the brain hemispheres and eventually flows into the space surrounding the spinal cord. CSF drains away mainly through the arachnoid villi into the dural venous system (Davson and Segal, 1996; Nicholson, 1999) (Figure 13). The flow of CSF is a result of pressure gradients which are generated by pulsatile arterial blood flow and by gradients generated by the continuous absorption and production of CSF. The CSF dynamics during fetal life have received little attention but it is suggested that arachnoid villi are not present before birth and CSF clearance is a function of the lymphatic system (Mollanji et al., 2012). Although the central nervous system parenchyma does not contain lymphatic vessels, drainage may occur through the cribiform plate (located at the roofs of the nasal cavity) into extracranial lymphatic vessels (Mollanji et al., 2012).

1.2.2 The role of embryonic CSF

The role of CSF was rather interestingly described by C. Nicolson (1999): " CSF is to the brain what the Great Lakes and waterways are to North America: a system of interconnected fluid spaces that influence the local climate and the environment of the territory that encloses them, while providing a conduit for traffic in goods and services".

CSF appears to interact with the neuroepithelium in an interdependent and co-operative way to promote brain growth, morphogenesis and histiogenesis (Gato and Desmond, 2009). As the neural plate invaginates to form the neural tube and the neuropores fuse, amniotic fluid is trapped inside the primitive ventricular lumen (Johansson et al., 2008). From then on, there are a number of processes taking place that lead to the production of the embryonic CSF (Gato and Desmond, 2009). Production of embryonic CSF begins when fluid starts to accumulate into the ventricular lumen as it enters via an osmotic gradient. This fluid influx is thought to be controlled by Na^+K^+ATPase pumps (Na^+ influx) as well as proteoglycan secretion from the neuroepithilium. Alfonso et al., (1998) demonstrated in an animal model that an increase in Na^+ influx leads to expansion of the ventricles and expansion of the whole brain while Lowery and Sive (2005) showed that Na^+K^+ATPase mutants where unable to inflate their ventricles and supported that ion transport is essential for inflation of the ventricles during development. They also suggested

that ventricular morphogenesis requires an intact polarised neuroepithelium for the formation of the neural tube, efficient activity of the Na^+K^+ATPase pumps for inflation of the ventricles and localised cell proliferation. Gato et al., (1993) demonstrated that osmosis which is created by accumulation of osmotic molecules such as proteoglycans and Na^+ is responsible for regulation of CSF pressure and that these molecules enter the lumen by either crossing through the epithelium or are secreted by the neuroepithium cells.

It should be noted that the choroid plexus is formed around the end of the embryonic period (6-9 weeks), well after the accumulation of embryonic CSF, so it does not appear to be involved in CSF production at these early developmental stages (O'Rahilly and Muller, 1990). This accumulation of fluid leads to an increase in pressure inside the ventricular lumen which promotes brain growth. Desmond et al., (2005) used chick embryos and demonstrated that intraluminar pressure increases 10% at each developmental stage as the embryo develops. In addition they showed that an increase in intraluminar pressure leads to increased mitotic activity of the neuroepithelium cells, while a decrease in pressure leads to a reduction in brain volume (Desmond and Jacobson, 1977). Also, the pressure applied on the neuroepithilum stimulates cell proliferation possibly through tension receptors thus promoting brain growth (Gato and Desmond, 2009). Gilmore et al. (2008) in a study in neonates with ventriculomegaly suggested that changes in ventricular size may lead to changes in CSF flow and subsequently leading to an increase in neuroepithilium.

Moreover, embryonic CSF is able to alter neuroepithelial cell behaviour by means of biologically active components. While in the adult brain, there are only traces of proteins contained in the CSF, embryonic and fetal CSF contain high concentrations of proteins including signalling, growth factors, enzymes and proteases (Dziegielewska et al., 2001; Parada et al., 2006; Zappaterra et al., 2007). It appears that this protein rich environment is essential in brain ventricle development as neuroepithelial proliferation occurs primarily at the ventricular surface. CSF is essential for brain development as indicated by the groups of Gato et al., (2005) and Miyan et al., (2006) who showed that chick and rat cell lines are unable to proliferate or undergo neurogenesis in a chemically defined medium while when CSF is added, cell survival, replication and neurogenesis were stimulated. CSF may also regulate gene expression through different stages of development thus affecting brain growth (Parada et al., 2006). CSF contains

multiple factors expressed at different stages of development such as NGF, BDNF, neurotrophin-3 (NT-3) and insulin-like factor (IGF-1). These neurotrophins have an important role in the regulation of survival, differentiation and synaptogenesis of neurons in the developing brain (Cohen et al., 1996; Salehi and Mashayekhi, 2006). Transfer of molecules from blood to brain and CSF occurs via intercellullar junctions in the brain barrier interface which are known to be present from early stages of brain development for a wide range of metabolically essential molecules such as glucose, amino acids and hormones (Saunders et al., 2012).

1.2.3 Cavum septum pellucidum

The 'maverick' of brain CSF spaces is the cavum septum pellucidum (CSP) (Figure 14). The CSP is the fluid-filled cavity found between the lateral ventricles in almost all developing human fetuses (Mott et al., 1992). In the 1950s it was termed the fifth ventricle however this term has proven inaccurate as the CSP is not part of the ventricular system. The CSP is not a ventricle as it does not contain choroid plexus, does not communicate directly with the ventricular system and does not have ependymal lining (Alonso et al., 1989). It is anatomically, functionally and developmentally closely related to the corpus callosum. The CSP comprises the anterior pellucidum and the cavum vergae (Figure 14) (Raybaud, 2010). Due to its central location it is a marker of normal brain midline development and its absence or enlargement is associated with various CNS malformations such as agenesis of the corpus callosum, holoprosencephaly and septo-optic dysplasia. It is easily recognised and routinely imaged in fetal and neonatal scans (Callen et al., 2008).

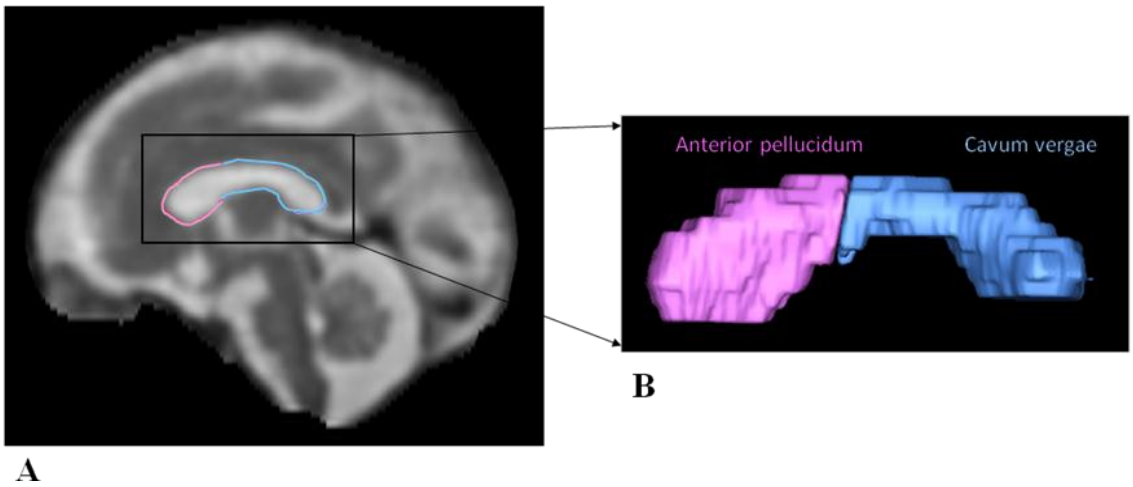


Figure 14. Cavum septum pellucidum

(A) T2-weighted MRI scan of a 28^{+1} week old fetus showing the outline of the CSP in the sagittal view (B) 3D volume representation of the CSP components, the anterior pellucidum and cavum vergae.

By 6 months of age it is generally closed, while patency in has been reported in 2.4% of normal adults (Bodensteiner et al., 1998). An increase in patency rates has been reported in schizophrenia, epilepsy, chromosomal disorders, Tourette's syndrome, obsessive compulsive disorder, in boxers as a result of head trauma and in infants as a result of vigorous shaking. It remains unclear whether CSPs that are patent in late childhood and adulthood have closed and reopened or have remained patent from fetal life. It is also unclear whether cava that are excessively wide during fetal and early neonatal life remain patent into adult life.

Studies on the fetal CSP have followed its development through linear measurements, showing a pattern of increase in size in early gestation and then decrease in late gestation: the CSP forms and disappears (Falco et al., 2000; Jou et al., 1998; Serhatlioglu et al., 2003). It first appears around 12 to 14 weeks, it increases until 28 weeks of gestation and decreases thereafter and closes by term or early in neonatal life. It is generally said to close from posterior to anterior (Winter et al., 2010). Hypotheses as to the means by which it closes vary (Winter et al., 2010).

Animal studies have shown that early in gestation (week 12), cells of the subventricular zone proliferate and form wedge-shape groups that extend continuously across the brain midline forming a glial sling which serves as a guide for developing callosal axons (Hankin et al., 1988;

Raybaud, 2010; Shu et al., 2003). Crossing the midline, the glial sling cells begin to die and a large serous-filled cavity appears. This space is the beginning of the CSP. The relationship between formation of the CSP and the ventricular system and whether the septal leaves are CSF permeable is unclear. Some pressure or osmotic gradient within ventricular CSF may cause the cavum to increase in size. It is difficult to understand the development of the cavum in abnormal cases as there are no previous studies looking at 3D CSP evolution in normal fetuses. The ventricles start to form well before the CSP and it is hypothesised that aberrant formation of the ventricular system may affect normal CSP development.

1.2.4 Cortical development

The cerebral cortex is a complex structure organised in a laminar and radial fashion. Development of the cortex is a dynamic process and defects underlie many developmental disorders of higher brain function. Unlike most organs where cells are produced near their final location, neurons designated to form the cortex are generated at a distance from the cortex. The cortex is formed in an inside-out manner with neurons born in the ventricular zone adjacent to the cerebral ventricles (Rakic, 2006; Rakic and Lombroso, 1998). Cortical development and organisation is regulated by the basic coordinated morphogenetic processes of proliferation, apoptosis, migration and differentiation of both neurons and glia (Chan et al., 2002). At week 6 of human gestation, the neopallium lining the lateral ventricles consists of 2 zones, the neuroepithelium and the preplate (Zecevic, 1993). The majority of neuroepithilial progenitor cells (conventionally called radial glia) go through several mitotic cycles thus expanding the pool of neural precursor cells and ultimately give rise to several types of cells within the cerebral cortex (Bystron et al., 2008). Post-mitotic nuclei re-enter the cell cycle resulting in two daughter cells which both remain attached to the ventricular surface (symmetric division) and extend to the cortical plate to guide migrating neurons (Chenn and McConnell, 1995; Lui et al., 2011). Asymmetric division generates a replacement radial glial cell and either a mature cortical neuron that migrates to the appropriate cortical layer or an intermediate progenitor cell that migrates to the subventricular zone (Molnar, 2011). The intermediate progenitor cell undergoes 1-3 symmetric divisions to amplify neurogenesis. At week 7, the subventricular zone appears just above the ventricular zone which gives rise to circuit neurons and glia (Zecevic, 1993). Elongated GFAP (glial fibrillary acidic protein) positive radial glial cells dominate the cerebral wall in the human fetus and serve as guides for migrating neurons by extending from the neuroepithilium to the cortical plate. Immature neurons migrate from the ventricular zone to the overlying cortical plate by using the scaffolding of the radial glial cells as a substrate (Rakic, 1971; Rakic and Lombroso, 1998). Neurons migrate in an inside out gradient formation of the cortical layers and distinct zones start to arise. The zones from the ventricular surface to the cortex include the ventricular zone, subventricular zone, intermediate zone, cortical plate (within the preplate) and marginal zone (Bystron et al., 2008; Kostovic and Jovanov-Milosevic, 2006) (Figure 15).

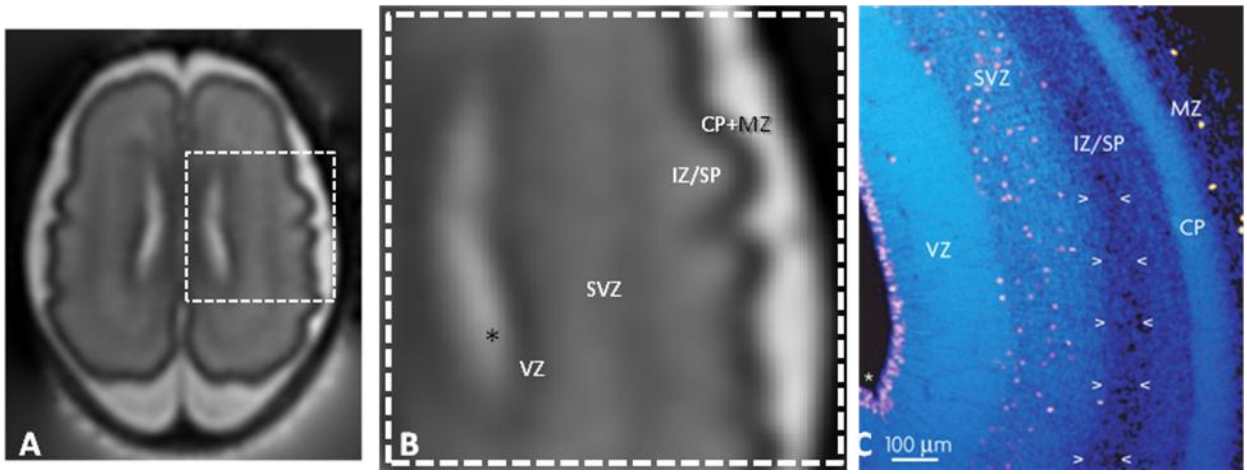


Figure 15. Formation of layers in the human cerebral wall

(A) T2-weighted image of a normal fetus aged 28^{+1} weeks (B) Layers of the cerebral tissue as seen on an amplification of image (A). (C) Layers of the cerebral tissue as seen on human embryonic tissue E56. Nuclei are shown in blue using Bisbenzimide staining while mitotic cells are shown in pink using Phosphohistone-H3 staining. (Image C reproduced from Bystron 2008).

Ventricle (asterisk), ventricular zone (VZ), subventricular zone (SVZ), intermediate zone and subplate (IZ/SP), cortical plate (CP) and marginal zone (MZ).

The location of a neuron in the cortical layers depends on the position of the precursor cell in the ventricular zone thus the cytoarchitecture and topographic maps depend on the spatial distribution of the progenitor cells in the ventricular zone (Rakic, 2006). The laminar position and phenotype of the cortical neurons is dependent on the time of their origin. At about week 10, the intermediate zone and cortical plate expand due to symmetric division (Choi, 1988; Kostovic and Vasung, 2009) while weeks 12-15 represent the peak of proliferation in the ventricular zone and preplate (Simonati et al., 1999). Neurons continue to migrate from the ventricular and subventricular zones towards the cortical plate and congregate above it (Ayoub and Kostovic, 2009). Earliest-born neurons migrate and settle in the deepest cortical layers while later generated neurons occupy more superficial layers and the cortex is formed in an inside-out manner (Rakic, 2006; Rakic and Lombroso, 1998). By week 15, the ventricular zone is no longer increasing indicating that migration of young neurons and cell proliferation are balanced. By week 16, the size of the ventricular zone starts to decrease as germinal matrix cells have started to migrate (Simonati et al., 1999). The subplate begins to form at around 13-15 weeks of gestation and starts to disappear from gestational week 35 and until the end of the second

postnatal month (Kendler and Golden, 1996; Kostovic and Judas, 2010; Kostovic and Rakic, 1990). On MRI the hypointense zone of the subplate starts to disappear from 28 gestational weeks (Perkins et al., 2008). It is a distinct transient layer located directly beneath the cortical plate with a functional role in normal development of cerebral cortical structure and connectivity (McQuillen et al., 2003). The subplate consists of migratory and postmigratory neurons, growth cones, axons, dendrites, synapses and glial cells (Kostovic and Rakic, 1990). While the cortical plate contains no synapses during the mid-fetal period the subplate contains presynaptic and postsynaptic elements and synapses from the thalamus, basal forebrain, brainstem and glutamatergic subplate neurons and is therefore a major site for synaptic interactions (Kostovic and Judas, 2010).

By week 24 the size of the ventricular and subventricular zones has reduced further. Proliferation in the ventricular/subventricular areas has been reduced while mitotic activity has increased in the intermediate zones and subplate. Progenitor cell proliferation in the intermediate and subplate zones starts to increase from week 20, peaks around 23-25 weeks, and decreases in the third trimester (Kendler and Golden, 1996). By the end of the fetal period the subventricular zone has almost disappeared. Proliferation follows a latero-medial gradient in the neocortex. Coinciding with proliferation, migration and differentiation is apoptosis which has an important role in adjusting the initial progenitor size and for CNS morphogenesis (Chan et al., 2002). Early in gestation apoptosis is involved in the development and morphogenesis of the neural tube supporting the role of apoptosis in adjusting the initial progenitor pool size (Kuan et al., 2000). At around 4.5 weeks apoptotic activity is seen in the ventricular zone but is very low. By week 6-7 apoptosis in the ventricular zone increases five-fold and there is evidence of apoptosis in the preplate (Zecevic and Rakic, 2001). By week 11 apoptosis has commenced in all cortical layers although it is most prominent in the proliferative zones. Between 12 and 22 weeks, apoptosis increases significantly throughout the telencephalon. After 32 weeks, apoptosis continues in all cortical layers. It is suggested that apoptosis during the embryonic period coincides with the process of proliferation and early migration and has a role in regulating the size of neuronal population while during fetal life it is synchronous with differentiation and synaptogenesis and probably involved in the establishment of neuronal circuitry (Rakic and Zecevic, 2000). An excess of neurons is produced during brain development many of which are discreetly removed

through normal developmental apoptosis, a process via which the developing brain is "sculpted" (Kalinichenko and Matveeva, 2008). This process by which exuberant neuronal branches and connections are removed is essential for establishing the functional organisation of circuitry. Delayed apoptosis may result in atypical patterns of connectivity which would be associated with cognitive dysfunction (Tau and Peterson, 2010).

1.2.4.1 Cortical folding

The surface of the fetal brain is initially smooth (lissencephalic) and as gestation progresses it becomes highly convoluted (gyrencephalic). Gyral elevations and sulcal indentations appear in different brain regions at separate gestational time points and develop at dissimilar rates creating complex patterns. Cortical folding involves a dynamic interaction between several developmental processes including neuronal proliferation, migration and differentiation, glial cell proliferation, apoptosis, axonal development and synaptogenesis (Grove and Fukuchi-Shimogori, 2003; Monuki and Walsh, 2001; O'Leary and Nakagawa, 2002; Rakic, 2006; Sur and Rubenstein, 2005).

The most widely accepted theory describing the underlying mechanisms of cortical folding is the VanEssen (1997) tension-based theory of gyral morphogenesis. Neurites exhibit a number of mechanical properties allowing them to adjust their length and maintain a steady tension. As immature neurites grow and extend they generate substantial mechanical tension (stress) and stretch to a length proportional to the tension exerted (Dennerll et al., 1988). When the tension is released then the neurite will shorten slightly while if stretched further it will become wavy like a rubber band. Elongation occurs when the tension overcomes a certain threshold whilst retraction occurs when the tension is released. During development the fetal brain undergoes significant changes in size and shape, at a time when neurons are establishing long-distance connections and must therefore continuously adjust their size. In order for the brain to form a rigid structural framework this tension is counterbalanced by hydrostatic pressure exerted by intrinsic pressure differential across the cellular plasma membrane (VanEssen, 1997). Cortical convolutions occur at specific spatial patterns. Previous studies have suggested that differential growth of cortical layers may explain cortical folding patterns however lesions in preterm infants affecting long-

distance connections alter cortical folding (Dehay et al., 1996; Toro and Burnod, 2005). According to the tension-based theory, folding is tension mediated. Mechanical tension created by populations of white matter axons "pull" together the pliable cortical sheet. A gyrus is formed when the crease is directed towards the exterior and the length of the axons within the gyrus is reduced (VanEssen, 1997). Cortical regions that are strongly interconnected are pulled together forming a gyrus. When tension directs the crease towards the interior sulci are formed.

However, neuroimaging data using diffusion tensor imaging (DTI) to visualise axonal fibre connections in humans, chimpanzees and macaque monkeys support an axonal "pushing" theory of cortical folding. The group of Nie et al., (2011) showed that fibre endings concentrate on gyral regions with 5.2 times higher axonal fibre density than in sulcal regions. In addition, gyral-gyral connections were highly dominant followed by gyral-sulcal. According to the axonal pushing theory, in early brain development thalamocortical, callosal and cortico-cortical axons grow guided by signalling molecules (O'Leary et al., 2007) and constantly "push" the cortical plate such that cortical layers expand in tangential directions. Mechanical constraint due to the fact that cortical area is almost three times larger than the cranial area causes cortical regions to fold inwards leading to the formation of sulci (Nie et al., 2010).

1.3 Aims and Hypothesis

The main aim of this thesis is to investigate brain development and characterise the volumetric, maturational and micro-structural changes in the fetal and neonatal brain in the presence of isolated ventriculomegaly. We hypothesise that isolated fetal ventriculomegaly is a marker of altered brain development characterised by relative overgrowth and aberrant white matter development.

Specific aims

1. Establish whether there is evidence of relative overgrowth and/ or aberrant development in multiple intracranial structures in fetuses with ventriculomegaly and how these relate to ventricular volume.
2. Design a detailed protocol for the evaluation of cortical development and establish whether ventriculomegaly is associated with delayed or abnormal cortical maturation.
3. Assess differences in brain metabolite ratios between fetuses with isolated ventriculomegaly and normal fetuses.
4. Assess white matter development in neonates with antenatally diagnosed ventriculomegaly.
5. Assess the neurodevelopmental outcome of children with antenatal isolated ventriculomegaly at 1 and 2 years of age and correlate developmental scores with MR measurements.

1.4 Magnetic Resonance Imaging

Magnetic resonance imaging is a non-invasive imaging technique that has been increasingly used for imaging the developing fetus due to its safety profile, high resolution and soft tissue contrast. MRI provides a unique opportunity to study *in vivo* brain development and provide additional information in clinical cases of congenital abnormalities.

1.4.1 Physics of Magnetic Resonance Imaging

1.4.1.1 Precession

The most abundant atom in the human body is Hydrogen (^1H) with a nucleus comprising of a single proton. The single positively charged hydrogen proton spins very fast around an axis producing a small magnetic field.

Each hydrogen nucleus is spinning on a given axis and when there is no external magnetic field the nuclei are randomly orientated (Figure 16A). When an external magnetic field (B_0) is applied though they align with the magnetic field parallel or anti-parallel (Figure 16B). Aligned protons also "wobble" around their axis. This type of movement is termed precession. During precession the axis of the spinning proton spins forming a cone shape. The frequency of the precession is proportional to the magnetic field strength and is defined by the Larmor equation:

$$\omega_0 = \gamma B_0$$

Where ω_0 = Precessional or Larmor frequency (MHz)

γ = Gyro magnetic Ratio (MHz/T)

B_0 = Magnetic field strength (T)

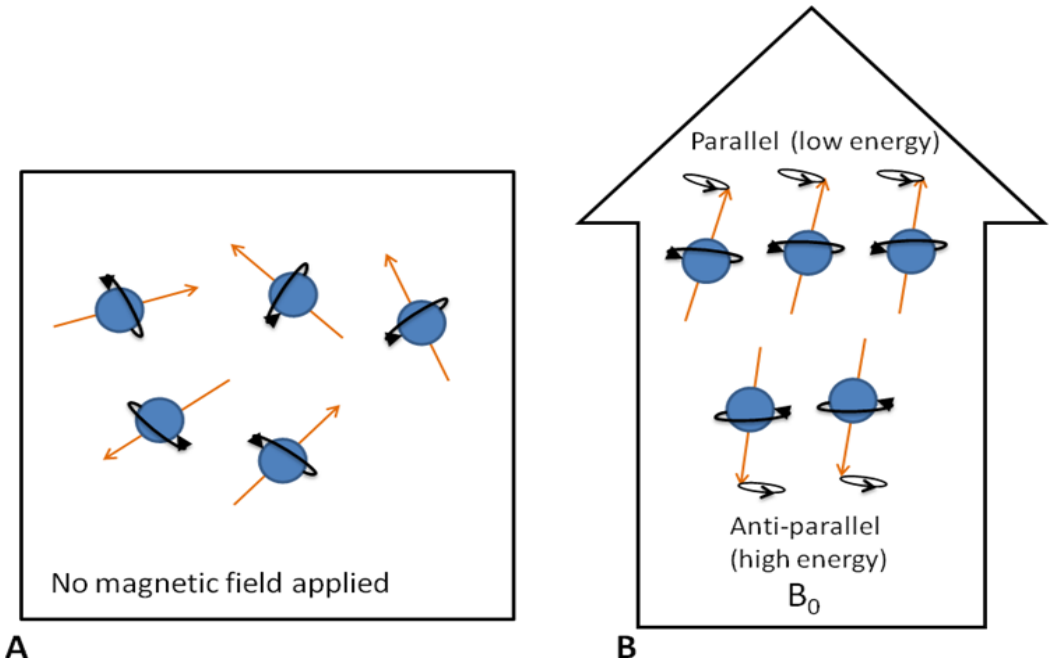


Figure 16. Precession

(A) When no external magnetic field is applied, hydrogen atoms are randomly orientated. (B) When an external magnetic field B_0 is applied the hydrogen atoms align parallel or anti-parallel with the magnetic field. During alignment the atoms spin around their own axis (precess).

1.4.1.2 The Zeeman effect

The two alignments (parallel or anti-parallel) are on different energy levels. Nuclei that align parallel to the magnetic field are in a low energy state and are termed spin up nuclei whilst nuclei that are aligned anti-parallel are in a high energy state and are termed spin down. This is the Zeeman effect. Nuclei are continually oscillating between the two states although the preferred state of alignment is the one that needs less energy. To favour a low energy state, there are more protons aligned parallel or low energy state than anti-parallel or high energy state. The excess amount of protons aligned parallel within a magnetic field are proportional to B_0 and the total magnetic field for the excess protons is known as the net magnetisation vector or M_0. Therefore the larger the B_0 the greater the difference in energy levels and the greater the excess number of protons aligned parallel to the magnetic field. The net magnetisation vector is in a direction along/longitudinal to the external magnetic field therefore it is called longitudinal magnetisation.

1.4.1.3 Excitation

A radiofrequency (RF) pulse is applied and the protons absorb that energy and resonate moving to a higher energy state. The frequency of the RF pulse is equal to the Larmor frequency in order to excite the protons (resonance). The addition of this RF pulse is termed excitation and it leads to an increase in the number of nuclei in the high energy state. This results in the movement of the net magnetisation vector out of alignment from the B_0 and pointing in the direction which the precessing protons point (transverse magnetisation). The angle to which this occurs is termed the flip angle and its amplitude depends on the amplitude of the radio-frequency pulse, normally 90°

.

1.4.1.4 Signal detection

The constant changing in the magnetic vector induces an electric current which is the MRI signal detected by an antenna. After the application of the radiofrequency pulse, the hydrogen protons lose the energy they absorbed and return from a high energy state to their lower energy state, realigning with B_0. The established transverse magnetisation starts to disappear (transverse relaxation) while the longitudinal magnetisation increases to the original state (longitudinal relaxation). The net magnetisation vector realigns with B_0 and some of the absorbed radiofrequency energy is being retransmitted to the surroundings. Part of the energy induces an increase in temperature of the surrounding tissue referred to as lattice. The process in which the excited protons release the absorbed energy back into the surrounding lattice and re-establishing the thermal equilibrium is known as T_1 Relaxation or longitudinal relaxation. The time course whereby the system returns to equilibrium is described by an exponential curve. As protons move together, their magnetic field begins to interact (spin-spin interaction). The temporary and random interaction between 2 spins leads to a loss of phase and a loss of signal known as T_2 Relaxation or transverse relaxation. The signal decay due to T_2 relaxation is denoted by an exponential curve. The image is not generated directly from the signal received. The signal is encoded in an intermediate form, the k-space. The data in k-space are transformed into the final image using Fourier transformation.

1.4.1.5 Pulse Timing Parameters

The RF pulses can be described using pulse sequences, indicating frequency and repetition. The time between each pulse is termed as the repetition time (TR). Echo time (TE) is the time between the peak of the 90˚ RF pulse to the peak of the signal induced in the coil or how long the magnetisation remains in the transverse plane before being refocused. Images with different contrasts are produced by altering the TE and by choosing the appropriate repetition time. In certain tissues the transverse magnetisation may decay faster compared to other regions. When the signal is delayed then less signal is detected from this region which therefore appears darker.

1.4.2 MR safety

MRI is considered a safe imaging modality for assessing the developing fetus and currently there is no evidence suggesting a harmful effect to the mother or the fetus. Guidelines are given by the National Radiological Protection Board (NRPB) (1991), the International Non-Ionizing Radiation Committee of the International Radiation Protection Association (ICNIRP) and the National Radiological Protection Board (NRPB). Establishing the risk from MRI to the fetus is complex as there is variation of magnet field strengths, gradient strengths and RF pulse sequences used but most importantly we do not understand what reaches the fetus and what the effect is at the different gestational ages. Current guidelines recommend that MRI is avoided during the first trimester except in cases with compelling maternal reasons.

1.4.2.1 Animal studies

Animal research regarding MR safety during pregnancy has been reported in numerous studies. Heinrichs et al., (1988) exposed pregnant mice in a 0.35T MR scanner at mid-gestation and found no gross effects but found some evidence of reduced crown-rump length. The study by Yip et al., (1994b) investigated exposure of chick embryos to 1.5T magnet for 6 hours at different developmental time points and observed an increase in abnormalities and mortality after birth. In a further study by the same group looking at effects at the molecular level, there was no difference in cell proliferation, migration or axonal outgrowth (Yip et al., 1994a; Yip et al., 1994b). Exposure of pregnant mice to 4T MRI did not show any alteration in fetal or postnatal

growth after long term exposure (9 hours) during day 9 (neural tube growth) and day 12 (reproductive system development) (Magin et al., 2000).

1.4.2.2 Human studies

Myers et al. (1998) compared fetal growth in a group of 74 normal fetuses (recruited as healthy volunteers) exposed to 0.5T MRI and a control group of 148 fetuses that did not undergo fetal MRI. There was no difference in fetal growth between the groups. Three studies (Michel et al., 2002; Poutamo et al., 1998; Vadeyar et al., 2000) have monitored fetal heart rate during MRI and did not detect any variance in heart rate during the scan.

1.4.2.3 Static Magnetic Field

Review of the literature on the safety of strong static magnetic field suggests there is no firm or established evidence of any adverse effect on human health (Schenck, 2000). Studies on cell cultures exposed to a static magnetic field ranging from 0.49T to 8T showed no effect on cell viability, growth or ability to differentiate (Kula and Drozdz, 1996; Sato et al., 1992; Ueno et al., 1994). Mevissen et al. (1994) exposed pregnant rats to a static magnetic field of 30mT throughout their gestation and reported increased risk of fetal loss. Additional studies exposing embryos from different species at a static magnetic field early in gestation have shown evidence of altered early embryonic development with duration of exposure being a significant factor. A large study on human pregnant MRI workers revealed no significant association between fertility, length of gestation, birthweight, pregnancy outcome and offspring gender with working with MRI (Kanal et al., 1993).

1.4.2.4 Time-varying magnetic gradient fields

The concerns for the fetus regarding the pulsed electromagnetic gradient fields are biological and acoustic noise. In terms of biological effects, it has been questioned whether low frequency electromagnetic fields are associated with an increased risk of spontaneous abortion (Li et al., 2002). However *in vitro* and *in vivo* animal and human studies have revealed no measurable

effects (De Wilde et al., 2005). More studies are needed to establish whether there is any effect from time-varying gradients used in MRI. A major concern has been acoustic noise which is produced by the rapid switching of the currents within the gradient coils in the presence of a strong magnetic field. This leads to the generation of Lorentz forces which make the coils vibrate and produce the characteristic knocking noise. Acoustic noise and the effect on the fetus has been of great concern to the MRI community as the mother's hearing is protected with headphones and it is unclear how much sound is attenuated as it passes though the abdomen and amniotic fluid to the fetus. Studies however have been inconclusive. The levels of acoustic noise measured during a MR examination are high and range from 80 to 120dB with a 30dB attenuation for the fetus (Glover et al., 1995; Price et al., 2001). However transition of sound in-utero occurs in a complex way with sound being attenuated and frequency being increased (Lecanuet et al., 1998). A report for the American Academy of Paediatric concluded that there was evidence of high frequency hearing loss, reduced gestation length and a decrease in birth weight in exposure over 90dB (Etzel et al., 1997). However, Reeves et al. (2010) assessed the cochlear function of 96 neonates that had undergone fetal MRI and did not show an increase in hearing impairment. In the study by Kok et al. (2004) 41 children that had undergone fetal MRI (1.5T) during the third trimester were followed up between 1 and 3 years and no harmful effects on neurodevelopment related to antenatal MRI were observed. More research is required to ascertain the effect of acoustic noise on the developing fetus.

1.4.2.5 RF pulse and heating

The risk associated with RF energy is an increase in maternal and subsequently fetal temperature. An elevation in temperature can be hazardous for the developing fetus (Edwards et al., 2003). A raised temperature may occur in humans through fever or other forms of heating. Although a specific temperature threshold has not been established it is accepted that a temperature rise of 2-2.5 ˚C in humans above the normal body temperature for over 24 hours may have an adverse effect on the developing fetus including abortion, growth restriction and developmental defect (Chambers et al., 1998; Edwards et al., 2003; Kline et al., 1985). The stage of gestation in human studies has been broad. Abnormalities are induced as elevated temperatures can affect cell proliferation, migration, differentiation and normal developmental

apoptosis. The nature of defect is dependent on the elevation, the duration of increased temperature and the developmental stage when this occurred. The sensitivity of the fetus to heat varies and depends on the state of development with various "windows" during fetal life where the risk is high and the fetus is especially vulnerable (Edwards et al., 1995). Sensitivity of different organs to heat is dependent on the stage of development with the susceptibility period being just before and after the commencement of cell proliferation. Therefore fetal organs are most susceptible while they are forming and are relatively resistant to heat once they have formed making the brain most sensitive during the embryonic and mid gestation period. The fetus has no homeostatic mechanisms to control its own temperature and is therefore dependent on regulation by the maternal temperature and placental blood flow. The fetus has a temperature of +0.5 ˚C above the maternal temperature (Schroder and Power, 1997). Manufactures design MRI systems in accordance to an international standard (IEC_60601-2-33, 2002) and must establish the specific absorption rates (SAR) for each pulse sequence conforming to guidelines. The ICNIRP guidelines (2004) state: 'It seems reasonable to assume that adverse developmental effects will be avoided with a margin of safety if the body temperature of pregnant women does not rise by more than 0.5 ˚C and the temperature of the fetus is less than 38 ˚C'. In a study by Hand et al. (2010) a mathematical model was used to estimate the regional heat absorption during fetal scanning in both 1.5T and 3T and showed that maximum heat absorption was in the mother and levels in the fetus appeared safe.

1.4.3 Imaging the fetus using ultrasound and MRI

Since the first application of MRI to study the fetal brain in 1983 (Smith et al., 1983), its clinical use has increased dramatically and significant progress and great advances have been made in the acquisition and post-processing of images (Figure 17).

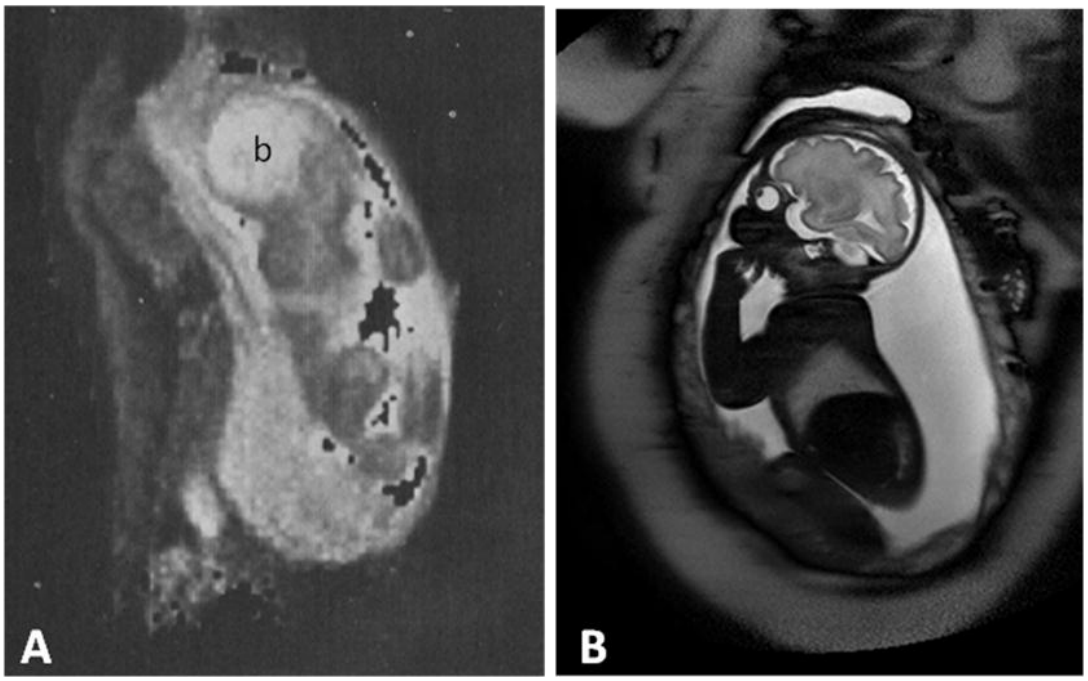


Figure 17. Fetal MR imaging through the years

(A) T_1 -weighted MR image of a 32 week old fetus performed in 1984 (b:brain, image reproduced from Smith et al. (1984), (B) T2-weighted MR image of a 30^{+5} weeks old fetus performed in 2012.

However it wasn't until the early 1990s that fetal MRI was revolutionised with the development of the single-shot rapid acquisition sequence during which each slice is acquired in less than a second providing good quality images in the presence of fetal motion.

MRI is an excellent complimentary imaging modality to ultrasound and is used when confirmation or additional information is requested for a diagnosed or suspected abnormality or in pathological cases where brain changes may not be detectable by ultrasound. MRI has a large field of view allowing visualisation of the whole uterus and fetal body and is not limited by fetal position. Great soft tissue contrast renders it excellent for visualising the different intracranial structures whilst image quality is not largely affected by the presence of excessive adipose tissue. Visualisation is also not affected in clinical conditions with low volume of amniotic fluid

(oligohydramnios). It also provides good visualisation of the posterior fossa an area difficult to visualise on ultrasound after 33 weeks, allows direct visualisation of both sides of the fetal brain and is an excellent modality for visualisation and assessment of cortical folding (Coakley et al., 2004; Glenn, 2006). However MRI is expensive and time-consuming. Maternal claustrophobia and discomfort during the scan are common complaints compared to ultrasonography whilst the small diameter of the bore may not allow imaging of patients with a high BMI. In addition, MRI is contraindicated in patients that have ferrous metal inside their body. Fetal motion affecting image acquisition and degrading quality has been a major limitation however this can be overcome with more recent advances in image acquisition and post-processing techniques (Jiang et al., 2007). Lastly, ultrasound may be superior to MRI for visualisation of some cysts and for calcification.

1.4.4 Fetal CNS assessment

T_2-weighted images are the mainstay in antenatal MRI to assess normal and pathological brain anatomy as they provide excellent delineation between fluid and tissue. The fetal brain is assessed for the presence of structural abnormalities on T2-weighted single shot fast spin echo (ssFSE) sequences obtained in transverse, coronal and sagittal planes. ssFSE sequences are used as they provide good quality images even in the presence of fetal motion due to the fast acquisition time of each slice. The T_2 time of fat is shorter compared to water, therefore the transverse component of magnetisation of fat decays faster and the magnitude of transverse magnetisation of fat is small while the magnitude of transverse magnetization in water is large. Consequently, water has a high signal and appears bright while fat has a low signal and appears dark on T2-weighted images. CSF fluid around the brain provides excellent contrast of the cerebral surface and developing gyration.

1.4.4.1 Fetal brain volumetry

Fetal MRI studies have successfully measured brain parenchyma and volumes of intracranial structures across gestational age in order to establish normative growth trajectories (Clouchoux et al., 2011; Corbett-Detig et al., 2011; Gong, 1998; Grossman et al., 2006; Hu et al., 2009; Limperopoulos et al., 2010; Rajagopalan et al., 2011a; Scott et al., 2011). However the majority

of studies have produced brain volumes using non-reconstructed data, sensitive to fetal motion (Clouchoux et al., 2011; Gong, 1998; Grossman et al., 2006; Hu et al., 2009). Critical limitations of fetal brain MRI include fetal and maternal motion, which lead to incomplete brain volumes, creation of artefacts and degraded image quality. Measurement errors may occur due to thick slice acquisitions and inter-slice motion induced differences in out-of-plane views. Maternal sedation is used in some centres outside the UK to minimise maternal and fetal motion however motion still exists due to diaphragmatic movement from maternal breathing. These data would be inappropriate for reliable quantification of the developing intracranial structures and comparison with high-risk groups or normal controls as they may not be accurate enough for ascertaining small but significant differences between groups. As described later, to overcome this issue in the current project we have used the Snapshot MRI with Volume Reconstruction (SVR) technique (Jiang et al., 2007), developed in our department, which provides image datasets of high resolution, high signal-to-noise ratio and full brain coverage essential for reliable volumetric analysis (Figure 18).

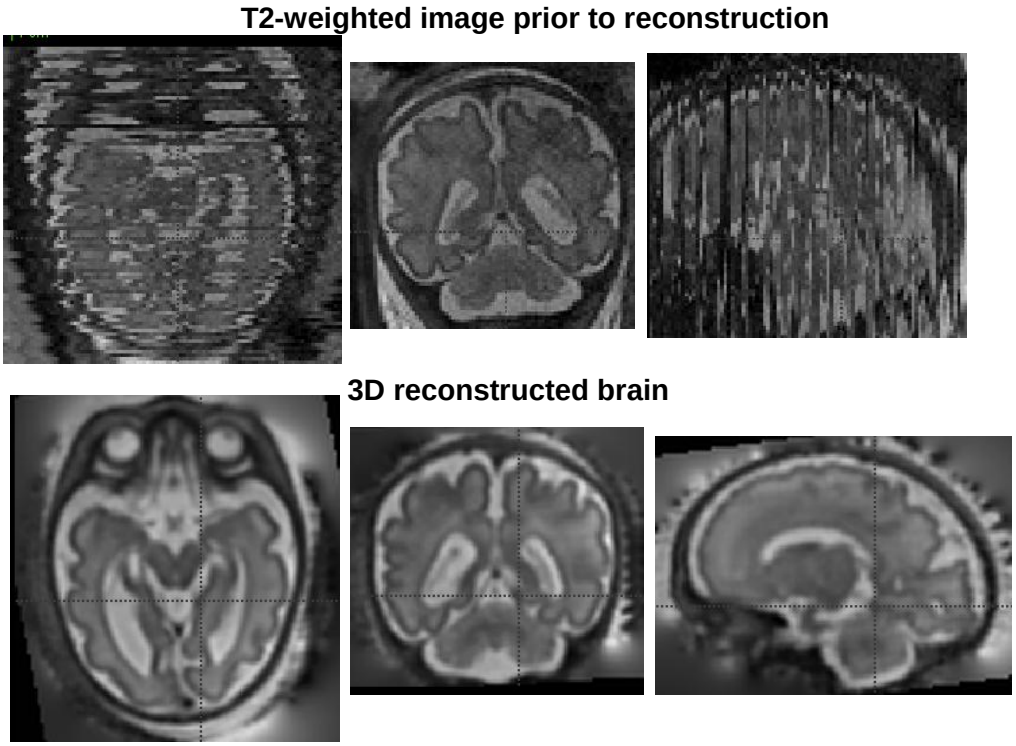


Figure 18. Example of fetal dataset before and after reconstruction

Before reconstruction (T2-weighted image prior to reconstruction) slices are corrupted due to fetal motion with lines of low signal intensity representing missing data while after registration of multiple acquisitions and reconstruction (3D reconstructed brain) there is no missing data and image quality has improved.

Segmentation of brain structures may be performed manually or using automated software. Manual segmentation of brain structures involves the examiner tracing around the structure of interest on each slice delineating the region of interest. The delineated area is multiplied by the voxel thickness to produce volumetric values. Whilst manual segmentation provides accurate data and is considered the 'gold standard' it is time-consuming and a laborious method of volumetric analysis thus impeding the analysis of large amount of data. While automatic methods have been successfully used for segmentation of intracranial structures, fetal brain volumetry is a new field that has emerged in the past decade with a number of studies developing automated methods for quantifying the fetal brain (Gholipour et al., 2011; Gong, 1998; Scott et al., 2011). Automatic techniques may be intensity-based, driven by differences in signal intensity between brain structures. However, reliable automatic segmentation in the fetal brain is hindered by the low contrast between the different brain structures because of image degradation due to fetal motion, increased water content throughout the cerebrum and presence of unmyelinated white matter. Whilst the contrast between CSF and cortical gray matter is adequate for delineation between the two, the gray matter/white matter boundary may not be easy to distinguish and mislabelling due to partial volume may result in incorrect tissue classifications. Another approach is the atlas-based approach. This relies on the construction of a probabilistic atlas generated from manually segmented brains at the age of interest. Any new case can be aligned on the constructed atlas to generate structural segmentations based on established algorithms using prior knowledge (Aljabar et al., 2009; Gousias et al., 2008; Kuklisova-Murgasova et al., 2011).

1.4.4.2 Methods for assessing cortical folding

Folding of the cerebral cortex during development follows a highly orchestrated sequence of gyral and sulcal formation. A number of studies have attempted to quantify the maturation of the cerebral cortex using different techniques. The majority of studies use an observational approach for the study of cortical maturation. This approach generates a timeline of appearance of different cortical landmarks and has been performed on post-mortem and MR studies (Afif et al., 2007), on fetuses (Garel et al., 2003a; Levine and Barnes, 1999; Toi et al., 2004) and neonates (Childs et al., 2001; van der Knaap et al., 1996). The gyrification index which is an overall

measurement of cortical maturation has also been used in previous studies, and calculated as the ratio of whole gyral contour length to their outer exposed surface (Armstrong et al., 1995; Kesler et al., 2006; Zilles et al., 1988). Recent advances in post-processing techniques have also allowed for the use of computational methods with the use of algorithms for the delineation of the sulcal patterns during development (Clouchoux et al., 2012; Mangin et al., 2004; Scott et al., 2011).

1.4.4.3 ^{1}H magnetic resonance spectroscopy

In addition to structural data, advances in MR techniques allow us to assess the function of the developing brain using ^{1}H magnetic resonance spectroscopy (^{1}HMRS). ^{1}HMRS has been commonly used to assess the neonatal brain and less frequently the fetal brain. It provides data in the output form of a chemical spectrum of metabolites. It can assess the metabolic profile of different brain tissue by measuring small molecular weight amino acids, carbohydrates, fatty acids and lipids. This technique was used to assess and compare the metabolic profile of normal fetuses and those with isolated ventriculomegaly. The frequency at which a proton generates a signal depends on the tissue in which it is incorporated therefore the metabolic fingerprint of a tissue varies according to the brain region studied and can be altered in structural damage, biochemical and genetic conditions. This is known as chemical shift and is expressed in terms of parts per million (ppm) (Gilles and Nelson, 2012).

As mentioned previously, the MR signal to create anatomical images is generated by the ^{1}H protons in water. In ^{1}HMRS, the signal is generated by the protons attached to other molecules and is visualised as a spectrum of peaks at different radiofrequencies representing protons in different chemical environments. Therefore the chemical shift provides information regarding the molecular group containing the hydrogen atoms. The RF pulses used in ^{1}HMRS are known as 'pulse Fourier transform spectroscopy'. The signal is recorded as a function of voltage against time, which for a single RF pulse is denoted as the free induction decay (FID). The FID is analysed using the Fourier transformation mathematical process to produce a spectrum with the constituent frequencies.

Although the area under the peak is proportional to the number of protons producing the signal there are additional factors that influence the MR signal such as relaxation time, coupling of the sample to the coil, pulse sequence used and acquisition method. Therefore absolute concentrations cannot be established without controlling all confounding factors. Consequently, relative concentrations of metabolite ratios are often used for quantification and are more robust than absolute quantification. These are expressed as ratios to a peak with a known concentration or to a stable metabolite in the spectrum. A limitation is the certainty that a metabolite is stable particularly in the developing or injured brain. Metabolites that are mobile and not incorporated into cell membranes or myelin can be measured with ^{1}HMRS.

Peaks in the spectra represent different metabolites and are identified by their frequency in parts per million (ppm) relative to a standard. The area below the peak represents the metabolite concentration in a given voxel. The height and width of the peaks is also influenced by the spin lattice and spin-spin relaxation and the exponential decay times. Mobile molecules generate narrow peaks while molecules attached to other structures produce short and broad resonances. Metabolites that have been successfully measured in the fetus are myo-inositol (MI), choline (Cho), creatine (Cr), N-acetylaspartate (NAA), lactate (Lac) (Figure 19).

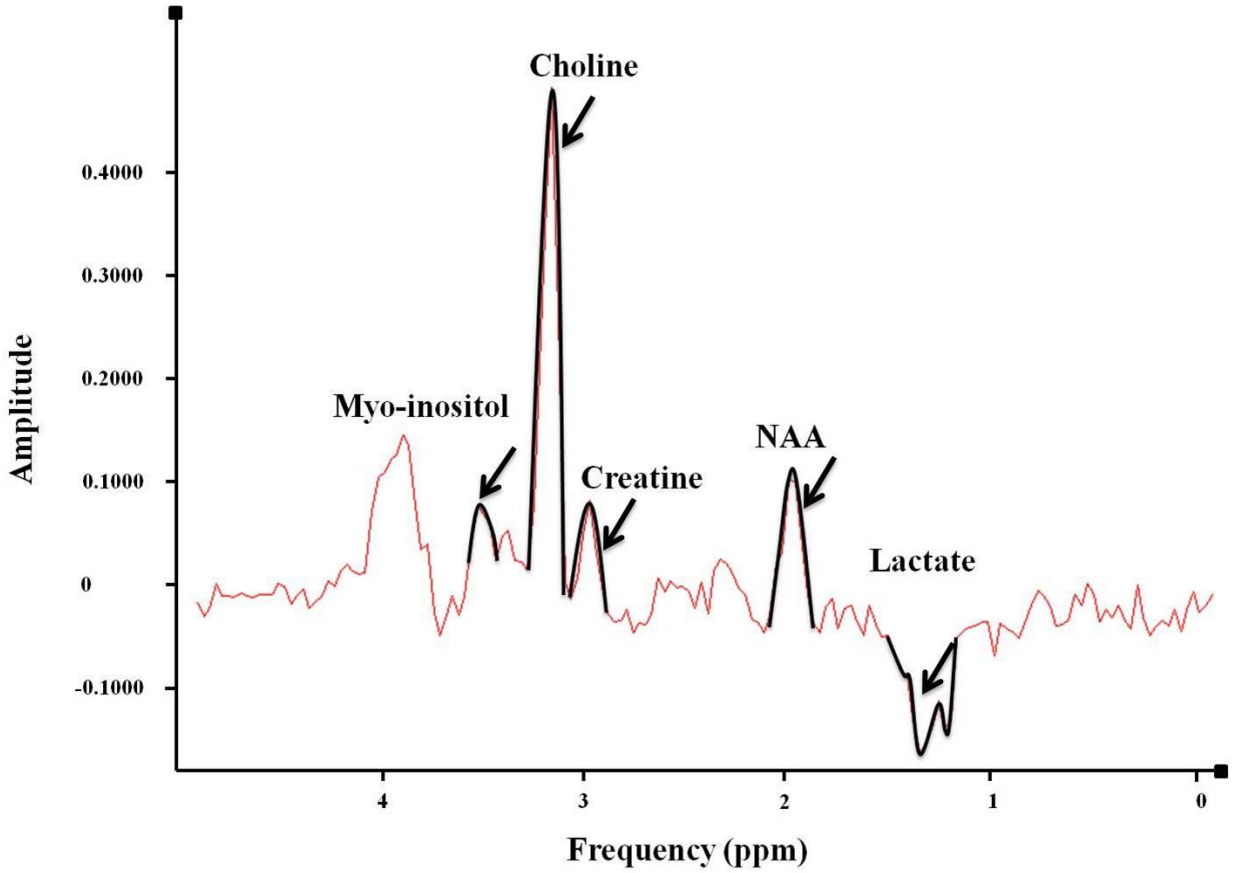


Figure 19. ^{1}HMRS fetal spectrum

^{1}HMRS spectrum from a normal control 24^{+6} weeks old fetus. The resonance peaks for myo-inositol (3.5 ppm), choline (3.2 ppm), creatine (3 ppm), NAA (2 ppm), lactate (1.3 ppm, bifid inverted peak) are indicated.

1.4.4.3.1 N-acetylaspartate

The NAA signal is detected at 2.0ppm and reflects both NAA and NAAG. In the normal brain NAA is synthesised in neuronal mitochondria from acetyl-CoA and N-acetyltransferase. It then diffuses along axons and is transferred to oligodendrocytes (Ariyannur et al., 2008; Gilles and Nelson, 2012; Moffett et al., 2007; Patel and Clark, 1979) where it is used for myelin and protein synthesis and energy production. NAA increases as the brain matures (Brighina et al., 2009). NAA is clinically important as a reduction may indicate altered mitochondrial function or neuronal/axonal damage or loss (Gilles and Nelson, 2012; Roelants-van Rijn et al., 2004).

1.4.4.3.2 Creatine

Creatine peak is detected at 3.0ppm and reflects both creatine and phosphocreatine. These molecules are in rapid chemical exchange in order to replenish ATP levels and are involved in energy metabolism. Cell cultures indicate that creatine is concentrated in astrocytes and oligodendrocytes (Urenjak et al., 1993). In autopsy studies in preterm and term infants creatine concentrations have shown regional variation with higher levels measured in the basal ganglia and thalami (Brighina et al., 2009; Huppi et al., 1995). It is probably required for energy production during myelination as the basal ganglia and thalami are highly metabolically active during myelination (Hegde et al., 2011). During gestation creatine is assumed to be relatively stable within a specific brain region and has been used by previous studies as a reference metabolite (Kok et al., 2002; Story et al., 2011a; Story et al., 2011b).

1.4.4.3.3 Choline

Choline is a complex peak comprised of several Cho-containing metabolites and detected at 3.2ppm. This peak is representative of only 10% of the choline present in a tissue as the majority of choline is incorporated in substances such as myelin and is not detectable using ^{1}HMRS. Cho-compounds are involved in the synthesis and breakdown of phospholipids and therefore cell membrane formation. It is found in high levels in glial cells but is also involved in acetylcholine synthesis therefore in neuronal uptake (Katz-Brull et al., 2002). Choline is of interest in tumour spectroscopy as cancer cells have abnormal membrane metabolism and abnormal choline. During normal development choline levels have been shown to decrease with progressive myelination due to the high levels of substrate needed for the formation of cell membranes (Girard et al., 2006a; Kok et al., 2002; Story et al., 2011b).

1.4.4.3.4 Myo-inositol

Myo-inositol is detected at 3.5ppm and is a pentose sugar synthesised from glucose-6-phosphate. It is an essential constituent of living cells and is involved in maintaining osmolyte homeostasis via the sodium/myo-inositol transporter (Brighina et al., 2009). It is important for neuronal plasticity and regulation of cell growth and is found in high concentrations in the CNS. While

initially thought that inositol was predominantly localised in glia and was an astrocyte marker, higher concentrations have also been found in neuronal populations (Novak et al., 1999). In adults an increase in MI is seen in gliomas and multiple sclerosis reactional gliosis whilst reduced levels are present in herpetic encephalitis. MI is also increased after acute perinatal brain injury due to an increase of osmolytes after hypoxia-ischaemia and in chronic cases of perinatal white matter injury in preterms (Robertson et al., 2000; Robertson et al., 2001).

1.4.4.3.5 Lactate

Lactate is detected at 1.33ppm and is not detected in the normal adult brain. It is a product of anaerobic glycolysis and increased levels have been detected in human neonates after a hypoxic insult, the higher the levels the worse the neurological outcome (Roelants-Van Rijn et al., 2001). However, animal studies have shown that the developing brain, in contrast to the adult brain, has the ability to metabolise lactate (Hernandez et al., 1980). Studies suggest a role for lactate as a fuel source in the developing brain and low levels have been detected in preterm infants and in term newborns with a normal brain appearance. These levels subsequently decrease (Cady et al., 1996; Tabernero et al., 1996; Tyson et al., 2003).

1.4.5 Imaging the neonate

MR imaging although a relatively new technique has been extensively used to visualise the neonatal brain and allows clinicians to assess normal development, to detect lesions and to predict outcome. Advances in imaging techniques extend the role of MR imaging beyond visual confirmation of normality and pathology and allow for objective volumetric measurement of intracranial structures, measurement of specific MR properties such as T1 and T2 and diffusion coefficients, quantification of white matter tract properties, quantification of metabolites and functional information (Arichi, 2012; Ball et al., 2010; Malamateniou et al., 2012; Ramenghi et al., 2009; Rutherford et al., 2010; Rutherford, 2002b; Varela et al., 2012; Xue et al., 2007). The purpose of this study extends beyond understanding brain development during fetal life. In a cohort of fetuses brain development was assessed during the neonatal period using volumetric analysis to assess intracranial volumetric changes after birth and also DTI to assess the microstructure of white matter tracts.

1.4.5.1 Diffusion Tensor Imaging

Diffusion Tensor Imaging has been extensively used in the neonatal and adult brain to provide information regarding tissue microstructure by quantifying the 3D micromovements of water molecules and providing voxelwise, scalar measures of water diffusion in different brain tissue. In CSF, the movement of water is isotropic, meaning that it is equivalent in all directions as water diffuses freely. In white matter water movement is strongly anisotropic (directional) with the majority of diffusion occurring parallel to the direction of the white matter tracts. Water motion is restricted along the axis of the tracts due to the structured and coherent formation and myelination of white matter bundles. Two basic properties are measured using the overall amount of water diffusion and the directionality (anisotropy) of diffusion. These properties are measured at each voxel. Therefore, DTI can indirectly identify and characterise white matter pathways and provide information regarding brain connectivity.

In addition to providing information on white matter fibre tracking it can assess tissue microstructure and maturation status of different brain regions. Anisotropic diffusion is an effect of the tissue microstructure and changes in anisotropy can reflect changes in tissue

microstructure. High values of diffusion in white matter may indicate poorly developed, immature or structurally compromised white matter (Smith et al., 2006).

1.4.5.1.1 Quantification

A measure of the molecular diffusion of water is the apparent diffusion coefficient (ADC) which depicts all forms of water motion including diffusion, perfusion and flow. Therefore ADC represents intracellular, extracellular and intravascular diffusion environments. In white matter however, the motion of water is highly anisotropic and in order to depict the directions and degree of anisotropy it is necessary to consider diffusion as a tensor (3x3 matrix) (Nucifora et al., 2007; Roberts and Schwartz, 2007). The tensor is described in terms of three coordinate axes with the main axis representing the preferred direction of diffusion (Figure 20). This eigenvector indicates the direction of greatest diffusion within a voxel. For convenience, diffusivity is represented in the form of a three-dimensional ellipsoid. Equal to all directions diffusion would be represented by a sphere. While the eigenvectors define the diffusion orientation of the ellipsoid, the eigenvalues (λ_1, λ_2, λ_3) represent the degree of directional preference. The sum of the principle diffusivities is represented by the Fractional Anisotropy (FA) which is an index ranging from 0 (isotropic) to 1 (fully anisotropic). FA quantifies the strength of directionality of a tract structure. An example of an ADC and an FA map in a normal neonate is shown in Figure 21.

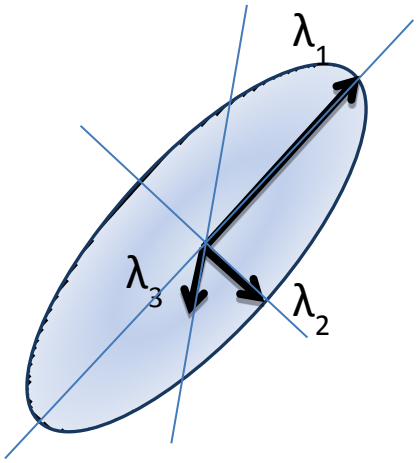


Figure 20. Diffusion ellipsoids

Diffusivity is represented as a 3D ellipsoid. The eigenvalues (λ_1, λ_2,λ_3) represent the degree of directional preference.

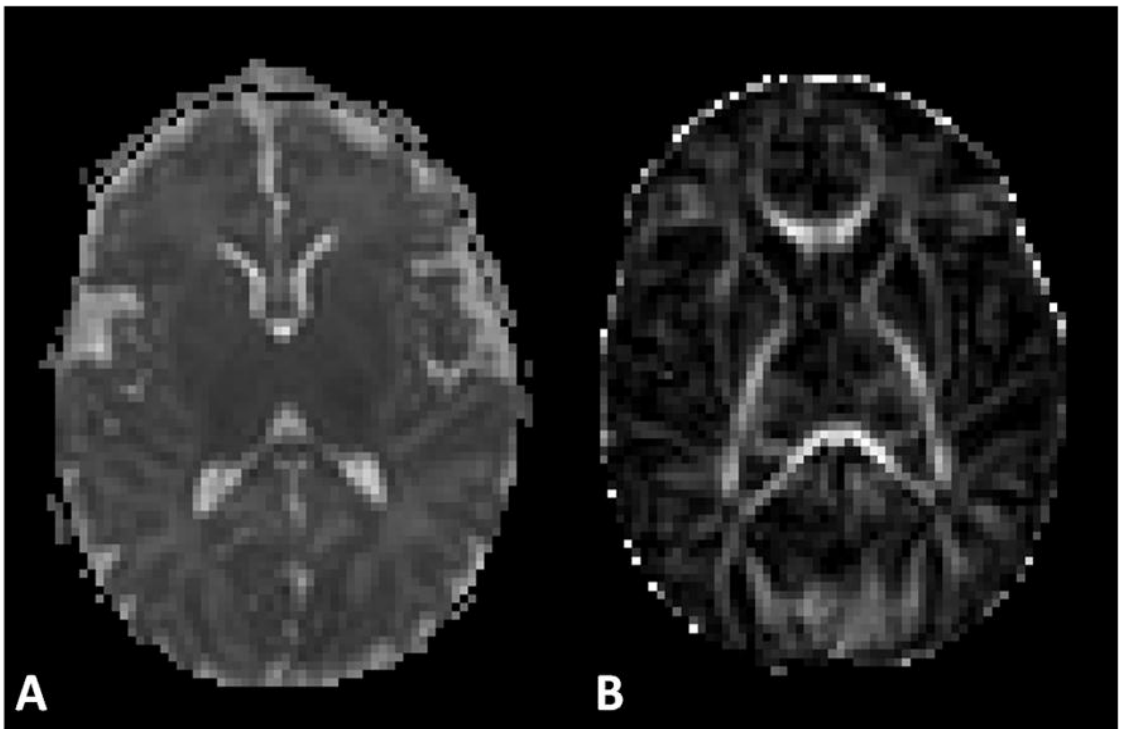


Figure 21. DTI Imaging: ADC and FA maps

DTI of a normal neonatal brain (A) ADC map; bright areas indicate isotropic water diffusion while darker areas indicate restricted water diffusion. (B) FA map; bright areas indicate high FA values and increased directionality of water diffusion.

Many studies of neonatal DTI have used regions of interest to obtain diffusion measurements directly from diffusion tensor images. However this approach is subjective and laborious and does not allow for comparison of large number of subjects. In addition, in order to analyse data from multiple subjects, FA images must be aligned in order to draw valid conclusion from the subsequent voxelwise analysis. These problems are addressed with the use of Tract-Based Spatial Statistics (TBSS), a powerful technique for analysis of DTI data that allows for multi-subject analysis with increased sensitivity and reduced subjectivity (Smith et al., 2006). The TBSS protocol includes tuned nonlinear registration and projection into an alignment-invariant tract representation (mean FA skeleton) and is described in detail in chapter 2.4.3. TBSS is a reproducible and objective voxelwise assessment of the white matter allowing the detection of changes consistent across subjects while avoiding the bias of location selection.

2 Materials and Methods

2.1 Ethics

Ethical approval for the study entitled "Quantification of fetal brain growth and development using magnetic resonance imaging" was granted by the Hammersmith Hospital Ethics Committee (ethics No. 07/H0707/105) and written informed consent obtained from all participants. Fetuses were referred to our department from antenatal ultrasound departments in hospitals across London, in order to further assess brain development. The reasons for referral are summarised in Table 3. Healthy volunteers were recruited from the antenatal clinic in Queen Charlotte's and Chelsea Hospital and through voluntary enrolment through patients and colleagues. As part of the research study all participants were offered neurodevelopmental follow up of their children. In summary, the follow up program included a brain scan and neurological examination during the neonatal period or at term equivalent after birth and a neurodevelopmental assessment at 1 and 2 years of age.

Reasons for referral for performance of an MRI fetal scan
Brain abnormality detected on ultrasound
Non-CNS abnormality detected on ultrasound
Maternal infection
Previous sibling with CNS abnormality
Complications during twin pregnancy

Table 3. Reasons for referral for a fetal MRI scan

2.2 Study population

2.2.1 Normal control cohort

Normal control fetuses were carefully selected from the total cohort of fetuses referred to our department from women who were either healthy pregnant volunteers, who had had a previous child with a confirmed abnormality, or who had had a suspected fetal abnormality on ultrasound not detected on MRI. The inclusion criterion was normal brain appearance on fetal MR examination as established by an experienced neuroradiologist. The clinical MR examination consisted of evaluation of the extra-cerebral space, ventricular system, cortex, white matter, corpus callosum, basal ganglia and thalami, internal capsule, cerebellum and brainstem. A normal appearance on fetal MRI however may not exclude subtle brain changes or developmental delay later in childhood thus it was considered important to follow-up these children ensuring their later neuro-development was within the normal range. Exclusion criteria for participation as a normal control were: poor MR image quality, delivery complications with abnormal neurological signs, birth-weight below the 3rd centile, congenital malformations or infection, chromosomal abnormality, twin pregnancy, premature delivery (<36 weeks), abnormal clinical neonatal examination, abnormal findings on neonatal MR examination, and abnormal neurodevelopmental examination at either one or two years of age.

2.2.2 Isolated ventriculomegaly cohort

Fetuses presenting with ventricular dilatation on clinical antenatal ultrasound were referred to our department for further assessment of the developing brain. Fetuses diagnosed with isolated ventriculomegaly were included in the ventriculomegaly group. Exclusion criteria were: additional brain abnormalities, positive infection or chromosomal abnormality screening, maternal drug use, twin pregnancy, intra-utero growth restriction, birth-weight below the 3rd centile or poor image quality. Upon diagnosis of fetal ventriculomegaly all pregnant women were advised by their obstetrician to undertake a TORCH screening test performed on maternal blood. Amniocentesis was recommended to exclude the presence of chromosomal abnormalities and fetal infections. To ascertain a negative infection status all TORCH results were reviewed. To exclude genetic syndromes all delivery summaries were reviewed for any indication of

dysmorphic facial features or additional undiagnosed congenital malformations which could indicate an underlying genetic syndrome. Clinical notes were also collected during the neonatal MRI and neurological examination and during the assessments at year 1 and 2 were reviewed. Maternal drug use was checked through review of the maternal medical notes. Birth weight and delivery history was recorded as indicated on the delivery summary for each newborn. Intra-utero growth restriction was defined as an estimated fetal weight below the 5th centile in association with ultrasound Doppler abnormalities (Damodaram et al., 2012).

2.3 Fetal Imaging

Expectant mothers were provided with an information sheet entailing the study information and details about the procedure prior to the scan date. Information sheets provided to patients and healthy volunteers are available in the Appendix 1 and 2. A video of the fetal MRI procedure for the parents has been produced in the department and is available online via the following link http://vimeo.com/37368763 Upon the day of examination, written informed consent was obtained from all participants and a detailed metal check questionnaire was completed to establish suitability for entering a strong magnetic field. Informed consent was obtained for a conventional clinical scan, acquisition, storage and use of research images, and permission to contact parents after delivery. Mothers were asked to lie in a lateral tilt to avoid compression of the inferior vena cava by the enlarged uterus which could lead to dizziness and loss of consciousness. A 32-channel coil was placed around the maternal abdomen and proximal to the fetal head. Scanning duration did not exceed 60 minutes; image acquisition was not continuous but was intermittent with small time frames of geometry setting of the next scan. Core body temperature was measured prior to and after the scan using an electronic ear thermometer. After the scan, all parents were provided with a questionnaire regarding their experience for later completion (Appendix 3)

2.3.1 MR safety

2.3.1.1 Temperature

Although maternal temperature is not routinely measured in other imaging departments and there are no national guidelines regarding maternal core body temperature and fetal imaging procedures, we have established a set of local rules based on review of the current literature and experience. Temperature was recorded in all participants prior to and after the scan. In accordance to the IRCNIP guidelines (2004) described earlier we have set an upper threshold for maternal temperature of 37.5 °C (equivalent to a fetal temperature of 38 °C). Therefore if the recorded maternal temperature prior to the scan was equal or above 37.5 °C the scan was not performed and was rescheduled for another day. Hospital scrubs were provided to ensure metal free clothing was worn and to avoid any increase in temperature due to personal clothing. Traditional clothing such as burkas were removed. Air conditioning inside the bore of the magnet was turned on to provide additional cooling. Placement of hands on the abdomen was discouraged. Heat absorption by the fetus was reduced further by interchanging low and high SAR sequences in addition to having short breaks for geometry setting between sequences. Room temperature was set to 18 °C and periodically monitored.

2.3.1.2 Noise

Headphones were provided to protect maternal hearing, provide music during the scan and to communicate with the mother.

2.3.2 Imaging

2.3.2.1 Data acquisition

A full clinical assessment was performed using an optimised protocol of different sequences for assessment of brain anatomy as described below.

Parameters	T2dyn	T2ssTSE	SNAPIR	T2*	PRESS 42	PRESS 136	PRESS 270
TE (ms)	160	127	9.5	80	45	136	270
TR (ms)	15000	1011	23000	3600	1500	1500	1500
Flip angle (deg)	90	90	180	90	-	-	-
Acquisition Voxel size (mm)	1.25x1.25x2.5	1.08x1.98x4	1.00x1.01x4	1.2x1.2x2	-	-	-
Slice gap (mm)	-1.25	0.4	0	-1.2	-	-	-
Reconstructed voxel size (mm)	1.18x1.18x2.5	0.84x0.84x4	0.96x0.97x4	0.63x0.63x2	-	-	-
FOV (mm)	320x340x95	430x352x114	320x340x88	400x400x65	-	-	-
SAR (W/Kg)	1.7	2	1	0.4	0.4	0.4	0.4

Table 4. Fetal imaging parameters

Structural scans included T2dyn, T2ss and SNAPIR. T2* was used for improved visualisation of haemorrhage. Spectroscopy sequences at echo times 42ms, 136ms and 270ms included PRESS 42, PRESS 136 and PRESS 270. T2dyn: T2 T2-weighted dynamic Single Shot Turbo Spin Echo, T2ss: T2-weighted Single Shot Turbo Spin Echo, SNAPIR: T1-weighted Snapshot Inversion-Recovery T2*:T2*-weighted Gradient Echo, PRESS: Point Resolved Spectroscopy.

2.3.2.1.1 T2-weighted Single Shot Turbo Spin Echo (ssTSE)

A rapidly acquired sequence in which the brain parenchyma appears hypointense and CSF appears hyperintense (Figure 22). T2-weighted ssFSE sequences were acquired in the transverse, coronal and sagittal planes with the parameters detailed in Table 4.

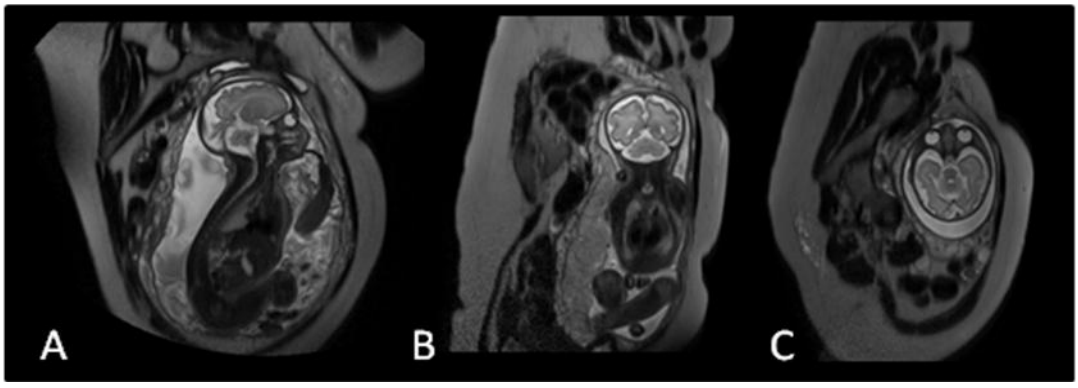


Figure 22. T2-weighted Single Shot Turbo Spin Echo

T2-weighted Single Shot Turbo Spin Echo sequences imaging a normal control 30^{+5} weeks old fetus in (A) sagittal (B) coronal and (C) transverse plane.

2.3.2.1.2 T2-weighted dynamic Single Shot Turbo Spin Echo (ssTSE)

This optimised sequence was designed in our department (Jiang et al., 2007) to overcome the issue of fetal motion and to enable the acquisition of complete datasets suitable for volumetric measurement (Figure 23). Multiple T2-weighted dynamic ssTSE overlapping slices (4 transverse, 2 coronal and 2 sagittal acquisitions) were obtained using the parameters detailed in Table 4 which were later post-processed offline for the production of 3D datasets.

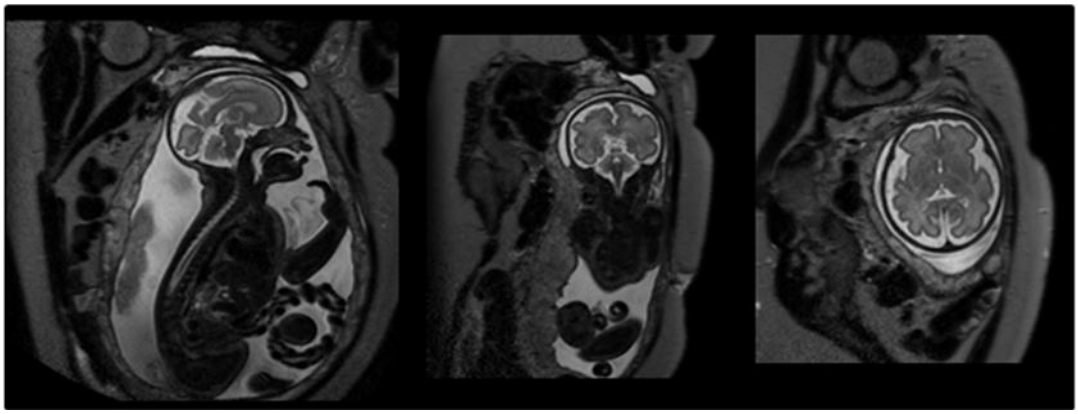


Figure 23. T2-weighted dynamic Single Shot Turbo Spin

T2-weighted dynamic Single Shot Turbo Spin sequences imaging a normal control 30^{+5} weeks old fetus in (A) sagittal (B) coronal (C) transverse plane.

2.3.2.1.3 T1-weighted Snapshot Inversion-Recovery

Conventional T1-weighted image sequences are long and therefore subject to artefact, even when combined with a maternal breath hold. A T1-weighted Snapshot Inversion-Recovery (SNAPIR) sequence, designed in our department (Malamateniou et al., 2011) was acquired as described in Table 4. This single shot sequence allows for confirmation of the normal or abnormal anatomy and visualising haemorrhage, fat and myelination near term. In contrast to conventional T1-weighted gradient echo sequences it is more robust to fetal motion thus providing better delineation of fetal brain anatomy (Figure 24).

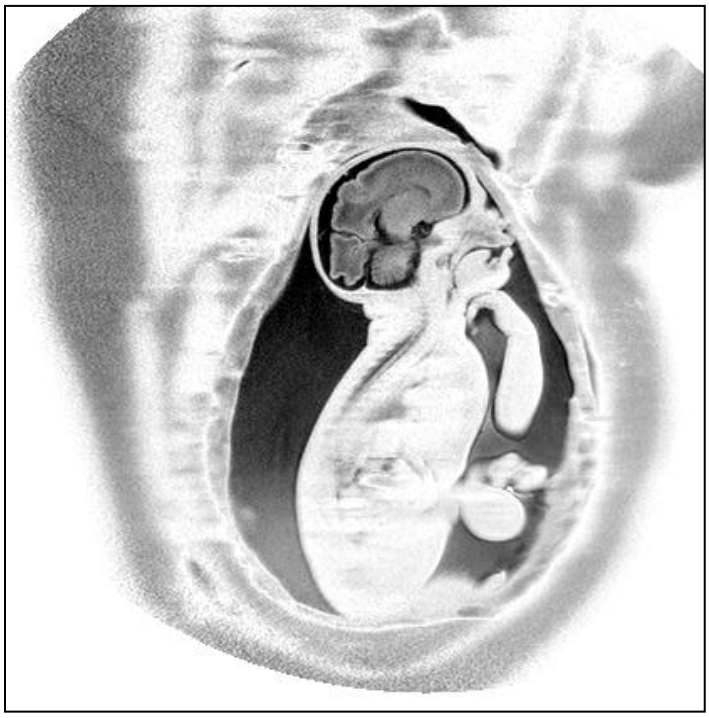


Figure 24. T1-weighted single shot Inversion-Recovery

T1-weighted Inversion-Recovery sequence imaging a normal control 30^{+5} weeks old fetus in a sagittal plane.

2.3.2.1.4 T2-weighted Gradient Echo*

T2* sequence is valuable for detecting hemosiderin present on iron molecules and visualising areas with haemorrhage. As illustrated in Figure 25 dark areas represent locations high in hemosiderin such as the germinal matrix, choroid plexus and internal cerebral veins.



Figure 25. T2*-weighted Gradient Echo

T2*-weighted Gradient Echo sequence imaging a normal control 34^{+4} weeks old fetus in a transverse plane. The great cerebral vein of Galen appears darker (arrowhead).

2.3.2.1.5 Magnetic Resonance Spectroscopy ^{1}H (echo times 42ms, 136ms, 270ms)

^{1}HMRS data were obtained using a Point Resolved Spectroscopy (PRESS) sequence. A 20x20x20mm voxel was placed centrally in the fetal brain sampling both white matter and gray matter. The positioning of the voxel is illustrated on Figure 26. Data were obtained at three different echo times of 42msec, 136msec and 270msec to allow for detection and quantification of different metabolites. Acquisition parameters are detailed in Table 4. A T2-weighted ssTSE sequence was obtained prior to the ^{1}HMRS sequence in order to establish fetal positioning and place the region of interest. The region of interest was selected by the operator at the time of scanning. Data were acquired in averages of 4 resulting in the production of 32 individual spectra at each echo. Acquiring data in packages allowed for elimination of individual corrupted spectra while the remaining usable spectra were summed. Acquisition was performed using water

suppression due to the large size of the water peak that may distort the baseline and obstruct metabolite quantification.

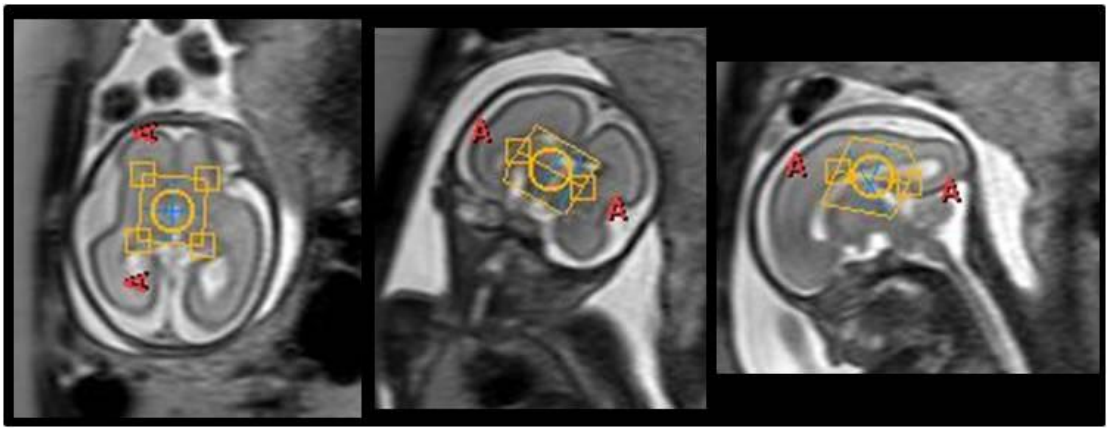


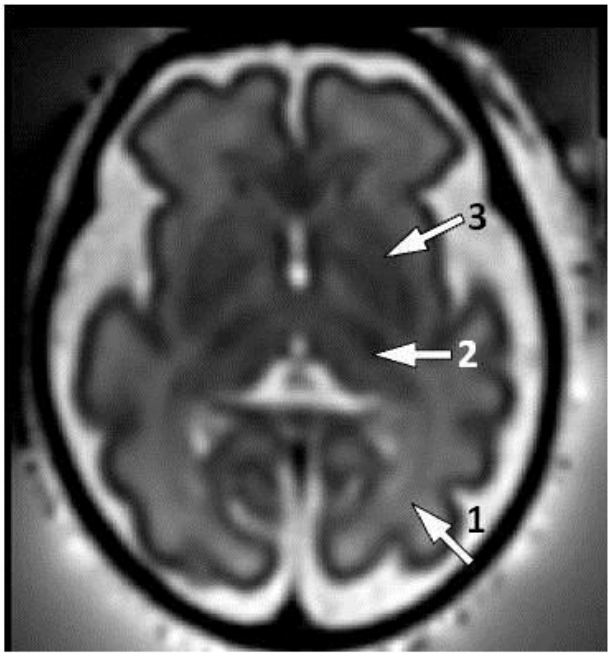
Figure 26. Voxel placement in fetal ^{1}HMRS

The voxel is placed centrally in the fetal brain sampling gray and white matter.

2.3.2.2 Post-processing of data

2.3.2.2.1 Clinical examination

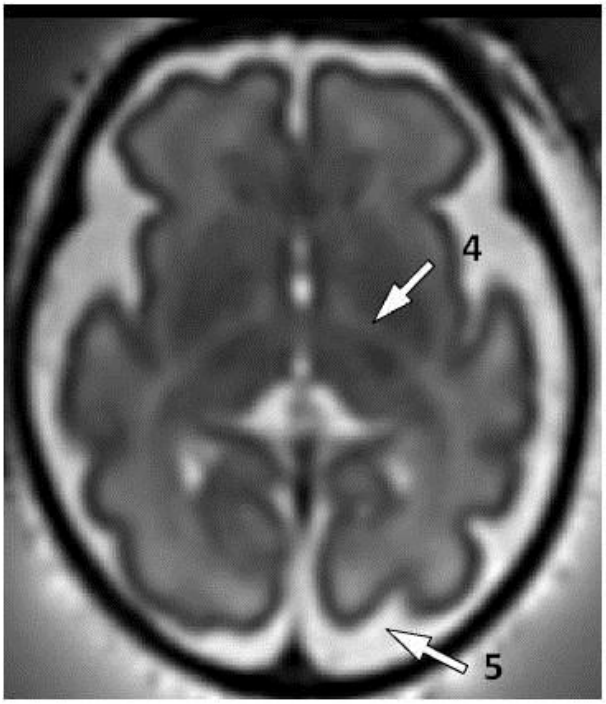
The imaging examination of all fetuses included coverage and subsequent assessment of white matter, basal ganglia and thalami, internal capsule, corpus callosum, extra-cerebral space, lateral ventricles, 3rd ventricle, 4rth ventricle, cavum septum pellucidum and vergae, orbits, cerebellum, vermis, brainstem, germinal matrix, cortex, biparietal diameter. An example of the clinical examination in a normal control fetus aged 30^{+5} weeks was performed as shown in Figure 27.



(1) White matter
Normal appearance/signal intensity

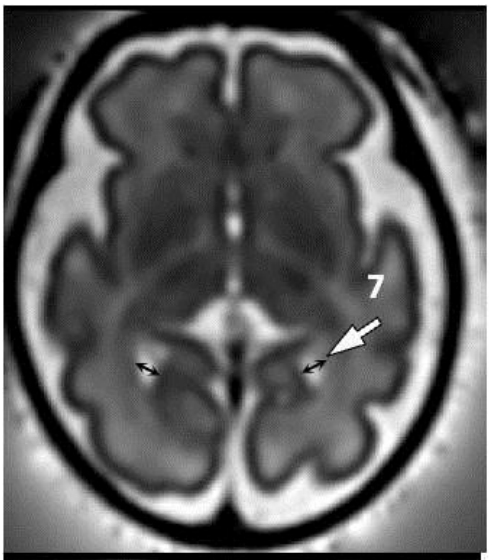
(2) Thalami
Normal appearance/signal intensity

(3) Basal ganglia
Normal appearance/signal intensity

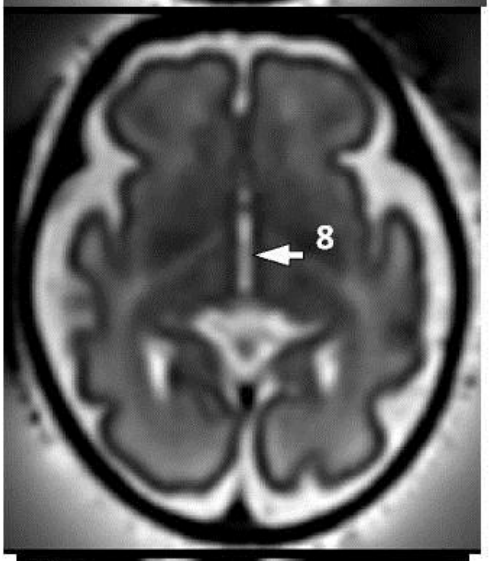


(4) Internal capsule
Present

(5) Extra-cerebral space
Normal



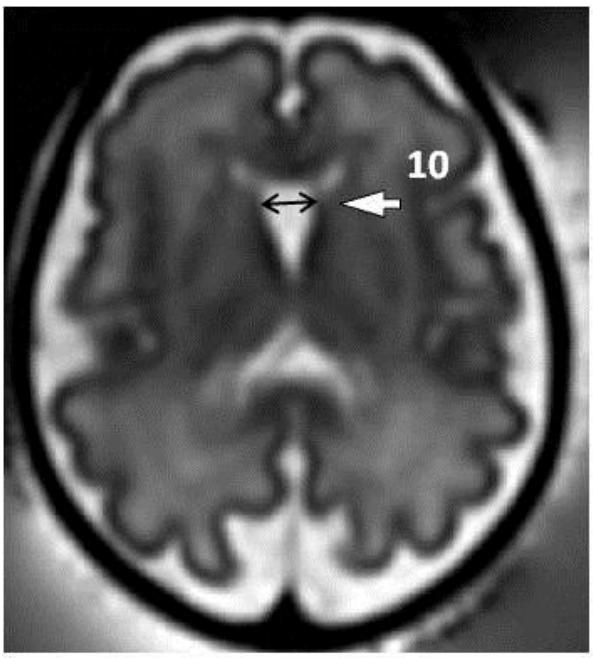
(7) Lateral ventricles
Normal size and shape



(8) Third ventricle
Normal appearance



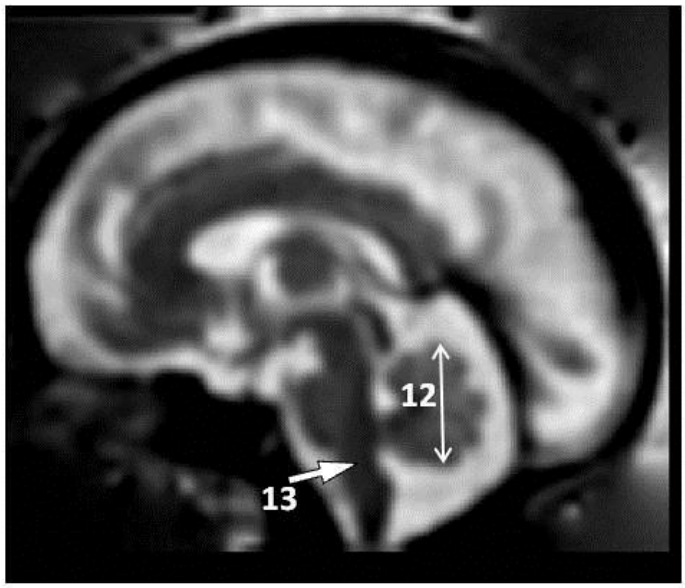
(9) Fourth ventricle
Normal appearance



(10) Cavum septum pellucidum
Normal size and shape

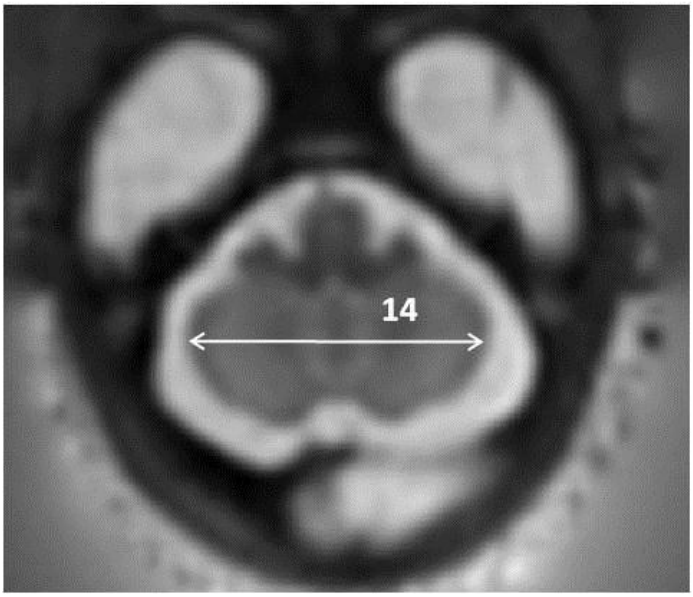


(11) Orbits
Normal appearance

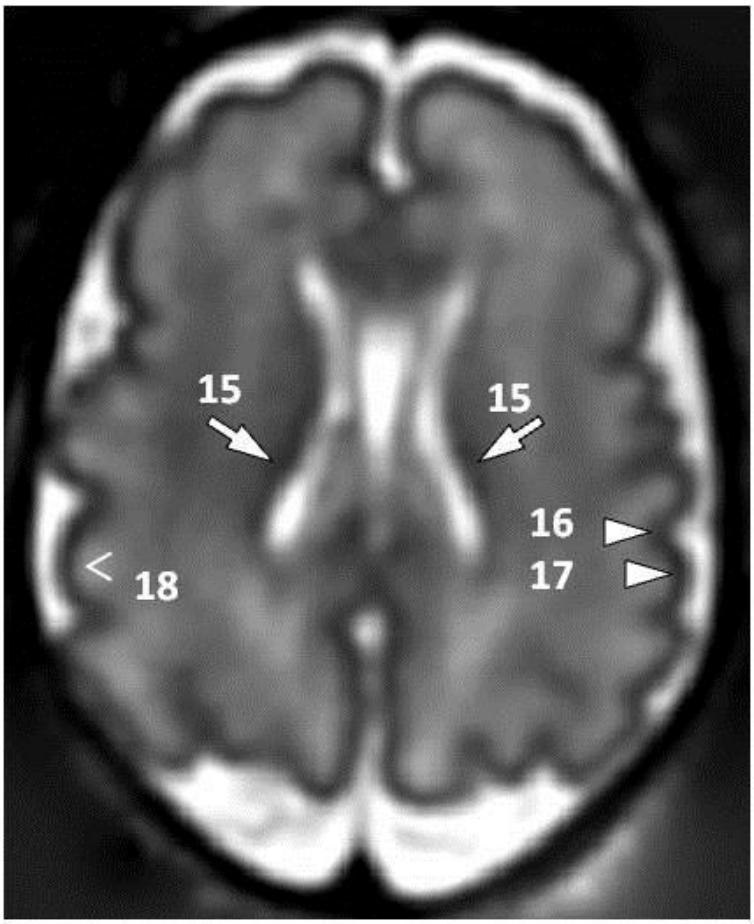


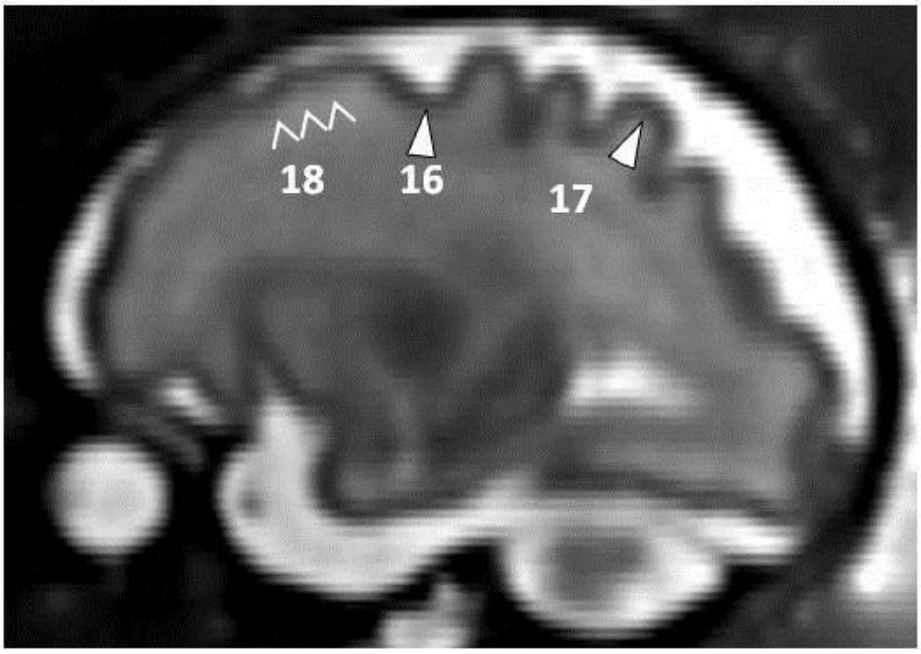
(12) Vermis
Normal size and appearance
(vermis height shown)

(13) Brainstem
Normal appearance



(14) Cerebellum
Normal size and appearance
(trans-cerebellar diameter shown)





(15) Germinal matrix
Normal appearance

(16-17) Cortex
Normal appearance
16 sulcus
17 gyrus

(18) Subplate
(areas of high signal intensity below the cortex)
Normal appearance

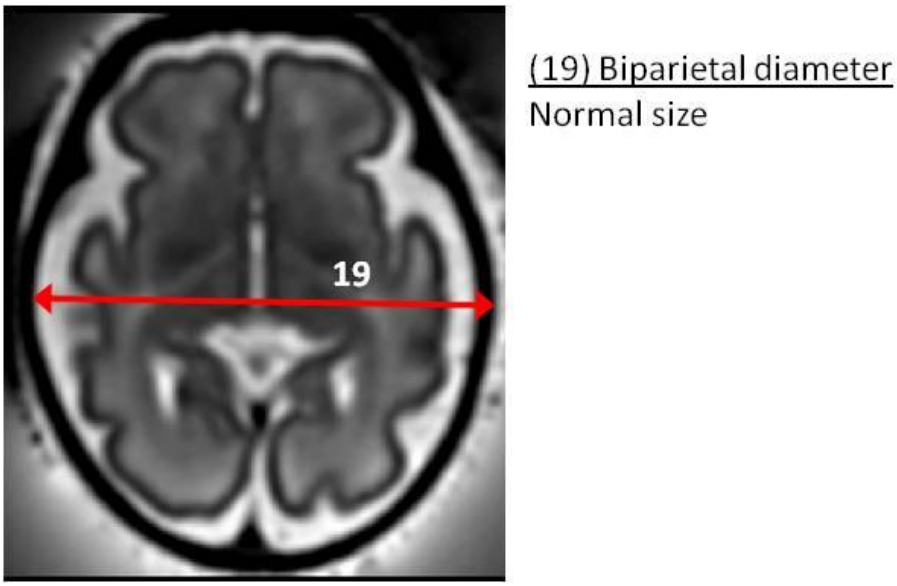


Figure 27. Fetal MRI clinical examination

Fetal MRI clinical examination in a normal control fetus aged 30^{+5} weeks.

2.3.2.2.2 Snapshot MRI with Volume Reconstruction (SVR)

The SVR technique (Jiang et al., 2007), developed in our department, provides image datasets of high resolution, high signal-to-noise ratio, aligned to orthogonal planes and with full brain coverage essential for reliable volumetric analysis (Figure 27). During scanning the fetal brain is scanned very fast with each slice acquired in less than 1 second therefore ensuring that each slice is of good quality even if the fetus is moving (Figure 28). Rarely fetal movement is faster than slice acquisition.

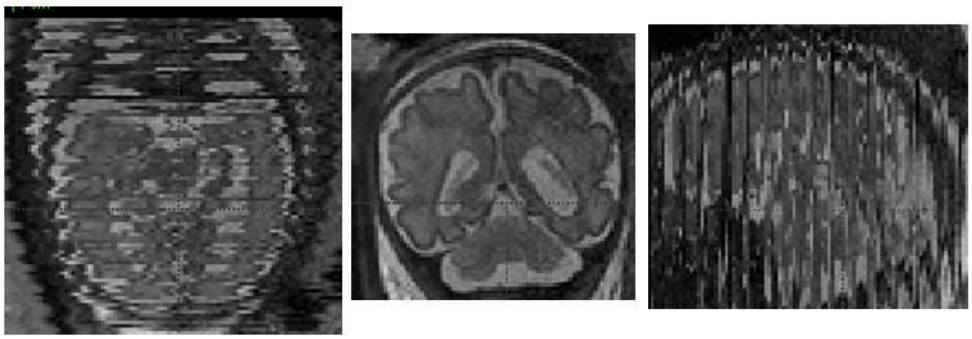


Figure 28. Fetal motion

Example of a single fetal dataset acquired in a coronal plane. Before registration of multiple acquisitions and reconstruction, slices are corrupted due to fetal motion and missing data are shown as missing lines in transverse and sagittal planes.

Multiple scans in all three planes are performed with overlapping slices in order to oversample the fetal brain and ensure that each part of the brain has been sampled even with significant motion. Image registration is then undertaken where each brain scan is registered into a common coordinate space in order to align the acquired slices. This is performed under the assumption that the brain has undergone unknown motion but has not changed in shape or size. The final result is a 3D high resolution with high signal-to-noise volumetric dataset that can be viewed in any plane.

The SVR protocol performed was the following: Eight T2 - weighted single shot Fast Spin Echo brain scans were acquired as described above (4 transverse, 2 coronal and 2 sagittal acquisitions) (Figure 29A). The files were converted from the DICOM format into a niftii format using the dcm2nii converter. The majority of maternal tissue was then removed from all 8 scans using ImageJ. Homogeneity of the image intensity values was calibrated (slope=1, intercept=0) to achieve uniformity thorough the images using mricroN. The scan with the least motion corruption and with full brain coverage was selected as a template and maternal tissue was removed in more detail from around the fetal skull using ImageJ. Using the best scan as a template the remaining 7 scans were manually transformed where they were spatially orientated and matched in close proximity to the template scan using Rview. All scans were then reviewed for image quality in every slice and the slices corrupted by motion artefacts where the anatomical detail had been lost were removed from the proceeding analysis. The 8 processed images and their transformations were entered into a script algorithm in Matlab (MathWorks, Natick, MA, USA) for registration and automatic reconstruction of the final 3D brain (Figure 29B).

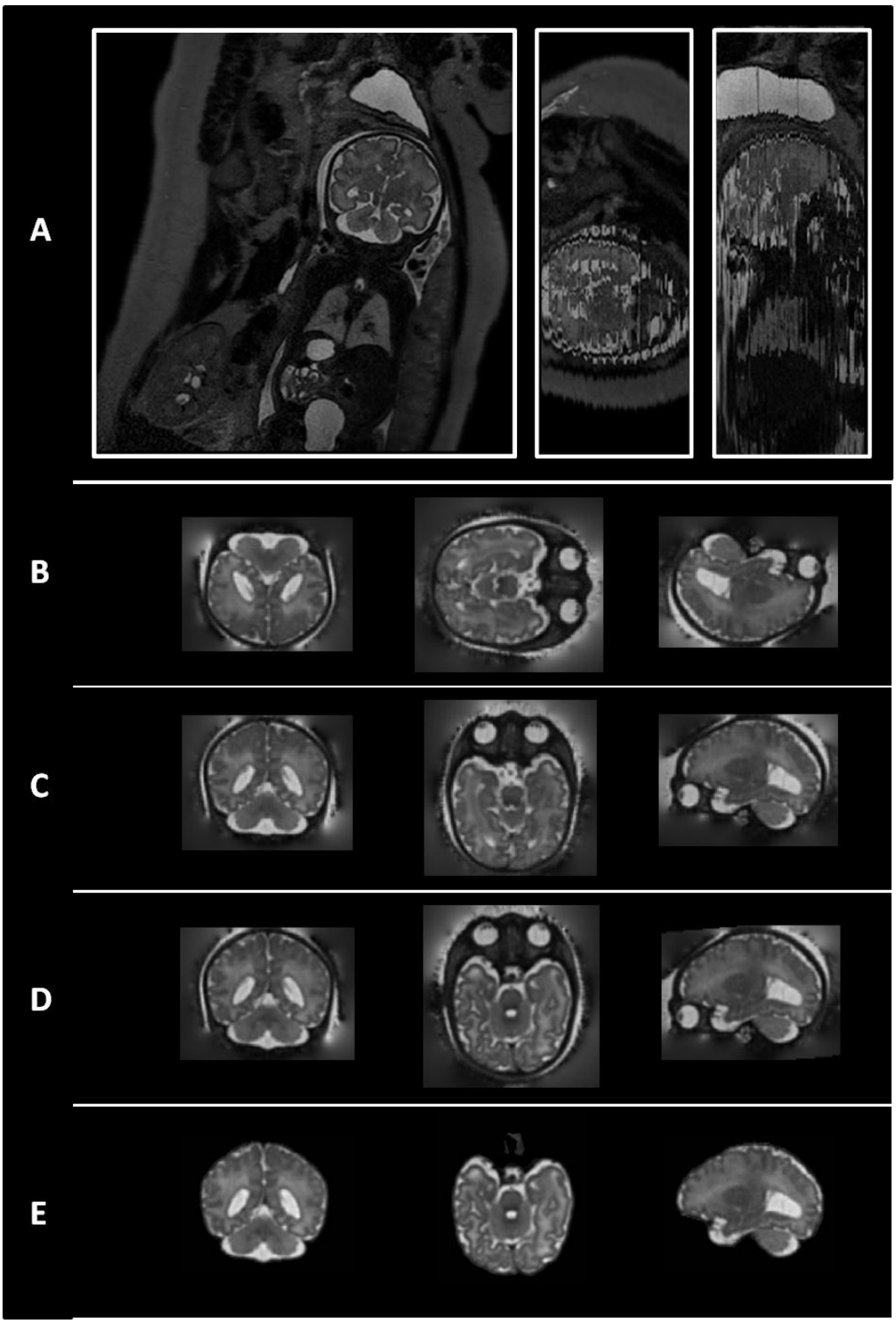


Figure 29. Post-processing of MR images

(A) Single loop of dynamic T2-ssFSE scan acquired in a coronal plane. (B) Reconstructed 3D brain. (C) Reconstructed 3D brain orientated in orthogonal planes. (D) Reconstructed orientated 3D brain resampled at a voxel size of 0.2x0.2x1 mm. (E) Reconstructed orientated 3D brain after removal of non-brain tissue.

2.3.2.2.2.1 Orientation

The fetal reconstructed brain was oriented manually using Rview in the standard axial, coronal and sagittal projections in order to achieve high reproducibility and homogeneity between subjects (Figure 29C). Image orientation is important in volumetric segmentation in order to increase homogeneity between images and reduce the observer's error.

2.3.2.2.2.2 Voxel size

The voxel size of the final reconstructed brain (1.18x1.18x1.18 mm) was too large for visual analysis and accurate volumetric segmentation (especially of small structures) as analysis would be prone to errors due to partial volume. The voxel size of the oriented image was converted from 1.18x1.18x1.18 mm to 0.2x0.2x1 mm (Figure 29D). The specific voxel size was chosen as it provided high image resolution and a feasible number of slices (~100) for manual segmentation and editing. A visual comparison between 6 different voxel sizes was performed in order to select the appropriate voxel size for volumetric segmentation. The first factor determining the selection of the voxel size was image quality in a transverse plane so as to minimise pixelation and partial volume for an accurate delineation of each structure. The second factor was to minimise the number of slices as manual segmentation is a laborious and time consuming task. Evaluation of different voxel sizes is shown in Figure 30. Removal of any tissue or fluid surrounding the fetal skull was then performed using the BET extraction tool in fsl4 in a Linux workstation (Figure 29E). The latter step provided faster and more accurate volumetric segmentation. Voxel size modifications were performed using Rview.

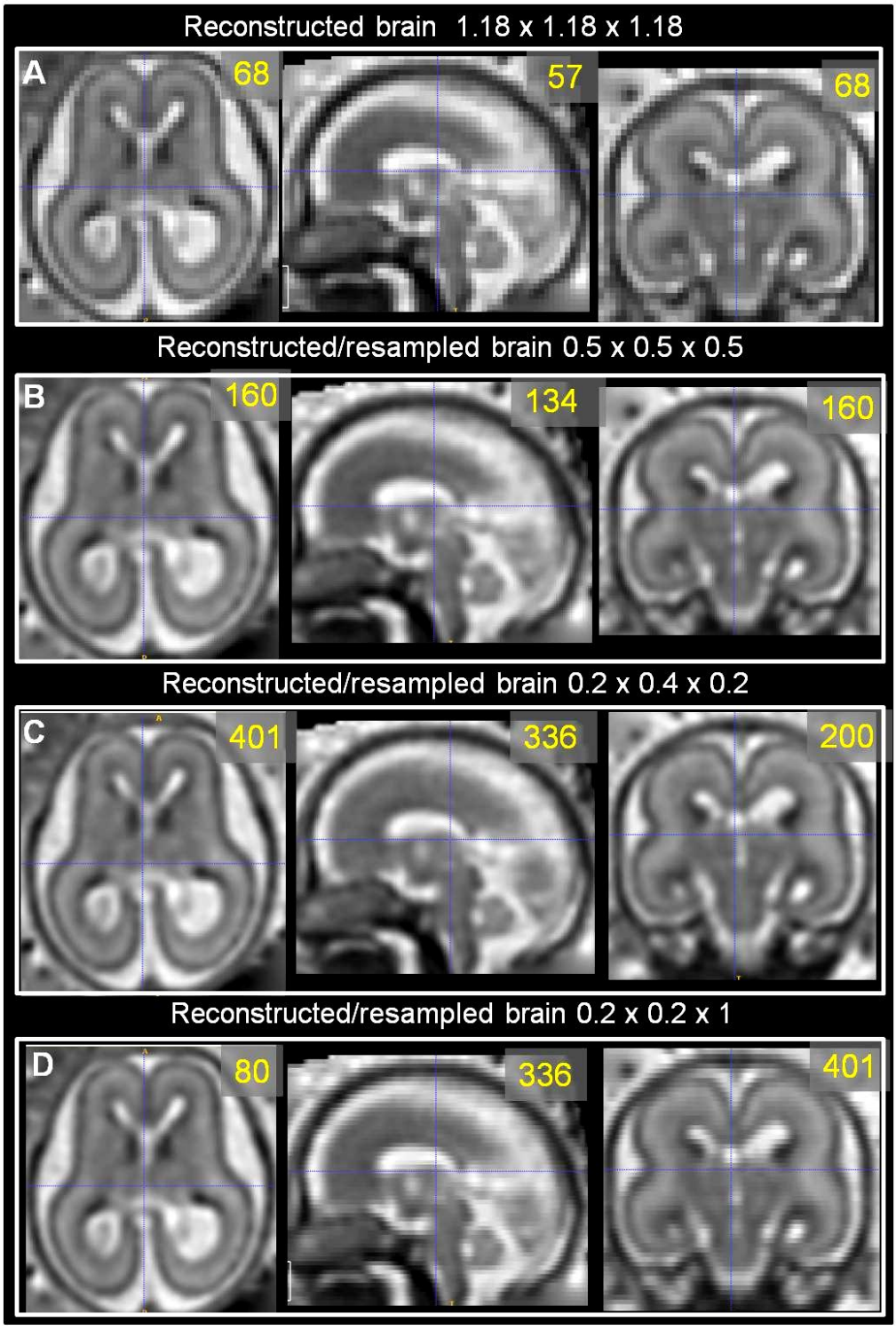


Figure 30. Selection of voxel size for volumetric analysis

(A) Voxel size 1.18x1.18x1.18mm, too pixelated for accurate volumetric analysis. (B) voxel size 0.5x0.5x0.5mm, slightly pixelated and large number of slices. (C) High resolution images in all planes, good for visual analysis, however slice number inappropriate for manual segmentation. (D) Good image quality in a transverse plane with sharp edges around the ventricular wall, appropriate slice number for manual segmentation.

(slice number for each plane is shown and is important for the determination of the voxel size with a feasible slice number for manual segmentation).

2.3.2.3 Measurements of intracranial structures

2.3.2.3.1 Linear measurements

Linear measurements were made using ImageJ. Atrial diameter was measured according to International Society of Ultrasound in Obstetrics and Gynaecology guidelines (ISUOG, 2007) at the level of the atrium, perpendicular to the ventricular axis from each side of the ventricular wall (Figure 31A) (Horsch et al., 2009,Salomon et al., 2011). Cavum septum pellucidum width was measured in a transverse plane at its largest width (Figure 31B).

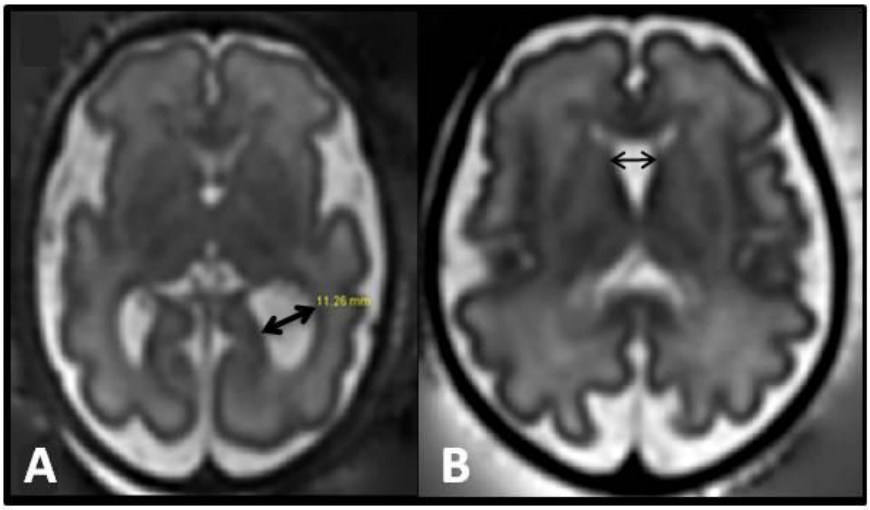


Figure 31. Linear measurements

Linear measurements included (A) atrial diameter (B) width of cavum septum pellucidum.

2.3.2.3.2 Volumetric analysis

2.3.2.3.2.1 Semi-automatic segmentation

Volumetric segmentation of intracranial structures was performed in a semi-automatic fashion using ITK-SNAP (Yushkevich et al., 2006). ITK-SNAP is a user supervised imaging software that allows for manual or the design of semi-automatic segmentation of medical images in three orthogonal planes simultaneously. As manual segmentation is a laborious and time-consuming task, effort was concentrated on optimising a semi-automatic technique for volumetric analysis through ITK-SNAP. Although ITK-SNAP is designed for adult MR images with high resolution

and well defined borders of the different brain structures, it can be optimised for fetal scans with high signal-to-noise and clear structural boundaries. Using a methodology called "region competition", the image intensities were thresholded and classified into background and foreground (region of interest). A range of intensities can be classified as a region of interest and this assignment is based on the user's specifications by visually assessing the image and manually setting the threshold. Regions of interest were filled using the "snake evolution" methodology where a snake refers to a closed curve representing a segmentation that evolves from a very rough estimate of the region of interest to a very close approximation of the structure. Snake evolution is governed by the velocity at every point of the snake which in turn depends on the shape of the snake at any given time and the intensities of the neighbouring pixels. The software allows the user to set upper and lower intensity thresholds, initialise the snake using spherical bubbles, set the velocities driving snake evolution and follow the process in real-time thus allowing for greater control over volume segmentation compared to automatic segmentation techniques. After completion of the automatic process, editing of the segmentation was performed manually using a drawing tablet (Intuos4, Wacom, Germany) in order to remove incorrectly filled areas and fill in areas were blurring did not allow for accurate thresholding. CSF containing structures provide clear intensity contrast at their borders make it ideal for a semi-automatic segmentation using ITK-SNAP. However structures such as the basal ganglia, thalami and cortex had to be segmented manually to achieve accurate delineation of their borders. Separation of the brain hemispheres was also performed manually.

2.3.2.3.2.2 Segmentation of intracranial structures

2.3.2.3.2.2.1 Lateral ventricles

Volume included the lateral ventricles and choroid plexuses and excluded the third and fourth ventricles and cavum septum pellucidum and vergae. The lateral ventricles and cavum septum pellucidum and vergae were separated by the septal leaves (Figure 32).

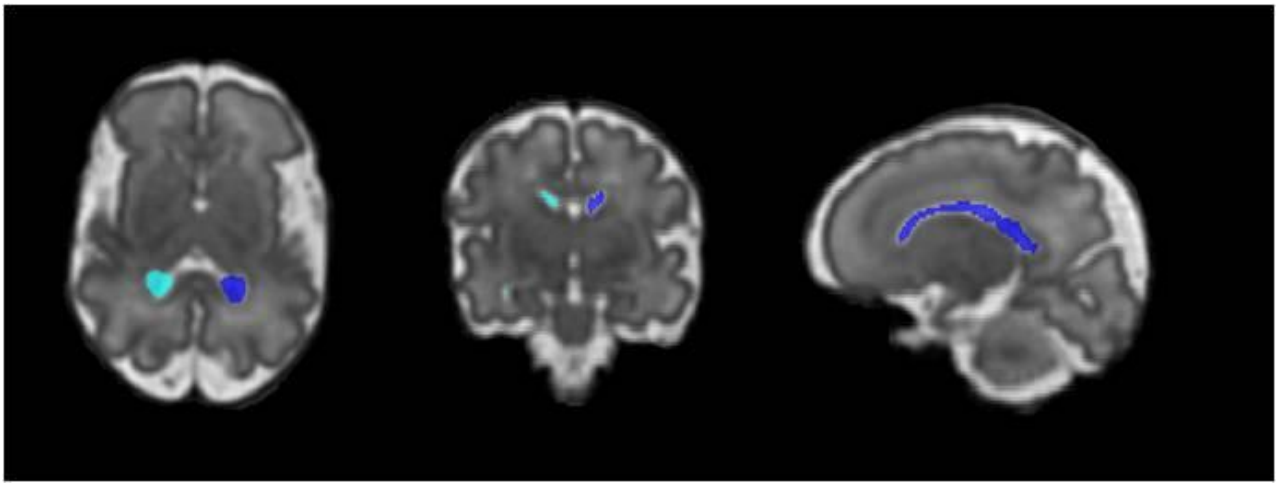


Figure 32. Volumetric segmentation of the lateral ventricles

2.3.2.3.2.2.2 Third ventricle

The third ventricle segmentation was bounded by the cerebrospinal fluid present between the membranous floor of the subthalamic level inferiorly, and the cavum septum pellucidum superiorly. While the anterior and posterior commissures defined the longitudinal aspects of the third ventricle, the thalamic hemispheres outlined the lateral borders. When present, the massa intermedia was excluded from the third ventricle segmentation. Ventricular segmentations were confirmed on sagittal slices (Figure 33).

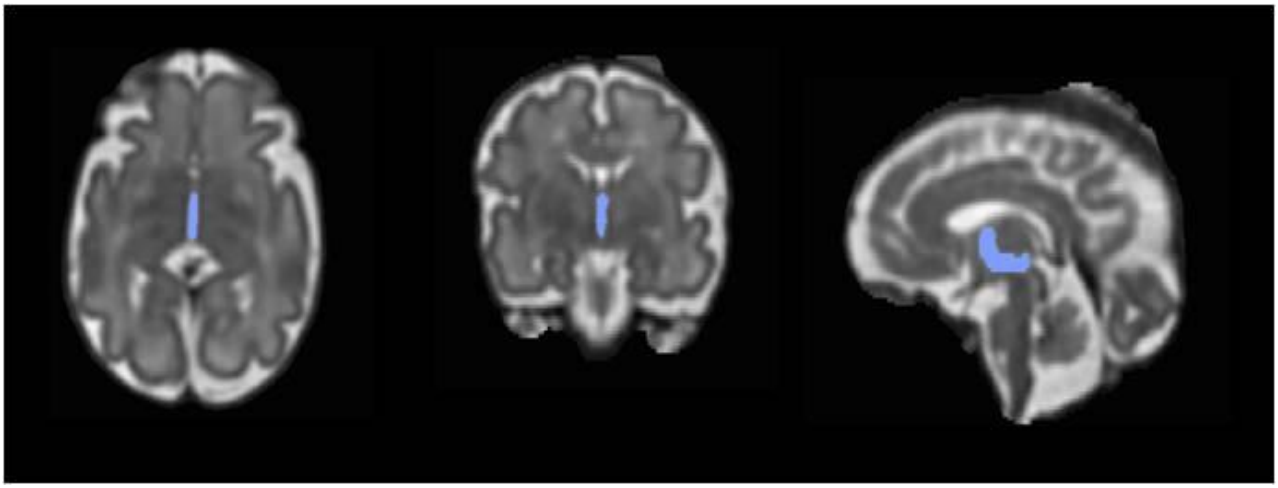


Figure 33. Volumetric segmentation of the third ventricle

2.3.2.3.2.2.3 Fourth ventricle

Omitting the cerebral aqueduct superiorly, the segmentation of the fourth ventricle began at the level of superior medullary velum and was halted at the obex inferiorly. On the transverse plane, the circumferential boundaries of the fourth ventricle were defined by the pons, cerebellar hemispheres and the vermis. Ventricular segmentations were confirmed on the sagittal plane (Figure 34).

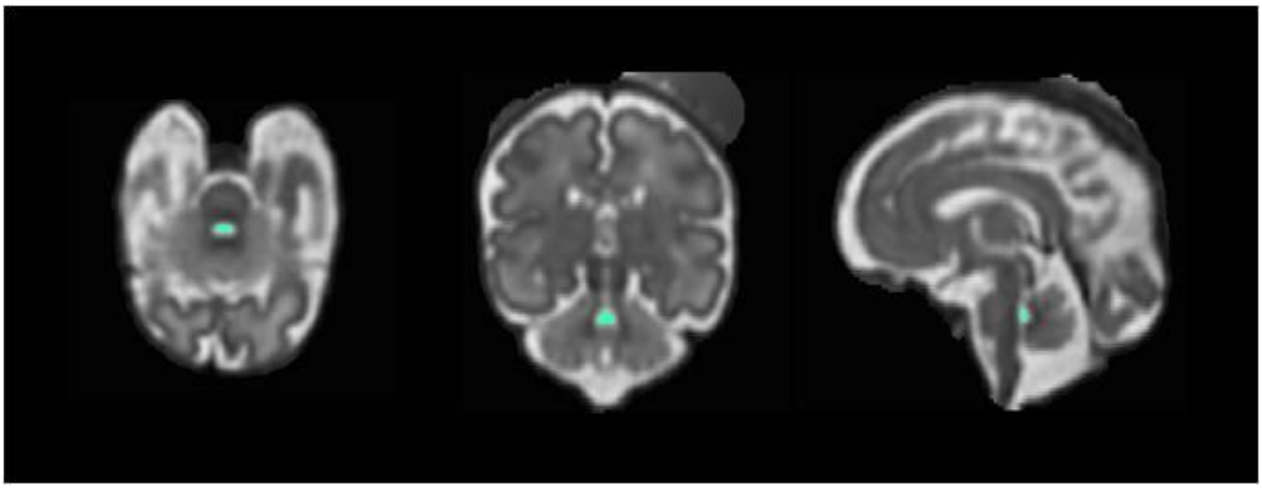


Figure 34. Volumetric segmentation of the fourth ventricle

2.3.2.3.2.2.4 Extra-cerebral CSF

Extra-cerebral CSF included all intracranial CSF space surrounding the supratentorial brain tissue and cerebellum and including the interhemispheric fissure space. CSF borders were outlined by the difference in intensity between the CSF and skull and CSF and cortex. The inferior boundary was defined by the differentiation of the cisterna magna (included) and spinal cord spinal canal. Intracranial veins were included in the segmentation (Figure 35).

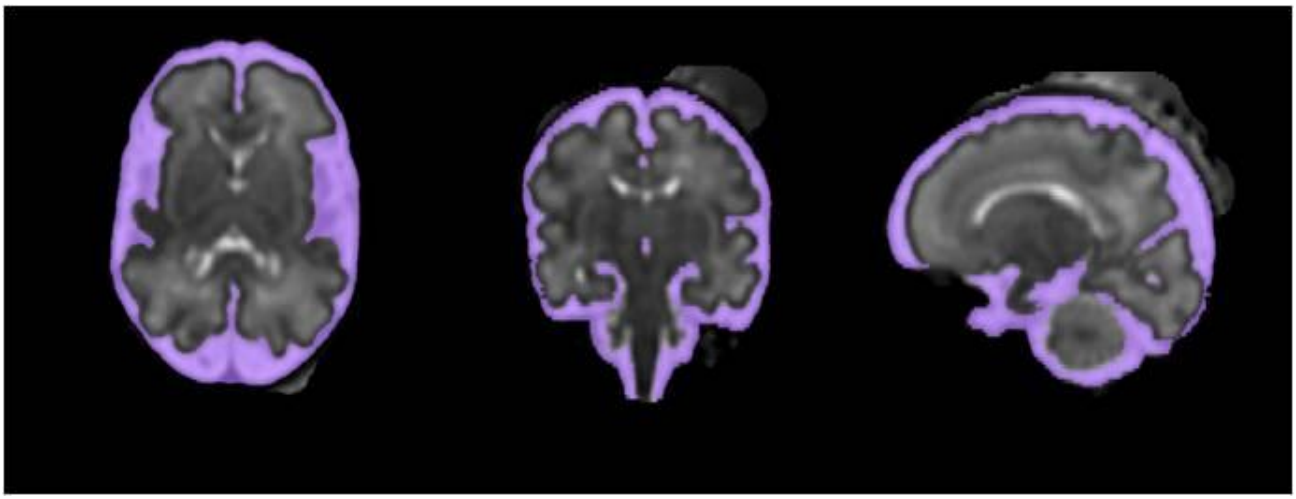


Figure 35. Volumetric segmentation of extra-cerebral CSF

2.3.2.3.2.2.5 Supratentorial brain tissue

Brain tissue volume was defined as the supratentorial brain tissue excluding all intracerebral CSF spaces, choroid plexuses, brainstem, cerebellum and pons (Figure 36). Left and right brain hemispheres were assigned and separation was performed manually (Figure 37). Laterality was established by locating the fetal heart, stomach and liver in a whole fetal body scan in a coronal plane with knowledge from ultrasound of no situs inversus or dextrocardia.

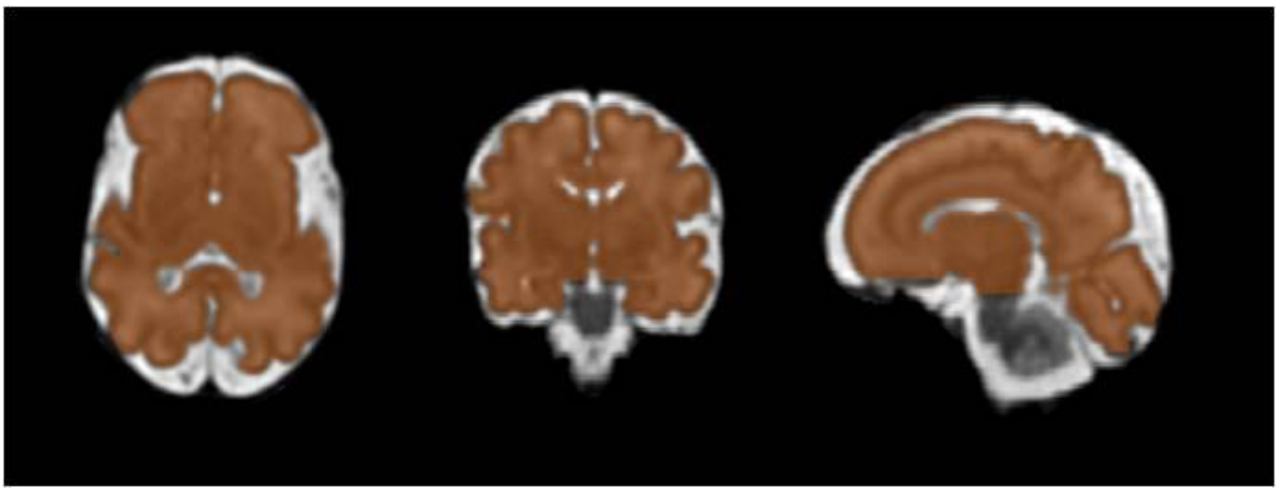


Figure 36. Volumetric segmentation of supratentorial brain tissue

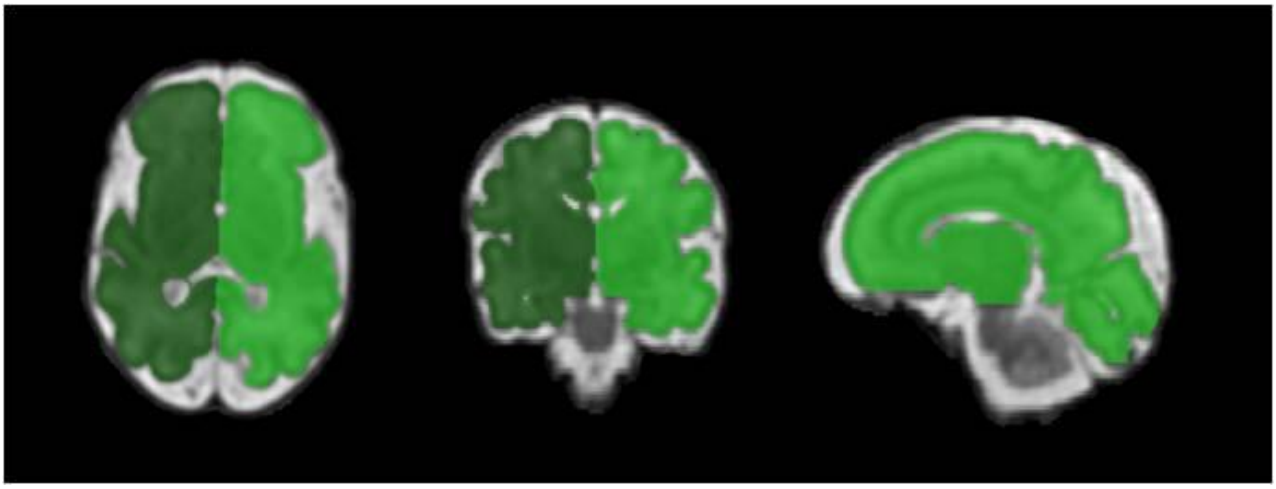


Figure 37. Volumetric segmentation of supratentorial brain tissue (hemispheres)

2.3.2.3.2.2.6 Cavum septum pellucidum

Superiorly the segmentation was initiated with the appearance of the CSP distinguished by the contrast difference due to CSF content just below the body of the corpus callosum. Anteriorly it was defined by the genu of the corpus callosum whilst laterally it was delimited by the septal leaves separating it from the lateral ventricles. Posteriorly the cavum vergae was delineated by the appearance of the internal cerebral veins in a sagittal plane. Inferiorly the CSP was distinguished from the third ventricle on the last slice where the genu of the corpus callosum was visible (Figure 38).

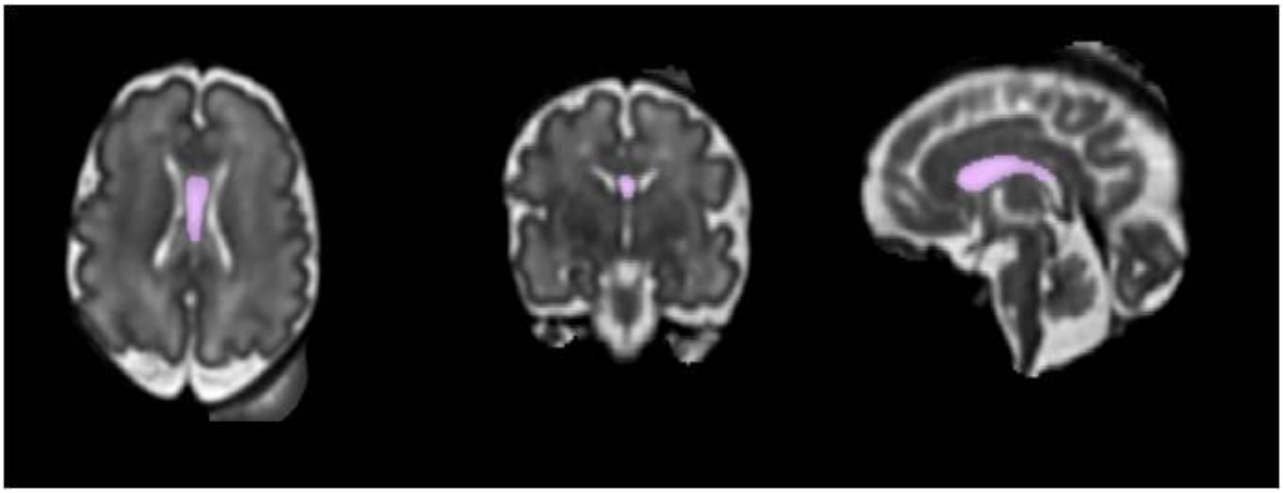


Figure 38. Volumetric segmentation of the cavum septum pellucidum

2.3.2.3.2.2.7 Basal Ganglia

The substructures of the basal ganglia included in this segmentation were caudate, putamen, globus pallidus and nucleus accumbens (Figure 39). Most superiorly, the segmentation was initiated with the visualisation of the caudate head and/or body (depending on the gestational age) outlined between the internal capsule and the hypointense subventricular germinal matrix of the lateral ventricles. Positioned anteriorly across slices with a rounded shape, the caudate head was segmented using the clear contrast between the external capsule anterolaterally, the rather poor delineation of the anterior limb of the internal capsule posterolaterally, and the subventricular zone at the border of the lateral ventricles medially. While the external capsule of the insular gyrus defined the lateral borders of putamen, the internal capsule with its anterior and posterior limbs outlined the borders of both the putamen and the globus pallidus, giving rise to an overall triangular shape. Visible inferiorly to the caudate head, the nucleus accumbens was also segmented in a small number of slices using the borders of anterior limb of the internal capsule, the accumbent neuroepithelium and subventricular zone, and the preoptic and hypothalamic areas. The inferior cut-off point was defined as the slice with no distinction between the basal ganglia and the subthalamic/midbrain structures.

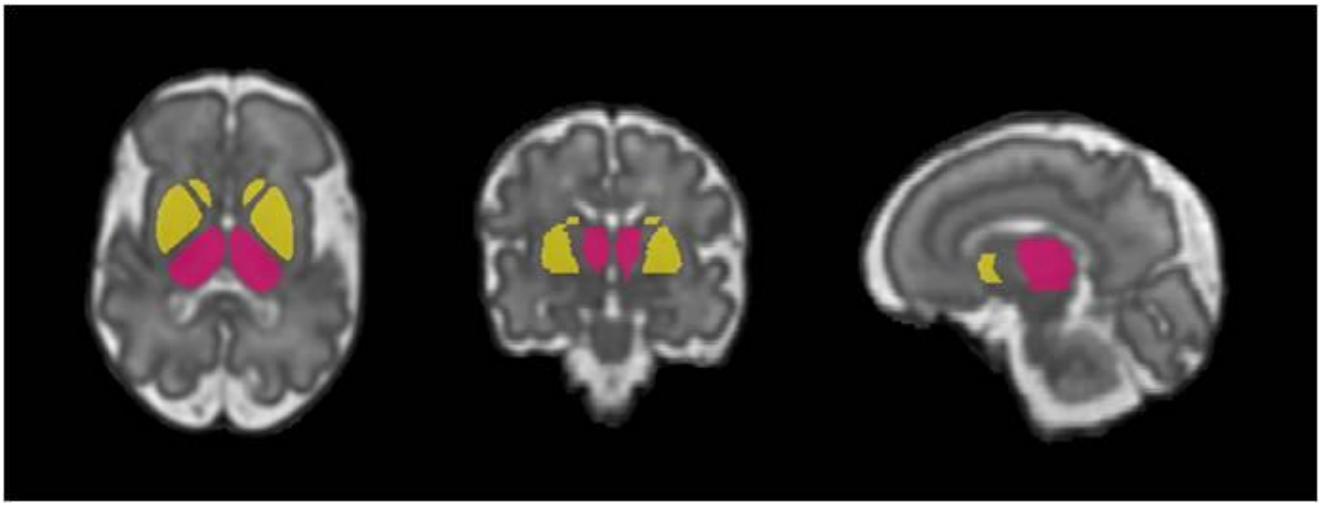


Figure 39. Volumetric segmentation basal ganglia (yellow) and thalami (pink).

2.3.2.3.2.2.8 Thalami

The thalamic segmentation consisted of all the nuclei that were defined by the tissue contrast of the internal capsule laterally, the atrial region of the lateral ventricles posteriorly, the third

ventricle medially and the hypothalamus anteriorly (Figure 39). The most superior slice was segmented with the visualization of the separation between the caudate head, and the thalamic nuclei bulging towards the body of the lateral ventricles, whereas the most inferior border was defined by the appearance of the tectum, due to the poor tissue contrast against the subthalamic region. While the pointed pretectal areas at the posterior third ventricular and medial thalamic region were excluded, the massa intermedia, joining the two hemispheres of the thalamus in some cases, was included in the segmentation.

2.3.2.3.2.2.9 Cortex

Cerebral cortical gray matter was manually segmented in a transverse plane by tracing around the outer cortical border (CSF-cortex) and inner cerebral cortex (cortex-white matter) in all slices (Figure 40).

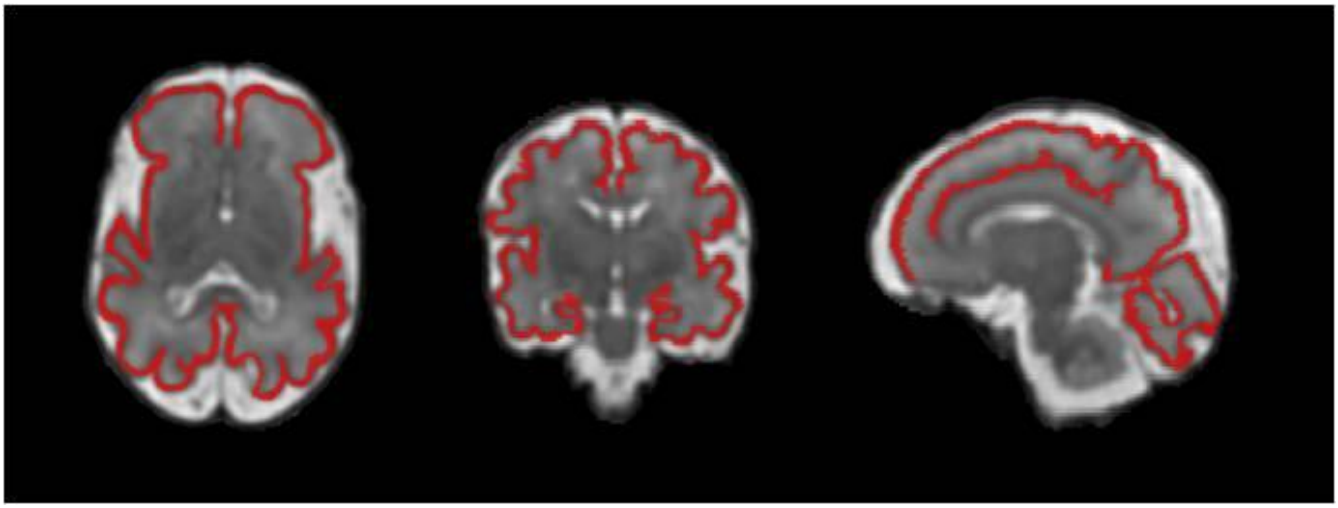


Figure 40. Volumetric segmentation of the cortex

After visual analysis of several normal control fetuses it was noted that specific cortical areas were not clearly visualised in all fetuses either due to image quality or because the limits surrounding developing structures at different gestations were unclear. In order to segment the cortex in a consistent way in all fetuses regardless of image quality and gestation and to avoid introducing error in "difficult areas" a detailed protocol was designed with rules defining uncertain cortical areas.

The cingulate gyrus was segmented up until the first convolution from the corpus callosum (Figure 41A).

The cortical regions including all lower signal intensity areas surrounding the interhemispheric fissure were included in the segmentation (Figure 41B).

The parieto-occipital sulcus was segmented up until the medial aspect of the hippocampus isthmus, not including the later (Figure 41C).

The calcarine sulcus was segmented in its entirety, including deep convolutions present in advance GAs (Figure 41D).

Cortical visualisation was compromised proximal to the inferior part of the frontal lobe due to partial volume of the frontal lobe and the eyes. The regions with obvious image blurring where excluded from the segmentation (Figure 41E-F).

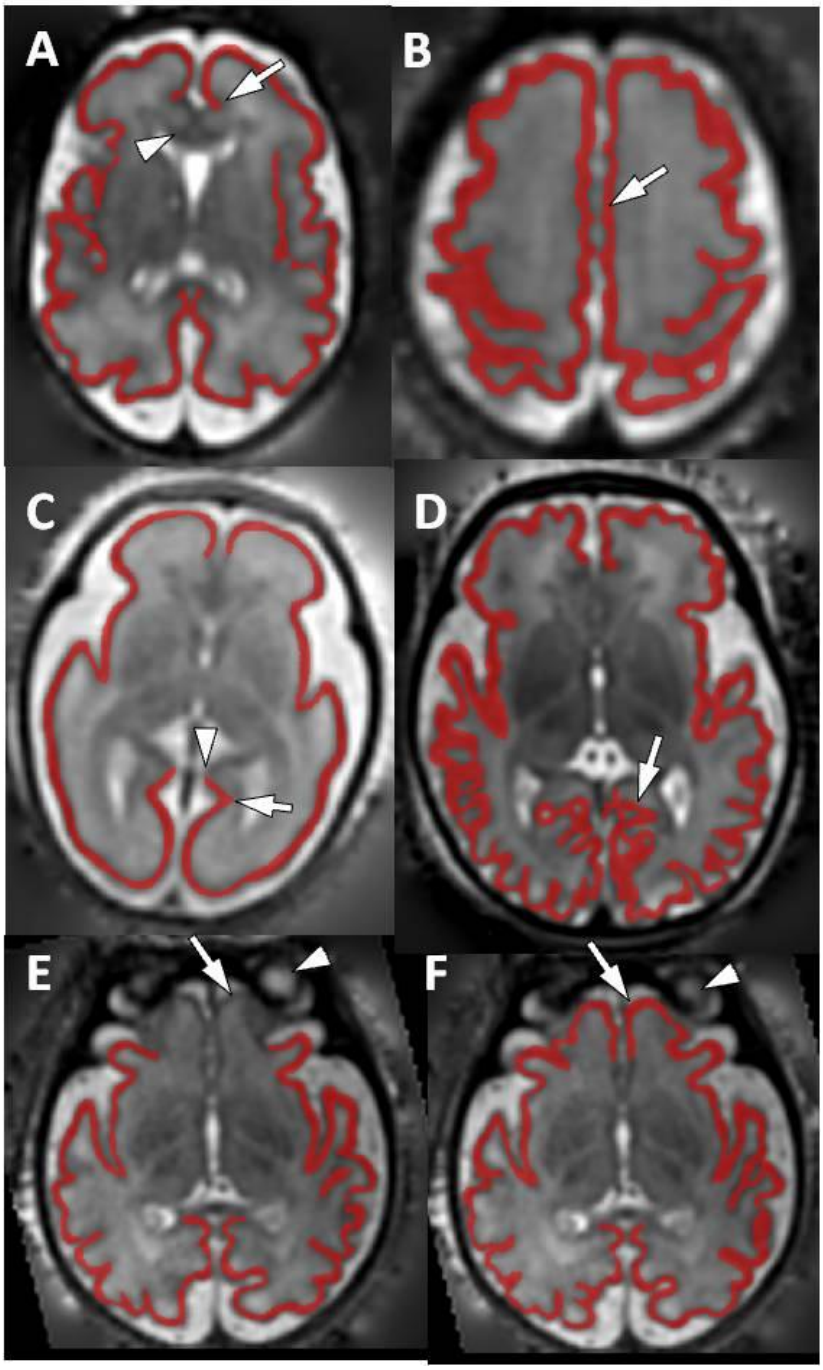


Figure 41. Cortical segmentation protocol

(A) The cingulate gyrus (arrow) was segmented up until the first convolution from the corpus callosum (arrow head).
(B) Around the interhemispheric fissure, the cortex was segmented including all lower signal intensity areas close to the interhemispheric fissure (arrow).
(C) The parietooccipital fissure (arrow) was included in the segmentation until medial border of the hippocampus isthmus (arrow head).
(D) The entirety of the calcarine sulcus including deep convolutions (arrow) was included in the segmentation.
(E) The cortex surrounding the inferior part of the frontal lobes was not included in the segmentation due to poor image quality due to partial volume. (F) Slice directly above (E) was included in the segmentation.

During the design of the protocol some cortical parts had to be excluded despite being visualised, therefore the segmented cortical volume may have introduced a small underestimation error in the measurement compared to the actual cortical volume. Designing a robust protocol that would provide consistent results regardless of image quality and gestation bias fulfilled the purpose of this study and we are aware that an underestimation error was introduced in all cortical measurements in both groups.

2.3.2.3.2.3 Work done by others

Volumetric segmentation of the basal ganglia, thalami, 3rd and 4th ventricles was performed by a colleague (DV). The design of the protocol for cortical volumetric segmentation was performed by me, however the manual segmentation was performed by a student I supervised (SE).

2.3.2.3.2.4 Duration of volumetric segmentations

The time required for segmentation of the different structures varied and were as following for one 28 week old fetus, total brain tissue and hemispheres (3 hours), cortex (8 hours), lateral ventricles (15 minutes), thalami (15 minutes), basal ganglia (30 minutes), cavum septum pellucidum and vergae (10 minutes). Factors determining segmentation duration included image quality, gestation and cortical complexity.

2.3.2.3.3 Cortical development

We wished to include both qualitative and quantitative analysis of the cortex, globally and regionally. Volumetric segmentation of the cortex can provide information about cortical size and growth trajectory through gestation however it cannot provide detailed information about cortical gyrification. A detailed protocol for evaluating cortical maturation was designed based on the cortical staging system by van der Knaap et al., (1996) which assessed the progress of cerebral gyration and sulcation in MR images of preterm and term neonates. In our study, the protocol designed assessed the development of the gyri and sulci during gestation by giving each one a score between 0 to 6 as illustrated in Figure 42. Sulci may receive a score from 0 to 6. Gyri may receive a score from 0 to 4 and 6. Gyri progress from score 4 directly to score 6 and do not receive a score of 5 due to their shape, the width does not equal 0 at any gestational age.

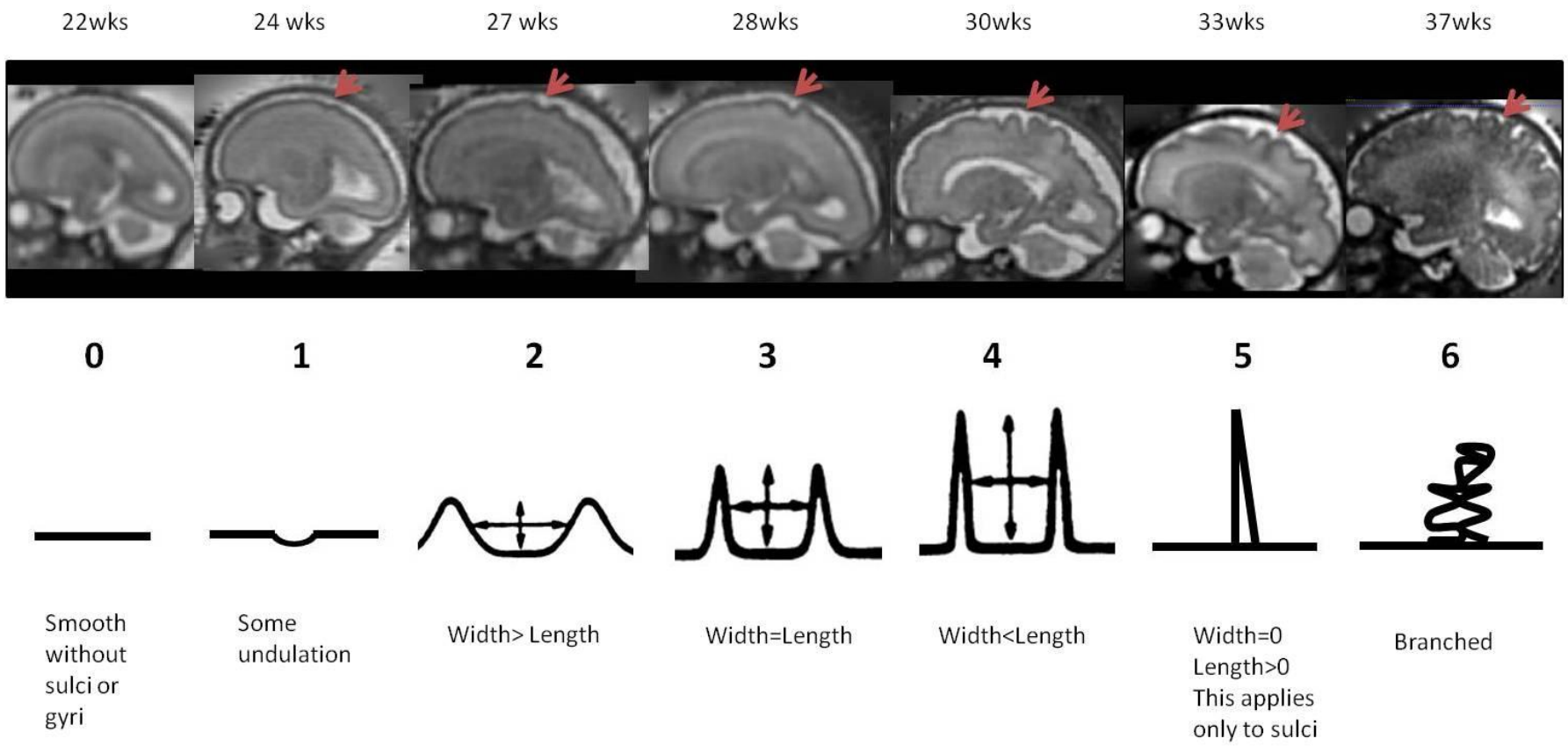


Figure 42. Cortical development scoring system

Gyri and sulci are assigned a score from 0 to 6 according to their appearance at each gestational age. As an example the development of the central sulcus is shown. Sulci may receive a score from 0 to 6. Gyri may receive a score from 0 to 4 and 6. Gyri progress from score 4 directly to score 6 and do not receive a score of 5 due to their shape as the width does not equal 0 at any GA.

The cortical maturation scoring system allows for the detection of delays in sulcation or gyrification. Whist all previous studies have visually assessed cortical maturation using the van der Knaap et al., (1996) scoring system, in the current project we have additionally measured the dimensions of the cortical landmarks in different planes. The scoring system can depict a delay in the development of the cortex but not a change in size or shape. Therefore a quantitative approach is essential for investigating changes in the size or shape of cortical landmarks. Furthermore, the size of each gyrus and sulcus was assessed by measuring the height and width at a specific plane. The major cortical landmarks from each brain lobe detected during gestation were selected for evaluation. These are presented in Table 5 and the measurements are shown in Figures 43-49.

Frontal lobe	Precentral gyrus
	Superior frontal gyrus
	Superior frontal sulcus
	Middle frontal gyrus
	Inferior frontal gyrus
	Inferior frontal sulcus
Frontal/Parietal border	Central sulcus
Parietal lobe	Postcentral gyrus
	Parieto-occipital fissure
Temporal lobe	Superior temporal gyrus
	Superior temporal sulcus
	Middle temporal gyrus
	Inferior temporal gyrus
Frontal/parietal/temporal border	Sylvian fissure
Occipital lobe	Calcarine sulcus
Limbic lobe	Cingulate sulcus

Table 5. Cortical landmarks assessed

Cortical landmarks selected were representative of each brain lobe.

The factors for deciding which plane and slice to measure each landmark were as follows: the landmark was easily identifiable in a consistent way in all gestational ages and also evolved throughout gestation in accordance to the scoring system. Exceptions were the Sylvian fissure and cingulate gyrus which could not be assessed with this scoring system due

to their complex configuration, the assessment was individualised for each. Sylvian fissure development was assessed using the ratio of the maximum distance from frontal to temporal boundaries along the insula-temporal cortex to the minimum distance from frontal to temporal borders of the operculum (Figure 47). The cingulate sulcus was assessed by measuring the maximum distance of the sulcus in a sagittal plan. The detailed protocol is available in Appendix 5.

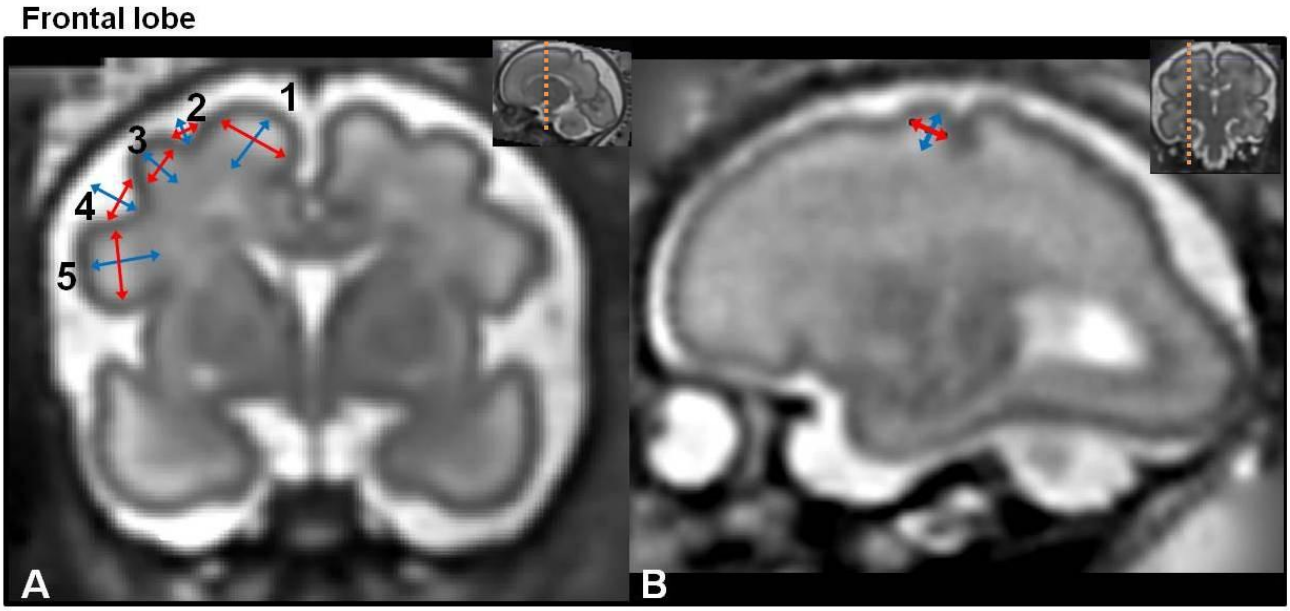


Figure 43. Cortical landmarks of the frontal lobe

Cortical landmarks of the frontal lobe included (A)(1) superior frontal gyrus (2) superior frontal sulcus (3) middle frontal gyrus (4) inferior frontal sulcus (5) inferior frontal gyrus (B) precentral gyrus. Measurements of cortical folding included height (blue) and width (red) of gyri and sulci. (Note areas of high signal intensity below the cortex constituting the subplate).

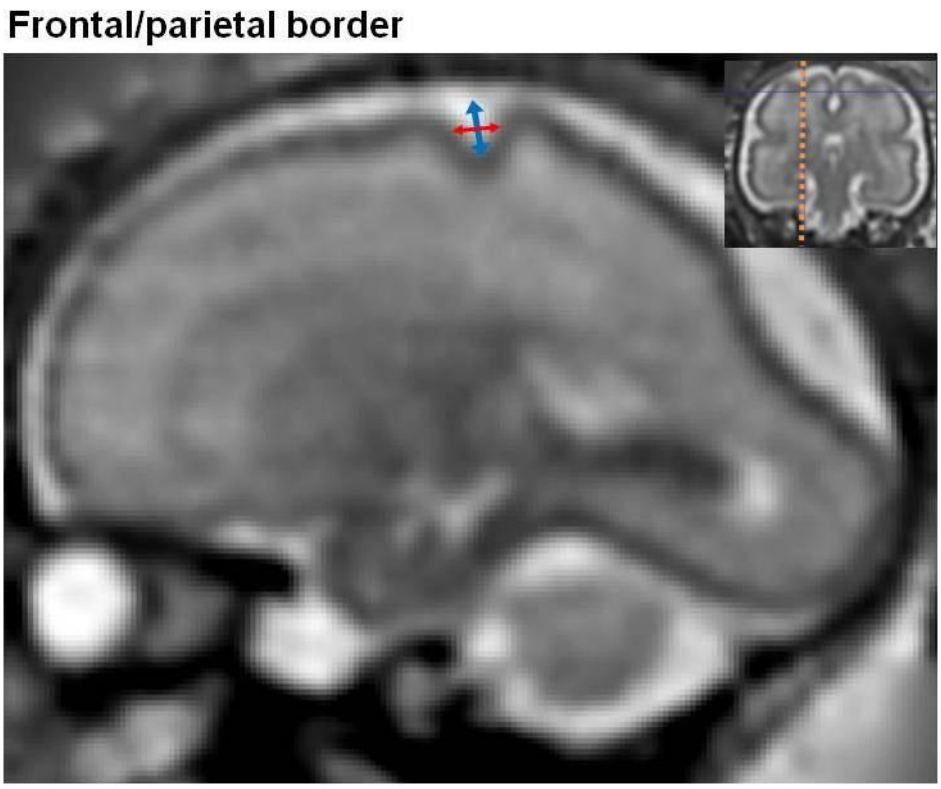


Figure 44. Cortical landmarks of the frontal/parietal border

Cortical landmarks of the frontal/parietal border included the central sulcus. Measurements of cortical folding of the central sulcus included height (blue) and width (red).

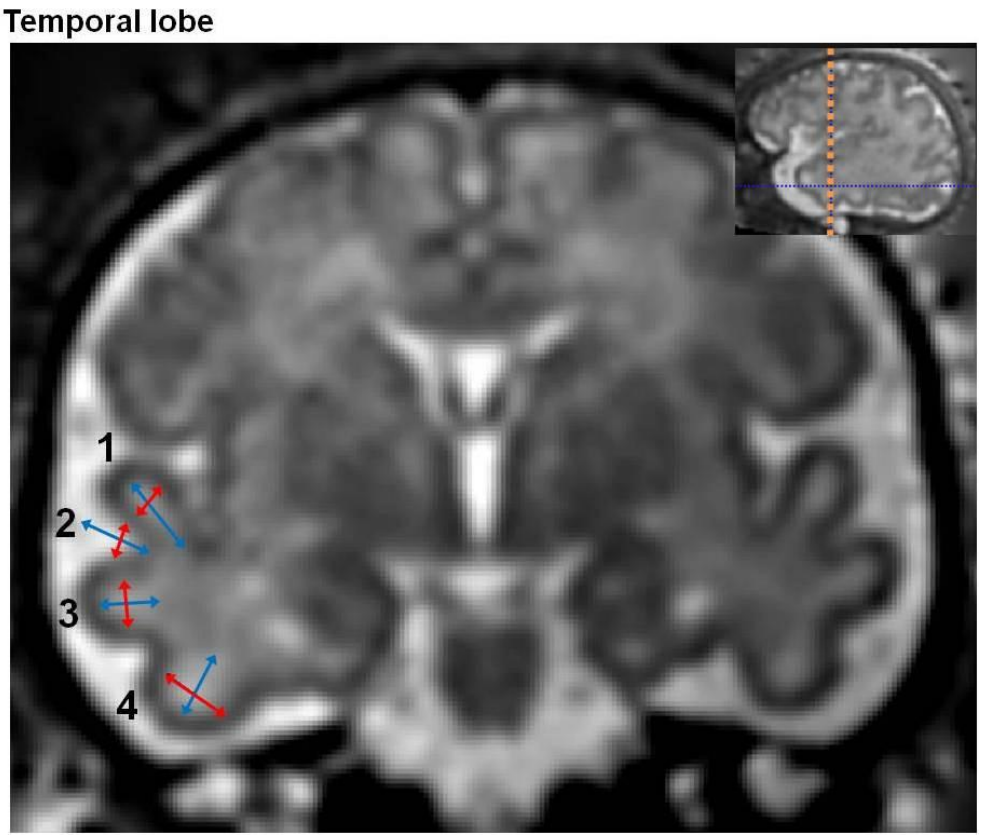


Figure 45. Cortical landmarks of the temporal lobe

Cortical landmarks of the temporal lobe included (1) superior temporal gyrus (2) superior temporal sulcus (3) middle temporal gyrus (4) inferior temporal gyrus. Measurements of cortical folding included height (blue) and width (red) of gyri and sulci.

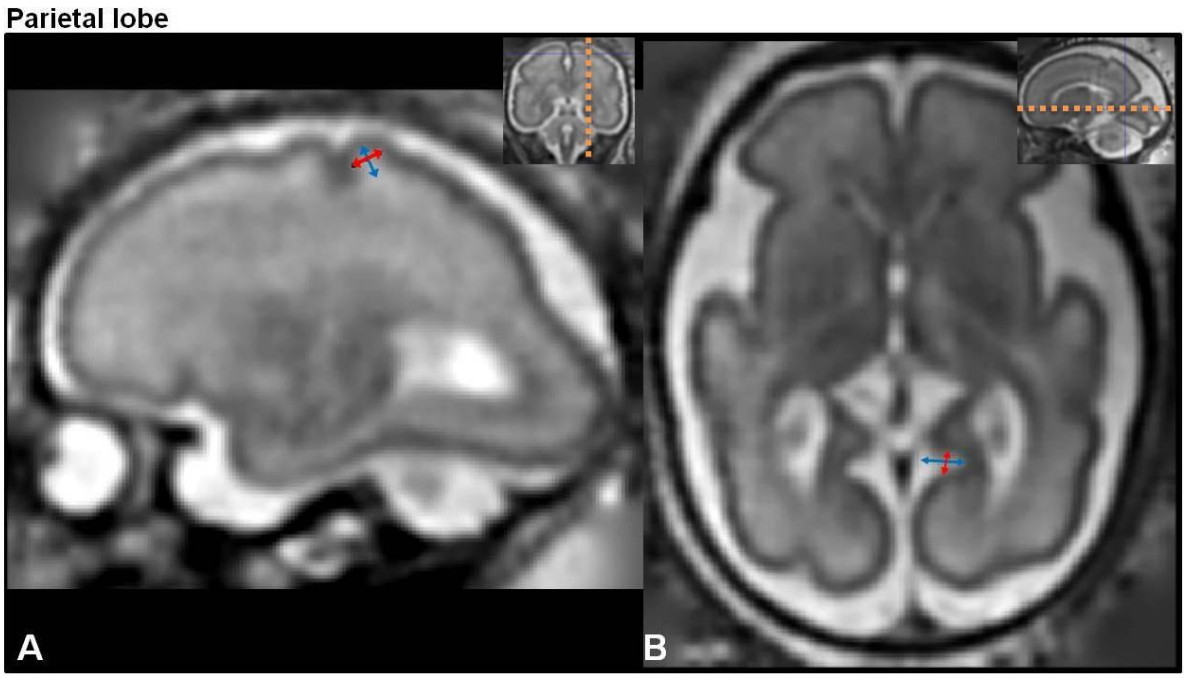


Figure 46. Cortical landmarks of the parietal lobe

Cortical landmarks of the parietal border included (A) the postcentral gyrus and (B) parieto-occipital fissure. Measurements of cortical folding of the cortical landmarks included height (blue) and width (red).

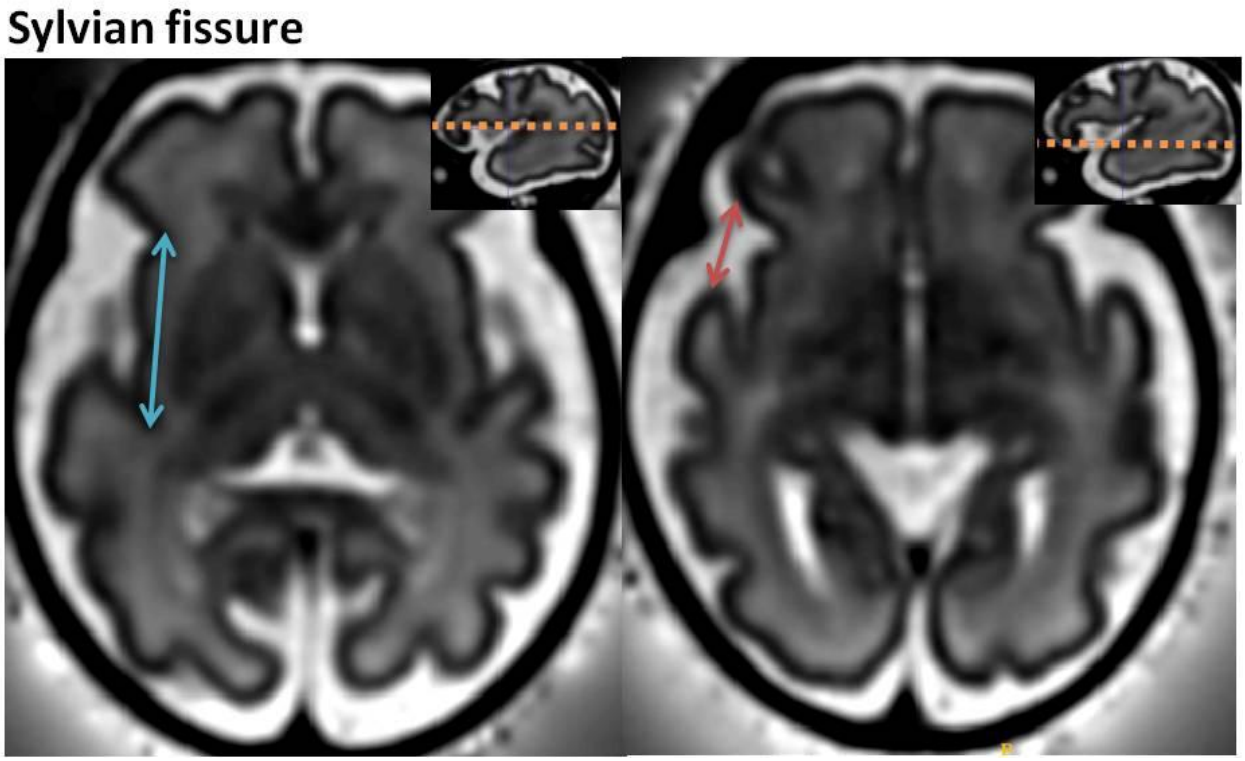


Figure 47. Cortical landmarks of the frontal/parietal/ temporal border

Cortical landmarks of the frontal/parietal/temporal border included the Sylvian fissure. Sylvian fissure development was assessed using the ratio of (A) the maximum distance from frontal to temporal boundaries along the insula-temporal cortex to (B) the minimum distance from frontal to temporal borders of the operculum.

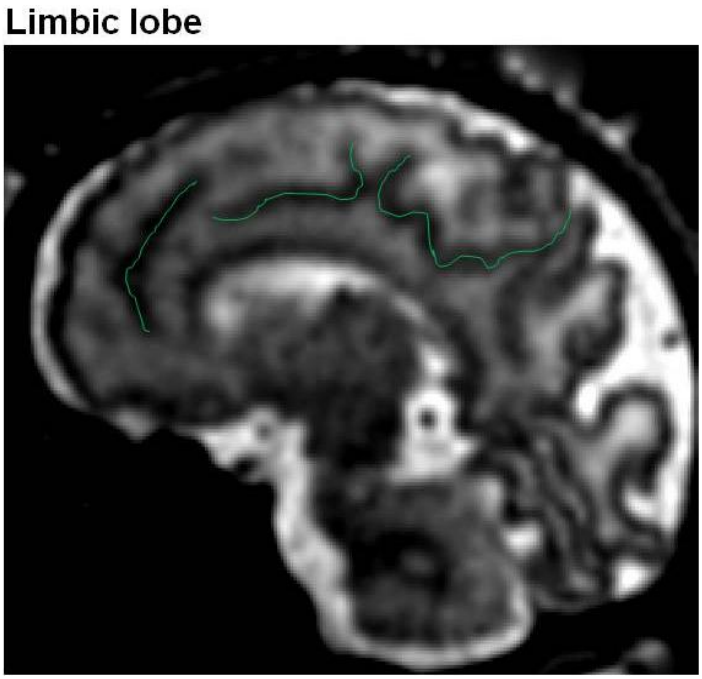


Figure 48. Cortical landmarks of the limbic lobe

Cortical landmarks of the limbic lobe included the cingulate gryus. Cortical development of the cingulate sulcus was assessed using the length of the cingulate sulcus (green) on a sagittal plane.

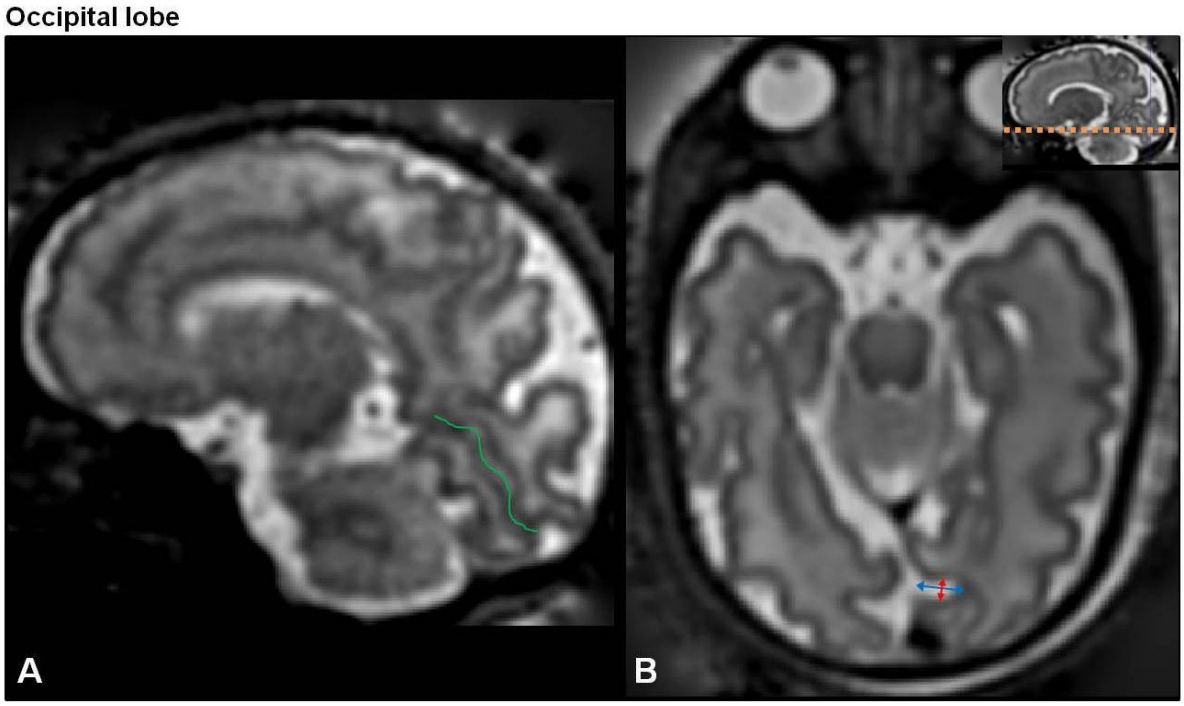


Figure 49. Cortical landmarks of the occipital lobe

Cortical landmarks of the occipital lobe included the calcarine sulcus. Cortical development of the calcarine sulcus was assessed using (A) the length of the cingulate sulcus in a sagittal plane (green) and (B) the height (blue) and width (red) on a transverse plane.

2.3.2.3.3.1 Image pre-processing

Consistency between images in terms of orientation was crucial for the assessment of the cortex and probably one of the most important steps in this process. As the measurements recorded were small the risk of introducing error due to improper orientation was high. All images previously orientated for volumetric analysis were re-checked visually and compared to each other in order to achieve homogeneity between the images in both groups. The voxel size was changed to 0.5x0.5x0.5 mm in order to achieve an isotropic voxel and achieve similar image quality in all planes and increase consistency in measurements. In order to ascertain consistency in all measurements each measurement was performed separately across all fetuses instead of evaluating all landmarks in each fetus in a single attempt. Laterality of the cerebral hemispheres was assigned according to the position of the fetal heart, stomach and liver as visualised in a T2-weighted MR image in a coronal plane with the knowledge from ultrasound of no situs inversus or dextrocardia. In the control group measurements were divided into left and right hemispheric sides whilst in the ventriculomegaly group according to the presence of the larger and smaller ventricle according to the atrial diameter. In bilateral cases the largest volume was used to depict the larger ventricle. The height and width was measured and recorded using ImageJ. All outliers were re-measured.

2.3.2.4 Spectroscopy

2.3.2.4.1 Post-processing of 1HMRS spectra

Analysis of ^{1}HMRS spectra and quantification of metabolites was performed offline using jMRUI (www.mrui.uab.es/mrui/mrui_homePage.shtml, version 2.2), a widely used and freely available graphical user interface allowing for analysis of 1D spectra.

2.3.2.4.2 Quality assessment

An initial quality assessment of the acquired spectra was performed during scanning as the scanner software allows for immediate display of the data. In addition, the quality of individual spectra was assessed offline using jMRUI. Spectrum quality was evaluated according to the signal-to-noise ratio (height of metabolite peaks compared to background noise) and spectral resolution (peak width and differentiation between metabolites). Aberrant spectra indicative of fetal motion were removed and the remaining spectra were summed into a final spectrum. An example of a motion corrupted spectrum not available for analysis is presented in Figure 50.

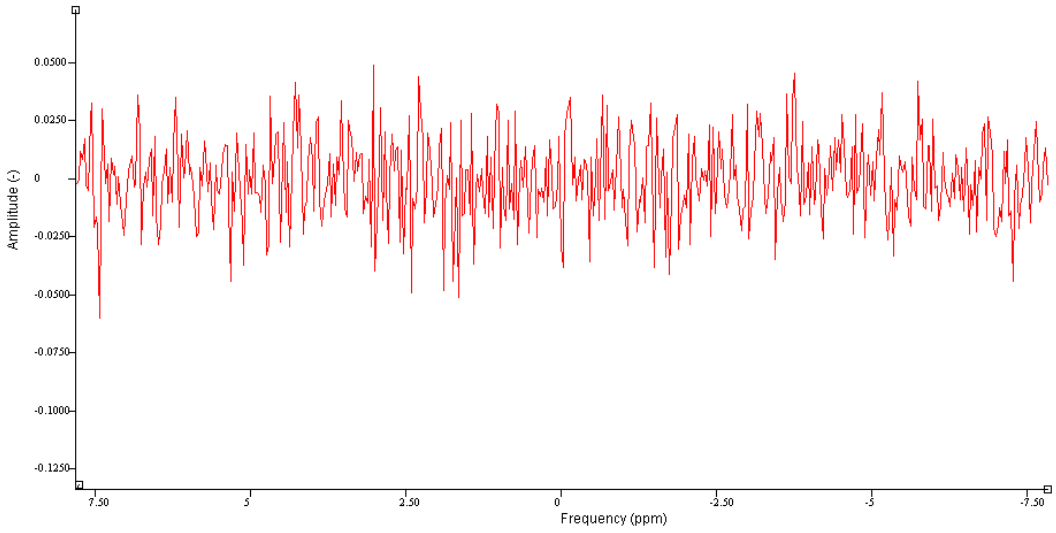


Figure 50. Motion corrupted fetal spectrum at echo time 136ms

Spectra that have been corrupted due to fetal motion are identified by the absence of a water peak (water peak should be present at 4.7 ppm).

2.3.2.4.3 Noise reduction

The signal of the metabolites in a FID is affected by the noise in the detector channels. A line broadening filter was applied which multiplies the signal by an exponentially decaying function leading to an increase in the signal-to-noise ratio but also broadening of the peaks (Drost et al., 2002). Noise reduction was followed by removal of the water peak at 4.7 ppm.

2.3.2.4.4 Phasing the spectrum

Quantification of metabolites requires evaluating the area under the peaks therefore distortion of the baseline may affect the accuracy of the areas. Phase adjustment of the spectrum was manually adjusted in order to achieve a flat baseline and for all points to have the same phase.

2.3.2.4.5 Quantification

Expected peaks were identified at each echo time based on their position within the spectrum as illustrated in Table 6. The top and midpoint of each peak were identified and a curve was fit by the software for each metabolite peak. Once curves had been fitted for all metabolites the ratios were calculated. The metabolite ratios calculated at each echo time are shown in Table 6. The inter-rater and intra-rater intraclass correlation coefficients were calculated for each echo time.

Echo Time (ms)	Metabolite ratios
42	*MI*:Cho *MI*:Cr Cho:Cr
136	NAA:Cho NAA:Cr Cho:Cr Lactate presence
270	NAA:Cho NAA:Cr Cho:Cr Lactate presence

Table 6. 1HMRS echo time and metabolite detection

The metabolite ratios calculated at each echo time are shown. Abbreviations: myo-inositol (MI), choline (Cho), creatine (Cr), N-acetylaspartate (NAA), lactate (Lac)

2.3.2.4.6 Work done by others

Analysis of spectra acquired at 136ms in the control cohort was performed by a colleague (LS) and data have been previously published (Story et al., 2011a).

2.4 Neonatal Imaging

Neonatal MRI was performed in order to assess the evolution of the ventricular dilatation, exclude additional abnormalities not detected on antenatal MRI and to assess white matter tissue microstructure. Post-processing of MR images included volumetric analysis of intracranial structures using an automated software and TBSS analysis of DTI data for the assessment of white matter.

2.4.1 Patient preparation

All participants enrolled in the fetal research program were offered a neonatal MRI scan which was performed from their day of delivery and up to 10 weeks after birth (ethics No. 07/H0707/105). Informed parental consent was obtained prior to each scan. A metal checklist was completed before the scan to ensure the infant was free of ferrous metals and safe to enter the magnetic field.

MRI was performed on a 3T Phillips system (Phillips, Best, The Netherland) using an eight channel phased array head coil. Before the scan, all neonates were assessed by an experienced paediatrician and a detailed neurological assessment was performed (Mercuri et al., 2005). Infants were imaged either in natural sleep or under light sedation (chloral hydrate 30-50 mg/kg dose orally administered) to minimise motion. Infants were wrapped and positioned supine and their head was immobilised using a polystyrene bead filled pillow which adjusted to the head size using vacuum air removal. Neonates were monitored throughout with ECG and pulse oximetry and a paediatrician was present throughout the scan. Imaging parameters of structural scans and DTI are detailed in Tables 7 and 8.

Physiological parameters including heart rate, oxygen saturation and temperature were monitored before and during the scan. Ear protection was used in all infants and included moulded earplugs made of silicone-based putty (President putty, Coltene/Whaledent, New Jersey, USA) and neonatal adhesive earmuffs (Natus MiniMuffs, Natus Medical Inc, CA, USA). An experienced neonatologist supervised all the examinations (Rutherford, 2002a).

Parameters	T2 SENSE	T2 dyn	Dual Echo	T1
TE (ms)	160	160	100	4.6
TR (ms)	1000	1000	1000	17
Flip angle (deg)	90	90	90	180
Acquisition Voxel size (mm)	1.15x1.18x2	0.98x0.99x2	1.15x1.18x2	0.82x0.97x1
Slice gap (mm)	-1	-1	-1	0
Reconstructed voxel size (mm)	0.86x0.86x2	0.86x0.87x2	0.86x0.86x2	0.82x0.82x0.5
FOV (mm)	220x220x107	220x176x101	220x220x141	210x157x120
SAR (W/Kg)	0.1	0.2	0.2	2.4

Table 7. Neonatal MRI scanning parameters

Parameters	DTI
TE (ms)	49
TR (ms)	1000
Flip angle (deg)	90
***b* value (s/mm^2)**	750
SENSE factor	2
Directions	32
Acquisition Voxel size (mm)	2 x 2.03 x 2
Slice gap (mm)	0
Reconstructed voxel size (mm)	1.75 x 1.75 x 2
FOV (mm)	224 x 224 x 98
SAR (W/Kg)	0.1

Table 8. Neonatal DTI scanning parameters

2.4.2 Neonatal volumetry

2.4.2.1 Overview

Volumetric segmentation was performed using a fully automatic segmentation algorithm designed in our department as described in Xue et al. (2007). This technique is intensity-based and uses the Expectation-Maximization (EM) algorithm which enables parameter estimation in probabilistic models (Do and Batzoglou, 2008) in conjunction to a Markov random field (MRF) and Mislabelled partial volume voxel detection and removal (MLPV). The EM-MRF-MLPV analysis was performed in Matlab (MathWorks, Natick, MA, USA).

2.4.2.2 Pre-processing

T2-SENSE images of the ventriculomegaly and control cohorts were reviewed for the presence of motion, image quality and brain coverage (Figure 51A). When these images were inappropriate for volumetric analysis (motion artefact or not full brain coverage) then the T2 dynamic ssFSE were used. A 3D reconstructed dataset was generated using the T2 dynamic ssFSE images as described in chapter 2.3.2.2.2. When both T2-SENSE and T2 dynamic ssFSE scans were not available a dual echo scan was used for volumetric analysis. Acquisition parameters were similar between the sequences allowing for comparable volumetric results. Imaging parameters are summarised in table 7.

Brain extraction was performed to exclude non-brain tissue using fsl4 in a Linux workstation (Figure 51B). In order to minimise the effects of intensity variability, inhomogeneity correction was applied using the Medical Image Processing Analysis and Visualization (MIPAV) (version 5.4.3). Label propagation via image registration was used for the exclusion of the brainstem and cerebellum in all images.

2.4.2.3 Expectation-Maximization (EM) algorithm

Each class label (CSF, gray matter and white matter) will have different image intensities for every voxel and the EM algorithm allows for every tissue class to be modelled by a Gaussian distribution. The EM algorithm requires an initial estimate of the class intensities of each tissue therefore initialising was performed via *k*-means clustering to assign each voxel to a

specific tissue class. The EM algorithm consists of two steps, the expectation step during which each voxel is classified according to a specific tissue label and the maximisation step which updates the estimated Gaussian distribution. The algorithm maximises the data likelihood and updates the tissue classification via iterations of the expectation and maximisation steps.

2.4.2.4 Markov Random Field

After completion of the voxel-wise tissue classification many voxels on the CSF-cortex boundary are incorrectly classified as white matter. A similar problem occurs at the CSF-non brain boundary where many voxels are classified as white matter due to the signal intensity at the border of the structures. In order to constrain spatial homogeneity of tissue labelling MRFs are commonly used. A first-order neighbourhood system was used for the removal of mislabelled voxels according to which the prior probability that a voxel belong to a specific tissue class depends on the neighbouring tissue class. The six nearest neighbouring voxels on the 3D image grid were used. Therefore voxels were assigned to a specific tissue class depending on their neighbouring voxel classification.

2.4.2.5 Mislabelled partial volume voxel detection and removal

Due to the large number of misclassified voxels in the CSF-cortex, EM and MRF alone are not sufficient to remove all incorrectly labelled voxels (Figure 51C). If many incorrect voxels are adjacent to each other this will prohibit them from being corrected. The MLPV removal is a knowledge-based approach and specifies that if a voxel classified as white matter has first order neighbouring voxels classified as CSF and cortex simultaneously then that voxel has been incorrectly labelled. The rule that no white matter voxel can appear in a CSF-cortex boundary is also applied for mislabelled voxels in the CSF-non brain boundary. Finally, the generated segmentations were reviewed in ITK-SNAP and incorrect labelling surrounding the cerebrum was manually removed using a drawing tablet (Intuos4, Wacom, Germany). Due to time constraints we only performed volumetric segmentation of the lateral ventricles and supratentorial brain tissue while delineation of white matter and cortex is currently underway (Figure 51D).

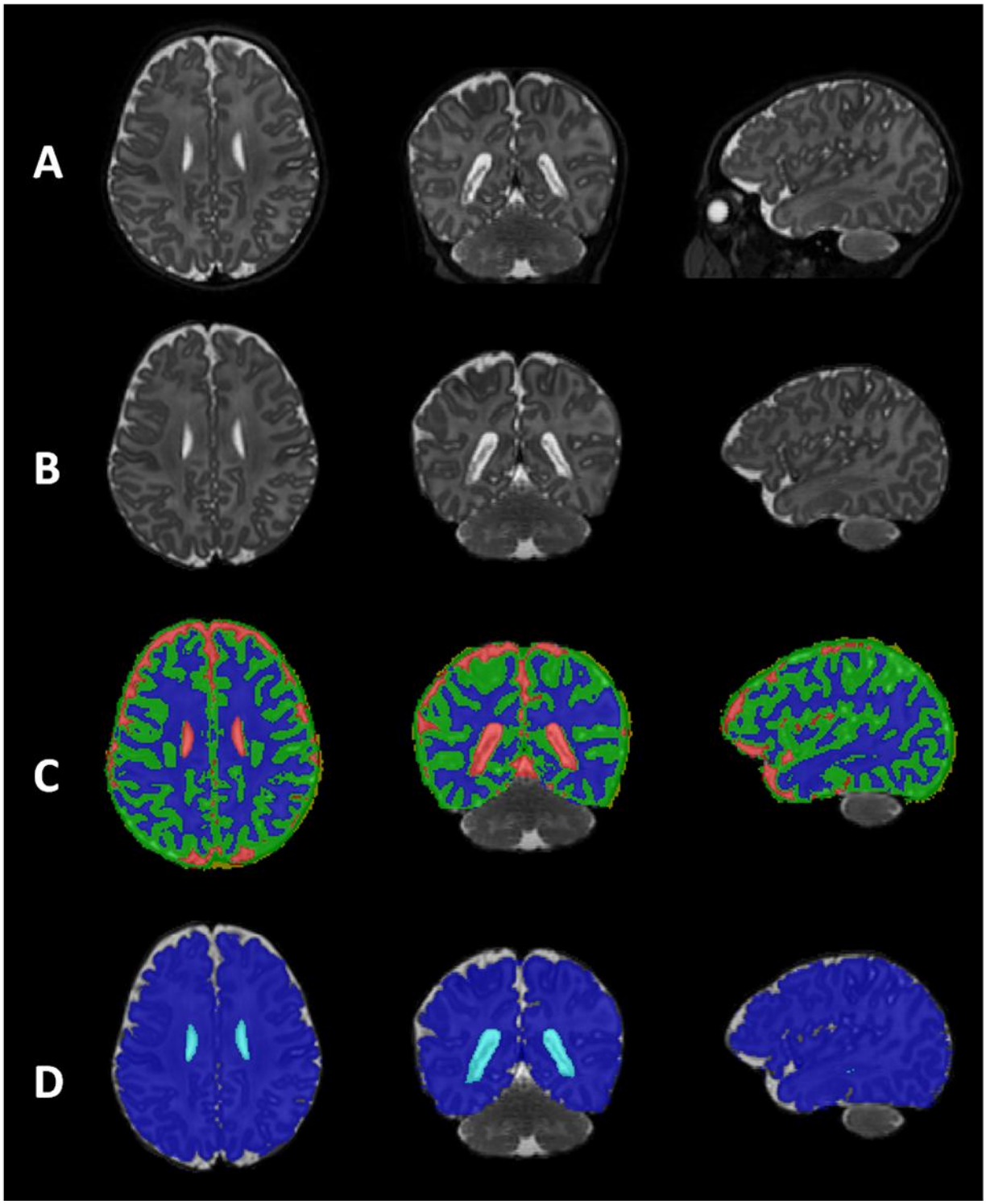


Figure 51. Automatic volumetric analysis in a neonatal brain
(A) T2-SENSE image of a neonate aged 43^{+3} postmenstrual weeks. (B) Neonatal brain after removal of non-brain tissue and inhomogeneity correction. (C) Automatic segmentation of intracranial structures as generated by Expectation-Maximization (EM) algorithm. Measurements are inaccurate without further editing due to voxel mislabelling. (D) Volumetry segmentation of supratentorial brain tissue and lateral ventricles after manual editing and correcting.

2.4.3 Diffusion Tensor Imaging

2.4.3.1 Pre-processing

DTI analysis was performed using FMRIB's Diffusion Toolbox (FDT v2.0), a freely available and comprehensive library of tools for the analysis of DTI brain imaging data (FSL v4.1; www.fmrib.ox.ac.uk/fsl; Smith et al. (2004)). Analysis was performed on a Linux workstation. All 32 volumes of acquired diffusion weighted data were visually checked for artefacts and motion distortion and corrupted volumes were removed. When more than 4 volumes had to be removed, the whole dataset was discarded. Removal of non-brain tissue was performed on the data using BET (v2.1). The generated mask was used for performing Brain Extraction in all DTI data for a specific subject. During data acquisition eddy currents in the gradients coils induce distortions in the images which are different for each gradient direction. Eddy Current Correction was applied to correct for these distortions and for head movement by affine registration of the DTI data to the reference b_0 image.

2.4.3.2 Image registration

An optimised protocol (Ball et al., 2010) designed for voxel-wise registration of neonatal data was used for the processing of the generated FA data. The first step included linear registration of the FA maps to each other using FMRIB's Linear Registration Tool (FLIRT v5.5; default settings). The FA maps were then registered using FMRIB's Non-Linear Registration Tool (FNIRT v1.0; parameters defined in FA_2_FMRIB58_1mm configuration file) for accurate alignment. The FA map of each subject was registered to the map of every other subject and the warp field was recorded. The FA map with the minimum mean warp displacement score was chosen as a target. Each subject's FA map was then aligned in the target space and the mean FA map and mean FA skeleton were generated. The mean FA skeleton represents the centre of all white matter tracts that are common to the group. The skeleton was thresholded at FA>0.1 in order to remove cerebral sinuses and CSF incorrectly represented in the skeleton and only to include the major white matter tracts. Each subject's aligned FA data were projected onto the mean FA skeleton.

2.4.3.3 Tract-Based Spatial Statistics

TBSS (v1.2) was used to assess the relationship between FA and presence of ventriculomegaly. The FA values of the control and ventriculomegaly groups were compared using voxel-wise cross-subject statistics controlling for postmenstrual age at scan and gestational age at birth. The results were corrected for multiple comparisons by using the family-wise error correction following threshold-free cluster enhancement (Smith and Nichols, 2009). $P < 0.05$ was considered statistically significant.

2.4.3.4 Work done by others

The steps of image pre-processing, image registration and TBSS analysis were performed by a colleague (GL).

2.5 Neurodevelopmental assessments

All parents were invited for a detailed neurodevelopmental assessment of their child at year 1 and 2. Assessments were performed by the clinical psychologist or paediatric neurologist. On the day of the assessment the child's weight, height and head circumference were measured. The Griffiths Mental Development Scales (GMDS) assessment was performed at year 1 and the Bayley Scales of Infant Development-III (BSID-III) assessment was performed at year 2. A strong association has been found between the GMDS and the BSID tests (Ramsay and Fitzhardinge, 1977). While the two tests may be used interchangeably the numerical scores are not equivalent. The GMDS has traditionally been the mainstay of developmental assessment for infants in the UK however in recent years an increasing number of studies have been using the BSID test as part of their follow-up. Due to the wide use of the BSID and in order for our data to be comparable with other studies the BSID was used for assessing the development of children at 2 years. The GMDS was used for the 1 year assessment due to the fact that it is shorter in duration and thus more appropriate for children at that age. Development scores at year 2 are more predictive of later outcome however assessments at 1 year of age allow for the detection of obvious developmental abnormalities and aid in keeping parental contact.

2.5.1 Griffiths Mental Development Scales

The GMDS assessment is a developmental test for children aged 0-2 years (Huntley, 1995). It is composed of 5 separate scales: Locomotor, Personal-Social, Hearing and Speech, Eye-Hand Co-ordination and Performance. The Locomotor sub-scale assesses the gross motor skills of the child and includes co-ordination, balance and general movements. The Personal-Social sub-scale assesses the development of skills related to social development and independence. The Hearing and Language sub-scale assesses active listening, expressive and receptive language development. The Eye and Hand Co-ordination includes fine motor skills, visual attention skills and manual dexterity. The Performance scale assesses how skills are used in novel situations and problem solving.

2.5.1.1 Scoring

Each task in the GMDS assessment is marked with 0 or 1; with 0 representing failure to perform a task and 1 successful performance. Upon completion of the assessment the total number of items passed in each sub-scale is added up producing the total raw score for each sub-scale. The raw scores for each sub-scale can be converted into standardised scores including age equivalent, sub- and general-Quotients, and percentile equivalents of the sub-quotients (Table 9). The raw score corresponding to each developmental age represents the average score obtained by all children tested in the standardisation sample who were that age. The sub-Quotients (SQ) and Developmental Quotients (DQ) take in to account how the child's raw scores vary around the mean score for each month of age. These are calculated for each sub-scale and for the total raw score. The sum of the total scores of all subtests and divided by the number of tests represents the total DQ. The DQ has a mean of 100 and a standard deviation of 12 while the SQ has a mean of 100 and a standard deviation of 16. DQ scores below 88 (1SD) and SQ scores below 84 (1SD) indicate developmental delay. The percentile scores are derived from the sub-quotients.

Sub-scale	Total Raw score	Age equivalent score	Sub- and General Quotient	Percentile score
Locomotor	•	•	•	•
Personal-Social	•	•	•	•
Hearing and Language	•	•	•	•
Eye and Hand Co-ordination	•	•	•	•
Performance	•	•	•	•
Total Scale	•	•	•	

Table 9. Griffiths Mental Development Scales

Areas of development assessed using the Griffiths Mental Development Scales and the scoring system.

2.5.2 Bayley Scales of Infant and Toddler Development-III

The BSID-III is a developmental test that assesses the developmental functioning of infants and young children between 1 month and 42 months of age (Bayley, 2006). The BSID-III assesses development in 3 domains; Cognition, Language (expressive and receptive) and Motor (fine and gross). The cognitive scale assesses sensorimotor development, exploration and manipulation, object relatedness, concept formation, memory and other aspects of cognitive processing. The Language scale is composed of the receptive communication and expressive communication subtests. The receptive communication assesses vocabulary development, preverbal behaviour and verbal comprehension. The expressive communication assesses preverbal communication and morpho-synaptic development. The motor scale was composed of the fine motor and gross motor subtests. The fine motor scale included items for assessing children's skills related to functional hand skills, such as grasping and object manipulation. The gross motor subtest assessed movement of the limbs and torso. Items evaluated static positioning, dynamic movement and co-ordination. The BSID-III also included a Social-Emotional scale, however this was not part of the routine examination and behaviour was informally assessed by the psychologist based on observation during the testing session.

2.5.2.1 Scoring

Each task in the BSID-III is marked with 0 or 1 with 0 representing failure to perform a task and 1 successful performance. At the end of the assessment the total raw scores are calculated by summing the number of completed tasks for each subtest (Table 10). Scaled scores are calculated for all subtests and are derived from the subtest total raw scores and range from 1-19 with a mean of 10 and a standard deviation of 3. Composite scores are derived from various sums of subtest scaled scores and are generated for the Cognitive, Language and Motor scales. The composite scores can be used to compare a child's performance across all 3 BSID-III scales. They are scaled to a metric with a range from 40-160, a mean of 100 and a standard deviation of 15. Developmental delay was classified when composite scores were below 85 (1SD) and scaled scores were below 7 (1SD). Percentile ranks are calculated indicating the performance of a child relative to that of children in the standardisation sample. Percentile ranks range from 1 to 99 with a mean and median of 50.

Scale or Subtest	Total Raw score	Scaled score	Composite score	Percentile Rank	Developmental Age Equivalent
Cognitive Scale	●	●	●	●	●
Language Scale			●	●	
Receptive Communication subtest	●	●			●
Expressive Communication subtest	●	●			●
Motor scale			●	●	
Fine motor subtest	●	●			●
Gross motor subtest	●	●			●

Table 10. Bayley Scales of Infant and Toddler Development-III

Areas of development assessed using the Bayley Scales of Infant and Toddler Development-III and the scoring system.

2.5.3 Ages and Stages Questionnaires

In our study, questionnaires were provided only in cases where the parents refused to attend a formal assessment and when we were unable to get in contact with parents and would otherwise have no follow-up data. Ages and Stages Questionnaires–III (ASQ-3) are parent-completed developmental questionnaires that assess a child's development in the areas of communication, gross motor, fine motor, problem solving and personal-social. An example of a questionnaire for a 24 month old infant is presented in the Appendix 3. Each questionnaire comprises 30 questions spanning the aforementioned developmental areas written in simple, straight-forward language and a series of overall questions to elicit parental concerns. They can be administered between 1 months and 5.5 years of age and the items required for completion of the tasks can generally be found in a family's home. The ASQ-3 serves as a first-level screening system and can identify infants or young children who are delayed in their development. The validity of the ASQ has been examined by comparing with several professionally administered standardised assessments including the BSID. Overall agreement on children's classifications was 86%, while studies comparing ASQ-2 and BSID-II in preterm infants at 2 years of age have shown sensitivity range from 73%-100% and specificity from 65%-87% (Gollenberg et al., 2010; Woodward et al., 2011). ASQ-3 is a reliable screening system for identifying children with development delay however it should be considered that specificity is low.

Work done by others

The GMDS and BSID-III assessments were performed by a paediatrician (AC) and a clinical psychologist (BH).

2.6 Statistics

Statistical analysis was performed using SPSS (Statistical Package for the Social Sciences) software package version 17 (SPSS Chicago, IL, USA). Normality of distribution was assessed using the Shapiro-Wilk goodness-of-fit test and the Q-Q plots for each variable. Data not normally distributed was log-transformed to achieve normal distribution. Log transformed data was tested for normality as described. Analysis of covariance (ANCOVA) on log-transformed data was used to compare results between groups when corrected for GA. A confidence level of 0.05 was considered significant. Correlation between variables was assessed using the Spearman's correlation coefficient (Spearman's r) on non-parametric data. Slope comparisons between groups were performed in StatsDirect statistics software using Grouped Linear Regression Analysis with a covariance as this function was not available in SPSS. Intra-rater and inter-rater variability was assessed using the intra-class correlation coefficient calculated and Bland-Altman plots on SPSS.

2.6.1 Power calculations

From previous published fetal MR volumetric and spectroscopy studies (29 intrauterine growth restriction [IUGR] v 46 controls) a significant decrease was detected in brain structure volumes and in metabolic status in association with IUGR (Damodaram et al., 2012; Story et al., 2011a). In this study we therefore anticipate that we have a large enough sample size to be able to detect and identify a significant difference ($p<0.05$)

3 Results

3.1 Contribution of MRI in the sonographic diagnosis of ventriculomegaly

3.1.1 Background

While sonography is the mainstay for the antenatal diagnosis of ventriculomegaly, there is increasing evidence for the value of MRI in providing additional diagnostic information. As the prognosis for fetuses with ventriculomegaly largely depends on the presence or absence of additional CNS abnormalities it is essential to perform a detailed assessment of the fetal brain. There are two clinical considerations in fetal ventriculomegaly regarding prognosis, the degree of dilatation and the presence of additional abnormalities. Whilst there is good correlation in atrial diameter measurement between the two techniques, studies have evaluated the diagnostic value of MRI following an ultrasound diagnosis of isolated ventriculomegaly and have reported a detection rate of additional abnormalities ranging from 14%-17% (Benacerraf and Shipp, 2007; Griffiths et al., 2010; Manganaro et al., 2009). Providing additional information and increasing the accuracy of diagnosis is important for parental counselling. The absence of additional abnormalities in this high risk group provides re-assurance to parents while in non-isolated cases accurate information is important for decision making and management of the pregnancy.

3.1.2 Aims

To evaluate the contribution of MRI in the sonographic diagnosis of fetal ventriculomegaly. To estimate the risk of additional CNS abnormalities in mild and moderate/severe ventriculomegaly.

3.1.3 Cohort

During the study period of November 2007 to May 2011, a total of 492 fetuses were referred from antenatal clinics or from the Fetal Medicine Unit in Queens Charlotte's and Chelsea Hospital for a MRI scan in our department; 110 cases with a sonographic diagnosis of

ventriculomegaly. All ultrasound and referral reports were reviewed and patients were grouped according to the sonography findings, into isolated and non-isolated ventriculomegaly. 66 fetuses were diagnosed on ultrasound with isolated ventriculomegaly and 44 with non-isolated ventriculomegaly. The mean GA at MRI scan was 27.4 weeks and the GA range was 18.5-37.3 weeks.

3.1.4 Detection of additional abnormalities on MRI

In the 66 isolated cases, MRI was in agreement to ultrasound in 54 cases (82%) where no additional abnormalities were detected and MRI confirmed the presence of isolated ventriculomegaly. MRI detected additional findings to those on ultrasound in 12 cases (18%). Abnormalities are summarised in Table 11 and included cerebellar haemorrhage, basal ganglia abnormality, agenesis of the corpus callosum, corpus callosum hypoplasia, cerebellar infarction, cerebellar structural abnormalities, subependymal heterotopia, abnormal white matter signal intensity, decreased white matter volume, cortical abnormalities, delayed cortical folding, presence of large parenchymal cysts. In 5 isolated cases, the maximum atrial diameter measurement was measured to be below 10 mm, however all measurements were ≥9 mm (range 9-9.7 mm) (Table 12).

#	Atrial diameter on US (mm)	Atrial diameter on MRI (mm)	GA at MRI (weeks)	Additional findings detected on MRI
1	11	12	29.6	Subependymal cysts in the caudothalamic notch, abnormal cortex, abnormal signal intensity in white matter
2	n/a	11.9	32.8	Delayed cortical folding, decreased white matter volume, small cerebellum.
3	12.3/13	12.2/12.7	26.1	Widening of the interhemispheric fissure and hypoplasia of the corpus callosum.
4	10.8	10.3	29	Large bilateral cysts within the caudate nuclei and smaller bilateral cysts within the temporal poles and within the posterior inferior lentiform nuclei.
5	9.4/9.6	9.8/10.5	29.8	Abnormal cerebellum fused with no obvious vermis, unusual cavum.
6	12.5	11	29.8	Hypoplastic corpus callosum, asymmetrical cerebellum, small vermis, small pons.
7	13.9	16.9	29.8	Subependymal heterotopia and abnormal cortex.
8	19/15	23.2/15.3	30.1	Dilated 4th ventricle, bilateral cerebellar haemorrhage, obvious abnormal signal intensity within the basal ganglia suggestive of an acute hypoxic ischemic episode.
9	15	14.9	31	Subependymal heterotopia.
10	11.3	11.6/13.5	31.7	Agenesis of the corpus callosum.
11	13/8.9	14.0/10.0	33.4	Small cerebellum with infarction in left cerebellar hemisphere, prominence of 3rd ventricle.
12	moderate	11.6	36.4	Large subependymal cyst within ventricle.

Table 11. Additional findings detected on MRI

MRI detected additional findings to those on ultrasound in 12 cases. In cases 2 and 12 the atrial diameter measurements on ultrasound were not available. Case 7 had progressive ventriculomegaly and the MRI was performed 1 month after the ultrasound.

#	Atrial diameter on US (mm)	Atrial diameter on MRI (mm)	GA at MRI (weeks)
1	11*	9.7	24
2	11	<10	33.1
3	11	9.5	32.3
4	11	9	28.1
5	11.5	9	28.1

Table 12. Discrepancy between ultrasound and MRI on the diagnosis of ventriculomegaly

MRI was performed after referral for ventriculomegaly. Atrial diameter measurements were below 10 mm on MRI in 5 cases. *Case 1 had an atrial diameter of 11 mm on anomaly scan, while on the ultrasound performed the same day as the MRI in a tertiary centre the atrial diameter measurement was 9.1 mm.

In the 44 non-isolated cases, MRI confirmed the CNS abnormalities detected on ultrasound. Abnormalities included, vermis hypoplasia, cerebellar hypoplasia, agenesis of the corpus callosum, dandy walker malformation, choroid cysts, Arnold-chiari malformation and presence of inter-hemispheric cyst. MRI detected further additional abnormalities in 17 of the cases (38.6%) in respect to ultrasound. These abnormalities included cerebellar and vermis hypoplasia, brainstem hypoplasia, thin cortical mantle, agenesis of the corpus callosum, cortical mantle abnormal signal intensity consistent with calcification, white matter abnormalities, cortical abnormalities, vermis rotation, delayed cortical folding, haemorrhage, abnormal corpus callosum, basal ganglia and thalamic abnormalities, cerebellar hemispheres fusion, Arnold-chiari malformation, cerebellar infarction, subependymal heterotopia, abnormal pons, intraventricular haemorrhage, porencephalic cyst and germinal matrix haemorrhage. In 3 cases the maximum atrial diameter measurement was below 10 mm (range 9.5-9.6 mm). MRI demonstrated only increased ventricular size (10-13.5 mm) and no other abnormalities in 5 cases (11.4%) in whom ultrasound had queried the presence of Blakes pouch/enlarged cisterna magna, agenesis of the corpus callosum, midline shift, a vermis defect.

3.1.5 Ventricular size and risk of additional abnormalities

The risk of finding additional CNS abnormalities was assessed with regard to ventricular atrial diameter and subjects were divided into mild (<12 mm) and moderate/severe (>12 mm) groups. As mentioned, according to the ultrasound reports, 66 cases were diagnosed with isolated ventriculomegaly and 44 cases with non-isolated ventriculomegaly. From the 66 isolated cases, 41 had an atrial diameter <12 mm (mild) and 25 cases had an atrial diameter >12mm (moderate/severe). From the non-isolated cases there were 21 mild cases and 23 moderate/severe. The risk of additional findings detected on MRI in mild cases was 12% for isolated cases and 9.5% for non-isolated. The risk of additional findings in moderate/severe cases was 28% for isolated cases and 65% for non-isolated (Figure 52).

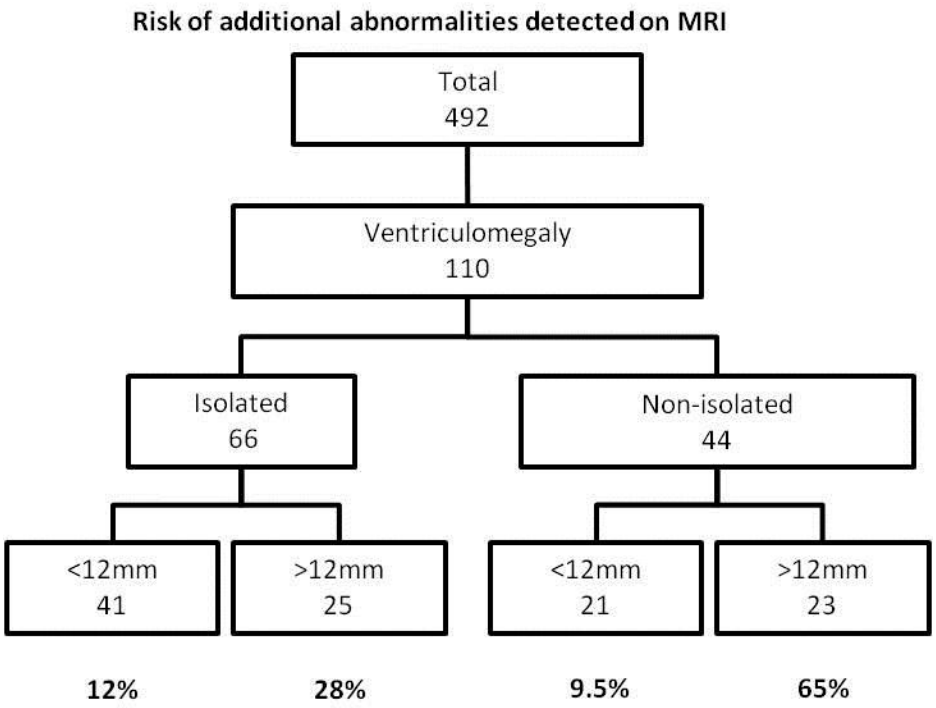


Figure 52. Risk of additional abnormalities detected on MRI

The risk of detecting additional abnormalities is higher in cases with an atrial diameter measurement > 12mm.

3.1.6 Discussion

Our study indicates that MRI is a valuable imaging technique and can provide additional information in respect to ultrasound in fetuses diagnosed with ventriculomegaly.

The risk of detecting additional abnormalities was higher in non-isolated cases compared to isolated cases (38.6% vs 18% respectively) as shown in previous studies (Benacerraf and Shipp, 2007). The risk of additional findings was highest when the atrial diameter exceeded 12 mm and more significant in non-isolated cases, similar to previous studies (Benacerraf and Shipp, 2007; Griffiths et al., 2010; Morris et al., 2007). The lowest risk of finding additional abnormalities was detected in mild ventriculomegaly cases with isolated and non-isolated cases having a similar risk.

However we have not evaluated the clinical significance of the presence of additional abnormalities in order to establish the potential impact of MRI on this group of fetuses. This would include reviewing the details as to whether the additional information provided by MRI altered the parent's decisions towards the progression of the pregnancy and whether it had an effect on clinical management of the pregnancy, delivery and future clinical referrals. In our cohort none of the cases diagnosed with isolated ventriculomegaly on MRI proceeded into termination of pregnancy. In the non-isolated group, 15 women proceeded to termination of pregnancy. Simon et al. (2000) showed that MRI altered pregnancy management in 46% out of 52 cases while Levine et al. (2003) showed that MRI changed the diagnosis in 31.7% of fetuses, altered management in 13.5% of cases and 49.7% in parental counselling. Importantly, in 11.4% of our cases diagnosed with non-isolated ventriculomegaly, MRI radically altered the diagnosis by excluding any additional abnormalities (except of ventriculomegaly) providing great reassurance to parents. All 5 cases continued with the pregnancy. The majority of studies agree that MRI is important in adding information in a diagnosis of ventriculomegaly (Benacerraf and Shipp, 2007; Griffiths et al., 2010; Manganaro et al., 2009) although some studies suggest that a detailed sonographic examination from an experienced technician is equivalent to MRI in the diagnosis of fetal brain abnormalities (Malinger et al., 2004; Monteagudo and Timor-Tritsch, 2009).

In terms of the type of abnormalities detected, our study found similar abnormalities detected on MRI to previous studies (Benacerraf and Shipp, 2007; Manganaro et al., 2009; Mehta and Levine, 2005; Salomon et al., 2006; Valsky et al., 2004). Abnormalities were located in regions known to be challenging to visualise using sonography and included the cortex, white matter, corpus callosum and cerebellum. Subtle abnormalities in these regions may be difficult to visualise on ultrasound. In cases where the ultrasound diagnosis is unclear or an abnormality is suspected, MRI can be used as an alternative imaging modality. In 3 cases with isolated ventriculomegaly and 2 cases with ventriculomegaly and subependymal heterotopia MR images had to be reconstructed to provide non-rotated images for evaluation of cortical folding.

MRI can also further the understanding of the appearance of specific abnormalities and thus improve detection on sonography, as in cases of diagnosis of heterotopia which were exclusively diagnosed on MRI (Benacerraf and Shipp, 2007). In our cohort there were 3 cases diagnosed with subependymal heterotopia. With increased understanding of the appearance of the disorder it may also be detected on sonography. Recent studies have shown that sonography techniques have improved significantly and evaluation of these regions is becoming accessible (Pistorius et al., 2010; Pugash et al., 2012).

After diagnosis of ventriculomegaly has been made, it is important to monitor the size of the lateral ventricles and ascertain whether the dilatation progresses, is stable or the ventricles normalise. Progression of the dilatation is associated with a worse outcome compare to cases where the ventricles remain stable or normalise (Melchiorre et al., 2009a). Ultrasound has an advantage over MRI in monitoring the ventricular size due to the inexpensive and time-efficient nature of the modality.

In conclusion, we have shown in our cohort that the risk of identifying additional abnormalities on MRI after an ultrasound referral of ventriculomegaly, is lowest in mild cases. When the atrial diameter exceeded 12 mm the risk doubled in isolated cases and increased 6-fold in non-isolated cases. Further work can evaluate in which of our cases MRI

had a significant impact on clinical management, diagnosis and parental counselling. While it must be emphasised that ultrasound is the screening modality of choice for the assessment of the fetal brain, MRI is an excellent complimentary imaging technique in the diagnosis of fetal ventriculomegaly and can provide additional information regarding the presence of additional abnormalities.

3.2 Volumetric quantification of intracranial structures from 22-38 weeks of gestation and after birth

3.2.1 Background

The latter half of gestation (20-40 gestational weeks) is a dynamic period during which the human brain shows accelerated growth manifesting in increases in volume, cortical complexity and changes in the molecular and cellular composition of the different cerebral regions. In the first part of this chapter, we assessed the volumetric changes of the different intracranial structures occurring between 22-38 weeks of gestation in a cohort of normal fetuses. Global and regional growth trajectories were constructed and used as a reference to compare with fetuses diagnosed with isolated ventriculomegaly in order to identify potential alterations in brain development. Additionally, in a subpopulation of these fetuses, volumetric analysis of intracranial structures was performed during the neonatal period. We compared neonatal brain structures in infants with antenatally diagnosed ventriculomegaly and normal controls in order to assess changes that persist after birth.

3.2.2 Aims

1. In a cohort of fetuses with antenatally diagnosed isolated ventriculomegaly: To establish whether there is evidence of relative overgrowth and/ or aberrant development in multiple intracranial structures (brain parenchyma, cortex, white matter, basal ganglia, thalami, CSF spaces including 3rd and 4th ventricles, cavum septum pellucidum and vergae and extra-axial space) and how these relate to the volume of the lateral ventricles.
2. To establish whether volumetric changes evident during fetal life persist after birth.

3.2.3 Fetal volumetry

3.2.3.1 Normal control cohort

During the study period of November 2007-August 2011, a total of 89 fetuses had a normal brain appearance on fetal MRI and were enrolled as normal controls. 31 cases were excluded in accordance with our exclusion criteria: poor image quality due to fetal motion (7), positive infection screening (6), declined follow-up post delivery (4), abnormal brain appearance in neonatal MRI (5), birth-weight below the 3rd centile (3), preterm delivery and neurodevelopmental delay (1), pregnancy complications and abnormal brain appearance on neonatal MRI (1), chromosome 22 duplication (1), neurodevelopmental delay and dyskinetic disorder (1), neonatal hypotonia and bradycardia (1), neonatal death related to non-CNS abnormalities (1).

In the remaining 58 fetuses, MRI was performed at a median age of 28.8 weeks GA (range 22.4-38.9 weeks) (Figure 53). Two fetuses were scanned twice during gestation (28.1 and 38.7 gestational weeks). The 58 mothers of included control fetuses consisted of 41 healthy volunteers and 17 women who had had a previous child with a confirmed abnormality or who had had a suspected fetal abnormality on ultrasound excluded on MRI. The number of fetuses and the reason for scanning are summarised in Table 13. In summary, 60 MR scans of 58 fetuses were included in the control group (30 males/30 females).

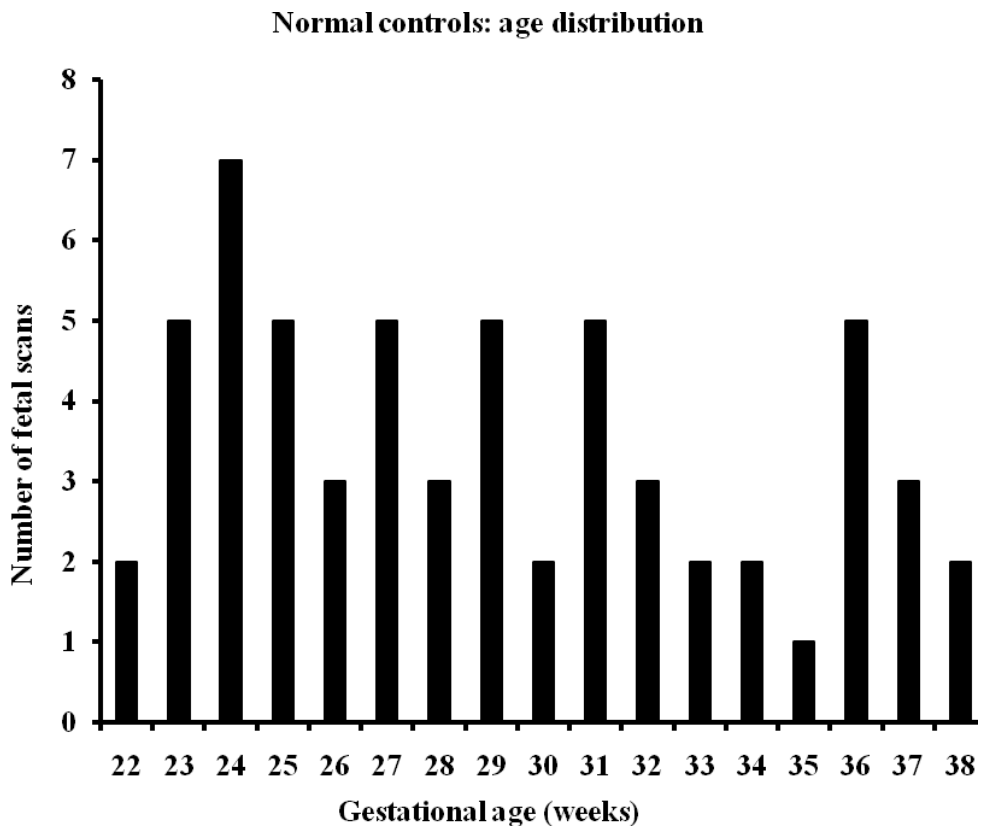


Figure 53. Gestational age distribution histogram in normal controls

Histogram of the gestational age distribution at time of MR scans in normal fetuses (n=60). Fetal gestational age was estimated from a first trimester dating ultrasound scan.

Participants	No. of cases
Healthy volunteers	41
Sibling diagnosed with pontocerebellar hypoplasia	3
Sibling diagnosed with agenesis of the corpus callosum	2
Sibling diagnosed with microcephaly and polymicrogyria	1
Sibling with antenatal brain haemorrhage	1
Sibling diagnosed with Ohtohara syndrome	1
Sibling neonatal death	1
Right side suprarenal cyst	1
Query of agenesis of corpus callosum	1
Ultrasound diagnosis of ventriculomegaly not detected on MRI	1
Resolved cystic hygroma	1
Suspected vertebral abnormality	1
Increased nuchal fold but normal karyotype	1
Diaphragmatic hernia	1
Left side congenital cystic adenomatoid malformation	1
Total	58

Table 13. Normal control cohort participants

The normal control cohort consisted, in the majority, of healthy volunteers, fetuses with a suspected CNS abnormality not present on MRI, fetuses with non-CNS abnormalities. 37 children had a normal neurodevelopmental assessment at either 1 or 2 years of age. 3 children declined follow-up, 14 we were unable to contact and 4 children are currently <12 months.

3.2.3.1.1 Lateral ventricles

The lateral ventricles were assessed using the atrial diameter, the volume of each lateral ventricle and the total (left and right) lateral ventricular volume. Measurements are summarised in Table 14. There was a small increase in the above measurements with increasing GA as indicated by a moderate correlation value in atrial diameter (Spearman's r=0.437, p<0.0001), volume of each lateral ventricle (Spearman's r=0.472, p<0.0001) and total lateral ventricular volume (Spearman's r=0.511, p<0.0001) with GA (Figures 54-56). The total lateral ventricular volume increased at a relative growth rate of 0.03% per gestational week increasing from an average volume of 2.27 cm^3 at week 22 to 4.43 cm^3 at week 38. Increased inter-subject variation however was evident in all ventricular measurements. Atrial diameter and lateral ventricle volume correlated well in both left (Spearman's r=0.742, p<0.0001) and right (Spearman's r=0.752, p<0.0001) lateral ventricles (Figure 57).

Ventricular measurement		**Range**	**Mean**	**SD**	**R^2**
Atrial diameter (mm)	Left	3.5 - 8.9	6.58	1.31	0.3
	Right	3 - 8.1	5.91	1.43	0.13
Lateral ventricle volume (cm^3)	Left	0.56 - 3.83	1.81	0.74	0.221
	Right	0.57 - 3.1	1.51	0.68	0.24
Total lateral ventricular volume (cm^3)		1.43 - 6.7	3.32	1.28	0.28

Table 14. Ventricular measurements using MRI in normal controls

When taking in account brain laterality, left atrial diameter and ventricle volumes were significantly larger compared to the right side with a difference of 20.2% (p=0.008) and 12.5% (p=0.004) respectively. There was no significant difference in atrial diameter (p=0.519), left (p=0.317) or right (p=0.669) lateral ventricle volumes or total lateral ventricular volume (p=0.304) between sexes in the control cohort however males had a trend to larger ventricular measurements. In males, the left lateral ventricle was significantly larger to the right (p=0.008) while in females this difference did not reach significance (p=0.08).

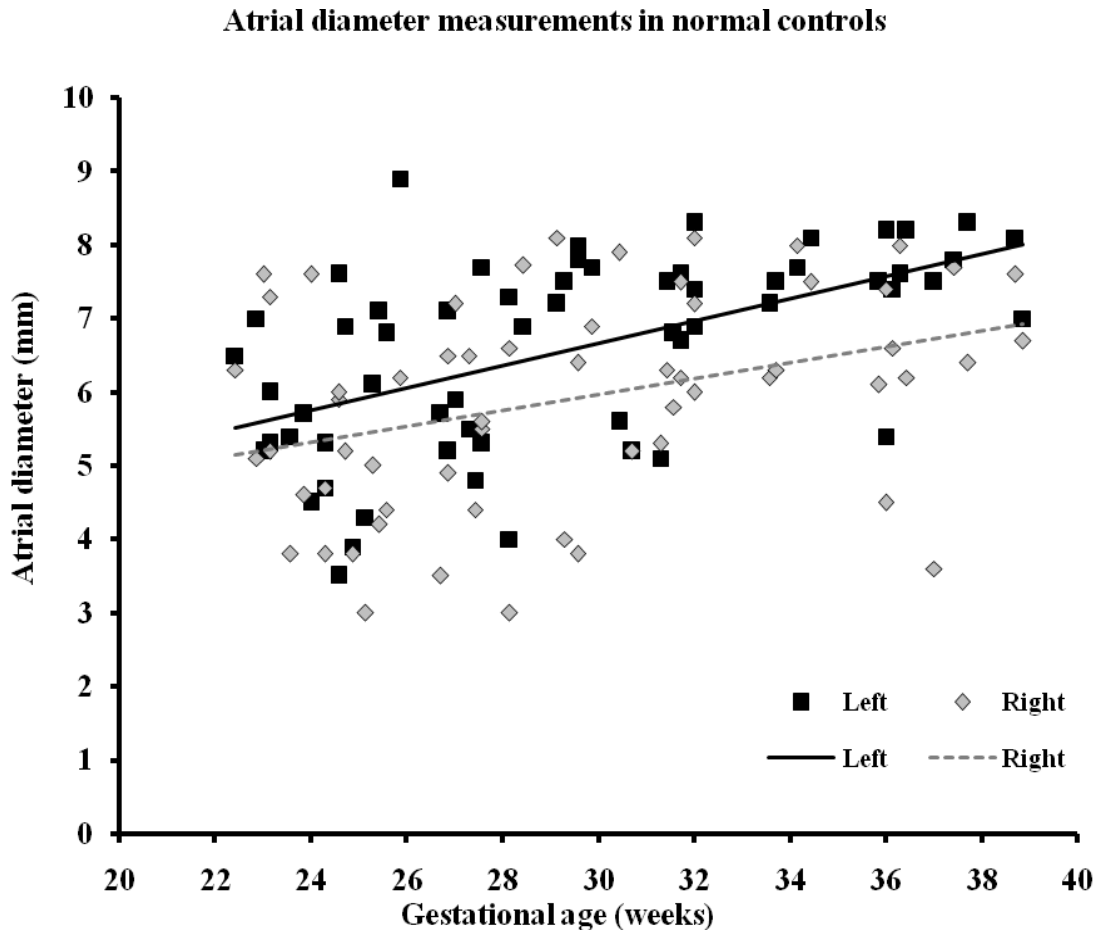


Figure 54. Atrial diameter measurements using MRI in normal controls

There was a small increase in atrial diameter with increasing GA (Spearman's r=0.437, p<0.0001). Atrial diameter of the left lateral ventricle was significantly larger compared to the right (p=0.008).

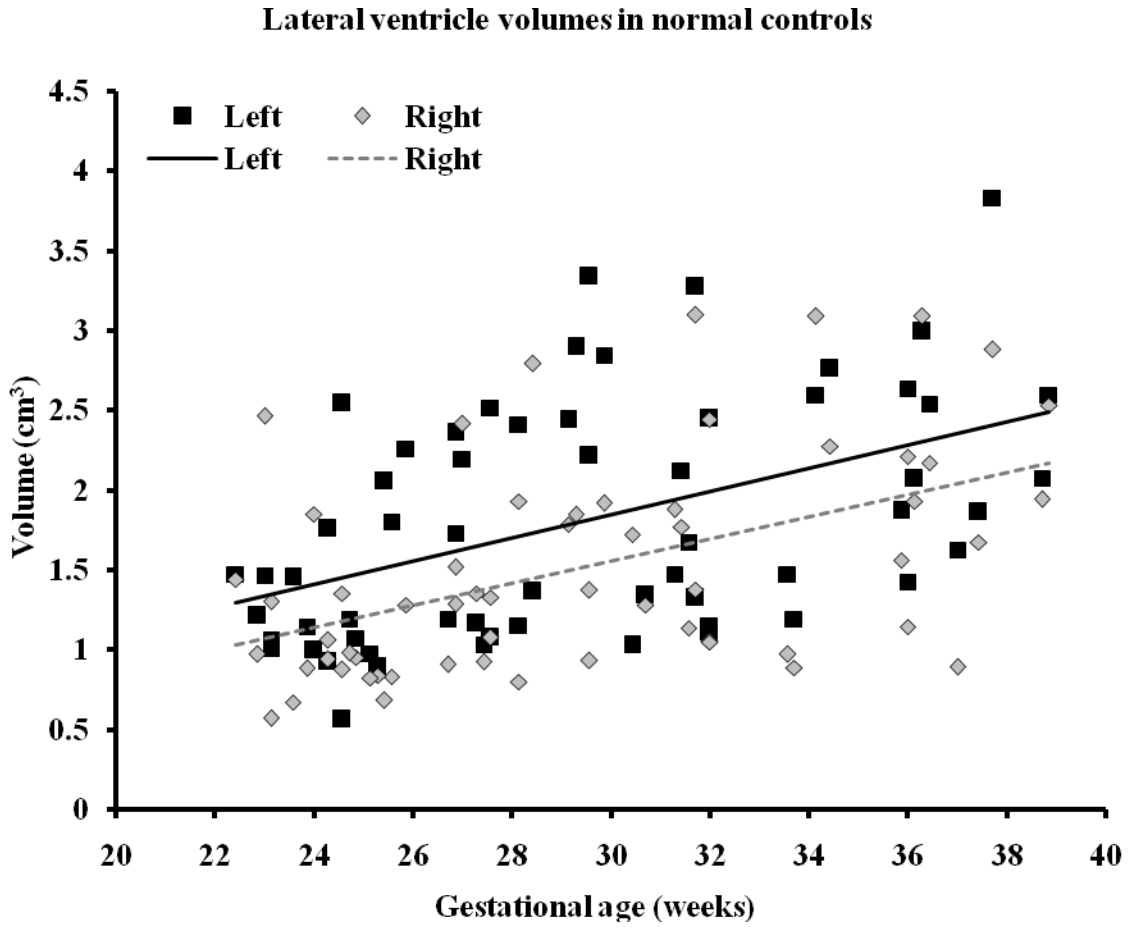


Figure 55. Lateral ventricle volumes in normal controls

There was a small increase in the volume of each lateral ventricle with increasing GA (Spearman's r=0.472, p<0.0001) The volume of the left lateral ventricle was significantly larger compared to the right (p=0.004).

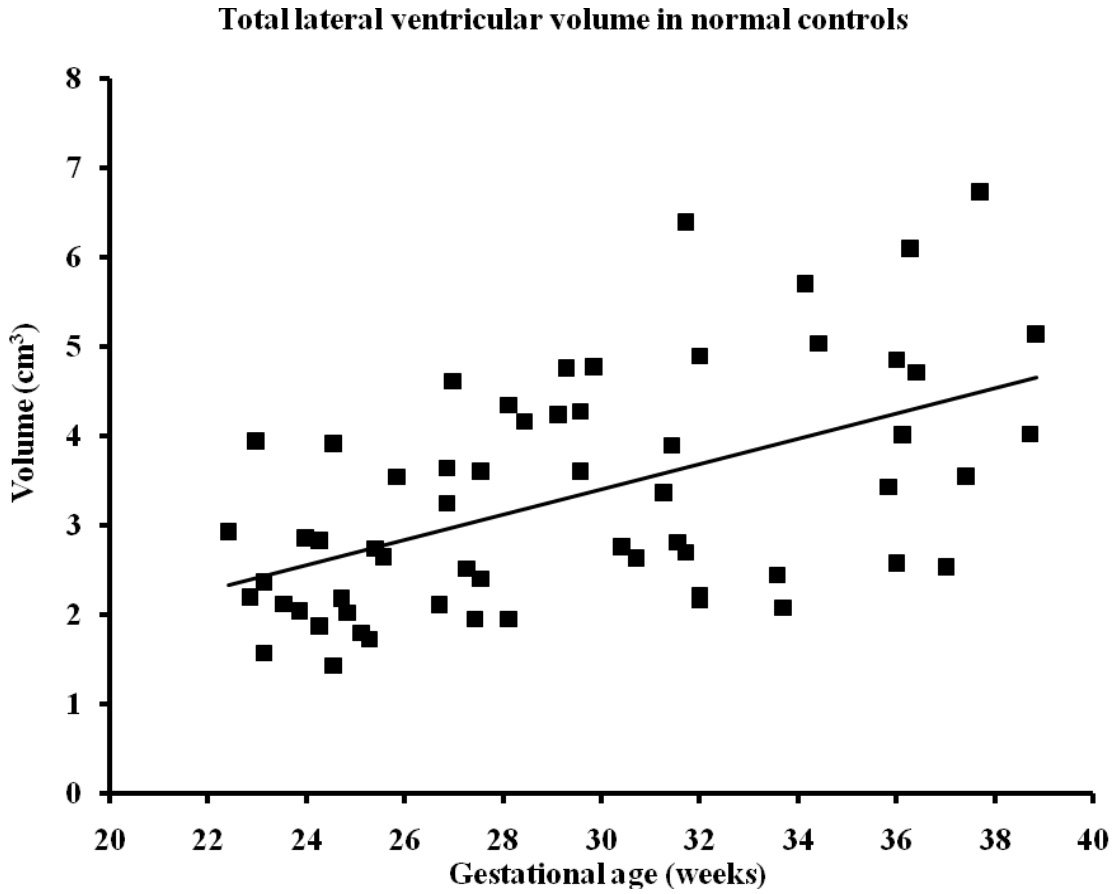


Figure 56. Total lateral ventricular volume in normal controls

There was a small increase in total lateral ventricular volume with increasing GA in normal controls (Spearman's r=0.511, p<0.0001).

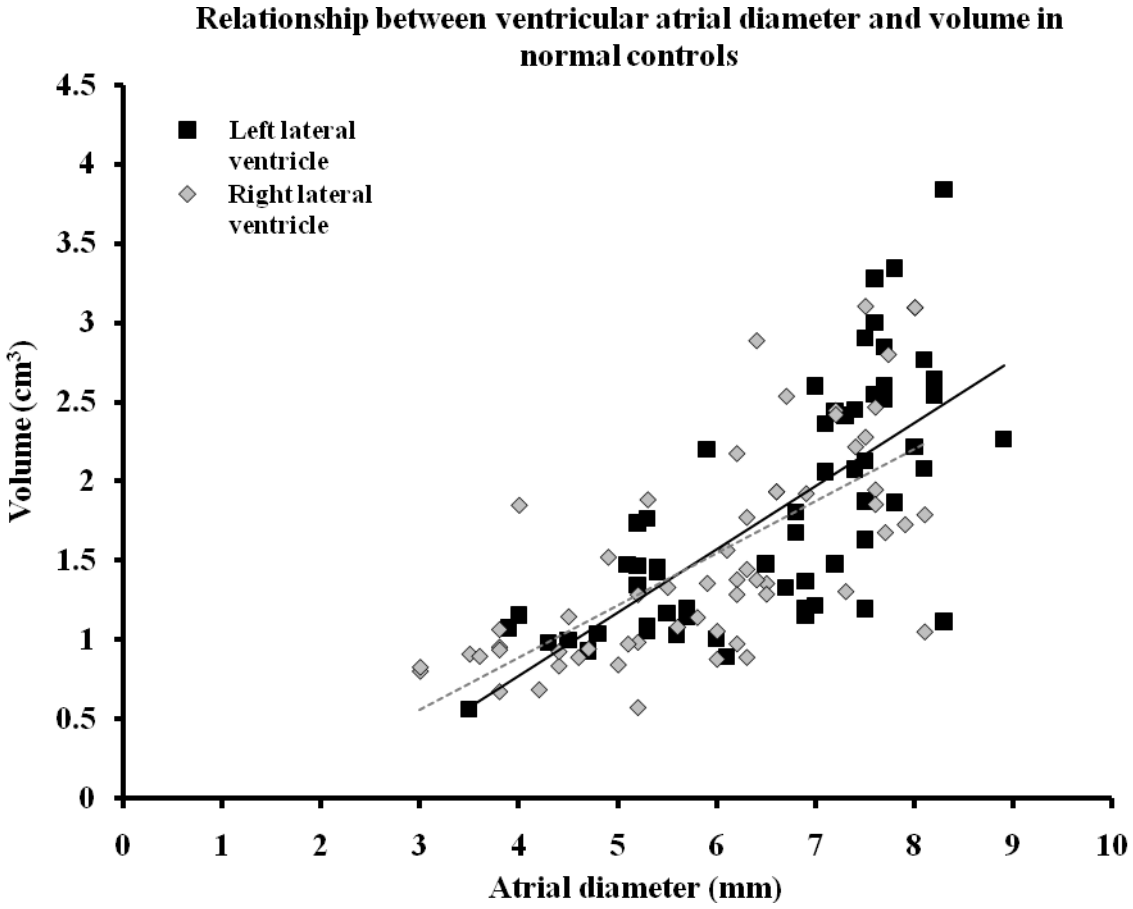


Figure 57. Relationship between ventricular atrial diameter and volume in normal controls

Atrial diameter and lateral ventricle volume correlated well in both left (Spearman's r=0.742, p<0.0001) and right (Spearman's r=0.752, p<0.0001) lateral ventricles.

3.2.3.1.2 Third and fourth ventricles

The third and fourth ventricles increased in volume with increasing GA (Spearman's r=0.927, p<0.0001; Spearman's r=0.733, p<0.0001 respectively) (Figures 58 and 59) (Table 18). There was a small increase in the volume of the third ventricle at a relative growth rate of 0.098% per week increasing from 0.074 cm^3 at week 22 to 0.359 cm^3 at week 38. Similarly, there was a small increase in the volume of the fourth ventricle during GA at a relative growth rate of 0.129% per week, increasing from 0.013 cm^3 at week 22 to 0.093 cm^3 at week 38. The goodness of fit for both third and fourth ventricles was similar for linear and exponential curves. There was no significant difference in the volume of the third (p=0.891) or fourth (p=0.155) ventricles between sexes, however males had a trend for larger volumes.

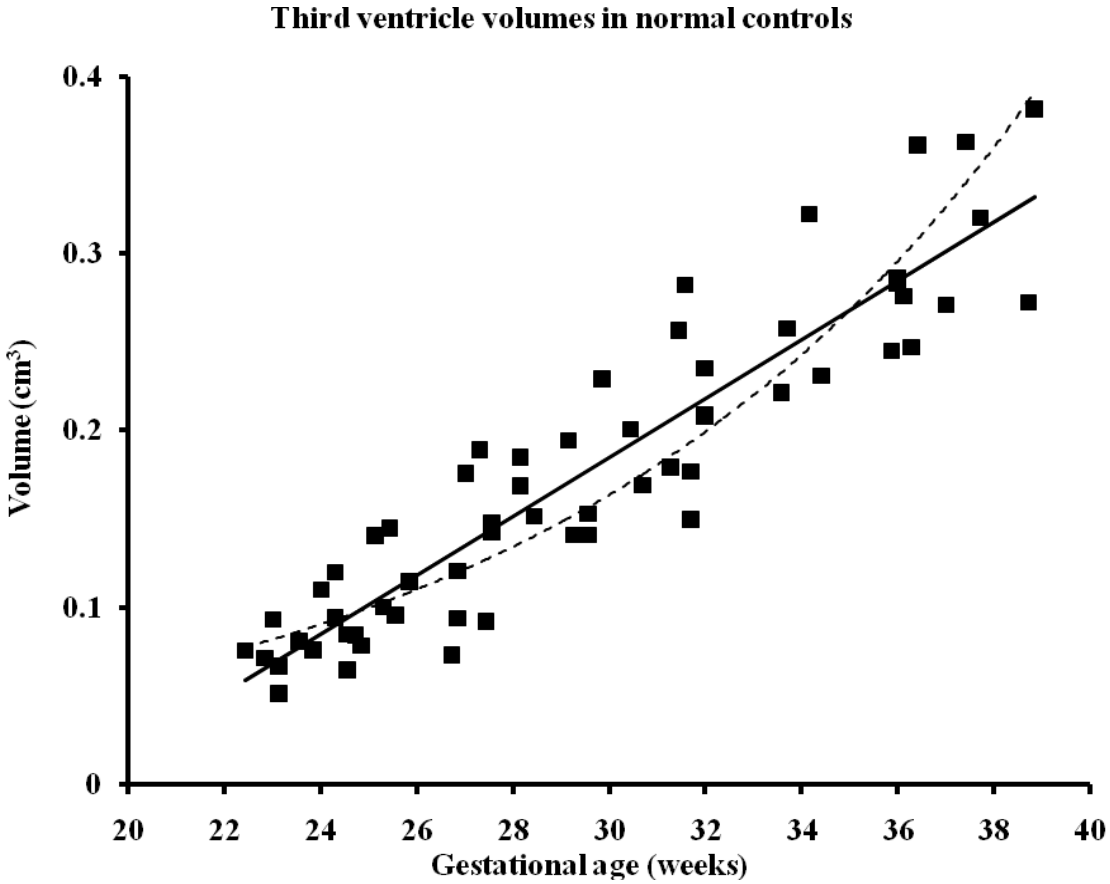


Figure 58. Third ventricle volumes in normal controls

The volume of the third ventricle increased with increasing GA in normal controls (Spearman's r=0.927, p<0.0001). Lines of best fit; stippled line=exponential, solid line=linear.

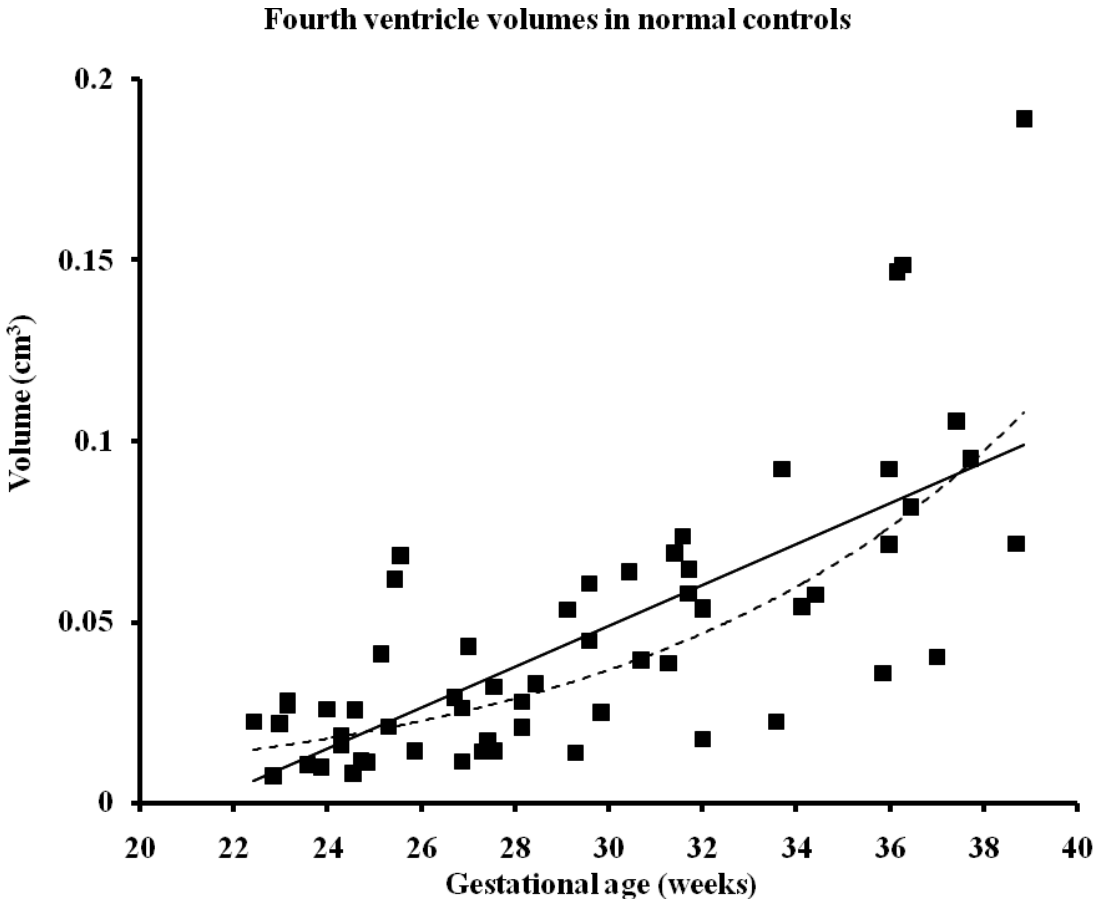


Figure 59. Fourth ventricle volume in normal controls

The volume of the fourth ventricle increased with increasing GA in normal controls (Spearman's r=0.733, p<0.0001). Lines of best fit; stippled line=exponential, solid line=linear.

3.2.3.1.3 Extra-cerebral CSF

Extra-cerebral CSF increased with GA at a relative growth rate of 0.06% per week from 22.68 cm^3 at week 22 cm^3 to 98.52 at week 38 (Spearman's r=0.873, p<0.0001) (Figure 60) (Table 18). While exponential and linear curves fitted the data similarly, the curve that best represented that data was a 2nd order polynomial due to the large scatter of data after 30 gestational weeks. This may indicate a decrease in the growth rate after 31 weeks.

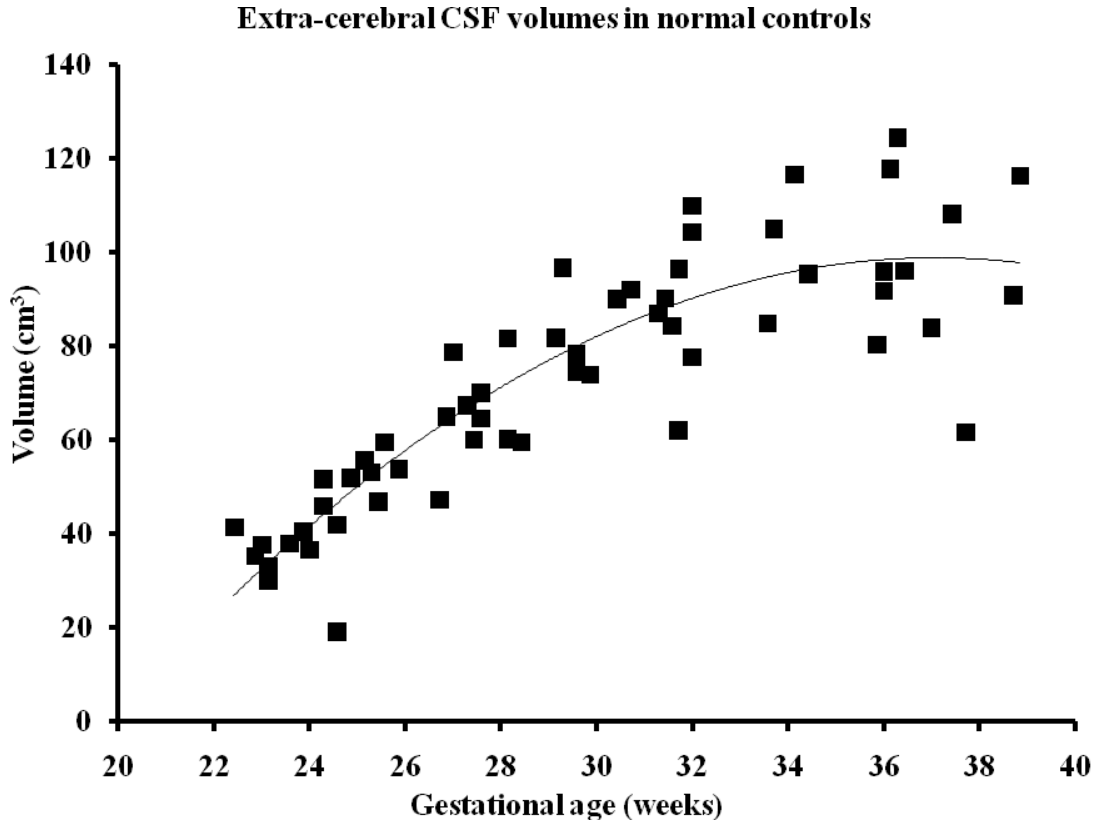


Figure 60. Extra-cerebral CSF volumes in normal controls

Extra-cerebral CSF volumes increased with GA with increasing GA in normal controls (Spearman's r=0.873, p<0.0001). A reduction in growth rate was evident at around 30-32 gestational weeks.

3.2.3.1.4 Cavum septum pellucidum

The CSP was assessed using the CSP width and the volume of the structure. Due to the large scatter of the measurements the data for the width and volume are presented in two ways, the raw measurements against GA (Figures 61 and 63) and also the mean measurement for each gestational week against GA (Figures 62 and 64). CSP width increased from 3.5 mm at week 22, peaked at 6.8 mm at 30 weeks and then decreased. A 2^{nd} order polynomial was fitted in the data to illustrate the complex changes occurring during gestation. Similarly the volume of the CSP increased between 22 to 30 weeks when it reached a peak and decreased from 30 to 38 weeks. CSP width and volume correlated well (Spearman's $r=0.777$, $p<0.0001$), there was however a large scatter of the data.

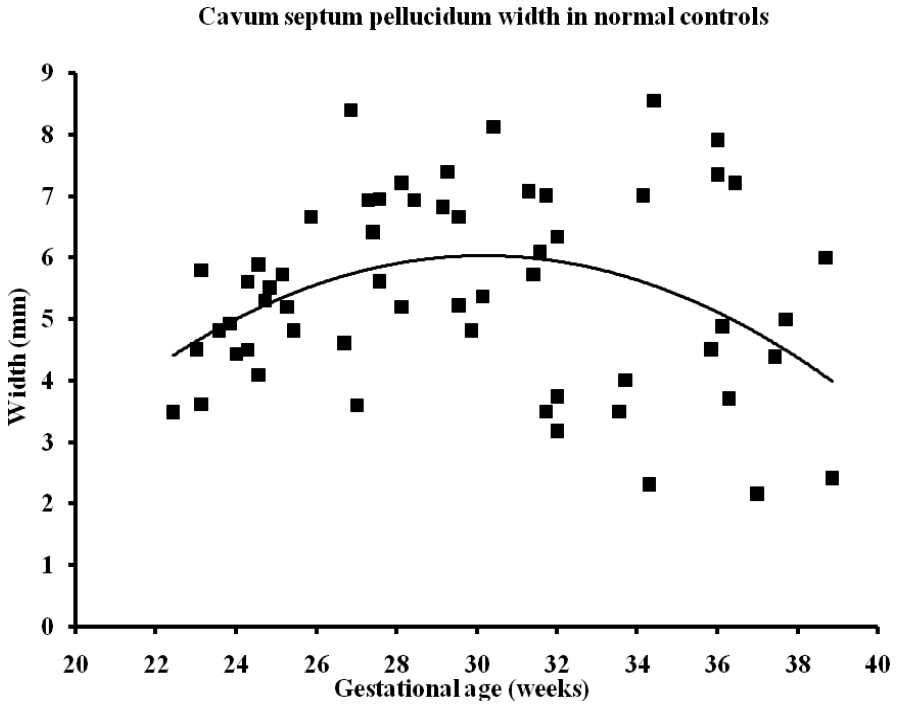


Figure 61. Cavum septum pellucidum width in normal controls

Cavum septum pellucidum width increased from week 22 until week 30 and decreased thereafter.

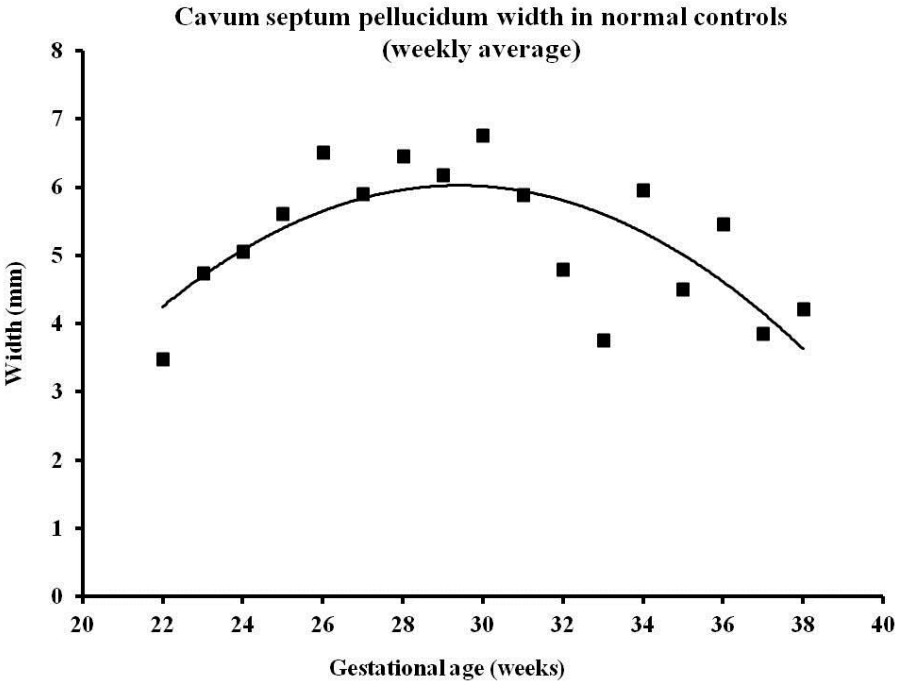


Figure 62. Cavum septum pellucidum width in normal controls (weekly average)

Cavum septum pellucidum width increased from week 22 until week 30 and decreased thereafter. Data are presented as a mean per gestational week.

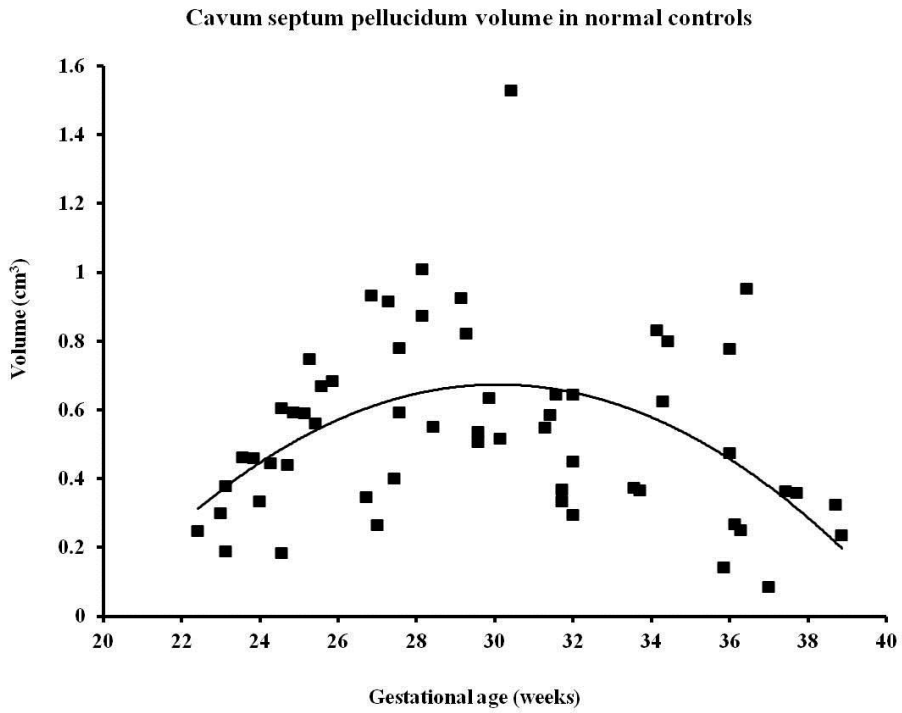


Figure 63. Cavum septum pellucidum volume in normal controls

Cavum septum pellucidum volume increased from week 22 until week 30 and decreased thereafter.

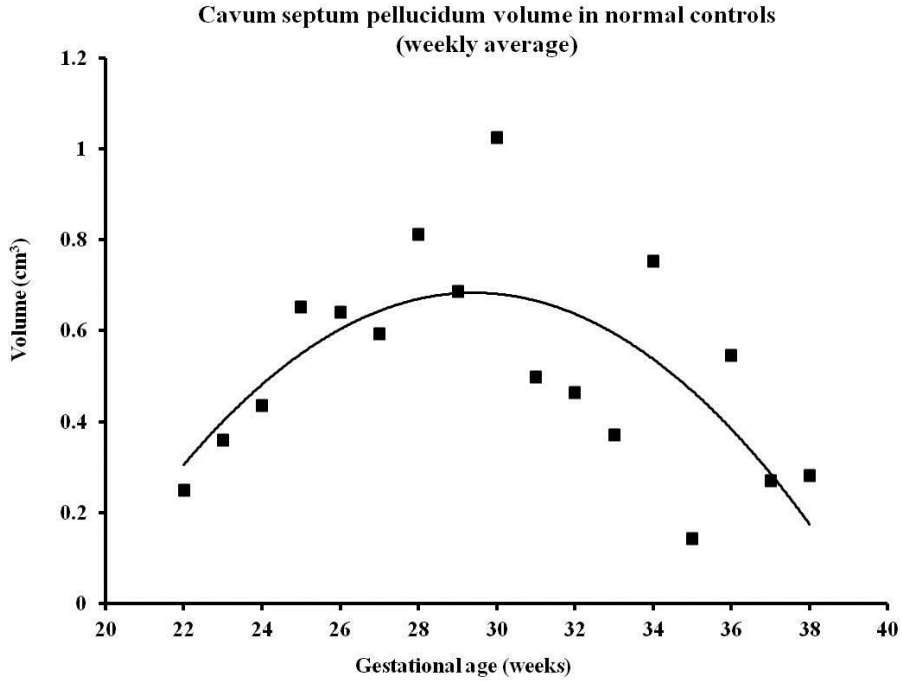


Figure 64. Cavum septum pellucidum volume in normal controls (weekly average)

Cavum septum pellucidum volume increased from week 22 until week 30 and decreased thereafter. Data are presented as a mean per gestational week.

3.2.3.1.5 Supratentorial brain tissue

Total supratentorial brain tissue volume increased at a relative growth rate of 11.65% with increasing GA, from 53.67 cm^3 at week 22 to 346.7 cm^3 at week 38 (Spearman's r=0.976, p<0.0001) (Figure 65) (Table 18). The goodness of fit was similar for linear and exponential curves, however an exponential curve was selected as it visually appears to represent the data better. There was no difference in the volumes of left and right hemispheres (p=0.966) (Figure 66). There was no significant difference between total brain tissue volume (p=0.817) between the sexes although males had a trend for larger brain tissue volumes.

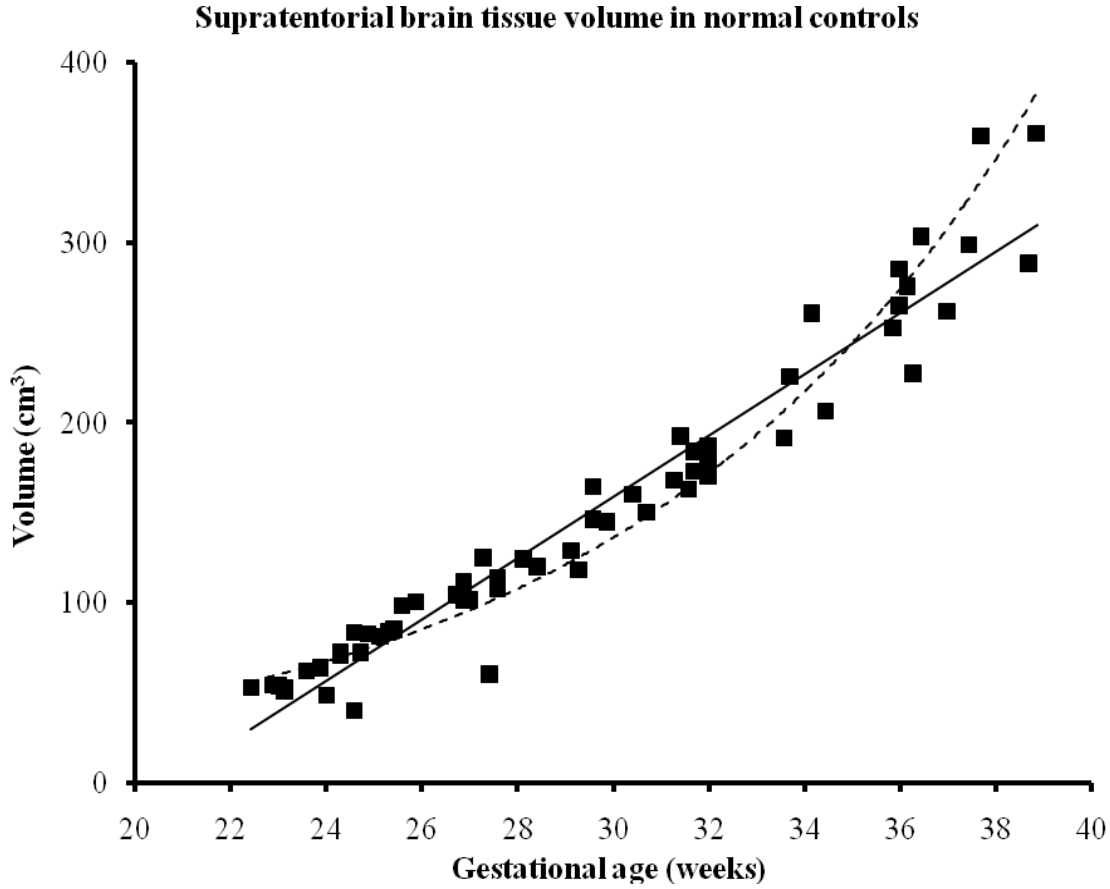


Figure 65. Supratentorial brain tissue volume in normal controls

Supratentorial brain tissue increased with increasing GA in normal controls (Spearman's r=0.976, p<0.0001). Lines of best fit; stippled line=exponential, solid line=linear.

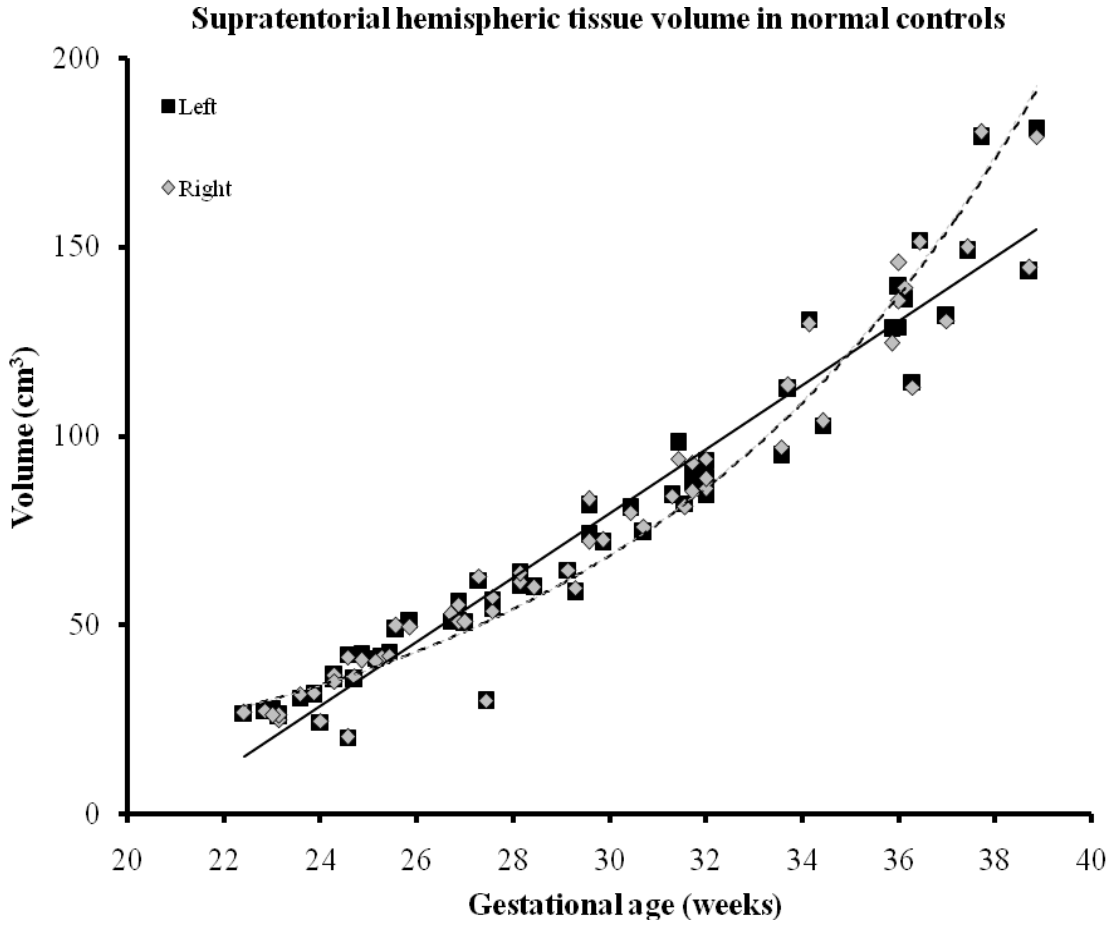


Figure 66. Supratentorial hemispheric brain tissue in normal controls

There was no difference in the volumes of left and right hemispheres (p=0.966). Lines of best fit; stippled line=exponential, solid line=linear.

3.2.3.1.6 Cortical gray matter

Total cortical gray matter volume was measured in 19 control cases (GA range 22.42-37.17 weeks, mean 29.29 weeks). There was no significant difference between the complete group (n=60) and this subgroup in GA, brain volume or ventricular volume. Between 22 and 37 weeks GA there was an exponential increase in cortical gray matter volume at a relative growth rate of 13.2% (Figure 67). Cortical volume increased from 11.01 cm^3 at week 22 to 105.58 cm^3 at week 38 (Spearman's r=0.873, p<0.0001) (Table 18).

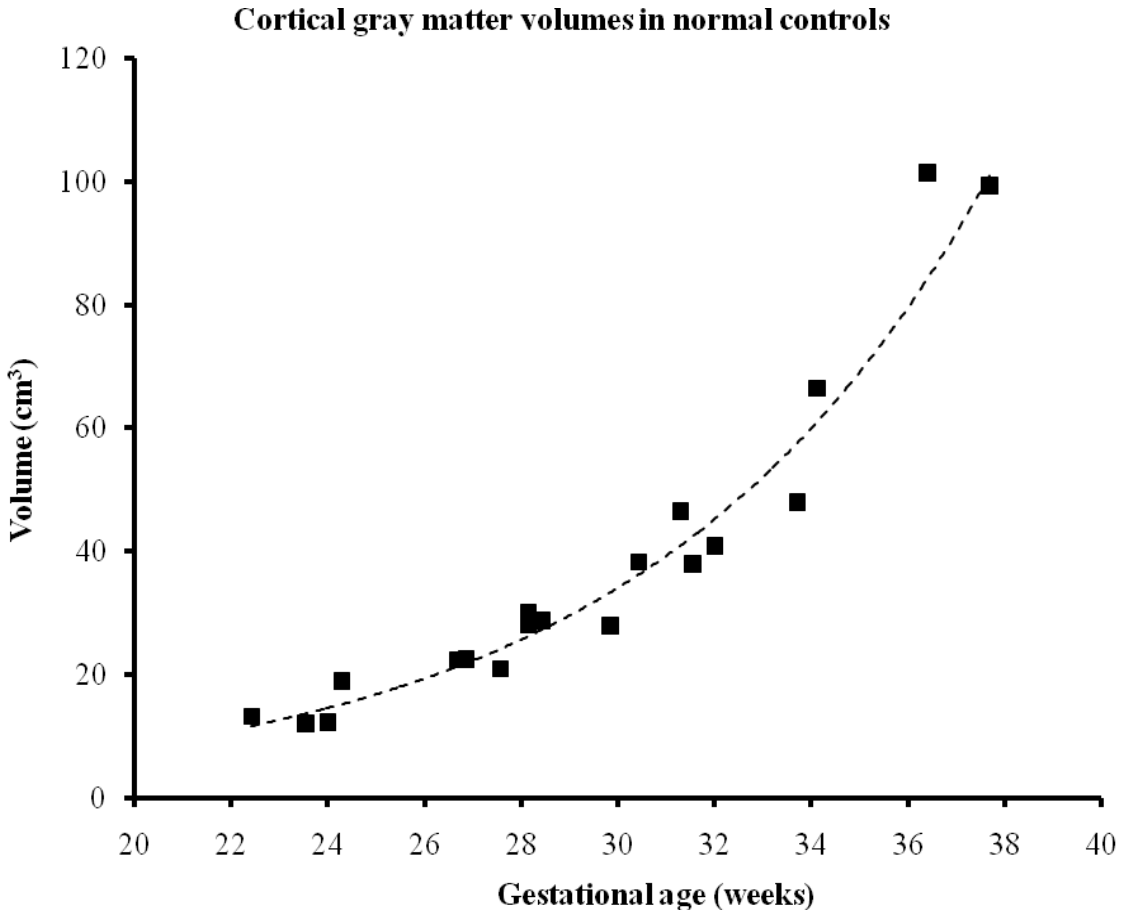


Figure 67. Cortical gray matter volume in normal controls

Cortical volumes increased with increasing GA (Spearman's r=0.873, p<0.0001).

3.2.3.1.7 Thalami

Total thalamic volumes were measured in the subgroup of 19 normal control cases. Thalamic volume increased exponentially (Spearman's r=0.993, p<0.0001) at a relative growth rate of 13.13% per week from 0.88 cm^3 at week 22 to 7.52 cm^3 at week 38 (Figure 68) (Table 18).

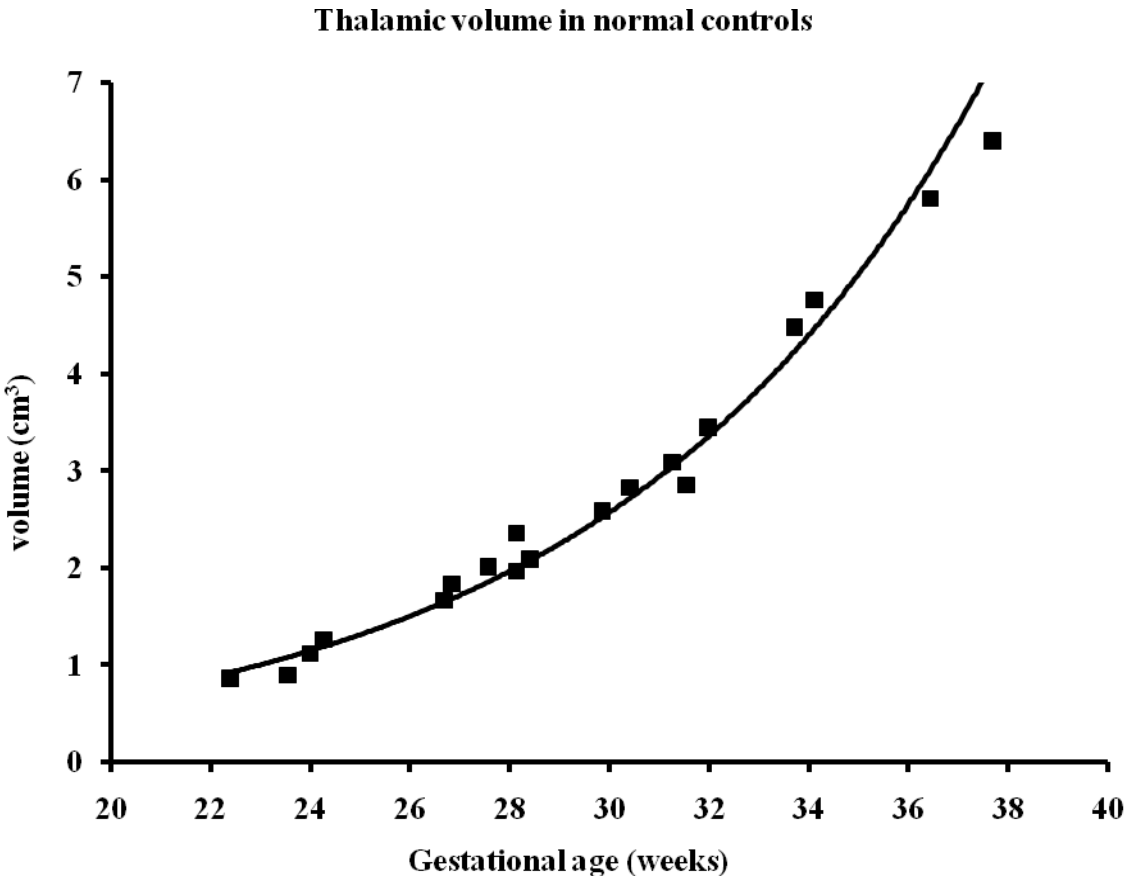


Figure 68. Thalamic volume in normal controls

Thalamic volumes increased with increasing GA (Spearman's r=0.993, p<0.0001).

3.2.3.1.8 Basal ganglia

The volumes of the basal ganglia were measured in 19 normal controls cases. The volumes increased with increasing GA at a relative growth rate of 11.39 cm^3 per week from 1.17 cm^3 at week 22 to 7.94 cm^3 at week 38 (Spearman's r=0.975, r<0.0001) (Figure 69) (Table 18). Both linear and exponential curves fitted the data.

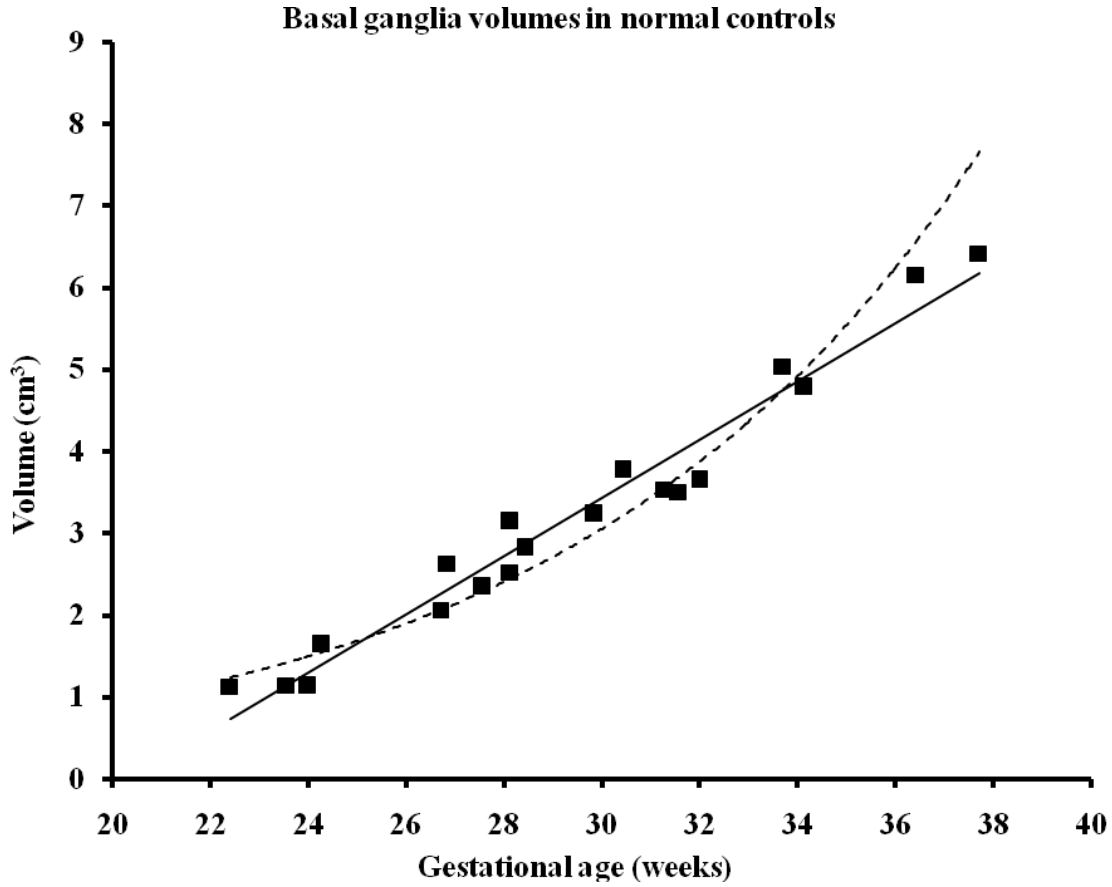


Figure 69. Basal ganglia volumes in normal controls

Basal ganglia volumes increased with increasing GA in normal controls (Spearman's r=0.975, r<0.0001). Lines of best fit; stippled line=exponential, solid line=linear.

3.2.3.1.9 White matter

White matter volumes were calculated in 19 controls cases by subtracting thalamic, cortical and basal ganglia volumes from the supratentorial brain tissue measurements. White matter volumes increased at a relative growth rate of 12.27% per week from 39.15 cm^3 at week 22 to 272.25 cm^3 at week 38 (Spearman's r=0.986, p<0.0001) (Figure 70) (Table 18).

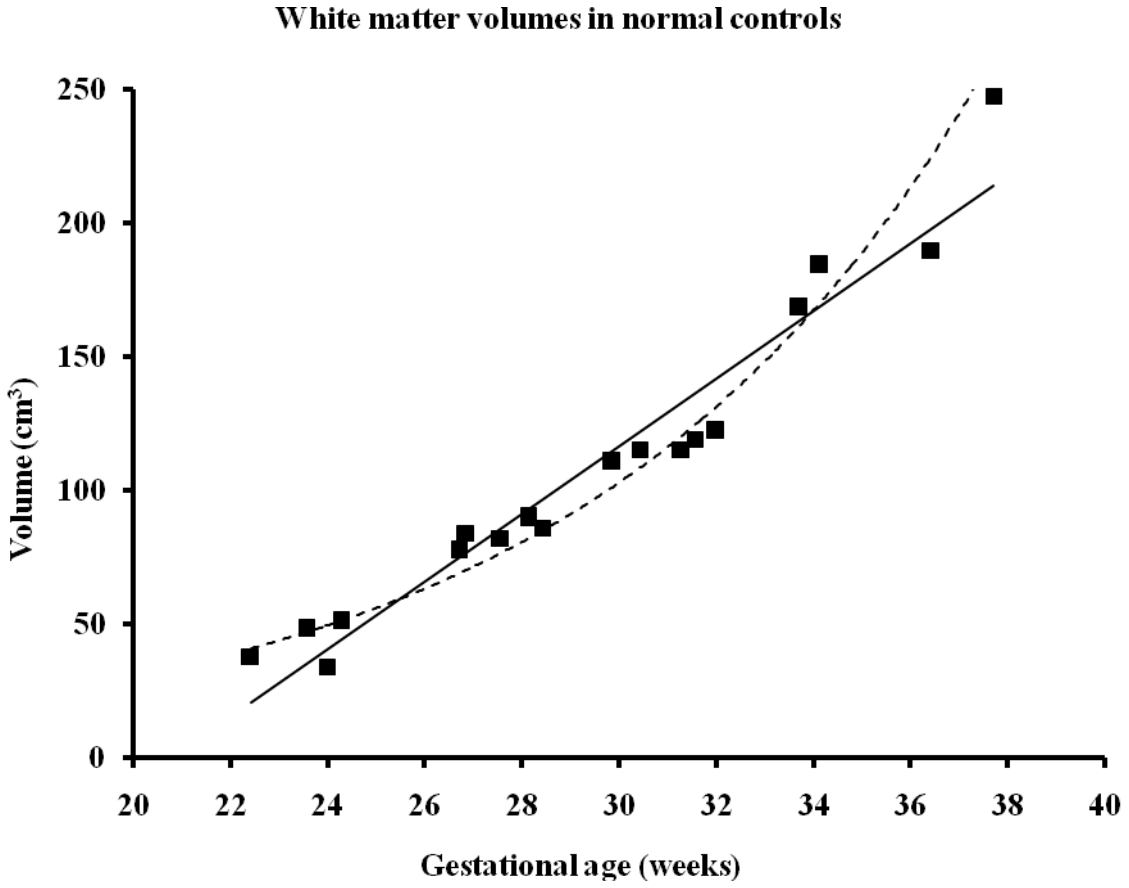


Figure 70. White matter volumes in normal controls

White matter volumes in increased with increasing GA in normal controls (Spearman's r=0.986, p<0.0001). Lines of best fit; stippled line=exponential, solid line=linear.

3.2.3.1.10 Correlations of ventricular size and intracranial measurements

There was a significant correlation between total lateral ventricular volume and supratentorial brain parenchyma (Spearman's r=0.54, p<0.0001), extra-cerebral CSF (Spearman's r=0.499, p<0.0001), third ventricle (Spearman's r=0.549, p<0.0001), fourth ventricle (Spearman's r=0.457, p<0.0001) and thalamic volumes (Spearman's r=0.389, p=0.05) (Table 15). There was no significant correlation between total lateral ventricular volume and cortex (Spearman's r=0.305, p=0.102), basal ganglia (Spearman's r=0.289, p=0.115) and white matter volumes (Spearman's r=0.34, p=0.077).

Correlation of total ventricular size and intracranial measurements

	Total Brain Tissue	Cortex	Basal Ganglia	Thalami	White Matter	Third Ventricle	Fourth Ventricle	Extra-cerebral CSF
Normal controls (Spearman's r)	0.54**	0.305	0.289	0.389*	0.34	0.549**	0.457**	0.499**

Table 15. Correlation of total ventricular volume and intracranial volumetric measurements

Spearman r values are presented for each relationship. * p<0.05 and p>0.0001 ** = p<0.0001

3.2.3.2 Comparison of volumetric results of ventriculomegaly cohort to normal controls

Isolated ventriculomegaly cohort

A total of 114 fetuses presented with an ultrasound diagnosis of dilatation of the lateral ventricles during the study period. Out of the 114 cases, 66 were excluded according to the exclusion criteria: additional brain abnormalities (56), IUGR (1), positive infection/chromosomal abnormality (8), maternal drug abuse (1). None of the included cases had signs consistent with obstruction to CSF flow or atrophy of the surrounding tissue on fetal MRI. 48 fetuses (34 males/14 females) were diagnosed with isolated ventriculomegaly with a 2D atrial diameter range of 10-17 mm. In 33 of the 48 fetuses the ventriculomegaly was unilateral (other atrial diameter <10 mm). 15 fetuses were scanned twice and one was scanned three times during gestation. In summary 65 MR scans of 48 cases were included in the isolated ventriculomegaly group (median GA 30 weeks, range 22-37.3 weeks, 48 males/17 females) (Figure 71). There was no significant difference in GA between groups (p=0.685).

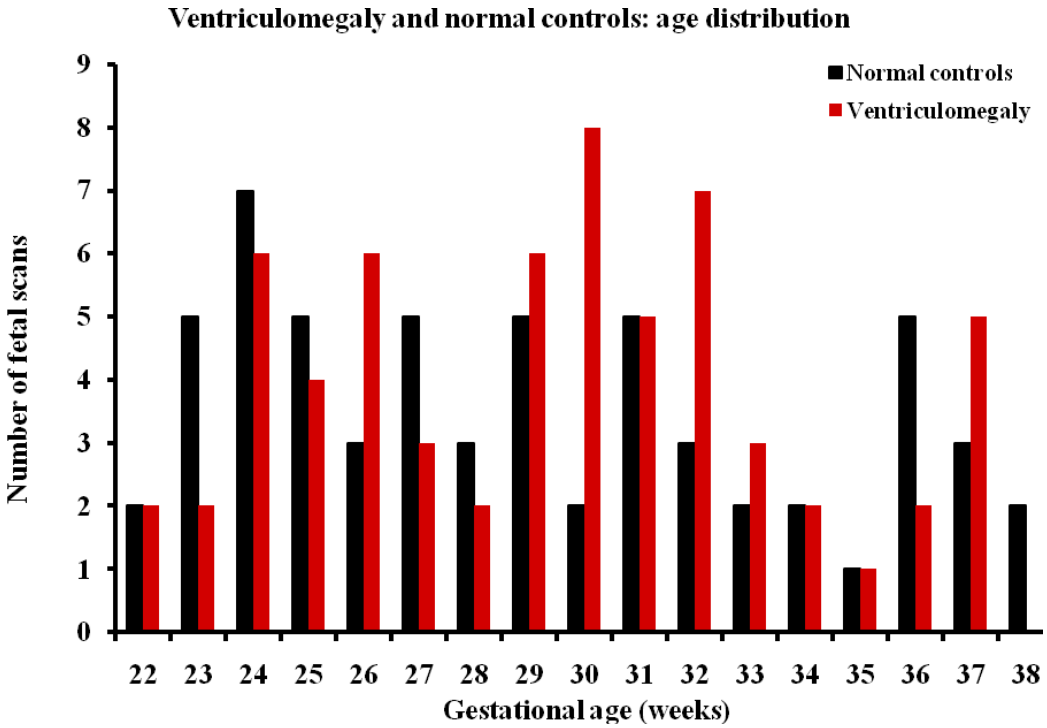


Figure 71. Gestational age distribution histogram in ventriculomegaly and normal controls

Histogram of the age distribution of fetal MR scans in the ventriculomegaly (red) and normal control (black) groups. Fetal gestational age was estimated from a first trimester dating ultrasound scan.

3.2.3.2.1 Lateral ventricles

Measurements of atrial diameter, lateral ventricle volume and total lateral ventricular volume are summarised in Table 16. There was no correlation between atrial diameter and GA (Spearman's r=0.086, p=0.249). There was a moderate correlation between lateral ventricle volume (Spearman's r=0.502, p<0.0001) and total (left and right) lateral ventricular volume (Spearman's r=0.481, p<0.0001) with GA.

It should be noted that lateral ventricle in the ventriculomegaly cohort refers to the largest ventricle in both unilateral and bilateral cases. In bilateral cases, only the largest ventricle was used for the analysis.

Ventricular measurement	**Range**	**Mean**	**SD**	**R^2**
Atrial diameter (mm)	10 - 17	11.99	1.46	0.036
Lateral ventricle volume (cm^3)	3.6 - 12.2	6.34	1.89	0.238
Total lateral ventricular volume (cm^3)	5.06 - 21.39	10.09	3.27	0.174

Table 16. Ventricular measurements in ventriculomegaly

All fetuses with an ultrasound diagnosis of ventriculomegaly had significantly larger lateral ventricle volumes than controls (295%, p<0.0001) (Figure 72). The range of ventricular measurements were 10-16.5 mm (atrial diameter), 3.6-12.2 cm^3 (lateral ventricle volume) and 5.06-21.39 cm^3 (total lateral ventricular volume). One control case of a 37^{+5} week old fetus had a normal atrial diameter of 8.3 mm but a lateral ventricle volume of 3.8 cm^3, within the lower ventriculomegaly range. With the exception of this control case, the volume of the each lateral ventricle between the two groups did not overlap. Conclusions regarding the evolution of the dilatation cannot be drawn for the ventriculomegaly group as each case had a different ventricular size.

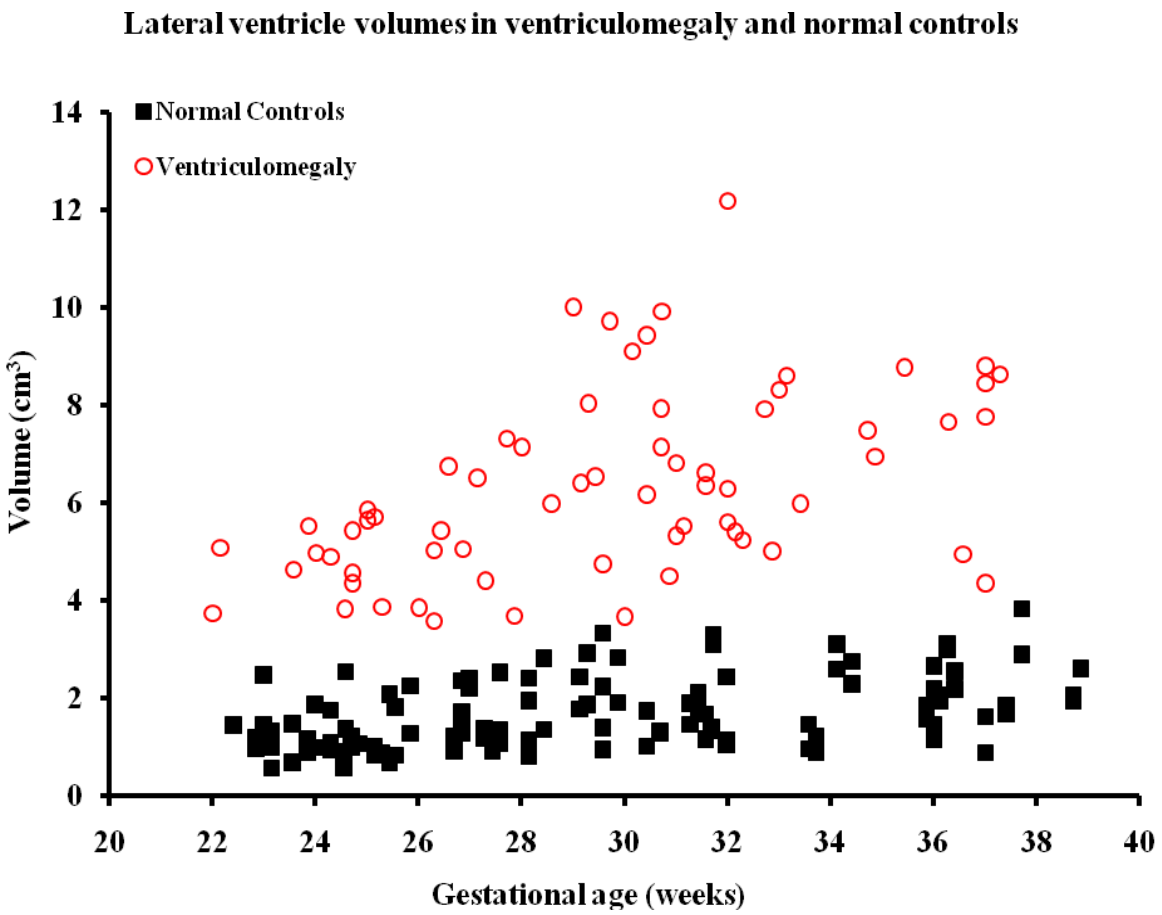


Figure 72. Lateral ventricle volume in controls and ventriculomegaly from 22 to 38 weeks

Fetuses with ventriculomegaly had significantly larger lateral ventricle volumes than controls (295%, $p<0.0001$). The ventriculomegaly data shown depict the large ventricle in the unilateral cases and the largest ventricle only of the bilateral cases.

Atrial diameter and lateral ventricle volume correlated well in the ventriculomegaly cohort (Spearman's=0.56, p<0.0001) (Figure 73) in both the ventricle with an atrial diameter >10 mm and the ventricle <10 mm.

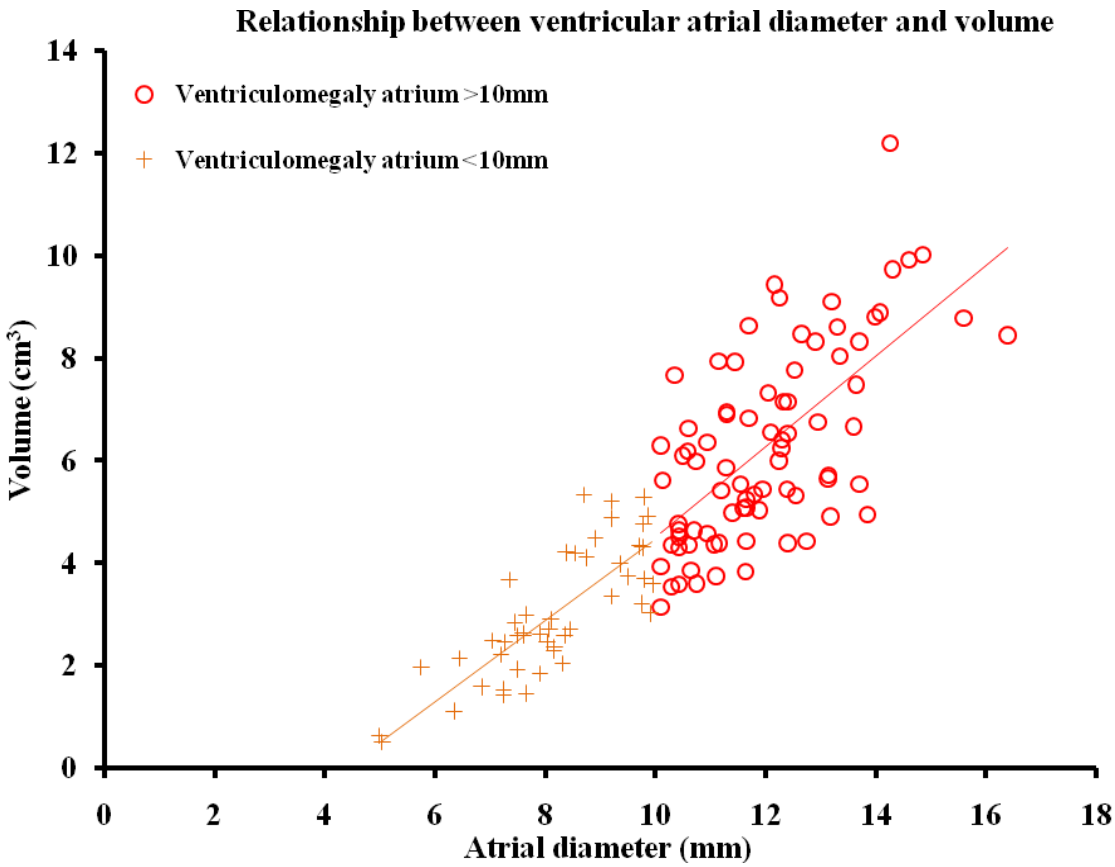


Figure 73. Relationship between ventricular atrial diameter and volume in ventriculomegaly

Atrial diameter and volume correlated well (r=0.6, p<0.00001) in the ventriculomegaly cohort. The ventriculomegaly atrium >10mm data shown depict the large ventricle of the unilateral cases and both enlarged ventricles in bilateral cases. The ventriculomegaly atrium <10mm represent the non-ventriculomegaly side in the unilateral cases.

33 of the 48 cases had unilateral ventriculomegaly as classified by an atrial diameter above 10 mm in only one ventricle. While the volumes of the lateral ventricles did not overlap between the groups, in 17 out of 33 unilateral cases, the volume of the normal sized lateral ventricle (atrial diameter < 10 mm) was in the ventriculomegaly range (atrial diameter mean 9.2 mm, range 7.4-9.9 mm; lateral ventricle volume mean 4.4 cm^3, range 3.6-5.3 cm^3) (Figure 74).

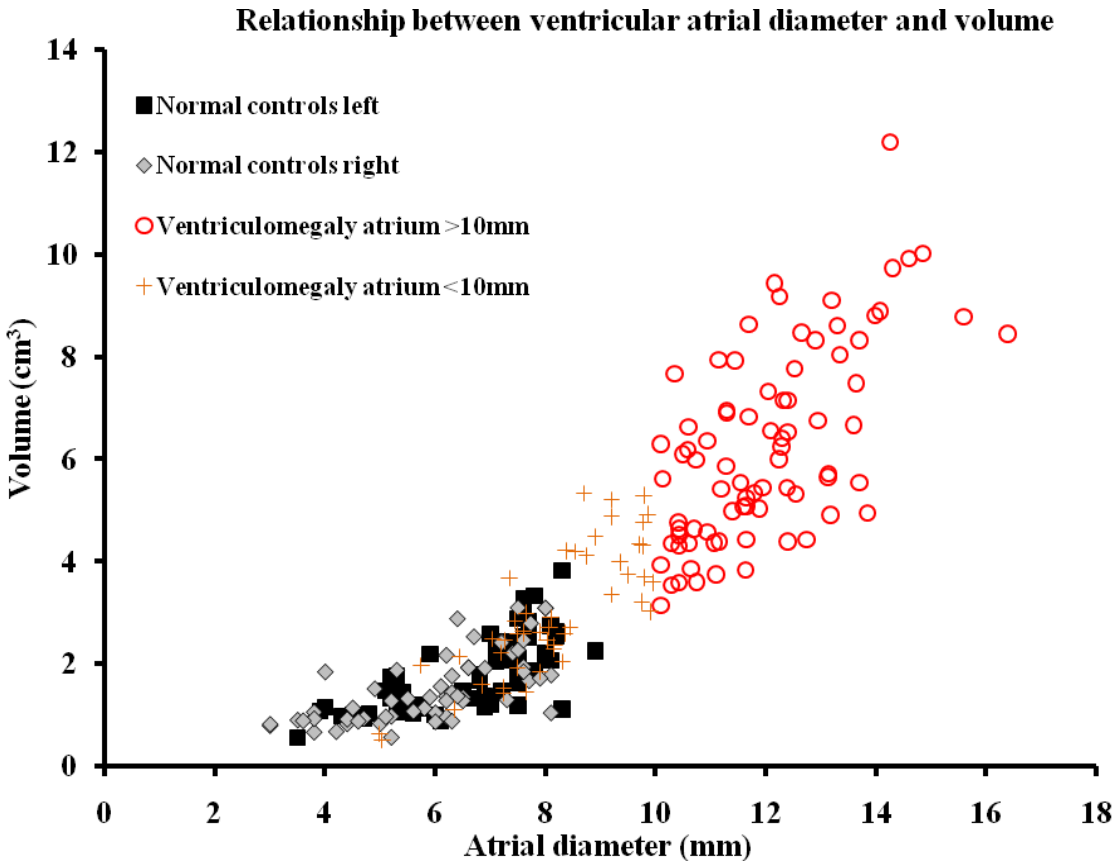


Figure 74. Relationship between ventricular atrial diameter and volume in controls and ventriculomegaly

Atrial diameter and volume correlated well in normal controls ($r=0.754$, $p<0.00001$) and ventriculomegaly ($r=0.6$, $p<0.00001$). The ventriculomegaly atrium> 10mm data shown depict the large ventricle of the unilateral cases and both enlarged ventricles of bilateral cases.

3.2.3.2.2 Third and fourth ventricles

The third and fourth ventricles increased with GA at a relative growth rate of 0.088% and 0.119% per week respectively (Table 18). The volume of the third and fourth ventricles were larger in the ventriculomegaly group compared to controls by 23% ($p<0.0001$) and 75% ($p<0.0001$) respectively at a GA of 29.6 weeks (Figures 75 and 76) (Table 18).

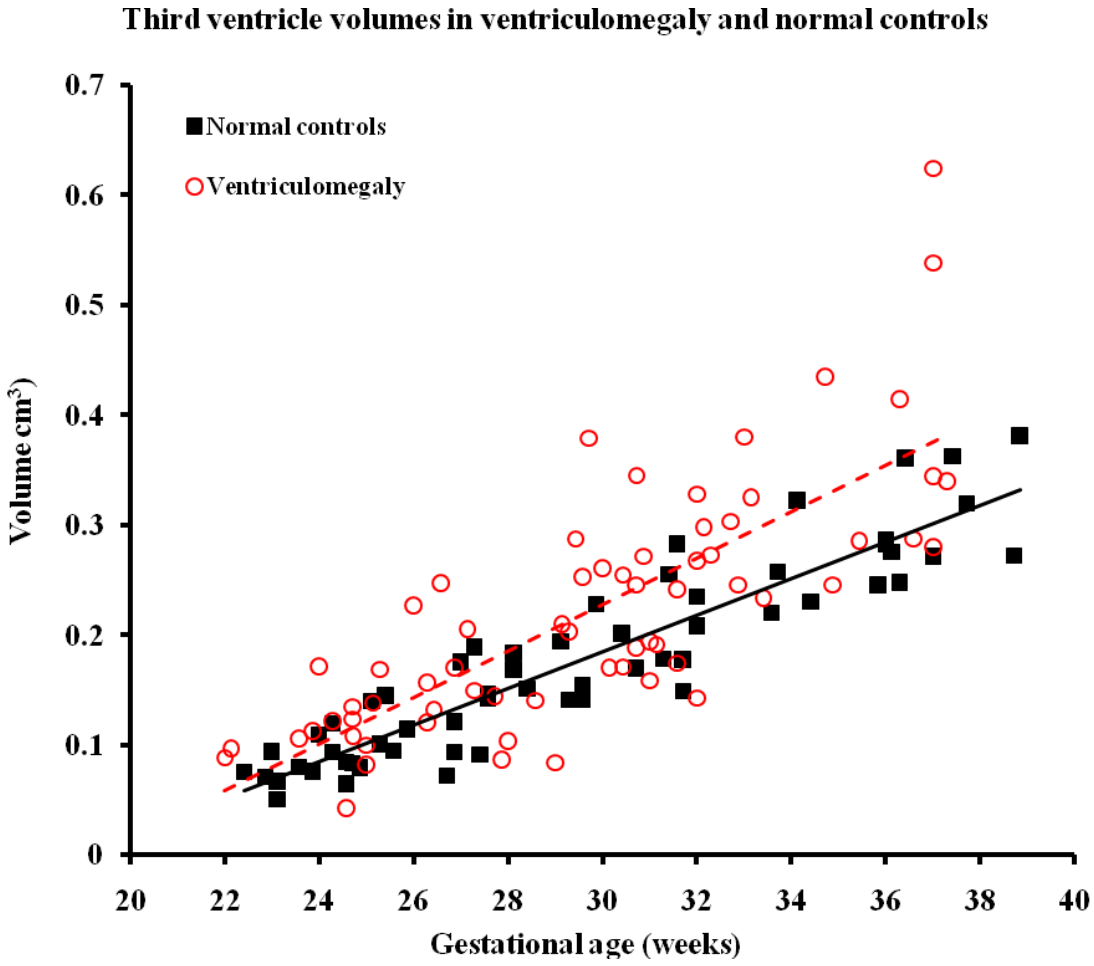


Figure 75. Third ventricle volumes in ventriculomegaly and normal controls

The volume of the third ventricle was significantly larger in the ventriculomegaly cohort by 23% ($p<0.0001$).

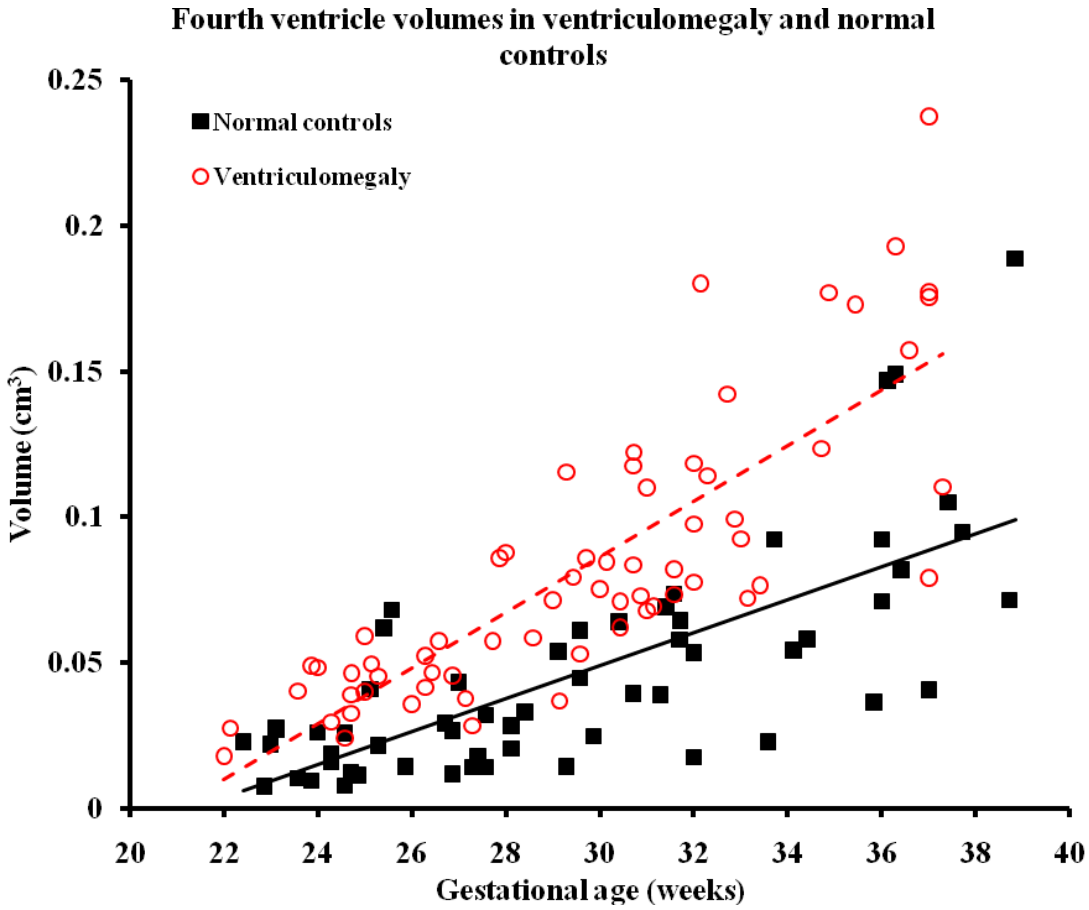


Figure 76. Fourth ventricle volumes in ventriculomegaly and normal controls

The volume of the fourth ventricle was significantly larger in the ventriculomegaly cohort by 75% ($p<0.0001$).

3.2.3.2.3 Extra-cerebral CSF

Extra-cerebral CSF volumes increased with GA in the ventriculomegaly group at a relative growth rate of 0.1% per week. The ventriculomegaly cohort had significantly larger extra-cerebral CSF volumes compared to the control group by 14% (p=0.002) at week 29.6 (Figure 77) (Table 18).

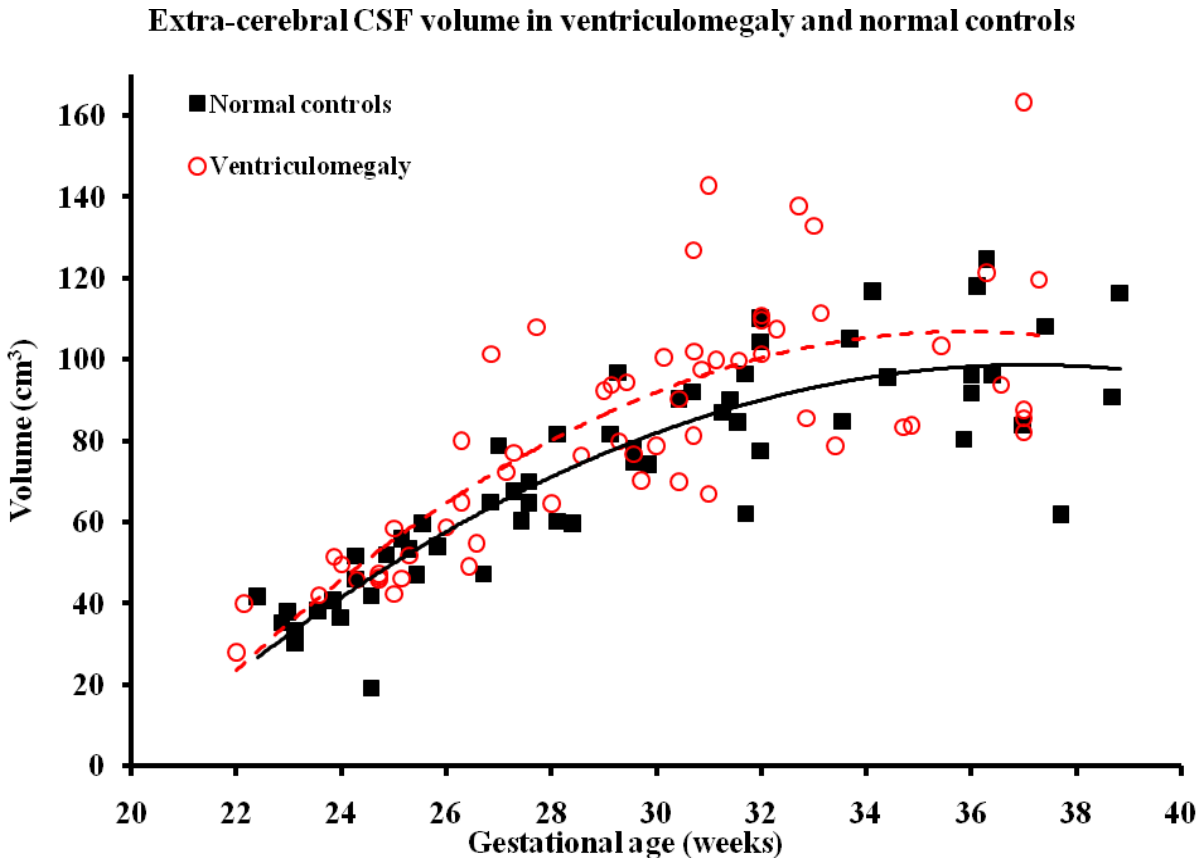


Figure 77. Extra-cerebral CSF volumes in ventriculomegaly and normal controls

Extra-cerebral CSF volume was significantly larger in the ventriculomegaly cohort by 14% (p=0.014).

3.2.3.2.4 Cavum septum pellucidum

In the ventriculomegaly group, CSP width increased from 3.5 mm at week 22, peaked at 6.7 mm at 30 weeks and then decreased. The majority of cava showed absence or thinning of the cavum vergae after 30 weeks. There was no significant difference in CSP width between the ventriculomegaly and control cohorts (p=0.377) (Figure 78). There was large variation between 34 to 36 weeks due to the limited number of cases. The volume of the CSP increased between 22 to 30 weeks when it reached a peak and then decreased from 30 to 38 weeks (Figure 79), showing a similar evolution pattern to the control cohort. CSP volume was significantly larger in the ventriculomegaly group (p=0.014). CSP width and volume correlated well (Pearson's r=0.77, p<0.0001), there was however a large scatter in the data (Figure 8). The anterior pellucidum was more prominent in the ventriculomegaly group.

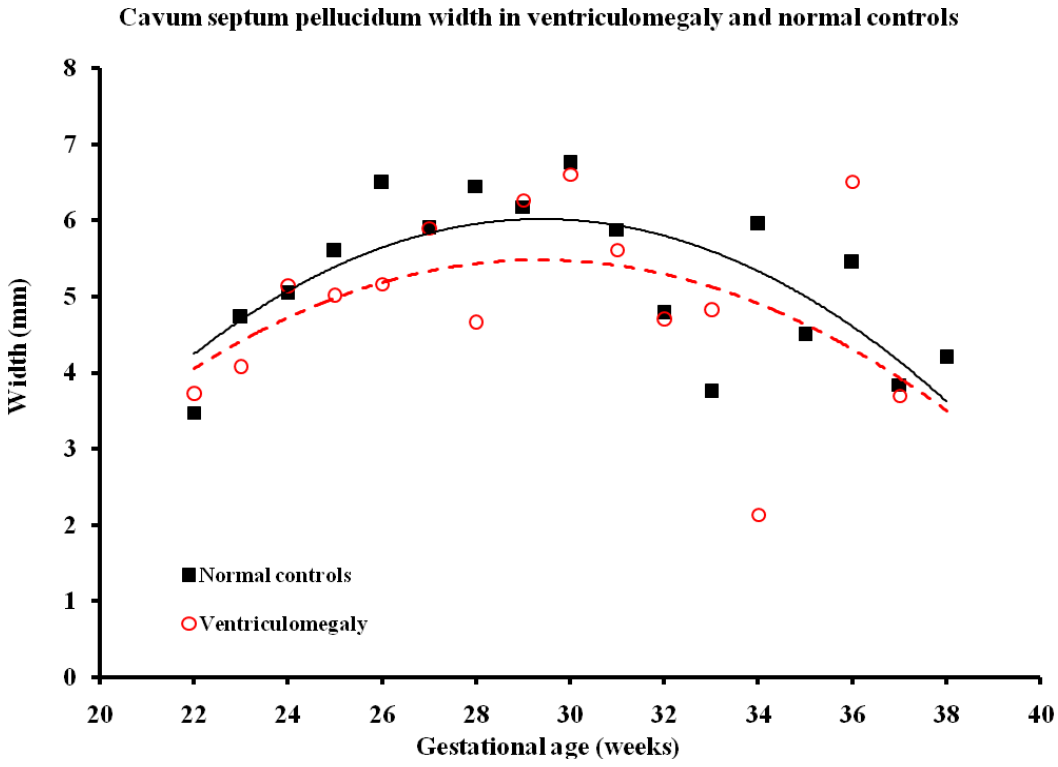


Figure 78. Cavum septum pellucidum width in ventriculomegaly and normal controls

There was no difference in CSP width between the ventriculomegaly and normal control cohort.

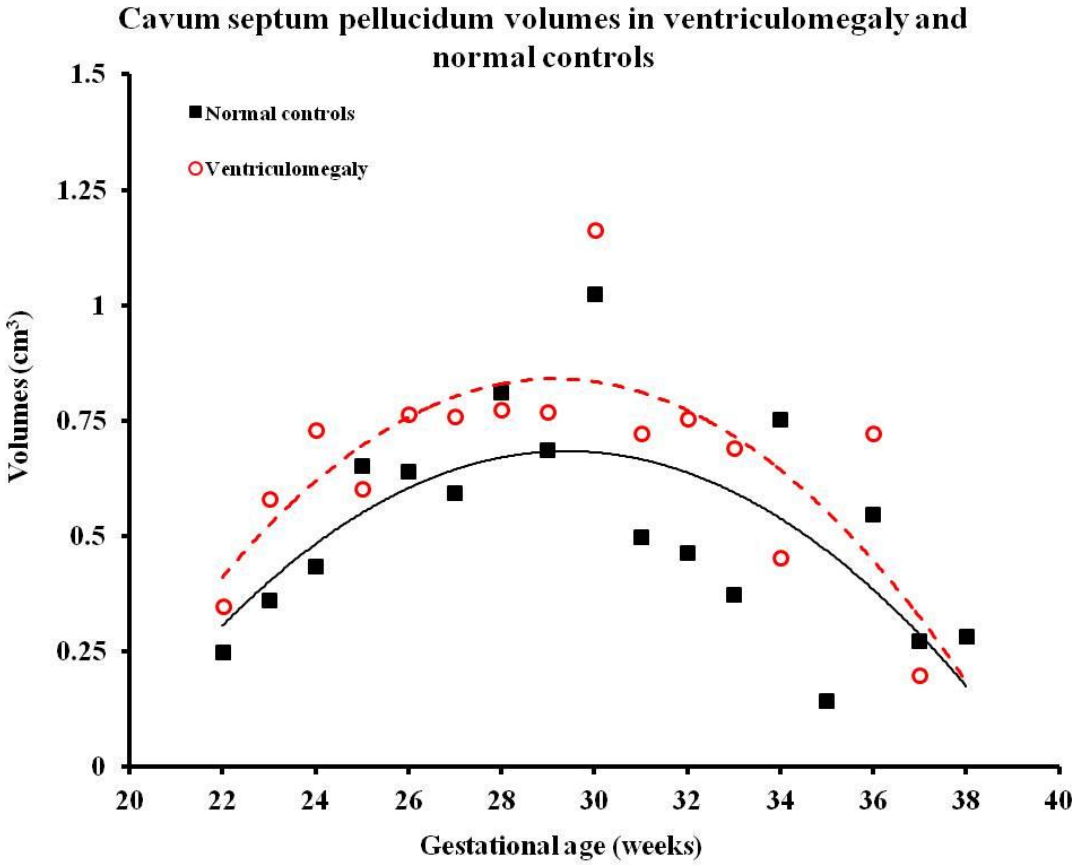


Figure 79. Cavum septum pellucidum volumes in ventriculomegaly and normal controls

CSP volumes were larger in the ventriculomegaly cohort compares to the normal control cohort (p=0.014).

3.2.3.2.5 Supratentorial brain tissue

Total supratentorial brain parenchyma volume increased exponentially with increasing GA at a relative growth rate of 11.65% and 12.35% in the control and ventriculomegaly groups respectively, which was not statistically different (Table 18). When comparing between groups and correcting for GA, fetuses with isolated ventriculomegaly had significantly larger total brain tissue volumes than controls (9.6%, $p<0.0001$) (Figure 80). In unilateral cases, the hemisphere containing the enlarged ventricle was 12.1% larger ($p<0.0001$) compared to both right and left hemispheres in the control cohort (Figure 80). The hemisphere containing the normal sized ventricle was also significantly larger than both right and left hemispheres in the normal control cohort (11.7%, $p<0.0001$) (Figure 81). There was no significant difference between the two hemispheres in fetuses with unilateral ventriculomegaly ($p=0.667$) (Figure 82). Significance was unchanged when data from repeat scans were excluded and when controlling for sex.

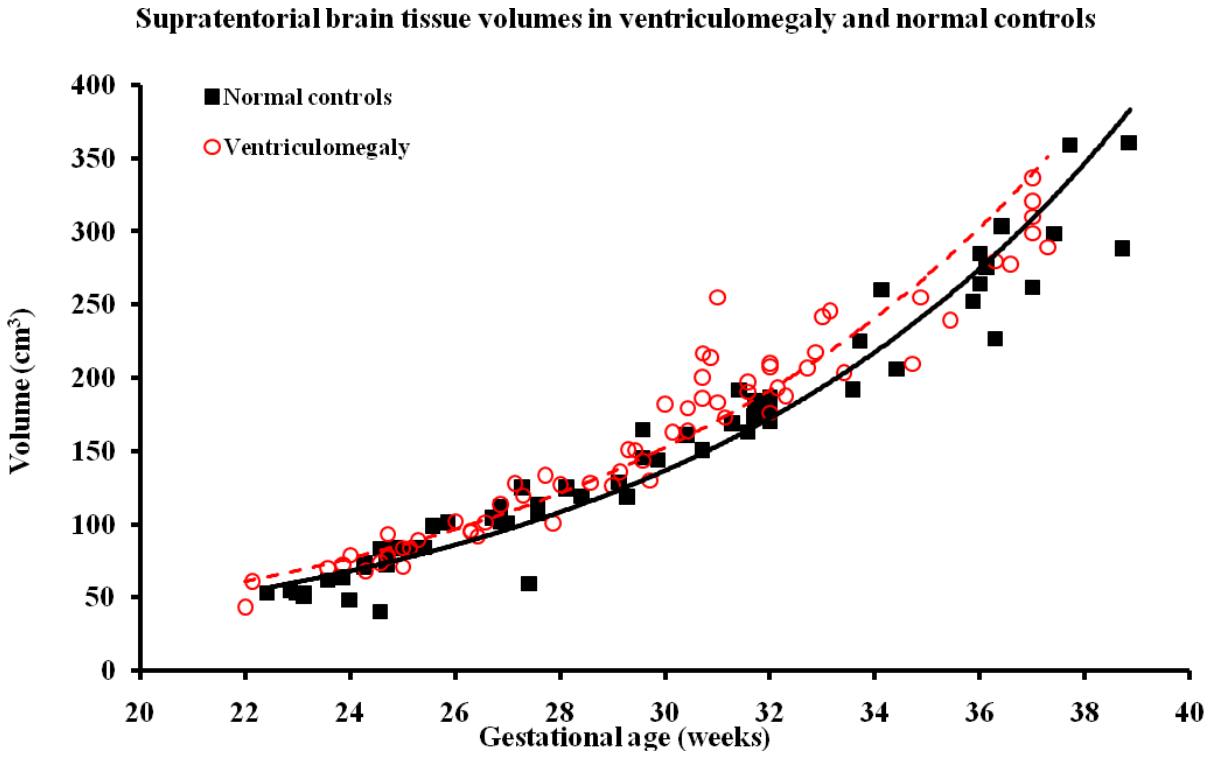


Figure 80. Supratentorial brain tissue volumes in ventriculomegaly and normal controls

Fetuses with isolated ventriculomegaly had significantly larger supratentorial brain tissue volumes compared to normal controls by 9.6% ($p<0.0001$).

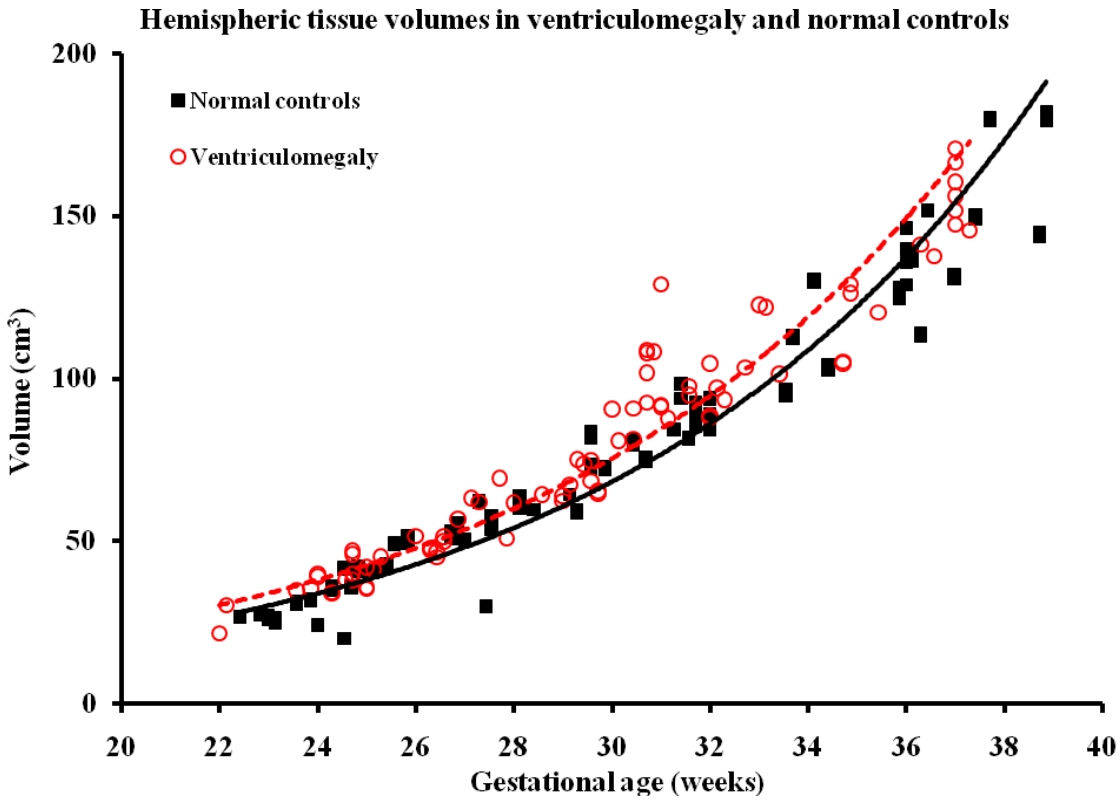


Figure 81. Supratentorial hemispheric brain tissue volumes in ventriculomegaly and normal controls

The hemisphere containing the enlarged ventricle was 9.8% larger ($p<0.0001$) compared to both right and left hemispheres in the control group. Left and right hemispheric data points of the control group are indistinguishable for better clarity. The ventriculomegaly data shown depict the hemisphere containing the enlarged ventricle in the unilateral cases and the hemisphere containing the largest ventricle only in the bilateral cases.

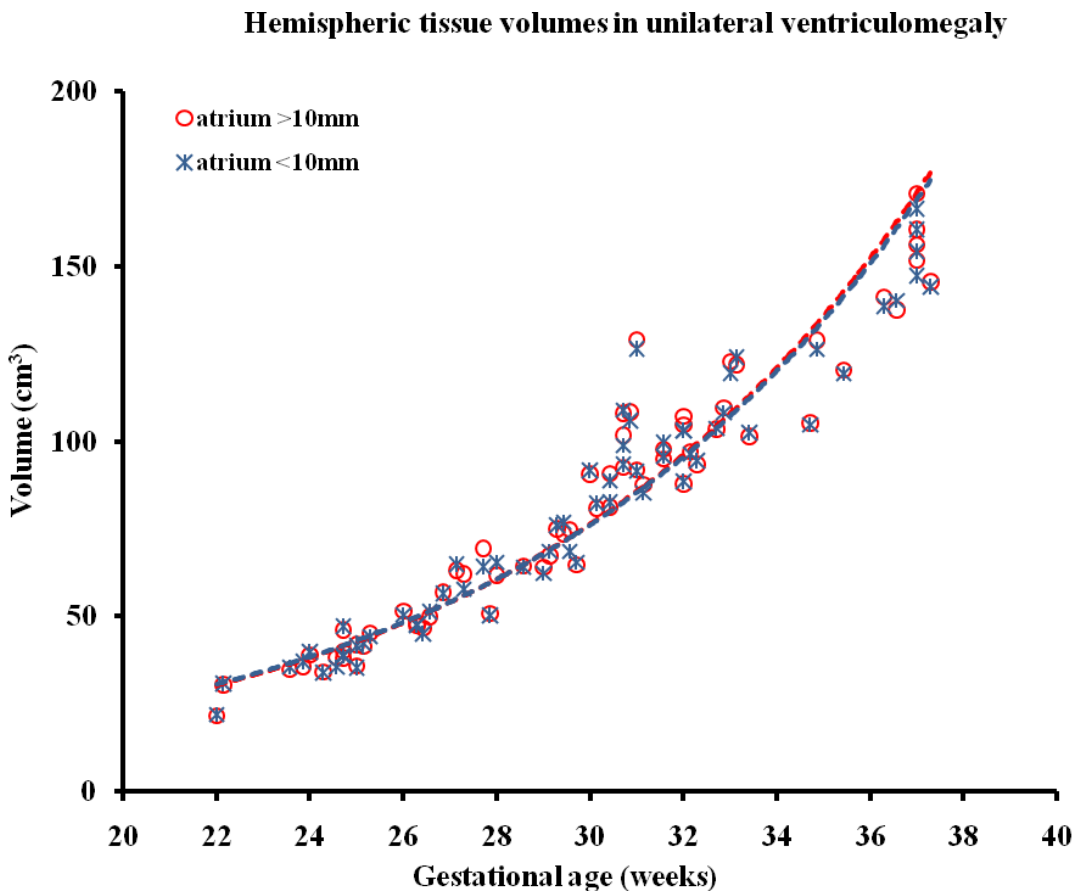


Figure 82. Hemispheric tissue volumes in unilateral ventriculomegaly

There was no significant difference between the two hemispheres in fetuses with unilateral ventriculomegaly (p=0.667).

3.2.3.2.6 Cortical gray matter

Total cortical gray matter volume was measured in 19 ventriculomegaly cases (GA range 22.14-37.29 weeks, mean 30.16 weeks). There was no significant difference between the complete group and this subgroup in GA, brain volume and ventricular volume. As expected, when comparing between subgroups, brain volumes were significantly larger in the ventriculomegaly fetuses compared to controls (p=0.027). The ventriculomegaly group also had significantly larger cortices than the controls across the GA range studied (17.2%, p=0.002), even when corrected for brain volume (14.6%, p=0.008) (Figure 83).

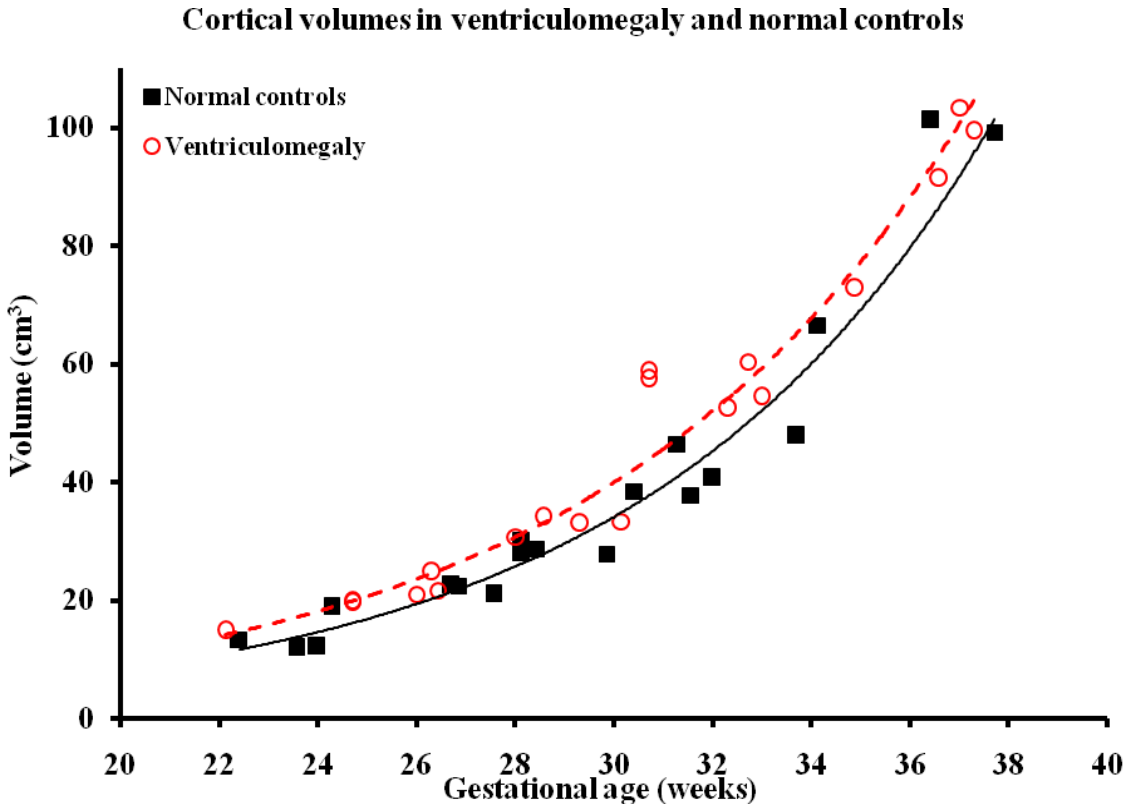


Figure 83. Cortical volume in ventriculomegaly and normal controls

Fetuses with ventriculomegaly had significantly larger cortices compared to normal controls by 17.25 (p=0.002).

3.2.3.2.7 White matter

White matter increased with GA (Spearman's r=0.963, p<0.0001) at a relative growth rate of 9.27% per week (Table 18). When comparing between groups there was no significant difference in white matter volume (p=0.637), even when correcting for brain tissue volume (0.228) (Figure 84).

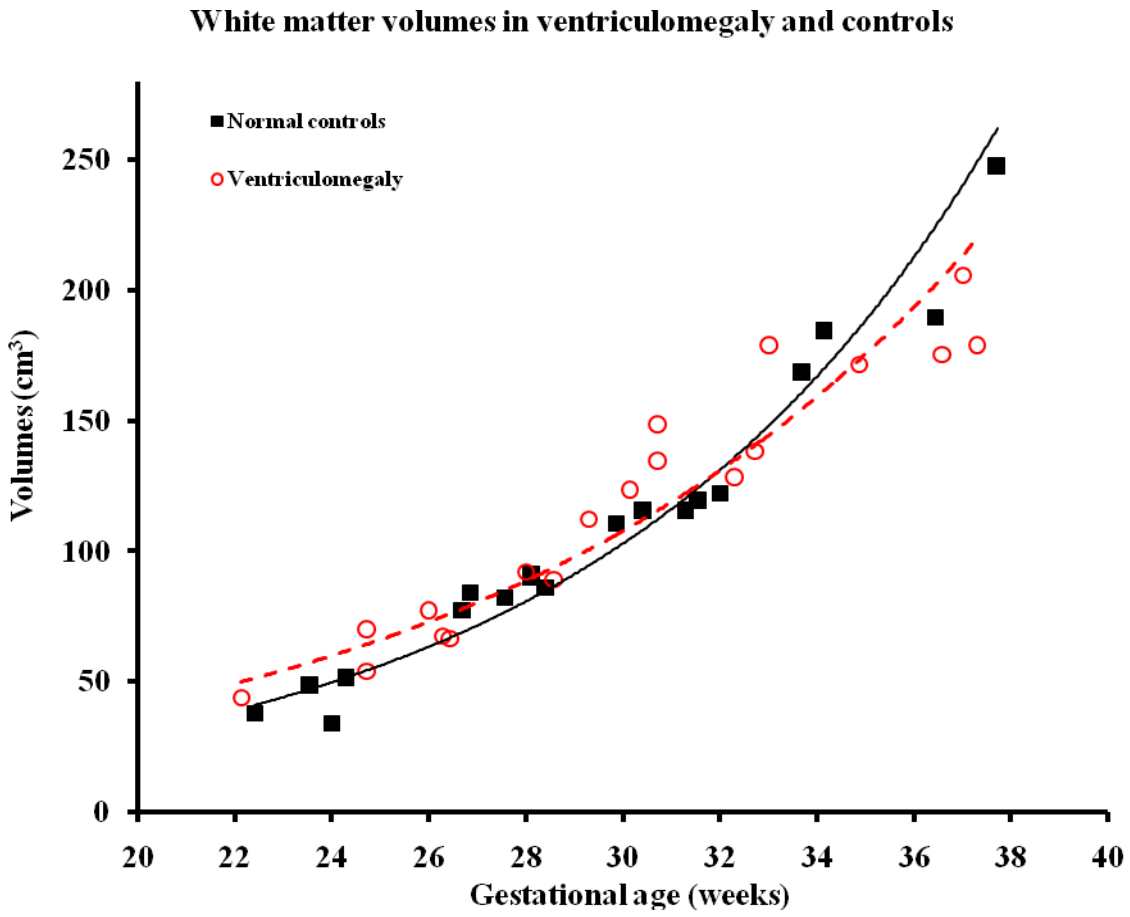


Figure 84. White matter volumes in ventriculomegaly and normal controls

There were no significant difference in white matter volumes between the cohorts (p=0.228).

3.2.3.2.8 Basal ganglia

In the ventriculomegaly group, basal ganglia volumes increased at a relative growth rate of 9.29% per week (Spearman's r=0.946, p<0.0001) (Table 18). There was no difference in volume between the two groups (p=0.29) (Figure 85).

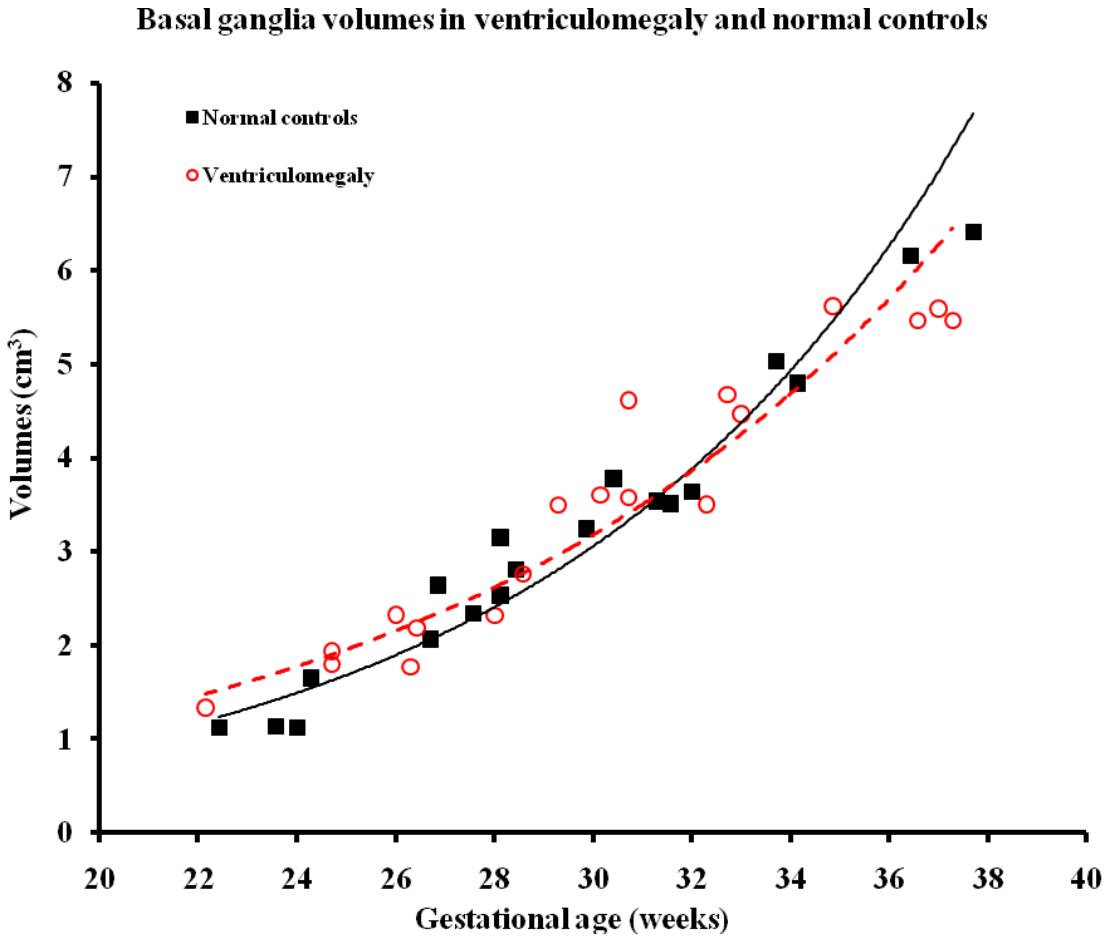


Figure 85. Basal ganglia volumes in ventriculomegaly and normal controls

There were no significant differences in basal ganglia volumes between the cohorts (p=0.29).

3.2.3.2.9 Thalami

Thalami increased with GA at a relative growth rate of 10.61% per week (Spearman's r=0.98, p<0.0001) (Table 18). When comparing between groups, there was no significant different in volume (p=0.656) (Figure 86).

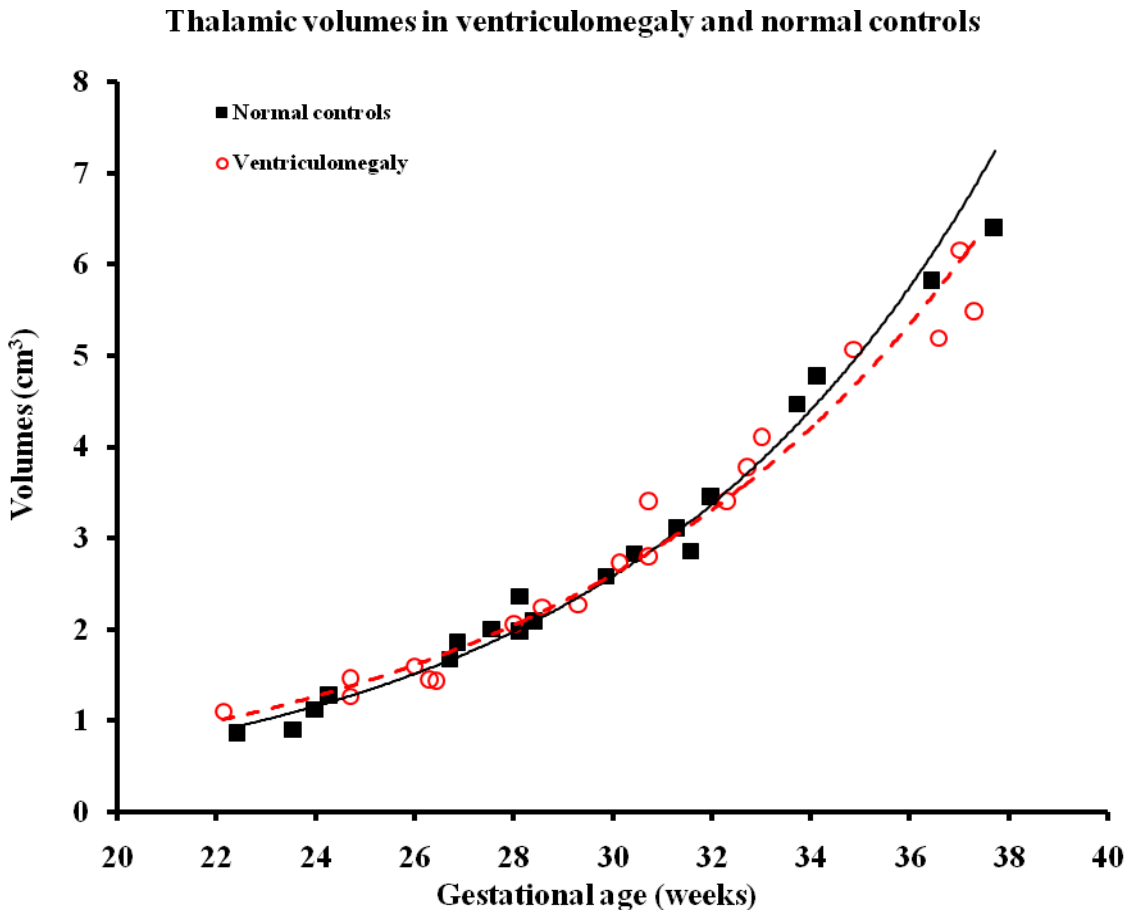


Figure 86. Thalamic volumes in ventriculomegaly and normal controls

There were no significant differences in thalamic volumes between the cohorts (p=0.656).

3.2.3.2.10 Correlations with ventricular size

As described earlier, in the normal controls group the total ventricular volume correlated with the total brain tissue, thalamic, third ventricle, fourth ventricle and extra-cerebral CSF volumes while there was no correlation with cortical or white matter volume. On the contrary, in the ventriculomegaly group the total ventricular volume significantly and positively correlated with all measurements. Results are summarised in Table 17.

Correlation of total ventricular size and intracranial measurements

	Total Brain Tissue	**Cortex**	**Basal Ganglia**	**Thalami**	**White Matter**	**Third Ventricle**	**Fourth Ventricle**	**Extra-cerebral CSF**
Normal controls (Spearman's r)	0.54**	0.305	0.289	0.389*	0.34	0.549**	0.457**	0.499**
Ventriculomegaly (Spearman's r)	0.475**	0.544*	0.640*	0.649*	0.630*	0.449**	0.567**	0.457**

Table 17. Correlation of total ventricular volume and intracranial volumetric measurements

Spearman r values are presented for each relationship. * $p<0.05$ and $p>0.0001$ ** = $p<0.0001$

To further assess the relationship between total lateral ventricular volume and brain tissue during gestation we assessed the cases that had multiple scans (Figure 87). The paired volumetric data from both scans were plotted against GA and compared against the normal controls. While the majority of ventriculomegaly paired data have slopes with similar trends there were 2 cases that exhibited large changes in volume. The total lateral ventricular volumes of one fetus that was scanned three times during gestation showed a steep increase and doubled in volume from 25 to 32 weeks (case +). However the increase in ventricular volume was not accompanied by a change in the total brain tissue volume slope compared to the controls or ventriculomegaly group. Another case of a fetus scanned twice during GA, showed a decrease in total lateral ventricular volume from 29.7 to 34.7 weeks (case ▲). Similarly to the previous case there was no difference in the slope of brain tissue volume compared to controls or ventriculomegaly.

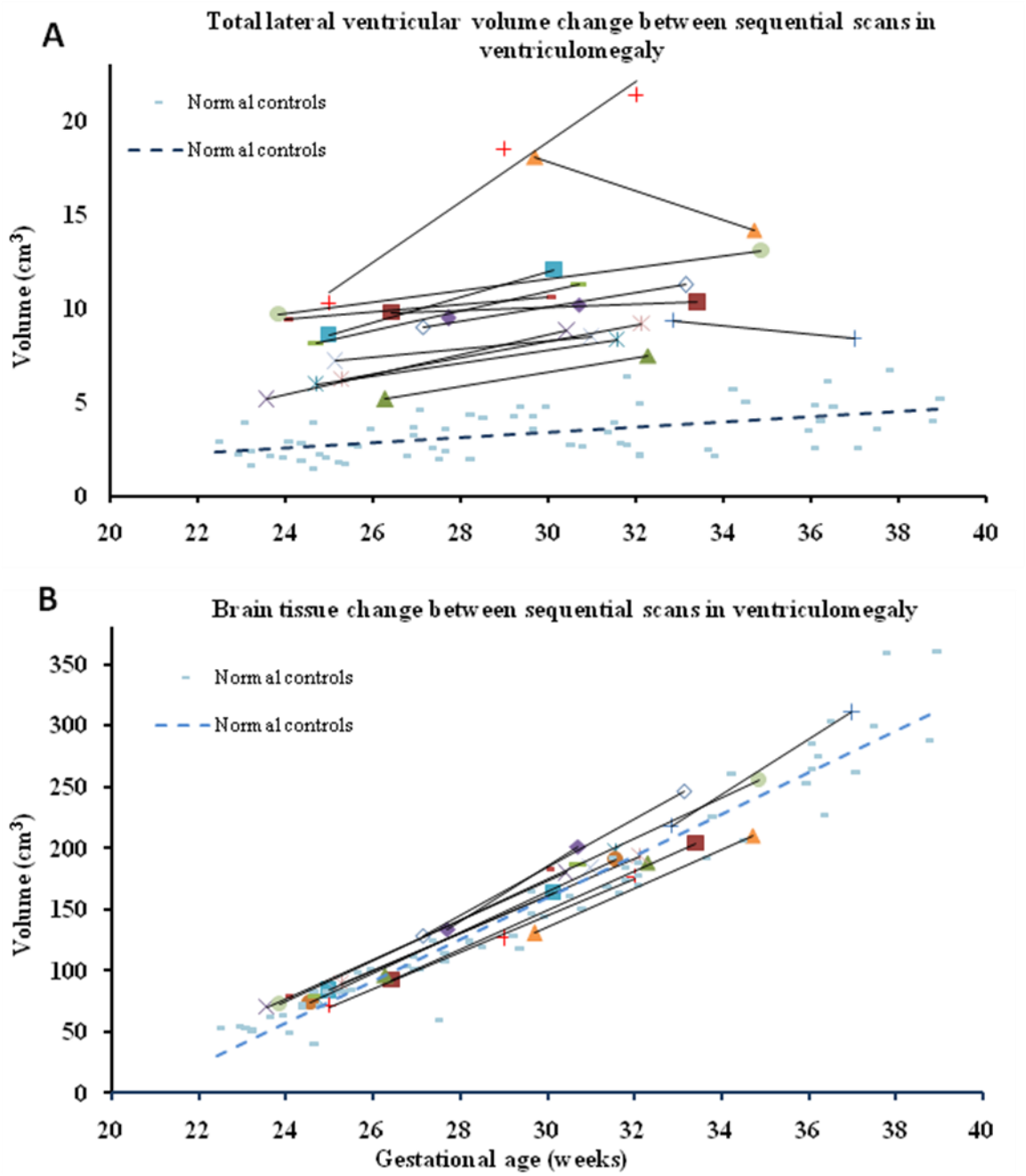


Figure 87. Ventricular and supratentorial brain tissue changes in serial scans

(A) Total ventricular volume change between sequential scans in ventriculomegaly. Fifteen fetuses were scanned twice during gestation and 1 fetuses had 3 scans. (B) Brain tissue volume change between sequential scans in ventriculomegaly. A change in the total ventricular volume was not accompanied with significant deviation in supratentorial brain tissue.

The volumetric results for both the control and ventriculomegaly cohorts are summarised in Table 18.

	Total Lateral Ventricles	Total Brain Tissue	Cortex	Basal Ganglia	Thalami	White Matter	Third Ventricle	Fourth Ventricle	Extra-cerebral CSF
Normal controls									
Spearman's r	0.511**	0.976**	0.964**	0.975**	0.993**	0.986**	0.927**	0.733**	0.873**
Relative Growth Rate (%/week)	3.43	11.65	13.15	11.39	13.13	12.27	0.098	0.129	0.06
Average volume (cm^3)									
at 22 GW	2.27	53.67	11.01	1.17	0.88	39.15	0.074	0.013	22.68
at 26 GW	2.68	85.56	19.37	1.89	1.51	63.58	0.110	0.022	57.67
at 30 GW	3.17	136.41	34.09	3.05	2.57	103.25	0.163	0.035	81.98
at 34 GW	3.75	217.47	60.00	4.93	4.40	167.66	0.242	0.057	95.59
at 38 GW	4.43	346.70	105.58	7.94	7.52	272.25	0.359	0.093	98.52
Ventriculomegaly									
Spearman's r	0.481**	0.968**	0.971**	0.946**	0.98**	0.963**	0.803**	0.849**	0.769**
Relative Growth Rate (%/week)	5.58	12.35	12.50	9.29	10.61	9.27	0.088	0.119	0.10
Average volume (cm^3)									
at 22 GW	7.31	61.10	13.84	1.46	0.99	49.41	0.092	0.029	23.66
at 26 GW	8.44	96.56	23.48	2.16	1.60	73.01	0.137	0.046	64.73
at 30 GW	9.74	152.59	39.85	3.18	2.60	107.88	0.203	0.074	91.97
at 34 GW	11.24	241.14	67.62	4.69	4.20	159.40	0.301	0.119	105.38
at 38 GW	12.97	381.07	114.74	6.92	6.79	235.53	0.446	0.192	104.96

Table 18. Volumetric results for control and ventriculomegaly cohorts

Correlation of each intracranial structure and GA is indicated by the Spearman's r value. Relative growth rate (%/per week) represents the percent volume increase relative to the average volume of the structure.** $p<0.0001$.

3.2.3.3 Statistics

Volumetric data were not normally distributed and were therefore log-transformed to achieve normal distribution. Log transformed data were tested for normality and achieved normal distribution. Analysis of covariance (ANCOVA) on log-transformed data was used to compare results between groups when corrected for GA. Correlation between variables was assessed using the Spearman's correlation coefficient (Spearman's r) correcting for GA, unless otherwise specified.

3.2.3.3.1 Intra-rater and inter-rater variability for volumetric analysis

Intra and inter-rater reliability for the left and right lateral ventricle segmentations and left and right hemispheres were performed between 2 raters (VK,DV) in 5 fetal datasets (at GA 23.14, 23.57, 24.57, 25.57, 36.29 weeks). The ICC for both intrarater and interater variability was 0.99 ($p<0.0001$) suggesting negligible variability between raters and excellent reproducibility in the same rater. In order to evaluate the spatial overlap accuracy of the segmentations between raters the Dice similarity coefficient was measured for the segmentation of the lateral ventricles in 10 cases. The Dice similarity coefficient, similar to the Pearsosn's r, has a range of -1 to +1 with values close to 1 indicating highly similar data. The Dice similarity coefficient was calculated at 0.9 indicating excellent agreement between raters. For cortical segmentations, intra and inter-rater reliability were performed between 2 raters (SE,NM) by calculating the cortical volume of five consecutive transverse slices. This was performed for five different fetal datasets (at GA 24.71, 26.29, 28.57, 30.43, 32.00 weeks). The mean intra-rater difference for the cortical volume was 1.2% and mean inter-rater difference was 2.7%.

3.2.4 Neonatal volumetry

3.2.4.1 Normal controls

The normal control cohort consisted of 24 neonates scanned in the neonatal unit during the study period from March 2007 to February 2012. Fourteen neonates were enrolled in the fetal research program and had undergone fetal MR imaging. Ten neonates were enrolled as normal controls in the following MR research studies of the preterm brain (Optimising functional MRI techniques in the study of neuronal development in preterm infants, 07/H0707/101; Computational analysis of brain abnormalities and neurodevelopmental impairments in preterm infants, 04/Q0406/125). Seven neonates had high signal intensity in the white matter, normal for their postmenstrual age. The mean post-menstrual age at scan was 42.5 weeks and the range from 37.9-49.1 weeks. The mean GA at birth was 39.2 weeks and the range from 37-41.7 weeks. Cohort characteristics are presented in Table 19.

Normal control cohort characteristics			
Male		12	
Female		12	
Gestational age at birth (weeks)		39.2	(37-41.7)
Post-menstrual age at scan (weeks)		42.5	(37.9-49.1)
Birthweight (g)		3279	(2410-4242)
Apgar scores	1 minute	9	(8-10)
	5 minutes	10	(9-10)

Table 19. Normal control cohort characteristics

3.2.4.2 Isolated ventriculomegaly

During the study period from August 2008 to April 2012, 27 neonates with a diagnosis of antenatal isolated ventriculomegaly underwent MR imaging. 26 neonates were enrolled in the research program and had undergone fetal MRI. One neonate had not had fetal MR imaging as the mother felt claustrophobic during the scan. This subject was a sibling of one of the fetal participants and had an ultrasound and a neonatal MR diagnosis of isolated ventriculomegaly.

One neonate was excluded from the analysis because of poor image quality due to motion. In summary, 26 neonates were used for the analysis with a mean post-menstrual age at scan at 45.3 weeks and range 41.4-50.4 weeks (Figure 88). The mean GA at birth was 39.5 weeks and the range was 34.3-41.4 weeks. Cohort characteristics are presented in Table 20. While there was no difference in the age at birth between cohorts there was a significant different in the post-menstrual age at scan (p=0.001) with the ventriculomegaly cohort being scanned at a later age.

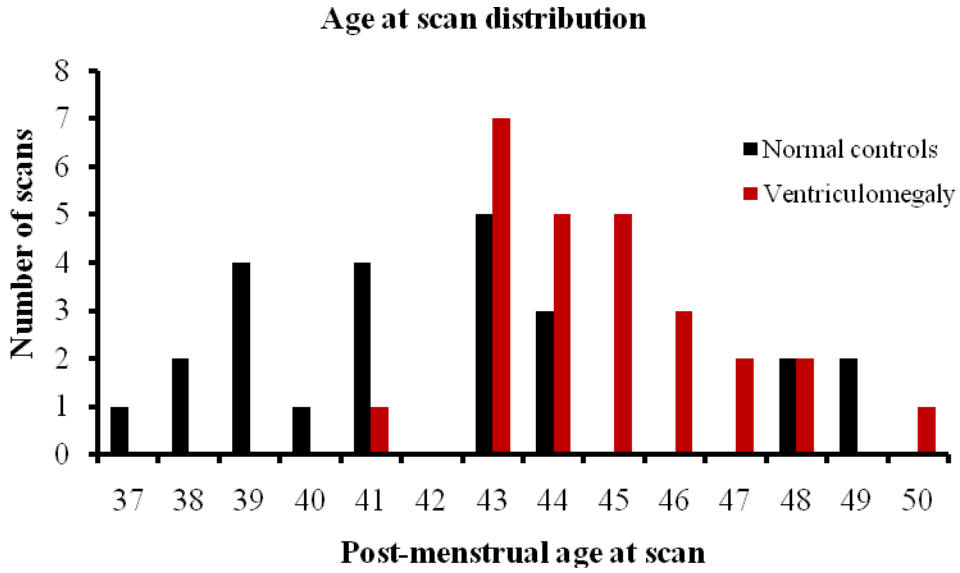


Figure 88. Histogram of age distribution of post-menstrual age at scan in the ventriculomegaly and normal control groups

Fetal gestational age was estimated from a first trimester dating ultrasound scan.

Ventriculomegaly cohort characteristics			
Male		19	
Female		7	
Gestational age at birth (weeks)		39.5	(34.3-41.4)
Post-menstrual age at scan (weeks)		45.3	(41.4-50.4)
Birthweight (g)		3427	(2530-4260)
Apgar scores	1 minute	9	(7-10)
	5 minutes	10	(9-10)

Table 20. Ventriculomegaly cohort characteristics

There were no additional CNS structural abnormalities detected on neonatal MRI to alter the diagnosis of isolated ventriculomegaly. However mild changes in brain appearance were reported on clinical MR examination and have been summarised in Table 21.

Findings on neonatal MRI	No. of cases
Increased extra-cerebral space	10
Thinning of the corpus callosum	9
Increased signal intensity in white matter	8
Signs of delayed gyrification	3

Table 21. Additional findings on neonatal MRI in the ventriculomegaly cohort

The findings detected on neonatal MRI in the ventriculomegaly cohort did not alter the diagnosis of isolated ventriculomegaly.

Statistics

Between group comparison was performed using analysis of covariance (ANCOVA). All comparisons and correlations were corrected for gestational age at birth and postmenstrual age at scan.

3.2.4.3 Volumetric analysis

3.2.4.3.1 Lateral ventricles

In the normal control group, the total lateral ventricular volume increased with postnatal age after birth and correlated significantly with age at scan when corrected for gestational age at birth (Pearson's r=0.665, p=0.0003) (Figures 89 and 90). Neonates with ventriculomegaly had significantly larger lateral ventricle volumes compared to controls (206% larger, p<0.0001) (Figure 89). There was overlap in lateral ventricle volumes in 2 cases. The volumes of both lateral ventricles in a ventriculomegaly case were within the limits of the normal control volumes. This neonate had two fetal scans, the first at 22 weeks showed 11 mm unilateral ventriculomegaly whilst in the second scan at 32 weeks the lateral ventricles had normalised and were below 10 mm. One control neonatal case had a lateral ventricle volume in the ventriculomegaly range. In the ventriculomegaly cohort, there was correlation between the antenatal lateral ventricle volume and neonatal lateral ventricle volume (Pearson's r=0.66, p=0.001).

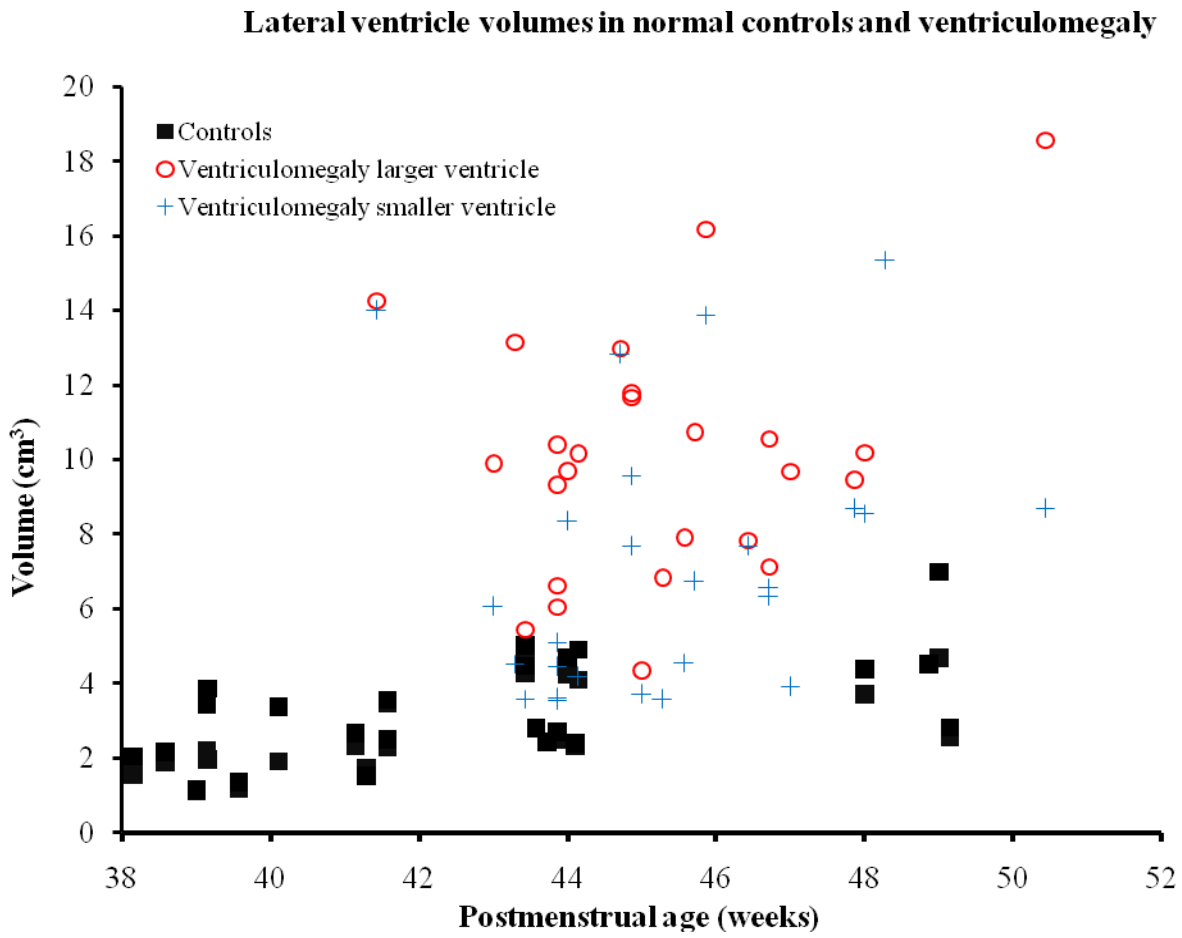


Figure 89. Lateral ventricle volumes in normal controls and neonates with antenatal ventriculomegaly

Neonates with antenatal ventriculomegaly had significantly larger lateral ventricle volumes than controls (206%, $p<0.0001$). There was overlap in 2 cases. Lateral ventricle volumes in the controls cohort represent right and left ventricles.

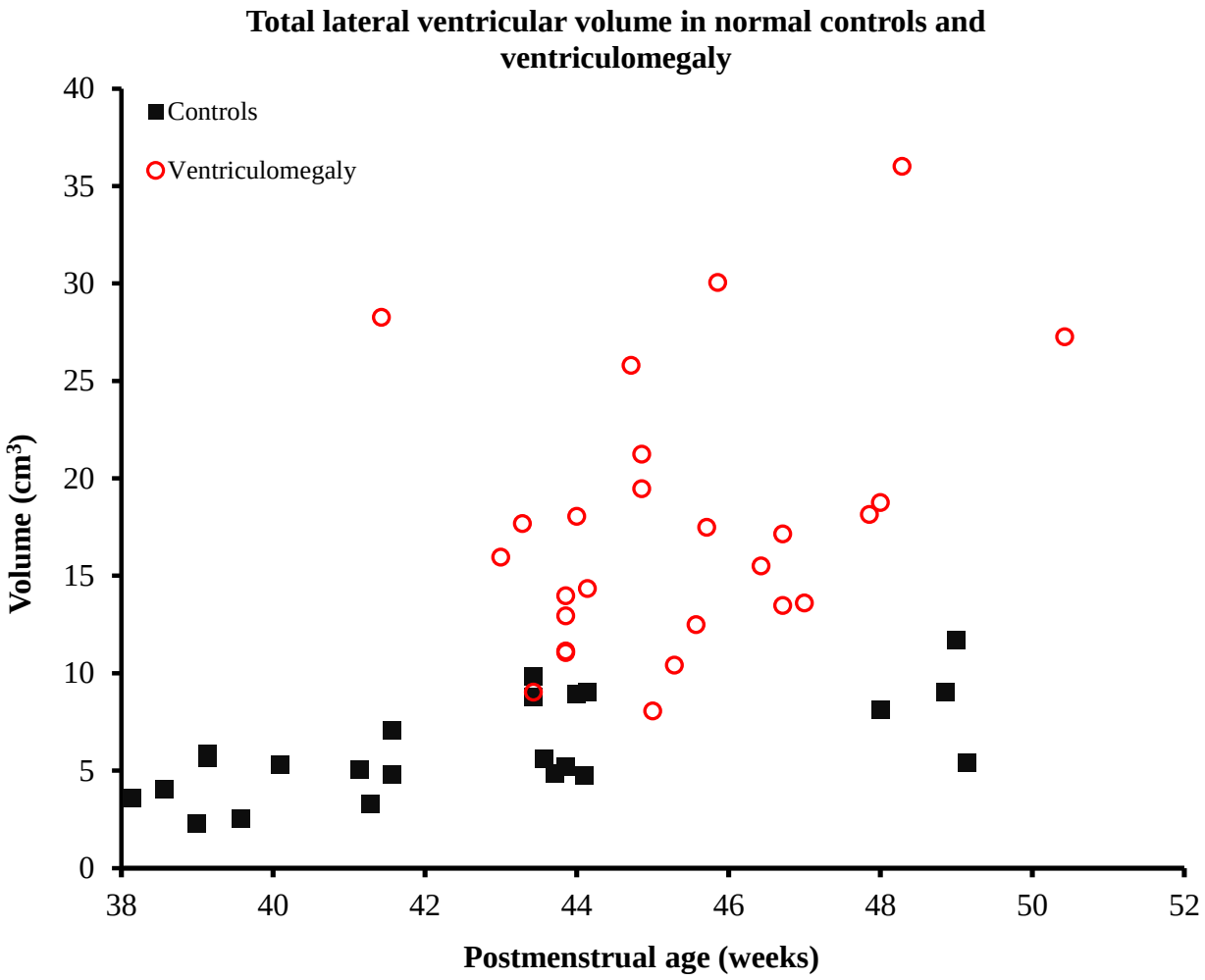


Figure 90. Total lateral ventricular volume in normal controls and neonates with antenatal ventriculomegaly
Neonates with antenatal ventriculomegaly had significantly larger total lateral ventricular volumes than controls ($p<0.0001$). There was overlap in 4 cases.

3.2.4.3.2 Supratentorial brain tissue volume

Supratentorial brain tissue volume increased in both groups with postmenstrual age and correlated with postmenstrual age at scan when corrected for GA at birth (Controls: Spearman's $r=0.772$, $p<0.0001$; Ventriculomegaly: Spearman's $r=0.423$, $p=0.018$) (Figure 90). When comparing between groups, neonates with antenatal ventriculomegaly had significantly larger total brain tissue volumes than controls (14.8% larger, $p=0.002$). This difference was not statistically significant when looking at each gender separately, probably due to the small sample size (males $p=0.071$, females $p=0.938$).

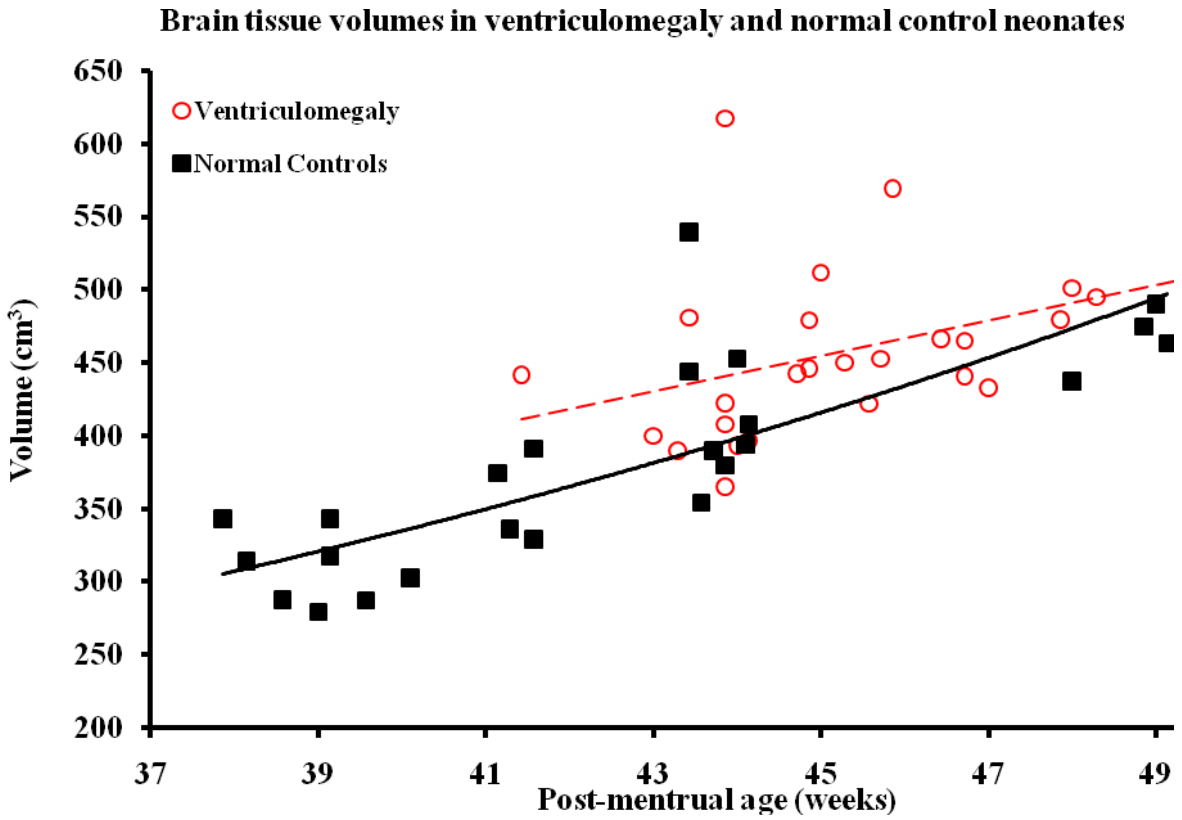


Figure 91. Supratentorial brain tissue volumes in normal controls and neonates with antenatal ventriculomegaly

Neonates with antenatal ventriculomegaly had significantly larger supratentorial brain tissue volumes compared to normal controls by 14.8% (p=0.002).

Out of the 26 neonates, 18 were also included in the fetal volumetric analysis. To ensure the neonatal subgroup was representative of the fetal group these 18 cases were identified on the fetal chart of supratentorial brain tissue volumes against GA (Figure 92). The selection of cases appear to be representative of the fetal cohort.

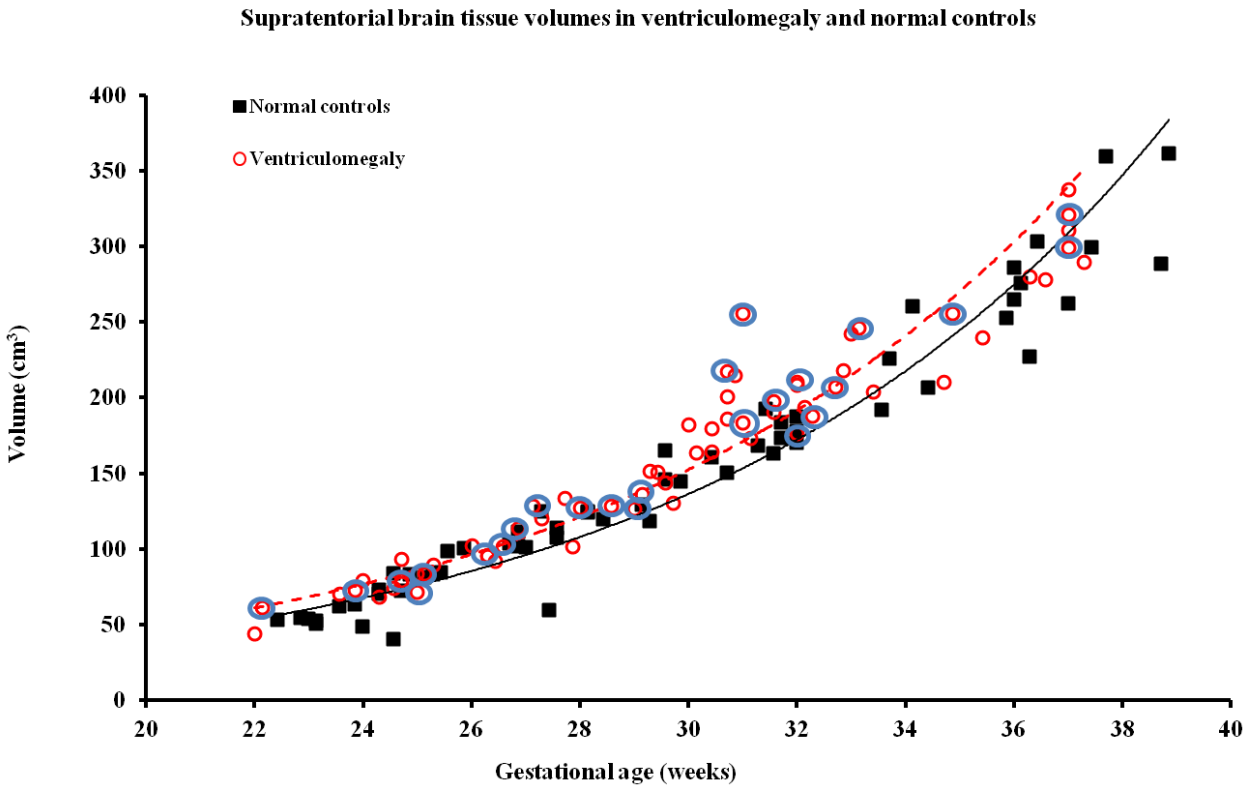


Figure 92. Fetal cases with antenatal ventriculomegaly used in neonatal volumetric analysis

Fetal sub-population used for neonatal volumetric analysis appears representative of the total fetal population. Selected cases are highlighted in blue circles.

3.2.4.3.3 Correlation between lateral ventricles and supratentorial brain tissue volumes

In the control group, total lateral ventricular volume correlated with supratentorial brain tissue volume when corrected for postmenstrual age at scan and GA at birth (Spearman's r=0.639, p=0.0001). On the contrary in the ventriculomegaly group there was no correlation between total lateral ventricular volume and brain tissue volume when corrected for postmenstrual age at scan and GA at birth (Spearman's r=0.303, p=0.07).

3.2.5 Discussion

In this study, using volumetric MRI of the fetal brain we present the first *in vivo* MRI evidence indicating brain overgrowth in fetuses with isolated ventriculomegaly. Fetuses with ventriculomegaly had significantly increased brain tissue volumes when compared to controls with enlargement restricted to the cortical gray matter. The third and fourth ventricles and extra-cerebral CSF were also enlarged. White matter, thalamic, and basal ganglia volumes were not significantly different between cohorts. Brain overgrowth and ventriculomegaly also persisted during neonatal life.

In normal fetuses, supratentorial brain tissue increased between 22 to 38 weeks GA at a relative growth rate of 11.65% per week. This is comparable to previous fetal MR volumetric studies performed on reconstructed datasets with growth rates ranging from 10.22% to 17% (Clouchoux et al., 2011; Rajagopalan et al., 2011a). Cortical volume in our normal fetuses increased at a relative growth rate of 13.15%, in agreement with the study of Scott and colleagues (Scott et al., 2011) in 34 normal fetuses between 20 and 31 weeks GA. In addition, cortical volume increased at a higher rate than supratentorial brain volume in our control cohort, as previously shown in the fetal (Scott et al., 2011) and in the preterm brain (Kapellou et al., 2006).

Ultrasound studies have shown that the atrial diameter remains relatively stable in the second and third trimesters although an increase in absolute values is observed (Almog et al., 2003). Our results showed a small but significant increase in absolute ventricle volumetric values from 22 to 38 weeks of gestation. Previous fetal MRI volumetric studies have been inconclusive as to whether the volume of the lateral ventricles increases (Scott et al., 2011; Snijders and Nicolaides, 1994), decreases (Clouchoux et al., 2011) or remains stable (Kazan-Tannus et al., 2007) during gestation. This variability may be due to heterogeneous cohorts and inclusion of the third ventricle or the CSP in the measurements. As shown in our study, enlargement of the lateral ventricles with increasing gestation was associated with enlargement of the third and fourth ventricles, CSP and extra-cerebral CSF.

As expected, fetuses with ventriculomegaly diagnosed on 2D measurement of the atrial diameter (on ultrasound and MRI) had significantly larger lateral ventricle volumes compared to controls.

In our cohort, boys were more likely to have ventriculomegaly than girls with a female/male ratio of 1:2.4; consistent with previous studies (Gilmore et al., 2008; Melchiorre et al., 2009a). Interestingly, in 1/3 of the unilateral ventriculomegaly cases, the normal measuring ventricle (atrium <10 mm) demonstrated a ventricular volume outside the normal range. In addition, whilst atrial diameter and volume of the lateral ventricles correlated well in both cohorts, data were scattered in the ventriculomegaly cohort. For example, an atrial diameter of 12.3 mm corresponded to volumes ranging from 4.4-9.2 cm^3. The atrial diameter only reflects the size of the posterior aspect of the lateral ventricles however enlargement may also be present in the anterior part of the ventricles. Whilst atrial diameter may be an accurate tool for the diagnosis of ventriculomegaly it does not appear to be sensitive to intra-group volumetric differences potentially impairing its ability to predict subsequent clinical neurodevelopmental outcome.

Fetuses with isolated ventriculomegaly had significantly larger total brain tissue volumes than controls supporting the hypothesis that ventriculomegaly may be associated with brain overgrowth which is apparent from mid gestation. Interestingly, in unilateral cases both hemispheres were enlarged and brain overgrowth was not localised to the hemisphere containing the larger ventricle.

In the control cohort, whilst total lateral ventricular volume correlated with other ventricles, extra-cerebral CSF, total brain and thalamic volume, there was no correlation with the other brain structures. On the contrary, in the ventriculomegaly cohort, total ventricular volume correlated well with all measured intracranial structures suggesting an altered relationship between the ventricles and developing structures in this cohort.

There have been four published studies on MR brain volumetry comparing fetuses with ventriculomegaly to controls (Grossman et al., 2006; Kazan-Tannus et al., 2007; Pier et al., 2011; Scott et al., 2012). Three studies were performed on non-reconstructed T2 MR datasets, not corrected for fetal motion and these did not find any significant differences in brain parenchyma volume between cohorts (Grossman et al., 2006; Kazan-Tannus et al., 2007; Pier et al., 2011). Results from these studies are difficult to interpret due to the selection criteria of normal control fetuses, non-homogeneous ventriculomegaly population and volumetric analysis on non-

reconstructed MR datasets known to be sensitive to fetal motion. These issues have been addressed in our study by the use of registered volumetric datasets, the rigid entry criteria of normal controls and the follow up of all participants to ensure normal development. In addition, a homogeneous "developmental" ventriculomegaly cohort was selected for analysis by excluding cases with chromosomal abnormalities, infection, brain parenchyma damage or additional abnormalities. Scott et al. (Scott et al., 2012) performed a volumetric comparison of intracranial structures between fetuses with isolated ventriculomegaly (n=16) and control subjects (n=16) at an age range from 22-25.5 weeks. Structures were automatically segmented. They found no significant difference in brain tissue or cortical volume between groups. We repeated our analysis in a subgroup of our cohorts using the same age range (22-25.5 weeks) and found that fetuses with isolated ventriculomegaly had significantly enlarged brain tissue volumes over a similar age range (p=0.038) (ventriculomegaly n=14 and controls n=18). Increased accuracy of the manual segmentation method may account for the detection of a volumetric difference.

Ventricular dilatation persisted after birth with the ventriculomegaly cohort having significantly larger lateral ventricle volumes compared to controls. In one case with ventriculomegaly, that had undergone two fetal scans, the lateral ventricles had "normalised" in the second scan (atrial diameter <10 mm). In the neonatal scan, the "normalised" case had lateral ventricle volumes in the control range however the supratentorial brain tissue volume was well above the control range and more specifically it was the third largest data point. There was no correlation between total lateral ventricular volume and supratentorial brain tissue while there was a significant correlation in the control group. The clinical MR examination also revealed mild visually apparent changes in brain appearance that were not consistent with a specific disorder nor altered the diagnosis of isolated ventriculomegaly. The most common change reported was increased extra-cerebral space which is in accordance to the volumetric result during fetal life. Thinning of the corpus callosum was reported in 9 cases however the clinical significance of this finding is unknown and callosal volumetric studies are warranted. Signs of delayed gyrification reported in 3 cases are in accordance with delayed appearance of cortical landmarks discussed in chapter 3.3. There were no signs of delayed gyrification during fetal life (scans performed at 28, 28^{+5} and 30^{+5} gestational weeks) visually overt high signal intensity within the white matter was reported in 8 cases. When reviewing the fetal MR clinical reports high signal intensity in the white matter

was reported in one case scanned at 37 gestational weeks. Quantitative analysis with DTI is underway. In addition, neonates with ventriculomegaly had significantly larger supratentorial brain tissue volumes compared to controls although we have not determined whether brain overgrowth is attributed to cortical overgrowth as shown in the fetal volumetric analysis.

Our volumetric results including the absolute volumetric ranges and relative growth rates of the white matter and deep gray matter (basal ganglia and thalami) in the control cohort are comparable with the study of Scott et al. (2011) in normal fetuses from 20 to 31 gestational weeks. Interestingly, when comparing between our two cohorts, there were no significant differences in the basal ganglia, thalamic and white matter volumes between control fetuses and those with ventriculomegaly. The brain overgrowth documented in our study was attributed to an increase in cortical volume. Our results from the fetal volumetric analysis are consistent with the study of Gilmore and colleagues (Gilmore et al., 2008) which used volumetric T1 datasets acquired postnatally and showed that neonates with isolated ventriculomegaly (n=34) (diagnosed on antenatal ultrasound) had significantly larger cortical gray matter volumes than control subjects (n =34) by 10.9% whilst there was no difference in absolute white matter volume (decreased when corrected for intracranial volume). In their small follow-up study (ventriculomegaly n=11, controls n=12) they showed that ventricular enlargement persisted at the age of 2 years and was then associated with increases in both gray and white matter volumes (Lyall et al., 2012). The authors suggested that increased surface area along the enlarged ventricular wall may result in a larger number of progenitor neurons. Indeed the human cortical germinal zone has several cytoarchitectonically distinct zones, that contain the various progenitor populations in different proportions (Hansen et al., 2010; Smart et al., 2002). Cortical overgrowth from an increase in progenitor neurons from the germinal zone would require the presence of ventriculomegaly from early in gestation and would not account for overgrowth documented in fetuses with VM diagnosed later in pregnancy with a normal appearance at 20 weeks. Over migration for these areas after 20 weeks would be more likely due to glial populations as late migrating inhibitory neurons arise from different regions in the ganglionic eminence. In our study, while the majority of fetuses were diagnosed with ventriculomegaly on their anomaly ultrasound scan performed around 20 weeks, 3 fetuses had a normal anomaly scan and developed ventriculomegaly at a later age. Greater brain parenchyma and cortical gray

matter volume could also be due to lack of normal developmental apoptosis in the developing brain (Kuan et al., 2000) rather than an increased number of migrating cells. Early in gestation apoptosis is involved in the development and morphogenesis of the neural tube supporting the role of apoptosis in adjusting the initial progenitor pool size (Kuan et al., 2000). At around 4.5 weeks apoptotic activity is seen in the ventricular zone but is very low. By week 6-7 apoptosis in the ventricular zone increases five-fold and there is evidence of apoptosis in the preplate (Zecevic and Rakic, 2001). By week 11 apoptosis has commenced in all cortical layers although it is most prominent in the proliferative zones. Between 12 and 22 weeks apoptosis increases significantly throughout the telencephalon. After 32 weeks apoptosis continues in all cortical layers. Apoptosis is an integral part of cortical development, initially related to morphogenesis, proliferation and regulation of progenitor size and during the late fetal and postnatal period to synaptogenesis. Previous studies in preterm and IUGR infants (Peterson et al., 2000; Tolsa et al., 2004) have shown that cortical volume and outcome data correlate well; the cortex mediates cognitive abilities, and a reduction in cortical volume has been associated with neurodevelopmental delay. Interestingly, fetuses with isolated ventriculomegaly also have an increased risk of neurocognitive delay (Leitner et al., 2009; Lyall et al., 2012; Sadan et al., 2007) but according to this study exhibit increased cortical volumes. This implies that it may be the quality of the cortical tissue and its connections not the absolute volume that relates to neurocognitive outcome. An increase in cortical volume could be due to an increase in cell numbers, synapses or in the extracellular matrix. Ventriculomegaly has been associated with brain and cortical overgrowth in a rat model of gestational Vitamin D deficiency. Cortical overgrowth in the affected rats was associated with an increase in proliferating cells and a decrease in apoptotic cells in the studied cortical regions of the cingulate and dentate gyri (Eyles et al., 2003). However it is unclear which cell types contributed to the larger brains.

Cortical development and organisation is regulated by the basic coordinated morphogenetic processes of proliferation, apoptosis, migration and differentiation of both neurons and glia (Haveman and Lavorel, 1975). Apoptosis is prominent in areas that undergo dramatic morphogenetic changes and is essential for the regulation of the proper size and shape of the cortex during development. Several animal knockout studies have shown that alterations in genes regulating developmental apoptosis lead to changes in cortical size and shape (Chenn and Walsh,

2002; Depaepe et al., 2005; Oppenheim et al., 2001). Cortical overgrowth has been described in children with neurofibromatosis Type 1 and cortical volume has correlated with the degree of learning disability (Moore et al., 2000). The presence of brain overgrowth in autistic children at the ages of 2-4 years is well established (Courchesne et al., 2011a). Cortical gray matter and white matter enlargement have been found in MRI volumetric studies in children with autism with enlargement most prominent in the frontal lobe (Carper and Courchesne, 2005; Courchesne et al., 2001; Hazlett et al., 2011). An excess of cerebral cortical neurons (67% increase) has been found at autopsy in 7 autistic patients (age median 4 years, range 2-16 years) compared to controls which could underlie the volume increases in cerebral gray matter reported (Courchesne et al., 2011b). In our cases white matter was not enlarged during fetal life and it was not possible to analyse the lobes of the brain separately. The group of Lyall et al. (2012) detected increases in white matter volume at 2 years of age but not in the neonatal period in fetuses with antenatally diagnosed ventriculomegaly.

There are several limitations to the current study. Cortical volume segmentations were performed only in a subset of fetuses due to the extensive work required to perform detailed and accurate manual segmentations. However, we are currently developing and assessing an automatic protocol for cortical segmentation. In addition, developmental data for the fetuses in our study are currently being collected. Detailed neurodevelopmental assessments using the Griffiths Mental Development Scales and BSID-III Scales of Infant and Toddler Development are performed at 1 and 2 years respectively and a battery of autism tests including the Autism Diagnostic Observation Schedule (ADOS) and Autism Diagnostic Interview-Revised (ADI-R) at 3 years. The question of homogeneity of the ventriculomegaly cohort has arisen on many occasions and it has been an issue not addressed in previous studies. In order to achieve homogeneity we excluded cases of infection and chromosomal abnormalities, metabolic syndromes and cases with ventriculomegaly and associated CNS abnormalities. The only limitation that may influence homogeneity in our cohort would be ventricular size. Previous studies have shown that moderate/severe ventricular size is associated with an abnormal outcome. However we thought important to include cases of all ventricular sizes in order to correlate the volume of the lateral ventricles with other MR biometric parameters measured.

In this study we have demonstrated brain overgrowth, restricted to cortical enlargement, in association with fetal ventriculomegaly while brain overgrowth persisted into neonatal life. Cortical overgrowth may occur secondary to disruption in the regulation of cell proliferation and apoptosis and subsequent altered brain connectivity may explain the high risk of later neurodevelopmental delay in these children. Importantly, brain overgrowth persisted during neonatal life in the cohort of fetuses with ventriculomegaly scanned as neonates although further analysis is required in order to determine whether brain overgrowth is attributed to cortical overgrowth and to subjectively quantify changes in white matter signal intensity and tract volume e.g. corpus callosum using advanced MR techniques such as DTI and tractography.

3.3 Assessment of cortical development and maturation

Cortical development occurs with an invariable temporospatial schedule and has therefore been relied upon by neuropathologists as an accurate marker of fetal brain maturation. Deviations from this highly orchestrated sequence of gyral-sulcal formation may be associated with later neurocognitive deficits. Cognitive impairment is thought to have a neurobiological origin within the developing cerebral cortex. Therefore, investigating cortical development in-utero may provide a useful tool for predicting outcome amongst those fetuses affected with ventriculomegaly. In this chapter we have characterised the developmental stages of the fetal cortex during normal development and compared these normative indices to fetuses with isolated ventriculomegaly.

3.3.2 Aims

To design a detailed protocol for the evaluation of cortical development and establish whether ventriculomegaly is associated with delayed or abnormal cortical maturation.

3.3.3 Normal control cohort

The normal control cohort consisted of 72 fetuses scanned at a mean GA of 29.4 weeks and a GA range from 22.4-38.9 weeks. Six fetuses were scanned twice during gestation and one fetus was scanned three times.

3.3.3.1 Gestational age of early sulcation

Gestational age at scan and presence of early sulcation (score 1) of each sulcus and gyrus is presented in a whisker box plot in Figure 93 to depict the variation in the appearance of sulci and gyri between fetuses. The GA range at which each landmark has a score of 1 in 25-75% of fetuses is presented in Table 22 and results are comparable with previous studies using MRI and ultrasound.

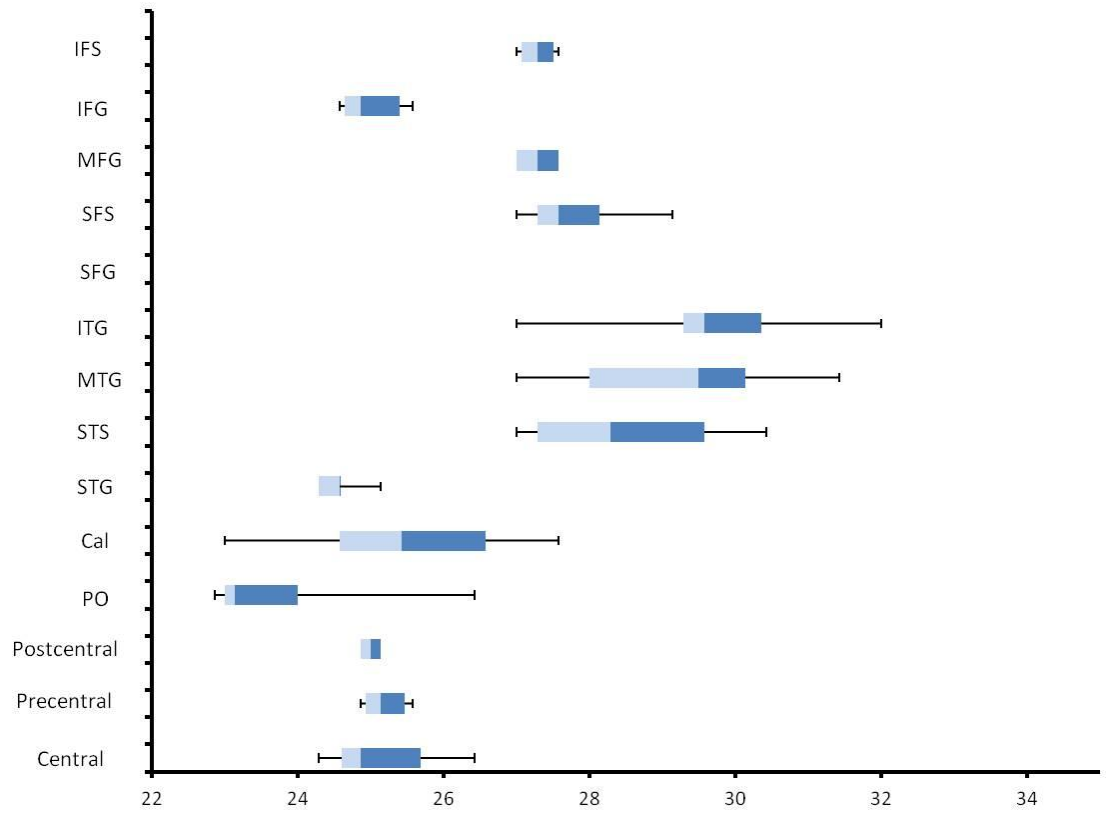


Figure 93. Gestational age and presence of early sulcation (score 1) of cortical landmarks in normal controls

The boxes represent the gestational age range at which 25-75% of fetuses had a score of 1. Box plot represents the median (light blue/dark blue boundary), lower (light blue) and upper (dark blue) quartiles and minimum and maximum values (box plot wiskers).

PO: parieto-occipital fissure, Cal: calcarine, STG: superior temporal gyrus, STS: superior temporal sulcus, MTG: middle temporal gyrus, ITG: inferior temporal gyrus, SFG: superior frontal gyrus, SFS: superior frontal sulcus, MFG: middle frontal gyrus, IFG: inferior frontal gyrus, IFS: inferior frontal sulcus, Postcentral: postcentral gyrus, Precentral: precentral gyrus, Central: central sulcus.

	Fetal MRI				Ultrasound
	This study	Levine	Garel		Pistorius
Cortical landmarks	25-75%	>75%	25-75%	Fogliarini	25-75%
Sylvian fissure	Before 22	16-17		Before 20	Before 22
Parieto-occipital fissure	23	18-19	22-23		22
Postcentral gyrus	24-25	26-27		27	
Central sulcus	24-25	26-27	24-25	24	26
Calcarine sulcus	24-27	18-19	22-23	24	
Cingulate sulcus	26-27	26-27			
Superior temporal gyrus	24				
Superior temporal sulcus	27-29	26-27	30	28	25
Middle temporal gyrus	27-30				
Inferior temporal gyrus	29-30				
Precentral gyrus	24-25	26-27		27	
Inferior frontal gyrus	24-25				
Superior frontal gyrus	27				
Middle frontal gyrus	27				
Inferior frontal sulcus	27	30-31	27		
Superior frontal sulcus	27-28		24-25		

Table 22. Gestational age of early appearance (score 1) of cortical landmarks in normal controls

Gestational age of early appearance of cortical landmarks as detected in our study and in comparison with previous fetal studies using MRI and ultrasound (Fogliarini et al., 2005; Garel, 2004; Levine and Barnes, 1999; Pistorius et al., 2010). The Sylvian fissure was present in all fetuses.

The strength of association for each cortical landmark between development scores and GA in the normal control cohort is presented in Table 23. Cortical development scores were highly correlated with GA and were similar for all areas.

Cortical landmark	Central sulcus	Pre central gyrus	Post central gyrus	Parieto-occipital fissure	Calcarine sulcus	Sylvian fissure ratio	Cingulate length	Superior frontal gyrus
Spearman's r	0.946**	0.962**	0.945**	0.913**	0.938**	0.909**	0.943**	0.939**
Cortical landmark	Superior frontal sulcus	Middle frontal gyrus	Inferior frontal gyrus	Inferior frontal sulcus	Superior temporal gyrus	Superior temporal sulcus	Middle temporal gyrus	Inferior temporal gyrus
Spearman's r	0.932**	0.925**	0.958**	0.929**	0.928**	0.925**	0.938**	0.913**

Table 23. Correlation of cortical development scores with GA in normal controls

Correlation was assessed using the Spearman's correlation coefficient (r). * $p<0.05$ and $p>0.0001$ ** $p<0.0001$

The height of each sulcus and gyrus increased with increasing GA and correlated strongly with increasing GA in the normal control cohort (Table 24). The width of different cortical landmarks either decreased or remained stable with increasing GA as summarised in Table 24.

Cortical landmark	**Central sulcus**	**Pre central gyrus**	**Post central gyrus**	**Parieto-occipital fissure**	**Calcarine sulcus**	**Superior frontal gyrus**	**Superior frontal sulcus**
Height	0.938**	0.934**	0.938**	0.887**	0.831**	0.613**	0.760**
Width	-0.296	-0.21*	-0.49**	-0.679**	-0.405*	0.212	-0.106
Cortical landmark	**Middle frontal gyrus**	**Inferior frontal gyrus**	**Inferior frontal sulcus**	**Superior temporal gyrus**	**Superior temporal sulcus**	**Middle temporal gyrus**	**Inferior temporal gyrus**
Height	0.786**	0.66**	0.739**	0.922**	0.781**	0.757**	0.665**
Width	0.225	0.224**	0.151	-0.268*	-0.28*	-0.182	-0.026

Table 24. Correlation of height and width of cortical landmarks with GA in normal controls

Correlation was assessed using the Spearman's correlation coefficient (r). * = $p<0.05$ and >0.0001 ** = <0.0001

The cortical development scores and linear measurements for each cortical landmark assessed in the normal control cohort are presented in Figures 94-101.

3.3.3.2 Frontal lobe

(Precentral gyrus, superior frontal gyrus, superior frontal sulcus, middle frontal gyrus, inferior frontal gyrus, inferior frontal sulcus)

In the normal control cohort, the cortical development scores and height of all five landmarks representing the frontal lobe increased with GA. The width of the superior, middle and inferior gyri increased and correlated weakly with GA and was significant only for the inferior gyrus. The width of the superior frontal sulcus and precentral gyrus decreased with GA although it did not reach significance. The results for the frontal lobe are presented in Figures 94-96. There were 9 control fetuses with one degree of asymmetry and 1 control fetus with two degrees of asymmetry in the precentral gyrus. There were 5 control fetuses with one grade of asymmetry for the superior frontal gyrus, 6 control fetuses with one grade of asymmetry and 1 control fetus with a two grade asymmetry in the superior frontal sulcus. The middle frontal gyrus showed one grade of asymmetry in 1 control fetus and two grades of asymmetry in another control fetus. Five control fetuses showed one grade of asymmetry in the inferior frontal gyrus and 5 control fetuses in the inferior frontal sulcus. In five control fetuses the asymmetry was present in more than one landmarks of the frontal lobe.

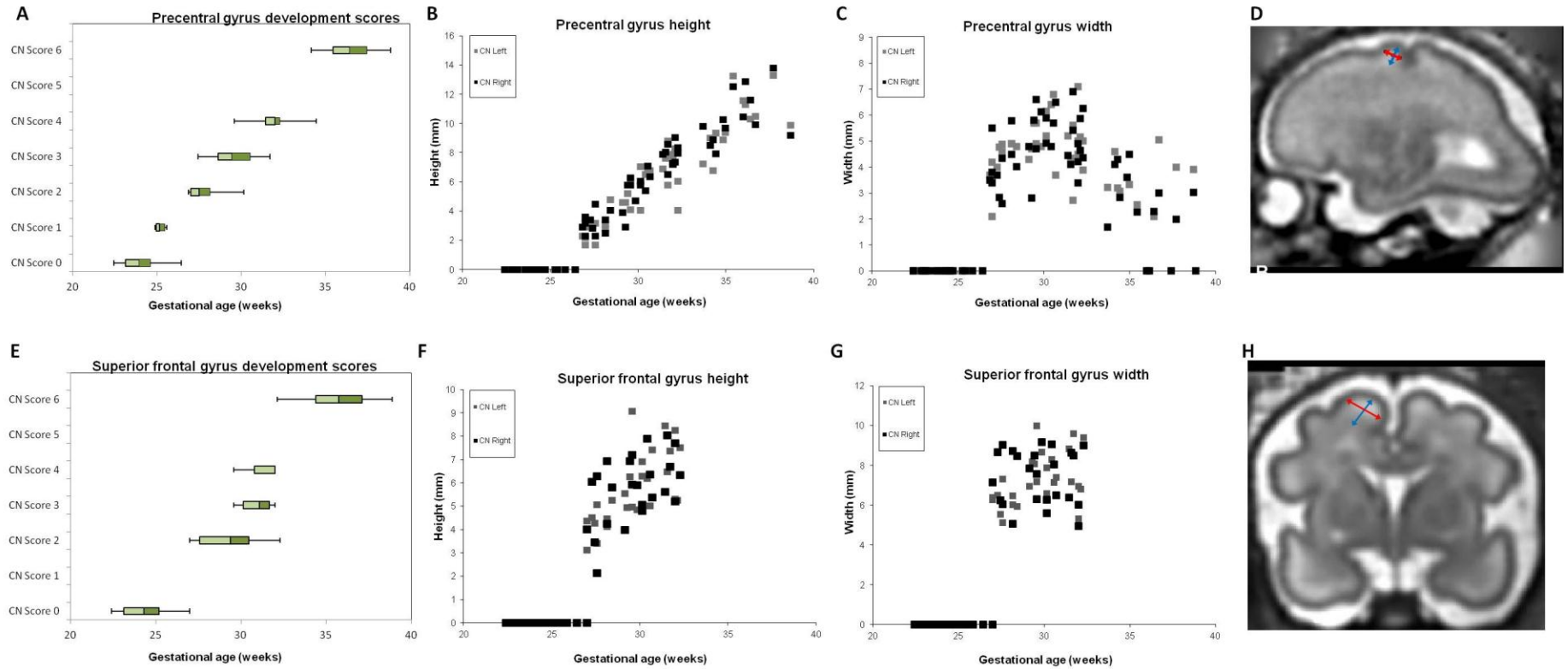


Figure 94. Precentral gyrus and superior frontal gyrus development in normal controls

(A-D) Precentral gyrus development in normal controls (A) Development scores (B) Height, (C) Width, (D) Linear measurements of height (blue) and width (red). Development score ($r=0.962$, $p<0.0001$) and height ($r=0.934$, $p<0.0001$) increased whilst the width decreased with GA ($r=-0.21$, $p<0.05$).

(E-H) Superior frontal gyrus development in normal controls (E) Development scores (F) Height, (G) Width, (H) Linear measurements of height (blue) and width (red). Development score ($r=0.939$, $p<0.0001$) and height ($r=0.613$, $p<0.0001$) increased whilst the width remained stable with GA ($r=0.212$, $p>0.05$). Only one case had a score of 1.

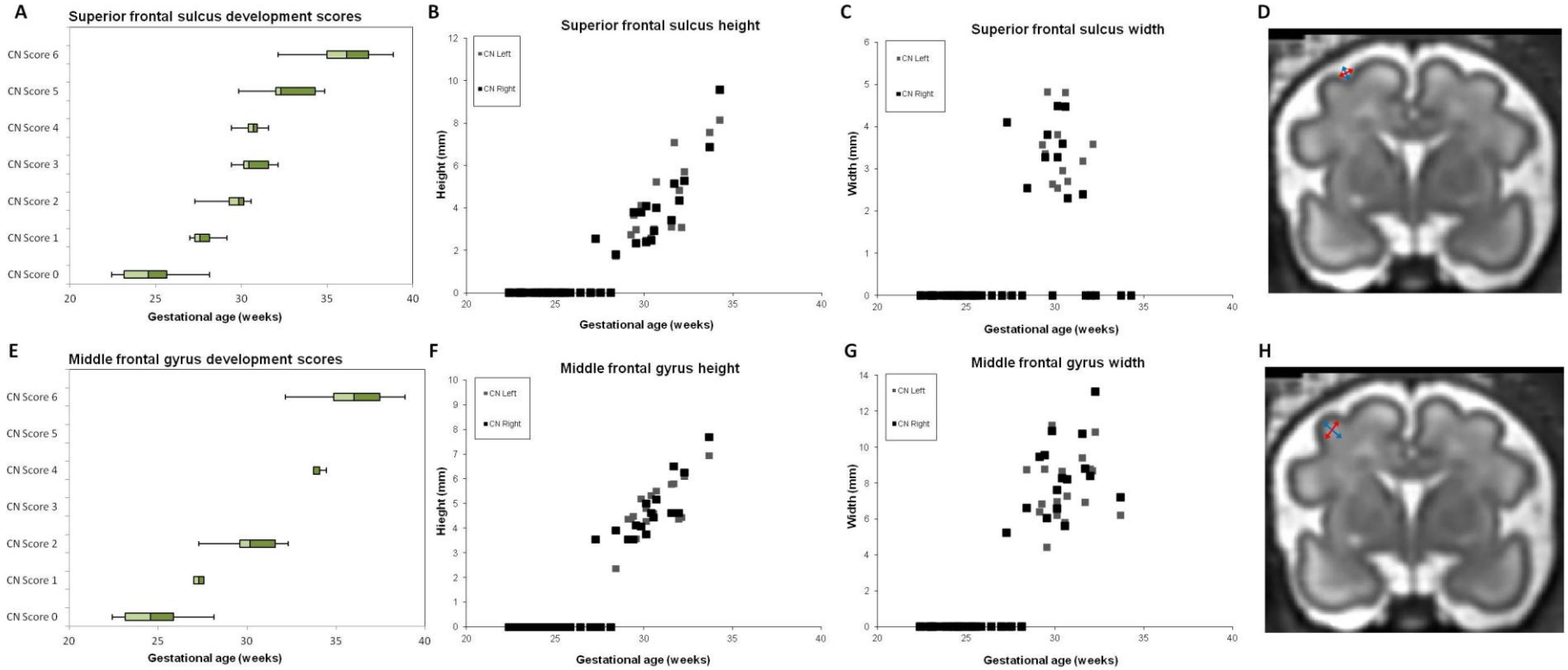


Figure 95. Superior frontal sulcus and middle frontal gyrus development in normal controls

(A-D) Superior frontal sulcus development in normal controls (A) Development scores (B) Height, (C) Width, (D) Linear measurements of height (blue) and width (red). Development score ($r=0.932$, $p<0.0001$) and height ($r=0.76$, $p<0.0001$) increased whilst the width remained stable with GA ($r=-0.106$, $p>0.05$).
(E-H) Middle frontal gyrus development in normal controls (E) Development scores (F) Height, (G) Width, (H) Linear measurements of height (blue) and width (red). Development score ($r=0.925$, $p<0.0001$) and height ($r=0.786$, $p<0.0001$) increased whilst the width remained stable with GA ($r=0.225$, $p>0.05$).

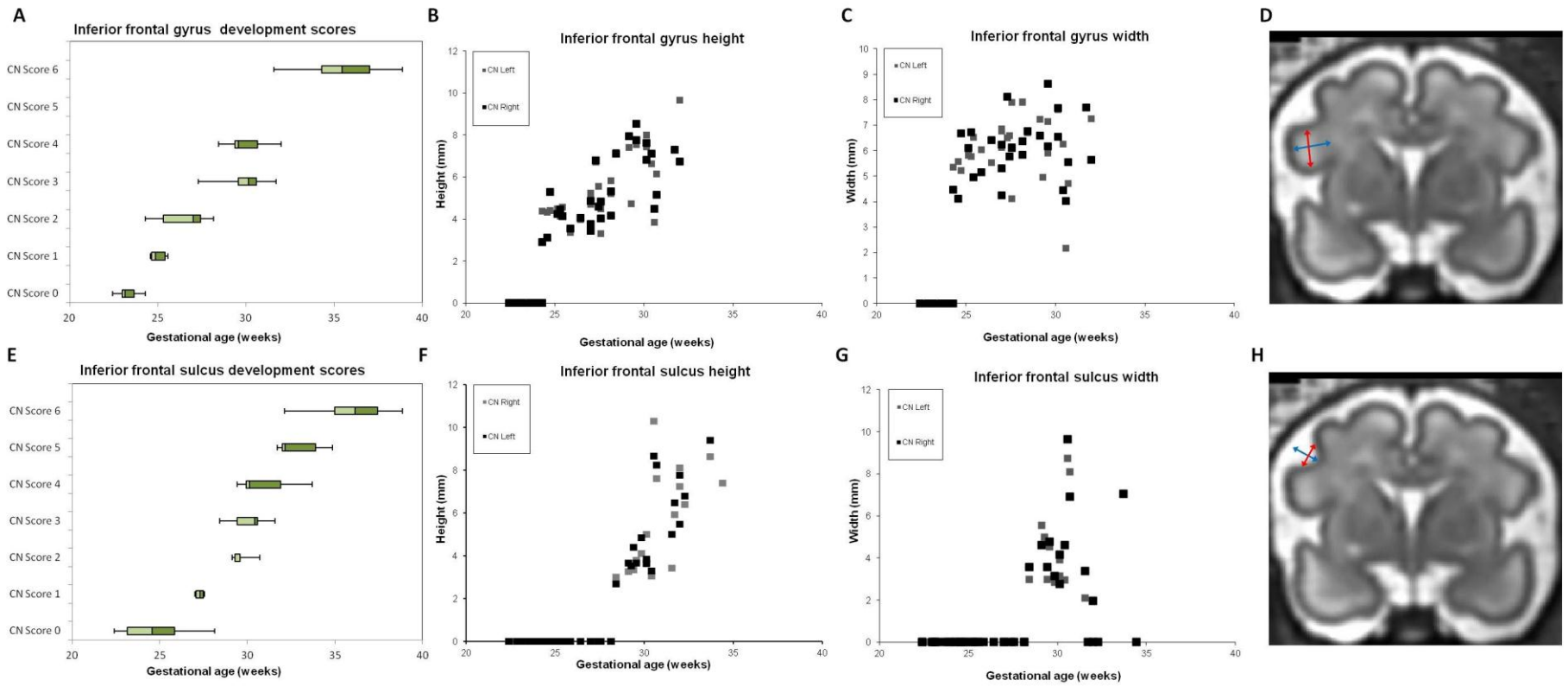


Figure 96. Inferior frontal gyrus and inferior frontal sulcus development in normal controls

(A-D) Inferior frontal gyrus development in normal controls

Development score ($r=0.958$, $p<0.0001$), height ($r=0.66$, $p<0.0001$) and width ($r=0.224$, $p<0.0001$) increased with GA. (A) Development scores (B) Height, (C) Width, (D) linear measurements of height (blue) and width (red).

(H-E) Inferior frontal sulcus development in normal controls

Development score ($r=0.929$, $p<0.0001$) and height ($r=0.739$, $p<0.0001$) increased whilst the width remained stable with GA ($r=0.151$, $p>0.05$). (E) Development scores (F) Height, (G) Width, (H) Linear measurements of height (blue) and width (red).

3.3.3.3 Frontal/parietal border and frontal/parietal/temporal border

(Central sulcus and Sylvian fissure)

In the normal control cohort, the cortical development score and height of the central sulcus increased with GA (score: Spearman's $r=0.962$, $p<0.0001$; height: Spearman's $r=0.938$, $p<0.0001$) whilst the width showed a trend for decrease although this was not statistically significant (Spearman's $r=0.962$, $p>0.05$) (Figure 97A-D). Four control fetuses had one grade asymmetry while all other fetuses were symmetrical.

The Sylvian fissure development ratio increased with GA (Spearman's $r=0.909$, $p<0.0001$) (Figure 97E-H). As the fissure matured the maximum distance from frontal to temporal boundaries along the insula-temporal cortex increased (Spearman's $r=0.959$, $p<0.0001$) while the minimum distance frontal to temporal borders of the operculum decreased with GA (Spearman's $r=-0.749$, $p<0.0001$).

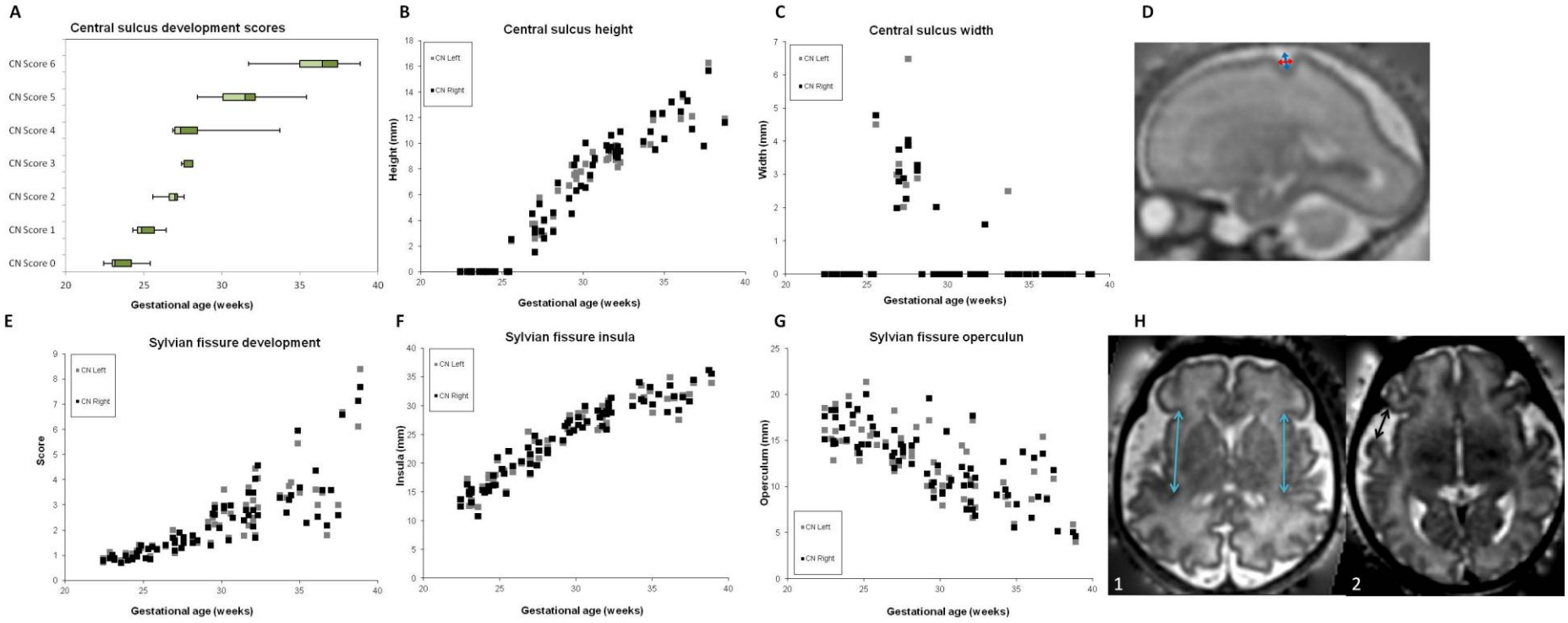


Figure 97. Central sulcus and Sylvian fissure development in normal controls

(A-D) Central sulcus development in normal controls (A) Development scores (B) Height, (C) Width, (D) linear measurements of height (blue) and width (red). Development score ($r=0.946$, $p<0.0001$) and height ($r=0.938$, $p<0.0001$) increased whilst the width remained stable with GA ($r=-0.296$, $p>0.05$).
(E-H) Sylvian fissure development in normal controls (A) Development score representing the ratio of the insula distance to the opercular distance, (B) Insular distance (C) Opercular distance, (H1-H2) Linear measurements of (1) insula (blue) (2) operculum (black). The development score ($r=0.959$, $p<0.0001$) and insula distance ($r=0.959$, $p<0.0001$) increased whilst the operculum distance ($p=-0.749$, $p<0.0001$) decreased with GA.

3.3.3.4 Parietal lobe

(Postcentral gyrus, parieto-occipital fissure)

In the normal control cohort, the development score and height of the postcentral gyrus increased with GA (score Spearman's r=0.945, p<0.0001; height Spearman's r=0.938, p<0.0001) while the width of the gyrus significantly decreased (Spearman's r=-0.49, p<0.0001) (Figure 98A-D). There were 3 control fetuses with one grade of asymmetry while the rest of the fetuses were symmetrical.

The development score of the parieto-occipital fissure and the height increased with GA (score Spearman's r=0.945, p<0.0001; height Spearman's r=0.938, p<0.0001) while the width of the sulcus significantly decreased (Spearman's r=0.647, p<0.0001) (Figure 98E-H). Seven control fetuses showed one grade of asymmetry. There were 4 control fetuses with one grade of asymmetry and 1 control fetus with 2 grades of asymmetry.

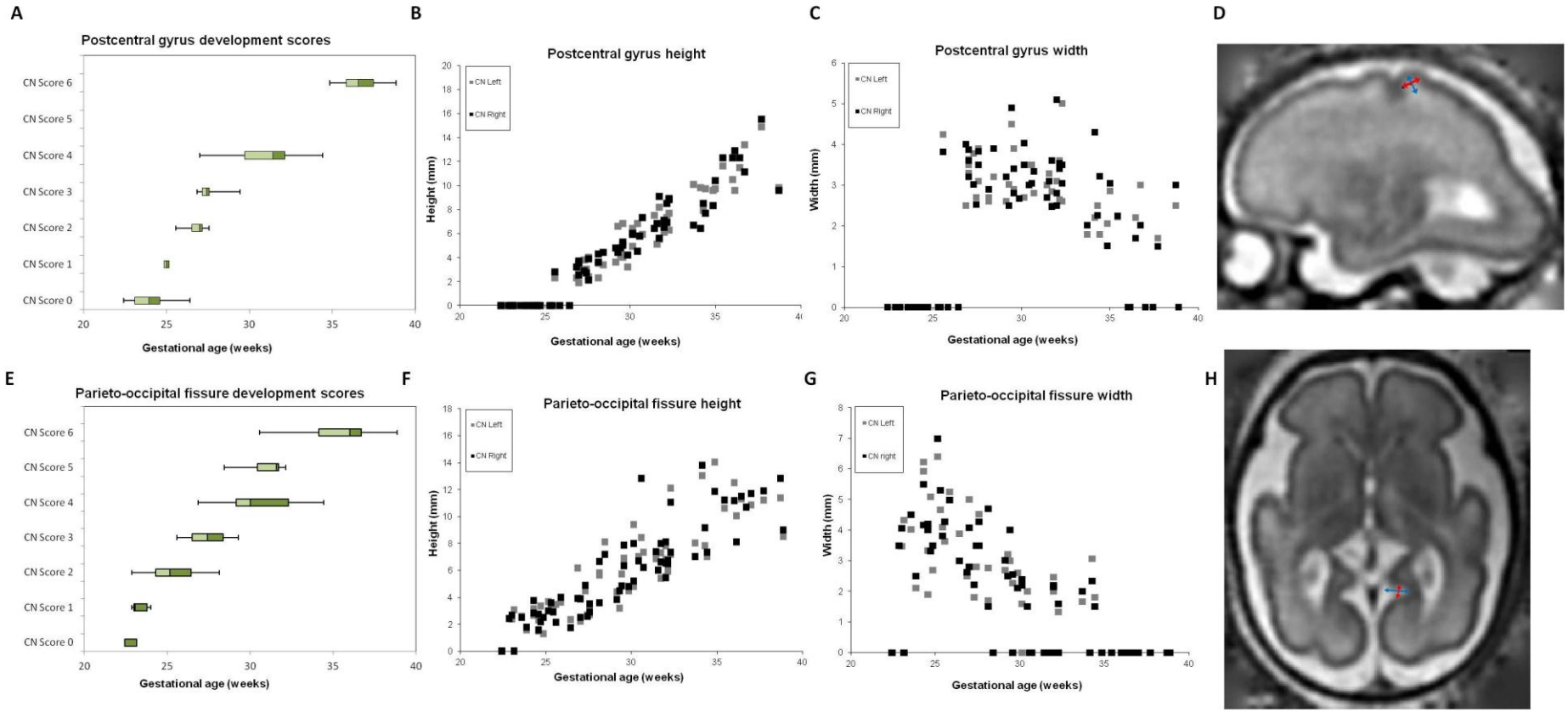


Figure 98. Postcentral gyrus and parieto-occipital fissure development in normal controls

(A-D) Postcentral gyrus development in normal controls (A) Development scores (B) Height, (C) Width, (D) Linear measurements of height (blue) and width (red). Development score ($r=0.945$, $p<0.0001$) and height ($r=0.938$, $p<0.0001$) increased whilst the width decreased with GA ($r=-0.49$, $p<0.001$).

(E-H) Parieto-occipital fissure development in normal controls (E) Development scores (F) Height, (G) Width, (H) Linear measurements of height (blue) and width (red)**.** Development score ($r=0.913$, $p<0.0001$) and height ($r=0.887$, $p<0.0001$) increased whilst the width decreased with GA ($r=-0.679$, $p<0.001$).

3.3.3.5 Temporal lobe

(Superior temporal gyrus, superior temporal sulcus, middle temporal gyrus, inferior temporal gyrus)

In the normal control cohort, the cortical development scores and height of all four landmarks representing the temporal lobe increased with GA. The width of all landmarks decreased although there was a weak correlation with GA and it did not reach significance for the middle temporal and inferior temporal gyrus. Results for the temporal lobe are presented in Figures 99 and 100. There were 4 control fetuses with one grade of asymmetry and 1 control fetus with two grades of asymmetry in the superior temporal gyrus. For the temporal sulcus there were 8 control fetuses with one grade of asymmetry, 2 control fetuses with two grades of asymmetry and 1 control fetus with three grades of asymmetry. For the middle temporal gyrus there were 6 control fetuses with one grade of asymmetry and 1 control fetus with two grades of asymmetry. Lastly for the inferior temporal gyrus there were 4 control fetuses with one grade of asymmetry and 1 control fetus with two grades of asymmetry. In 4 control fetuses asymmetry was present in more than one landmark of the temporal lobe.

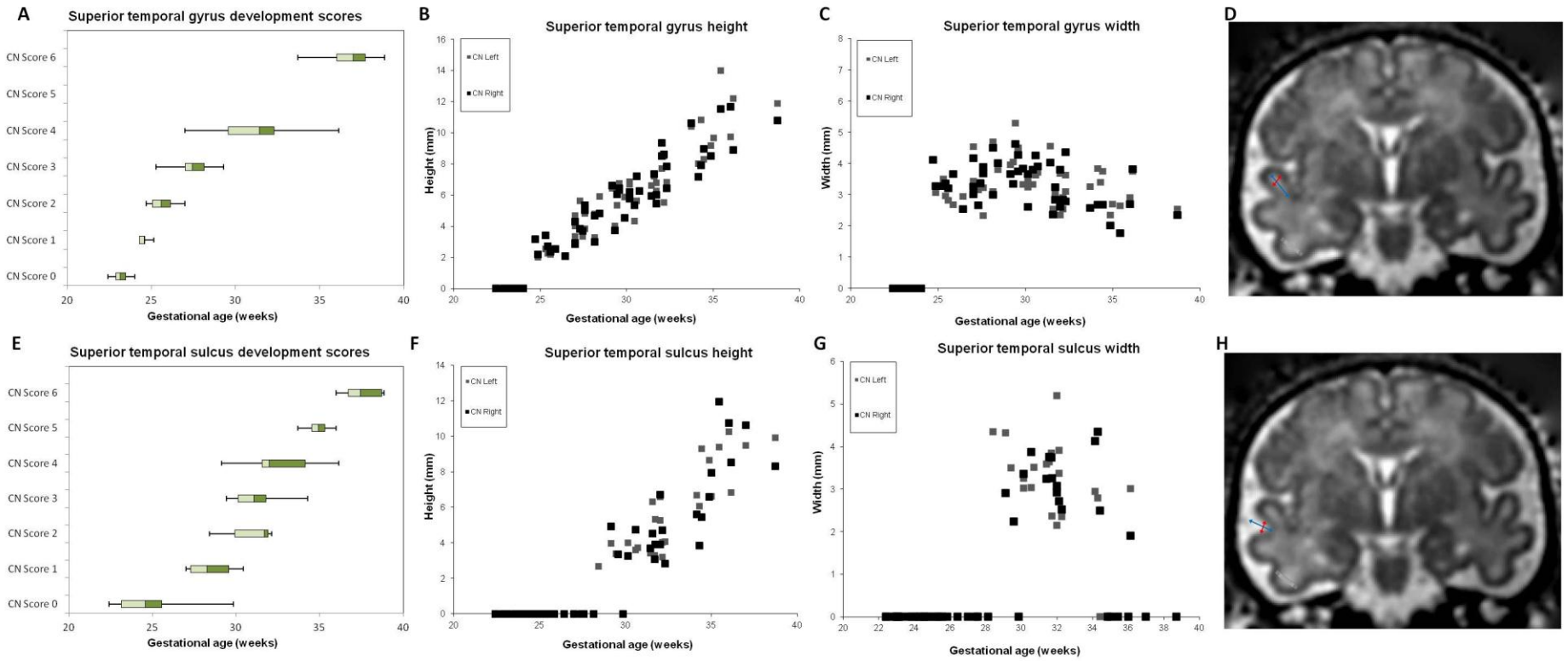


Figure 99. Superior temporal gyrus and superior temporal sulcus development in normal controls

(A-D) Superior temporal gyrus development in normal controls (A) Development scores (B) Height, (C) Width, (D) Linear measurements of height (blue) and width (red). Development score ($r=0.613$, $p<0.0001$) and height ($r=0.922$, $p<0.0001$) increased whilst the width decreased with GA ($r=-0.268$, $p<0.05$).
(E-H) Superior temporal sulcus development in normal controls (E) Development scores (F) Height, (G) Width, (H) Linear measurements of height (blue) and width (red). Development score ($r=0.925$, $p<0.0001$) and height ($r=0.781$, $p<0.0001$) increased whilst the width decreased with GA ($r=-0.28$, $p<0.05$).

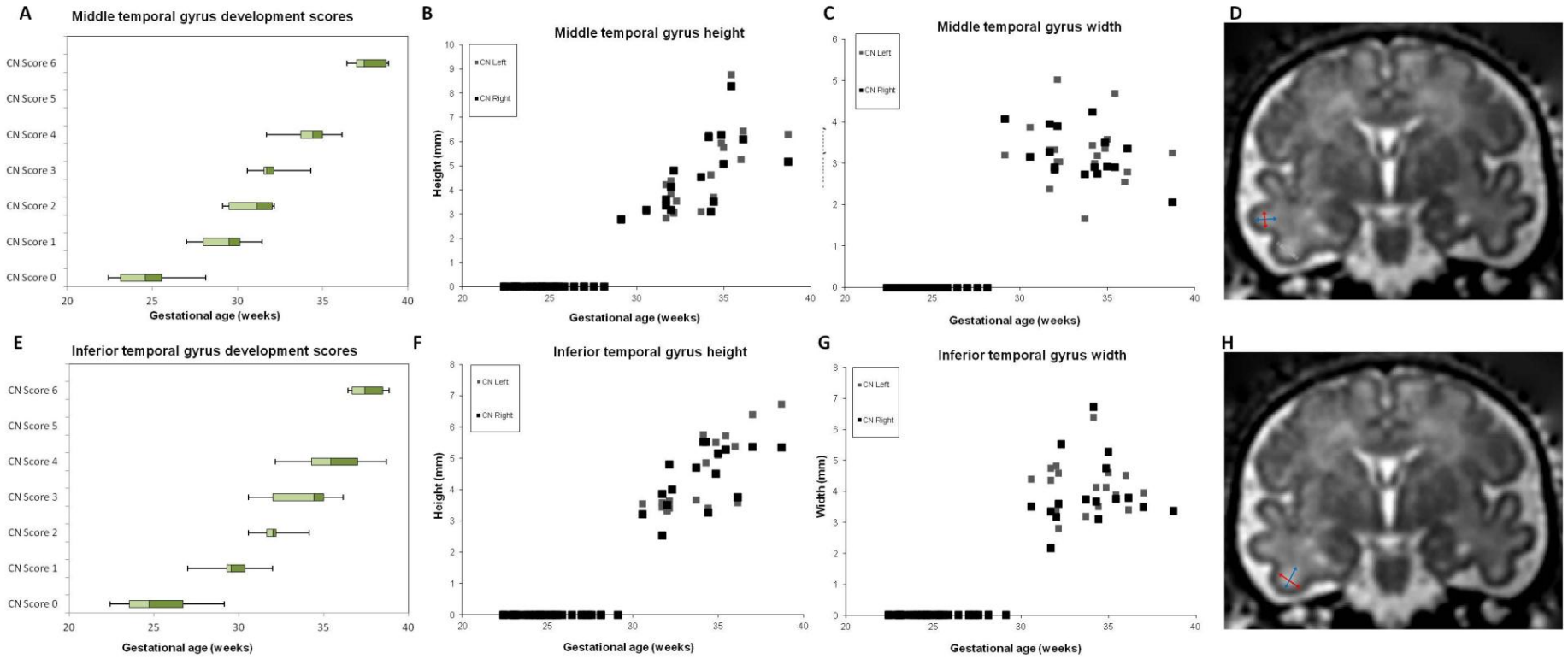


Figure 100. Middle temporal gyrus and inferior temporal gyrus development in normal controls

(A-D) Middle temporal gyrus development in normal controls (A) Development scores (B) Height, (C) Width, (D) Linear measurements of height (blue) and width (red). Development score ($r=0.938$, $p<0.0001$) and height ($r=0.757$, $p<0.0001$) increased whilst the width remained stable with GA ($r=-0.182$, $p>0.05$).
(E-H) Inferior temporal gyrus development in normal controls (E) Development scores (F) Height, (G) Width, (H) Linear measurements of height (blue) and width (red). Development score ($r=0.913$, $p<0.0001$) and height ($r=0.665$, $p<0.0001$) increased whilst the width remained stable with GA ($r=-0.026$, $p>0.05$).

3.3.3.6 Occipital lobe

(Calcarine sulcus)

In the normal control cohort, the cortical development score, calcarine height and length increased with GA (score Spearman's r=0.938, p<0.0001; height Spearman's r=0.771, p<0.0001; length Spearman's r=0.923, p<0.0001) while the width decreased with GA (Spearman's r=-0.521, p<0.0001) (Figure 101A-F). Seven control fetuses had one grade of asymmetry.

3.3.3.7 Limbic lobe

(Cingulate sulcus)

In the normal control cohort, the cingulate sulcus length increased with increasing GA (Spearman's r=0.943,p<0.0001) (Figure 101G-H)**.** There was no significant difference in cingulate sulcus length between the left and right hemispheres (p=0.945).

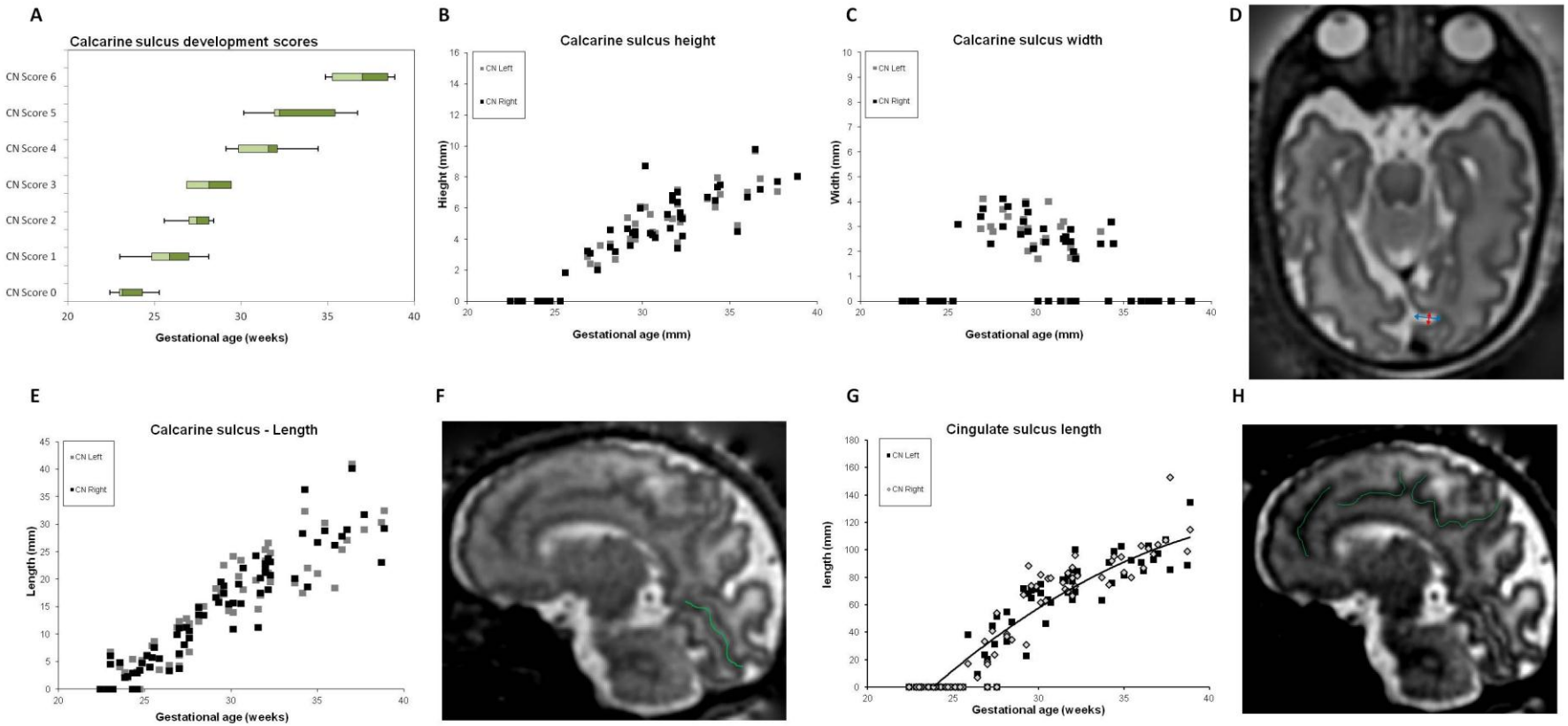


Figure 101. Calcarine sulcus and cingulate sulcus development in normal controls

(A-F) Calcarine sulcus development in normal controls (A) Development scores (B) Height, (C) Width, (D) Linear measurements of height (blue) and width (red), (E) Length, (F) Linear measurement of length (blue). Development score ($r=0.938$, $p<0.0001$) length ($r=0.923$, $p<0.0001$) and height ($r=0.771$, $p<0.0001$) increased whilst the width remained stable with GA ($r=-0.521$, $p<0.0001$).

(G-H) Cingulate sulcus development in normal controls (G) Length, (H) Linear measurements of length (blue). Cingulate sulcus length increased with GA ($r=0.943$, $p<0.0001$).

3.3.4 Comparison with ventriculomegaly cohort

The ventriculomegaly cohort consisted of 63 fetuses scanned at a mean GA of 29.7 weeks and a GA range of 22-37.3 weeks. 14 fetuses were scanned twice during gestation while one fetus was scanned three times.

3.3.4.1 Gestational age of early sulcation

The gestational age at which the individual landmarks had most immature configuration (score 1) in the ventriculomegaly cohort and normal control cohort are presented in a whisker box plot in Figure 102. There was an apparent delayed appearance in the ventriculomegaly cohort of all cortical landmarks assessed, by an average of 2 gestational weeks. The delay was statistically significant for the majority of sulci and gyri with the exception of the central sulcus, superior frontal sulcus, inferior frontal sulcus and superior temporal gyrus in which although a delay in appearance was evident it did not reach statistical significance.

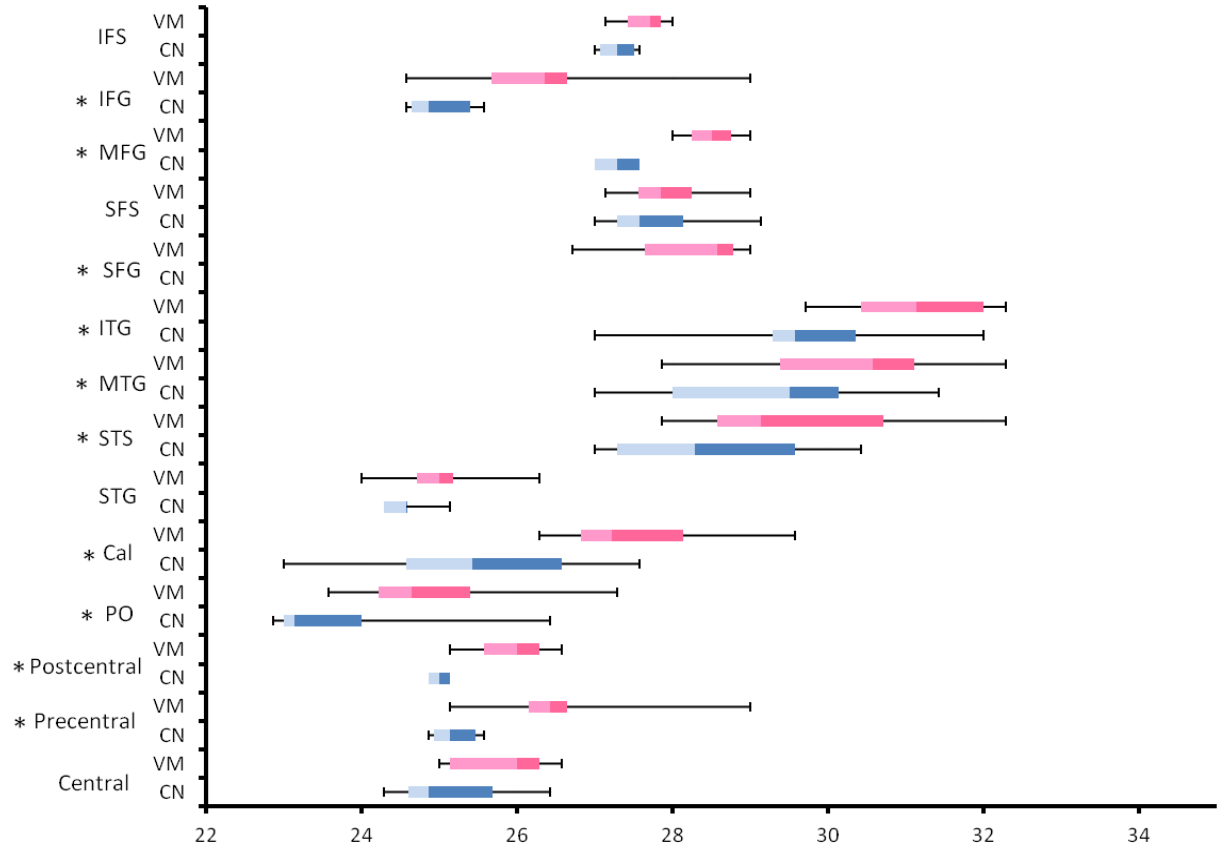


Figure 102. Gestational age of early sulcation (score 1) of cortical landmarks in normal controls (blue) and ventriculomegaly (pink) cohorts

Box plot represents the median (light/dark colour boundary), lower (light colour) and upper (dark colour) quartiles and minimum and maximum values (box plot whiskers).

PO: parieto-occipital fissure, Cal: calcarine, STG: superior temporal gyrus, STS: superior temporal sulcus, MTG: middle temporal gyrus, ITG: inferior temporal gyrus, SFG: superior frontal gyrus, SFS: superior frontal sulcus, MFG: middle frontal gyrus, IFG: inferior frontal gyrus, IFS: inferior frontal sulcus.

The strength of association between development scores and GA for the ventriculomegaly cohort is presented for each cortical landmark in Table 25. Cortical development scores highly correlated with GA and were similar for all areas.

Cortical landmark	Central sulcus	Pre central gyrus	Post central gyrus	Parieto-occipital fissure	Calcarine sulcus	Sylvian fissure ratio	Cingulate length	Superior frontal gyrus
Spearman's r	0.891**	0.944**	0.932**	0.91**	0.926**	0.883**	0.898**	0.925**
Cortical landmark	**Superior frontal sulcus**	**Middle frontal gyrus**	**Inferior frontal gyrus**	**Inferior frontal sulcus**	**Superior temporal gyrus**	**Superior temporal sulcus**	**Middle temporal gyrus**	**Inferior temporal gyrus**
Spearman's r	0.947**	0.937**	0.915**	0.929**	0.864**	0.924**	0.923**	0.894**

Table 25. Correlation of cortical development scores with GA in ventriculomegaly

Correlation was assessed using the Spearman's correlation coefficient (r). * =<0.05 and >0.0001 ** = <0.0001

In the ventriculomegaly cohort, the height of each sulcus and gyrus increased and strongly correlated with GA. The width of different cortical landmarks varied with increasing GA for each landmark as summarised in Table 26.

Cortical landmark	Central sulcus	Pre central gyrus	Post central gyrus	Parieto-occipital fissure	Calcarine sulcus	Superior frontal gyrus	Superior frontal sulcus
Height	0.843**	0.878**	0.931**	0.833**	0.659**	0.626*	0.603*
Width	-0.182	-0.343*	-0.180	-0.776*	-0.532*	0.498*	-0.304
Cortical landmark	**Middle frontal gyrus**	**Inferior frontal gyrus**	**Inferior frontal sulcus**	**Superior temporal gyrus**	**Superior temporal sulcus**	**Middle temporal gyrus**	**Inferior temporal gyrus**
Height	0.829**	0.867**	0.736*	0.963**	0.665**	0.753*	0.767**
Width	0.439*	0.598*	0.055	0.001	-0.382*	-0.763**	-0.077

Table 26. Correlation of height and width of cortical landmarks with GA in ventriculomegaly

Correlation was assessed using the Spearman's correlation coefficient (r). Asterisk indicates significance * p<0.05 and p>0.0001 ** p<0.0001

The cortical development score and linear measurements for each cortical landmark assessed in the control and ventriculomegaly cohorts are presented in Figures 103-110.

3.3.4.2 Frontal lobe

(Precentral gyrus, superior frontal gyrus, superior frontal sulcus, middle frontal gyrus, inferior frontal gyrus, inferior frontal sulcus)

Precentral gyrus

In the ventriculomegaly cohort, the cortical development score and height of the precentral gyrus increased with GA (score Spearman's r=0.944, p<0.0001; height Spearman's r=0.878, p<0.0001) while the width decreased during gestation (Spearmans's r=-0.343, p<0.05). There was a significant difference in GAs in cortical development scores 1 and 2 between ventriculomegaly and control cohorts (p=0.017 and p=0.045 respectively) with higher GA values in the ventriculomegaly cohort (Figure 103A-D). There was no difference in scores 3, 4 and 6 between ventriculomegaly and control cohorts. There were 5 fetuses with ventriculomegaly with one grade asymmetry with 2 fetuses more advanced in the non-ventriculomegaly case. There were 2 fetuses with ventriculomegaly with two grades of asymmetry both more advanced on the ventriculomegaly side. There was no difference in height (p=0.531) or width (p=0.532) of the precentral gyrus between ventriculomegaly and control cohorts.

Superior frontal gyrus

In the ventriculomegaly cohort, the cortical development score, height and width of the superior frontal gyrus increased with GA (score Spearman's r=0.925, p<0.0001; height Spearman's r=0.626, p<0.05; width Spearman's r=0.498, p<0.05). There was no difference in GAs in scores 1, 2, 4 and 6. The ventriculomegaly group had lower GA values in score 3 compared to the control group (p=0.022), however the number of cases was limited (Figure 103E-H). There were 2 fetuses with ventriculomegaly with one grade of asymmetry. One fetus was more advanced on the non-ventriculomegaly side. There was no difference in the height of the superior frontal gyrus between ventriculomegaly and control cohorts (p=0.724). There was a significant difference in the width of the superior frontal gyrus between ventriculomegaly and control cohorts with higher values in the ventriculomegaly group (p=0.001). This difference however was not significant when removing the three outliers (p=0.076).

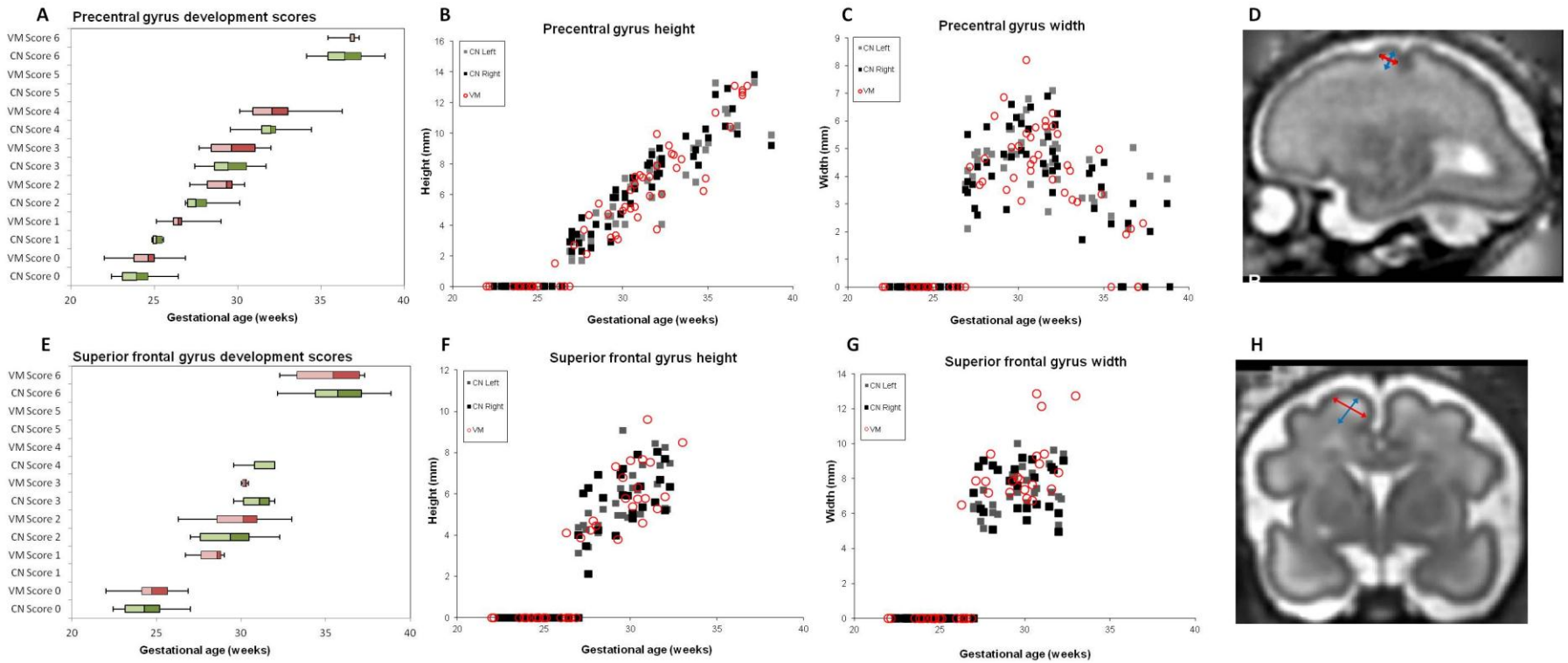


Figure 103. Precentral gyrus and frontal gyrus development in normal control and ventriculomegaly cohorts

(A-D) Precentral gyrus development in normal control (green/black) and ventriculomegaly (red) cohorts (A) Development scores (B) Height, (C) Width, (D) Linear measurements of height (blue) and width (red). There was a significant delay in development scores 1 (p=0.017) and 2 (p=0.045) in the ventriculomegaly cohort. There was no difference in the height (p=0.531) or width (p=0.532) between cohorts.

(E-H) Superior frontal gyrus development in normal control (green/black) and ventriculomegaly (red) cohorts (E) Development scores (F) Height, (G) Width, (H) Linear measurements of height (blue) and width (red). There was a significant difference in score 3 between cohorts although numbers were limited. There was no significant difference in height between cohorts (p=0.724) between cohorts. The width was significantly increased (p=0.001) in the ventriculomegaly cohort, however significance was lost when removing the 3 outliers (0.076).

Data shown include both left and right sides for controls and only the side with the larger ventricle for fetuses with ventriculomegaly.

Superior frontal sulcus

In the ventriculomegaly cohort, the cortical development score and height of the superior frontal sulcus increased with GA (score Spearman's $r=0.947$, $p<0.0001$; height Spearman's $r=0.603$, $p<0.05$) while there was a weak non-significant decrease in the width of the sulcus with GA (Spearman's $r=-0.304$, $p>0.05$). The was no difference in the GA in any of the cortical development scores between ventriculomegaly and control cohorts (Figure 104A-D). There were 3 fetuses with ventriculomegaly with one grade asymmetry with 1 fetus being more advanced on the non-ventriculomegaly side. There was 1 fetus with ventriculomegaly with three grade asymmetry with a higher score on the non-ventriculomegaly side. There was no difference in the height ($p=0.994$) or width ($p=0.451$) of the superior frontal sulcus between ventriculomegaly and control cohorts.

Middle frontal gyrus

In the ventriculomegaly cohort, the cortical development score, height and width of the middle frontal gyrus increased with GA (score Spearman's $r=0.937$, $p<0.0001$; height Spearman's $r=0.829$, $p<0.0001$; width Spearman's $r=0.439$, $p<0.05$). However there was missing data in scores 3 and 4. The ventriculomegaly cohort had significantly higher GA values in score 1 compared to controls ($p=0.016$). The was no difference in GAs in scores 2 and 6 (Figure 104E-H). There were 2 fetuses with ventriculomegaly with one grade asymmetry with the non-ventriculomegaly side being more advanced. There was 1 fetus with ventriculomegaly with a four grade asymmetry more advanced on the non-ventriculomegaly side. There was no difference in the height ($p=0.624$) or width ($p=0.558$) of the middle frontal gyrus between ventriculomegaly and control cohorts.

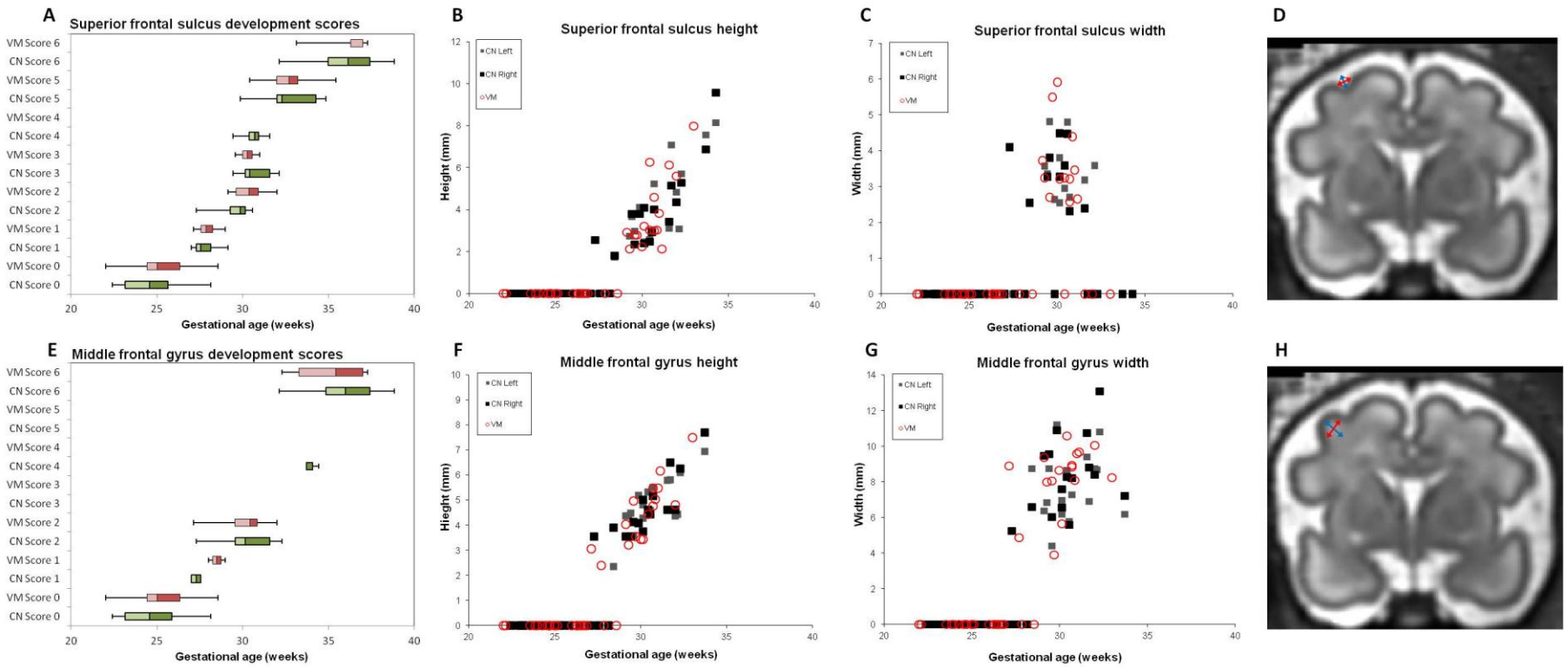


Figure 104. Superior frontal sulcus and middle frontal gyrus development in normal control and ventriculomegaly cohorts

(A-D) Superior frontal sulcus development in normal control (green/black) and ventriculomegaly (red) cohorts (A) Development scores (B) Height, (C) Width, (D) Linear measurements of height (blue) and width (red). There was no difference in development scores ($p>0.05$), height ($p=0.994$) or width ($p=0.451$) between cohorts.

(E-H) Middle frontal gyrus development in normal (green/black) and ventriculomegaly (red) cohorts (E) Development scores (F) Height, (G) Width, (H) Linear measurements of height (blue) and width (red). There was a significant delay in development score 1 in the ventriculomegaly cohort ($p=0.016$). There was no difference in height (0.624) or width ($p=0.558$) between cohorts.

Data shown include both left and right sides for controls and only the side with the larger ventricle for fetuses with ventriculomegaly.

Inferior frontal gyrus

In the ventriculomegaly cohort, the cortical development score, height and width of the inferior frontal gyrus increased with GA (score Spearman's $r=0.915$, $p<0.0001$; height Spearman's $r=0.876$, $p<0.0001$; width Spearman's $r=0.598$, $p<0.05$). There was no difference in GAs in cortical development scores of 2, 3, 4 and 6 between ventriculomegaly and control cohorts (Figure 105A-D). There was a significant difference in GA in score 1 with the ventriculomegaly cohort exhibiting higher GA values ($p=0.048$). There were 2 fetuses with ventriculomegaly with one grade of asymmetry and both were advanced on the non-ventriculomegaly side. There was a significant difference in the height of the inferior frontal gyrus with the ventriculomegaly group having higher values at a mean of 0.68 mm at 27.9 weeks ($p=0.022$). In addition, the ventriculomegaly group had higher width measurements compared to controls at a mean of 0.59 mm ($p=0.022$). When removing the one outlier the significance was lost ($p=0.06$).

Inferior frontal sulcus

In the ventriculomegaly cohort, the cortical development score and height of the inferior frontal sulcus increased with GA while the width remained stable through gestation (score: Spearman's $r=0.929$, $p<0.0001$; height: Spearman's $r=0.736$, $p<0.05$; width: Spearman's $r=0.055$, $p>0.05$). There was no difference in GA in any of the cortical development scores between ventriculomegaly and control cohorts (Figure 105E-H). There were 2 fetuses with ventriculomegaly with one grade asymmetry more advanced on the non-ventriculomegaly side. There was no significant difference in the height ($p=0.681$) or width ($p=0.227$) of the inferior frontal sulcus between ventriculomegaly and control cohorts.

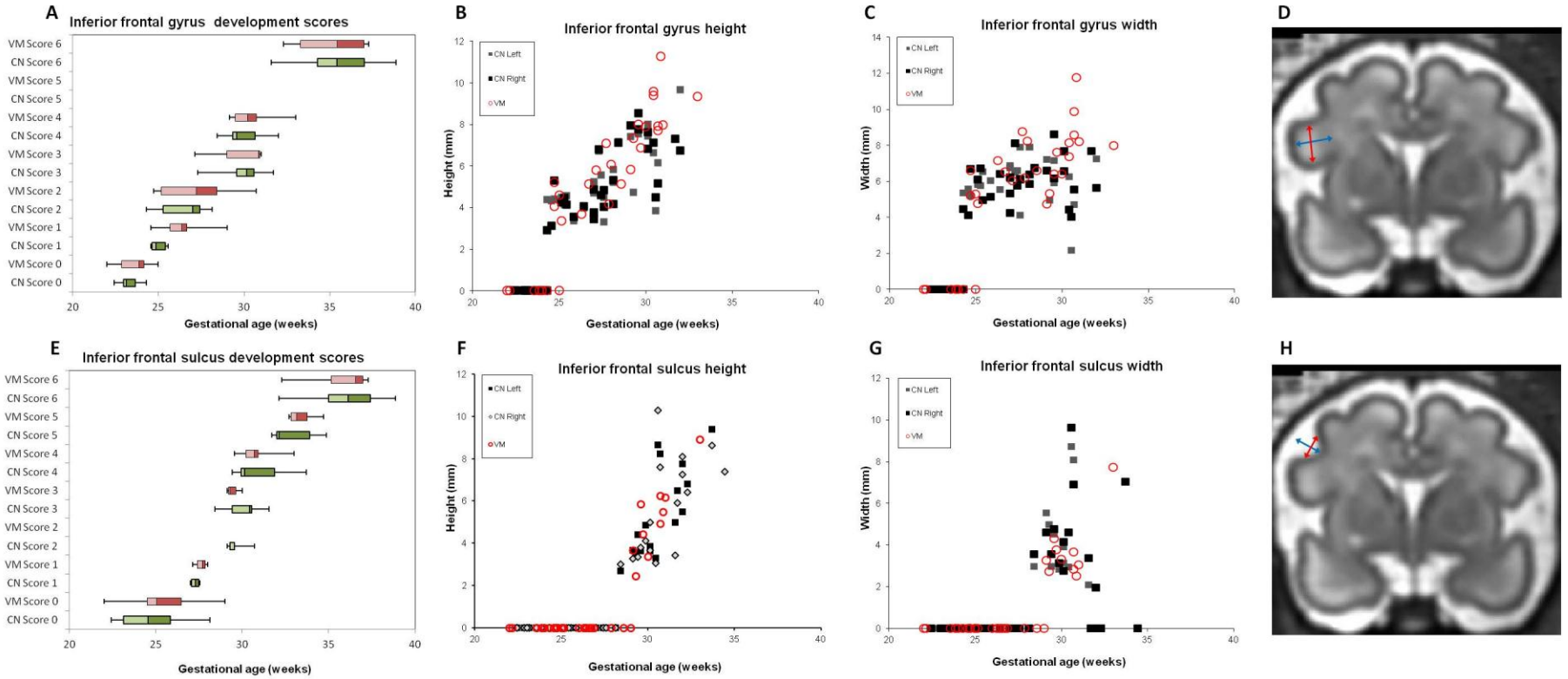


Figure 105. Inferior frontal gyrus and inferior frontal sulcus development in normal control and ventriculomegaly cohorts

(A-D) Inferior frontal gyrus development in normal control (green/black) and ventriculomegaly (red) cohorts (A) Development scores (B) Height, (C) Width, (D) Linear measurements of height (blue) and width (red). There was a significant delay in development score 1 in the ventriculomegaly cohort (p=0.048). The height was significantly increased in the ventriculomegaly cohort (p=0.022). The width was significantly increased (p=0.022) in the ventriculomegaly cohort however significance was lost when removing the 1 outlier (p=0.06).

(E-H) Inferior frontal sulcus development in normal control (green/black) and ventriculomegaly (red) cohorts (E) Development scores (F) Height, (G) Width, (H) Linear measurements of height (blue) and width (red). There was no difference in development scores (p>0.05), height (p=0.681) or width (p=0.227) between cohorts.

Data shown include both left and right sides for controls and only the side with the larger ventricle for fetuses with ventriculomegaly.

3.3.4.3 Frontal/parietal border and frontal/parietal/temporal border

(Central sulcus and Sylvian fissure)

Central sulcus

In the ventriculomegaly cohort, the cortical development score and height of the central sulcus increased with GA (score Spearman's r=0.891, p<0.0001; height Spearman's r=0.843, p<0.0001) whilst the width showed a weak trend for decrease although this was not statistically significant (Spearman's r=-0.182, p>0.05) (Figure 106A-D). Four fetuses with ventriculomegaly had one grade asymmetry while all other fetuses were symmetrical. Two of the 4 fetuses with ventriculomegaly had a lower score on the ventriculomegaly side. When comparing the GAs at each development score the ventriculomegaly cohort had lower GAs for scores 1, 4, 5 and 6. Only score 5 had a significant difference between ventriculomegaly and control cohorts (p=0.0009). Scores 2 and 3 had limited number of cases. There was no significant difference in the height or width of the central sulcus between ventriculomegaly and control cohorts (height p=0.844, width p=0.259).

Sylvian fissure

In the ventriculomegaly cohort, the Sylvian fissure development ratio increased with GA (Spearman's r=0.883, p<0.0001). As the fissure matured the maximum distance from frontal to temporal boundaries along the insula-temporal cortex increased (Spearman's r=0.955, p<0.0001) while the minimum distance frontal to temporal borders of the operculum decreased (Spearman's r=-0.65, p<0.0001). There was no difference between ventriculomegaly and control cohorts in the maximum distance from frontal to temporal boundaries along the insula-temporal cortex (p=0.369) or the development ratio (p=0.106) (figure 106E-H). There was a significant difference (p=0.03) in the minimum distance frontal to temporal borders of the operculum with the ventriculomegaly cohort having higher values. The mean distance at 29.1 weeks in the control group was 11.96 mm while in the ventriculomegaly cohort the mean distance was 12.97 mm.

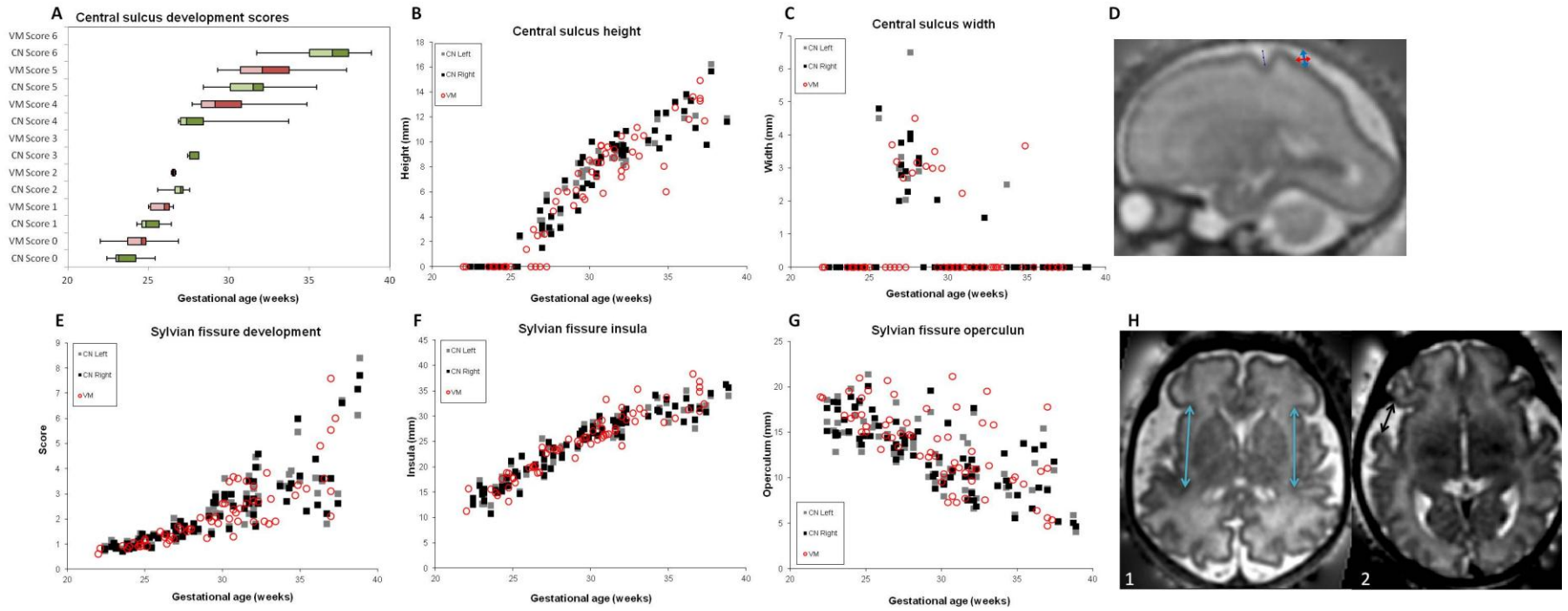


Figure 106. Central sulcus and Sylvian fissure development in normal control and ventriculomegaly cohorts

(A-D) Central sulcus development in normal control (green/black) and ventriculomegaly (red) cohorts (A) Development scores (B) Height, (C) Width, (D) Linear measurements of height (blue) and width (red). There was a significant delay in score 5 in the ventriculomegaly cohort (p=0.009). There was no difference in the height (p=0.844) or width (p=0.259) between cohorts.

(E-H) Sylvian fissure development in normal control (green/black) and ventriculomegaly (red) cohorts (A) Development score representing the ratio of the insula distance to the opercular distance, (B) Insular distance (C) Opercular distance, (H1-H2) Linear measurements of (1) insula (blue) (2) operculum (black). There was no significant difference in the score or insular distance between cohorts. The opercular distance was significantly increased in the ventriculomegaly cohort (p=0.03).

Data shown include both left and right sides for controls and only the side with the larger ventricle for fetuses with ventriculomegaly.

3.3.4.4 Parietal lobe

(postcentral gyrus, parieto-occipital fissure)

Postcental gyrus

In the ventriculomegaly cohort, the development score and height of the postcentral gyrus increased with GA (score Spearman's r=0.932, p<0.0001; height Spearman's r=0.931, p<0.0001) while the width of the gyrus showed a weak non-significant decrease (Spearman's r=-0.18, p>0.05) (Figure 107A-D). There were 7 fetuses with ventriculomegaly with one grade of asymmetry with the lower scores on the ventriculomegaly side. There were 6 fetuses with ventriculomegaly with two grades of asymmetry with the lower score on the ventriculomegaly side. There was 1 fetus with ventriculomegaly with 3 grades of asymmetry with the lower score on the ventriculomegaly side. When comparing between ventriculomegaly and control cohorts, the GAs in each development score were higher in the ventriculomegaly group. The ventriculomegaly cohort showed a delay in appearance of each score however this reached significance only in scores 1 and 4. There was no significant difference in the height (p=0.138) or width (p=0.61) of the postcentral gyrus between ventriculomegaly and control cohorts.

Parieto-occipital fissure

In the ventriculomegaly cohort, the development score and height of the parieto-occipital increased with GA (score Spearman's r=0.91, p<0.0001; height Spearman's r=0.833, p<0.0001) while the width decreased with GA (Spearman's r=-0.776, p<0.05) (Figure 107E-H). There were 4 fetuses with ventriculomegaly with one degree of asymmetry with 2 more advanced on the non-ventriculomegaly side. There was 1 fetus with ventriculomegaly with 2 degrees of asymmetry with the ventriculomegaly side being more advanced. When comparing between ventriculomegaly and control cohorts, the GAs in each development were higher in the VM group. Significance was reached for scores 1, 2, 3 and 5. The height of the fissure was significantly decreased in the ventriculomegaly group by an average of 0.6 mm at 30.2 weeks. The width of the fissure was significantly increased in the ventriculomegaly cohort by an average of 0.8 mm at 28.4 weeks.

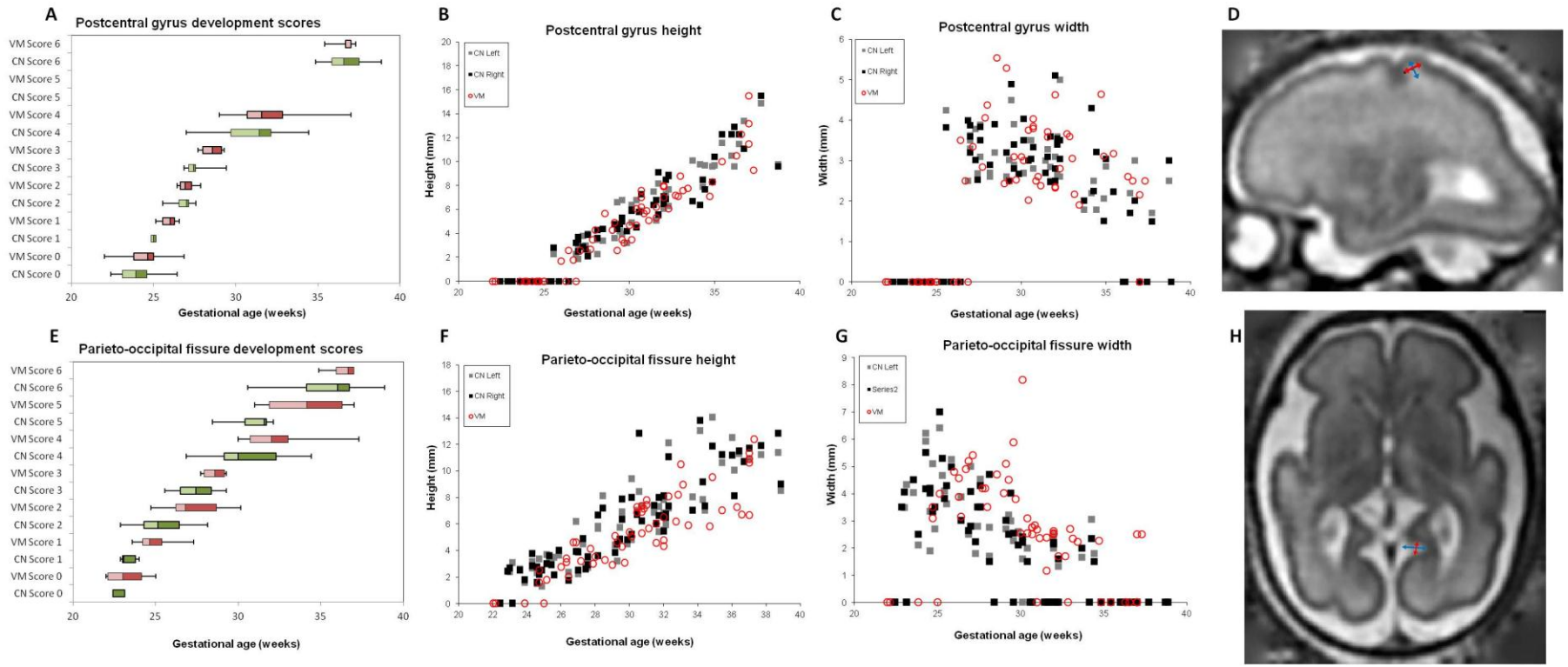


Figure 107. Postcentral gyrus and parieto-occipital fissure development in normal control and ventriculomegaly cohorts

(A-D) Postcentral gyrus development in normal control (green/black) and ventriculomegaly (red) cohorts (A) Development scores (B) Height, (C) Width, (D) Linear measurements of height (blue) and width (red). There was a significant delay in scores 1 ($p=0.054$) and 4 ($p=0.053$) in the ventriculomegaly cohort. There was no difference in the height ($p=0.138$) or width ($p=0.61$) between cohorts.

(E-H) Parieto-occipital fissure development in normal control (green/black) and ventriculomegaly (red) cohorts (E) Development scores (F) Height, (G) Width, (H) Linear measurements of height (blue) and width (red). There was a significant delay in scores 1 ($p=0.004$), 2 ($p<0.0001$), 4 ($p=0.007$) and 5 ($p<0.0001$). The height was significantly reduced ($p=0.012$) whilst the width was significantly increased ($p<0.0001$) in the ventriculomegaly cohort.

Data shown include both left and right sides for controls and only the side with the larger ventricle for fetuses with ventriculomegaly.

3.3.4.5 Temporal lobe

(superior temporal gyrus, superior temporal sulcus, middle temporal gyrus, inferior temporal gyrus)

In the ventriculomegaly cohort, the development score and height of all landmarks of the temporal lobe increased with GA. The width of the superior temporal sulcus and gyrus decreased with GA while the width of the superior and inferior temporal gyri remained stable with increasing GA. Results for the temporal lobe are presented in Figures 108-109.

Superior temporal gyrus

In the superior temporal gyrus, the ventriculomegaly cohort had higher GAs at scores 1, 2 and 4, with only score 4 being significant (Figure 108A-D). In score 3 the ventriculomegaly cohort had lower GA values that controls and score 6 did not have sufficient numbers to compare. There was one grade asymmetry in 4 fetuses with ventriculomegaly all more advanced on the non-ventriculomegaly side. There was 1 fetus with ventriculomegaly with two grade asymmetry more advanced on the non-ventriculomegaly side. There was no difference in the height ($p=0.783$) of the superior temporal gyrus between ventriculomegaly and control cohorts while the difference in width measurements was borderline significant ($p=0.057$) with the higher values in the ventriculomegaly group. The average width in the control group at 30.4 weeks was 3.27 mm and in the ventriculomegaly group 3.51 mm.

Superior temporal sulcus

In the superior temporal sulcus, there was no difference in GAs between cohorts in the different cortical development scores except for score 1 ($p=0.037$) (Figure 108E-H). There were 6 fetuses with ventriculomegaly with one grade asymmetry, out of which 5 were more advanced on the non-ventriculomegaly side. There was 1 fetus with ventriculomegaly with a three grade asymmetry more advanced on the non-ventriculomegaly side. There was no difference in the height ($p=0.109$) or width ($p=0.693$) of the superior temporal sulcus between ventriculomegaly and control cohorts.

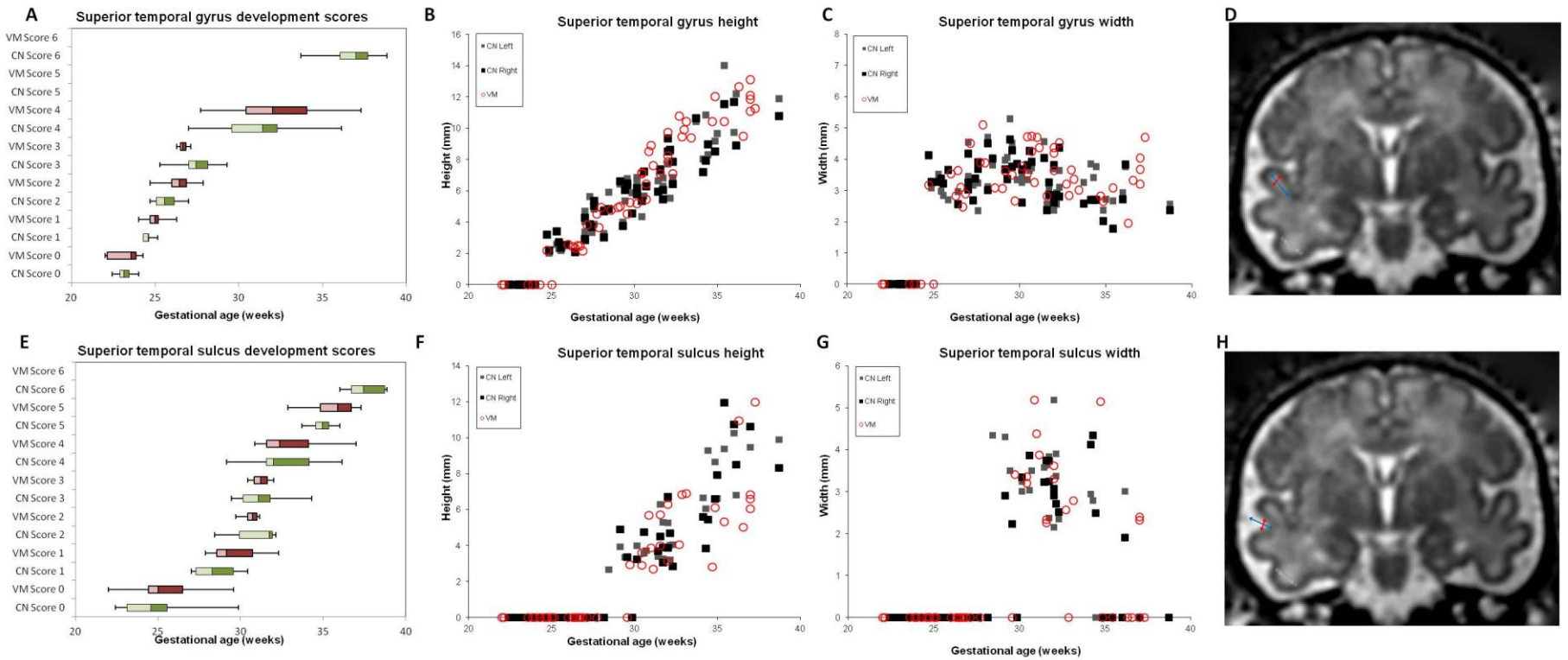


Figure 108. Superior temporal gyrus and superior temporal sulcus development in normal control and ventriculomegaly cohorts

(A-D) Superior temporal gyrus development in normal control (green/black) and ventriculomegaly (red) cohorts (A) Development scores (B) Height, (C) Width, (D) Linear measurements of height (blue) and width (red). There was a significant delay in score 5 (p=0.035) in the ventriculomegaly cohorts. There was no significant difference in height (p=0.783) whilst the width was increased (p=0.057) in the ventriculomegaly cohort.

(E-H) Superior temporal sulcus development in normal control (green/black) and ventriculomegaly (red) cohorts (E) Development scores (F) Height, (G) Width, (H) Linear measurements of height (blue) and width (red). There was a significant delay score 1 in the ventriculomegaly cohort. There was no difference in the height (p=0.109) or width (p=0.693) between cohorts.

Data shown include both left and right sides for controls and only the side with the larger ventricle for fetuses with ventriculomegaly.

Middle temporal gyrus

In the middle temporal gyrus, the ventriculomegaly cohort had higher GA values in scores 1 (p=0.021) and 4 (p=0.01) while there was no difference in scores 2, 3 and 5 (p=0.93, p=0.64, p=0.48 respectively) (Figure 109A-D). There were 7 fetuses with ventriculomegaly with one grade asymmetry, 5 of which were more advanced on the non-ventriculomegaly side. There was 1 fetus with ventriculomegaly with two grade asymmetry more advanced on the ventriculomegaly side. There was no difference in the height (p=0.299) or width (p=0.329) of the middle temporal gyrus between ventriculomegaly and control cohorts.

Inferior temporal gyrus

In the inferior temporal gyrus, the ventriculomegaly cohort had higher GA values in scores 1 and 4 (significant for score 1). There were 8 fetuses with ventriculomegaly with one grade asymmetry, in 7 of which the non-ventriculomegaly side was more advanced (Figure 108E-H). There was a significant difference in the height of the inferior temporal gyrus (p=0.004) with a mean difference of 0.64 mm at 34 weeks. There was no difference in the width of the inferior temporal gyrus between ventriculomegaly and control cohorts (p=0.332).

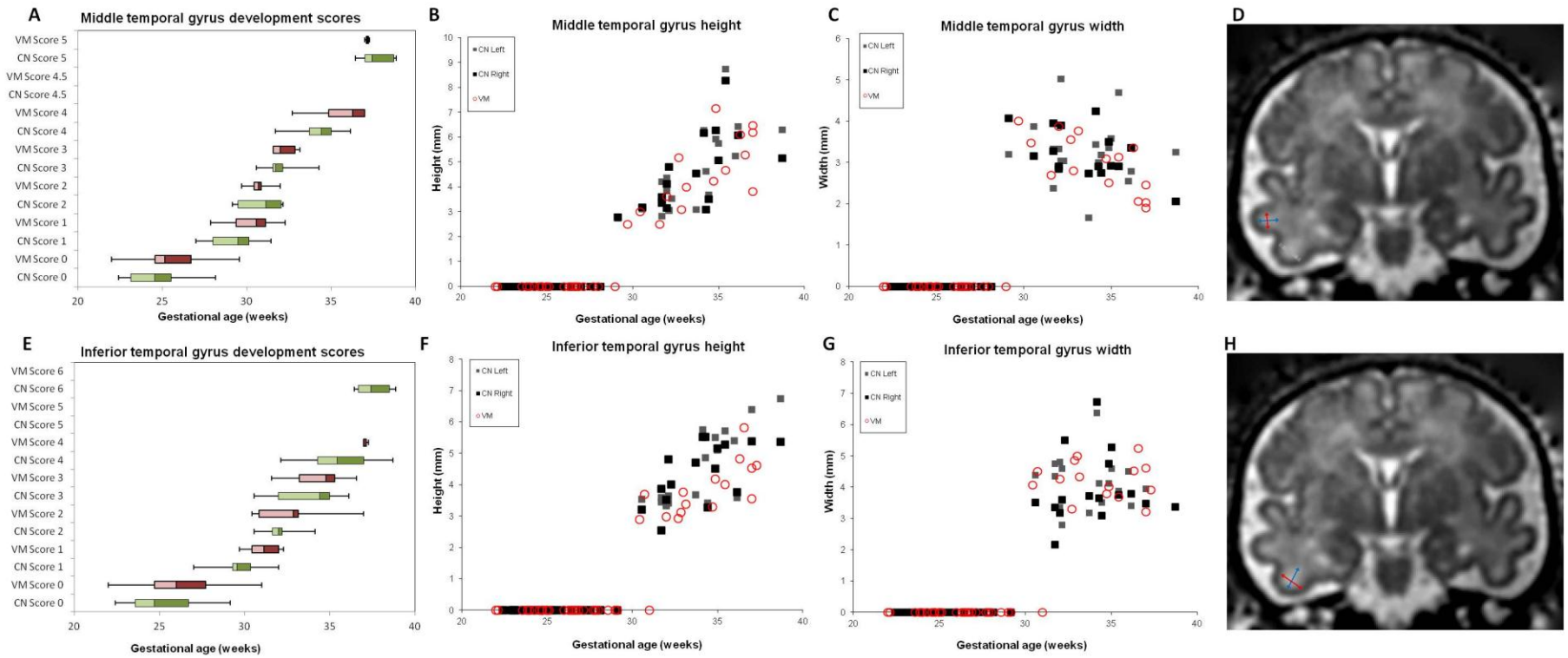


Figure 109. Middle temporal gyrus and inferior temporal gyrus development in normal control and ventriculomegaly cohorts

(A-D) Middle temporal gyrus development in normal control (green/black) and ventriculomegaly (red) cohorts (A) Development scores (B) Height, (C) Width, (D) Linear measurements of height (blue) and width (red). There was a delay in scores 1 (p=0.021) and 4 (p=0.01) in the ventriculomegaly cohort. There was no difference in height (p=0.299) or width (p=0.329) between cohorts.

(E-H) Inferior temporal gyrus development in normal control (green/black) and ventriculomegaly (red) cohorts (E) Development scores (F) Height, (G) Width, (H) Linear measurements of height (blue) and width (red). There was a delay in score 1 (p=0.003) in the ventriculomegaly cohort. The height was significantly reduced (p=0.004) in the ventriculomegaly cohort whilst there was no difference in the width between cohorts.

Data shown include both left and right sides for controls and only the side with the larger ventricle for fetuses with ventriculomegaly.

3.3.4.6 Occipital lobe

(Calcarine sulcus)

In the ventriculomegaly cohort, the development score and height of the calcarine sulcus increased with GA (score Spearman's r=0.926, p<0.0001; height Spearman's r=0.0.659, p<0.0001) while the width decreased (Spearman's r=-0.532, p<0.05) (Figure 110A-F). There were 13 fetuses with ventriculomegaly with one grade of asymmetry with 12 being more advanced on the non-ventriculomegaly side. There were 2 fetuses with ventriculomegaly with two grades of asymmetry, both more advance on the non-ventriculomegaly side.

When comparing between ventriculomegaly and control cohorts, the GAs in development scores 1, 2, 3 and 4 were higher in the ventriculomegaly group. There was no difference in score 5 while in score 6 there were insufficient numbers in the ventriculomegaly cohort. Score 3 had a clear difference between ventriculomegaly and control cohorts however significance was borderline (p=0.06). There was no difference in the height of the sulcus (p=0.126), however the width was significantly larger in the ventriculomegaly cohort by 0.8 mm at 30^{+5} weeks.

3.3.4.7 Limbic lobe

(Cingulate sulcus)

In the ventriculomegaly cohort, the cingulate sulcus length increased with increasing GA (Spearman's r=0.898, p<0.0001)**.** There was no difference in length between the groups (p=0.474) (Figure 110G-H).

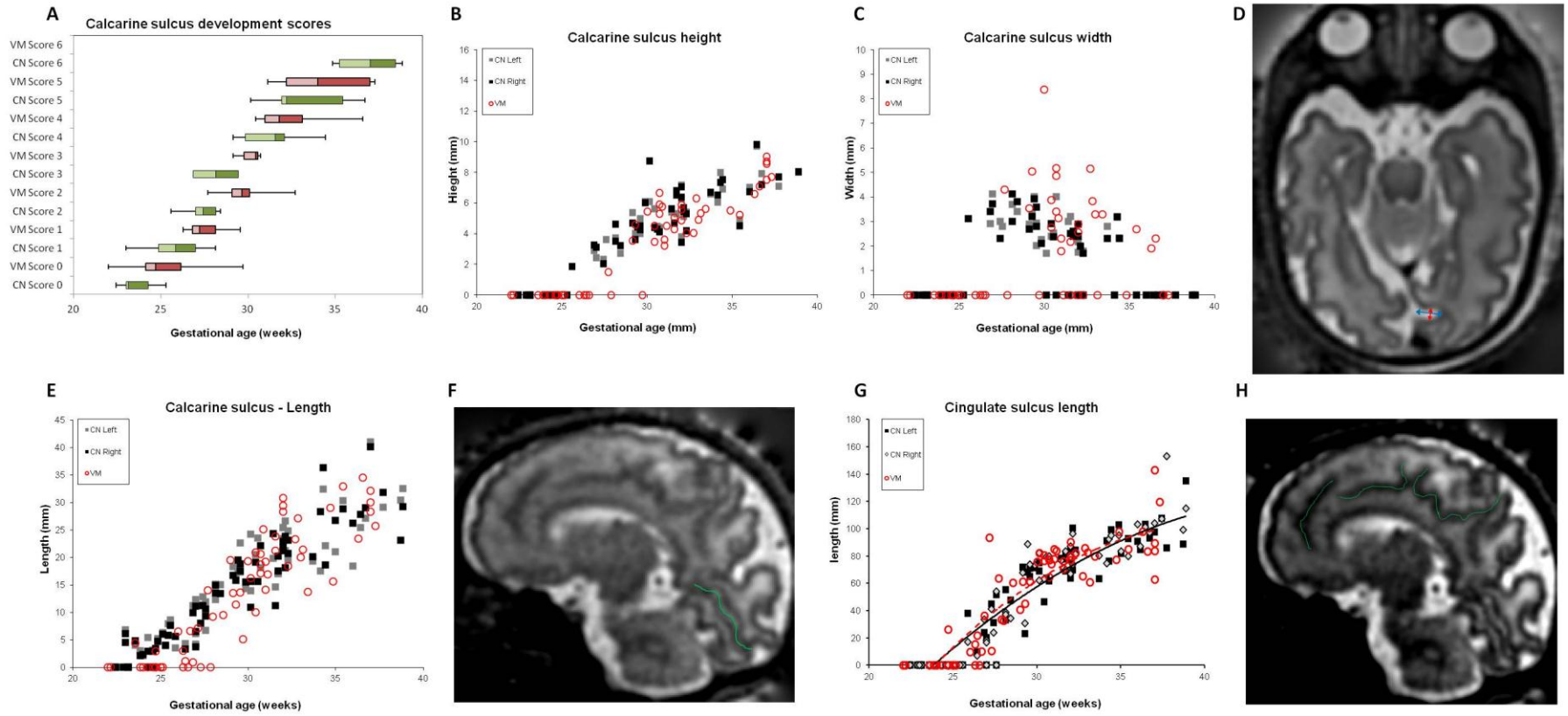


Figure 110. Calcarine sulcus and cingulate sulcus development in normal control and ventriculomegaly cohorts

(A-F) Calcarine sulcus development in normal control (green/black) and ventriculomegaly (red) cohorts (A) Development scores (B) Height, (C) Width, (D) Linear measurements of height (blue) and width (red), (E) Length, (F) Linear measurement of length (blue). There was no difference in the length of the cingulate sulcus between cohorts (p=0.474).

(G-H) Cingulate sulcus development in normal control (black) and ventriculomegaly (red) cohorts (G) Length, (H) Linear measurements of length (blue). There was a significant delay in scores 1 (p=0.0004), 2 (p=0.004) 3 (p=0.06), and 4 (p=0.047) in the ventriculomegaly cohort. There was no significant difference in the length (p=0.158) or height (p=0.126) between cohorts. The width was significantly increased (p=0.0002) in the ventriculomegaly cohort.
Data shown include both left and right sides for controls and only the side with the larger ventricle for fetuses with ventriculomegaly.

3.3.5 Statistics

To access the strength of the association between the development score and GA, Spearman correlation coefficient (r) was used. Degrees/grades of asymmetry refer to the number of difference in score between hemispheres. Cortical asymmetry in the ventriculomegaly cohort was assessed only in the unilateral cases. All measurements were performed by the same examiner (VK) to exclude confounding factors of inter-observer variability. To ensure reproducibility between the same examiner, 40 linear measurements (including height and width) of the superior temporal gyrus were performed twice. The ICC was calculated at 0.969 ($p<0.0001$) indicated excellent reproducibility of measurements. Between group comparisons were performed using ANOVA. Detailed results presented so far in this chapter are not corrected for multiple comparisons.

3.3.5.1 Correction for multiple comparisons

In order to correct for multiple comparisons performed and minimise the Type-1 error the Bonferroni correction was applied to the results of the cortical analysis by multiplying all p values by the total number of measurements performed (n=32). The results prior to and after correction are presented in Table 27. When comparing between cohorts and applying the Bonferroni correction significance remained for the width and score 2 of the parieto-occipital fissure and for the width, score 1 and score 2 for the calcarine sulcus.

	Linear measurements			Development scores					
Cortical landmarks	**Height**	**Width**	**Length**	**score 1**	**score 2**	**score 3**	**score 4**	**score 5**	**score 6**
Central sulcus	NS	NS	n/a	NS	NS	NS	NS	0.009	NS
Precentral gyrus	NS	NS	n/a	0.017	0.045	NS	NS	n/a	NS
Postcentral gyrus	NS	NS	n/a	0.054	NS	NS	0.053	n/a	NS
Parieto-occipital fissure	0.008	**0.00002**	n/a	0.054	**0.0001**	NS	0.007	0.019	NS
Superior frontal gyrus	NS	NS	n/a	NS	NS	0.022	NS	n/a	NS
Superior frontal sulcus	NS	NS	n/a	NS	NS	NS	NS	NS	NS
Middle frontal gyrus	NS	NS	n/a	0.016	NS	NS	NS	NS	NS
Inferior frontal gyrus	0.043	NS	n/a	0.048	NS	NS	NS	n/a	NS
Inferior frontal sulcus	NS	NS	n/a	NS	NS	NS	NS	NS	NS
Superior temporal gyrus	NS	0.057	n/a	NS	NS	NS	0.035	n/a	NS
Superior temporal sulcus	NS	NS	n/a	0.037	NS	NS	NS	NS	NS
Middle temporal gyrus	NS	NS	n/a	0.021	NS	NS	0.01	n/a	NS
Inferior temporal gyrus	0.004	NS	n/a	0.003	NS	NS	NS	n/a	NS
Calcarine sulcus	NS	**0.001**	NS	**0.0004**	**0.001**	0.022	0.041	NS	NS
Cingulate length	n/a	n/a	NS	n/a	n/a	n/a	n/a	n/a	n/a

Table 27. Inter-group comparisons of cortical measurements

P values for inter-group comparisons of linear measurements and development scores not corrected for multiple comparisons. Results that remain significant after Bonferroni correction are highlighted in red. NS non-significant ($p>0.05$), n/a not available (measurement was not performed).

3.3.6 Discussion

In this study, we describe regional differences in cortical development between fetuses with isolated ventriculomegaly and control fetuses. Between 22 and 38 weeks of gestation there were differences in gyrification in cortical regions including a delayed appearance of cortical gyri and sulci representative of each brain lobe. The major differences in cortical maturation that persisted throughout gestation were detected in the calcarine sulcus and parieto-occipital fissure although a delay was evident throughout the cerebral cortex but did not reach significance. More cortical asymmetries between hemispheres were detected for the calcarine sulcus in the ventriculomegaly cohort with the ventriculomegaly side being more delayed. The Sylvian fissure showed aberrant development with a significant increase in the opercular distance length.

Normal controls

The process of development and maturation of gyri and sulci can be quantified/documented in the fetus using the revised cortical development scheme which appropriately depicts gradual stages of cortical folding and maturation as indicated by the highly significant correlation values between development scores and GA. This individual delineation of sulci and gyri allows the detection of a differential temporal maturation pattern related to brain spatial location. Our findings on the timescale of gyrification corroborate previous *in vivo* studies although not all landmarks assessed in our study are included in previous imaging studies (Fogliarini et al., 2005; Garel, 2004; Levine and Barnes, 1999; Pistorius et al., 2010). Some variation exists which may be due to the strict anatomic criteria used in our study. Gyrification scoring and measurements were performed on specific image slices to achieve consistency between measurements and obtain comparable results. In addition variation amongst studies may be due to inaccuracies in the determination of gestational ages, small cohorts and inclusion of twin pregnancies. A simplified but accurate way for scoring normal development would be a visual score of several sulci or gyri at each gestational age.

The earliest appearing landmark which was already present at 22 weeks was the Sylvian fissure which is recognisable at around 14 weeks as a smooth lateral depression (primary Sylvian fissure) (Toi et al., 2004). As the temporal and parietal lobes form and enlarge they

overgrow the insula, a process known as operculisation which proceeds in a well-defined manner. By term, the insular is completely embedded by the operculum (Chen et al., 1996). The second appearing landmark was the parieto-occipital fissure which appeared at week 23 weeks of gestation and between 34-36 weeks complex folds had started to appear. The appearance of the parieto-occipital fissure was followed by the superior temporal gyrus which was the earliest appearing cortical landmark in the anterior part of the temporal lobe at week 24. The remaining landmarks of the temporal lobe, including the inferior and middle temporal gyri and superior temporal sulcus, do not appear until weeks 27-30. Between 24-27 weeks the calcarine begins to form which is followed by the appearance of the postcentral gyrus and central sulcus at weeks 24-25 and the precentral gyrus at week 26. At weeks 24-25 the inferior frontal gyrus also starts to form while the rest of the frontal lobe landmarks including the inferior and superior frontal sulci and middle frontal gyrus all start to form at weeks 27-28. The latest appearing landmarks include the inferior and middle temporal gyri and superior temporal sulcus which start to form at weeks 27-30. The cingulate sulcus which was assessed using the full length of the sulcus appears at approximately 27-29 weeks and forms in a posterior to anterior manner. The asynchronous development of the cortex may reflect differential development of underlying white matter connections during the fetal period.

Isolated ventriculomegaly

When comparing the gestational age of the early form of each cortical landmark between cohorts, the ventriculomegaly cohort showed delayed appearance of all cortical landmarks studied although significance was not reached for the inferior and superior frontal and central sulci. Interestingly altered cortical development was not restricted to the regions proximal to the ventricular dilatation suggesting altered global brain development. However, except for the calcarine and parieto-occipital fissure we were not able to establish whether cortical maturation delay persisted throughout gestation in all brain regions because of the time required for full maturation of each sulcus. It is evident that a delay in reaching different developmental scores was present however statistical significance was not achieved in many cases. The data may be suggestive of delay in cortical maturation throughout gestation however this would have to be confirmed in a larger sample size. In addition as there is

normal variability in the appearance of cortical folding in normal fetuses this introduced 'noise' into the data not allowing for statistical significance to be achieved with small numbers. Alteration in the shape of cortical regions was detected for the calcarine sulcus (width), parieto-occipital fissure (height and width), inferior frontal gyrus (height), superior temporal gyrus (width), and inferior temporal gyrus (height). There was no obvious alteration in shape detected on visual assessment. A delay in cortical development score may be accompanied by an increased width and/or decreased height of the landmarks. These results are consistent with a delay in the maturation of the different cortical regions with the exception of the inferior frontal gyrus where the height of the gyrus was significantly higher in the ventriculomegaly cohort.

The Bonferroni correction was applied to correct for multiple comparisons and significant differences remained in the calcarine and parieto-occipital landmarks. Although the Bonferroni is a conservative approach for correction it may be inappropriate to assume that individual cortical sulci and gyri are developing independent to each other. The data suggest that there are significant changes in cortical folding more prominent in the calcarine and parieto-occipital areas.

There have been few studies reporting cortical gyrification differences between high-risk and control cohorts. The mean time lag of appearance of cortical landmarks between ventriculomegaly and control cohorts observed in our study was approximately 2 weeks. There was some overlap between cohorts in the GA range as shown in the mean and SD plots presented in the Appendix 6.5. Levine and Barnes (1999) compared the gestational age of appearance of different cortical regions in 9 fetuses with isolated mild ventriculomegaly on MRI with the expected age of appearance based on neuroanatomical studies. Similar to our study, they reported a 2-week mean lag in the time of appearance of the cortical regions studied. Scott et al. (2012) used curvature analysis to compare cortical development in 16 fetuses with isolated ventriculomegaly (10-15 mm) and 16 controls over a gestational age period of 22-25.5 weeks. They reported reduced cortical folding only in the parieto-occipital fissure in fetuses with ventriculomegaly but the lack of difference in cortical regions identified in comparison to our study may be due to the limited gestational period studied.

When reviewing our data during the gestational period 22-25.5 weeks a difference in the age of appearance was only observed in the parieto-occipital fissure as the majority of cortical folds have not yet appeared. Cortical development has also been assessed in preterm infants as a substrate for neurodevelopment impairment and studies have shown delayed cortical development at term equivalent age (Ajayi-Obe et al., 2000; Kapellou et al., 2006).

Fetuses with ventriculomegaly also exhibited altered development of the Sylvian fissure. While there was no difference in the length of the insula, the open distance length of the operculum was larger in the ventriculomegaly cohort. If the increased opercular distance was simply an effect of an enlarged brain it would be expected that the insular distance would be increased as well giving a stable ratio and therefore similar maturational status. Our results suggest altered development of the operculum in fetuses with ventriculomegaly. Increased interopercular distance ('open operculum') accompanied with a normal insular and normal appearing frontal lobe has been described as the most common opercular abnormality by Chen et al. (1996) in 58 infants presenting with macrocephaly, microcephaly, seizures, developmental delay and tonal abnormalities. The authors reported that there were no other associated cerebral abnormalities while 50 cases did not have an obvious underlying disease. Because the operculum encompasses regions involved in language, speech, auditory and secondary somatic sensory and motor function aberrant development or malformation at this area may cause impairments with developmental delay (Barkovich et al., 1992; Chen et al., 1996). It is unclear whether the changes in cortical development detected in our study have a functional impact on the later neurodevelopment of these children, long-term outcome studies are required to investigate an association.

Regional delays in gyrification may indicate abnormal cortical development and a neurobiological substrate for neurodevelopmental deficits in children with antenatal ventriculomegaly. As discussed previously there have been several theories regarding the mechanisms of cortical folding. The tension-based theory supports that cortical folding is an effect of mechanical tension excreted by white matter fibre bundles (VanEssen, 1997). Cortical regions that are strongly interconnected are "pulled together" leading to the formation of sulci. Imaging studies however support that white matter fibre endings

concentrate on gyri and growing axons result in expansion of the gyral regions in tangenital directions (Nie et al., 2011). Although there is a debate regarding the precise underlying mechanisms of cortical folding, it is agreed that white matter fibre and synaptic development play an important role in the fine-tuning of cortical development. Thus our data on altered cortical development may reflect abnormal cortical connectivity as a substrate for later impairment.

3.4 Assessment of metabolite ratios during gestation

3.4.1 Background

Fetal brain development involves changes in biochemistry as well as morphology and ^{1}HMRS is an invaluable tool for studying the *in vivo* metabolism in normal development and pathology. However little is known about the biochemical changes that occur during fetal brain development due to the technical limitations of ^{1}HMRS which include fetal motion. In this chapter we have used an optimised approach to quantify the metabolic changes occurring during normal development in fetuses from 22 to 38 weeks of gestation and compare these with changes in metabolism associated with isolated ventriculomegaly. Data were obtained at three different echo times of 42msec, 136msec and 270msec to allow for detection and quantification of different metabolites

3.4.2 Aim

To assess differences in brain metabolite ratios between fetuses with isolated ventriculomegaly and normal fetuses at three different echo times.

3.4.3 Reproducibility

The 136ms echo time datasets in the normal control cohort were analysed by another examiner (LS) and have been previously published (Story et al., 2011a). To ensure reproducibility of pre-processing between investigators, 8 spectra were analysed by both the same and two different investigators and the results were compared. Datasets from 8 normal fetuses (echo time 136ms) were blindly analysed by 2 different investigators (VK and LS) and the ratios of NAA:Cho, NAA:Cr, Cho:Cr were calculated and the presence of lactate recorded. The same 8 datasets were analysed twice on separate occasions by the same investigator (VK) to evaluate intra-rater variation. The inter-rater and intra-rater intraclass correlation coefficients were 0.972 ($p<0.0001$) and 0.964 ($p<0.0001$) respectively suggesting excellent agreement between rates and within the same rater.

3.4.4 Spectral acquisition at echo time 136ms

3.4.4.1 Cohorts

53 normal controls and 46 fetuses diagnosed with isolated ventriculomegaly were included in the analysis. At an echo time of 136ms, 71% of the spectra obtained in the normal control and 67% from the ventriculomegaly cohorts were suitable for analysis. Therefore, 37 interpretable spectra were obtained from the control (GA range 21.3-38.3, mean 30.7 weeks) and 31 from the ventriculomegaly cohort (GA range 22-37, mean 29.4 weeks). 3 fetuses with ventriculomegaly and 1 normal control fetus had spectroscopy data from two separate scans at different GAs. The remaining spectra were uninterpretable due to fetal motion.

NAA, choline and creatine were identified in all spectra. In 1 case although choline was identified it was not detected by the software due to the small size of the peak. An example of a typical spectrum is shown in Figure 111.

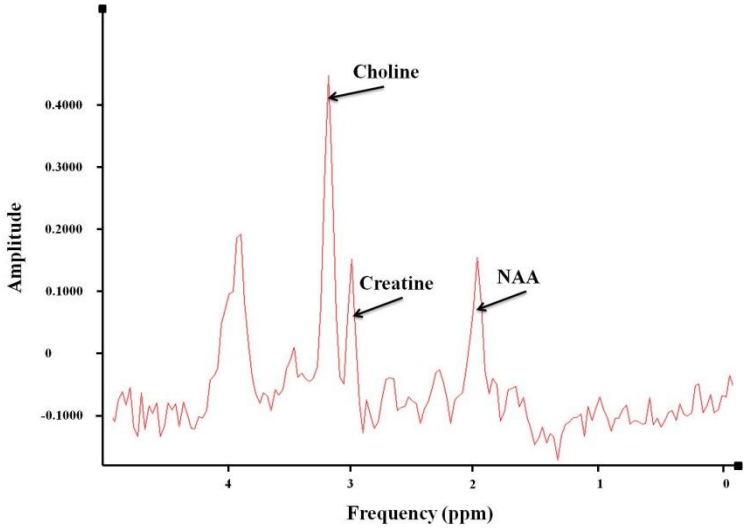


Figure 111. Fetal spectrum at 136ms of a normal control fetus at 32^{+2} gestational weeks

Representative fetal spectrum acquired at echo time 136ms. Choline, creatine and NAA peaks are distinguished.

3.4.4.2 Metabolite ratios during gestation in normal control fetuses at echo time 136ms

In the control group NAA:Cho and NAA:Cr increased with increasing GA (Spearman's r=0.595, p<0.0001; Spearman's r=0.309, p=0.031 respectively) while Cho:Cr ratios decreased (Spearman's r=-0.275, p=0.049) (Figure 112).

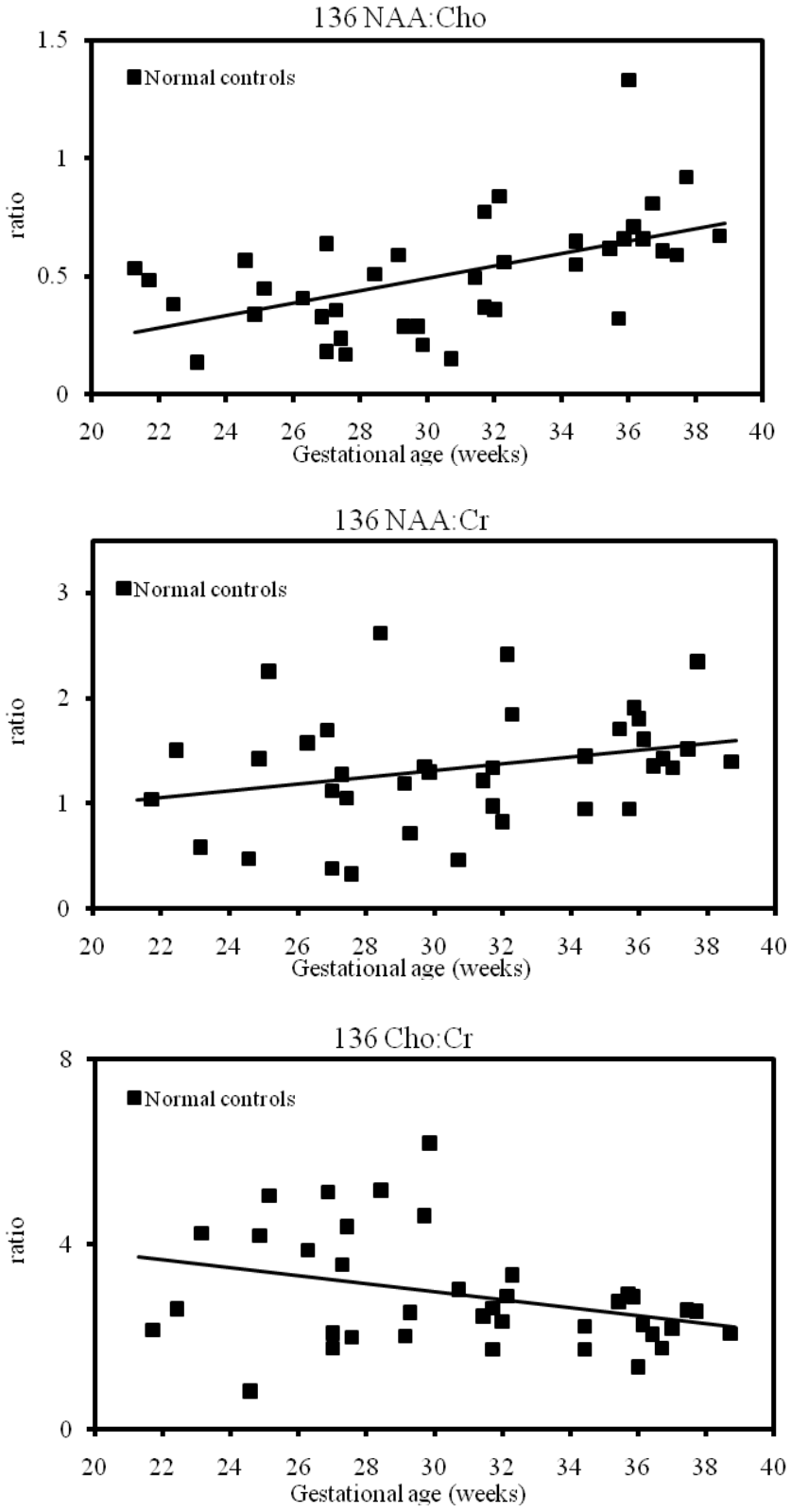


Figure 112. NAA:Cho, Cho:Cr and NAA:Cr ratios varying with gestation in normal control fetuses acquired at an echo time of 136ms

Lactate was present in 5 normal fetuses (GA range 24.57-37.71 weeks). There was no difference in NAA:Cho (p=0.813), NAA:Cr (p=0.772) or Cho:Cr (p=0.39) ratios in the control cohort between fetuses with and without lactate.

3.4.4.3 Differences in metabolite ratios between normal controls and fetuses with ventriculomegaly at echo time 136ms

In the ventriculomegaly cohort, NAA:Cho increased with GA (Spearman's r=0.577, p<0.0001), NAA:Cr remained stable (Spearman's r=0.21, p=0.129) and Cho:Cr decreased (Spearman's r=-0.338, p=0.031). The NAA:Cho ratios corrected for GA were significantly lower in fetuses with ventriculomegaly compared to controls (p=0.004) (Figure 113). There was no significant difference in the NAA:Cr and Cho:Cr ratios between ventriculomegaly and control cohorts (p=0.231 and p=0.087 respectively). In the ventriculomegaly group, lactate was present in 7 fetuses while in an additional 1 fetus the presence of lactate was equivocal. There was no difference in NAA:Cho (p=0.813), NAA:Cr (p=0.105) or Cho:Cr (p=0.058) ratios in the ventriculomegaly cohort between fetuses with and without lactate. The GA range of the 7 fetuses with lactate was 24.7-33.7 weeks and the atrial diameter range was 10-15.3 mm. There was no difference in GA or atrial diameter between fetuses with and without lactate. There was no difference in GA between fetuses with ventriculomegaly and controls with lactate present.

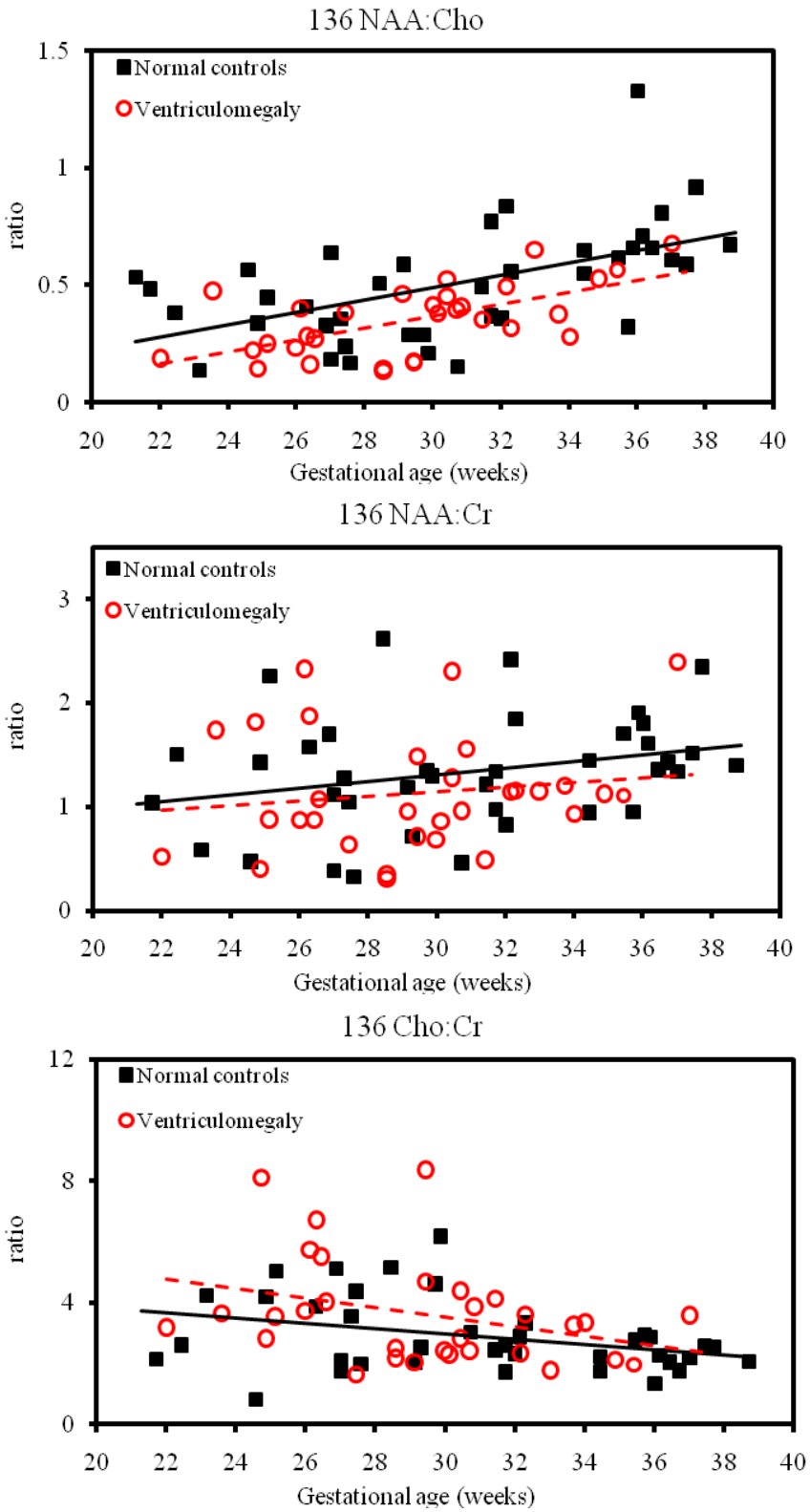


Figure 113. NAA:Cho, Cho:Cr and NAA:Cr ratios varying with gestation in normal control fetuses and fetuses with isolated ventriculomegaly acquired at an echo time of 136ms

Fetuses with ventriculomegaly had significantly lower NAA:Cho (p=0.004) ratios while there was no difference in Cho:Cr (p=0.231) and NAA:Cr (p=0.087) ratios.

3.4.5 Spectral acquisition at echo time 270ms

41 normal controls and 36 fetuses diagnosed with isolated ventriculomegaly were included in the analysis. At an echo time of 270ms, 56% of the spectra obtained in the control and 66% from the ventriculomegaly cohorts were suitable for analysis. Therefore, 23 interpretable spectra from the control (GA range 22.4-38.7, mean 30.8 weeks) and 24 interpretable spectra from the ventriculomegaly cohort were obtained (GA range 22.1-37.4, mean 29.4 weeks). The remaining spectra were uninterpretable due to fetal motion. An example of a representative spectrum is shown in Figure 114.

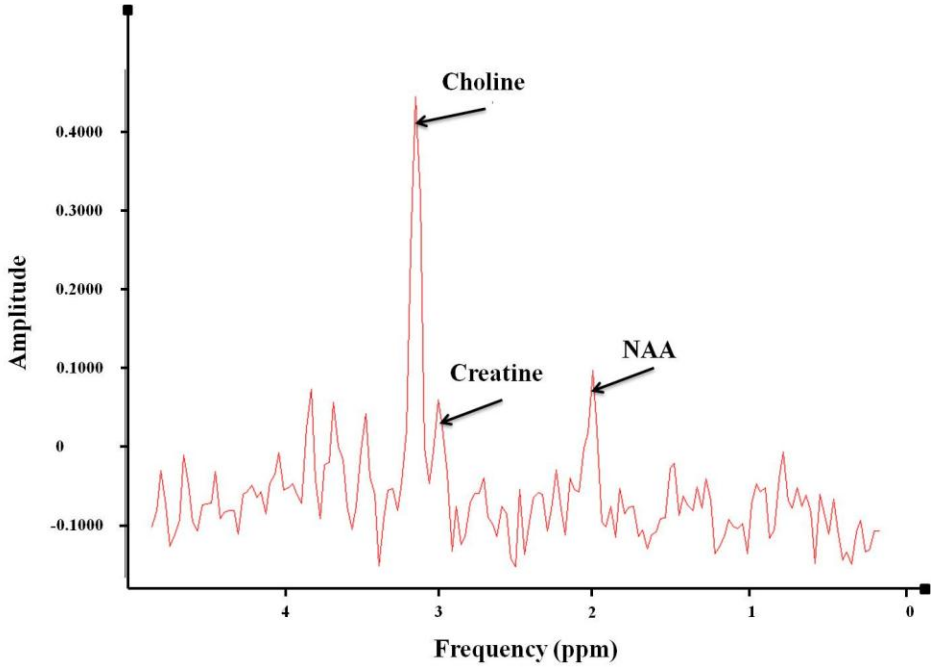


Figure 114. Fetal spectrum at 270ms in a normal control fetus at 24^{+4} gestational weeks

Representative fetal spectrum acquired at echo time 270ms. Choline, creatine and NAA peaks are distinguished.

3.4.5.1 Metabolite ratios during gestation in normal control fetuses at echo time 270ms

In the control group NAA:Cho increased with increasing GA (Spearman's r=0.69, p<0.0001) while NAA:Cr showed a weak non-significant increase (Spearman's r=0.296, p=0.085) and Cho:Cr ratios remained stable (Spearman's r=0.034, p=0.44) (Figure 115). Lactate was present in 6 normal control fetuses.

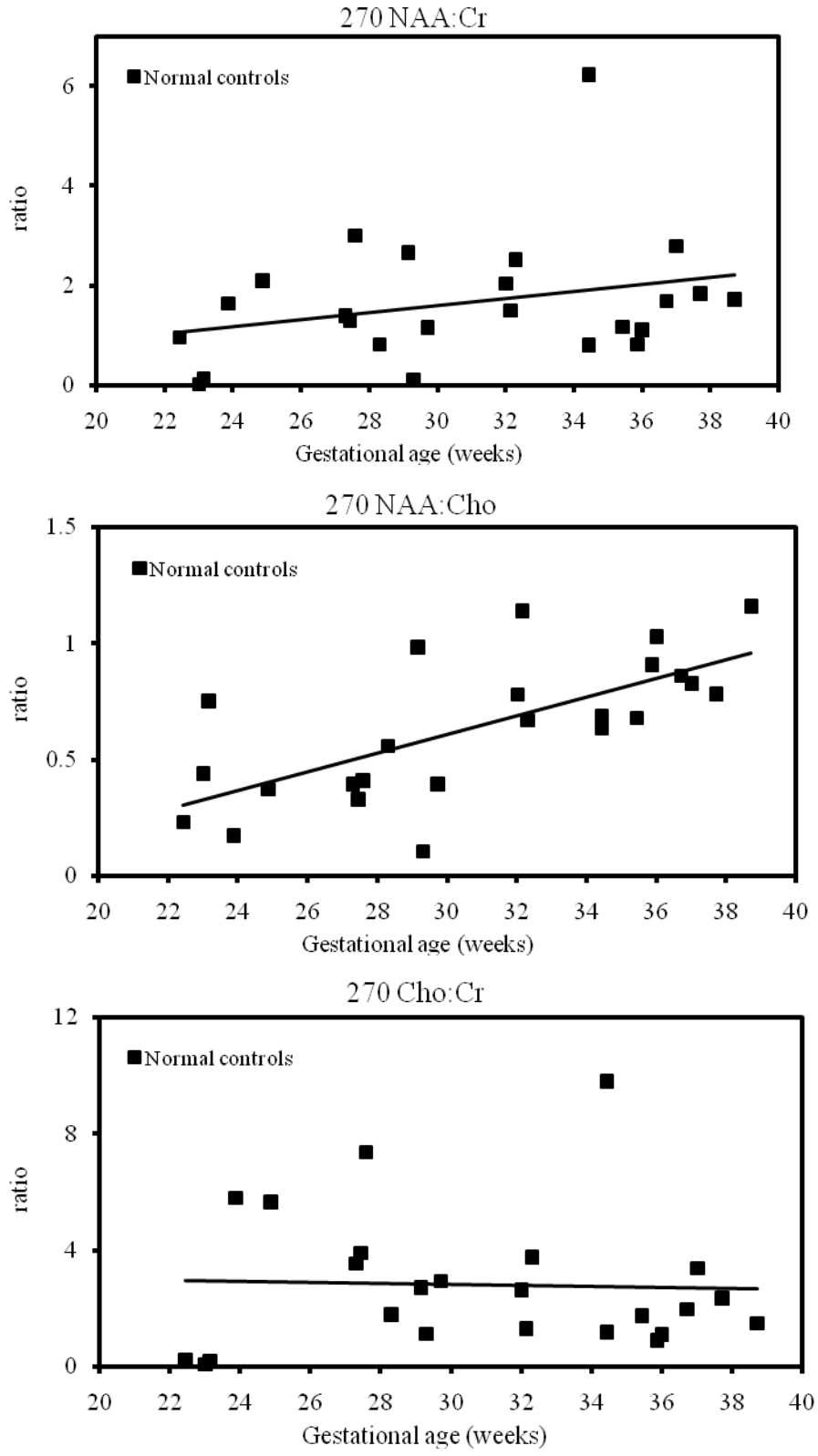


Figure 115. NAA:Cho, Cho:Cr and NAA:Cr ratios varying with gestation in normal control fetuses acquired at an echo time of 270ms

3.4.5.2 Differences in metabolite ratios between normal control and fetuses with ventriculomegaly at echo time 270ms

In the ventriculomegaly cohort, NAA:Cr, NAA:Cho and Cho:Cr ratios were stable through gestation (Spearman's r=0.237, p=0.132, r=0.124, p=0.281, r=-0.11, p=0.48 respectively). There was no difference in the NAA:Cr, NAA:Cho and Cho:Cr ratios between ventriculomegaly and control cohorts (p=0.560, p=0.581 and p=0.111 respectively) (Figure 116). In the ventriculomegaly cohort, lactate was present in 11 fetuses while in an additional 4 fetuses the presence of lactate was equivocal.

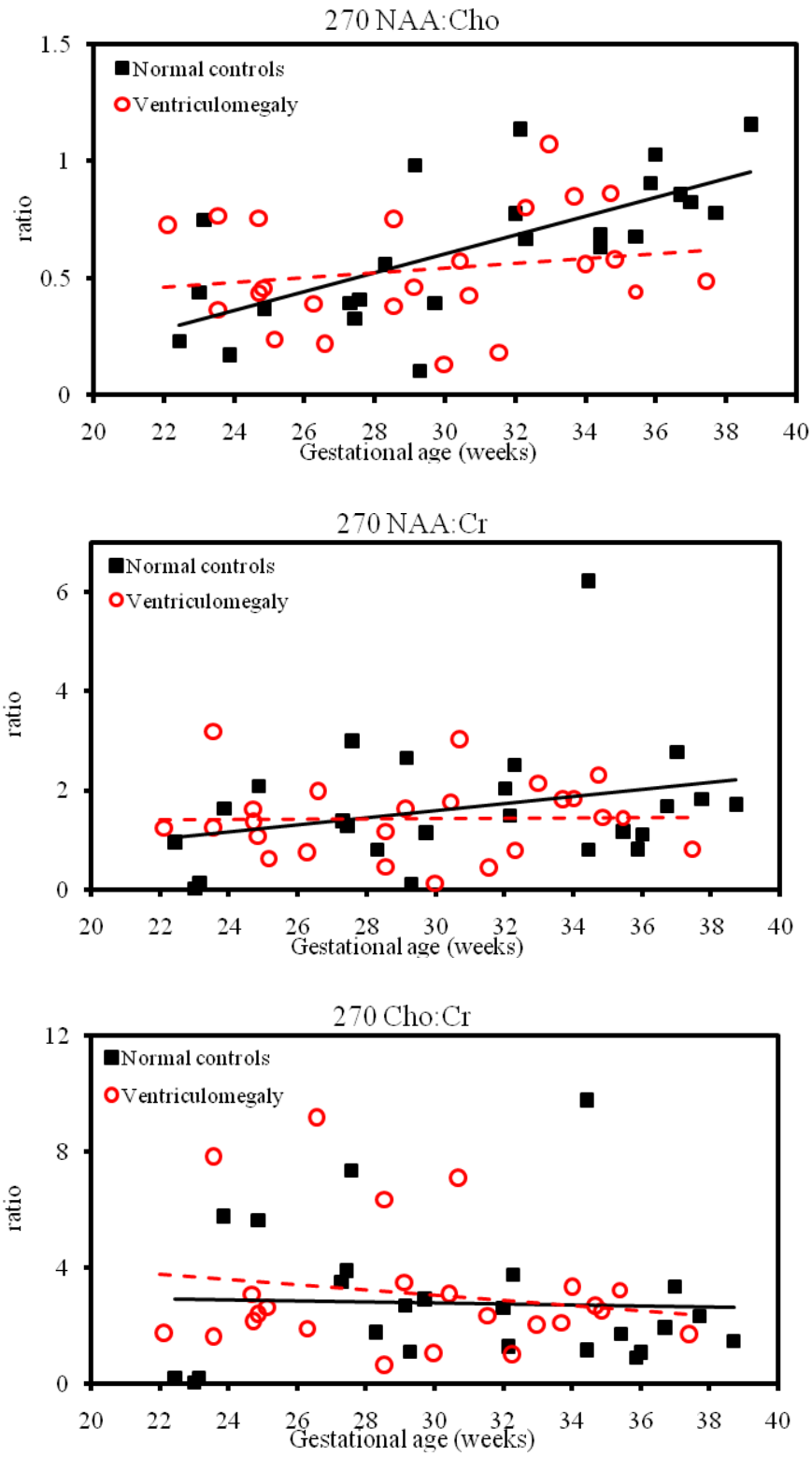


Figure 116. NAA:Cho, Cho:Cr and NAA:Cr ratios varying with gestation in normal control fetuses and fetuses with isolated ventriculomegaly acquired at an echo time of 270ms

There was no significant difference in NAA:Cho, Cho:Cr and NAA:Cr rations between cohorts.

3.4.6 Lactate presence at 136ms and 270ms

In 22 normal control fetuses, data were interpretable in both 136ms and 270ms echo times allowing for comparison. Five fetuses at echo time 136ms had a lactate peak while only 2 of those fetuses also had a lactate peak at echo time 270ms. An additional 3 fetuses had a lactate peak in echo time 270ms not present in 136ms. An example of a discrepancy case is shown in Figure 117.

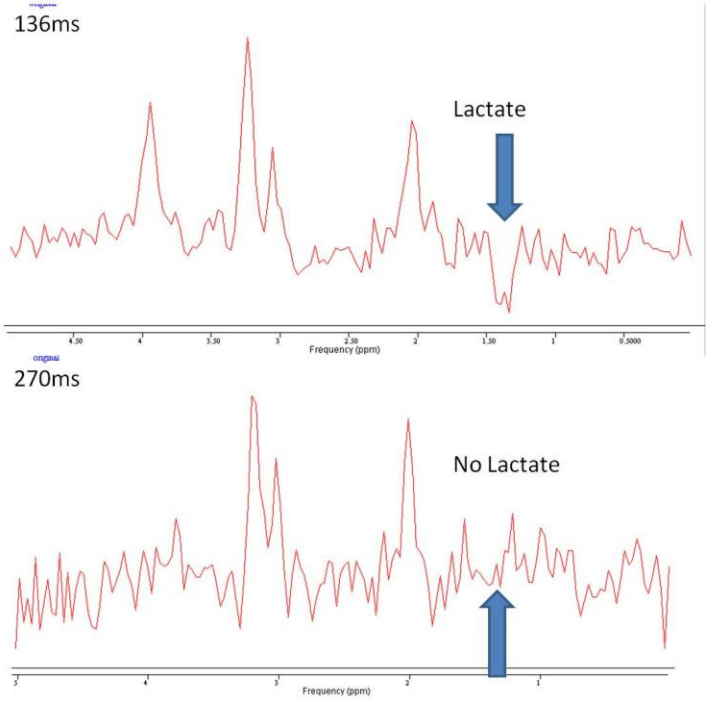


Figure 117. Lactate detection at 136ms and 270ms echo times

Discrepancy of lactate peak in a 37^{+5} old fetus at echo times 136ms and 270ms. An obvious lactate peak is present at 136ms but not at 270ms.

3.4.7 Spectral acquisition at echo time 42ms

37 normal controls and 41 fetuses diagnosed with isolated ventriculomegaly were included in the analysis. At an echo time of 42ms, 62% of the spectra from the control and 73% from the ventriculomegaly cohorts were suitable for analysis. Therefore, 23 interpretable spectra from the control (GA range 23.1-37.4, mean 31.6 weeks) and 30 interpretable spectra from the ventriculomegaly group (GA range 22-37.4, mean 29 weeks) were obtained. The remaining

spectra were uninterpretable due to fetal motion. An example of a representative spectrum is shown in Figure 118.

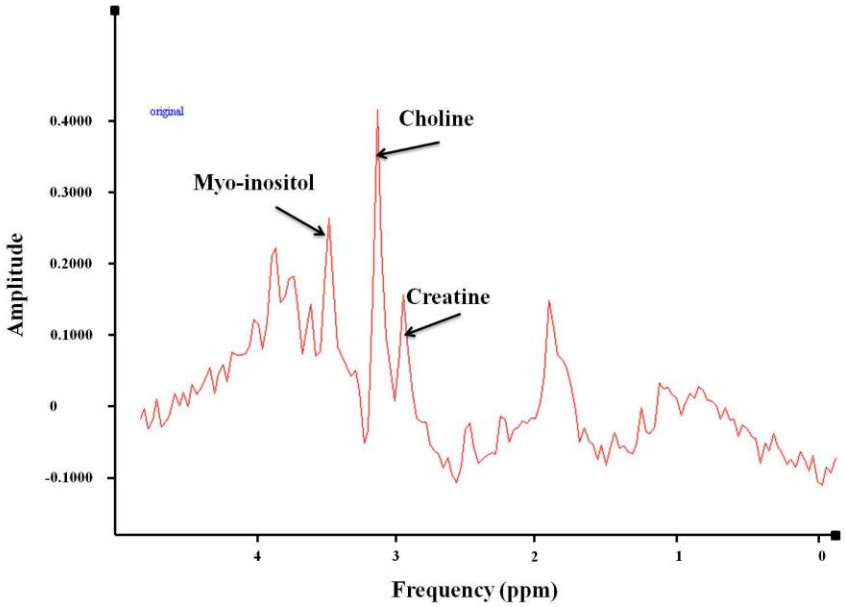


Figure 118. Fetal spectrum at 42ms

Representative fetal spectrum acquired at echo time 42ms. Myo-inositol, choline and creatine peaks are distinguished.

3.4.7.1 Metabolite ratios during gestation in normal control fetuses at echo time 42ms

In the control group MI:Cho ratios were stable with increasing GA (Spearman's r=0.049, p=0.412) while MI:Cr and Cho:Cr ratios showed a weak non-significant decrease (Spearman's r=-0.295, p=0.081; Spearman's r=-0.289, p=0.081) (Figure 119).

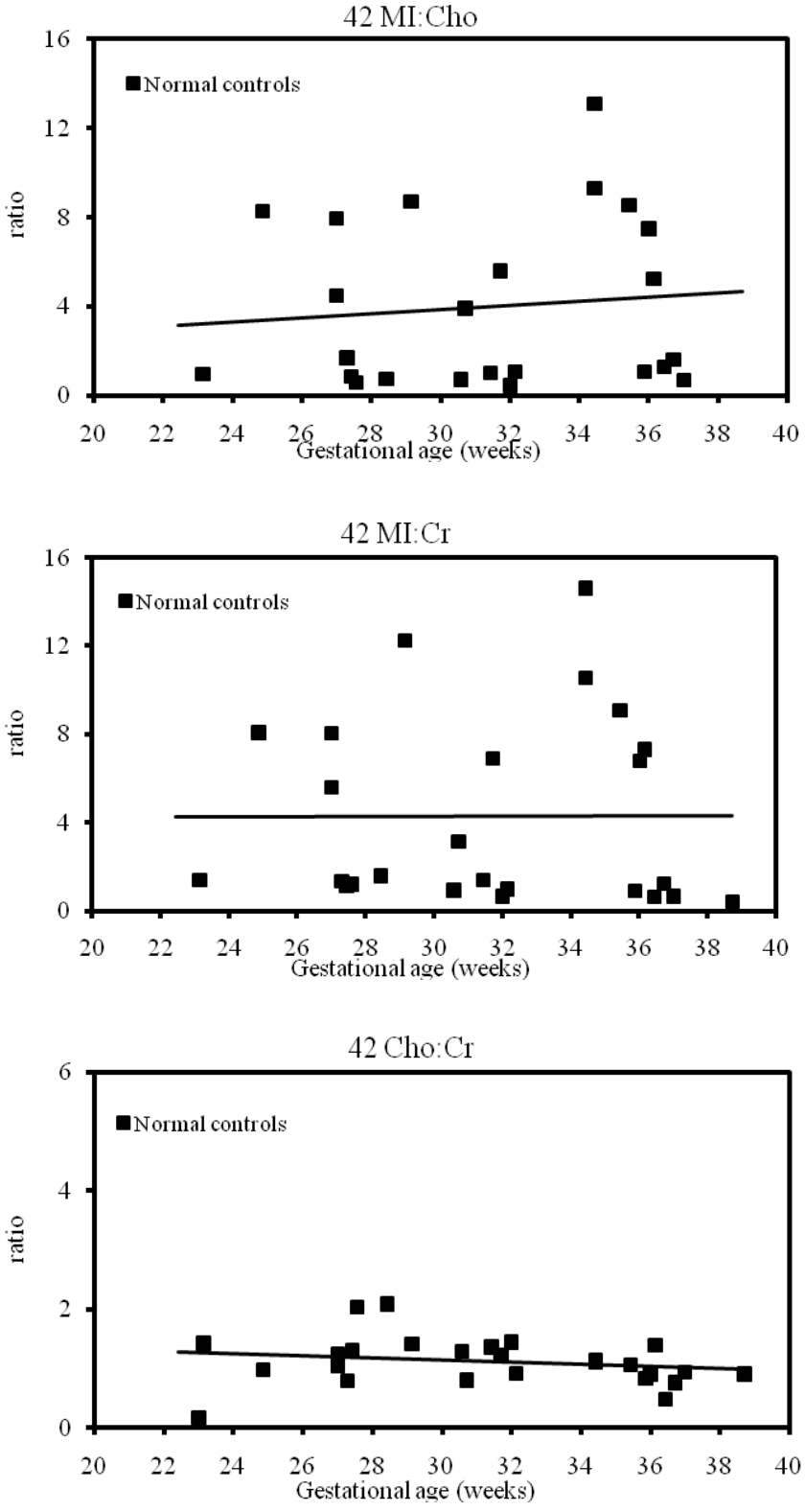


Figure 119. MI:Cho, MI:Cr and Cho:Cr ratios varying with gestation in normal control fetuses acquired at an echo time of 42ms

3.4.7.2 Differences in metabolite ratios between normal controls and fetuses with ventriculomegaly at echo time 42ms

In the ventriculomegaly cohort, MI:Cho, MI:Cr and Cho:Cr ratios were stable with increasing GA (Spearman's r=-0.23, p=0.111, r=-0.243, p=0.098, r=-0.057, p=0.382 respectively). The MI:Cho and MI:Cr ratios corrected for GA were significantly lower in fetuses with ventriculomegaly compared to controls (p=0.001 and p=0.028 respectively) while the Cho:Cr were significantly higher in the ventriculomegaly cohort (p=0.028) (Figure 120).

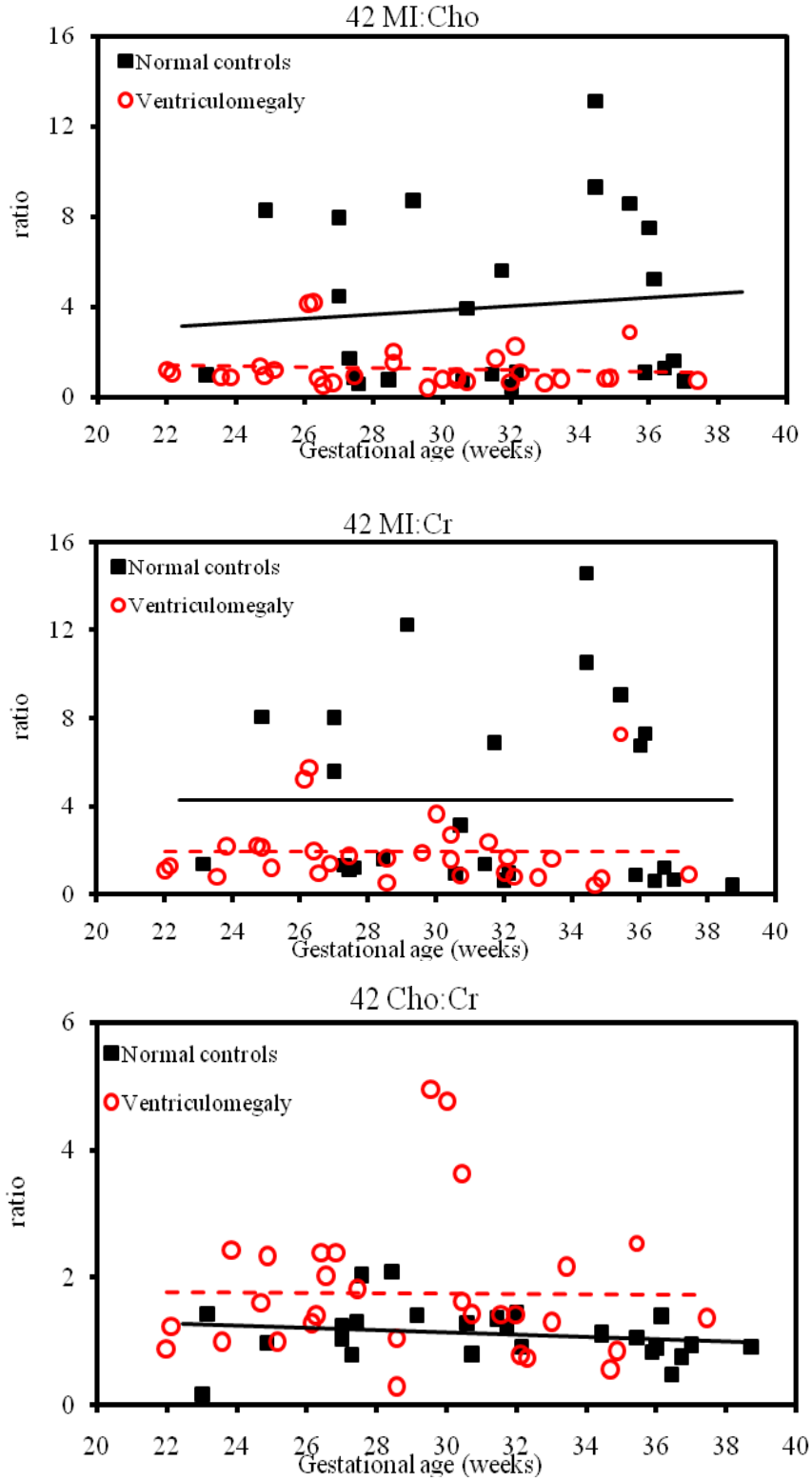


Figure 120. MI:Cho, MI:Cr and Cho:Cr ratios varying with gestation in normal control fetuses and fetuses with isolated ventriculomegaly acquired at an echo time of 42ms

Fetuses with ventriculomegaly had significantly lower MI:Cho (p=0.001) and MI:CR (p=0.028) ratios while Cho:Cr ratios were significantly higher (p=0.028) compared to the control cohort.

3.4.8 Discussion

This study has demonstrated that fetuses with isolated ventriculomegaly had significant alterations in their metabolic pattern compared to normal control fetuses. More specifically, NAA:Cho, MI:Cho, MI:Cr ratios were significantly lower in fetuses with ventriculomegaly whilst Cho:Cr were significantly higher at echo time 42ms in the ventriculomegaly cohort compared to controls. However there was no significant difference in Cho:Cr ratios at echo times 136ms and 270ms.

Normal controls

In the normal control cohort, NAA:Cho and NAA:Cr ratios increased with GA at echo times 136ms and 270ms while Cho:Cr ratios decreased in echo times 136ms and 42ms. These results are in accordance with the study by Kok et al. (2002) in a cohort of 35 fetuses from 30 to 41 weeks GA. They showed that NAA:Cho and NAA:Cr increased whilst Cho:Cr ratios decreased with advancing GA and suggested that these changes reflected brain maturation. The NAA:Cho increase with advancing gestation shown in our results may be due to increasing NAA and may reflect the development of dendrites and synapses and proliferation and differentiation of oligodendrocytes (Fenton et al., 2001). Decreasing choline levels may also account for the observed increase in NAA:Cho ratios (Girard et al., 2006b). The choline peak comprises of glycerophosphocholine, phosphocoline and free choline and the prominence of the peak likely represents the high levels of substrate required for the formation of cell membranes and myelin synthesis (Huppi and Inder, 2001). Both glial and neurons are involved in its uptake (Girard et al., 2006a). Previous fetal studies measuring the absolute levels of choline during gestation have been conflicting as to whether the levels decrease (Girard et al., 2006a) or remain stable (Kok et al., 2002). These differences may be due to the different GA ranges studied. The decrease in NAA:Cr ratios may be attributed to an increase in NAA levels and relatively stable creatine levels during gestation. The creatine peak comprises of creatine and phosphocreatine which are involved in energy production. Previous studies have shown that absolute creatine levels are stable during gestation and have suggested that it is an ideal reference for quantification of other metabolites (Heerschap et al., 2003; Kok et al., 2002).

At an echo time of 42ms, the MI:Cho ratios were stable whilst the MI:Cr decreased, this may reflect a decrease in the MI levels and relatively stable creatine levels and decreasing choline levels. Girard et al. (2006b) was able to calculate absolute levels of MI in the fetal brain from 22 to 39 weeks GA based on assumptions of spin relaxation times and brain tissue water content. They found a decrease in myo-inositol levels with GA and later suggested that this may reflect the high density of glial cells in between 22 and 28 weeks (Girard et al., 2006a).

In the normal control cohort, lactate was detected in 5 normal control fetuses at an echo time of 136ms and 6 normal control fetuses at an echo time of 270ms. Agreement between echo times 136ms and 270ms was observed in only 2 fetuses. There has been controversy regarding the role of lactate in the fetal brain as studies using animal models indicated that it is a product of anaerobic glycolysis and accumulates in cases of acute hypoxia, while in human neonates lactate production is a result of a hypoxic insult (van Cappellen van Walsum et al., 1998). When reviewing our cases in which lactate was present 1 fetus was aged 37^{+5} weeks GA and the woman ruptured her membranes shortly after her MRI scan and retrospectively reported of tightenings during the scan. It is possible that she was in the early stages of labour and lactate levels were reflecting transient hypoxaemia. The rest of the normal control fetuses however were between 24 and 34 weeks in gestation. The role of lactate as a supplementary fuel for activated neurons has also been debated (Korf, 2006). It is suggested that lactate synthesised by astrocytes may be used by neurons as an aerobic substrate under certain circumstances (Pellerin et al., 2007). In the study by Leth et al. (1995) lactate was present in 10 out of 13 preterm appropriately grown for gestational age infants and they showed that its concentrations were inversely related to postmenstrual age. The authors suggested that lactate may support brain metabolism. In a study by Roelants-van Rijn et al. (2004) lactate was present in preterm infants appropriately grown for gestational age. These children were assessed at 2 years of age using the GMDS and had a normal developmental quotient. Lactate has also been detected in amniotic fluid samples during the second trimester of pregnancy in fetuses at risk for genetic disorders referred for an amniocentesis but with a normal karyotype (Cohn et al., 2009).

Alteration in metabolite ratios between fetuses with isolated ventriculomegaly and normal controls

Fetuses with ventriculomegaly had significantly lower NAA:Cho (136ms), MI:Cho and MI:Cr (42ms) and significantly higher Cho:Cr (42ms and 136ms) compared to normal controls when corrected for GA. There was no difference in NAA:Cr levels in either 136ms or 270ms echo times. There was no difference detected in any metabolite ratios in echo time 270ms. Specific metabolic patterns have not been previously identified for fetuses with isolated ventriculomegaly.

The observed reduction in NAA:Cho may be due to a reduction in NAA and/or increase in choline. A reduction in NAA may reflect immaturity, neuronal/axonal damage or neuronal viability however no overt structural lesions were present in our cohort on fetal MRI (Baslow et al., 2003). NAA is also found in oligodendrocyte type-2 astrocyte progenitor cells and immature oligodendrocytes and is essential for myelin synthesis. The acetate portion is used for myelin synthesis while the aspartate for energy production. NAA levels increase during normal development reflecting synaptic complexity and increasing myelination (Girard et al., 2006b; Kok et al., 2002). Therefore lower levels may reflect delayed or abnormal white matter development. Indeed, human studies indicate that midgestation is the beginning of a critical period for myelination processes that extends until the second postnatal year (Brighina et al., 2009; Kinney et al., 1994). Therefore reduced NAA levels may reflect alterations in the myelination process during the fetal period. A meta-analysis of ^{1}HMRS in children with autism demonstrated a significant reduction in NAA levels in the cerebrum highly significant in the frontal lobe and the authors suggested that this may indicate a relative increase in glial cells (Aoki et al., 2012). They commented that if brain enlargement in autism was a consequence of increased neuronal numbers this should be accompanied by an increase in NAA levels. Therefore the reduction in NAA most likely represents decreased neuron density induced by brain enlargement due to increased glial numbers (dilution effect). In contrast, autopsy data from a small cohort of children with autism have shown increased neuronal numbers in the frontal lobe (Courchesne et al., 2011b). In addition, NAA is synthesised in neuronal mitochondria and is considered to reflect mitochondrial function (Clark, 1998). Therefore changes in NAA levels may reflect dysfunction of mitochondrial

energy metabolism in the absence of neuronal loss. A reduction in NAA levels has been detected in IUGR fetuses and has been attributed to mitochondrial dysfunction as suggested from many animal models of IUGR (Story et al., 2011a). Other explanations may involve a cellular redistribution of NAA resulting in changes in the ratio of free to bound NAA. ^{1}HMRS can only detect unbound molecules therefore a redistribution may alter the NAA signal.

The observed reduction in MI:Cho and MI:Cr in combination to increased levels of Cho:Cr may indicate a reduction in myo-inositol levels and/or increase in choline. The group of Kok et al. (2003) compared ^{1}HMRS data from normal fetuses and fetuses with isolated hydrocephalus (n=2), hydrocephalus with spina bifida (n=4) and hydrocephalus with agenesis of the corpus callosum (n=4). They did not define how they diagnosed fetuses with isolated hydrocephalus therefore it is unclear whether these were fetuses with isolated ventriculomegaly similar to our cohort, most probably not. The GA range studied was 28 to 37 weeks. They showed that hydrocephalic fetuses had significantly reduced levels of inositol to creatine ratios and suggested that this reflected reduced inositol levels as creatine is relatively stable during gestation. They concluded that inositol may influence the development of the fetal CNS early and later during pregnancy. In an animal model with susceptibility to neural tube defects it has been shown that inositol is essential for the closure of the neural tube therefore is important for brain morphogenesis (Cogram et al., 2004; Greene and Copp, 1997). Myo-inositol has a role in the inositol/lipid cycle and is involved in signal transduction, steroid synthesis and intracellular calcium regulation. Myo-inositol stimulates embryonic cell proliferation via activation of protein kinase C leading to normal closure of the neural tube in transgenic mice (Cogram et al., 2004; van Straaten and Copp, 2001). Increased myo-inositol levels have been reported in the brain of adults with Down's syndrome (Beacher et al., 2005; Huang et al., 1999) while myo-inositol concentration significantly (negatively) has been correlated with cognitive performance (Beacher et al., 2005). Beacher et al. (2005) suggested that this increase may reflect an underlying metabolic process linked to neuronal dysfunction and is probably due to an up-regulation of the metabolite's transport associated with an extra copy of the gene on chromosome 21.

Choline levels may be increased in the ventriculomegaly cohort as indicated by a reduction in NAA:Cho, MI:Cho and an increase in Cho:Cr. Creatine levels appear unchanged between our cohorts. Studies in fetuses aged 22-28 weeks have shown that as gestation progresses choline levels decrease (Girard et al., 2006b). This decrease has been ascribed to accelerated myelination during the third trimester as choline is incorporated into the myelin constituent lipids (Inder and Huppi, 2000; Kok et al., 2002). Increased choline levels may indicate a failure of choline to incorporate into myelin lipids thus higher levels of unbound choline being present. This may lead to delayed white matter development and myelination.

The fact that lactate was identified in both normal control fetuses and fetuses with ventriculomegaly suggests that it is not simply a marker of acute hypoxia and may have a role in normal fetal development. Although lactate was present in higher percentage of fetuses with ventriculomegaly compared to controls we are unable to ascertain whether higher concentrations were present in the ventriculomegaly cohort.

Limitations

^{1}HMRS is sensitive to fetal motion as indicated by the large number of cases that were unusable due to movement. In addition, sampling specific brain regions is not feasible in the fetus due to the large voxel size required for adequate signal-to-noise and due to fetal motion. Differences in metabolite ratios between cohorts at echo time 136ms were not replicated in echo time 270ms. Due to technical difficulties it is not always possible to acquire usable spectra at each echo time in every fetus which probably explains variations between the same metabolite ratios between echo times. Different echo times may alter the ability to identify different metabolite ratios. At short echo times there is better signal-to-noise ratio for the detection of metabolites however lipids signals may be present while in longer echo times there is a clearer baseline and lipid signals are significantly reduced allowing for easier quantification of metabolites. Due to different intrinsic metabolite T2 relaxation times between long and short echo times the normal spectra heights may appear significantly different.

Conclusions

In our study we have shown that fetuses with ventriculomegaly had significantly lower NAA:Cho, MI:Cho and MI:Cr ratios whilst significantly higher Cho:Cr ratios. These results may indicate a reduction in NAA and myo-inositol and an increase in choline. These changes may reflect a delay or impairment in white matter development in fetuses with isolated ventriculomegaly.

3.5 Assessment of white matter microstructure in neonates with ventriculomegaly

3.5.1 Background

While conventional MRI is able to delineate early structural developmental events such as cortical gyrification, DTI provides quantitative data on anatomical connectivity. It has been extensively used to characterise microstructural changes associated with normal and abnormal development via quantification of the physical integrity and maturity of white matter fibres. Thus providing an insight into white matter microstructure and organisation, important early markers or later neurodevelopmental outcome (Counsell et al., 2008; Groppo et al., 2012; Tusor et al., 2012). The quantitative parameters of DTI include the Apparent Diffusion Coefficient (ADC) which depicts the degrees of water diffusion and the Fractional Anisotropy (FA) which reflects the degree of directional preference of water diffusion (Roberts and Schwartz, 2007). An optimised protocol (Ball et al., 2010) designed for voxel-wise registration of neonatal data was used for the processing of the generated FA data. The FA maps of each subject were aligned and registered to each other to create the mean FA map representing the mean of all aligned FA images and the mean FA skeleton which represents the centre of all white matter tracts that are common to all subjects. Tract-Based Spatial Statistics (TBSS) analysis was used to assess the relationship between FA and presence of ventriculomegaly by comparing the FA values throughout the white matter tracts between the control and ventriculomegaly cohorts. TBSS is an automated, observer-independent technique for assessing FA throughout the white matter tracts on a voxelwise basis across groups of subjects (Smith et al., 2006). Therefore in this chapter we have used TBSS to compare white matter microstructure in term born neonates with antenatally diagnosed isolated ventriculomegaly, with a cohort of control term-born neonates with normal brain appearances.

3.5.2 Aim

To assess white matter development in neonates with antenatal ventriculomegaly.

3.5.3 Cohorts

3.5.3.1 Normal controls

The normal control group consisted of 25 term-born neonates with a normal brain appearance on MR, either enrolled in the fetal research program (n=10) or enrolled as normal controls in the following MR research studies of the preterm brain (n=15) (Optimising functional MRI techniques in the study of neuronal development in preterm infants, 07/H0707/101; Computational analysis of brain abnormalities and neurodevelopmental impairments in preterm infants, 04/Q0406/125). The mean GA at birth was 39.6 weeks (range 38-41.7 weeks) and mean post-menstrual age at scan was 41.9 weeks (range 39-49.1 weeks). Cohort characteristics are presented in Table 28.

Normal control cohort characteristics			
Male		13	
Female		12	
Gestational age at birth (weeks)		39.6	(38-41.7)
Post-menstrual age at scan (weeks)		41.9	(39-49.1)
Birthweight (g)		3364	(2410-4242)
Apgar scores	1 minute	9	(8-10)
	5 minutes	10	(9-10)

Table 28. Normal control cohort characteristics

Gestational age at birth, post-menstrual age at scan and birthweight are presented as mean (range). Apgar scores are presented as median (range).

Neurological examination in normal control neonates

A complete neurological and visual examination was performed prior to the scan in all term neonates with a normal brain appearance. A normal neurological and visual examination was reported in all 25 neonates.

3.5.3.2 Isolated ventriculomegaly

The ventriculomegaly cohort was the same as in chapter 3.2.4.3 for the neonatal volumetric analysis. All neonates had antenatally diagnosed isolated ventriculomegaly detected on ultrasound and confirmed on MRI. From the 26 neonates used previously for volumetric analysis, 4 cases had significant motion and DTI data from these cases were discarded. The remaining 22 neonates had a mean GA at birth 39.8 weeks (range 36-41.4 weeks) and mean post-menstrual age at scan 45.4 weeks (range 41.4-50.4 weeks). Cohort characteristics are presented in Table 29. There was a significant difference in post-menstrual age at scan with neonates with ventriculomegaly being scanned at a later age by an average of 3.4 weeks ($p<0.0001$). There was no significant difference in gestational age at birth between cohorts. The results presented are corrected for both gestational age at birth and post-menstrual age at scan.

Ventriculomegaly cohort characteristics			
Male		16	
Female		6	
Gestational age at birth (weeks)		39.8	(36-41.4)
Post-menstrual age at scan (weeks)		45.4	(41.4-50.4)
Birthweight (g)		3462	(2528-4260)
Apgar scores	1 minute	9	(7-10)*
	5 minutes	10	(9-10)*

Table 29. Ventriculomegaly cohort characteristics

Gestational age at birth, post-menstrual age at scan and birthweight are presented as mean (range). Apgar scores are presented as median (range). * apgar scores were not available in 4 neonates.

Neurological examination in neonates with ventriculomegaly

A complete neurological examination was performed in all neonates with antenatal ventriculomegaly prior to the scan. A normal neurological examination was reported in 18 out of 22 neonates. In the remaining cases the examination revealed 3 cases with head lag/lower neck tone and 1 case with reduced central tone and head lag. Visual examination was normal for all 22 neonates.

3.5.4 FA quantification

The mean FA map constructed from the normal control and ventriculomegaly cohorts is shown in Figure 121. The mean FA skeleton overlaid on the mean FA map is shown in Figure 122. Intergroup statistical comparisons were performed on the mean FA map in order to identify which regions on the mean white matter skeleton in each cohort had higher, lower or of no statistical difference FA values. All statistical comparisons were corrected for gestational age at birth and post-menstrual age at scan. FA values were significantly lower in the ventriculomegaly cohort in the splenium of the corpus callosum, sagittal stratum bilaterally and right posterior corona radiate (Figures 123-125). The tracts that go through these white matter regions are presented in Table 30. There was no significant difference in FA in the rest of the white matter tracts between cohorts.

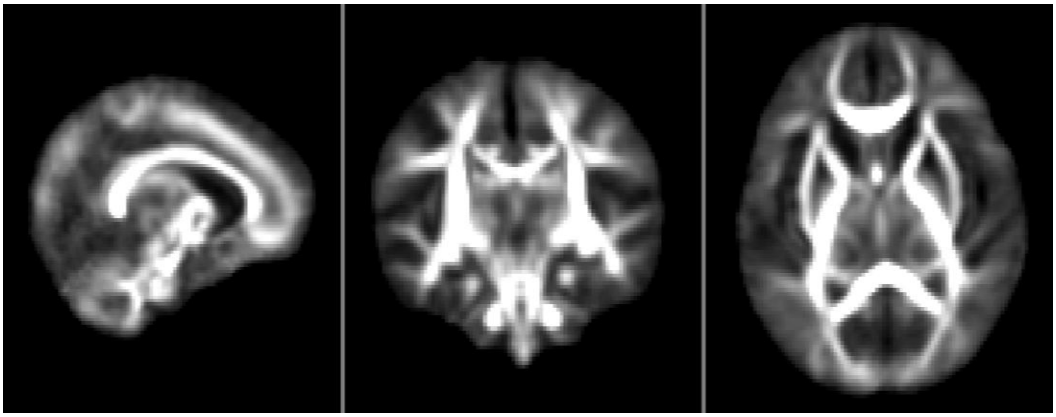


Figure 121. Mean FA images
Mean FA images of white matter tracts constructed from the normal control and ventriculomegaly cohorts. Data shown in (A) sagittal (B) coronal and (C) transverse planes.

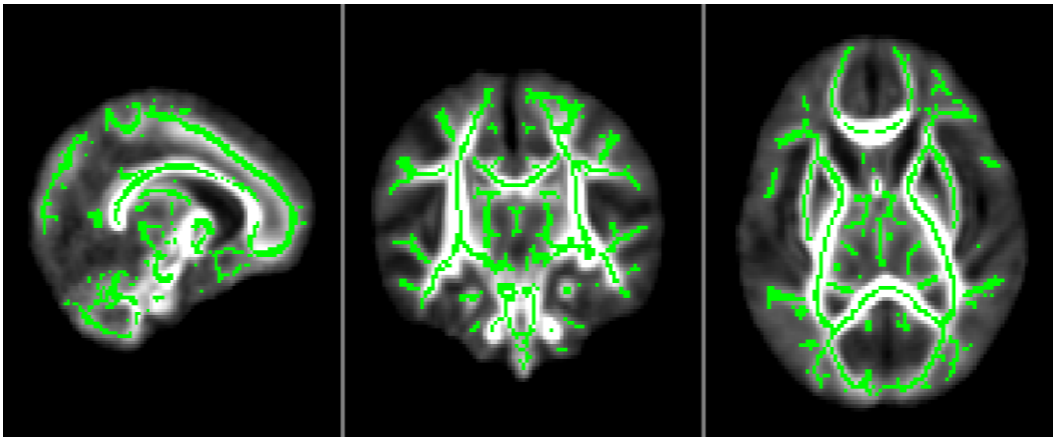


Figure 122. Mean FA skeleton
Mean FA skeleton (green) overlain on mean FA images constructed from the normal control and ventriculomegaly cohorts. Data shown in (A) sagittal (B) coronal and (C) transverse planes.

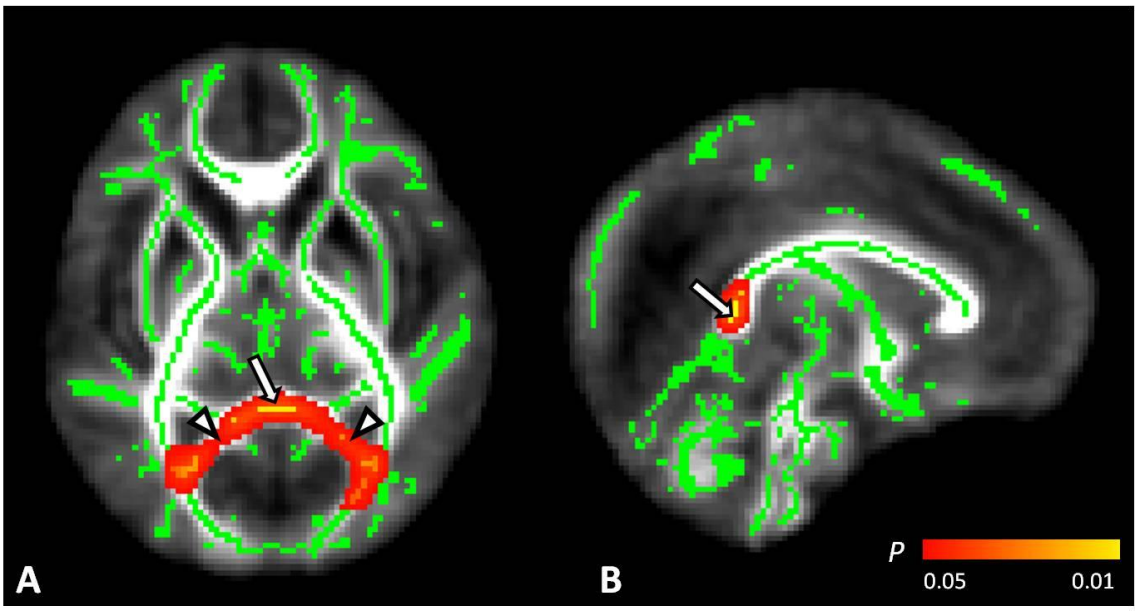


Figure 123. Splenium of the corpus callosum

FA values in the splenium (arrows) of the corpus callosum were significantly lower in the ventriculomegaly cohort as shown in (A) transverse and (B) sagittal planes. The fibres passing through the splenium of the corpus callosum form the forceps major (arrowheads). Tapetum projections originate from the splenium and sweep inferiorly along the lateral margin of the posterior horn of the lateral ventricles. Mean FA skeleton (green) was overlain on the mean FA images constructed from the normal control and ventriculomegaly cohorts.

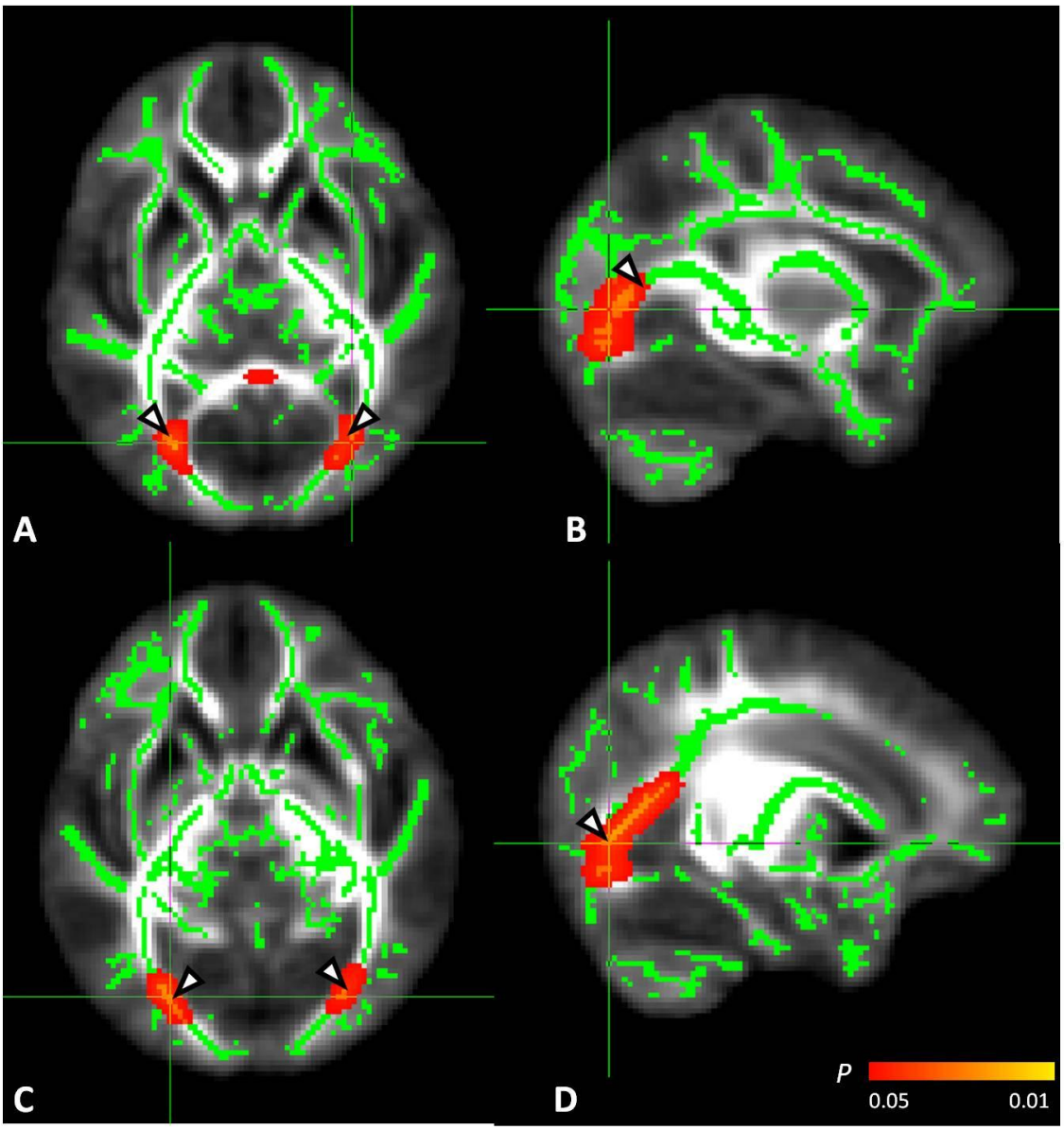


Figure 124. Sagittal stratum

FA values in the sagittal striatum (arrowheads) were significantly lower in the ventriculomegaly cohort as shown in (A,C) transverse and (B,D) sagittal planes. The sagittal striatum consists of the inferior and superior longitudinal fasciculus, inferior fronto-occipital fasciculus and optic radiations. Mean FA skeleton (green) was overlain on the mean FA images constructed from the normal control and ventriculomegaly cohorts.

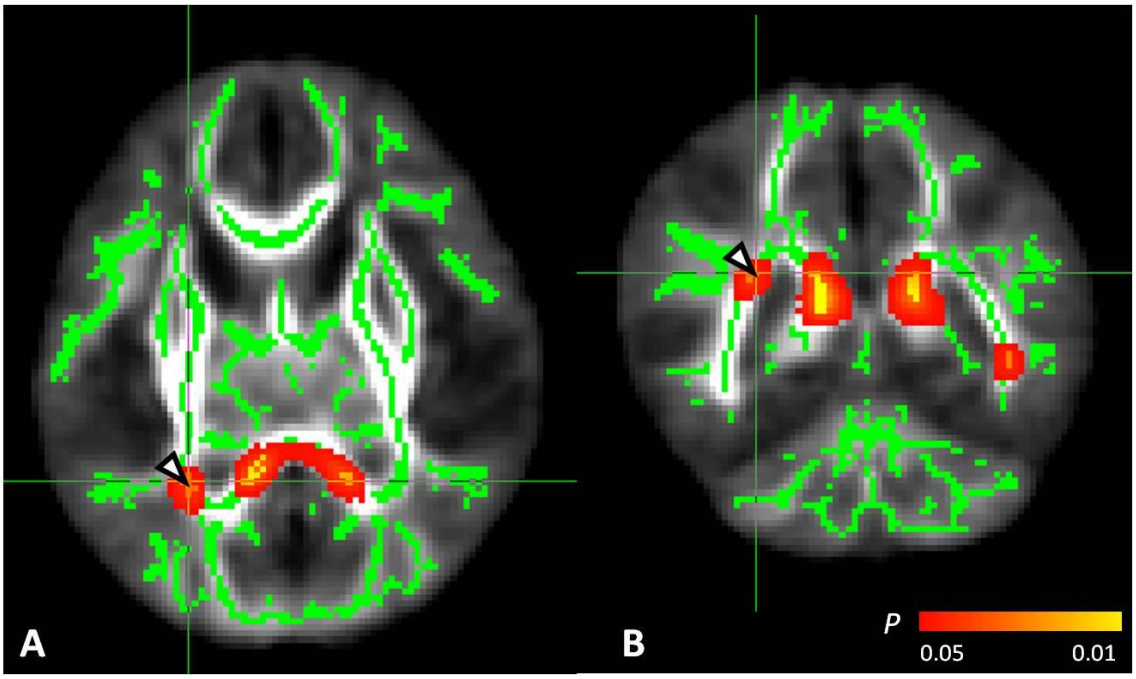


Figure 125. Posterior corona radiata

FA values in the right posterior corona radiate (arrowheads) were significantly lower in the ventriculomegaly cohort as show in (A) transverse and (B) coronal planes. The tracts going through the posterior corona radiata include the inferior and superior longitudinal fasciculus, inferior fronto-occipital fasciculus, corticopontine tracts and posterior thalamic radiations (mainly consisting of the optic radiations). Mean FA skeleton (green) was overlain on the mean FA images constructed from the normal control and ventriculomegaly cohorts.

White matter region	White matter tracts
Splenium of corpus callosum	Forceps major Tapetum
Sagittal stratum	Inferior longitudinal fasciculus Superior longitudinal fasciculus Inferior fronto-occipital fasciculus Optic radiations
Posterior corona radiata	Inferior longitudinal fasciculus Superior longitudinal fasciculus Inferior fronto-occipital fasciculus Corticopontine Posterior thalamic radiations

Table 30. White matter regions and tracts

White matter regions and tracts that run through the specific regions. Table constructed from data described in (Oishi et al., 2010; Wakana et al., 2004).

3.5.5 Discussion

TBSS analysis in this study has demonstrated that in neonates with antenatally diagnosed isolated ventriculomegaly, white matter microstructure as determined by FA, showed altered development. Reductions in FA values, compared to term born control neonates with normal imaging, were detected in white matter regions including the splenium of the corpus callosum, sagittal stratum bilaterally and right posterior corona radiate.

Neurobiological basis of FA changes

In normal development white matter maturation is accompanied by an increase in FA which is likely influenced by early neurogenesis, fibre organisation, pre-myelination and myelination (Huppi et al., 1998; Neil et al., 1998; Wimberger et al., 1995)**.** At term age myelination has only occurred in the posterior limb of the internal capsule and the brainstem (Yakovlev and Lecours, 1967) therefore a reduction in FA probably reflects deficits or delays in pre-myelination including increased axonal thickness, alteration in axonal permeability and pre-myelination wrapping of the oligodendrocytes around axons (Wimberger et al., 1995). During the pre-myelination stage an increase in FA is attributed to numerous histological changes including an increase in the number of axonal microtubule-associated proteins, a change in axon calibre, changes in axonal membrane (Na^+/K^+ activity) and an increase in the number of oligodendrocytes (Fields and Waxman, 1988; Wimberger et al., 1995). The highest FA values in the immature brain are in the genu and splenium of the corpus callosum (Partridge et al., 2004) due to their compactness and high degree of parallel organisation. A more sustained increase in FA is noted during myelination of the posterior limb of the internal capsule in the newborn infant and is visible on T_1 and T_2 weighted images. In addition to myelination, other factors influence FA changes such as axon compactness, relative membrane permeability to water, internal axonal structure and tissue water content. DTI is an indirect method of assessing white matter microstructure and the reduction in FA may have different aetiologies as described above. Post-mortem studies in cases with isolated ventriculomegaly would provide insights into the underlying mechanism leading to a reduction in FA. However, there are currently no post-mortem studies in this population as the majority of cases have a good outcome and a high survival rate. In chapter

3.4 we showed a potential increase in choline in fetuses with ventriculomegaly which may reflect alterations in myelin synthesis and therefore a reduction in FA as observed during neonatal life.

Comparison with previous neonatal DTI studies

In our study we have found that neonates with isolated ventriculomegaly have significantly reduced FA values compared to controls in the splenium of the corpus callosum, sagittal stratum bilaterally and right posterior corona radiate. White matter microstructure has been previously assessed using DTI in 34 neonates with antenatally diagnosed isolated ventriculomegaly and compared with 34 age- and sex-matched controls (Gilmore et al., 2008). Analysis was performed using a region of interest approach on non-registered images and FA was compared between groups in pre-determined regions including the corpus callosum and the corticospinal tracts. They showed that neonates with ventriculomegaly had a significant reduction in FA in the central splenium, left cortical splenium, left cortical corticospinal and right central corticospinal regions. Subsequently they developed a population-based registration method, similar to our methodology, and compared FA values in predetermined regions of interest including the genu and splenium of the corpus callosum and the corticospinal tracts (Goodlett et al., 2009). The comparison was performed between 13 neonates with isolated ventriculomegaly and 85 term controls. They showed a significant reduction only in the splenium of the corpus callosum. Our study is in agreement with the results from this study showing a reduction in FA values in the splenium of the corpus callosum. Unfortunately their investigation did not include FA quantification throughout the white matter tracts therefore we are unable to compare our results any further.

Additional studies on white matter microstructure in neonates have been performed in preterm-born children imaged at term equivalent age (Anjari et al., 2007; Skiold et al., 2010; van Kooij et al., 2012). The brain appearance of the neonates included in these studies was considered normal. Van Kouij et al. (2012) performed DTI in 63 preterm-born term equivalent neonates with no evidence of lesions on MRI and reported a positive relationship between FA in the body and the splenium of the corpus callosum and cognitive outcome at 2 years corrected age. FA throughout the white matter significantly correlated with fine motor

scores at 2 years corrected age, with particular significance including the corpus callosum, corona radiata, superior longitudinal fasciculus, and inferior longitudinal and fronto-occipital fasciculi. Additional studies using DTI and TBSS have been performed on preterm infants with no evidence of focal lesions compared to term-born neonates. Reductions in FA in white matter regions (Anjari et al., 2007; Skiold et al., 2010) have been reported, there is however no overlap between the regions identified in these studies and our study. Correlation between FA values and outcome was not performed in these studies.

White matter tracts and function

Our study revealed reductions in FA in the splenium of the corpus callosum, right posterior corona radiate and sagittal striatum. Multiple white matter tracts run in parallel through these regions and it is not possible to extrapolate which white matters tracts specifically contribute to the changes in FA observed. The majority of white matter pathways highlighted in our study and including the superior and inferior longitudinal fasciculi, inferior fronto-occipital fasciculus, splenium of the corpus callosum and posterior thalamic radiations are involved mainly in language circuitry and also in cognitive and attention skills (Catani, 2007; Doricchi and Tomaiuolo, 2003; Dramsdahl et al., 2012; Duffau et al., 2002; Gazzaniga, 2000; Hynd et al., 1995; Leclercq et al., 2010; Nosarti et al., 2004; Qiu et al., 2011; Tanabe et al., 1987). The regions highlighted in our study do not contain major tracts involved in motor functioning. This would be expected as outcome studies in children with antenatally diagnosed ventriculomegaly have shown an increased risk of abnormal development outcome mostly in cognitive, behavioural and communication domains with few motor impairments documented (Beeghly et al., 2010; Bloom et al., 1997; Gomez-Arriaga et al., 2012; Leitner et al., 2009; Lyall et al., 2012; Sadan et al., 2007).

Neurological examination

The presence of head lag or low neck tone may be a sign of later neurological impairment however as part of a normal otherwise neurological exam it is unclear whether it is predictive of later deficits.

Limitations

There was a significant difference in post-menstrual age at scan between cohorts, with the neonates with ventriculomegaly being scanned at a later age compared to controls. However FA values should increase with postmenstrual age and therefore higher values would have been expected in the ventriculomegaly cohort. The reason for this difference in postmenstrual age at scan lies in the recruitment of the normal controls enrolled in the different studies. Term-controls for studies other than the fetal research program recruited their participants shortly after birth in Queen Charlotte's and Chelsea Hospital. However participants enrolled in the fetal research program were invited for a scan after the parents had left the hospital while the majority were born in other London hospital therefore delaying the day of scan.

Due to spatial resolution limitation of current DTI methods, distinction between pathways crossing the same white matter regions is not possible with the current method although additional techniques such as DTI-tractography can be used for the delineation of individual groups of white tracts (Mori et al., 2002). Specificity of tracts is lost when tracts run parallel or merge together. At the resolution achieved *in vivo*, it is inevitable that the voxels will contain fibre population with different orientations. These areas also introduce bias due to intra-subject variation.

While there is a higher proportion of male subjects in the ventriculomegaly cohort we have not controlled for sex in the TBSS analysis due to the restricted participant numbers. However, a study (Geng et al., 2012) in preterm-born children imaged at term (with normal brain appearance) showed no difference in FA in white matter tracts between males and females. While not performed during this study a comparison between sex in the controls should be included in future work.

Conclusions

Antenatally diagnosed isolated ventriculomegaly is a significant risk factor for later development delay. Previous studies have shown that the areas of development mostly affected in these children include language, behaviour, attention and cognitive skills (Beeghly et al., 2010; Bloom et al., 1997; Gomez-Arriaga et al., 2012; Leitner et al., 2009; Lyall et al., 2012; Sadan et al., 2007). We have shown that neonates with antenatally diagnosed ventriculomegaly exhibit significant reductions in FA in white matter tracts involved in language, cognition and attention. These results may be consistent with a delay in maturation or abnormal development of the specific white matter tracts. Future work should involve the detailed neurodevelopmental assessment of the children enrolled in this study with specific aim to correlate changes in FA with specific developmental scores.

3.6 Neurodevelopmental outcome in children with antenatal ventriculomegaly (Preliminary results as part of on-going study)

In this chapter we present preliminary results of the neurodevelopmental outcome of a small cohort of children with isolated antenatal ventriculomegaly enrolled in our study. Follow-up is still on-going and currently the participant numbers are small however they provide an insight in the developmental deficits present in this cohort and allow for comparison with the current literature.

3.6.1 Aim

To assess the neurodevelopmental outcome of children with antenatal isolated ventriculomegaly at 1 and 2 years of age and correlate developmental scores with MR measurements.

3.6.2 Developmental assessments at year 1 of age

All fetuses with an antenatal diagnosis of isolated ventriculomegaly enrolled in the research program were invited for a developmental assessment at year 1 and year 2 of age. Assessment at 1 year of age was performed using the Griffiths Mental Development Scales (GMDS). A total of 45 children were diagnosed with ventriculomegaly and born during the period of March 2008-July 2011 and were invited for a developmental assessment when they reached their first year of age. A complete assessment was performed in 28 children representing a 62.2% follow up rate at a mean chronological age of 12.5 (± 1.5) months and a range of 9-16.5 months (Table 31). 17 infants did not take part due to the following reasons: refusal to attend for an assessment (6), unable to contact parents (5), assessment missed (5), neonatal death due to non-CNS abnormalities (1). There was no significant difference (p=0.483) in atrial diameter between the children that had an assessment and those that did not attend. Parental filled questionnaires were posted to the parents that we were unable to contact and those that refused to attend for an assessment. In 2 cases completed questionnaires were sent back. In addition, in 2/5 cases that the assessments were missed at 1

year of age the infants were assessed at 2 years of age. Therefore some information was available on 32 out of 44 children (71%).

Neurodevelopmental assessment at 1 year of age		
Total children assessed	28 out of 45	
Male	22	
Female	6	
Age (months)	12.5 (±1.5)	(9-16.5)
Atrial diameter (mm)	11.8 (±1.2)	(10.1-14.8)

Table 31. Year 1 cohort characteristics

For the age and atrial diameter, measurements are shown in mean (SD) and range.

According to the results of the GMDS, 71.4% of the children assessed had scores within the normal range in all the developmental scales.

In the Locomotor domain 26 children (92.8%) showed normal development while 1 infant showed borderline delay and 1 infant severe delay. Two children with normal motor development had reduced tone in their lower limbs and both were re-assessed at 2 years of age. In one case this normalised while it persisted in the second case. No children had signs consistent with cerebral palsy.

On the Language and Hearing scale, 20 children (71.4%) had normal language development while 8 children (28.6%) showed mild delay.

On the Personal-Social and Eye-Hand Co-ordination scales all children had scores within the normal range.

The Performance scores revealed normal development in 25 cases, borderline scores in 2 cases (7%) and mild delay in 1 case (3.6%).

Three children (10.7%) had poor attention skills and difficulty concentrating during the assessment as observed by the clinical psychologist although this was not formally assessed.

Two cases that completed ASQ assessments and scores within the normal range in all sub-scales.

As a provisional analysis and accepting follow up is not complete and numbers are small, the sub-quotient scores for each sub-scale in the GMDS were correlated with the atrial diameter, larger lateral ventricle volume and total lateral ventricular volume (Table 32). There was a significant negative correlation between eye and hand co-ordination and total lateral ventricular volume (Spearman's r=-0.4, p=0.019). However this correlation did not withstand Bonferroni correction for multiple comparisons. There was also a negative correlation, of borderline significance (p~0.06), between atrial diameter and eye and hand co-ordination scores and performance scores.

	Language and Hearing	Personal and social	Locomotor	Eye and hand co-ordination	Performance	DQ
Atrial diameter	0.07	-0.04	-0.08	-0.28	-0.29	-0.13
Larger lateral ventricle volume	-0.04	-0.07	-0.11	-0.25	-0.07	-0.1
Total lateral ventricular volume	-0.07	-0.18	-0.19	**-0.4***	-0.22	-0.24

Table 32. Relationship between MR measurements and GMDS outcome scores at year 1

Eye and hand co-ordination scores correlated negatively with the total lateral ventricular volume. Correlation was assessed using the Spearman's r. * $p<0.05$

3.6.3 Developmental assessments at year 2 of age

A total of 25 children were diagnosed with antenatal ventriculomegaly and born in the period of March 2008-July 2011 and were invited for a developmental assessment when they reached their second year of age. Assessments at 2 years of age were performed using the Bayley Scales of Infant and Toddler Development-III (BSID-III). A complete assessment was performed in 16 children (64%) at a mean chronological age of 25.2 (±3) months and a range of 19.5-33 months (Table 33). 12 children had assessments at both years 1 and 2. There were 9 children that did not have an assessment for reasons including refusal to attend (5), unable to contact parents (3) and neonatal death (1). There was no significant difference (p=0.261) in atrial diameter between the children that had an assessment and those that did not attend. Questionnaires were sent to the parents that declined to attend or those who we were unable to contact. One of the cases that declined assessment and 1 case that we were unable to contact completed the questionnaires. Out of the 16 children that attended, 13 were assessed using the BSID-III and 3 were assessed using the GMDS.

Neurodevelopmental assessment at 2 years of age		
Total children assessed	16 out of 25	
Male	11	
Female	5	
Age (months)	25.2 (±3)	(19.5-33)
Atrial diameter (mm)	12.2 (±1.6)	(10.1-16.4)

Table 33. Year 2 cohort characteristics

For the age and atrial diameter, measurements are shown in mean (SD) and range.

According to the results of the BSID-III for 13 children and the GMDS for 3 children, only 37.5% of the children assessed had scores within the normal range in all developmental scales.

On the Gross Motor scale, 14 children (87.5%) showed normal development and 2 children (12.5%) were delayed in their gross motor skills. No children had signs consistent with cerebral palsy. In the Fine Motor scales 1 child had delayed development while another child

had borderline scores. Only one of these children had both fine motor and gross motor delay. One child with normal motor development had slightly lower tone in his knees, hips and shoulders.

On the Language scale, only 8 children (50%) had normal language skills, of which two had scores in the borderline/lower normal range, one of which was raised in a bilingual environment. Delayed language development was detected in 8 children (50%). One of the children with severe language delay had signs of autism.

The Cognitive scale scores revealed normal cognitive development in 14 children (87.5%) while 4 children (25%) had delayed cognitive scores. All children with delayed cognitive development also had language delay. One child with language delay had cognitive scores in the lower normal range.

As observed by the clinical psychologist seven children (43.8%) had a short attention span and 5/7 of those also had language delay. However attention skills were not formally assessed.

Two cases that completed ASQ assessments showed scores within the normal range in all sub-scales.

Whilst the numbers are very small we did some preliminary statistical analysis as follows. In the 8 children with language delay at 2 years of age the mean atrial diameter was 12.9 mm (±1.7) and a range of 11-16.4 mm while in the 8 children with normal language development for their age the mean atrial diameter was 11.8 mm (±1.5) and a range of 10.1-14.1 mm. There was no significant difference between the atrial diameter measurements between the two groups however all children with language delay had an atrial diameter >11 mm.

The scores for each sub-scale in the BSID-III were correlated with the atrial diameter, larger lateral ventricle volume and total lateral ventricular volume (Table 34). There was a significant negative correlation between fine motor scores and atrial diameter (Spemann's r=-

0.64, p=0.017) however significance was lost after applying the Bonferroni correction. There was a negative correlation of borderline significance (p~0.05) between atrial diameter and cognitive scores (prior to Bonferroni correction). These correlations have been limited by the small number of data available for statistical analysis. BSID-III data were only available for 11 children as 1 autistic child did not complete any tasks and 3 children had the GMDS at 2 years. These 3 children without BSID-III scores had the largest ventricular atrial diameters in the cohort and all had language delay while 2 also had motor delay. In addition, volumetric data were not available in 1 case due to excessive fetal motion prohibiting brain reconstruction.

	Cognitive	Language (Receptive)	Language (Expressive)	Language sum	Fine motor	Gross motor	Motor sum
Atrial diameter	-0.47	-0.40	-0.25	-0.38	**-0.64***	0.01	-0.45
Larger lateral ventricle volume	0.25	0.27	0.20	0.29	0.03	0.06	0.12
Total lateral ventricular volume	0.36	0.33	0.16	0.36	0.08	0.16	0.21

Table 34. Relationship between MR measurements and BSID-III outcome scores at year 2

Fine motor scores correlated negatively with the total lateral ventricular volume. Correlation was assessed using the Spearman's r. * $p<0.05$

There were 3 children that were born preterm (32^{+4}-36^{+3} weeks) and were assessed at year 1 and year 2 of age. One child born at 35 weeks GA had scores within normal limits in all developmental scales however the neurological exam showed reduced tone in knees, hips and shoulders at both assessments. One child born at 32^{+4} weeks GA showed normal development in all scales at 1 and 2 years of age. One child was born at 36^{+3} weeks GA and at year 1 of age had language delay while at year 2 was delayed in the language, cognitive and motor scales.

Children assessed at both year 1 and year 2

Twelve children were assessed at year 1 and year 2 of age. The results of the developmental assessments are summarised in Table 35.

#	Development at year 1	Development at year 2
1	normal	***language/cognitive delay***
2	normal	***borderline fine motor***
3	normal	normal
4	normal	***language/cognitive delay***
5	normal	***language/cognitive delay***
6	normal	normal
7	normal	normal
8	***language delay***	***language/cognitive/motor delay***
9	normal	***language/cognitive***
10	***language delay***	***borderline language***
11	***language/performance delay***	***borderline language***
12	***language/motor delay***	***language/motor delay***

Table 35. Comparison between developmental outcomes at 1 and 2 years of age in 12 cases

3.6.4 Discussion

While the majority of children (71.4%) at year 1 had a normal neurodevelopmental outcome, only 37.5% of children at 2 years of age had scores within the normal range in all developmental domains. The deficits detected in this preliminary cohort were mostly within language and cognitive domains. At 2 years of age, 50% of children had significant language delay requiring referral to speech and language therapy. Language delay was associated with cognitive delay in half of the cases. All cases with language delay had an atrial diameter above 11 mm. As observed by the clinical psychologist, children with language delay also had difficulties concentrating and had short attention span although this was not formally assessed. Out of the 8 cases that had language delay only 2 cases were identified at 1 year of age indicating as expected that follow-up studies before 2 years of age will underestimate the risk of this abnormal outcome. There was a significant negative correlation between fine motor scores and ventricular size at year 1 and year 2. These results require verification with a larger number of participants.

Our study is in agreement with the study by Sadan et al. (2007) who assessed 20 children with antenatal isolated ventriculomegaly (10-15 mm) at a mean age of 32.3 months (1-42 months) using the BSID-II. They showed that the deficits present in their cohort were mostly of a mental (including language) and behavioural nature while motor development was the least affected. 25% of the children required early intervention. Lyall et al. (2012) assessed 28 children with antenatal ventriculomegaly at 2 years of age and found reduced developmental scores in expressive language and fine motor scales while there was no difference in gross motor, visual perception and receptive language. Gomez-Arriaga et al. (2012) assessed 18 children diagnosed with antenatal ventriculomegaly (10-12 mm) at a mean age of 4.4 years and found that the areas with the highest number of affected children were the personal-social, adaptive (including attention) and motor areas followed by cognitive and language areas. They commented that 60% of the motor deficits were minor deviations from normality. The reasons for an increased incidence of motor problems may be due to that diagnosis of isolated ventriculomegaly made solely on ultrasound. Therefore some of the cases diagnosed as isolated ventriculomegaly may have had additional abnormalities not detected on antenatal ultrasound, such as subependymal heterotopia and agenesis of the

corpus callosum. Bloom et al. (1997) assessed 22 children with antenatal ventriculomegaly (10-15 mm) at a mean age of 21.6 months using the BSID-II and the Vineland Behaviour scales. They reported that 8 out of the 22 children assessed had developmental delay whilst their scoring analysis revealed significantly reduced scores in the ventriculomegaly group for mental and motor development. There was no difference in scores in the behaviour scale. Atrial diameter and mental developmental index score correlated negatively ($r=-0.5$, $p=0.001$). Similarly to the previous study, ultrasound was the sole diagnostic modality for isolated ventriculomegaly therefore cases with additional abnormalities may be present in their group. As reported by the authors, one case required placement of a ventriculoperitoneal shunt at 2 months of age which is atypical for isolated ventriculomegaly.

There have been only 2 studies that have used MRI to confirm no additional abnormalities after an ultrasound referral of ventriculomegaly and have excluded cases with chromosomal abnormalities and positive infection screening (Beeghly et al., 2010; Leitner et al., 2009). Leitner et al. (2009) showed that children ($n=28$) with antenatal isolated bilateral ventriculomegaly as assessed at 4.4 years had significantly reduced attention span and working memory scores compared to controls and suggested that these specific difficulties could later influence academic performance at school. Similarly, a number of the children in our study were reported to have a short attention span and difficulty focusing. Beeghly et al. (2010) reported that while the average scores in mental, motor and behaviour development were within normal limits, individual scores in either sub-scale varied from severely or mildly delayed to within normal limits. Surprisingly the average motor score at 1 year of age was significantly higher (more advanced skills) in the ventriculomegaly cohort compared to controls.

We investigated the relationship between developmental scores at year 1 and year 2 and ventricular size. While the number of children assessed to date is limited there was a significant negative correlation between fine motor scores and ventricular size. Fine motor skills included the tasks of block stacking, drawing and manipulation of small objects. Such tasks involve somatosensory and visual perception, motor control and different cognitive processes. Larger numbers of cases are required to validate these results.

There were 2 children that had delayed motor development at year 2. One child had persistent ventriculomegaly as was shown on fetal scans (GA 22 and 31 weeks, ~12 mm) and after birth on serial cranial ultrasounds and two MRIs (PMA 45.9 weeks 10.7 mm and 50.4 weeks moderate/severe ventriculomegaly). The ventricles had an abnormal shape while the thalami appeared fused in the latest MRI. One could argue that this case should be excluded from out cohort. The second child with motor delay had mild ventriculomegaly as a fetus (10.7 mm) while in the neonatal MRI at 43^{+2} weeks the ventricles had normalised (atrial diameter <10 mm) and no other brain abnormality was detected. This child also experienced problems in the first year of life due to lactose intolerance.

Of interest 1 child in our young cohort showed autistic features including lack of response to name, severely delayed language development, lack of facial expressions, avoidance of eye-contact, lack of interaction and repetitive motor behaviour at 25.5 months of age. A diagnosis of autism is usually not made until approximately the age of 4 because features of the disorder may not be evident or may be subtle before 3-4 years of age. Developments in clinical diagnosis including increased expertise and use of standardised diagnostic instruments (ADOS and ADI-R) show that diagnosis can be reliable, valid and stable from the age of 2 years (Kleinman et al., 2008; Lord et al., 2006). The children in our cohort where not tested specifically for autistic spectrum disorders and therefore we cannot at the moment ascertain the incidence of autism in our study. As part of our future plan we aim to test our cohort using a battery of autism tests including the ADOS and ADI-R at 3 years. Ideally follow-up should be extended to school age as mild manifestation of developmental delay including communication disorders and attention deficits and learning disorders may not be apparent at an earlier age.

In conclusion, in our preliminary data we have shown that children with antenatal ventriculomegaly have increased risk of language, cognitive and attention difficulties at 2 years of age while there is evidence of a relationship between fine motor scores and ventricular size. However, neurodevelopmental follow-up in these children is still on-going and the data presented in this chapter are preliminary and require further validation.

4. Main discussion

Fetal ventriculomegaly is the most common CNS abnormality and is associated with neurodevelopmental impairments in childhood. When isolated, the aetiology of the dilatation is usually unknown and the outcome is only partially predicted by the atrial diameter. The neurodevelopmental outcome of these children is variable and includes language, cognitive and behavioural deficits while the reasons for this variability are not well understood. Much of the initial research has focused on outcome prediction and characterisation of the nature of deficits whilst classifying the degree of the dilatation according to the atrial diameter. A very limited number of studies exist investigating brain development in fetuses with ventriculomegaly and these have been unable to detect any brain volumetric differences when compared to controls (Grossman et al., 2006; Kazan-Tannus et al., 2007; Pier et al., 2011; Scott et al., 2012). Ventriculomegaly has been associated with cerebral overgrowth in a fetal rat model (Eyles et al., 2003), in children with Soto's syndrome (Leventopoulos et al., 2009; Palmen et al., 2005), hemimegalencephaly (Kalifa et al., 1987), and high-functioning children with autism (Palmen et al., 2005). Therefore we hypothesise that fetal ventriculomegaly is a marker of altered brain development characterised by relative brain overgrowth. The main aims and findings of this thesis are summarised in Table 36.

Aims	Methods	Main findings
To establish whether there is evidence of relative overgrowth and/ or aberrant development in multiple intracranial structures in fetuses with ventriculomegaly	Manual segmentation of fetal intracranial structures	Fetuses with ventriculomegaly had significantly increased brain volumes and enlargement was restricted to the cortical gray matter.
To establish whether volumetric changes evident during fetal life persist after birth.	Automatic segmentation of neonatal intracranial structures	Ventricular and brain volumes were increased in neonates with antenatal ventriculomegaly.
To design a detailed protocol for the evaluation of cortical development. To establish whether ventriculomegaly is associated with delayed or abnormal cortical maturation.	Cortical scoring system	There was a delay in the appearance of cortical landmarks in fetuses with ventriculomegaly. The delay persisted in the calcarine sulcus and parieto-occipital fissure.The sylvian fissure showed aberrant development with an increased opercular distance.
To assess differences in brain metabolite ratios between fetuses with isolated ventriculomegaly and normal fetuses.	^{1}HMRS	NAA:Cho, MI:Cho and MI:Cr ratios were lower whilst Cho:Cr ratios were higher in fetuses with ventriculomegaly.
To assess the white matter development in neonates with antenatal ventriculomegaly.	DTI	FA was decreased in the splenium of the corpus callosum, sagittal stratum bilaterally and right posterior corona radiate in neonates with antenatal ventriculomegaly.
To assess the neurodevelopmental outcome of children with antenatal isolated ventriculomegaly at 1 and 2 years of age and correlate with MR measurements.	Neurodevelopmental assessments	Preliminary data: At 2 years of age, 62.5% of children had developmental delay. 32% had language delay, 16% cognitive delay and 8% delayed motor development.

Table 36. Main aims and findings of this thesis

This study has longitudinally assessed 60 MR scans of normal control fetuses between 22.4-38.9 gestational weeks and 65 MR scans of fetuses with isolated ventriculomegaly between 22-37.3 gestational weeks using volumetric analysis on reconstructed images. We have shown that isolated ventriculomegaly in the presence of a normal karyotype and a normal infection status is associated with increased supratentorial brain volume which is apparent from mid gestation. Volumetric analysis of intracranial structures revealed that brain enlargement was restricted to the cortical gray matter while there was no significant difference in white matter and central gray matter volumes. An altered relationship was present between ventricular size and the developing brain structures in the ventriculomegaly

cohort. Our results are in contrast to previous fetal MR volumetric studies that have shown no difference in brain tissue or cortical volume in fetuses with isolated ventriculomegaly (Grossman et al., 2006; Kazan-Tannus et al., 2007; Pier et al., 2011; Scott et al., 2012). However these studies have had several limitations including use of non-homogeneous ventriculomegaly populations, inappropriate criteria for selection of normal controls and volumetric analysis performed on non-reconstructed MR datasets known to be sensitive to fetal motion. These limitations have been taken in to account during the design of this study. Our study is in agreement with Gilmore et al. (2008) who showed that neonates with antenatally diagnosed isolated ventriculomegaly have increased cortical volumes compared to controls. Furthermore, we have followed up a subgroup of these fetuses and quantified volumetric changes of brain parenchyma after birth and have shown that brain overgrowth persists in neonatal life. Volumetric delineation of cortical gray matter and white matter is currently underway to assess whether brain overgrowth is attributed to cortical overgrowth in neonatal life. Greater brain parenchyma and cortical gray matter volume may be due to lack of normal developmental apoptosis in the developing brain, a process essential for brain morphogenesis during gestation and synaptogenesis during the late fetal and postnatal period. Several animal knockout studies have shown that alterations in genes regulating developmental apoptosis lead to changes in cortical size and shape (Chenn and Walsh, 2002; Depaepe et al., 2005; Oppenheim et al., 2001). In previous studies in preterm and IUGR infants abnormal neurocognitive outcome has been associated with a reduction in cortical volume. However, fetuses with isolated ventriculomegaly are at increased risk of neurocognitive delay but according to our study exhibit increased cortical volumes. This suggests that it may be the quality of the connections and not the absolute cortical volume relating to later neurocognitive outcome.

Due to the neurocognitive nature of deficits reported in children with fetal ventriculomegaly and the notion of the neurobiological origin of cognitive impairment within the developing cortex we aimed to assess the temporospatial schedule of formation of sulci and gyri. To assess cortical development and quantify cortical maturation during fetal life we designed a detailed protocol for the evaluation of cortical development similar to the cortical scoring system used by van der Knaap et al. (1996) in preterm infants. While previous studies have

evaluated cortical folding in large brain areas we have selected individual gyri and sulci representative of each brain lobe and performed a detailed assessment of cortical folding. We have demonstrated that this was a feasible and reproducible modality to quantify cortical development in the fetal brain. The normal control fetuses were assessed to create a normative reference dataset which was used for comparison with fetuses with isolated ventriculomegaly. We have found regional differences in cortical development between fetuses with isolated ventriculomegaly and control fetuses. The gestational age of the early form of gyri and sulci was delayed in the ventriculomegaly cohort by approximately 2 weeks with delay present in all brain lobes studied. Our results are in agreement with the study by Levine and Barnes (1999) that reported a 2-week mean lag in the time of appearance of cortical gyrification. While there was evidence of persistent delay throughout gestation in several cortical areas, significance was only reached for the calcarine suclus and parieto-occipital fissure. The data did not withstand Bonferroni correction for multiple comparisons except for the calcarine and parieto-occipital landmarks suggesting that changes in cortical folding are more prominent in these cortical regions. Our results are in agreement with the study by Scott et al. (2012), using curvature analysis, showing reduced cortical folding in the parieto-occipital fissure in fetuses with isolated ventriculomegaly. A cortical region that could not be assessed with the cortical scoring system, due to its complex formation, was the Sylvian fissure. It was included in our analysis because it encompasses regions involved in language processing and was evaluated using a different approach. Interestingly we found altered development in the Sylvian fissure with an increased opercular distance length with a normal insular length. The functional impact of this finding needs further investigation. While the underlying mechanisms that drive the formation of cortical undulation are unclear, the major hypotheses (Nie et al., 2011; VanEssen, 1997) support that white matter fibre and synaptic development are involved in the regulation of cortical gyrification and therefore changes in cortical development may reflect aberrant white matter connectivity.

The next component of the study assessed the metabolic profile of the developing brain in normal control fetuses and fetuses with isolated ventriculomegaly. In the normal fetal brain it was shown that the ratios of metabolites NAA:Cr and NAA:Cho increased with increasing GA at echo times 136ms and 270ms and Cho:Cr decreased with advancing gestation at echo

times 136ms and 42ms. These findings may be attributed to increasing levels of NAA during development reflective of increased myelination and synaptic complexity while a decrease in choline levels may reflect the high demands for cell membrane formation during this period and increased myelination. At echo time 42ms, MI:Cr metabolite ratios decreased with advancing GA which may be attributed to stable Cr levels and decreasing myo-inositol levels reflecting the high density of glial cells in between 22 and 28 weeks (Girard et al., 2006a). When comparing between our cohorts a significant alteration in brain metabolism was detected, with fetuses with ventriculomegaly exhibiting lower NAA:Cho levels compared to controls. This alteration most likely is attributed to reduced NAA levels and may reflect delayed white matter development and alterations in the pre-myelination processes. NAA is a neuronal marker, however is also present in oligodendrocytes. A reduction in NAA has been deleted in IUGR fetuses and attributed to mitochondrial dysfunction in the absence of neuronal loss (Story et al., 2011a). A reduction in NAA has also been reported in autistic children and suggested it reflects decreased neuronal density as a consequence of increased glial numbers (Aoki et al., 2012). In addition, we detected decreased MI:Cho and MI:Cr ratios and increased Cho:Cr levels indicating a reduction in myo-inositol levels and/or increase in choline. Myo-inositol is essential for the closure of the neural tube and brain morphogenesis and decreased levels may reflect an underlying metabolic process linked to altered CNS development. Lastly, choline levels have been shown to decrease in normal fetuses as choline molecules are incorporated into myelin lipids. Therefore an increase in choline levels in fetuses with ventriculomegaly may reflect higher levels of unbound choline molecules present after failure to incorporate into myelin lipids. This may lead to delayed white matter development and myelination. In conclusion, these changes in the metabolic profile of fetuses with isolated ventriculomegaly may reflect a delay or impairment in white matter development.

While there was no difference in white matter volume in fetuses with ventriculomegaly during gestation, alterations in cortical development, in volume and maturation, and changes in the metabolic profile in the context of increased risk for developmental delay suggested delayed or impaired white matter development. In order to assess white matter development we used DTI and TBSS to compare white matter microstructure in neonates with antenatal

ventriculomegaly (imaged during fetal life) compared to controls. We showed a significant reduction in FA in white matter regions including the splenium of the corpus callosum, sagittal stratum and right posterior corona radiate. The white matter pathways highlighted in our study are involved in the circuitry of language, attention and cognition. Our results are in agreement with Goodlett et al. (2009) that showed a reduction in FA in the splenium of the corpus callosum in neonates with isolated ventriculomegaly compared to controls. A reduction in FA may reflect a delay in maturation or abnormal development of the specific white matter tracts. More specifically a reduction in FA during neonatal life probably reflects deficits or delays in pre-myelination including increased axonal thickness, alteration in axonal permeability and pre-myelination wrapping of the oligodendrocytes around axons (Wimberger et al., 1995). Neurodevelopmental assessments of these children at 2 years of age are currently underway with the aim to correlate changes in FA with development scores in cognitive, language and motor domains.

Finally, we have assessed the neurodevelopmental outcome in a small number of children enrolled in our study however the data presented are preliminary and part of an on-going study. We have shown that from the children assessed at 2 years of age, only 37.5% of children with isolated antenatal ventriculomegaly had a normal outcome. The deficits detected in this preliminary cohort were mostly within language and cognitive domains. Only 2 children had delayed motor development. Although not formally assessed but observed by the clinical psychologist half of the children had a short attention span and difficulty concentrating during the assessment. Our results are in agreement with the current literature supporting that children with isolated ventriculomegaly are at increased risk of abnormal development with delays in language and cognitive skills, while motor skills were the least affected (Bloom et al., 1997; Gomez-Arriaga et al., 2012; Leitner et al., 2009; Sadan et al., 2007). While small numbers did not allow for comparison of MR measurements between cases with an abnormal outcome and those with normal development we have assessed the relationship between developmental scores and ventricular size. Ventricular size showed a negative correlation with fine motor scores at 1 and 2 years of age, however these results require further verification.

In conclusion, we have shown that brain development during fetal and neonatal life is altered in the presence of isolated ventriculomegaly. There are macro- and microstructural differences associated with isolated ventriculomegaly and including measures of total brain size and cortical gray matter, cortical gyrification, metabolite levels and white matter connections. These changes may form the neural basis of later abnormal neurodevelopment and further correlation with developmental scores may aid outcome prediction.

5. Future work

5.1 Volumetric segmentation of the cerebellum in fetuses with ventriculomegaly

While we performed volumetric analysis of supratentorial brain parenchyma and all CSF spaces, structures below the tentorium were not included, these comprise the cerebellum and brainstem. These structures were not segmented during this study firstly because ventricular enlargement was thought to be restricted to the lateral ventricles and therefore hypothesised that any alterations in brain development would be restricted to supratentorial structures. Secondly, in the study of Gilmore et al. (2008) in neonates with antenatal ventriculomegaly there was no difference in cerebellar volume when compared to a control cohort. However our results indicate that enlargement of the lateral ventricles is accompanied by enlargement of the fourth ventricle therefore cerebellar development may also be altered in the presence of ventriculomegaly. In addition, there has been increasing recognition of the role of the cerebellum in cognitive processing (Steinlin, 2007) therefore cerebellar development should be included in future work.

5.2 Volumetric segmentation of white matter and gray matter in neonates with ventriculomegaly

While we have shown that neonates with antenatal ventriculomegaly have increased supratentorial brain tissue volume we have been unable to demonstrate (due to time constraints) whether this enlargement was restricted to cortical overgrowth as shown during fetal life. While the volumetric algorithm used in chapter 3.2.2 has delineated between white matter and cortex, manual editing is required for the correction of mislabelled voxels. Segmentation of these structures is currently underway.

5.3 Neurodevelopmental follow up in children with antenatal ventriculomegaly

As mentioned in chapter 3.6, neurodevelopmental follow in children with ventriculomegaly is on-going. The future aim of this part of the study is to correlate the developmental scores of children with ventriculomegaly with MR measurements including ventricular and brain size, cortical gyrification and FA values.

The assessments currently performed do not include behaviour and attention skills evaluation. Therefore as part of our follow-up assessment we aim to use a battery of autism tests including the Autism Diagnostic Observation Schedule (ADOS) and Autism Diagnostic Interview-Revised (ADI-R) at 3 years in order to formally characterise the behavioural phenotype of these children.

5.4 Correlation of neurodevelopmental outcome and white matter development

Neurodevelopmental data are currently being collected for the 22 neonates with ventriculomegaly that had DTI performed. Future work should aim to assess the relationship between diffusion parameters and specific neurodevelopmental performance at 2 years of age. Previous studies have shown that neurodevelopmental performance can be predicted by FA values in white matter on DTI analysed by TBSS (Beaulieu, 2002; Peters et al., 2011; Tusor et al., 2012).

5.5 Vitamin D and brain development: a pilot study

As discussed in the introduction, the aetiology of fetal isolated ventriculomegaly is unknown. There has been a newborn rat model of gestational Vitamin D deficiency (Eyles et al., 2003) with a brain phenotype of ventriculomegaly and cortical overgrowth similar to the findings described in our study in the fetus with ventriculomegaly. These changes were attributed to a disruption in the balance between neuronal stem cell proliferation and programmed cell death in the offspring (Eyles et al., 2003; Feron et al., 2005). In the recent years there has been increasing interest in the role of Vitamin D in the brain, a previously understudied area however these is no human study investigating the effect of maternal Vitamin D deficiency on the developing fetal brain. We have completed a retrospective pilot study to determine the

feasibility of measuring Vitamin D levels in stored booking bloods obtained at 12 weeks of gestation. We have recently received ethics and funding to proceed with a larger prospective study to determine the effect of maternal Vitamin D deficiency in normal control fetuses. This chapter summarises the background, design and results of the pilot study and concludes with the main aims of the larger prospective study on the effect of Vitamin D deficiency on brain development.

Background

The fetus relies on placental transfer of 25(OH)D whilst Vitamin D deficiency in pregnancy is of epidemic proportions (Hollis and Wagner, 2006). In of one of the few studies of pregnant women from ethnic minorities in the UK more than 50% of women had a plasma 25(OH)D level in the deficient range (Datta et al., 2002). The consequences for the fetus extend beyond the traditional effects on bone development although splaying of the fetal femora has now been documented on ultrasound as early as 19 weeks gestation (Mahon et al., 2010). Infantile rickets is on the increase, (Holick, 2006; Kreiter et al., 2000) women who breast feed placing their infants at the highest risk (Ziegler et al., 2006). In a London study 1.6 neonates per 1000 deliveries presented with symptomatic vitamin D deficiency such as seizures (Sharma et al., 2009). Vitamin D deficiency during pregnancy is also important in fetal "imprinting" and may affect immunity (Harvey et al., 2010) and chronic disease susceptibility such as type II diabetes later in life. The relationship between multiple sclerosis and latitude and season at birth points strongly to an association with vitamin D (Holick, 2006). Neonatal Vitamin D deficiency has also been linked to adult psychiatric diseases such as schizophrenia (McGrath et al., 2010). A recent study has also shown that maternal Vitamin D insufficiency is associated with offspring language impairments at 5 and 10 years of age (Whitehouse et al., 2012).

There is to date no information about the effect of maternal vitamin D deficiency on the developing human brain however gestational vitamin D deficiency causes permanent changes in the developing rat brain. Maternal deficiency alters brain gene and protein expression and disrupts the balance between neuronal stem cell proliferation and

programmed cell death in the offspring (Levenson and Figueiroa, 2008). Vitamin D receptors are particularly concentrated in the subventricular zone and Vitamin D can regulate cell proliferation. Recent studies have demonstrated a partially reversible brain phenotype in rat pups born to Vitamin D deficient dams (Eyles et al., 2003). Rat pups demonstrated an increased brain size and ventriculomegaly. The cortices of deficient pups were also larger compared with controls. This brain phenotype was attributed to increased mitosis and a decrease in apoptosis in central and cortical gray matter which was confirmed at histology. In this study the dam and consequently the rat pups were rendered extremely deficient with levels of <10 nmol/L equivalent. In pups that were given Vitamin D from birth ventriculomegaly improved but did not normalise. Brain development is recognised to involve a fine balance of cell growth and division and cell death and programmed cell death is essential for normal brain development. These deficient pups show abnormal behaviour with hyperlocomotion. Adult rats with antenatal deficiency show cognitive and memory deficits (Becker et al., 2005) and a similar deficient mouse model has shown that the offspring of vitamin D deficient dams scored poorly on behavioural tests as adults despite being supplemented with Vitamin D from birth (Fernandes de Abreu et al., 2010). There is sufficient animal evidence supporting a role for Vitamin D in brain development combined with the knowledge that the VDR is present in key regions in the human brain to warrant a study to look at the effects of maternal deficiency on fetal brain growth development. Vitamin D deficiency is common in our antenatal population, yet treatment is inexpensive.

Retrospective analysis

Hypothesis

We hypothesise that fetuses from vitamin D deficient mothers will show altered human brain development when compared to normal controls. More specifically we expect the brain phenotype of Vitamin D deficient fetuses to be characterised by increased brain tissue and cortical gray matter volume and enlarged lateral ventricular volume.

Aims of retrospective pilot study

To measure Vitamin D levels in stored booking bloods.

Compare maternal Vitamin D levels between normal controls and isolated ventriculomegaly fetuses.

Correlate ventricular and supratentorial brain tissue volumes with Vitamin D levels.

Ethical approval

Ethical approval for an amendment in the original ethics (07/H0707/105) for retrospective measurement of vitamin D levels in the study participants was granted by the West London Research Ethics Committee. Contact with participants was made via telephone to provide information about the study and invite participation. Consent forms and detailed information about the study were posted to all interested participants. Participants who returned signed informed consent forms were included in the study. The results were posted to the GPs of all participants.

Quantification of Vitamin D levels

Maternal vitamin D levels were measured retrospectively in stored booking serum samples. Serum samples were stored at the Virology department in Charing Cross Hospital at -20°C. An aliquot of 250μl was used for the analysis. Measurements were performed in the Clinical Biochemistry department in Charing Cross Hospital according to the standardised protocol for measuring Vitamin D levels in clinical samples. The range of storage time was from 6 to 33 months. Previous studies have shown that Vitamin D is a highly stable molecule at temperatures below -20 °C and reliable measurements can be obtained on sera samples stored up to 40 years. Liquid chromatography mass spectrometry was used for the analysis. $25(OH)D_2$ and $25(OH)D_3$ were measured in all samples. Total Vitamin D levels were defined as the sum of $25(OH)D_2$ and $25(OH)D_3$. Clinical Vitamin D cut-off levels (on total Vitamin D levels) were defined as following: Deficient <40nmol/L, Insufficient 40-69nmol/L, Replete >70nmol/L.

Imaging and volumetric analysis

Imaging and volumetric analysis of intracranial structures was performed as described in chapter 2.3.2. Volumetric measurements of the lateral ventricles and supratentorial brain tissue were performed on 3D-reconstructed datasets in the normal control and ventriculomegaly cohorts.

Results

Cohorts

Normal controls

The normal control cohort consisted of 10 fetuses with normal brain appearance on fetal MR that were already enrolled in the research program. The mean age at scan was 28^{+6} weeks and the range was 23 to 36 weeks.

Isolated ventriculomegaly

The isolated ventriculomegaly cohort consisted of 16 fetuses diagnosed with isolated ventriculomegaly on fetal MR and were already enrolled in the research program. The mean age at scan was 27^{+2} weeks and the range was 22 to 37 weeks.

Vitamin D levels and ethnicity

Women were divided according to their ethnicity into two groups including Asian/African American (Group A, n=10) and Caucasian (Group B, n=16). All women from both cohorts were included. There was a significant difference between groups A and B (p=0.018) with a median of 37 (SD ±18) and 57 (SD ±24) nmol/L respectively (Appendix 6, Figure 1). In group A, none of the women had measurements in the replete range, 6/10 were Vitamin D deficient while 4/10 were insufficient. In group B, 4/16 were deficient, 7/16 were insufficient and 5 had replete levels.

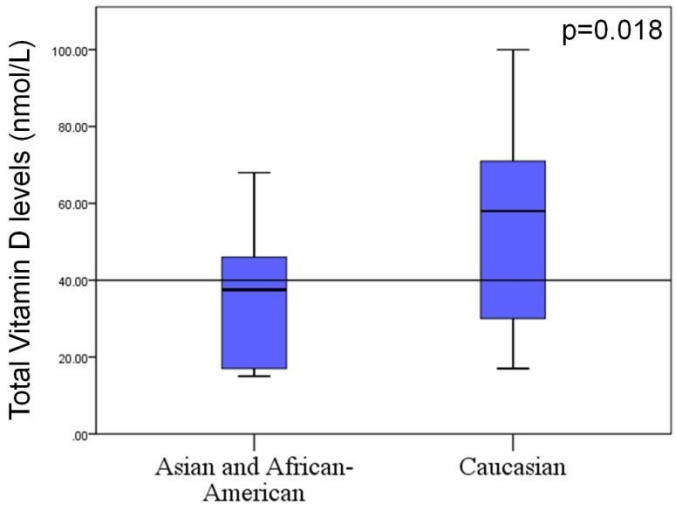


Figure 126. Total Vitamin D levels and ethnicity

$25(OH)D_2$ levels obtained through the diet were only detectable in 2 cases. In the rest of the cases only the $25(OH)D_3$ levels contributed to the total Vitamin D levels.

Vitamin D levels and brain development

Total Vitamin D levels were compared between the control and ventriculomegaly cohorts and there was no significant difference in total Vitamin D levels between the cohorts. In both the control and ventriculomegaly groups, however, deficient cases (<40nmol/L) had larger lateral ventricles and supratentorial brain tissue volumes although this was not statistically significant (Appendix 6, Figure 2). There was no significant correlation between vitamin D levels and ventricular or supratentorial brain tissue volume adjusted for gestational age.

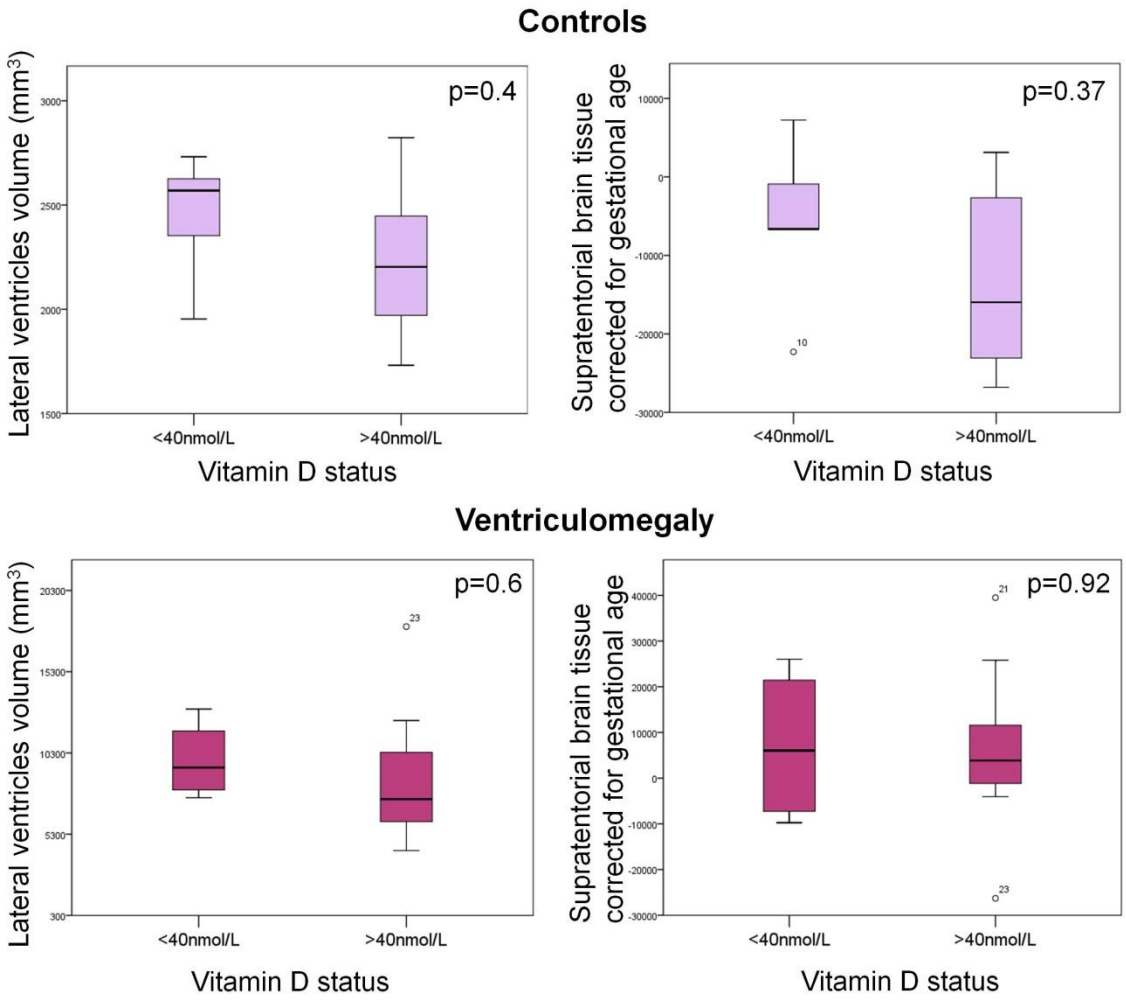


Figure 127. Vitamin D status and intracranial structures in controls and fetuses with ventriculomegaly

Correlation of Vitamin D levels and intracranial structures

In the control cohort, there was no significant correlation between Vitamin D levels and supratentorial brain tissue (Spearman's r=-0.262, p=0.464) or total ventricular volume (Spearman's r=-0.091, p=0.802) when corrected for GA. Similarly, in the ventriculomegaly cohort there was no significant correlation between Vitamin D levels and supratentorial brain tissue (Spearman's r=-0.146, p=0.603) or total ventricular volume (Spearman's r=-0.275, p=0.321) when corrected for GA.

Discussion and prospective work

We have completed a retrospective pilot study to determine the feasibility of measuring Vitamin D levels in stored booking bloods obtained at around 12 weeks of gestation. We measured the Vitamin D levels in maternal samples of 10 normal fetuses and 16 fetuses with isolated ventriculomegaly. Vitamin D levels were successfully measured in all samples and we showed that 50% of cases were deficient. Ethnicity was a determining factor. Deficient cases had larger lateral ventricles and brain tissue volumes although this was not statistically significant, possibly due to the small cohort size. In addition we showed that Vitamin D intake through the diet was negligible.

Prospective study

We have recently received ethics and funding to proceed with a larger prospective study to determine the effect of maternal Vitamin D deficiency in normal control fetuses. The expectant mothers are currently being recruited from the Queen Charlotte's and Chelsea antenatal clinic at the time of their anomaly ultrasound scan at around 20 gestational weeks. Eligibility for participation is determined by an uncomplicated pregnancy and a normal brain appearance on ultrasound. We are collecting information on ethnicity, practice of skin covering, Body Mass Index (BMI), Vitamin D intake and daily sun exposure using detailed questionnaires (Appendix 6). All mothers are recruited into the ongoing MR study of fetal brain development. The aims of the study are summarised below:

Aims

1. To prospectively acquire fetal MR imaging from normal control fetuses from uncomplicated pregnancies with a normal antenatal ultrasound.
2. To ascertain the levels of maternal Vitamin D deficiency from the maternal booking bloods.
3. To determine the effect of maternal Vitamin D deficiency at the time of booking on the structure and metabolic function of the developing brain and
4. To assess the effect of any alterations in brain development on later neurocognition and behaviour.

Appendix

Appendix 1. Information Sheet for Patients

You will be given a copy of this information sheet

Study Title:

Quantification of fetal brain development and growth using magnetic resonance imaging

Invitation to take part

We are inviting you to take part in a research study, which uses a technique called magnet resonance to image your baby. Before you decide it is important for you to understand why the research is being done and what it will involve. Please take time to read the following information carefully and discuss it with friends, relatives and your GP if you wish. Ask us if there is anything that is not clear or if you would like more information. Take time to decide whether or not you wish to take part.

What is the purpose of this study?

Magnetic resonance imaging is a method of obtaining pictures of the inside of the body. While ultrasound is excellent for showing the anatomy of the normal fetus (baby), magnetic resonance is usually better for detecting and assessing both normal structures and abnormalities. This is why your obstetrician may have referred you for an MR scan. We are interested in developing the MR technique further to improve our abilities to detect abnormalities and to try and understand more about their impact on your child's later development.

We therefore plan to image your baby once or twice prior to delivery. Where possible we also seek your permission to scan your baby after delivery and in the event of a premature delivery at term equivalent age. We would also like to assess your child's development over the first few years.

We are also keen to understand the effect of maternal illness or complications of pregnancy on the developing baby's brain. In particular we would like to assess the effect of maternal Vitamin D. Vitamin D levels are often low in pregnancy, particularly in women who are dark skinned or cover their skin when outdoors but the effects, if any, of a low level on the developing baby's brain are not understood.

The MR technique uses a large magnet and radio waves. It does not involve the use of either X-rays or radiation. It is not believed to have any hazard associated with it, although care is necessary to keep certain metallic objects away from the magnet and, at the present time, we exclude women who are in the first three months of an uncomplicated pregnancy. This is only a precaution as there are no reports of any side effects even in the very young fetus. However in the first months of pregnancy the fetus is very small and many structures are not completely formed therefore we do not feel that, very early MR imaging would be particularly useful with current MR techniques. MR can also be used to obtain information about the way a tissue is functioning, this is called MR spectroscopy.

Why have I been chosen?

We seek permission for these studies from:
Women with complicated pregnancies,
Women where antenatal ultrasound has shown a possible problem with the fetus,
Women with normal pregnancies and normal fetuses.

Do I have to take part?

It is up to you to decide whether or not to take part. If you do decide to take part you will be given this information sheet to keep and be asked to sign a consent form. If you decide to take part you are still free to withdraw at any time and without giving a reason. This will not affect the standard of care you receive. If you do not wish to take part we will only take those images that we consider necessary to help with the management of your pregnancy. We still require your permission to do this.

What will happen to me if I take part?

If you have been referred for an MR scan by your doctor this will be performed as usual. You will be asked to lie feet first inside a magnet. Your head will be level with the opening of the magnet. We will make you as comfortable as possible. You will hear a knocking noise during the procedure. We will give you some headphones and you can listen to some music during the scan if you wish. Your partner or a friend or relative may accompany you into the scanning room once they have had a safety check. You will be given an alarm bell to sound at any time if you are upset or worried during the examination. If the procedure does not suit you for any reason, it can be stopped at any time.

For the purposes of this research we wish to collect some extra images from your baby's brain. We may also collect MR spectroscopy information from your baby's brain and liver and your placenta. We need information on these organs to increase our understanding of their role when a baby is not growing well. The total duration of the examination is unlikely to be longer than 45 minutes. If you become uncomfortable we can stop the scan. It is possible to continue scanning after you have had a break or a change in position.

No extra blood tests will be necessary. Vitamin D levels will be measured on a small sample of your blood that was taken at the time of booking for antenatal care and is stored in the hospital.

You may like to go online and watch a short video explaining the MRI procedure in more detail and what you can expect when you come for your scan: http://vimeo.com/37368763

What do I have to do?

For your scans we will ask you to lie as still as possible within a magnetic scanner while the machine produces images.

What is the procedure that is being tested?

The procedures being tested are magnetic resonance imaging and spectroscopy. We will be optimising the scanner's abilities to obtain the most detailed information possible about the

unborn baby. These developments will allow us, for instance, to accurately measure areas of a baby's brain at different gestations and to identify an area of injury soon after it has occurred.

What are the side effects of taking part?

The examination itself is not believed to have any side effects for you or your baby. The machine is enclosed and people who cannot travel in a lift because of claustrophobia may find it unacceptable. However your head will be level with the opening and not remain deep in the scanner. Occasionally we find that the magnet is not wide enough to take women who are large e.g. twin pregnancy or women who are nearing term. The machine is noisy when it is acquiring images and that is why we give you some headphones whilst you are being scanned. We can play music through these and if you want you could bring your own CD.

What are the possible disadvantages and risks of taking part?

The basic examination is not believed to have hazards associated with it when operated within National Radiological Protection Board Guidelines (which we do).

What are the possible benefits of taking part?

A scan may have been requested by your doctor to help him/her with the management of your pregnancy. The further MR images that we take may be of benefit to you in improving the diagnostic information of your baby. Otherwise the benefit is likely to be in improving the diagnostic technique for the benefit of others.

As part of this study we would like to follow your baby's development. You may find information that is produced from these assessments reassuring or it may help plan any treatment or extra therapy that your baby may require.

What if new information becomes available?

MRI may just confirm the findings on your antenatal ultrasound or it may show an abnormality that has not been detected previously. This improved detection is why you may have been referred for an MRI. All the findings on your scan will be discussed with yourself and with your obstetrician. This will allow your obstetrician to advise on the management of your pregnancy with all the available information.

What happens when the research study stops?

The present research has been continuing for over 20 years and the results have been published regularly. We intend to continue this.

What if something goes wrong?

In the unlikely event of you suffering any adverse effects as a consequence of your participation in the study you will be compensated through the Imperial College School of Medicines "No Fault Compensation Scheme".

Will my taking part in this study be kept confidential?

The information obtained from your study is covered by the Data Protection Act. The computerised information is protected by a software and hardware barrier and the records are handled in the same way as hospital records. We also seek permission to include clinical details about your pregnancy in the study, for instance your gestation, ultrasound details of your baby. This information would be given to us by your obstetrician and would be handled confidentially. Any imaging data that is shared with colleagues in collaborating units will be anonymised.

If we measure Vitamin D levels on your stored blood we will send the result to your doctor who if your level is low will be able to discuss with you if any supplementation is necessary.

What will happen to the results of the research study?

The results are usually published in the medical literature. **No** patients' names will be included.

Who is organising and funding the research?

The research is organised and funded by the Medical Research Council, Imperial College School of Medicine and charities such as Action for Medical Research.

Who has reviewed the study?

The study has been reviewed by the Hammersmith Hospitals Research Ethics Committee.

Appendix 2. Information Sheet for Healthy Pregnant Volunteers

Study Title:

Quantification of fetal brain development and growth using magnetic resonance imaging.

Invitation to take part

You are being invited to take part in a research study. Before you decide it is important for you to understand why the research is being done and what it will involve. Please take time to read the following information carefully and discuss it with friends, relatives and your GP if you wish. Ask us if there is anything that is not clear or if you would like more information. Take time to decide whether or not you wish to take part.

What is the purpose of this study?

Magnetic resonance imaging (MRI) is a method of obtaining pictures of the inside of the body. While ultrasound is excellent for showing the anatomy of the normal fetus, MRI is usually better for detecting and assessing both normal structures and abnormalities. We are interested in developing the MR technique further to improve our abilities to both monitor brain growth and development and to detect abnormalities and to try and understand more about their impact on a child's later development. We are therefore asking your permission to image your baby prior to delivery and where possible after delivery. We would also like to assess your child's development during the first few years after birth.

We are also keen to understand the effect of maternal illness or complications of pregnancy on the developing baby's brain. In particular we would like to assess the effect of maternal Vitamin D. Vitamin D levels are often low in pregnancy, particularly in women who are dark skinned or cover their skin when outdoors but the effects, if any, of a low level on the developing baby's brain are not understood

The MRI technique uses a large magnet and radio waves. It does not involve the use of either X-rays or radiation. It is not believed to have any hazard associated with it, although care is

necessary to keep certain metallic objects away from the magnet and, at the present time, we exclude normal women who are in the first three months of an uncomplicated pregnancy. This is only a precaution as there are no reports of any side effects even in the very young fetus. However in the first months of pregnancy the fetus is very small and many structures are not completely formed therefore we do not feel that very early MR imaging would be particularly useful with current techniques. MR can also be used to obtain information about the way a tissue is functioning; this is called MR spectroscopy.

Why have I been chosen?

We seek permission for these studies from normal pregnant volunteers to increase our understanding about the normally developing brain and its relationship with the child's later development. The purpose is to obtain information about normal fetuses from uncomplicated pregnancies so that deviations from normal can be recognised. We would also plan to compare data on the normally growing fetus with that obtained on our population of preterm babies. Infants born preterm have a high risk of learning difficulties and we think this is because their brains develop differently outside of the womb.

Do I have to take part?

It is up to you to decide whether or not to take part. If you do decide to take part you will be given this information sheet to keep and be asked to sign a consent form. You will also be given an information sheet about scanning your baby after delivery. If you decide to take part you are still free to withdraw at any time and without giving a reason.

What will happen to me if I take part?

You will be asked to lie feet first inside a magnet and you will hear a knocking noise during the procedure. Your head will be level with the opening of the magnet. We will make you as comfortable as possible. Your partner or a friend or relative may accompany you into the scanning room once they have had a safety check. You will be given an alarm bell to sound at any time if you are upset or worried during the examination. If the procedure does not suit you for any reason, it can be stopped at any time. During the examination we will collect imaging data on your baby's brain. We may also collect MR spectroscopy information from

your baby's brain and liver and your placenta. We need normal information on these organs to increase our understanding of their role when a baby is not growing well. The total duration of the examination will be approximately 45 minutes. If you become uncomfortable we can stop the scan. It is possible to continue scanning after you have had a break or a change in position.

We seek your permission to perform two scans during pregnancy several weeks apart to allow us to measure growth over time. In addition we would like to be able to follow your baby's development after birth, as this will provide very useful information when quantifying our MR scans. The follow up would include a further MRI after delivery. Information about this is provided on a separate sheet.

No extra blood tests will be necessary. Vitamin D levels will be measured on a small sample of your blood that was taken at the time of booking for antenatal care and is stored in the hospital.

You may like to go online and watch a short video explaining the MRI procedure in more detail and what you can expect when you come for your scan: http://vimeo.com/37368763

What do I have to do?

For the fetal scans we will ask you to lie within a magnetic scanner while the machine produces images.

What is the procedure that is being tested?

The procedures being tested are magnetic resonance imaging and spectroscopy. We will be optimising the scanner's abilities to take the best possible images of your baby. These developments will then allow us to accurately measure areas of a baby's brain at different gestations using specially designed computer programmes and also to identify an area of injury soon after it has occurred.

What are the side effects of taking part?

The MR examination itself is not believed to have any side effects on you or your baby. The machine is enclosed and people who cannot travel in a lift because of claustrophobia may find it unacceptable. However your head will be level with the opening and not remain deep in the scanner. Occasionally we find that the magnet is not wide enough to take women who are large e.g. twin pregnancy or women who are nearing term. The machine is noisy when it is acquiring images and we therefore give you some headphones whilst you are being scanned. We can play music through these and if you want you could bring your own CD. The noise has not been reported to have any effects on the fetus.

What are the possible disadvantages and risks of taking part?

The basic examination is not believed to have hazards associated with it when operated within National Radiological Protection Board Guidelines (which we do).

What are the possible benefits of taking part?

The benefit from your examination is likely to be in improving the diagnostic technique for the benefit of others. We will however be able to check your baby's brain development and give you a copy of the images on a CD. We would also be able to check your toddler's overall development at 12 and 24 months and hopefully after school entry.

What if new information becomes available?

Whilst it is unlikely, MRI may detect an abnormality that has not been detected by your antenatal ultrasound. If unexpected information of potential clinical importance is found during the examination, we will discuss the matter with you and, if you give your permission, refer the matter to your GP or any other appropriate doctor. Most often the finding will be a normal variation and not clinically significant. In addition whilst we anticipate that your fetal magnetic resonance images will show normal appearances, this cannot be considered as a guarantee that your baby will have normal development throughout childhood. Some children with significant problems with their development have normal appearances on their MRI scans even when performed later in childhood.

What happens when the research study stops?

The present research has been continuing for over 20 years and the results have been published regularly. We intend to continue this.

What if something goes wrong?

In the unlikely event of you suffering any adverse effects as a consequence of your participation in the study you will be compensated through the Imperial College School of Medicines "No Fault Compensation Scheme".

Will my taking part in this study be kept confidential?

The information obtained from your study is covered by the Data Protection Act. The computerised information is protected by a software and hardware barrier and the records are handled in the same way as hospital records. We also seek permission to include clinical details about your pregnancy in the study, for instance your gestation, ultrasound details of your baby. This information would be given to us by your obstetrician and would be handled confidentially. Any image information sent out from our unit to colleagues in a collaborating unit will be anonomised.

If we measure Vitamin D levels on your stored blood specifically we will send the result to your doctor who if the level is low be able to discuss with you if any supplementation is necessary.

What will happen to the results of the research study?

The results are usually published in the medical literature. **No** patients' names will be included.

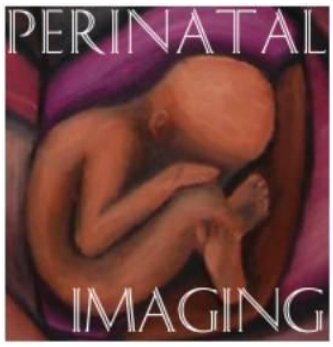
Who is organising and funding the research?

The research is organised and funded by the Medical Research Council, Imperial College School of Medicine and other funding bodies such as Action Medical Research

Who has reviewed the study?

The study has been reviewed by the Hammersmith Hospitals Research Ethics Committee.

Appendix 3. Parental Questionnaire



Fetal Imaging Programme

Parental Questionnaire

Dear Parents,

We are trying to improve our clinical and research service and would really value your views. It would be helpful if you could answer the following questions for us. The completed questionnaire will be anonymous unless you wish to give your name. We have given you a stamped addressed envelope to make it easier to let us have your replies.

Yours faithfully



Mary Rutherford
Professor in Perinatal Imaging

m.rutherford@imperial.ac.uk

Please put a circle around your chosen answer i.e. YES (NO) or tick the box

1. **Which hospital were you referred from?**

   Queen Charlottes Other hospital

2. **Why were you referred for an MRI scan? Because there was a problem with my**

   Baby's brain baby's body my pregnancy other

   None of the above I am a volunteer for research ☐

3. **How did you receive your appointment?**

   Hand/In person Phone Mail

4. **Were you able to confirm the appointment easily or contact us for more details?**

   YES NO

5. **Did you receive an information sheet about our research?**

   YES NO

6. **Did you have enough time to read through it?**

   YES NO

7. **Did you understand it?**

   YES NO

8. **Would you have preferred it to be in a different language from English?**

   YES NO

9. **If you answered "Yes" which language? _____**

10. Did you have the opportunity to ask any questions about the information sheet?

YES NO

11. Were you clear which aspects of your examination were research and which were clinical?

YES NO

12. Were the practical details about the scan and safety issues explained to you?

YES NO

13. Did you receive (on appointment letter and information sheet) the internet based video link showing further details of MR scan?

YES NO

14. Did you view it?

YES NO

15. Did you find it helpful?

YES NO

16. What further information would you have liked to receive prior to the scan?

YES NO

17. Was there anything about the scan itself that worried you?

18. In what ways could the scan have been better for you

19. Were you shown the images after the scan?

YES NO

If you answered NO did you want to see the images?

YES NO

20. Did you understand what you were told about the images?

YES NO

21. Could the discussion have been improved in anyway?

YES NO

22. Did you discuss the scan findings <u>again</u> with one of your doctors?

YES NO

23. Did you feel the scan helped you understand the problems affecting your baby or your pregnancy?

YES NO

24. Did you feel the scan was a help in making decisions about your pregnancy?

YES NO

25. As part of the research we have asked your permission to contact you again. Were you happy with this?

YES NO

26. We may have asked your permission for further scans of your baby. Did you agree?

YES NO

If you did not agree for further scans could we ask your reasons for saying no?

27. We may have asked whether we could follow your baby's development. Did you agree?

YES NO

If you did not agree for further scans could we ask your reasons for saying no?

28. Finally on a scale of 1-5, where 1 is not useful at all and 5 is very useful, do you feel that having the scan was a useful thing to have done?
(Please put a circle around the number.)

1 2 3 4 5

Thank you very much indeed for filling this in. We would be very grateful if you could put the questionnaire into the pre addressed and stamped envelope
Also we would welcome,

ANY EXTRA COMMENTS, IDEAS OR SUGGESTIONS:

Appendix 4. Ages and Stages Questionnaire

ASQ-3

24 Month Questionnaire *23 months 0 days through 25 months 15 days*

On the following pages are questions about activities children may do. Your child may have already done some of the activities described here, and there may be some your child has not begun doing yet. For each item, please fill in the circle that indicates whether your child is doing the activity regularly, sometimes, or not yet.

Important Points to Remember:

- ☑ Try each activity with your child before marking a response.
- ☑ Make completing this questionnaire a game that is fun for you and your child.
- ☑ Make sure your child is rested and fed.
- ☑ Please return this questionnaire by _____.

Notes:

_____

_____

_____

_____

At this age, many toddlers may not be cooperative when asked to do things. You may need to try the following activities with your child more than one time. If possible, try the activities when your child is cooperative. If your child can do the activity but refuses, mark "yes" for the item.

COMMUNICATION

	YES	SOMETIMES	NOT YET	
1. Without your showing him, does your child *point* to the correct picture when you say, "Show me the kitty," or ask, "Where is the dog?" *(She needs to identify only one picture correctly.)*	◯	◯	◯	____
2. Does your child imitate a two-word sentence? For example, when you say a two-word phrase, such as "Mama eat," "Daddy play," "Go home," or "What's this?" does your child say both words back to you? *(Mark "yes" even if her words are difficult to understand.)*	◯	◯	◯	____
3. Without your giving him clues by pointing or using gestures, can your child carry out at least *three* of these kinds of directions?	◯	◯	◯	____
◯ a. "Put the toy on the table." ◯ d. "Find your coat."				
◯ b. "Close the door." ◯ e. "Take my hand."				
◯ c. "Bring me a towel." ◯ f. "Get your book."				
4. If you point to a picture of a ball (kitty, cup, hat, etc.) and ask your child, "What is this?" does your child correctly *name* at least one picture?	◯	◯	◯	____
5. Does your child say two or three words that represent different ideas together, such as "See dog," "Mommy come home," or "Kitty gone"? *(Don't count word combinations that express one idea, such as "bye-bye," "all gone," "all right," and "What's that?")* Please give an example of your child's word combinations:	◯	◯	◯	____

E101240200

Ages & Stages Questionnaires®, Third Edition (ASQ-3™), Squires & Bricker
© 2009 Paul H. Brookes Publishing Co. All rights reserved.

COMMUNICATION (continued)

	YES	SOMETIMES	NOT YET	
6. Does your child correctly use at least two words like "me," "I," "mine," and "you"?	○	○	○	____

COMMUNICATION TOTAL ____

GROSS MOTOR

	YES	SOMETIMES	NOT YET	
1. Does your child walk down stairs if you hold onto one of her hands? She may also hold onto the railing or wall. *(You can look for this at a store, on a playground, or at home.)*	○	○	○	____
2. When you show your child how to kick a large ball, does he try to kick the ball by moving his leg forward or by walking into it? *(If your child already kicks a ball, mark "yes" for this item.)* 	○	○	○	____
3. Does your child walk either up or down at least two steps by herself? She may hold onto the railing or wall. 	○	○	○	____
4. Does your child run fairly well, stopping herself without bumping into things or falling? 	○	○	○	____
5. Does your child jump with both feet leaving the floor at the same time? 	○	○	○	____
6. Without holding onto anything for support, does your child kick a ball by swinging his leg forward? 	○	○	○	____ *

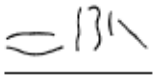
GROSS MOTOR TOTAL ____

**If Gross Motor Item 6 is marked "yes" or "sometimes," mark*

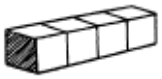
FINE MOTOR

	YES	SOMETIMES	NOT YET	
1. Does your child get a spoon into his mouth right side up so that the food usually doesn't spill?	○	○	○	___
2. Does your child turn the pages of a book by herself? *(She may turn more than one page at a time.)*	○	○	○	___
3. Does your child use a turning motion with his hand while trying to turn doorknobs, wind up toys, twist tops, or screw lids on and off jars?	○	○	○	___
4. Does your child flip switches off and on?	○	○	○	___
5. Does your child stack seven small blocks or toys on top of each other by herself? *(You could also use spools of thread, small boxes, or toys that are about 1 inch in size.)*	○	○	○	___
6. Can your child string small items such as beads, macaroni, or pasta "wagon wheels" onto a string or shoelace? 	○	○	○	___
			FINE MOTOR TOTAL	___

PROBLEM SOLVING

	YES	SOMETIMES	NOT YET	
1. After watching you draw a line from the top of the paper to the bottom with a crayon (or pencil or pen), does your child copy you by drawing a single line on the paper in *any direction*? *(Mark "not yet" if your child scribbles back and forth.)* Count as "yes"  Count as "not yet"	○	○	○	___
2. After a crumb or Cheerio is dropped into a small, clear bottle, does your child turn the bottle upside down to dump out the crumb or Cheerio? *(Do not show him how.) (You can use a soda-pop bottle or baby bottle.)*	○	○	○	___
3. Does your child pretend objects are something else? For example, does your child hold a cup to her ear, pretending it is a telephone? Does she put a box on her head, pretending it is a hat? Does she use a block or small toy to stir food?	○	○	○	___
4. Does your child put things away where they belong? For example, does he know his toys belong on the toy shelf, his blanket goes on his bed, and dishes go in the kitchen?	○	○	○	___
5. If your child wants something she cannot reach, does she find a chair or box to stand on to reach it (for example, to get a toy on a counter or to "help" you in the kitchen)?	○	○	○	___

PROBLEM SOLVING (continued)

	YES	SOMETIMES	NOT YET	
6. While your child watches, line up four objects like blocks or cars in a row. Does your child copy or imitate you and line up *four* objects in a row? *(You can also use spools of thread, small boxes, or other toys.)* 	○	○	○	____
			PROBLEM SOLVING TOTAL	____

PERSONAL-SOCIAL

	YES	SOMETIMES	NOT YET	
1. Does your child drink from a cup or glass, putting it down again with little spilling?	○	○	○	____
2. Does your child copy the activities you do, such as wipe up a spill, sweep, shave, or comb hair?	○	○	○	____
3. Does your child eat with a fork?	○	○	○	____
4. When playing with either a stuffed animal or a doll, does your child pretend to rock it, feed it, change its diapers, put it to bed, and so forth?	○	○	○	____
5. Does your child push a little wagon, stroller, or other toy on wheels, steering it around objects and backing out of corners if he cannot turn?	○	○	○	____
6. Does your child call herself "I" or "me" more often than her own name? For example, "I do it," more often than "Juanita do it."	○	○	○	____
			PERSONAL-SOCIAL TOTAL	____

OVERALL

Parents and providers may use the space below for additional comments.

1. Do you think your child hears well? If no, explain: ○ YES ○ NO

2. Do you think your child talks like other toddlers her age? If no, explain: ○ YES ○ NO

E101240500

Ages & Stages Questionnaires®, Third Edition (ASQ-3™), Squires & Bricker
© 2009 Paul H. Brookes Publishing Co. All rights reserved.

OVERALL (continued)

3. Can you understand most of what your child says? If no, explain: ○ YES ○ NO

4. Do you think your child walks, runs, and climbs like other toddlers his age? If no, explain: ○ YES ○ NO

5. Does either parent have a family history of childhood deafness or hearing impairment? If yes, explain: ○ YES ○ NO

6. Do you have any concerns about your child's vision? If yes, explain: ○ YES ○ NO

7. Has your child had any medical problems in the last several months? If yes, explain: ○ YES ○ NO

OVERALL (continued)

8. Do you have any concerns about your child's behavior? If yes, explain: ○ YES ○ NO

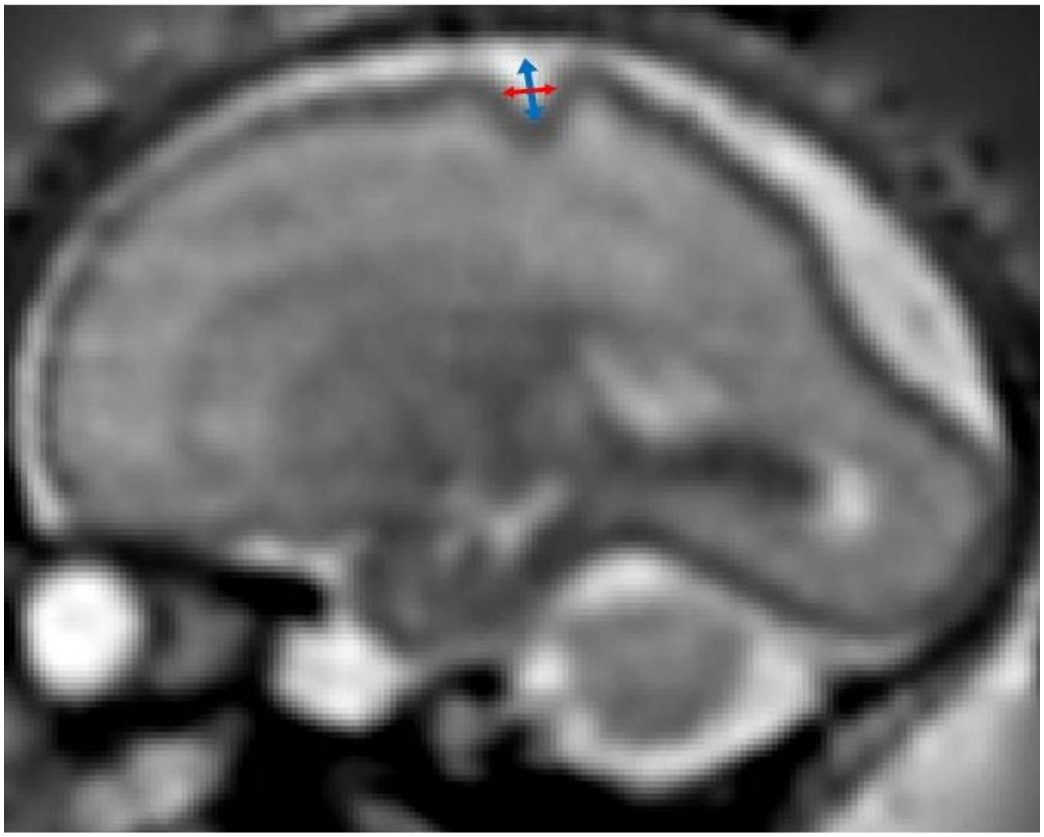
9. Does anything about your child worry you? If yes, explain: ○ YES ○ NO

Ages & Stages Questionnaires®, Third Edition (ASQ-3™), Squires & Bricker
© 2009 Paul H. Brookes Publishing Co. All rights reserved.

Appendix 5. Detailed protocol of cortical development assessment

Central sulcus (Height&Width)

The height and width of the central sulcus are measured at a sagittal plane at a slice where it has the maximum visible height, and when the cerebellum is present. The width is measured at the middle and perpendicular to the height measurement. To find the correct place to measure as you move laterally towards a midsaggital plane the sulcus appears to make a little "jump" and that is where the measurement is performed.

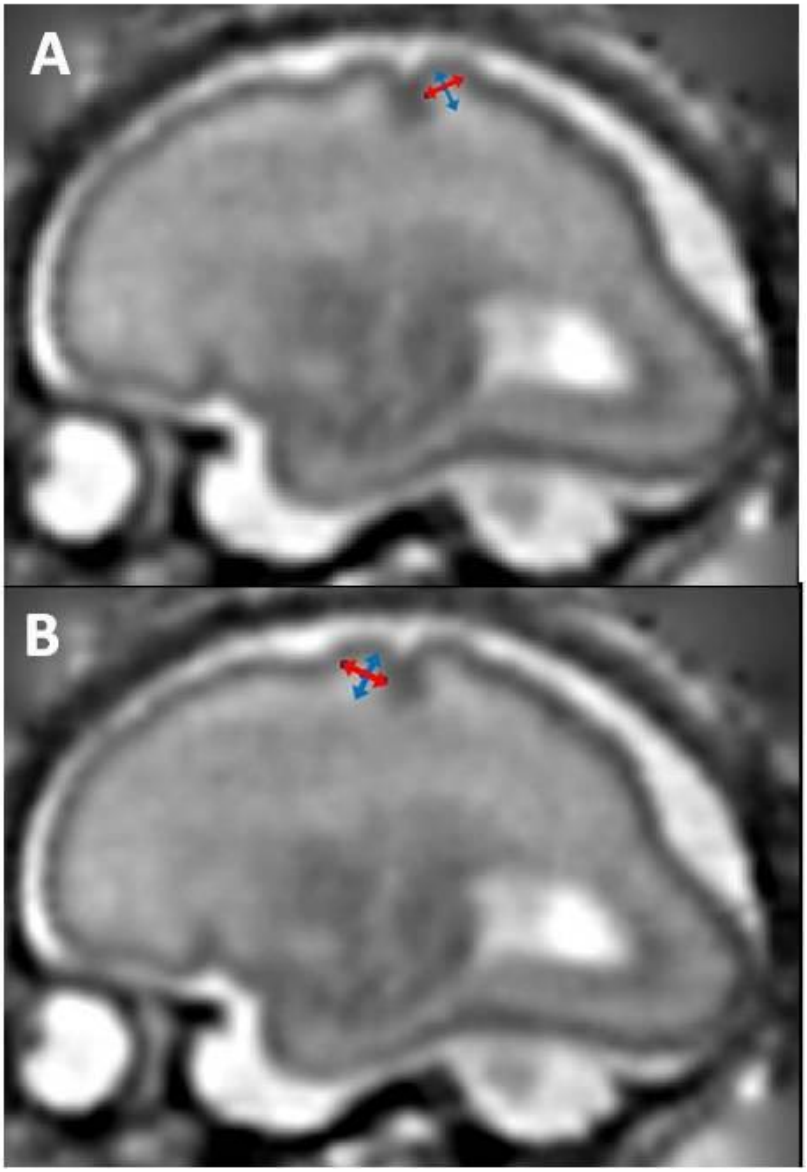


Central sulcus

Measurements of the central sulcus included height (blue) and width (red).

<u>Precentral and postcentral gyri</u>: <u>(Height&Width)</u>

Measured at a sagittal plane where the sylvian fissure is not visible and before the appearance of the brainstem and spinal cord. Both precentral and postcentral should appear in their most mature stage and symmetrical to each other. If either landmark is slightly curved the measurement is performed into segments.

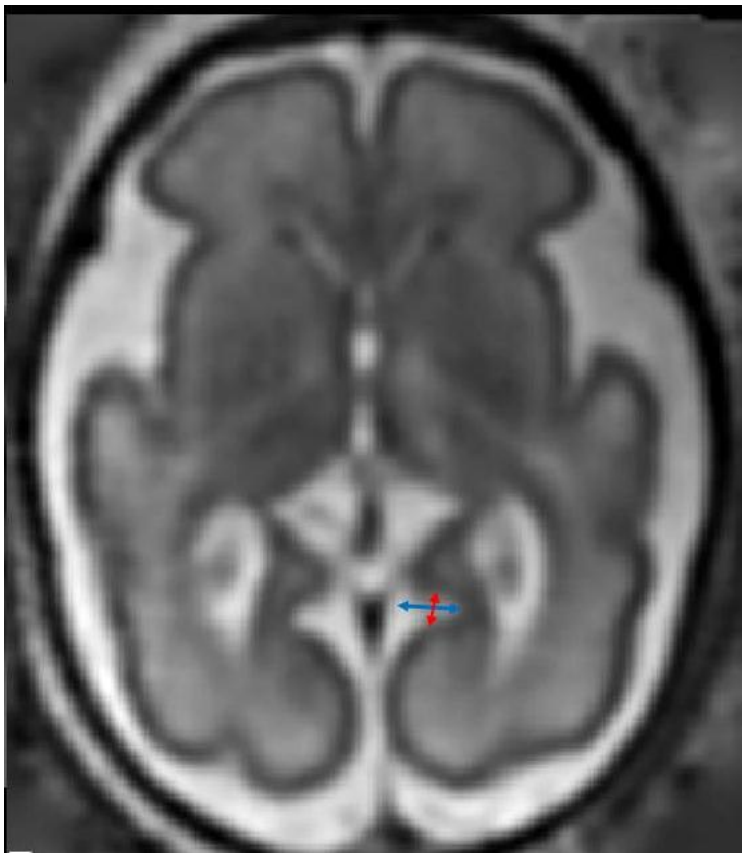


Postcentral and precentral and gyri

(A)Postcentral gyrus (B) Precentral gyrus. Measurements of cortical folding included height (blue) and width (red) of gyri and sulci.

Parieto-occipital fissure (Height&Width)

Measured in a transverse plane where the sulcus "dips" inside the atrium. Commonly on the same slice as for the measurement for maximum distance from frontal to temporal along the insula-temporal cortex.



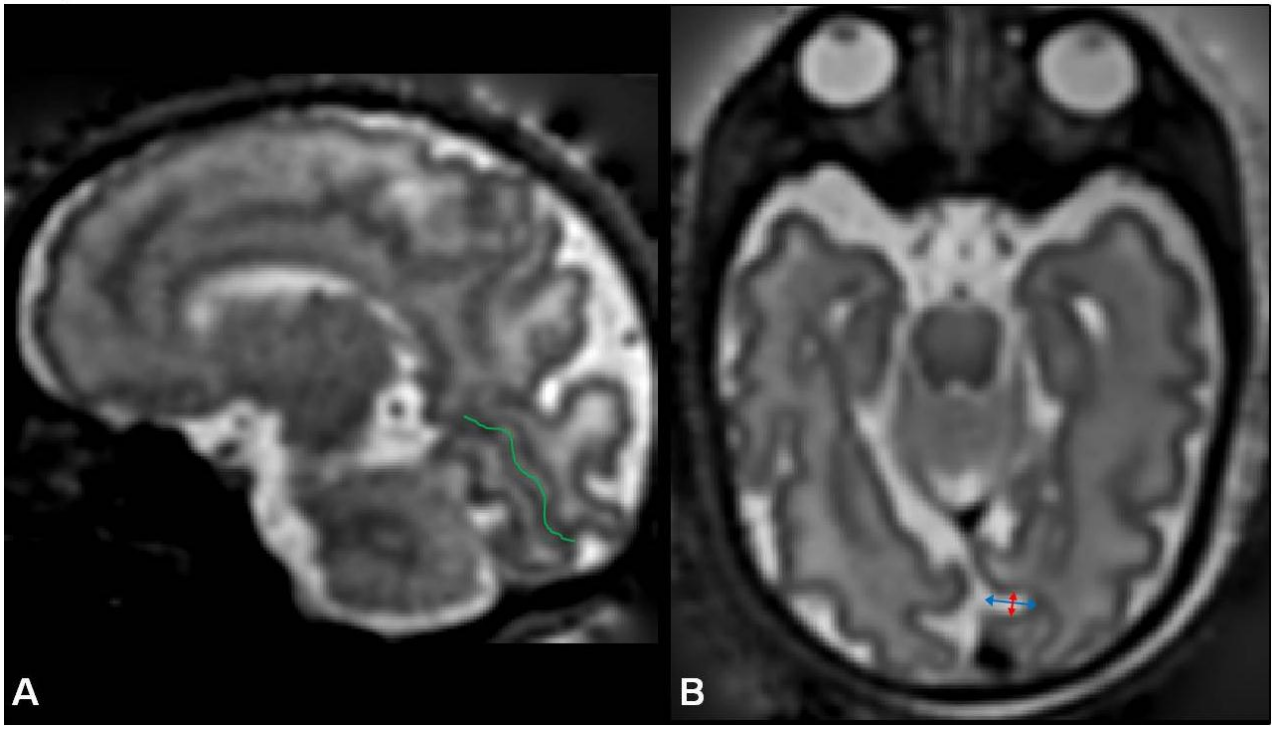
Parieto-occipital fissure

Measurements of cortical folding of the cortical landmarks included height (blue) and width (red).

Calcarine sulcus(Height&Width&length)

Length: measured in a sagittal plane at the slide where it appears longest and before it opens fully.

Height/Width: measured in a transverse plane, on the slide corresponding to the measurement performed on the sagittal. On the sagittal the cursor is positioned at the most posterior part in the centre of the loop formed. Commonly at eye level.



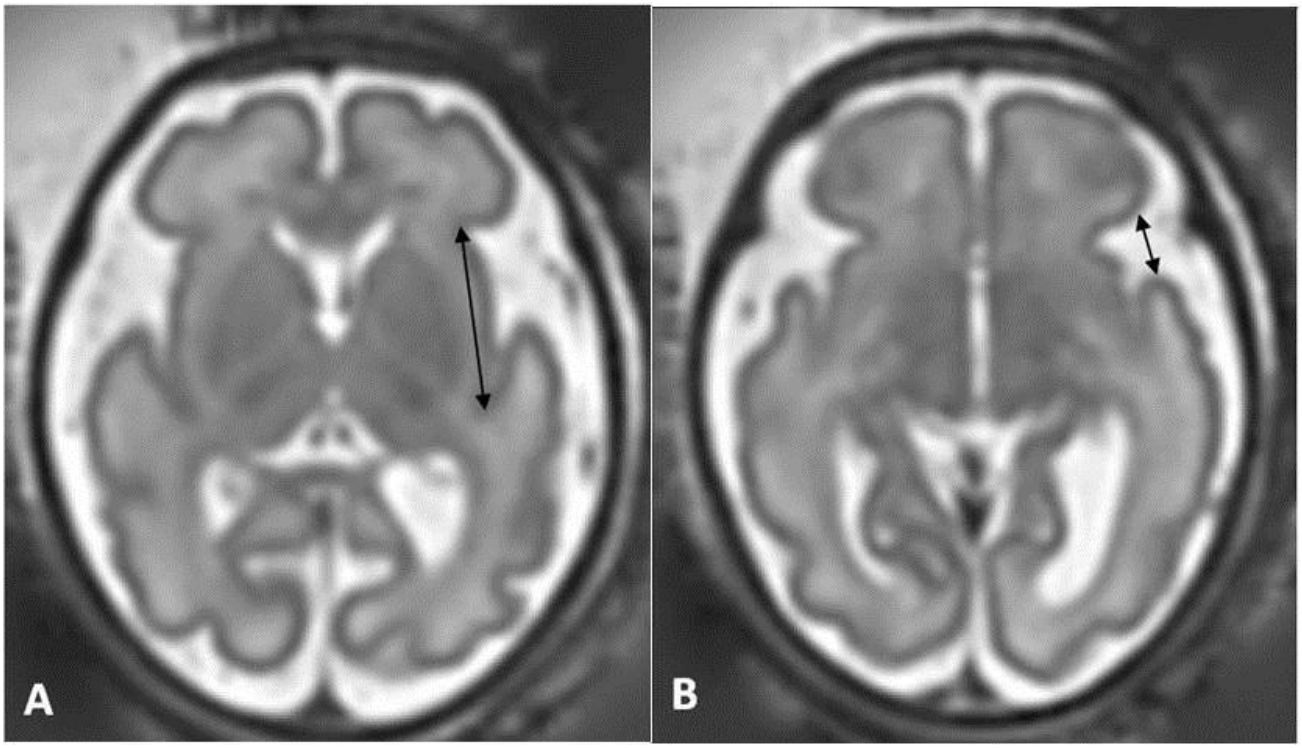
Calcarine sulcus

Cortical development of the calcarine sulcus was assessed using (A) the length of the cingulate sulcus in a sagittal plane (green) and (B) the height (blue) and width (red) on a transverse plane.

Sylvian fissure (2 linear measurements and their ratio)

Opercular distance= minimum distance from frontal to temporal of the operculum. Insular distance = maximum distance from frontal to temporal aslong the insula-temporal cortex.

Ratio = $\frac{\text{insular distance}}{\text{opercular distance}}$

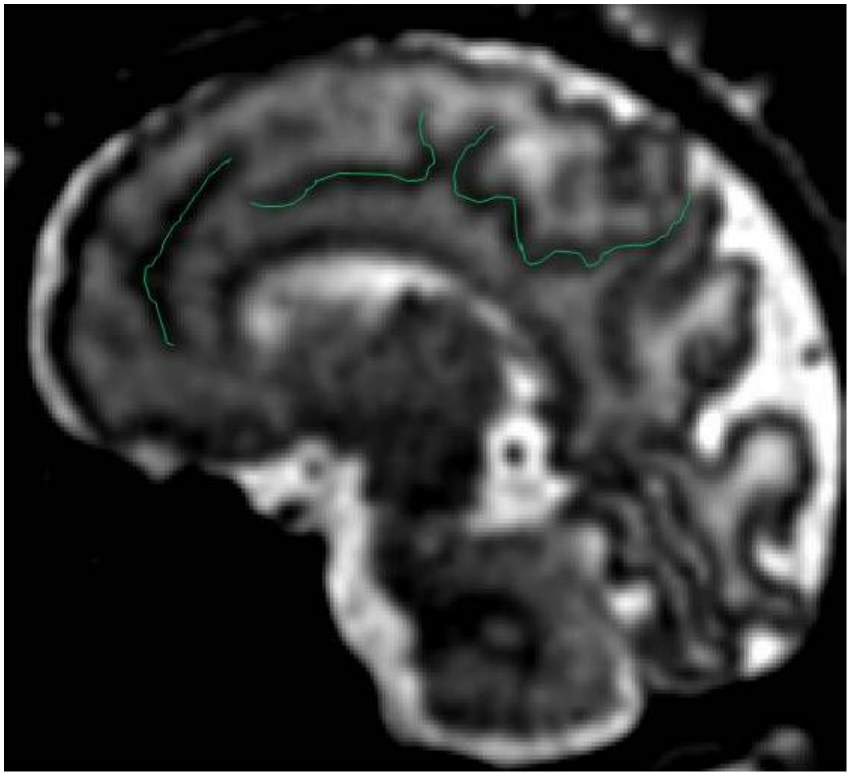


Sylvian fissure

Sylvian fissure development was assessed using the ratio of (A) the maximum distance from frontal to temporal boundaries along the insula-temporal cortex to (B) the minimum distance from frontal to temporal borders of the operculum.

Cingulate sulcus

In a sagittal plane length of the sulcus is measured at the slice where it has maximum length. If the cingulate appears in segments that might appear in slightly different slices then the segments are measured individually and added together. The paracingulate is not included in the measurement as it is not present in all fetuses.

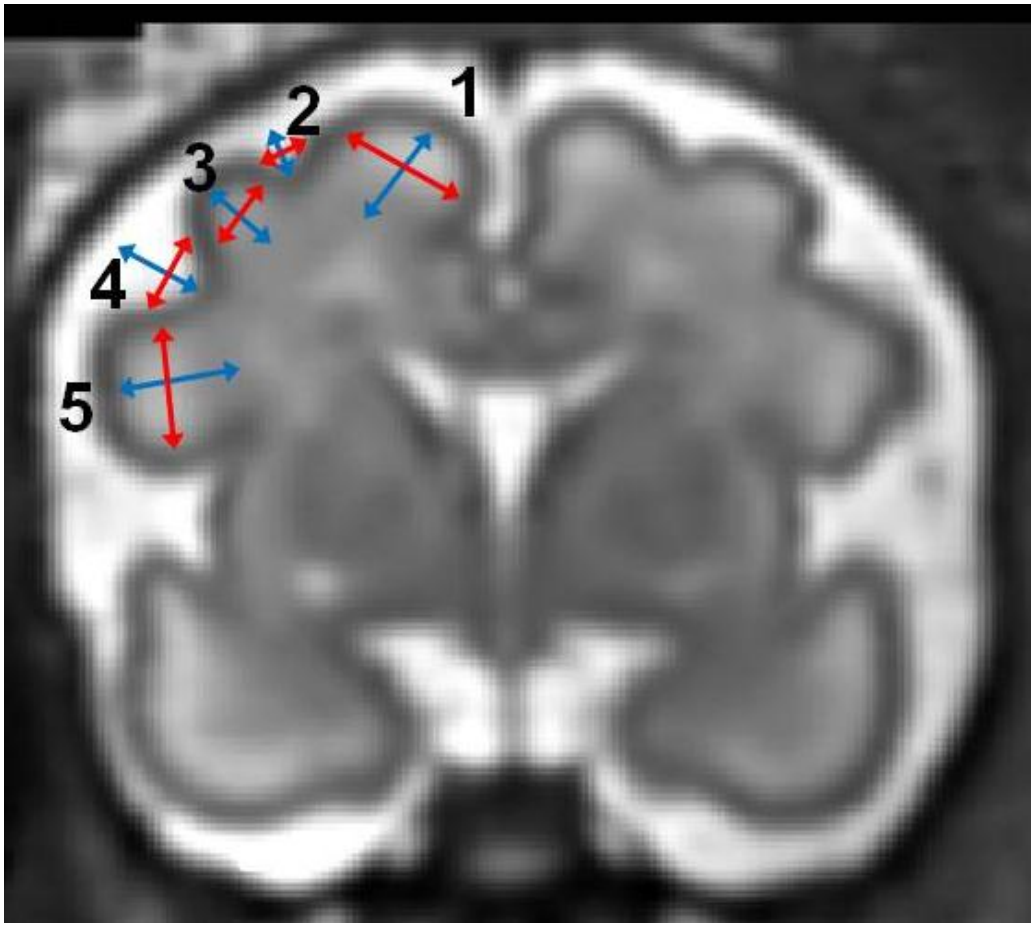


Cingulate sulcus

Cortical development of the cingulate sulcus was assessed using the length of the cingulate sulcus (blue) on a sagittal plane.

Frontal lobe

Superior frontal gyrus and sulcus/ middle frontal gyrus/ inferior frontal gyrus and sulcus: All measurements are made in a coronal plane on a slice where the anterior temporal lobes are present but not the brainstem. To locate the correct slice, the frontal sulcus is visualised in a transverse plane and the cursor is placed at 1/3 distance along the sulcal length from the anterior, in order to locate the corresponding coronal slice.

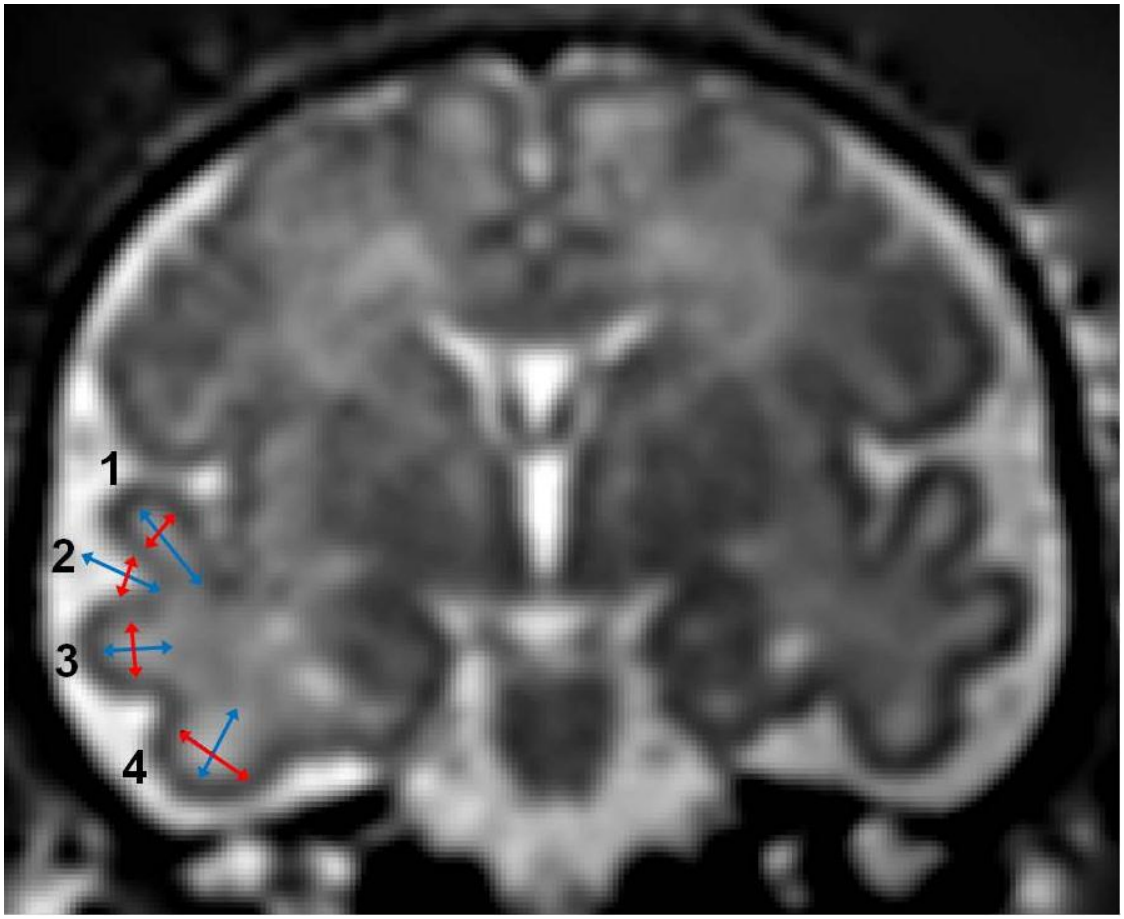


Frontal lobe

(1) superior frontal gyrus (2) superior frontal sulcus (3) middle frontal gyrus (4) inferior frontal sulcus (5) inferior frontal gyrus (B) precentral gyrus. Measurements of cortical folding included height (blue) and width (red) of gyri and sulci.

Temporal lobe

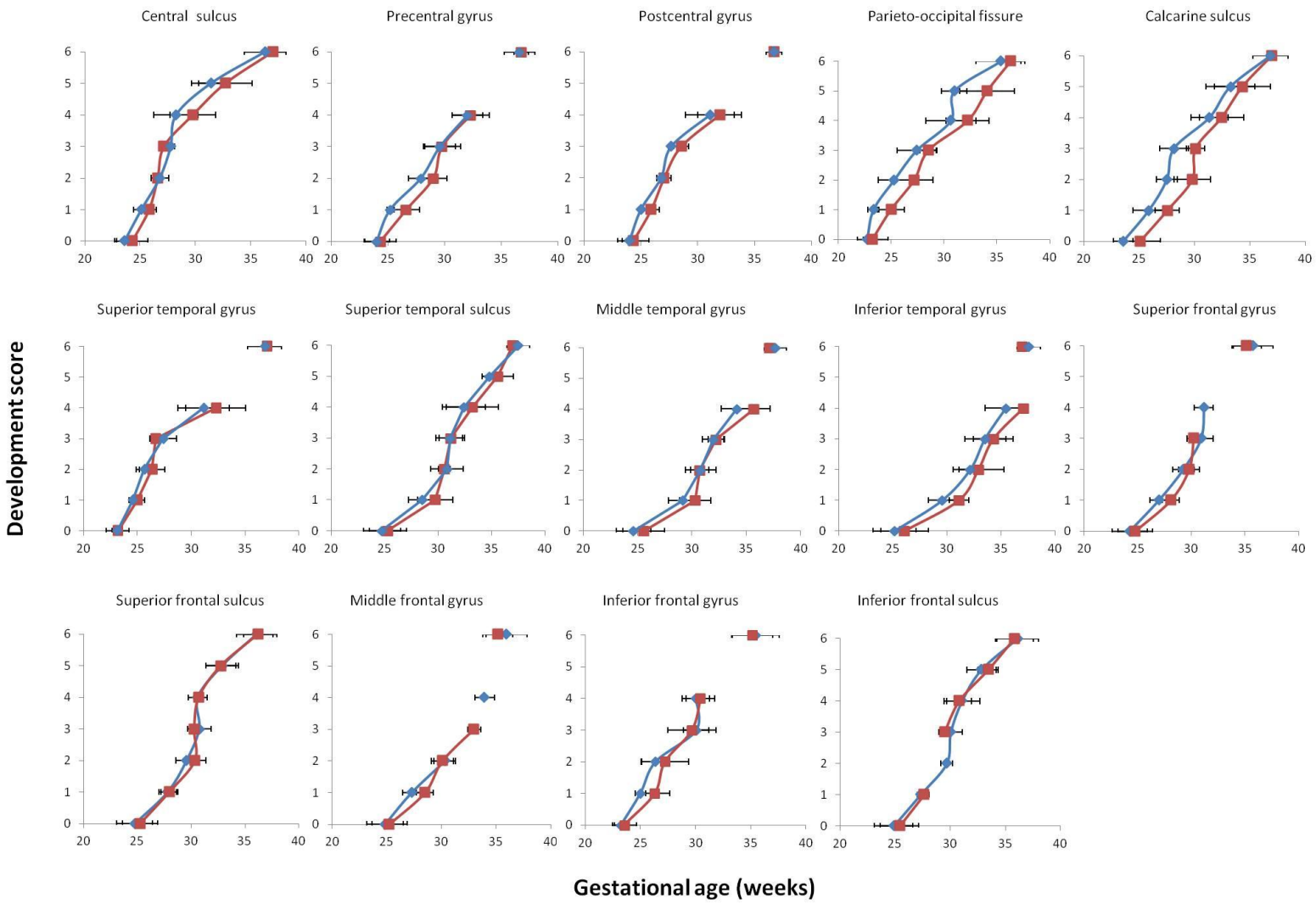
Superior temporal gyrus and sulcus/Middle temporal gyrus/ Inferior temporal gyrus: All measurements are made in a coronal plane before the appearance of the brainstem and spinal cord. Measurements are taken where the brainstem appears as a square. Late in gestation it is more clear to take the measurements a few slices more frontal just as the brainstem starts to appear.



Temporal lobe

(1) Superior temporal gyrus (2) superior temporal sulcus (3) middle temporal gyrus (4) inferior temporal gyrus. Measurements of cortical folding included height (blue) and width (red) of gyri and sulci.

Appendix 6. Cortical development: Mean and standard deviation of GA for different development scores



Appendix 7. Vitamin D Questionnaire

Do you know your vitamin D levels? Yes ☐ No ☐
If yes: Date last measured (mm/yy) and level _____

Do you take multivitamins? Yes ☐ No ☐

If so which product do you use? _____
When did you start taking the multivitamins? _____

Do you take Vitamin D supplements or calcium with Vitamin D?
Yes ☐ No ☐

If so, how many IU (units) per day? _____
When did you start taking Vitamin D? _____

Do you take cod liver oil? Yes ☐ No ☐

How much and how often? _____
When did you start taking cod liver oil? _____

Are you vegetarian/vegan? Yes ☐ No ☐

How many times per week do you eat oily fish? _____

What is your ethnic background? _____

What is your clothing style? (please circle)
Skin fully covered / only face uncovered / no traditional clothing

What is your occupation? _____

Have you received a suntan in the past 12 months? Yes ☐ No ☐

Have you used a tanning booth in the past 12 months? Yes ☐ No ☐

On average, how much sun exposure have you had during your pregnancy? (please circle)
<5minutes per day / 5-15 minutes per day / 15-30 minutes per day / >30 minutes per day

Do you use sunscreen? Yes ☐ No ☐

Do you suffer from any renal conditions? Yes ☐ No ☐_____

Have you got any family history of rickets, bone diseases or previous children affected?

Yes ☐ ☐ No _____

References

Afif, A., Bouvier, R., Buenerd, A., Trouillas, J., and Mertens, P. (2007). Development of the human fetal insular cortex: study of the gyration from 13 to 28 gestational weeks. Brain Struct Funct *212*, 335-346.

Ajayi-Obe, M., Saeed, N., Cowan, F.M., Rutherford, M.A., and Edwards, A.D. (2000). Reduced development of cerebral cortex in extremely preterm infants. Lancet *356*, 1162-1163.

Aljabar, P., Heckemann, R.A., Hammers, A., Hajnal, J.V., and Rueckert, D. (2009). Multi-atlas based segmentation of brain images: atlas selection and its effect on accuracy. NeuroImage *46*, 726-738.

Almog, B., Gamzu, R., Achiron, R., Fainaru, O., and Zalel, Y. (2003). Fetal lateral ventricular width: what should be its upper limit? A prospective cohort study and reanalysis of the current and previous data. J Ultrasound Med *22*, 39-43.

Alonso, J.R., Covenas, R., Lara, J., Pinuela, C., and Aijon, J. (1989). The cavum septi pellucidi: a fifth ventricle? Acta Anat (Basel) *134*, 286-290.

Alonso, M.I., Gato, A., Moro, J.A., and Barbosa, E. (1998). Disruption of proteoglycans in neural tube fluid by beta-D-xyloside alters brain enlargement in chick embryos. Anat Rec *252*, 499-508.

Anjari, M., Srinivasan, L., Allsop, J.M., Hajnal, J.V., Rutherford, M.A., Edwards, A.D., and Counsell, S.J. (2007). Diffusion tensor imaging with tract-based spatial statistics reveals local white matter abnormalities in preterm infants. NeuroImage *35*, 1021-1027.

Antonelli, A., Chiaretti, A., Amendola, T., Piastra, M., Di Rocco, C., and Aloe, L. (2004). Nerve growth factor and brain-derived neurotrophic factor in human paediatric hemimegalencephaly. Neuropediatrics *35*, 39-44.

Aoki, Y., Kasai, K., and Yamasue, H. (2012). Age-related change in brain metabolite abnormalities in autism: a meta-analysis of proton magnetic resonance spectroscopy studies. Translational psychiatry *2*, e69.

Arichi, T. (2012). Functional MRI of the developing neonatal brain: potential and challenges for the future. Dev Med Child Neurol *54*, 680.

Ariyannur, P.S., Madhavarao, C.N., and Namboodiri, A.M. (2008). N-acetylaspartate synthesis in the brain: mitochondria vs. microsomes. Brain Res *1227*, 34-41.

Armstrong, E., Schleicher, A., Omran, H., Curtis, M., and Zilles, K. (1995). The ontogeny of human gyrification. Cerebral cortex *5*, 56-63.

Arora, A., Bannister, C.M., Russell, S., and Rimmer, S. (1998). Outcome and clinical course of prenatally diagnosed cerebral ventriculomegaly. European journal of pediatric surgery *8 Suppl 1*, 63-64.

Ayoub, A.E., and Kostovic, I. (2009). New horizons for the subplate zone and its pioneering neurons. Cerebral cortex *19*, 1705-1707.

Ball, G., Counsell, S.J., Anjari, M., Merchant, N., Arichi, T., Doria, V., Rutherford, M.A., Edwards, A.D., Rueckert, D., and Boardman, J.P. (2010). An optimised tract-based spatial statistics protocol for neonates: applications to prematurity and chronic lung disease. NeuroImage *53*, 94-102.

Barkovich, A.J., Gressens, P., and Evrard, P. (1992). Formation, maturation, and disorders of brain neocortex. AJNR Am J Neuroradiol *13*, 423-446.

Baslow, M.H., Suckow, R.F., Gaynor, K., Bhakoo, K.K., Marks, N., Saito, M., Saito, M., Duff, K., Matsuoka, Y., and Berg, M.J. (2003). Brain damage results in down-regulation of N-acetylaspartate as a neuronal osmolyte. Neuromolecular Med *3*, 95-104.

Bayley, N. (2006). Bayley Scales of Infant and Toddler Development, 3rd edn (Psychological Corporation).

Beacher, F., Simmons, A., Daly, E., Prasher, V., Adams, C., Margallo-Lana, M.L., Morris, R., Lovestone, S., Murphy, K., and Murphy, D.G. (2005). Hippocampal myo-inositol and cognitive ability in adults with Down syndrome: an in vivo proton magnetic resonance spectroscopy study. Arch Gen Psychiatry *62*, 1360-1365.

Beaulieu, C. (2002). The basis of anisotropic water diffusion in the nervous system - a technical review. NMR Biomed *15*, 435-455.

Becker, A., Eyles, D.W., McGrath, J.J., and Grecksch, G. (2005). Transient prenatal vitamin D deficiency is associated with subtle alterations in learning and memory functions in adult rats. Behav Brain Res *161*, 306-312.

Beeghly, M., Ware, J., Soul, J., Plessis, A., Senapati, G.M., Robson, C.D., Robertson, R.L., Poussaint, Y., Barnewolt, C.E., Feldman, H.A., *et al.* (2010). Neurodevelopmental outcomes of fetuses referred for ventriculomegaly. Clinical Research *35*, 405-416.

Benacerraf, B.R., and Shipp, T.D. (2007). What does magnetic resonance Imaging add to the prenatal sonographic diagnosis of ventriculomegaly ? Ultrasound, 1513-1522.

Blaas, H.G., Eik-Nes, S.H., Berg, S., and Torp, H. (1998). In-vivo three-dimensional ultrasound reconstructions of embryos and early fetuses. Lancet *352*, 1182-1186.

Bloom, S.L., Bloom, D.D., DellaNebbia, C., Martin, L.B., Lucas, M.J., and Twickler, D.M. (1997). The developmental outcome of children with antenatal mild isolated ventriculomegaly. Obstet Gynecol *90*, 93-97.

Bodensteiner, J.B., Schaefer, G.B., and Craft, J.M. (1998). Cavum septi pellucidi and cavum vergae in normal and developmentally delayed populations. J Child Neurol *13*, 120-121.

Bosman, C., Boldrini, R., Dimitri, L., Di Rocco, C., and Corsi, A. (1996). Hemimegalencephaly. Histological, immunohistochemical, ultrastructural and cytofluorimetric study of six patients. Childs Nerv Syst *12*, 765-775.

Breedveld, G., de Coo, I.F., Lequin, M.H., Arts, W.F., Heutink, P., Gould, D.B., John, S.W., Oostra, B., and Mancini, G.M. (2006). Novel mutations in three families confirm a major role of COL4A1 in hereditary porencephaly. Journal of medical genetics *43*, 490-495.

Breeze, A.C., Alexander, P.M., Murdoch, E.M., Missfelder-Lobos, H.H., Hackett, G.A., and Lees, C.C. (2007). Obstetric and neonatal outcomes in severe fetal ventriculomegaly. Prenat Diagn *27*, 124-129.

Breeze, A.C., Dey, P.K., Lees, C.C., Hackett, G.A., Smith, G.C., and Murdoch, E.M. (2005). Obstetric and neonatal outcomes in apparently isolated mild fetal ventriculomegaly. J Perinat Med *33*, 236-240.

Brighina, E., Bresolin, N., Pardi, G., and Rango, M. (2009). Human fetal brain chemistry as detected by proton magnetic resonance spectroscopy. Pediatr Neurol *40*, 327-342.

Bromley, B., Frigoletto, F.D., Jr., and Benacerraf, B.R. (1991). Mild fetal lateral cerebral ventriculomegaly: clinical course and outcome. Am J Obstet Gynecol *164*, 863-867.

Buka, S.L., and Fan, A.P. (1999). Association of prenatal and perinatal complications with subsequent bipolar disorder and schizophrenia. Schizophr Res *39*, 113-119; discussion 160-111.

Burne, T.H., Becker, A., Brown, J., Eyles, D.W., Mackay-Sim, A., and McGrath, J.J. (2004). Transient prenatal Vitamin D deficiency is associated with hyperlocomotion in adult rats. Behav Brain Res *154*, 549-555.

Buss, R.R., and Oppenheim, R.W. (2004). Role of programmed cell death in normal neuronal development and function. Anat Sci Int *79*, 191-197.

Bystron, I., Blakemore, C., and Rakic, P. (2008). Development of the human cerebral cortex: Boulder Committee revisited. Nat Rev Neurosci *9*, 110-122.

Cady, E.B., Penrice, J., Amess, P.N., Lorek, A., Wylezinska, M., Aldridge, R.F., Franconi, F., Wyatt, J.S., and Reynolds, E.O. (1996). Lactate, N-acetylaspartate, choline and creatine concentrations, and spin-spin relaxation in thalamic and occipito-parietal regions of developing human brain. Magn Reson Med *36*, 878-886.

Callen, P.W., Callen, A.L., Glenn, O.A., and Toi, A. (2008). Columns of the fornix, not to be mistaken for the cavum septi pellucidi on prenatal sonography. J Ultrasound Med *27*, 25-31.

Carabalona, A., Beguin, S., Pallesi-Pocachard, E., Buhler, E., Pellegrino, C., Arnaud, K., Hubert, P., Oualha, M., Siffroi, J.P., Khantane, S., *et al.* (2012). A glial origin for periventricular nodular heterotopia caused by impaired expression of Filamin-A. Hum Mol Genet *21*, 1004-1017.

Cardoza, J.D., Goldstein, R.B., and Filly, R.A. (1988). Exclusion of fetal ventriculomegaly with a single measurement: the width of the lateral ventricular atrium. Radiology *169*, 711-714.

Carper, R.A., and Courchesne, E. (2005). Localized enlargement of the frontal cortex in early autism. Biol Psychiatry *57*, 126-133.

Castellanos, F.X., Giedd, J.N., Marsh, W.L., Hamburger, S.D., Vaituzis, A.C., Dickstein, D.P., Sarfatti, S.E., Vauss, Y.C., Snell, J.W., Lange, N., *et al.* (1996). Quantitative brain magnetic resonance imaging in attention-deficit hyperactivity disorder. Arch Gen Psychiatry *53*, 607-616.

Catani, M. (2007). From hodology to function. Brain *130*, 602-605.

Chambers, C.D., Johnson, K.A., Dick, L.M., Felix, R.J., and Jones, K.L. (1998). Maternal fever and birth outcome: a prospective study. Teratology *58*, 251-257.

Chan, W.Y., Lorke, D.E., Tiu, S.C., and Yew, D.T. (2002). Proliferation and apoptosis in the developing human neocortex. The Anatomical record *267*, 261-276.

Chen, C.Y., Zimmerman, R.A., Faro, S., Parrish, B., Wang, Z., Bilaniuk, L.T., and Chou, T.Y. (1996). MR of the cerebral operculum: abnormal opercular formation in infants and children. AJNR Am J Neuroradiol *17*, 1303-1311.

Chenn, A., and McConnell, S.K. (1995). Cleavage orientation and the asymmetric inheritance of Notch1 immunoreactivity in mammalian neurogenesis. Cell *82*, 631-641.

Chenn, A., and Walsh, C.A. (2002). Regulation of cerebral cortical size by control of cell cycle exit in neural precursors. Science *297*, 365-369.

Childs, a.M., Ramenghi, L.a., Cornette, L., Tanner, S.F., Arthur, R.J., Martinez, D., and Levene, M.I. (2001). Cerebral maturation in premature infants: quantitative assessment using MR imaging. Ajnr American Journal Of Neuroradiology *22*, 1577-1582.

Choi, B.H. (1988). Developmental events during the early stages of cerebral cortical neurogenesis in man. A correlative light, electron microscopic, immunohistochemical and Golgi study. Acta neuropathologica *75*, 441-447.

Clark, J.B. (1998). N-acetyl aspartate: a marker for neuronal loss or mitochondrial dysfunction. Dev Neurosci *20*, 271-276.

Clouchoux, C., Guizard, N., Evans, A.C., du Plessis, A.J., and Limperopoulos, C. (2011). Normative fetal brain growth by quantitative in vivo magnetic resonance imaging. AmJ Obstet Gynecol *206*, 173-178.

Clouchoux, C., Kudelski, D., Gholipour, A., Warfield, S.K., Viseur, S., Bouyssi-Kobar, M., Mari, J.L., Evans, A.C., du Plessis, A.J., and Limperopoulos, C. (2012). Quantitative in vivo MRI measurement of cortical development in the fetus. Brain Struct Funct *217*, 127-139.

Coakley, F.V., Glenn, O.A., Qayyum, A., Barkovich, A.J., Goldstein, R., and Filly, R.A. (2004). Fetal MRI : A Developing Technique for the Developing Patient History of Fetal MRI. Most, 243-252.

Cogram, P., Hynes, A., Dunlevy, L.P., Greene, N.D., and Copp, A.J. (2004). Specific isoforms of protein kinase C are essential for prevention of folate-resistant neural tube defects by inositol. Hum Mol Genet *13*, 7-14.

Cohen, R.I., Marmur, R., Norton, W.T., Mehler, M.F., and Kessler, J.A. (1996). Nerve Growth Factor and Neurotrophin-3 Differentially Regulate the Brain Oligodendrocytes. *16*, 6433-6442.

Cohn, B.R., Joe, B.N., Zhao, S., Kornak, J., Zhang, V.Y., Iman, R., Kurhanewicz, J., Vahidi, K., Yu, J., Caughey, A.B., *et al.* (2009). Quantitative metabolic profiles of 2nd and 3rd trimester human amniotic fluid using (1)H HR-MAS spectroscopy. Magma *22*, 343-352.

Corbett-Detig, J., Habas, P.A., Scott, J.A., Kim, K., Rajagopalan, V., McQuillen, P.S., Barkovich, A.J., Glenn, O.A., and Studholme, C. (2011). 3D global and regional patterns of human fetal subplate growth determined in utero. Brain Struct Funct *215*, 255-263.

Counsell, S.J., Edwards, A.D., Chew, A.T., Anjari, M., Dyet, L.E., Srinivasan, L., Boardman, J.P., Allsop, J.M., Hajnal, J.V., Rutherford, M.A., *et al.* (2008). Specific relations between neurodevelopmental abilities and white matter microstructure in children born preterm. Brain *131*, 3201-3208.

Courchesne, E., Campbell, K., and Solso, S. (2011a). Brain growth across the life span in autism: age-specific changes in anatomical pathology. Brain Res *1380*, 138-145.

Courchesne, E., Karns, C.M., Davis, H.R., Ziccardi, R., Carper, R.A., Tigue, Z.D., Chisum, H.J., Moses, P., Pierce, K., Lord, C., *et al.* (2001). Unusual brain growth patterns in early life in patients with autistic disorder: an MRI study. Neurology *57*, 245-254.

Courchesne, E., Mouton, P.R., Calhoun, M.E., Semendeferi, K., Ahrens-Barbeau, C., Hallet, M.J., Barnes, C.C., and Pierce, K. (2011b). Neuron number and size in prefrontal cortex of children with autism. JAMA *306*, 2001-2010.

D'Addario, V., Pinto, V., Di Cagno, L., and Pintucci, A. (2007). Sonographic diagnosis of fetal cerebral ventriculomegaly: an update. J Matern Fetal Neonatal Med *20*, 7-14.

Damodaram, M.S., Story, L., Eixarch, E., Patkee, P., Patel, A., Kumar, S., and Rutherford, M. (2012). Foetal volumetry using magnetic resonance imaging in intrauterine growth restriction. Early Hum Dev *88 Suppl 1*, S35-40.

Datta, S., Alfaham, M., Davies, D.P., Dunstan, F., Woodhead, S., Evans, J., and Richards, B. (2002). Vitamin D deficiency in pregnant women from a non-European ethnic minority population--an interventional study. BJOG *109*, 905-908.

Davson, and Segal (1996). Physiology of the CSF and blood-brain barriers (FL: CRC Press).

De Wilde, J.P., Rivers, A.W., and Price, D.L. (2005). A review of the current use of magnetic resonance imaging in pregnancy and safety implications for the fetus. Prog Biophys Mol Biol *87*, 335-353.

Dehay, C., Giroud, P., Berland, M., Killackey, H., and Kennedy, H. (1996). Contribution of thalamic input to the specification of cytoarchitectonic cortical fields in the primate: effects of bilateral enucleation in the fetal monkey on the boundaries, dimensions, and gyrification of striate and extrastriate cortex. J Comp Neurol *367*, 70-89.

Del Bigio, M.R. (1993). Neuropathological changes caused by hydrocephalus. Acta Neuropathol *85*, 573-585.

Dennerll, T.J., Joshi, H.C., Steel, V.L., Buxbaum, R.E., and Heidemann, S.R. (1988). Tension and compression in the cytoskeleton of PC-12 neurites. II: Quantitative measurements. J Cell Biol *107*, 665-674.

Depaepe, V., Suarez-Gonzalez, N., Dufour, A., Passante, L., Gorski, J.A., Jones, K.R., Ledent, C., and Vanderhaeghen, P. (2005). Ephrin signalling controls brain size by regulating apoptosis of neural progenitors. Nature *435*, 1244-1250.

Desmond, M.E., and Jacobson, A.G. (1977). Embryonic brain enlargement requires cerebrospinal fluid pressure. Dev Biol *57*, 188-198.

Desmond, M.E., Levitan, M.L., and Haas, A.R. (2005). Internal luminal pressure during early chick embryonic brain growth: descriptive and empirical observations. Anat Rec A Discov Mol Cell Evol Biol *285*, 737-747.

Devaseelan, P., Cardwell, C., Bell, B., and Ong, S. (2010). Prognosis of isolated mild to moderate fetal cerebral ventriculomegaly: a systematic review. J Perinat Med *38*, 401-409.

Do, C.B., and Batzoglou, S. (2008). What is the expectation maximization algorithm? Nature biotechnology *26*, 897-899.

Doricchi, F., and Tomaiuolo, F. (2003). The anatomy of neglect without hemianopia: a key role for parietal-frontal disconnection? Neuroreport *14*, 2239-2243.

Douglas, J., Hanks, S., Temple, I.K., Davies, S., Murray, A., Upadhyaya, M., Tomkins, S., Hughes, H.E., Cole, T.R.P., and Rahman, N. (2003). NSD1 mutations are the major cause of

Sotos syndrome and occur in some cases of Weaver syndrome but are rare in other overgrowth phenotypes. American journal of human genetics *72*, 132-143.

Dramsdahl, M., Westerhausen, R., Haavik, J., Hugdahl, K., and Plessen, K.J. (2012). Adults with attention-deficit/hyperactivity disorder - a diffusion-tensor imaging study of the corpus callosum. Psychiatry Res *201*, 168-173.

Drost, D.J., Riddle, W.R., Clarke, G.D., and Group, A.M.T. (2002). Proton magnetic resonance spectroscopy in the brain: report of AAPM MR Task Group #9. Medical physics *29*, 2177-2197.

Duffau, H., Capelle, L., Sichez, N., Denvil, D., Lopes, M., Sichez, J.P., Bitar, A., and Fohanno, D. (2002). Intraoperative mapping of the subcortical language pathways using direct stimulations. An anatomo-functional study. Brain *125*, 199-214.

Dziegielewska, K.M., Ek, J., Habgood, M.D., and Saunders, N.R. (2001). Development of the choroid plexus. Microsc Res Tech *52*, 5-20.

Edwards, M.J., Saunders, R.D., and Shiota, K. (2003). Effects of heat on embryos and foetuses. Int J Hyperthermia *19*, 295-324.

Edwards, M.J., Shiota, K., Smith, M.S., and Walsh, D.A. (1995). Hyperthermia and birth defects. Reproductive toxicology *9*, 411-425.

Etzel, R.A., Balk, S.J., Bearer, C.F., Miller, M.D., Shea, K.M., and Simon, P.R. (1997). Noise: A Hazard for the Fetus and Newborn. Pediatrics *100*, 724-727.

Eyles, D., Brown, J., Mackay-Sim, A., McGrath, J., and Feron, F. (2003). Vitamin D3 and brain development. Neuroscience *118*, 641-653.

Falco, P., Gabrielli, S., Visentin, A., Perolo, A., Pilu, G., and Bovicelli, L. (2000). Transabdominal sonography of the cavum septum pellucidum in normal fetuses in the second and third trimesters of pregnancy. Ultrasound Obstet Gynecol *16*, 549-553.

Falip, C., Blanc, N., Maes, E., Zaccaria, I., Oury, J.F., Sebag, G., and Garel, C. (2007). Postnatal clinical and imaging follow-up of infants with prenatal isolated mild ventriculomegaly: a series of 101 cases. Pediatr Radiol *37*, 981-989.

Fatemi, S.H., and Folsom, T.D. (2009). The neurodevelopmental hypothesis of schizophrenia, revisited. Schizophr Bull *35*, 528-548.

Fenton, B.W., Lin, C.S., Macedonia, C., Schellinger, D., and Ascher, S. (2001). The fetus at term: in utero volume-selected proton MR spectroscopy with a breath-hold technique--a feasibility study. Radiology *219*, 563-566.

Fernandes de Abreu, D.A., Nivet, E., Baril, N., Khrestchatisky, M., Roman, F., and Feron, F. (2010). Developmental vitamin D deficiency alters learning in C57Bl/6J mice. Behav Brain Res *208*, 603-608.

Feron, F., Burne, T.H., Brown, J., Smith, E., McGrath, J.J., Mackay-Sim, A., and Eyles, D.W. (2005). Developmental Vitamin D3 deficiency alters the adult rat brain. Brain Res Bull *65*, 141-148.

Fields, R.D., and Waxman, S.G. (1988). Regional membrane heterogeneity in premyelinated CNS axons: factors influencing the binding of sterol-specific probes. Brain Res *443*, 231-242.

Fogliarini, C., Chaumoitre, K., Chapon, F., Fernandez, C., Levrier, O., Figarella-Branger, D., and Girard, N. (2005). Assessment of cortical maturation with prenatal MRI. Part I: Normal cortical maturation. Eur Radiol *15*, 1671-1685.

Gaglioti, P., Danelon, D., Bontempo, S., Mombro, M., Cardaropoli, S., and Todros, T. (2005). Fetal cerebral ventriculomegaly: outcome in 176 cases. Ultrasound Obstet Gynecol *25*, 372-377.

Gaglioti, P., Oberto, M., and Todros, T. (2009). The significance of fetal ventriculomegaly: etiology, short- and long-term outcomes. Prenatal diagnosis *29*, 381-388.

Garel, C. (2004). MRI of the fetal brain. Normal development and cerebral pathologies (Springer).

Garel, C., Chantrel, E., Elmaleh, M., Brisse, H., and Sebag, G. (2003a). Fetal MRI: normal gestational landmarks for cerebral biometry, gyration and myelination. Childs Nerv Syst *19*, 422-425.

Garel, C., Luton, D., Oury, J.-F., and Gressens, P. (2003b). Ventricular dilatations. Child's nervous system : ChNS : official journal of the International Society for Pediatric Neurosurgery *19*, 517-523.

Gato, A., and Desmond, M.E. (2009). Why the embryo still matters: CSF and the neuroepithelium as interdependent regulators of embryonic brain growth, morphogenesis and histiogenesis. DevBiol *327*, 263-272.

Gato, A., Moro, J.A., Alonso, M.I., Bueno, D., De La Mano, A., and Martin, C. (2005). Embryonic cerebrospinal fluid regulates neuroepithelial survival, proliferation, and neurogenesis in chick embryos. Anat Rec A Discov Mol Cell Evol Biol *284*, 475-484.

Gato, A., Moro, J.A., Alonso, M.I., Pastor, J.F., Represa, J.J., and Barbosa, E. (1993). Chondroitin sulphate proteoglycan and embryonic brain enlargement in the chick. Anat Embryol (Berl) *188*, 101-106.

Gazzaniga, M.S. (2000). Cerebral specialization and interhemispheric communication: does the corpus callosum enable the human condition? Brain *123*, 1293-1326.

Geng, X., Gouttard, S., Sharma, A., Gu, H., Styner, M., Lin, W., Gerig, G., and Gilmore, J.H. (2012). Quantitative tract-based white matter development from birth to age 2years. NeuroImage *61*, 542-557.

Gholipour, A., Estroff, J.A., Barnewolt, C.E., Connolly, S.A., and Warfield, S.K. (2011). Fetal brain volumetry through MRI volumetric reconstruction and segmentation. Int J Comput Assist Radiol Surg *6*, 329-339.

Gilles, F., and Nelson, D.M. (2012). The developing human brain: growth and adversities, 1 edn (Mac Keith Press).

Gilmore, J.H., Smith, L.C., Wolfe, H.M., Hertzberg, B.S., Smith, J.K., Chescheir, N.C., Evans, D.D., Kang, C., Hamer, R.M., Lin, W., *et al.* (2008). Prenatal mild ventriculomegaly predicts abnormal development of the neonatal brain. BiolPsychiatry *64*, 1069-1076.

Girard, N., Fogliarini, C., Viola, A., Confort-Gouny, S., Fur, Y.L., Viout, P., Chapon, F., Levrier, O., and Cozzone, P. (2006a). MRS of normal and impaired fetal brain development. Eur J Radiol *57*, 217-225.

Girard, N., Gouny, S.C., Viola, A., Le Fur, Y., Viout, P., Chaumoitre, K., D'Ercole, C., Gire, C., Figarella-Branger, D., and Cozzone, P.J. (2006b). Assessment of normal fetal brain maturation in utero by proton magnetic resonance spectroscopy. Magn Reson Med *56*, 768-775.

Glenn, O.A. (2006). Fetal central nervous system MR imaging. Neuroimaging Clin N Am *16*, 1-17.

Glover, P., Hykin, J., Gowland, P., Wright, J., Johnson, I., and Mansfield, P. (1995). An assessment of the intrauterine sound intensity level during obstetric echo-planar magnetic resonance imaging. Br J Radiol *68*, 1090-1094.

Goldstein, R.B., La Pidus, A.S., Filly, R.A., and Cardoza, J. (1990). Mild lateral cerebral ventricular dilatation in utero: clinical significance and prognosis. Radiology *176*, 237-242.

Gollenberg, A.L., Lynch, C.D., Jackson, L.W., McGuinness, B.M., and Msall, M.E. (2010). Concurrent validity of the parent-completed Ages and Stages Questionnaires, 2nd Ed. with the Bayley Scales of Infant Development II in a low-risk sample. Child: care, health and development *36*, 485-490.

Gomez-Arriaga, P., Herraiz, I., Puente, J.M., Zamora-Crespo, B., Nunez-Enamorado, N., and Galindo, A. (2012). Mid-term neurodevelopmental outcome in isolated mild ventriculomegaly diagnosed in fetal life. Fetal Diagn Ther *31*, 12-18.

Gong, G.H., Roberts Q. Y. Roberts Garden A. S. Whitehouse A. S. (1998). Fetal and fetal brain volume estimation in the third trimester of human pregnancy using gradient echo MR imaging. Science *16*, 235-240.

Goodlett, C.B., Fletcher, P.T., Gilmore, J.H., and Gerig, G. (2009). Group analysis of DTI fiber tract statistics with application to neurodevelopment. NeuroImage *45*, 133-142.

Gould, D.B., Phalan, F.C., Breedveld, G.J., van Mil, S.E., Smith, R.S., Schimenti, J.C., Aguglia, U., van der Knaap, M.S., Heutink, P., and John, S.W. (2005). Mutations in Col4a1 cause perinatal cerebral hemorrhage and porencephaly. Science *308*, 1167-1171.

Gousias, I.S., Rueckert, D., Heckemann, R.A., Dyet, L.E., Boardman, J.P., Edwards, A.D., and Hammers, A. (2008). Automatic segmentation of brain MRIs of 2-year-olds into 83 regions of interest. NeuroImage *40*, 672-684.

Graham, E., Duhl, A., Ural, S., Allen, M., Blakemore, K., and Witter, F. (2001). The degree of antenatal ventriculomegaly is related to pediatric neurological morbidity. J Matern Fetal Med *10*, 258-263.

Greene, N.D., and Copp, A.J. (1997). Inositol prevents folate-resistant neural tube defects in the mouse. Nat Med *3*, 60-66.

Greene, N.D., and Copp, A.J. (2009). Development of the vertebrate central nervous system: formation of the neural tube. Prenat Diagn *29*, 303-311.

Griffiths, P.D., Reeves, M.J., Morris, J.E., Mason, G., Russell, S.A., Paley, M.N., and Whitby, E.H. (2010). A prospective study of fetuses with isolated ventriculomegaly investigated by antenatal sonography and in utero MR imaging. AJNR Am J Neuroradiol *31*, 106-111.

Groppo, M., Ricci, D., Bassi, L., Merchant, N., Doria, V., Arichi, T., Allsop, J.M., Ramenghi, L., Fox, M.J., Cowan, F.M., *et al.* (2012). Development of the optic radiations and visual function after premature birth. Cortex.

Grossman, R., Hoffman, C., Mardor, Y., and Biegon, A. (2006). Quantitative MRI measurements of human fetal brain development in utero. British journal of anaesthesia *33*, 463-470.

Grove, E.A., and Fukuchi-Shimogori, T. (2003). Generating the cerebral cortical area map. Annu Rev Neurosci *26*, 355-380.

Hand, J.W., Li, Y., and Hajnal, J.V. (2010). Numerical study of RF exposure and the resulting temperature rise in the foetus during a magnetic resonance procedure. Physics in medicine and biology *55*, 913-930.

Hankin, M.H., Schneider, B.F., and Silver, J. (1988). Death of the subcallosal glial sling is correlated with formation of the cavum septi pellucidi. J Comp Neurol *272*, 191-202.

Hansen, D.V., Lui, J.H., Parker, P.R., and Kriegstein, A.R. (2010). Neurogenic radial glia in the outer subventricular zone of human neocortex. Nature *464*, 554-561.

Harvey, L., Burne, T.H., McGrath, J.J., and Eyles, D.W. (2010). Developmental vitamin D3 deficiency induces alterations in immune organ morphology and function in adult offspring. J Steroid Biochem Mol Biol *121*, 239-242.

Hatzaki, A., Anagnostopoulou, E., Metaxa-Mariatou, V., Melissinos, C., Philalithis, P., Iliadis, K., Kontaxis, A., Liberatos, K., Pangratis, N., and Nasioulas, G. (2003). The impact of heterozygosity for the factor V Leiden and factor II G20210A mutations on the risk of thrombosis in Greek patients. Int Angiol *22*, 79-82.

Haveman, J., and Lavorel, J. (1975). Identification of the 120 mus phase in the decay of delayed fluorescence in spinach chloroplasts and subchloroplast particles as the intrinsic back reaction. The dependence of the level of this phase on the thylakoids internal pH. Biochim Biophys Acta *408*, 269-238.

Hazlett, H.C., Poe, M.D., Gerig, G., Styner, M., Chappell, C., Smith, R.G., Vachet, C., and Piven, J. (2011). Early brain overgrowth in autism associated with an increase in cortical surface area before age 2 years. Biochimica et biophysica acta *68*, 467-476.

Heerschap, A., Kok, R.D., and van den Berg, P.P. (2003). Antenatal proton MR spectroscopy of the human brain in vivo. Childs Nerv Syst *19*, 418-421.

Hegde, A.N., Mohan, S., Lath, N., and Lim, C.C. (2011). Differential diagnosis for bilateral abnormalities of the basal ganglia and thalamus. Radiographics *31*, 5-30.

Heinrichs, W.L., Fong, P., Flannery, M., Heinrichs, S.C., Crooks, L.E., Spindle, A., and Pedersen, R.A. (1988). Midgestational exposure of pregnant BALB/c mice to magnetic resonance imaging conditions. Magn Reson Imaging *6*, 305-313.

Hermann, B.P., Dabbs, K., Becker, T., Jones, J.E., Myers y Gutierrez, A., Wendt, G., Koehn, M.A., Sheth, R., and Seidenberg, M. (2010). Brain development in children with new onset epilepsy: a prospective controlled cohort investigation. Epilepsia *51*, 2038-2046.

Hernandez, M.J., Vannucci, R.C., Salcedo, A., and Brennan, R.W. (1980). Cerebral blood flow and metabolism during hypoglycemia in newborn dogs. Journal of neurochemistry *35*, 622-628.

Hilpert, P.L., Hall, B.E., and Kurtz, A.B. (1995). The atria of the fetal lateral ventricles: a sonographic study of normal atrial size and choroid plexus volume. AJR Am J Roentgenol *164*, 731-734.

Holick, M.F. (2006). Resurrection of vitamin D deficiency and rickets. J Clin Invest *116*, 2062-2072.

Hollis, B.W., and Wagner, C.L. (2006). Vitamin D deficiency during pregnancy: an ongoing epidemic. Am J Clin Nutr *84*, 273.

Hu, H.H., Guo, W.Y., Chen, H.Y., Wang, P.S., Hung, C.I., Hsieh, J.C., and Wu, Y.T. (2009). Morphological regionalization using fetal magnetic resonance images of normal developing brains. Eur J Neurosci *29*, 1560-1567.

Huang, W., Alexander, G.E., Daly, E.M., Shetty, H.U., Krasuski, J.S., Rapoport, S.I., and Schapiro, M.B. (1999). High brain myo-inositol levels in the predementia phase of

Alzheimer's disease in adults with Down's syndrome: a 1H MRS study. Am J Psychiatry *156*, 1879-1886.

Huntley, M. (1995). The Griffiths Mental Development Scales: From Birth to 2 years. Association for Research in Infant and Child Development (ARICD).

Huppi, P.S., Fusch, C., Boesch, C., Burri, R., Bossi, E., Amato, M., and Herschkowitz, N. (1995). Regional metabolic assessment of human brain during development by proton magnetic resonance spectroscopy in vivo and by high-performance liquid chromatography/gas chromatography in autopsy tissue. Pediatr Res *37*, 145-150.

Huppi, P.S., and Inder, T.E. (2001). Magnetic resonance techniques in the evaluation of the perinatal brain: recent advances and future directions. Seminars in neonatology : SN *6*, 195-210.

Huppi, P.S., Maier, S.E., Peled, S., Zientara, G.P., Barnes, P.D., Jolesz, F.A., and Volpe, J.J. (1998). Microstructural development of human newborn cerebral white matter assessed in vivo by diffusion tensor magnetic resonance imaging. Pediatr Res *44*, 584-590.

Hynd, G.W., Hall, J., Novey, E.S., Eliopulos, D., Black, K., Gonzalez, J.J., Edmonds, J.E., Riccio, C., and Cohen, M. (1995). Dyslexia and corpus callosum morphology. Archives of neurology *52*, 32-38.

IEC_60601-2-33 (2002). Particular requirements for the safety of magnetic resonance equipment for medical diagnosis. International electrical comission Genevea, Switzerland.

Inder, T.E., and Huppi, P.S. (2000). In vivo studies of brain development by magnetic resonance techniques. Mental retardation and developmental disabilities research reviews *6*, 59-67.

ISUOG (2007). The International Society of Ultrasound in Obstetrics and Gynecology. Sonographic examination of the fetal central nervous system: guidelines for performing the 'basic examination' and the 'fetal neurosonogram'. Ultrasound Obstet Gynecol *29*, 109-116.

Jackson, D.C., Irwin, W., Dabbs, K., Lin, J.J., Jones, J.E., Hsu, D.a., Stafstrom, C.E., Seidenberg, M., and Hermann, B.P. (2011). Ventricular enlargement in new-onset pediatric epilepsies. Epilepsia *52*, 2225-2232.

Jiang, S.Z., Xue, H., Glover, A., Rutherford, M., Rueckert, D., and Hajnal, J.V. (2007). MRI of moving subjects using multislice snapshot images with volume reconstruction (SVR): Application to fetal, neonatal, and adult brain studies. IEEE transactions on medical imaging *26*, 967-980.

Johansson, P.A., Dziegielewska, K.M., Liddelow, S.A., and Saunders, N.R. (2008). The blood-CSF barrier explained: when development is not immaturity. Bioessays *30*, 237-248.

Johnson, C.P., and Myers, S.M. (2007). Identification and evaluation of children with autism spectrum disorders. Pediatrics *120*, 1183-1215.

Joo, J.G., Toth, Z., Beke, A., Papp, C., Toth-Pal, E., Csaba, A., Szigeti, Z., Rab, A., and Papp, Z. (2008). Etiology, prenatal diagnostics and outcome of ventriculomegaly in 230 cases. Fetal Diagn Ther *24*, 254-263.

Jou, H.J., Shyu, M.K., Wu, S.C., Chen, S.M., Su, C.H., and Hsieh, F.J. (1998). Ultrasound measurement of the fetal cavum septi pellucidi. Ultrasound Obstet Gynecol *12*, 419-421.

Kalifa, G.L., Chiron, C., Sellier, N., Demange, P., Ponsot, G., Lalande, G., and Robain, O. (1987). Hemimegalencephaly: MR imaging in five children. Radiology *165*, 29-33.

Kalinichenko, S.G., and Matveeva, N.Y. (2008). Morphological characteristics of apoptosis and its significance in neurogenesis. Neurosci Behav Physiol *38*, 333-344.

Kalnin, A., Perkins, S.M., Johnson, C.S., Mathews, V.P., Egelhoff, J.C., Dunn, D.W., and Austin, J.K. (2009). MR Imaging findings in chilren with first recognised seizure. *39*, 404-414.

Kanal, E., Gillen, J., Evans, J.A., Savitz, D.A., and Shellock, F.G. (1993). Survey of reproductive health among female MR workers. Radiology *187*, 395-399.

Kapellou, O., Counsell, S.J., Kennea, N., Dyet, L., Saeed, N., Stark, J., Maalouf, E., Duggan, P., Jayi-Obe, M., Hajnal, J., *et al.* (2006). Abnormal cortical development after premature birth shown by altered allometric scaling of brain growth. PLoSMed *3*, e265.

Katz-Brull, R., Koudinov, A.R., and Degani, H. (2002). Choline in the aging brain. Brain Res *951*, 158-165.

Kazan-Tannus, J.F., Dialani, V., Kataoka, M.L., Chiang, G., Feldman, H.A., Brown, J.S., and Levine, D. (2007). MR volumetry of brain and CSF in fetuses referred for ventriculomegaly. British journal of anaesthesia *189*, 145-151.

Kelly, E.N., Allen, V.M., Seaward, G., Windrim, R., and Ryan, G. (2001). Mild ventriculomegaly in the fetus, natural history, associated findings and outcome of isolated mild ventriculomegaly: a literature review. Prenat Diagn *21*, 697-700.

Kendler, A., and Golden, J.A. (1996). Progenitor cell proliferation outside the ventricular and subventricular zones during human brain development. J Neuropathol Exp Neurol *55*, 1253-1258.

Kesler, S.R., Vohr, B., Schneider, K.C., Katz, K.H., Makuch, R.W., Reiss, A.L., and Ment, L.R. (2006). Increased temporal lobe gyrification in preterm children. Neuropsychologia *44*, 445-453.

Kinney, H.C., Karthigasan, J., Borenshteyn, N.I., Flax, J.D., and Kirschner, D.A. (1994). Myelination in the developing human brain: biochemical correlates. Neurochemical research *19*, 983-996.

Kinoshita, Y., Okudera, T., Tsuru, E., and Yokota, A. (2001). Volumetric analysis of the germinal matrix and lateral ventricles performed using MR images of postmortem fetuses. Am J Neuroradiol *22*, 382-388.

Kleinman, J.M., Ventola, P.E., Pandey, J., Verbalis, A.D., Barton, M., Hodgson, S., Green, J., Dumont-Mathieu, T., Robins, D.L., and Fein, D. (2008). Diagnostic stability in very young children with autism spectrum disorders. Journal of autism and developmental disorders *38*, 606-615.

Kline, J., Stein, Z., Susser, M., and Warburton, D. (1985). Fever during pregnancy and spontaneous abortion. American journal of epidemiology *121*, 832-842.

Kok, R.D., de Vries, M.M., Heerschap, A., and van den Berg, P.P. (2004). Absence of harmful effects of magnetic resonance exposure at 1.5 T in utero during the third trimester of pregnancy: a follow-up study. Magn Reson Imaging *22*, 851-854.

Kok, R.D., Steegers-Theunissen, R.P., Eskes, T.K., Heerschap, A., and van den Berg, P.P. (2003). Decreased relative brain tissue levels of inositol in fetal hydrocephalus. Am J Obstet Gynecol *188*, 978-980.

Kok, R.D., van den Berg, P.P., van den Bergh, A.J., Nijland, R., and Heerschap, A. (2002). Maturation of the human fetal brain as observed by 1H MR spectroscopy. Magn Reson Med *48*, 611-616.

Kolega, J. (1986). The cellular basis of epithelial morphogenesis. Developmental biology *2*, 103-143.

Korf, J. (2006). Is brain lactate metabolized immediately after neuronal activity through the oxidative pathway? Journal of cerebral blood flow and metabolism : official journal of the International Society of Cerebral Blood Flow and Metabolism *26*, 1584-1586.

Kostovic, I., and Jovanov-Milosevic, N. (2006). The development of cerebral connections during the first 20-45 weeks' gestation. Semin Fetal Neonatal Med *11*, 415-422.

Kostovic, I., and Judas, M. (2010). The development of the subplate and thalamocortical connections in the human foetal brain. Acta paediatrica *99*, 1119-1127.

Kostovic, I., and Rakic, P. (1990). Developmental history of the transient subplate zone in the visual and somatosensory cortex of the macaque monkey and human brain. J Comp Neurol *297*, 441-470.

Kostovic, I., and Vasung, L. (2009). Insights from in vitro fetal magnetic resonance imaging of cerebral development. Semin Perinatol *33*, 220-233.

Kramer, R.L., Yaron, Y., Johnson, M.P., Evans, M.I., Treadwell, M.C., and Wolfe, H.M. (1997). Differences in measurements of the atria of the lateral ventricle: does gender matter? Fetal Diagn Ther *12*, 304-305.

Kreiter, S.R., Schwartz, R.P., Kirkman, H.N., Jr., Charlton, P.A., Calikoglu, A.S., and Davenport, M.L. (2000). Nutritional rickets in African American breast-fed infants. J Pediatr *137*, 153-157.

Kriebs, J.M. (2008). Breaking the cycle of infection: TORCH and other infections in women's health. J Midwifery Womens Health *53*, 173-174.

Kuan, C.Y., Roth, K.A., Flavell, R.A., and Rakic, P. (2000). Mechanisms of programmed cell death in the developing brain. Trends Neurosci *23*, 291-297.

Kuklisova-Murgasova, M., Aljabar, P., Srinivasan, L., Counsell, S.J., Doria, V., Serag, A., Gousias, I.S., Boardman, J.P., Rutherford, M.A., Edwards, A.D., *et al.* (2011). A dynamic 4D probabilistic atlas of the developing brain. NeuroImage *54*, 2750-2763.

Kula, B., and Drozdz, M. (1996). A study of magnetic field effects on fibroblast cultures Part 1. The evaluation of the effects of static and extremely low frequency (ELF) magnetic fields on vital functions of fibroblasts. Bioelectrochemistry and Bioenergetics *39*, 21-26.

Lecanuet, J.P., Gautheron, B., Locatelli, A., Schaal, B., Jacquet, A.Y., and Busnel, M.C. (1998). What sounds reach fetuses: Biological and nonbiological modeling of the transmission of pure tones. Developmental psychobiology *33*, 203-219.

Leclercq, D., Duffau, H., Delmaire, C., Capelle, L., Gatignol, P., Ducros, M., Chiras, J., and Lehericy, S. (2010). Comparison of diffusion tensor imaging tractography of language tracts and intraoperative subcortical stimulations. J Neurosurg *112*, 503-511.

Lecuit, T., and Lenne, P.F. (2007). Cell surface mechanics and the control of cell shape, tissue patterns and morphogenesis. Nat Rev Mol Cell Biol *8*, 633-644.

Leijser, L.M., Srinivasan, L., Rutherford, M.A., Counsell, S.J., Allsop, J.M., and Cowan, F.M. (2007). Structural linear measurements in the newborn brain: accuracy of cranial ultrasound compared to MRI. Pediatr Radiol *37*, 640-648.

Leitner, Y., Stolar, O., Rotstein, M., Toledano, H., Harel, S., Bitchonsky, O., Ben-Adani, L., Miller, E., and Ben-Sira, L. (2009). The neurocognitive outcome of mild isolated fetal ventriculomegaly verified by prenatal magnetic resonance imaging. Am J Obstet Gynecol *201*, 215 e211-216.

Leth, H., Toft, P.B., Pryds, O., Peitersen, B., Lou, H.C., and Henriksen, O. (1995). Brain lactate in preterm and growth-retarded neonates. Acta paediatrica *84*, 495-499.

Levene, M.I., and Chervenak, F.A. (2009). Fetal and Neonatal Neurology and Neurosurgery, 4th edn (USA: Elsevier Limited).

Levenson, C.W., and Figueiroa, S.M. (2008). Gestational vitamin D deficiency: long-term effects on the brain. Nutr Rev *66*, 726-729.

Leventopoulos, G., Kitsiou-Tzeli, S., Kritikos, K., Psoni, S., Mavrou, A., Kanavakis, E., and Fryssira, H. (2009). A clinical study of Sotos syndrome patients with review of the literature. Biochemical pharmacology *40*, 357-364.

Levine, D., and Barnes, P.D. (1999). Cortical maturation in normal and abnormal fetuses as assessed with prenatal MR imaging. Radiology *210*, 751-758.

Levine, D., Barnes, P.D., Robertson, R.R., Wong, G., and Mehta, T.S. (2003). Fast MR imaging of fetal central nervous system abnormalities. Radiology *229*, 51-61.

Leviton, a., and Gilles, F. (1996). Ventriculomegaly, delayed myelination, white matter hypoplasia, and "periventricular" leukomalacia: how are they related? Pediatric neurology *15*, 127-136.

Lewis, D.A., and Levitt, P. (2002). Schizophrenia as a disorder of neurodevelopment. Annu Rev Neurosci *25*, 409-432.

Li, D.K., Odouli, R., Wi, S., Janevic, T., Golditch, I., Bracken, T.D., Senior, R., Rankin, R., and Iriye, R. (2002). A population-based prospective cohort study of personal exposure to magnetic fields during pregnancy and the risk of miscarriage. Epidemiology *13*, 9-20.

Limperopoulos, C., Tworetzky, W., McElhinney, D.B., Newburger, J.W., Brown, D.W., Robertson, R.L., Jr., Guizard, N., McGrath, E., Geva, J., Annese, D., *et al.* (2010). Brain volume and metabolism in fetuses with congenital heart disease: evaluation with quantitative magnetic resonance imaging and spectroscopy. Circulation *121*, 26-33.

Lipitz, S., Yagel, S., Malinger, G., Meizner, I., Zalel, Y., and Achiron, R. (1998). Outcome of fetuses with isolated borderline unilateral ventriculomegaly diagnosed at mid-gestation. Ultrasound Obstet Gynecol *12*, 23-26.

Liu, J.S. (2011). Molecular genetics of neuronal migration disorders. Current neurology and neuroscience reports *11*, 171-178.

Lord, C., Risi, S., DiLavore, P.S., Shulman, C., Thurm, A., and Pickles, A. (2006). Autism from 2 to 9 years of age. Arch Gen Psychiatry *63*, 694-701.

Loureiro, T., Ushakov, F., Maiz, N., Montenegro, N., and Nicolaides, K.H. (2012). Lateral ventricles in fetuses with aneuploidies at 11-13 weeks' gestation. Ultrasound Obstet Gynecol *40*, 282-287.

Lowery, L.A., and Sive, H. (2005). Initial formation of zebrafish brain ventricles occurs independently of circulation and requires the nagie oko and snakehead/atp1a1a.1 gene products. Development *132*, 2057-2067.

Lowery, L.A., and Sive, H. (2009). Totally tubular: the mystery behind function and origin of the brain ventricular system. BioEssays : news and reviews in molecular, cellular and developmental biology *31*, 446-458.

Lui, J.H., Hansen, D.V., and Kriegstein, A.R. (2011). Development and evolution of the human neocortex. Cell *146*, 18-36.

Lumsden, A., and Krumlauf, R. (1996). Patterning the vertebrate neuraxis. Science *274*, 1109-1115.

Lyall, A.E., Woolson, S., Wolfe, H.M., Goldman, B.D., Reznick, J.S., Hamer, R.M., Lin, W., Styner, M., Gerig, G., and Gilmore, J.H. (2012). Prenatal isolated mild ventriculomegaly is associated with persistent ventricle enlargement at ages 1 and 2. Early Hum Dev *88*, 691-698.

Lyoo, K., Noam, G., Lee, K., Kennedy, P., and Renshaw, F. (1996). The corpus callosum and lateral ventricles in children with attention-deficit hyperactivity disorder: a brain magnetic resonance imaging study. Biological psychiatry *40*, 1060-1063.

Madazli, R., Sal, V., Erenel, H., Gezer, A., and Ocak, V. (2011). Characteristics and outcome of 102 fetuses with fetal cerebral ventriculomegaly: experience of a university hospital in Turkey. J Obstet Gynaecol *31*, 142-145.

Magin, R.L., Lee, J.K., Klintsova, A., Carnes, K.I., and Dunn, F. (2000). Biological effects of long-duration, high-field (4 T) MRI on growth and development in the mouse. J Magn Reson Imaging *12*, 140-149.

Mahon, P., Harvey, N., Crozier, S., Inskip, H., Robinson, S., Arden, N., Swaminathan, R., Cooper, C., and Godfrey, K. (2010). Low maternal vitamin D status and fetal bone development: Cohort study. Journal of Bone and Mineral Research *25*, 14-19.

Malamateniou, C., Malik, S.J., Counsell, S.J., Allsop, J.M., McGuinness, A.K., Hayat, T., Broadhouse, K., Nunes, R.G., Ederies, A.M., Hajnal, J.V., *et al.* (2012). Motion-Compensation Techniques in Neonatal and Fetal MR Imaging. AJNR Am J Neuroradiol, [epub ahead of print].

Malamateniou, C., McGuinness, A.K., Allsop, J.M., O'Regan, D.P., Rutherford, M.A., and Hajnal, J.V. (2011). Snapshot inversion recovery: an optimized single-shot T1-weighted inversion-recovery sequence for improved fetal brain anatomic delineation. Radiology *258*, 229-235.

Malinger, G., Ben-Sira, L., Lev, D., Ben-Aroya, Z., Kidron, D., and Lerman-Sagie, T. (2004). Fetal brain imaging: a comparison between magnetic resonance imaging and dedicated neurosonography. Ultrasound Obstet Gynecol *23*, 333-340.

Malinger, G., Lev, D., Ben-Sira, L., Hoffmann, C., Herrera, M., Vinals, F., Vinkler, H., Ginath, S., Biran-Gol, Y., Kidron, D., *et al.* (2011a). Can syndromic macrocephaly be diagnosed in utero? Ultrasound Obstet Gynecol *37*, 72-81.

Malinger, G., Lev, D., Zahalka, N., Ben Aroia, Z., Watemberg, N., Kidron, D., Sira, L.B., and Lerman-Sagie, T. (2003). Fetal cytomegalovirus infection of the brain: the spectrum of sonographic findings. AJNR Am J Neuroradiol *24*, 28-32.

Malinger, G., Werner, H., Rodriguez Leonel, J.C., Rebolledo, M., Duque, M., Mizyrycki, S., Lerman-Sagie, T., and Herrera, M. (2011b). Prenatal brain imaging in congenital toxoplasmosis. Prenat Diagn, 881-886.

Manfredi, R., Tognolini, A., Bruno, C., Raffaelli, R., Franchi, M., and Pozzi Mucelli, R. (2010). Agenesis of the corpus callosum in fetuses with mild ventriculomegaly: role of MR imaging. Radiol Med *115*, 301-312.

Manganaro, L., Savelli, S., Francioso, A., Di Maurizio, M., Coratella, F., Vilella, G., Noia, G., Giancotti, A., Tomei, A., Fierro, F., *et al.* (2009). Role of fetal MRI in the diagnosis of cerebral ventriculomegaly assessed by ultrasonography. Radiol Med *114*, 1013-1023.

Mangin, J.F., Riviere, D., Cachia, A., Duchesnay, E., Cointepas, Y., Papadopoulos-Orfanos, D., Scifo, P., Ochiai, T., Brunelle, F., and Regis, J. (2004). A framework to study the cortical folding patterns. NeuroImage *23 Suppl 1*, 129-138.

Manoranjan, B., and Provias, J.P. (2010). Hemimegalencephaly: a fetal case with neuropathological confirmation and review of the literature. Acta Neuropathol *120*, 117-130.

McAllister, J.P., Maugans, T.A., Shah, M.V., and Truex, R.C. (1985). Neuronal effects of experimentally induced hydrocephalus in newborn rats. J Neurosurg *63*, 776-783.

McGrath, J.J., Burne, T.H., Feron, F., Mackay-Sim, A., and Eyles, D.W. (2010). Developmental vitamin D deficiency and risk of schizophrenia: a 10-year update. Schizophr Bull *36*, 1073-1078.

McQuillen, P.S., Sheldon, R.A., Shatz, C.J., and Ferriero, D.M. (2003). Selective vulnerability of subplate neurons after early neonatal hypoxia-ischemia. J Neurosci *23*, 3308-3315.

Mehta, T.S., and Levine, D. (2005). Imaging of fetal cerebral ventriculomegaly: a guide to management and outcome. Seminars in fetal & neonatal medicine *10*, 421-428.

Melchiorre, K., Bhide, A., Gika, A.D., Pilu, G., and Papageorghiou, A.T. (2009a). Counseling in isolated mild fetal ventriculomegaly. Ultrasound ObstetGynecol *34*, 212-224.

Melchiorre, K., Liberati, M., Celentano, C., Domizio, S., Puglielli, C., Buoni, S., Strambi, M., and Zannolli, R. (2009b). Neurological outcome following isolated 10-12 mm fetal ventriculomegaly. Arch Dis Child Fetal Neonatal Ed *94*, 311-312.

Melo (1999). Neuroimaging and Echocardiographic Findings in Sotos Syndrome To the Editor. American Journal of Medical Genetics *433*, 432-433.

Mercier, A., Eurin, D., Mercier, P.Y., Verspyck, E., Marpeau, L., and Marret, S. (2001). Isolated mild fetal cerebral ventriculomegaly: a retrospective analysis of 26 cases. Prenat Diagn *21*, 589-595.

Mercuri, E., Ricci, D., Pane, M., and Baranello, G. (2005). The neurological examination of the newborn baby. Early Hum Dev *81*, 947-956.

Mevissen, M., Buntenkotter, S., and Loscher, W. (1994). Effects of static and time-varying (50-Hz) magnetic fields on reproduction and fetal development in rats. Teratology *50*, 229-237.

Michel, S.C., Rake, A., Gotzmann, L., Seifert, B., Ferrazzini, M., Chaoui, R., Treiber, K., Keller, T.M., Marincek, B., and Kubik-Huch, R.A. (2002). Pelvimetry and patient acceptability compared between open 0.5-T and closed 1.5-T MR systems. Eur Radiol *12*, 2898-2905.

Millen, and Woollam (1962). The anatomy of the cerebrospinal fluid (Oxford University Press).

Miyan, J.A., Zendah, M., Mashayekhi, F., and Owen-Lynch, P.J. (2006). Cerebrospinal fluid supports viability and proliferation of cortical cells in vitro, mirroring in vivo development. Cerebrospinal Fluid Res *3*, 2.

Moffett, J.R., Ross, B., Arun, P., Madhavarao, C.N., and Namboodiri, A.M. (2007). N-Acetylaspartate in the CNS: from neurodiagnostics to neurobiology. Prog Neurobiol *81*, 89-131.

Mollanji, R., Papaiconomou, C., Boulton, M., Midha, R., Johnston, M., Granger, J.P., Physiol, A.J., Integr, R., and Physiol, C. (2012). Comparison of cerebrospinal fluid transport in fetal and adult sheep. Am J Physiol Regul Integr Comp Physiol *281*, 1215-1223.

Molnar, Z. (2011). Evolution of cerebral cortical development. Brain Behav Evol *78*, 94-107.

Monteagudo, A., and Timor-Tritsch, I.E. (2009). Normal sonographic development of the central nervous system from the second trimester onwards using 2D, 3D and transvaginal sonography. Prenatal diagnosis *29*, 326-339.

Monuki, E.S., and Walsh, C.A. (2001). Mechanisms of cerebral cortical patterning in mice and humans. Nat Neurosci *4 Suppl*, 1199-1206.

Moore, B.D., III, Slopis, J.M., Jackson, E.F., De Winter, A.E., and Leeds, N.E. (2000). Brain volume in children with neurofibromatosis type 1: relation to neuropsychological status. Neurology *54*, 914-920.

Mori, S., Kaufmann, W.E., Davatzikos, C., Stieltjes, B., Amodei, L., Fredericksen, K., Pearlson, G.D., Melhem, E.R., Solaiyappan, M., Raymond, G.V., *et al.* (2002). Imaging cortical association tracts in the human brain using diffusion-tensor-based axonal tracking. Magn Reson Med *47*, 215-223.

Morris, J.E., Rickard, S., Paley, M.N., Griffiths, P.D., Rigby, A., and Whitby, E.H. (2007). The value of in-utero magnetic resonance imaging in ultrasound diagnosed foetal isolated cerebral ventriculomegaly. Clin Radiol *62*, 140-144.

Mott, S.H., Bodensteiner, J.B., and Allan, W.C. (1992). The cavum septi pellucidi in term and preterm newborn infants. J Child Neurol *7*, 35-38.

Myers, C., Duncan, K.R., Gowland, P.A., Johnson, I.R., and Baker, P.N. (1998). Failure to detect intrauterine growth restriction following in utero exposure to MRI. Br J Radiol *71*, 549-551.

Nadel, A.S., and Benacerraf, B.R. (1995). Lateral Ventricular Atrium - Larger in Male Than Female Fetuses. Int J Gynecol Obstet *51*, 123-126.

Neil, J.J., Shiran, S.I., McKinstry, R.C., Schefft, G.L., Snyder, A.Z., Almli, C.R., Akbudak, E., Aronovitz, J.A., Miller, J.P., Lee, B.C., *et al.* (1998). Normal brain in human newborns: apparent diffusion coefficient and diffusion anisotropy measured by using diffusion tensor MR imaging. Radiology *209*, 57-66.

Nejat, F., Kazmi, S.S., and Ardakani, S.B. (2008). Congenital brain tumors in a series of seven patients. Pediatr Neurosurg *44*, 1-8.

Nichols, G.J., Martin, R.A., Wallace, G.B., and Fuchs, A.P. (2001). From neuron to brain, 4th edn (Sinauer Associates, Inc.).

Nicholson, C. (1999). Signals that go with the flow. TINS *22*, 143-145.

Nicolaides, K.H., Berry, S., Snijders, R.J., Thorpe-Beeston, J.G., and Gosden, C. (1990). Fetal lateral cerebral ventriculomegaly: associated malformations and chromosomal defects. Fetal Diagn Ther *5*, 5-14.

Nie, J., Guo, L., Li, G., Faraco, C., Stephen Miller, L., and Liu, T. (2010). A computational model of cerebral cortex folding. Journal of theoretical biology *264*, 467-478.

Nie, J., Guo, L., Li, K., Wang, Y., Chen, G., Li, L., Chen, H., Deng, F., Jiang, X., Zhang, T., *et al.* (2011). Axonal Fiber Terminations Concentrate on Gyri. Cerebral cortex, 1-9.

Nopoulos, P., Swayze, V., Flaum, M., Ehrhardt, J.C., Yuh, W.T.C., and Andreasen, N.C. (1997). Cavum septi pellucidi in normals and patients with schizophrenia as detected by magnetic resonance imaging. Biological psychiatry *41*, 1102-1108.

Nosarti, C., Rushe, T.M., Woodruff, P.W., Stewart, A.L., Rifkin, L., and Murray, R.M. (2004). Corpus callosum size and very preterm birth: relationship to neuropsychological outcome. Brain *127*, 2080-2089.

Novak, J.E., Turner, R.S., Agranoff, B.W., and Fisher, S.K. (1999). Differentiated human NT2-N neurons possess a high intracellular content of myo-inositol. Journal of neurochemistry *72*, 1431-1440.

Nucifora, P.G.P., Verma, R., Lee, S.-k., and Melhem, E.R. (2007). Diffusion-Tensor MR Imaging. Brain *245*.

O'Leary, D.D., Chou, S.J., and Sahara, S. (2007). Area patterning of the mammalian cortex. Neuron *56*, 252-269.

O'Leary, D.D., and Nakagawa, Y. (2002). Patterning centers, regulatory genes and extrinsic mechanisms controlling arealization of the neocortex. Curr Opin Neurobiol *12*, 14-25.

O'Rahilly, R., and Muller, F. (1990). Ventricular system and choroid plexuses of the human brain during the embryonic period proper. Am J Anat *189*, 285-302.

O'Rahilly, R., and Muller, F. (2008). Significant features in the early prenatal development of the human brain. Ann Anat *190*, 105-118.

Oishi, K., Faria, A., van Zijl Peter C. M., and Susumu, M. (2010). MRI Atlas of Human White Matter (Academic Press).

Oppenheim, R.W., Flavell, R.A., Vinsant, S., Prevette, D., Kuan, C.Y., and Rakic, P. (2001). Programmed cell death of developing mammalian neurons after genetic deletion of caspases. J Neurosci *21*, 4752-4760.

Oreskovic, D., and Klarica, M. (2010). The formation of cerebrospinal fluid: nearly a hundred years of interpretations and misinterpretations. Brain Res Rev *64*, 241-262.

Ouahba, J., Luton, D., Vuillard, E., Garel, C., Gressens, P., Blanc, N., Elmaleh, M., Evrard, P., and Oury, J.F. (2006). Prenatal isolated mild ventriculomegaly: outcome in 167 cases. BJOG *113*, 1072-1079.

Owen, M.J., O'Donovan, M.C., Thapar, A., and Craddock, N. (2011). Neurodevelopmental hypothesis of schizophrenia. Br J Psychiatry *198*, 173-175.

Palmen, S.J., Hulshoff Pol, H.E., Kemner, C., Schnack, H.G., Durston, S., Lahuis, B.E., Kahn, R.S., and Van Engeland, H. (2005). Increased gray-matter volume in medication-naive high-functioning children with autism spectrum disorder. Psychol Med *35*, 561-570.

Parada, C., Gato, A., Aparicio, M., and Bueno, D. (2006). Proteome analysis of chick embryonic cerebrospinal fluid. Proteomics *6*, 312-320.

Park, J.H., Park, Y.S., Suk, J.S., Park, S.W., Hwang, S.N., Nam, T.K., Kim, Y.B., and Lee, W.B. (2011). Cerebrospinal fluid pathways from cisterns to ventricles in N-butyl cyanoacrylate-induced hydrocephalic rats. J Neurosurg Pediatr *8*, 640-646.

Partridge, S.C., Mukherjee, P., Henry, R.G., Miller, S.P., Berman, J.I., Jin, H., Lu, Y., Glenn, O.A., Ferriero, D.M., Barkovich, A.J., *et al.* (2004). Diffusion tensor imaging: serial quantitation of white matter tract maturity in premature newborns. NeuroImage *22*, 1302-1314.

Patel, M.D., Filly, A.L., Hersh, D.R., and Goldstein, R.B. (1994). Isolated mild fetal cerebral ventriculomegaly: clinical course and outcome. Radiology *192*, 759-764.

Patel, M.D., Goldstein, R.B., Tung, S., and Filly, R.A. (1995). Fetal cerebral ventricular atrium: difference in size according to sex. Radiology *194*, 713-715.

Patel, T.B., and Clark, J.B. (1979). Synthesis of N-acetyl-L-aspartate by rat brain mitochondria and its involvement in mitochondrial/cytosolic carbon transport. The Biochemical journal *184*, 539-546.

Pellerin, L., Bouzier-Sore, A.K., Aubert, A., Serres, S., Merle, M., Costalat, R., and Magistretti, P.J. (2007). Activity-dependent regulation of energy metabolism by astrocytes: an update. Glia *55*, 1251-1262.

Perkins, L., Hughes, E., Srinivasan, L., Allsop, J., Glover, A., Kumar, S., Fisk, N., and Rutherford, M. (2008). Exploring cortical subplate evolution using magnetic resonance imaging of the fetal brain. Dev Neurosci *30*, 211-220.

Peters, S.U., Kaufmann, W.E., Bacino, C.A., Anderson, A.W., Adapa, P., Chu, Z., Yallampalli, R., Traipe, E., Hunter, J.V., and Wilde, E.A. (2011). Alterations in white matter pathways in Angelman syndrome. Dev Med Child Neurol *53*, 361-367.

Peterson, B.S., Vohr, B., Staib, L.H., Cannistraci, C.J., Dolberg, A., Schneider, K.C., Katz, K.H., Westerveld, M., Sparrow, S., Anderson, A.W., *et al.* (2000). Regional brain volume abnormalities and long-term cognitive outcome in preterm infants. JAMA *284*, 1939-1947.

Pier, D.B., Levine, D., Kataoka, M.L., Estroff, J.A., Werdich, X.Q., Ware, J., Beeghly, M., Poussaint, T.Y., Duplessis, A., Li, Y., *et al.* (2011). Magnetic resonance volumetric assessments of brains in fetuses with ventriculomegaly correlated to outcomes. J Ultrasound Med *30*, 595-603.

Pilu, G., Falco, P., Gabrielli, S., Perolo, A., Sandri, F., and Bovicelli, L. (1999). The clinical significance of fetal isolated cerebral borderline ventriculomegaly: report of 31 cases and review of the literature. Ultrasound Obstet Gynecol *14*, 320-326.

Pistorius, L.R., Smal, J., de Haan, T.R., Page-Christiaens, G.C., Verboon-Maciolek, M., Oepkes, D., and de Vries, L.S. (2008). Disturbance of cerebral neuronal migration following congenital parvovirus B19 infection. Fetal Diagn Ther *24*, 491-494.

Pistorius, L.R., Stoutenbeek, P., Groenendaal, F., de Vries, L., Manten, G., Mulder, E., and Visser, G. (2010). Grade and symmetry of normal fetal cortical development: a longitudinal two- and three-dimensional ultrasound study. Ultrasound Obstet Gynecol *36*, 700-708.

Poutamo, J., Partanen, K., Vanninen, R., Vainio, P., and Kirkinen, P. (1998). MRI does not change fetal cardiotocographic parameters. Prenat Diagn *18*, 1149-1154.

Pretorius, D.H., Drose, J.A., and Manco-Johnson, M.L. (1986). Fetal lateral ventricular ratio determination during the second trimester. J Ultrasound Med *5*, 121-124.

Price, D.L., De Wilde, J.P., Papadaki, A.M., Curran, J.S., and Kitney, R.I. (2001). Investigation of acoustic noise on 15 MRI scanners from 0.2 T to 3 T. J Magn Reson Imaging *13*, 288-293.

Pugash, D., Hendson, G., Dunham, C.P., Dewar, K., Money, D.M., and Prayer, D. (2012). Sonographic assessment of normal and abnormal patterns of fetal cerebral lamination. Ultrasound Obstet Gynecol, [epub ahead of print].

Qiu, M.G., Ye, Z., Li, Q.Y., Liu, G.J., Xie, B., and Wang, J. (2011). Changes of brain structure and function in ADHD children. Brain topography *24*, 243-252.

Rajagopalan, V., Scott, J., Habas, P.A., Kim, K., Corbett-Detig, J., Rousseau, F., Barkovich, A.J., Glenn, O.A., and Studholme, C. (2011a). Local tissue growth patterns underlying normal fetal human brain gyrification quantified in utero. J Neurosci *31*, 2878-2887.

Rajagopalan, V., Scott, J., Habas, P.A., Kim, K., Corbett-Detig, J., Rousseau, F., Barkovich, A.J., Glenn, O.A., and Studholme, C. (2011b). Local tissue growth patterns underlying normal fetal human brain gyrification quantified in utero. J Neurosci *31*, 2878-2887.

Rakic, P. (1971). Guidance of neurons migrating to the fetal monkey neocortex. Brain Res *33*, 471-476.

Rakic, P. (2006). A century of progress in corticoneurogenesis: from silver impregnation to genetic engineering. Cerebral cortex *16 Suppl 1*, 3-17.

Rakic, P., and Lombroso, P.J. (1998). Development of the cerebral cortex: I. Forming the cortical structure. J Am Acad Child Adolesc Psychiatry *37*, 116-117.

Rakic, S., and Zecevic, N. (2000). Programmed cell death in the developing human telencephalon. Eur J Neurosci *12*, 2721-2734.

Ramenghi, L.A., Rutherford, M., Fumagalli, M., Bassi, L., Messner, H., Counsell, S., and Mosca, F. (2009). Neonatal neuroimaging: going beyond the pictures. Early Hum Dev *85*, 75-77.

Ramsay, M., and Fitzhardinge, P.M. (1977). A comparative study of two developmental scales: the Bayley and the Griffiths. Early Hum Dev *1*, 151-157.

Raybaud, C. (2010). The corpus callosum, the other great forebrain commissures, and the septum pellucidum: anatomy, development, and malformation. Neuroradiology *52*, 447-477.

Raymond, A.A., Fish, D.R., Stevens, J.M., Sisodiya, S.M., Alsanjari, N., and Shorvon, S.D. (1994). Subependymal heterotopia: a distinct neuronal migration disorder associated with epilepsy. J Neurol Neurosurg Psychiatry *57*, 1195-1202.

Reeves, M.J., Brandreth, M., Whitby, E.H., Hart, A.R., Paley, M.N.J., Griffiths, P.D., and Stevens, J.C. (2010). Neonatal Cochlear Function: Measurement after Exposure to Acoustic Noise during in Utero MR Imaging. Radiology *257*, 802-809.

Roberts, T.P., and Schwartz, E.S. (2007). Principles and implementation of diffusion-weighted and diffusion tensor imaging. Pediatr Radiol *37*, 739-748.

Robertson, N.J., Kuint, J., Counsell, T.J., Rutherford, T.A., Coutts, A., Cox, I.J., and Edwards, A.D. (2000). Characterization of cerebral white matter damage in preterm infants using 1H and 31P magnetic resonance spectroscopy. Journal of cerebral blood flow and metabolism : official journal of the International Society of Cerebral Blood Flow and Metabolism *20*, 1446-1456.

Robertson, N.J., Lewis, R.H., Cowan, F.M., Allsop, J.M., Counsell, S.J., Edwards, A.D., and Cox, I.J. (2001). Early increases in brain myo-inositol measured by proton magnetic resonance spectroscopy in term infants with neonatal encephalopathy. Pediatr Res *50*, 692-700.

Roelants-Van Rijn, A.M., van der Grond, J., de Vries, L.S., and Groenendaal, F. (2001). Value of (1)H-MRS using different echo times in neonates with cerebral hypoxia-ischemia. Pediatr Res *49*, 356-362.

Roelants-van Rijn, A.M., van der Grond, J., Stigter, R.H., de Vries, L.S., and Groenendaal, F. (2004). Cerebral structure and metabolism and long-term outcome in small-for-gestational-age preterm neonates. Pediatr Res *56*, 285-290.

Rutherford, M. (2002a). MRI of the Neonatal Brain (London: WB Saunders).

Rutherford, M., Biarge, M.M., Allsop, J., Counsell, S., and Cowan, F. (2010). MRI of perinatal brain injury. Pediatr Radiol *40*, 819-833.

Rutherford, M., Srinivasan, L., Dyet, L., Ward, P., Allsop, J., Counsell, S., and Cowan, F. (2006). Magnetic resonance imaging in perinatal brain injury: clinical presentation, lesions and outcome. Pediatr Radiol *36*, 582-592.

Rutherford, M.A. (2002b). What's new in neuroimaging? Magnetic resonance imaging of the immature brain. European journal of paediatric neurology : EJPN : official journal of the European Paediatric Neurology Society *6*, 5-13.

Sadan, S., Malinger, G., Schweiger, A., Lev, D., and Lerman-Sagie, T. (2007). Neuropsychological outcome of children with asymmetric ventricles or unilateral mild ventriculomegaly identified in utero. BJOG *114*, 596-602.

Salehi, Z., and Mashayekhi, F. (2006). The role of cerebrospinal fluid on neural cell survival in the developing chick cerebral cortex: an in vivo study. Eur J Neurol *13*, 760-764.

Salomon, L.J., Bernard, J.P., and Ville, Y. (2007). Reference ranges for fetal ventricular width: a non-normal approach. Ultrasound Obstet Gynecol *30*, 61-66.

Salomon, L.J., Ouahba, J., Delezoide, A.L., Vuillard, E., Oury, J.F., Sebag, G., and Garel, C. (2006). Third-trimester fetal MRI in isolated 10- to 12-mm ventriculomegaly: is it worth it? BJOG *113*, 942-947.

Sari, A., Ahmetoglu, A., Dinc, H., Saglam, A., Kurtoglu, U., Kandemir, S., and Gumele, H.R. (2005). Fetal biometry: size and configuration of the third ventricle. Acta Radiol *46*, 631-635.

Sato, K., Yamaguchi, H., Miyamoto, H., and Kinouchi, Y. (1992). Growth of human cultured cells exposed to a non-homogeneous static magnetic field generated by Sm-Co magnets. Biochim Biophys Acta *1136*, 231-238.

Saunders, N.R., Liddelow, S.A., and Dziegielewska, K.M. (2012). Barrier mechanisms in the developing brain. Front Pharmacol *3*, 46.

Schenck, J.F. (2000). Safety of strong, static magnetic fields. J Magn Reson Imaging *12*, 2-19.

Schroder, H.J., and Power, G.G. (1997). Engine and radiator: fetal and placental interactions for heat dissipation. 403-414.

Scott, J.A., Habas, P.A., Kim, K., Rajagopalan, V., Hamzelou, K.S., Corbett-Detig, J.M., Barkovich, A.J., Glenn, O.A., and Studholme, C. (2011). Growth trajectories of the human fetal brain tissues estimated from 3D reconstructed in utero MRI. IntJ DevNeurosci *29*, 529-536.

Scott, J.A., Habas, P.A., Rajagopalan, V., Kim, K., Barkovich, A.J., Glenn, O.A., and Studholme, C. (2012). Volumetric and surface-based 3D MRI analyses of fetal isolated mild ventriculomegaly: Brain morphometry in ventriculomegaly. Brain Struct Funct, [Epub ahead of print].

Senat, M.V., Bernard, J.P., Schwarzler, P., Britten, J., and Ville, Y. (1999). Prenatal diagnosis and follow-up of 14 cases of unilateral ventriculomegaly. Ultrasound Obstet Gynecol *14*, 327-332.

Serhatlioglu, S., Kocakoc, E., Kiris, A., Sapmaz, E., Boztosun, Y., and Bozgeyik, Z. (2003). Sonographic measurement of the fetal cerebellum, cisterna magna, and cavum septum pellucidum in normal fetuses in the second and third trimesters of pregnancy. Journal of clinical ultrasound : JCU *31*, 194-200.

Sethna, F., Tennant, P.W., Rankin, J., and S, C.R. (2011). Prevalence, natural history, and clinical outcome of mild to moderate ventriculomegaly. Obstet Gynecol *117*, 867-876.

Sharma, S., Khan, N., Khadri, A., Julies, P., Gnanasambandam, S., Saroey, S., Jacobs, B., Beski, S., Coren, M., and Alexander, S. (2009). Vitamin D in pregnancy-time for action: a paediatric audit. BJOG *116*, 1678-1682.

Shu, T.Z., Li, Y., Keller, A., and Richards, L.J. (2003). The glial sling is a migratory population of developing neurons. Development *130*, 2929-2937.

Signorelli, M., Tiberti, A., Valseriati, D., Molin, E., Cerri, V., Groli, C., and Bianchi, U.A. (2004). Width of the fetal lateral ventricular atrium between 10 and 12 mm: a simple variation of the norm? Ultrasound Obstet Gynecol *23*, 14-18.

Simon, E.M., Goldstein, R.B., Coakley, F.V., Filly, R.A., Broderick, K.C., Musci, T.J., and Barkovich, A.J. (2000). Fast MR imaging of fetal CNS anomalies in utero. AJNR Am J Neuroradiol *21*, 1688-1698.

Simonati, A., Tosati, C., Rosso, T., Piazzola, E., and Rizzuto, N. (1999). Cell proliferation and death: morphological evidence during corticogenesis in the developing human brain. Microsc Res Tech *45*, 341-352.

Skiold, B., Horsch, S., Hallberg, B., Engstrom, M., Nagy, Z., Mosskin, M., Blennow, M., and Aden, U. (2010). White matter changes in extremely preterm infants, a population-based diffusion tensor imaging study. Acta paediatrica *99*, 842-849.

Smart, I.H., Dehay, C., Giroud, P., Berland, M., and Kennedy, H. (2002). Unique morphological features of the proliferative zones and postmitotic compartments of the neural epithelium giving rise to striate and extrastriate cortex in the monkey. Cerebral cortex *12*, 37-53.

Smith, F.W., Adam, A.H., and Phillips, W.D. (1983). NMR imaging in pregnancy. Lancet *1*, 61-62.

Smith, F.W., MacLennan, F., Abramovich, D.R., MacGilivray, I., and Hutchison, J.M. (1984). NMR imaging in human pregnancy: a preliminary study. Magn Reson Imaging *2*, 57-64.

Smith, S.M., Jenkinson, M., Johansen-Berg, H., Rueckert, D., Nichols, T.E., Mackay, C.E., Watkins, K.E., Ciccarelli, O., Cader, M.Z., Matthews, P.M., *et al.* (2006). Tract-based spatial statistics: voxelwise analysis of multi-subject diffusion data. NeuroImage *31*, 1487-1505.

Smith, S.M., Jenkinson, M., Woolrich, M.W., Beckmann, C.F., Behrens, T.E., Johansen-Berg, H., Bannister, P.R., De Luca, M., Drobnjak, I., Flitney, D.E., *et al.* (2004). Advances in functional and structural MR image analysis and implementation as FSL. NeuroImage *23 Suppl 1*, 208-219.

Smith, S.M., and Nichols, T.E. (2009). Threshold-free cluster enhancement: addressing problems of smoothing, threshold dependence and localisation in cluster inference. NeuroImage *44*, 83-98.

Smulian, J.C., Campbell, W.A., Rodis, J.F., Feeney, L.D., Fabbri, E.L., and Vintzileos, A.M. (1995). Gender-specific second-trimester biometry. Am J Obstet Gynecol *173*, 1195-1201.

Snijders, R.J.M., and Nicolaides, K.H. (1994). Fetal Biometry at 14-40 Weeks Gestation. Ultrasound in obstetrics & gynecology *4*, 34-48.

Srour, M., Rioux, M.F., Varga, C., Lortie, A., Major, P., Robitaille, Y., Decarie, J.C., Michaud, J., and Carmant, L. (2011). The clinical spectrum of nodular heterotopias in children: report of 31 patients. Epilepsia *52*, 728-737.

Steinlin, M. (2007). The cerebellum in cognitive processes: supporting studies in children. Cerebellum *6*, 237-241.

Story, L., Damodaram, M.S., Allsop, J.M., McGuinness, A., Patel, A., Wylezinska, M., Hagberg, H., Kumar, S., and Rutherford, M.A. (2011a). Brain metabolism in fetal intrauterine growth restriction: a proton magnetic resonance spectroscopy study. Am J Obstet Gynecol *205*, 483-488.

Story, L., Damodaram, M.S., Allsop, J.M., McGuinness, A., Wylezinska, M., Kumar, S., and Rutherford, M.A. (2011b). Proton magnetic resonance spectroscopy in the fetus. Eur J Obstet Gynecol Reprod Biol *158*, 3-8.

Sur, M., and Rubenstein, J.L. (2005). Patterning and plasticity of the cerebral cortex. Science *310*, 805-810.

Tabernero, A., Vicario, C., and Medina, J.M. (1996). Lactate spares glucose as a metabolic fuel in neurons and astrocytes from primary culture. Neurosci Res *26*, 369-376.

Tanabe, H., Sawada, T., Inoue, N., Ogawa, M., Kuriyama, Y., and Shiraishi, J. (1987). Conduction aphasia and arcuate fasciculus. Acta neurologica Scandinavica *76*, 422-427.

Tatli, B., Ozer, I., Ekici, B., Kalelioglu, I., Has, R., Eraslan, E., and Yuksel, A. (2012). Neurodevelopmental outcome of 31 patients with borderline fetal ventriculomegaly. Clin Neurol Neurosurg *114*, 969-971.

Tau, G.Z., and Peterson, B.S. (2010). Normal development of brain circuits. Neuropsychopharmacology *35*, 147-168.

Toi, A., Lister, W.S., and Fong, K.W. (2004). How early are fetal cerebral sulci visible at prenatal ultrasound and what is the normal pattern of early fetal sulcal development? Ultrasound Obstet Gynecol *24*, 706-715.

Tolsa, C.B., Zimine, S., Warfield, S.K., Freschi, M., Sancho, R.A., Lazeyras, F., Hanquinet, S., Pfizenmaier, M., and Huppi, P.S. (2004). Early alteration of structural and functional brain development in premature infants born with intrauterine growth restriction. PediatrRes *56*, 132-138.

Toro, R., and Burnod, Y. (2005). A morphogenetic model for the development of cortical convolutions. Cerebral cortex *15*, 1900-1913.

Tusor, N., Wusthoff, C., Smee, N., Merchant, N., Arichi, T., Allsop, J.M., Cowan, F.M., Azzopardi, D., Edwards, A.D., and Counsell, S.J. (2012). Prediction of neurodevelopmental outcome after hypoxic-ischemic encephalopathy treated with hypothermia by diffusion tensor imaging analyzed using tract-based spatial statistics. Pediatr Res *72*, 63-69.

Tyson, R.L., Gallagher, C., and Sutherland, G.R. (2003). 13C-Labeled substrates and the cerebral metabolic compartmentalization of acetate and lactate. Brain Res *992*, 43-52.

Ueno, S., Iwasaka, M., and Shiokawa, K. (1994). Early embryonic development of frogs under intense magnetic fields up to 8 T. . J Appl Phys *75*, 7165-7167.

Urenjak, J., Williams, S.R., Gadian, D.G., and Noble, M. (1993). Proton nuclear magnetic resonance spectroscopy unambiguously identifies different neural cell types. J Neurosci *13*, 981-989.

Vadeyar, S.H., Moore, R.J., Strachan, B.K., Gowland, P.A., Shakespeare, S.A., James, D.K., Johnson, I.R., and Baker, P.N. (2000). Effect of fetal magnetic resonance imaging on fetal heart rate patterns. Am J Obstet Gynecol *182*, 666-669.

Valsky, D.V., Ben-Sira, L., Porat, S., Yanai, N., Lewin, A., Nadjari, M., Gomori, J.M., and Yagel, S. (2004). The role of magnetic resonance imaging in the evaluation of isolated mild ventriculomegaly. J Ultrasound Med *23*, 525-526.

van Cappellen van Walsum, A.M., Heerschap, A., Nijhuis, J.G., Oeseburg, B., and Jongsma, H.W. (1998). Proton magnetic resonance spectroscopy of fetal lamb brain during hypoxia. Am J Obstet Gynecol *179*, 756-757.

van der Knaap, M.S., van Wezel-Meijler, G., Barth, P.G., Barkhof, F., Ader, H.J., and Valk, J. (1996). Normal gyration and sulcation in preterm and term neonates: appearance on MR images. Radiology *200*, 389-396.

van Kooij, B.J., de Vries, L.S., Ball, G., van Haastert, I.C., Benders, M.J., Groenendaal, F., and Counsell, S.J. (2012). Neonatal tract-based spatial statistics findings and outcome in preterm infants. AJNR Am J Neuroradiol *33*, 188-194.

van Straaten, H.W., and Copp, A.J. (2001). Curly tail: a 50-year history of the mouse spina bifida model. Anat Embryol *203*, 225-237.

VanEssen, D. (1997). A tension-based theory of morphogenesis and compact wiring in the central nervous systemy.

Varela, M., Groves, A.M., Arichi, T., and Hajnal, J.V. (2012). Mean cerebral blood flow measurements using phase contrast MRI in the first year of life. NMR Biomed *25*, 1063-1072.

Vergani, P., Locatelli, A., Strobelt, N., Cavallone, M., Ceruti, P., Paterlini, G., and Ghidini, A. (1998). Clinical outcome of mild fetal ventriculomegaly. Am J Obstet Gynecol *178*, 218-222.

Wakana, S., Jiang, H., Nagae-Poetscher, L.M., van Zijl, P.C., and Mori, S. (2004). Fiber tract-based atlas of human white matter anatomy. Radiology *230*, 77-87.

Weichert, J., Hartge, D., Krapp, M., Germer, U., Gembruch, U., and Axt-Fliedner, R. (2010). Prevalence, characteristics and perinatal outcome of fetal ventriculomegaly in 29,000 pregnancies followed at a single institution. Fetal Diagn Ther *27*, 142-148.

Whitehouse, A.J., Holt, B.J., Serralha, M., Holt, P.G., Kusel, M.M., and Hart, P.H. (2012). Maternal serum vitamin D levels during pregnancy and offspring neurocognitive development. Pediatrics *129*, 485-493.

Wilhelm, C., Keck, C., Hess, S., Korinthenberg, R., and Breckwoldt, M. (1998). Ventriculomegaly diagnosed by prenatal ultrasound and mental development of the children. Fetal Diagn Ther *13*, 162-166.

Wimberger, D.M., Roberts, T.P., Barkovich, A.J., Prayer, L.M., Moseley, M.E., and Kucharczyk, J. (1995). Identification of "premyelination" by diffusion-weighted MRI. Journal of computer assisted tomography *19*, 28-33.

Winter, T.C., Kennedy, A.M., Byrne, J., and Woodward, P.J. (2010). The cavum septi pellucidi: why is it important? J Ultrasound Med *29*, 427-444.

Woodward, B.J., Papile, L.A., Lowe, J.R., Laadt, V.L., Shaffer, M.L., Montman, R., and Watterberg, K.L. (2011). Use of the Ages and Stages Questionnaire and Bayley Scales of Infant Development-II in neurodevelopmental follow-up of extremely low birth weight infants. J Perinatol *31*, 641-646.

Wright, C., Rabe-Hesketh, S., Woodruff, W., David, W., Murray, M., and Bullmore, T. (2000). Meta-analysis of regional brain volumes in schizophrenia. The American journal of psychiatry *157*, 16-25.

Wyldes, M., and Watkinson, M. (2004). Isolated mild fetal ventriculomegaly. Archives of disease in childhood Fetal and neonatal edition *89*, F9-13.

Xue, H., Srinivasan, L., Jiang, S., Rutherford, M., Edwards, A.D., Rueckert, D., and Hajnal, J.V. (2007). Automatic segmentation and reconstruction of the cortex from neonatal MRI. NeuroImage *38*, 461-477.

Yakovlev, P.I., and Lecours, A.R. (1967). The myelogenetic cycles of regional maturation of the brain.

Yip, Y.P., Capriotti, C., Norbash, S.G., Talagala, S.L., and Yip, J.W. (1994a). Effects of MR exposure on cell proliferation and migration of chick motoneurons. J Magn Reson Imaging *4*, 799-804.

Yip, Y.P., Capriotti, C., Talagala, S.L., and Yip, J.W. (1994b). Effects of MR exposure at 1.5 T on early embryonic development of the chick. J Magn Reson Imaging *4*, 742-748.

Yushkevich, P.A., Piven, J., Hazlett, H.C., Smith, R.G., Ho, S., Gee, J.C., and Gerig, G. (2006). User-guided 3D active contour segmentation of anatomical structures: significantly improved efficiency and reliability. NeuroImage *31*, 1116-1128.

Zappaterra, M.D., Lisgo, S.N., Lindsay, S., Gygi, S.P., Walsh, C.A., and Ballif, B.A. (2007). A comparative proteomic analysis of human and rat embryonic cerebrospinal fluid. Journal of proteome research *6*, 3537-3548.

Zecevic, N. (1993). Cellular composition of the telencephalic wall in human embryos. Early Hum Dev *32*, 131-149.

Zecevic, N., and Rakic, P. (2001). Development of layer I neurons in the primate cerebral cortex. J Neurosci *21*, 5607-5619.

Ziegler, E.E., Hollis, B.W., Nelson, S.E., and Jeter, J.M. (2006). Vitamin D deficiency in breastfed infants in Iowa. Pediatrics *118*, 603-610.

Zilles, K., Armstrong, E., Schleicher, A., and Kretschmann, H.-J. (1988). The human pattern of gyrification in the cerebral cortex. Anat Embryol *179*, 173-179.

Zoossmann-Diskin, A., Gazit, E., Peleg, L., Shohat, M., and Turner, D. (2008). Thrombophilic polymorphisms in Israel. Blood Cells Mol Dis *41*, 230-233.